

SYNTHESIS AND BIOLOGICAL APPLICATIONS OF FLAVONOID BASED NATURAL PRODUCTS

Ph.D. THESIS

by

IRAM PARVEEN



**DEPARTMENT OF CHEMISTRY
INDIAN INSTITUTE OF TECHNOLOGY ROORKEE
ROORKEE – 247 667 (INDIA)
SEPTEMBER, 2018**

SYNTHESIS AND BIOLOGICAL APPLICATIONS OF FLAVONOID BASED NATURAL PRODUCTS

A THESIS

*Submitted in partial fulfilment of the
requirements for the award of the degree*

of

DOCTOR OF PHILOSOPHY

in

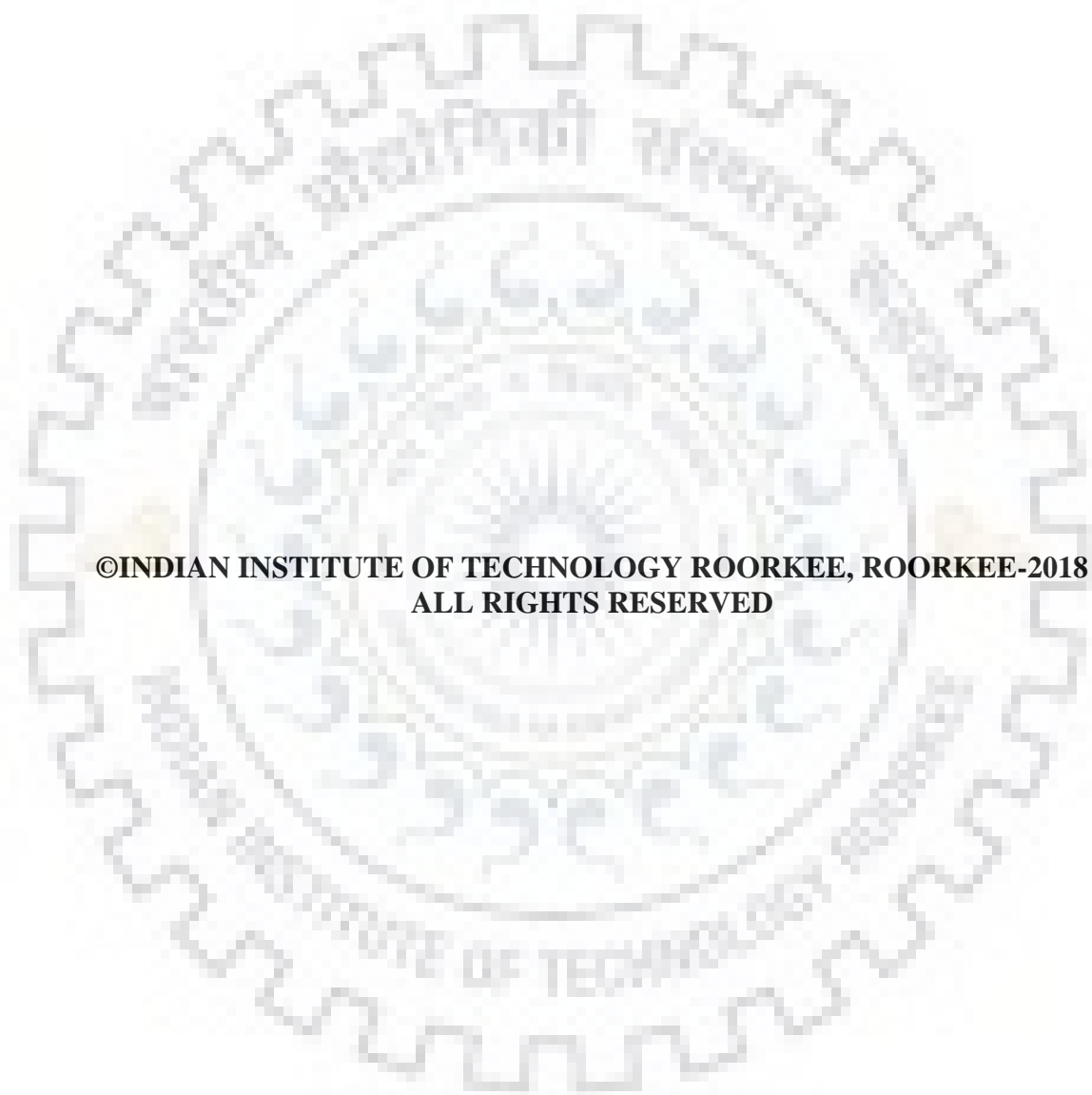
CHEMISTRY

by

IRAM PARVEEN



**DEPARTMENT OF CHEMISTRY
INDIAN INSTITUTE OF TECHNOLOGY ROORKEE
ROORKEE – 247 667 (INDIA)
SEPTEMBER, 2018**



**©INDIAN INSTITUTE OF TECHNOLOGY ROORKEE, ROORKEE-2018
ALL RIGHTS RESERVED**



INDIAN INSTITUTE OF TECHNOLOGY ROORKEE ROORKEE

CANDIDATE'S DECLARATION

I hereby certify that the work which is being presented in the thesis entitled “**SYNTHESIS AND BIOLOGICAL APPLICATIONS OF FLAVONOID BASED NATURAL PRODUCTS**” in partial fulfilment of the requirements for the award of the Degree of Doctor of Philosophy and submitted in the Department of Chemistry of the Indian Institute of Technology Roorkee, Roorkee is an authentic record of my own work carried out during a period from July, 2013 to September, 2018 under the supervision of Dr. Naseem Ahmed, Associate Professor, Department of Chemistry, Indian Institute of Technology Roorkee, Roorkee.

The matter presented in this thesis has not been submitted by me for the award of any other degree of this or any other institution.

(**IRAM PARVEEN**)

This is to certify that the above statement made by the candidate is correct to the best of my knowledge.

(Naseem Ahmed)
Supervisor

Dated: September, 2018

The Ph.D. Viva-Vice Examination of **Miss Iram Parveen**, Research scholar, has been held on.....

Chairman, SRC

Signature of External Examiner

This is to certify that the student has made all the corrections in the thesis.

Signature of Supervisor

Head of the Department



ACKNOWLEDGEMENT

First and foremost, I am submissively bowing down to the almighty for bestowing me with innumerable blessings and uncountable favors throughout my life. I am sincerely grateful to Him for my skills and capabilities and for the many chances He gave me to arrive here and hold my head high with self-esteem.

I would like to express my sincere gratitude to my Supervisor Dr. Naseem Ahmed, Department of Chemistry, IIT Roorkee who was always available for discussions. He has contributed a great deal to my understanding in research through valuable discussions, ideas and useful comments, which were a great source of my inspiration.

I take the opportunity to express my gratitude to my Student Research Committee (SRC) members Dr. Anuj Sharma and Dr. Rama Krishna Peddinti, Department of Chemistry and Dr. Parsenjit Mondal, Department of Chemical engineering, IIT Roorkee for extending me all possible help and offering valuable suggestions during the entire course. I am highly grateful to Prof. M. R. Maurya, Head of the Department of Chemistry, for providing me with necessary facilities and support to carry out my work. I am thankful to Mr. S. P. Singh, Mr. Madan Pal, Mr. Tiwari and other staff members, Department of Chemistry, for giving a helping hand to me on all occasions.

I also thank to the Head, Institute instrumentation center, IIT Roorkee for providing NMR and other necessary instrumentation facilities. I would like to thanks Ms. Neetu Singh and Prof. U. P. Singh, IIT Roorkee, for single crystal X-ray data collection and discussion at various stage of my research work. I wish to put on record my gratitude to the Editors & Reviewers for their comments/suggestions during publishing manuscripts and conference proceedings.

I would like to thank my seniors and labmates Dr. S. M. Abdul shakoor, Dr. Naveen Konduru, Dr. Shaily, Dr. Nishant, Dr. Gulab, Dr. Sumit, Waheed, Mauzey, Danish, Khawaja and Bhawana. I thank you all for your cooperation, help, maintaining excellent working atmosphere in the lab and sparing time for me whenever I needed it from you. I am also grateful to all the members of Chemistry Department for their cooperation and timely help which provided a suitable environment to develop my skills as a researcher. True friendship is the soul of a beautiful life. I consider myself truly blessed as I have always been in a good company of friends. Their daily smiles and laughter have made my time intensely delightful and certainly unforgettable. I would like to gratefully thanks to my special friends Dr. Nirma Maurya, Dr. Mandeep Kaur, Dr. Surinder Pal Kaur, Dr. Divya singhal, Dr. Neha Gupta, Dr. Nitika Sharma, Dr. Ankita Saini, Dr. Himanshu, Dr. Tawseef Ahmed Dar, Mandeep Khan, Shweta, Manju, Kavita, Garima, Madhusudan,

ACKNOWLEDGEMENT

Anshu, Neha dua and Pratima with whom I have shared the best time of my life and who were always there in the hour of need. I extended my warm thanks to my friends Maheen, Khushnuma, Samya, Kanika, Huma, Gulista, Saima and all my batch mates at AMU.

It is a privilege to express my sincerest and warm gratitude to all the teachers who have taught me since childhood. I always value their patience, labour and dedicated efforts that they undertook to make me learn. Their advices and scoldings will always remain close to my heart and I will keep seeking them for further guidance and knowledge.

I am thankful to IITR and UGC, India for providing me the fellowship. I am grateful to IITR for providing necessary infrastructure for my research work.

I am incredibly lucky to have been born in a family of caring and loving members. My family deserves special mention for their unflagging love and support in my life. This work would simply have been impossible without them. I am indebted to my beloved mother Smt. Jannat Khatoon and father Sh. Inayat Hussain Ansari for their love, affection, constant inspiration, unconditional support throughout my life. I also thank to my family members Sh. Farooqe Ahmed and Smt. Akhtarun Nisha for their love, encouragement and innumerable prayers. I extend my gratefulness and love to my elder brothers Amjad Ali, Parvez Alam Ansari, Asad, Danish, Adil and cute younger sister Mahek for their love, affection and for all the sweet memories. I am exceedingly thankful to my special gratitude to my younger brother Javed Akhter for his loving support and encouragement and being a pillar of strength for me.

As I conclude, my apologies and honest gratitude to all those whose names have been unintentionally left. I hold all of them in high regards and I know they will swarm around me with their best efforts whenever I need them.

Finally, I am thankful to almighty GOD, for his mercy and grace bestowed upon me during my entire life.

Iram Parveen

ABSTRACT

The thesis entitled “**Synthesis and Biological Applications of Flavonoid Based Natural Products**” is reported in six chapters.

The present work is aimed to design and synthesis of novel flavonoids-based derivatives involving C-C, C-O, C-N bonds formation using different reactions like Ullmann coupling, Aza-Michael ring opening and cyclization, C-H amination, dehalogenation reaction. The novel synthesized compounds were characterized through different spectral techniques such as ^1H NMR, ^{13}C NMR, IR, LC-MS, HRMS and x-ray diffraction and their biological evaluations were reported as anti-proliferative applications. The thesis has been divided into six chapters for the sake of convenience and clarity and organized as follows:

Chapter 1: Introduction

Flavonoids are found in most of the higher plants as secondary metabolites and are water soluble due to polyphenolic nature. These naturally occurring compounds are widely distributed in plants like vegetables, tea, soya bean, berries and other citrus fruits as dietary sources. They have exhibited antioxidant and chelating properties so have many health promoting effects. Some of the activities attributed to flavonoids include anti-allergic, anti-cancer, antioxidant, anti-inflammatory and anti-viral. Flavonoids as central core containing compounds are used as drugs such as xanthokeyismins A-C and dime fine for the treatment of bronchial asthma. Chromene and quinoline based conjugates belong to important class of natural and synthetic compounds displaying a broad spectrum of pharmacological activities including anticancer, antitubercular, anti-inflammatory, antimicrobial, antihistaminic, antihypertensive and anti-HIV activity.

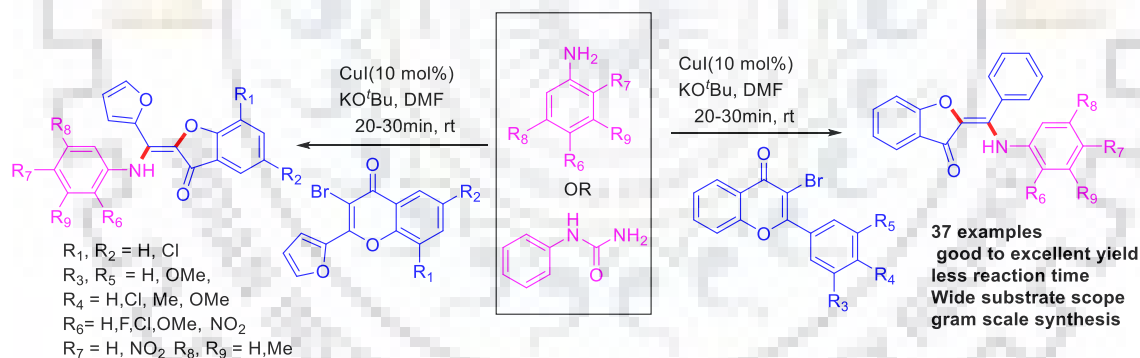
Natural product is a substance or compound, created *via* living organism such as - plants, fruits and microorganisms, etc. exclusively found in nature, formed with metabolism. For the development in the field of organic chemistry, natural products have participated a vital role by providing confronting synthetic targets in drug development and drug synthesis. Directly and indirectly, a huge percentage of drugs in modern medicine are originated from natural sources. Traditionally significant concept for the natural products is that it is applied as a therapeutic agent in different disease such as cancer infectious disease and reduced pain flavonoids, carotenoids, chromones, coumarins, alkaloids and quinolines etc. are considered as a significant part of natural products and usually utilized around the world due to their assorted pharmacological properties. In general, flavonoids, chromenes and quinolines have occupied a

ABSTRACT

considerable amount of research space owing to their diverse pharmacological, therapeutic and chemo-sensor applications.

Chapter 2. Route to Highly Functionalized stereospecific-Aminated Aurones from 3-bromo flavones with aniline and N-phenyl urea via a Domino- Aza Michael- ring opening-cyclization reaction

In this chapter, We describe the synthesis and characterization stereospecific aminated aurone scaffold by cascade Domino reaction (Aza Michael addition, ring opening and cyclization reaction) between 3-bromoflavone and aniline or N- phenyl urea is make known to continue economically in the presence of potassium tertiary but-oxide as a base and copper Iodide as a catalyst. Optimization of the reaction conditions and screening of copper Iodide 5 mol % best catalyst and 3 equivalents of KO^tBu best base and DMF is suitable solvent for the stereospecific aminated aurone which gave products in good yields to excellent yields (62-84%). This protocol is operationally successful with ease, avoids the requirement of additives and ligand, less reaction time, and offers broad substrate scope with high yielding.



Scheme: 1 Synthesis of stereospecific aminated aurone from 3-bromo flavone and aniline and N-phenyl urea.

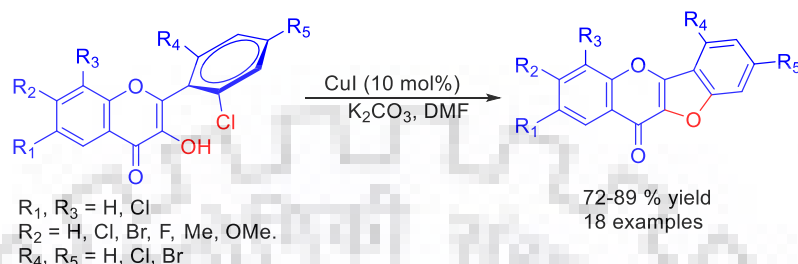
All synthesized compounds were fully characterized by ¹H-NMR, ¹³C-NMR, FT-IR, HR-MS and single crystal X-ray analysis.

Chapter 3: CuI mediated synthesis of heterocyclic flavone-benzofuran fused derivatives

In this chapter, A copper iodide catalyzed the coupling reaction of substituted 2-(2-chlorophenyl)-3-hydroxy-4H-chromen-4-ones with base *i.e.* K₂CO₃ followed by intramolecular cyclization between -OH (hydroxy) and -Cl (Chloro) group leads to

ABSTRACT

assembling of functionalized Flavone fused benzofuran derivative with good to excellent yield (75–90%), a natural product with a broad range of biological activities. This protocol involves less reaction time, low catalyst loading, ligand free, fast conversion and mild reaction condition.



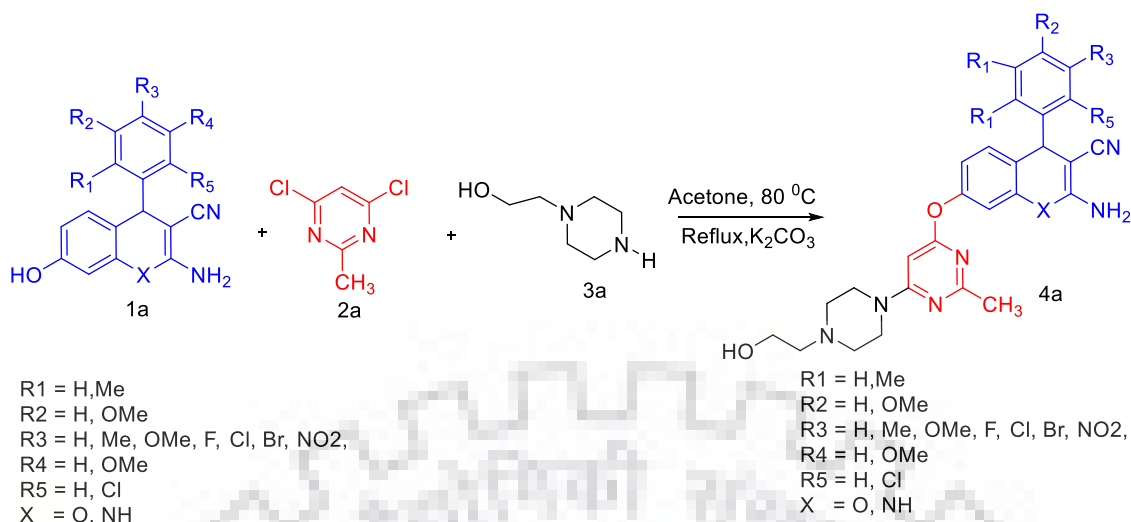
Scheme: 2 Synthesis of flavone fused benzofuran derivative.

All Synthesized compounds were fully characterized by ¹H NMR, ¹³C NMR, FT-IR and LCMS.

Chapter 4. Synthesis, estrogen receptor binding affinity and molecular docking of pyrimidine-piperazine-chromene and -quinoline conjugates

In this chapter, we report a simple, mild and efficient multi-component reaction in one pot synthesis and characterization of substituted 2-amino-7-((6-(4-(2-hydroxyethyl) piperazin-1-yl)-2-methylpyrimidin-4-yl)oxy)-4-phenyl-4*H*-chromene-3-carbonitrile and 2-amino-7-((6-(4-(2-hydroxyethyl)piperazin-1-yl)-2-methylpyrimidin-4-yl)oxy)-4-phenyl-1,4-dihydroquinoline-3-carbonitrile conjugates under mild reaction condition. The synthesised compounds (**5a -5t**) were assessed their antiproliferative activities against human embryonic kidney cells (HEK293) (Normal cell) and human breast cancer cell lines (MCF-7). Compounds **5f**, **5g**, **5o**, **5q** and **5s** showed better cytotoxic activities as (48 ± 1.70, 65 ± 1.13, 92 ± 1.18, 30 ± 1.17 and 16 ± 1.10) with (IC₅₀ < 50 mM) against human breast cancer line than curcumin drug (48 ± 1.11) as compare to other compounds. We also perform molecular docking with compounds **5f**, **5g** and **5o** against Bcl-2 protein which gave good binding affinity (ΔG = -9.08 kcal/mol, -8.29 kcal/mol and -7.70 kcal/mol). Furthermore, the structure-activity relationship (SAR) study exposed that the optimal amalgamation enhanced anti-proliferative activities when quinoline and chromene moiety attached with pyrimidine and piperazine moiety. All synthesized compounds were fully characterized by ¹H-NMR, ¹³C-NMR, FT-IR, LC-MS.

ABSTRACT

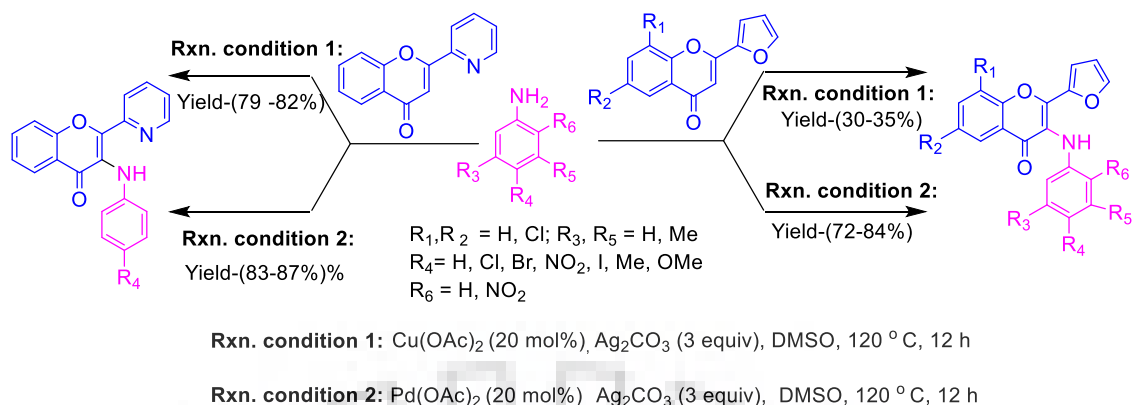


Scheme: 3 Synthesis of chromene and quinoline derivative with pyrimidine and piperazine and their biological evolution against human breast cancer cell line and human embryonic kidney cell line.

Chapter-5: Design, Synthesis, Molecular docking and Molecular Insights Inhibition studies of Microtubule Affinity Regulating Kinase 4 of novel 3-N-aryl substituted-2-heteroarylchromones for Cancer Therapy

In this chapter we describe a series of 3-N-aryl substituted-2-heteroarylchromones were designed and efficiently synthesized *via* Pd-mediated oxidative coupling using 2-heteroarylchromones and anilines as selective human Microtubule affinity regulating kinase 4 (MARK4) enzyme inhibitors, a recently identified anti-cancer drug target. Among 22 synthesized molecules, compounds para-iodo, para-nitro and para-methyl were identified as hit and exhibited excellent *in vitro* inhibitory effect against MARK4 with IC₅₀ value (50% of ATPase activity) at 2.12 ± 0.22 μM, 1.98 ± 0.34 μM and 5.56 ± 0.42 μM respectively. The fluorescence binding and dot blot assay were found in μM range for compounds para-iodo, para-nitro and para-methyl substituted derivative which indicates a better binding affinity. *In vitro* studies against the cancerous cells (MCF-7 and HepG2) revealed that the compounds para-iodo, para-nitro and para-methyl substituted derivative inhibit the cell viability, induce apoptosis and tau-phosphorylation. Cell viability studies gave the growth inhibition of cancerous cells with IC₅₀ values of 3.22 ± 0.42, 4.32 ± 0.23 μM and 16.22 ± 1.33 μM for human breast cancer cells (MCF-7) and 6.45 ± 1.12, 5.22 ± 0.72 μM and 19.12 ± 1.43 μM for human liver carcinoma cells (HepG2) respectively.

ABSTRACT



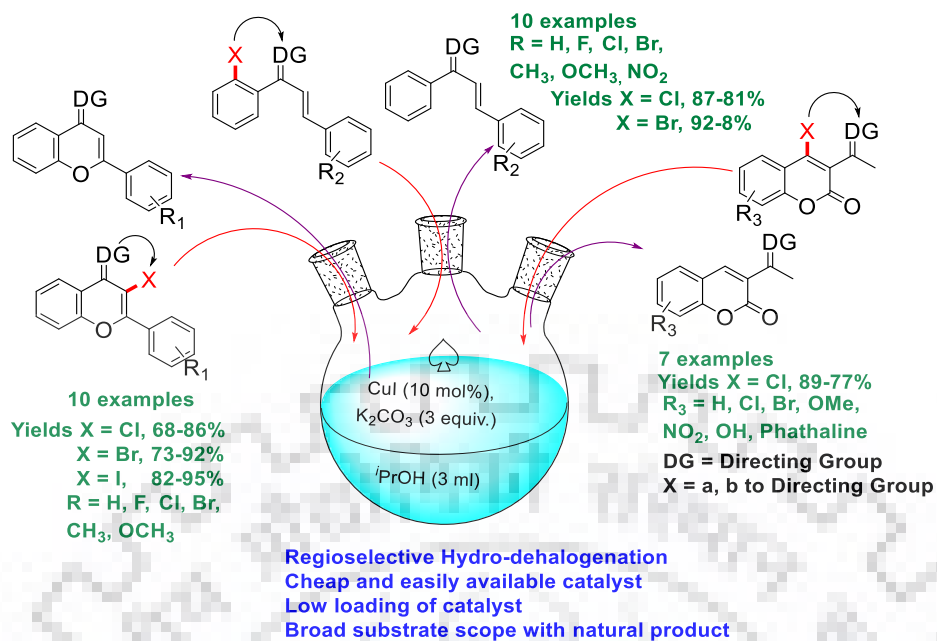
Scheme: 4 Synthesis of 3-N-aryl substituted-2-heteroarylchromones and their Microtubule Affinity Regulating Kinase 4 for human breast cancer cell line, human liver carcinoma cells and human embryonic kidney cell line.

Also, compounds *para*-iodo, *para*-nitro and *para*-methyl put the cancerous cells on oxidative stress as suggested by ROS quantification. Based on above studies, molecular docking of compounds *para*-iodo, *para*-nitro and *para*-methyl showed hydrogen bonding, charge or polar and van der Waals interactions by the active site residues of MARK4. These observations clearly showed that the compounds fit nicely in the active site with high binding affinity. Thus, compounds may be as potential inhibitors and further explored to design novel therapeutic molecules in the drug discovery against MARK4-related diseases. All synthesized compounds were fully characterized by ¹H-NMR, ¹³C-NMR, FT-IR, HRMS.

Chapter 6. Regioselective Hydrodehalogenation of Aromatic α - and β -Halo carbonyl Compounds by CuI in Isopropanol

An operationally simple copper-catalyzed hydro-dehalogenation of β '-halo-chalcone and α -halo-flavone has been developed with isopropanol used as a solvent and also serve as a hydride source in basic medium at 90 °C leads to the corresponding hydro dehalogenation chalcone and flavone products with high selectivity. By this reagent combination, Iodide, bromide and chloride can be reduced without any ligand involving good to excellent yield. The reduction is companionable with numerous electron-withdrawing or electron-donating groups. All synthesized compounds were fully characterized by ¹H-NMR, ¹³C-NMR, FT-IR, HRMS.

ABSTRACT



Scheme 5. Synthesis of β' -dehalogenated chalcone and α -flavone product from β -halochalcone and α -haloflavone.

ABBREVIATIONS

AChE	Acetylcholinesterase
AIDS	Acquired Immunodeficiency Syndrome
BCL-2	B-cell lymphoma 2
ACN	Acetonitrile
CAN	Ceric ammoniumnitrate
CHS	Chalcone Synthase
CHI	Chalcone Isomerase
CoA	Coenzyme A
CNS	Central Nervous System
COX	Cyclooxygenase
DNA	Deoxyribonucleic Acid
DCM	Dichloromethane
DCE	Dichloroethane
DMF	<i>N, N</i> -dimethylformamide
DMSO	Dimethyl sulfoxide
DIPEA	Diisopropylethylamine
ER	Estrogen Receptor
FLS	Flavonol Synthase
HEK-293	human embryonic kidney cells
HepG2	human hepatoma G2
HRMS	High Resolution Mass Spectrometry
HIV	Human Immunodeficiency Virus
IC ₅₀	Half maximal inhibitory concentration
LC-MS	Low Resolution Mass Spectrometry
LDL	Low-Density Lipoprotein
LOX	Lipoxygenase
MARK4	Microtubules affinity regulated kinase 4
MCF-7	Michigan Cancer Foundation-7
MTT	3-(4,5-Dimethylthiazol-2-yl)-2,5-diphenyltetrazolium bromide
MW	Microwave
PLA2	Phospholipases A2
ROS	Reactive oxygen species
SAR	Structure activity relationship
THF	Tetrahydrofuran

ABBREVIATIONS

μg	Microgram
ml	Millilitre
mmol	Millimole
m.p.	Melting point
μM	Micro Molar



LIST OF TABLES

<u>LIST OF TABLES</u>	Page No.
<u>CHAPTER-2</u>	
Table 2.1. Optimization of reaction conditions	54
Table 2.2. Important crystal data of compound 3b	60
<u>CHAPTER-3</u>	
Table 3.1. Optimization of reaction conditions	84
<u>CHAPTER-4</u>	
Table 4.1. Shows the calculated IC ₅₀ values of synthesized compounds on MCF-7 and HEK-293 cells	110
Table 4.2. Docking score of compounds 5f , 5g and 5o .	113
<u>CHAPTER-5</u>	
Table 5.1. Optimization of reaction conditions	129
Table 5.2. Molecular docking results showing binding energy and interacting residues from the active site of MARK4 with 6b , 6c and 6n derivatives	135
<u>CHAPTER-6</u>	
Table 6.1. Optimization of reaction condition	159

LIST OF SCHEMES

<u>LIST OF SCHEMES</u>	<u>Page no.</u>
<u>CHAPTER-1</u>	
Scheme 1.1. Biosynthesis pathway of chalcone	5
Scheme 1.2. Various chalcone derivatives from different starting material.	6
Scheme 1.3. Various flavonoid derivatives from 2-hydroxychalcone as starting material	7
Scheme 1.4. Various flavonoids derivatives from chalcone as starting material.	8
Scheme 1.5. Synthesis of bichalcone.	8
Scheme 1.6. Synthesis of Chromenochalcones	12
Scheme 1.7. Biosynthesis pathway of flavone	12
Scheme 1.8. Synthesis of flavone <i>via</i> different starting materials	13
Scheme 1.9. Synthetic transformation from flavone	14
Scheme 1.10. Synthesis of flavopiridol alkaloid as anticancer agent	16
Scheme 1.11. Synthesis of iso-prenylflavones	17
Scheme 1.12. Synthesis of 6 iodoflavone	18
Scheme 1.13. Synthesis of boronate flavone	18
Scheme 1.14. Synthesis of biflavone <i>via</i> Suzuki cross coupling reaction	18
Scheme 1.15. Biosynthesis pathway of flavone	19
Scheme 1.16. Synthesis of flavonol <i>via</i> Auwer synthesis and Algar-Flynn-Oyamada reaction	20
Scheme 1.17. Synthesis of flavonol	20
Scheme 1.18. Synthesis of kaempferol	21
Scheme 1.19. Synthetic transformations of flavonol.	21
Scheme 1.20. Biosynthesis pathway of Aurone	23
Scheme 1.21. Gold catalysed synthesis of (<i>Z</i>)-aurone <i>via</i> salicyldehyde and phenyl acetylene.	23
Scheme 1.22. synthesis of (<i>Z</i>)-aurone through 2-bromoacetophenone and <i>p</i> -chlorobenzaldehyde.	23
Scheme 1.23. Formation of aurone by 2-iodophenol and phenyl acetylene	24
Scheme 1.24. Synthesis of (2-(diphenylmethylene)-4-hydroxy benzofuran 3(2H)-one).	24

LIST OF SCHEMES

Scheme 1.25.	Synthesis of aurone by exocyclization of <i>O</i> -Alkynoylphenol	24
Scheme 1.26.	Synthesis of Aureusidin by Algar–Flynn–Oyamada reaction	24
Scheme 1.27.	Formation of 2-Benzylidene-benzofuran-3-ones as Flavopiridol Mimics	25
Scheme 1.28.	Synthesis of substituted aminated aurone	28
Scheme 1.29.	Synthesis of naturally and biologically active coumestrol	29
Scheme 1.30.	Total synthesis of hirtellanine A	29
Scheme 1.31.	Total synthesis of lupinalbin H	30
Scheme 1.32.	Synthesis of wadelolactone	31
Scheme 1.33.	Synthesis of tetracyclic fused furan compound	31
Scheme 1.34.	Synthesis of 3-N-aryl substituted-2-heteroarylchromones and their Microtubule Affinity Regulating Kinase 4 for human breast cancer cell line, human liver carcinoma cells and human embryonic kidney cell line	33
Scheme 1.35.	Dehalogenation of aryl chlorides using palladium/phosphite catalyst	34
Scheme 1.36.	Hydrodehalogenation of Halogenated Heteropentalenes	34
Scheme 1.37.	Hydrodehalogenation of halobenzenes with molecular hydrogen	35
Scheme 1.38.	Fe-catalysed hydrodehalogenation of aryl halide	35
Scheme 1.39.	Ru-catalysed hydrodehalogenation of aromatic halide.	35
Scheme 1.40.	Synthesis of β' -dehalogenated chalcone and α flavone product	35
<u>CHAPTER-2</u>		
Scheme 2.1.	Synthesis of 4, 5-Dialkoxyaurones	52
Scheme 2.2.	Synthesis of <i>Z</i> -aurone	52
Scheme 2.3.	Cyclization of <i>o</i> -alkynoylphenols	52
Scheme 2.4.	Synthesis of aminated aurone	53
Scheme 2.5.	Reaction of substituted flavone with substituted aniline	56
Scheme 2.6.	Reaction of substituted 3-bromo-2-(furan-2-yl)-4H-chromen-4-one and aniline.	57
Scheme 2.7.	Reaction of substituted 3-bromo flavone with N-phenyl urea	58

LIST OF SCHEMES

Scheme 2.8.	Reaction of aliphatic and aromatic amine with 3-bromochromone	58
Scheme 2.9.	Gram scale reaction	58
Scheme 2.10.	Synthesis of β -Aminated 2' Hydroxy chalcone	59
Scheme 2.11.	Reactivity measurement between nucleophiles	59
Scheme 2.12.	Reaction with benzamide, piperazine and 2-aminopyridine	61
Scheme 2.12.	Proposed Mechanism	61
 <u>CHAPTER-3</u>		
Scheme 3.1.	Synthesis of Ladder-Type Heteroarenes	82
Scheme 3.2.	Synthesis of Dibenzofuran	83
Scheme 3.3.	Synthesis of phenyldibenzofuran	83
Scheme 3.4.	Synthesis of heterocyclic flavones-benzofuran fused derivatives	86
Scheme 3.5	Proposed mechanism	88
 <u>CHAPTER-4</u>		
Scheme 4.1.	Synthesis of pyrimidine-piperazine-chromene and quinoline conjugates	103
Scheme 4.2.	Substrate scope of pyrimidine-piperazine-chromene and quinoline conjugates	104
 <u>CHAPTER-5</u>		
Scheme 5.1.	Scope of aniline for the direct C-H amination of 2-(furan-2-yl)-4H-chromen-4-one	131
Scheme 5.2.	Scope of substrates for the direct C-H amination of 2-(pyridin-2-yl)-4H-chromen-4-one	132
 <u>CHAPTER-6</u>		
Scheme 6.1.	Dehalogenation reaction of α -halo arene derivative.	160
Scheme 6.2.	Dehalogenation reaction of 3-halo flavone.	161
Scheme 6.3.	Dehalogenation reaction of β' -halochalcone.	162
Scheme 6.4.	Dehalogenation reaction of 3-acetyl-4-chlorocoumarin	163

LIST OF SCHEMES

Scheme 6.5.	Reaction of substituted flavone and Chalcone with Deuterated Isopropanol	163
Scheme 6.6.	Reactivity of Bromo derivatives	165
Scheme 6.7.	Proposed Mechanism	165



LIST OF FIGURES

<u>LIST OF FIGURES</u>	<u>Page No.</u>
<u>CHAPTER-1</u>	
Figure 1.1. Uses of natural product	1
Figure 1.2. Classification of flavonoid	2
Figure 1.3. Basic skelton flavan, isoflavan and neoflavan structure	3
Figure 1.4. General structures of flavonoid	3
Figure 1.5. General structures of neo-flavonoid and isoflavonoid	3
Figure 1.6. Some Natural and synthetic and semisynthetic flavonoids structure	4
Figure 1.7. Structure of and quercetin, chrysin, Flavone and biochanin A	4
Figure 1.8. Basic Skeleton of chalcone	4
Figure 1.9. Some naturally occurring biologically active chalcone derivatives	9
Figure 1.10. Some Synthetic biologically active chalcone derivatives	10
Figure 1.11. Prenyl, Geranyl and farnesyl chalcone	11
Figure 1.12. General structure of flavone	12
Figure 1.13. Some naturally occurring biologically active flavone derivatives	15
Figure 1.14. Some Synthetic biologically active Flavone derivatives	16
Figure 1.15. Basic skeleton of flavanol	19
Figure 1.16. Biologically active structure of flavanol	22
Figure 1.17. Basic skeleton of Aurone	22
Figure 1.18. Some structure of naturally occurring aurone	26
Figure 1.19. Structure of substituted aurone	27
Figure 1.20. Structure of aurone	27
Figure 1.21. structure of chromene and coumarin aurone scaffold	27
Figure 1.22. structure of ferrocene (organomettalic) and simple aurone	28
Figure 1.23. Some naturally occurring structure of Polycyclic Benzofuran derivative	28
Figure 1.24. Some synthetic structure of Polycyclic Benzofuran derivative	30
Figure 1.25. synthesis of chromene and quinoline derivative	32
Figure 1.26. Pyrimidine with piperazine conjugates	32
Figure 1.27 Chromene and quinoline pyrimidine piperazine conjugates	33

LIST OF FIGURES

CHAPTER-2

Figure 2.1. Biologically active aurone derivatives 51

CHAPTER-3

Figure 3.1. Biologically active benzofuroheterocyclic derivatives 81

Figure.3.2. LC-MS spectra of **4d** compound. 95

Figure.3.3. HRMS spectra of **4s** compound. 95

CHAPTER-4

Figure 4.1. Effect of synthesized compounds **5a** to **5e** on the viability of HEK293 cells. HEK293 cells were incubated with the denoted concentrations of each compound for 48 h. The cell viabilities were evaluated by MTT assay. Data represent three independent sets of experiments and results are shown as the mean \pm SD. 105

Figure 4.2. Effect of synthesized compounds **5f**, **5g**, **5o**, **5p** and **5s** on the viability of HEK293 cells. HEK293 cells were incubated with the denoted concentrations of each compound for 48 h. The cell viabilities were evaluated by MTT assay. Curcumin is used as a positive control. Data represent three independent sets of experiments and results are shown as the mean \pm SD. 106

Figure 4.3. Effect of synthesized compounds **5h** to **5l** on the viability of HEK293 cells. HEK293 cells were incubated with the denoted concentrations of each compound for 48 h. The cell viabilities were evaluated by MTT assay. Data represent three independent sets of experiments and results are shown as the mean \pm SD. 106

Figure 4.4. Effect of synthesized compounds **5m**, **5n**, **5p**, **5r** and **5t** on the viability of HEK293 cells. HEK293 cells were incubated with the denoted concentrations of each compound for 48 h. The cell viabilities were evaluated by MTT assay. Data represent three independent sets of experiments and results are shown as the mean \pm SD. 107

Figure 4.5. Effect of synthesized compounds **5a** to **5e** on the viability of human breast cancer MCF-7 cells. MCF-7 cells were incubated with the denoted concentrations of each compound for 108

LIST OF FIGURES

- 48 h. The cell viabilities were evaluated by MTT assay. Data represent three independent sets of experiments and results are shown as the mean \pm SD.
- Figure 4.6.** Effect of synthesized compounds **5f**, **5g**, **5o**, **5p** and **5s** on the viability of MCF-7 cells. MCF-7 cells were incubated with the denoted concentrations of each compound for 48 h. The cell viabilities were evaluated by MTT assay. Curcumin is used as a positive control. Data represent three independent sets of experiments and results are shown as the mean \pm SD 108
- Figure 4.7.** Effect of synthesized compounds **5h** to **5l** on the viability of human breast cancer MCF-7 cells. MCF-7 cells were incubated with the denoted concentrations of each compound for 48 h. The cell viabilities were evaluated by MTT assay. Data represent three independent sets of experiments and results are shown as the mean \pm SD 109
- Figure 4.8.** Effect of synthesized compounds **5m**, **5n**, **5p**, **5r** and **5t** on the viability of human breast cancer MCF-7 cells. MCF-7 cells were incubated with the denoted concentrations of each compound for 48 h. The cell viabilities were evaluated by MTT assay. Data represent three independent sets of experiments and results are shown as the mean \pm SD 109
- Figure 4.9.** (A) 2-amino-7-((6-(4-(2-hydroxyethyl) piperazin-1-yl)-2-methylpyrimidin-4-yl)oxy)-4-(p-tolyl)-1,4-dihydroquinoline-3-carbonitrile docked with Bcl-2. (B) Surface representation of Bcl-2 docked with 2-amino-7-((6-(4-(2-hydroxyethyl) piperazin-1-yl)-2-methylpyrimidin-4-yl)oxy)-4-(p-tolyl)-1,4-dihydroquinoline-3-carbonitrile 112
- Figure 4.10.** (A) 2-amino-7-((6-(4-(2-hydroxyethyl) piperazin-1-yl)-2-methylpyrimidin-4-yl)oxy)-4-phenyl-1,4-dihydroquinoline-3-carbonitrile docked with Bcl-2. (B) Surface representation of Bcl-2 docked with 2-amino-7-((6-(4-(2-hydroxyethyl) piperazin-1-yl)-2-methylpyrimidin-4-yl)oxy)-4-phenyl-1,4-dihydroquinoline-3-carbonitrile 112

LIST OF FIGURES

Figure 4.11. (A) 2-amino-4-(4-bromophenyl)-7-((6-(4-(2-hydroxyethyl)piperazin-1-yl)-2-methylpyrimidin-4-yl)oxy)-4H-chromene-3-carbonitriledocked with Bcl-2. (B) Surface representation of Bcl-2 docked with 2-amino-4-(4-bromophenyl)-7-((6-(4-(2-hydroxyethyl)piperazin-1-yl)-2-methylpyrimidin-4-yl)oxy)-4H-chromene-3-carbonitrile

Figure.4.12. LC-MS spectra of **5d** compound. 121

Figure.4.13. LC-MS spectra of **5j** compound. 121

CHAPTER-5

Figure 5.1. Kinase inhibition assay. (A). Shows the hydrolysis of Pi from ATP, position of Pi and ATP spots are indicated. Lane 1, negative control (without protein); lane 2, 100 nM MARK4 (positive control); and lanes labelled as 0.5, 1.0, 2.0, 3.0, 5.0 and 10.0, shows the concentration of compound **6b**, **6c** and **6n**. (B). Binding of MARK4 with radiolabelled oligos (C). Inhibition of kinase activity of MARK4 verified by DOT-blot assay by using radiolabelled oligos as substrate showing that all three selected molecules inhibits MARK4. 133

Figure 5.2. Molecular docking studies of (A) compound **6b**, (B) compound **6c** and (C) compound **6n**. Upper panel shows the pocket view of MARK4 binding with selected compounds. Lower panel is showing the 2D schematic diagram of interactions of MARK4 with selected compounds. Residues involved in hydrogen bonding, charge or polar interactions, van der Waals interactions are represented in different color 134

Figure 5.3. Fluorescence binding studies. Fluorescencespectra of MARK4 (5 μ M) with increasing concentration of (A) (A) compound **6b**, (B) compound **6c** and (C) compound **6n** (0–10 μ M). Excitation wavelength was fixed to 280 nm and emission was recorded in the range 300–400 nm. Lower pannel shows Modified Stern-Volmer plot used to calculate binding affinity (K_a) and number of binding sites (n). 136

LIST OF FIGURES

- Figure 5.4.** Cell proliferation studies. Effect of compound **6b**, **6c** and **6n** (A) 137
MCF-7 (Breast Cancer) and (B) HepG2 (Liver cancer) cells. Cells
were treated with increasing concentrations of compound **6b**, **6c**
and **6n** (0–200 μ M) for 48 h. Cell viabilities were shown as a
percentage of the number of viable cells to that of the control.
Each data point shown is the mean \pm SD from n = 3
- Figure 5.5.** **Apoptosis studies.** (A) Annexin-V staining of MCF-7 and HepG2 138
cells; cells were treated with IC50 concentrations of each
compound for 48 h and subsequently stained with FITC Annex
in-V. Stimulation of apoptosis was quantified by flow cytometry.
Representative flow images showing FITC-Annex in-V labeled
cells, which directly corresponds to the percentage of apoptotic
cells. Bar graphs of (B) MCF-7 and (C) HepG2 cells represents
the percentage of apoptotic cells stained with Annex in-V for
duplicate measurements \pm SD. p < 0.001, compared with the
control (untreated cells). Statistical analysis was done using one-
way ANOVA and t-test for unpaired samples. For anticancer
activities doxorubicin has been taken as positive control.
- Figure 5.6.** Representative flow cytometry histogram of MCF-7 cell fractions 140
stained with phosphorylated anti-tau antibodies, each histogram
represents the phosphorylation status of tau under different
treatments as mentioned in inset. (B). Showing the concentration
of ROS at different concentrations of selected compounds
- Figure.5.7.** HRMS spectra of **6n** compound. 151
- Figure.5.8.** HRMS spectra of **6l** compound 152
- CHAPTER-6**
- Figure 6.1** Deuterated HRMS spectrum of **8k** 164
- Figure 6.2** Deuterated HRMS spectrum of **8l** 164

LIST OF TABLES

<u>LIST OF TABLES</u>	Page No.
<u>CHAPTER-2</u>	
Table 2.1. Optimization of reaction conditions	54
Table 2.2. Important crystal data of compound 3b	60
<u>CHAPTER-3</u>	
Table 3.1. Optimization of reaction conditions	84
<u>CHAPTER-4</u>	
Table 4.1. Shows the calculated IC ₅₀ values of synthesized compounds on MCF-7 and HEK-293 cells	110
Table 4.2. Docking score of compounds 5f , 5g and 5o .	113
<u>CHAPTER-5</u>	
Table 5.1. Optimization of reaction conditions	129
Table 5.2. Molecular docking results showing binding energy and interacting residues from the active site of MARK4 with 6b , 6c and 6n derivatives	135
<u>CHAPTER-6</u>	
Table 6.1. Optimization of reaction condition	159



Chapter-1

Introduction

1.1. Introduction

1.1.1. General Introduction of Natural products

Natural product is a substance or compound, created *via* living organism such as - plants, fruits and microorganisms *etc.* and are exclusively found in nature, formed with secondary metabolism [1-2]. For the development in the field of organic chemistry, Natural products have played a vital role by providing confronting synthetic targets in drug development and discoveries. Directly and indirectly, a huge percentage of drugs in modern medicine originate from natural sources. Traditionally, the concept for the natural product is that it is applied as a therapeutic agent in different disease such as Cancer infectious disease [3]. Flavonoids, Carotenoids, Chromenes, coumarins, alkaloids and quinolones *etc.* are considered as a significant part of natural products and are usually utilized around the world due to their assorted pharmacological properties [4]. In Particular, flavonoids, chromene and quinoline have occupied a considerable interest, owing to their diverse pharmacological, therapeutic and chemosensor applicability's [5].

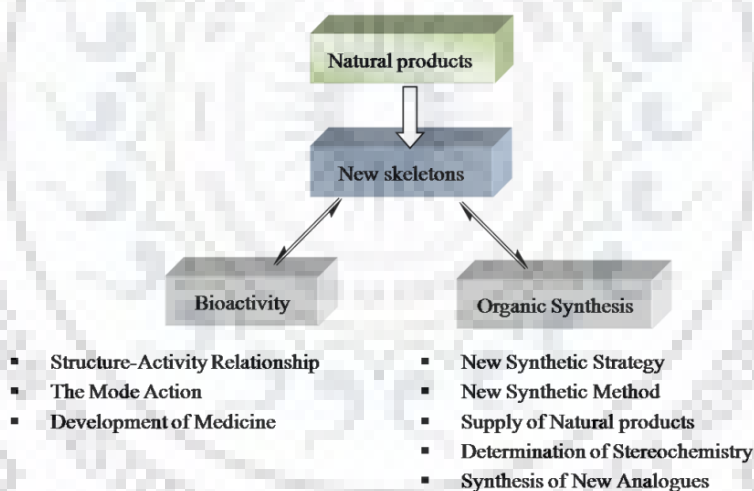


Figure.1.1. Uses of natural products.

1.2. Flavonoid

Flavonoids (or bioflavonoids) are main sort of natural compounds, firstly invented by Hungarian scientist *Albert Szent-Gyorgyi* in 1938 and comes from the Latin word "*flavus*" signifying yellow. They are an assorted group of phytonutrients (plant chemicals) found in almost all fruits and vegetables [6]. Flavonoids are usually found in plants as glycosylated derivatives and have numerous functions for flower coloration, including attracting insects for pollination and dispersal of seeds, transport of auxin, acting in defence systems, root and shoot development, modulation of reactive oxygen species, (e.g., as UV-B protectants and phytoalexins), signalling between plants and

microbes [7-9]. These compounds also have antioxidant and chelating properties and therefore show many health promoting effects [10]. In addition, they have antibacterial, antioxidant, anticancer effects, antiulcer, anti-viral, cardiovascular disorders, diabetes mellitus and celiac disease [11]. Moreover, epidemiologic studies propose studies a defensive quality of dietary flavonoids besides coronary heart disease [12].

Various additional properties ascribed to flavonoids include: Non-steroidal anti-inflammatory drugs (NSAIDS) intended for the rationales of dipping swelling, reducing fever, reducing pain affecting Alzheimer's $\alpha\beta$ production on the basis of NF κ B dependent mechanism and aromatase inhibitors enzyme [13-14].

1.2.1. Classification of flavonoids

Chemically flavonoids are polyphenolic constituents that support the flavan nucleus, which are classified on the basis of fifteen-carbon skeleton (C6-C3-C6) containing two benzene rings *i.e.* A and B joined through a pyran heterocyclic ring (C) (Figure 1.2) [15].

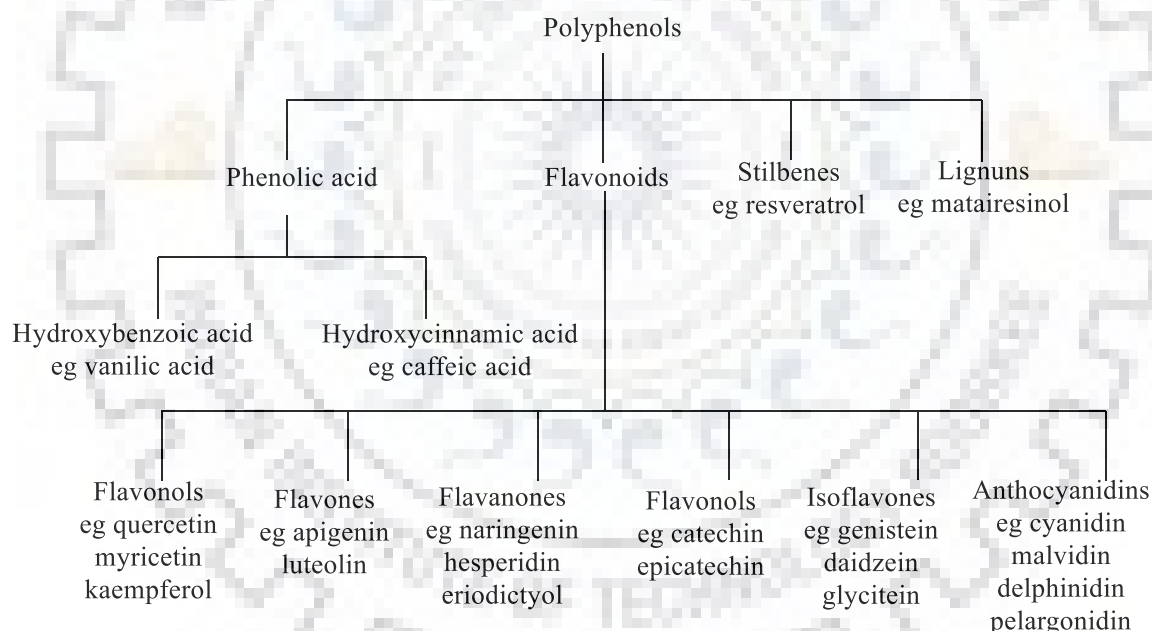


Figure.1.2. Classification of flavonoid

Flavonoids are classified into one of many subclasses which are different in the level of central ring oxidation, absence or presence of double bond, and form of substitution on the C ring. The flavonoid class on the basis of location of ring B at 2-position are called flavonoids *i.e.* 2-phenyl-benzopyrans, at 3-position is called isoflavonoids *i.e.* 3-phenyl-benzopyrans and at 4-position are called neoflavonoids *i.e.* 4-phenyl-benzopyrans (Figure 1.3). The major flavonoid groups when the B ring is attached with 2 carbon *i.e.* flavones, flavanones, flavonols, flavanols, chalcones, aurones (Figure 1.4). Isoflavonoids embrace isoflavones *i.e.* the analogue of flavones. Next is 4-aryl coumarin,

its reduced form is 3, 4-dihydro-4-aryl coumarin main neoflavonoids which derived from neoflavan structure (Figure 1.5) [16].

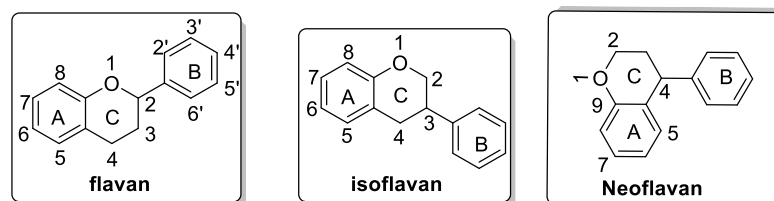


Figure.1.3. Basic skelton flavan, isoflavan and neoflavan structure.

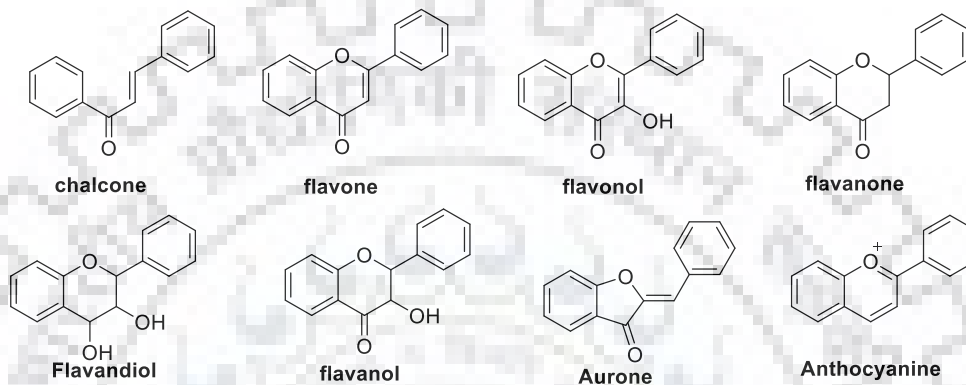


Figure.1.4. General structures of flavonoids.

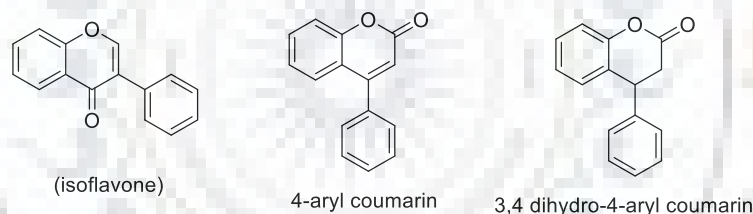
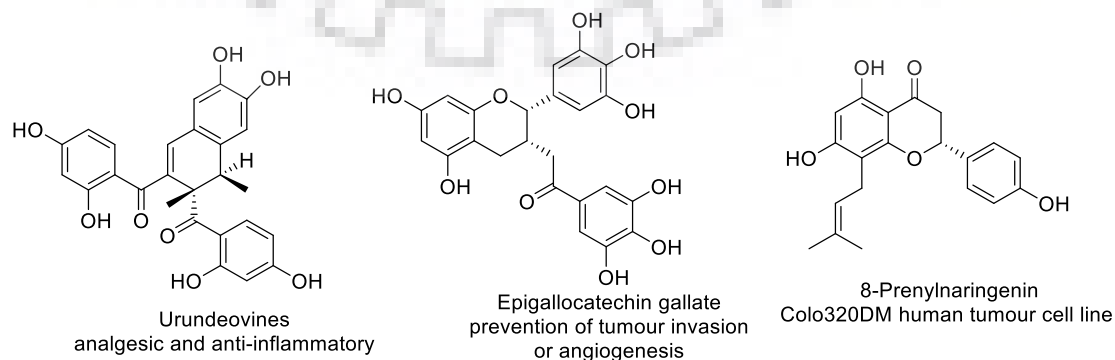


Figure.1.5. General structures of neo-flavonoid and isoflavonoid.

1.2.2. Natural Occurring Biologically Active Flavonoids

Some natural, synthetic and semi-synthetic flavonoids (Figure 1.6) have been extensively accounted to exhibit diverse biological activities and are of significant interest in the development of innovative therapeutic agents to treat different diseases [17-23].



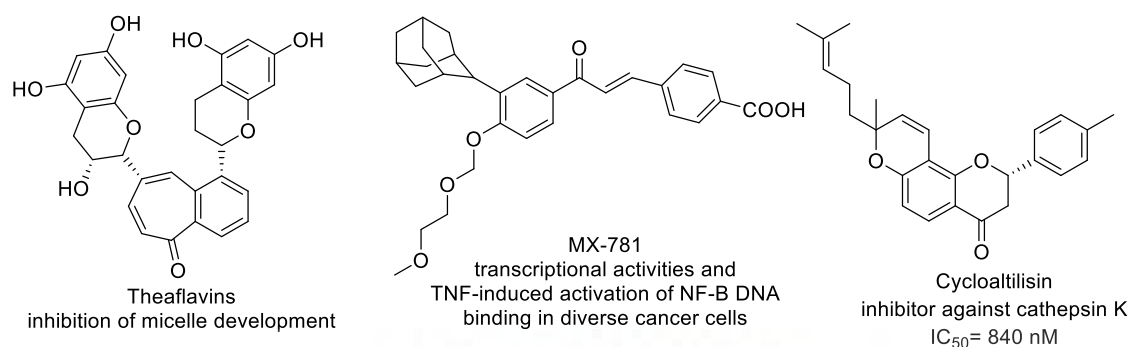


Figure.1.6. Some Natural and synthetic and semi-synthetic flavonoids structure.

Some alternations and inclusion of new functional groups like hydroxyl and aryl group in the flavonoids structure, lead to considerable alteration in biological activities, for *e.g.*; quercetin has more antioxidant activity as compared to the chrysin, owing to the presence of three supplementary hydroxyl groups [24], yet chrysin and flavone are more efficient in the inhibition of the human aromatase enzyme as compared to the biochanin A. (Figure 1.7) [25].

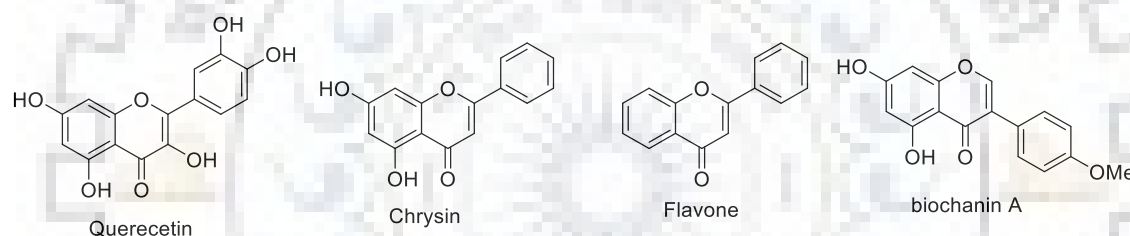


Figure.1.7. Structure of quercetin, chrysin, Flavone and biochanin A.

1.3. Chalcone

Chalcones (benzalacetophenone, benzylidene acetophenone and Phenyl styryl ketone), are defined as open- flavonoid that appearances of the central core aimed as a diversity of vital biologically active compounds, were primary isolated from Chinese liquorice (*Glycyrrhizae inflata*) which are important constituents of natural source. The term chalcone (α -phenyl- β -benzoyl ethylene) was firstly specified by Kostanecki and Tambor [26].

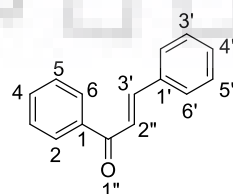


Figure.1.8. Basic Skelton of chalcone.

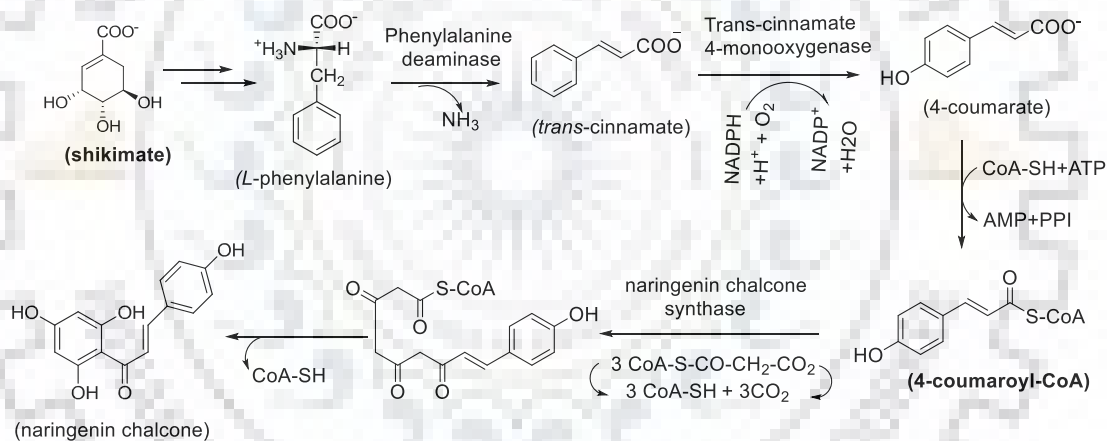
Chalcones have nearly planar or linear structure; the two rings are interconnected *via* an aliphatic three carbon chain and have completely delocalized- π -electron system due to the presence of conjugated double bonds. Chalcones are generally coloured compounds

on account of the occurrence of the chromophore (-ketoethylenic group) $-\text{CO}-\text{CH}=\text{CH}$ and auxochrome (Figure 1.8).

1.3.1. Methods for the synthesis of chalcone

1.3.1.1. Biosynthetic method of chalcone:

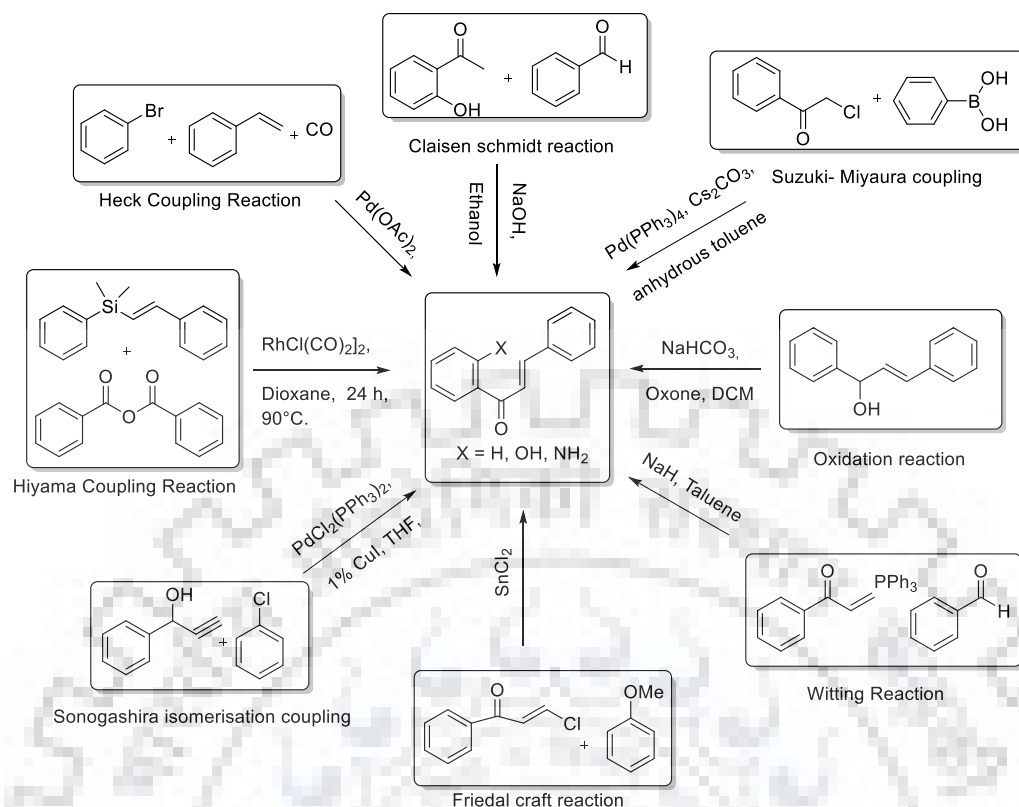
Chalcone biosynthesis set off from the phenylalanine amino acid originating from carbohydrate, which is synthesized by the shikimate arogenate pathway from chorismate. The key step is the formation of trans-cinnamate *via* deamination of phenylalanine in the presence of phenylalanine ammonia-lyase enzyme (PAL). Cinnamate 4-hydroxylase monooxygenase synthesized from 4-coumarate by the hydroxylation of trans-cinnamate. 4-coumaroyl-CoA is generated from the reaction of coenzyme A and 4-coumarate which is catalysed through the 4-coumarate-CoA ligase as of the phenylpropanoid pathway. It reacts with three acetate unit of malonyl-CoA producing naringenin chalcone by losing coenzyme A in presence of *naringenin chalcone synthase* (Scheme 1.1) [27].



Scheme.1.1. Biosynthesis pathway of chalcone.

1.3.1.2. Synthetic methods for chalcone preparation

Chalcone purification and extraction from plant is time taking and is a pricey method. Because of this, scientists decided to develop easy, cheap, less reaction time, efficient and effective methods in the laboratory. The general and easy method is the Claisen-Schmidt condensation by using acids and bases such as potassium hydroxide (KOH), sodium hydroxide (NaOH), Piperidine, Lithium hydroxide (LiOH), Calcium Oxide (CaO), Aluminium Oxide (Al₂O₃), Barium hydroxide (Ba(OH)₂), Titanium tetrachloride (TiCl₄), Zirconium tetrachloride (ZrCl₄) *etc.* is used in polar solvents.



Scheme.1.2. Various chalcone derivatives from different starting material.

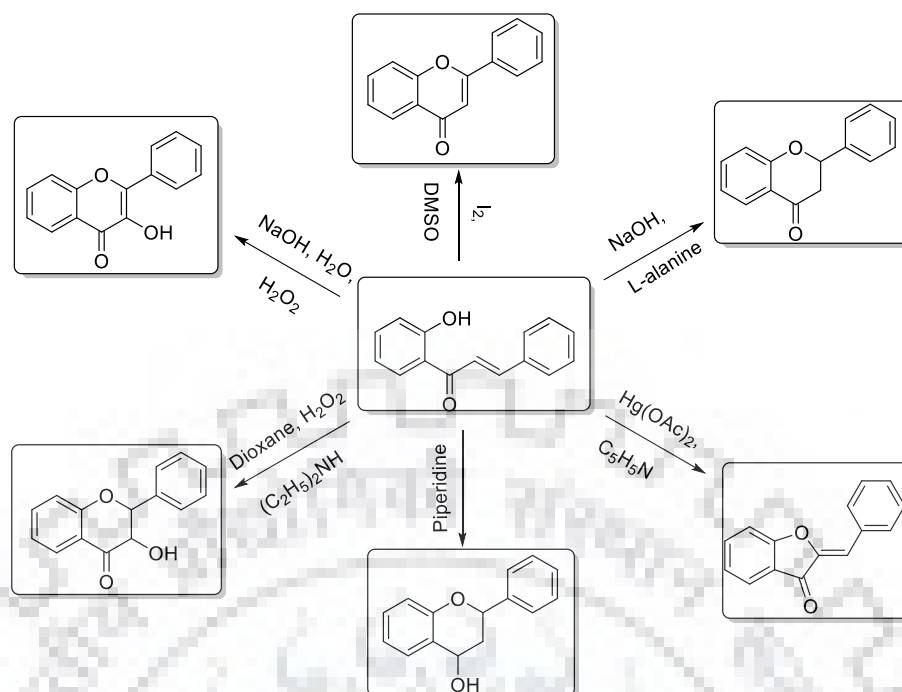
Additionally, some other striking protocols have been described such as palladium mediated Heck coupling reaction of styrene, Bromobenzene and carbonmonooxide [28]. Suzuki Miyaura coupling reaction between phenyl boronic acids and cinnamoyl chloride in the presence of palladium catalyst [29]. One more method is oxidation of 1, 3-diphenylpropenol with sodium bicarbonate and Oxone [30]. Further witting reaction *via* equimolar concentration of α -carbonylated ylide with aldehydes [31]. Chalcones have been also prepared directly by Friedel Crafts acylation 3-chloro-1-phenylprop-2-en-1-one and anisole [32]. Another approach is palladium catalysed reaction of chlorobenzene and 1-phenylprop-2-yn-1-ol by using copper iodide as a co-catalyst in THF [33]. Interestingly a new approach is also introduced using dieny silanes and desilylative acylation of styryl with Iridium catalyst through acid anhydrides [34].

1.3.2. Application of chalcones

1.3.2.1. Synthetic Application

1.3.2.1.1. Synthesis of flavonoids derivatives

Chalcones have a simple chemistry, 2-hydroxy chalcone is used as main synthon in the synthesis and biosynthesis of different flavonoids (scheme 1.3).

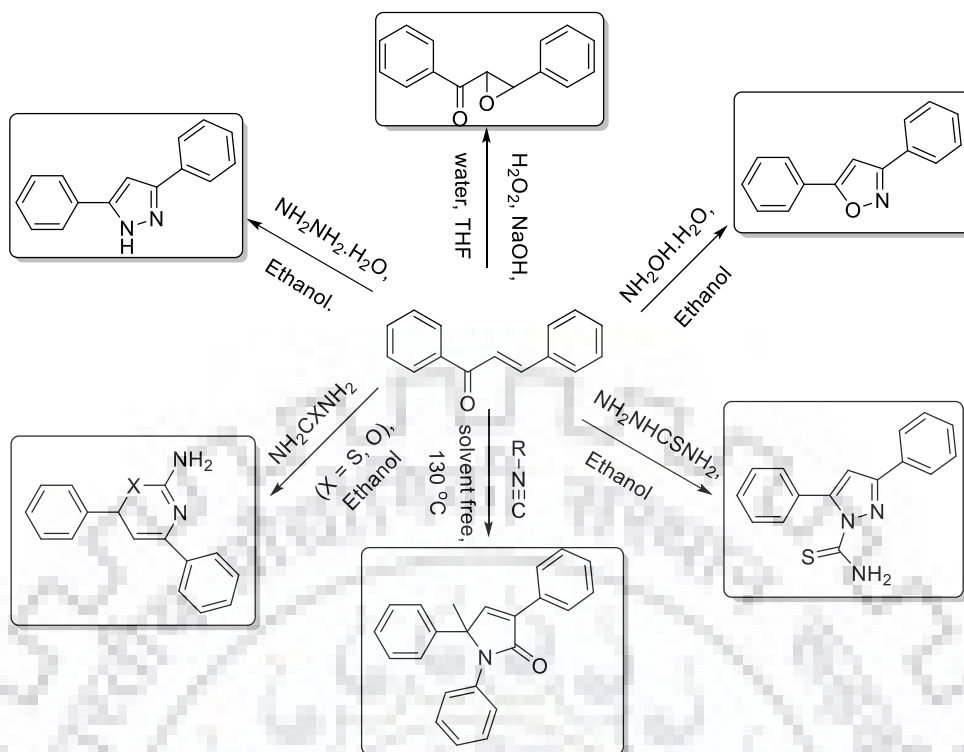


Scheme.1.3. Various flavonoid derivatives from 2-hydroxy chalcone as starting material.

Chemists have developed large number of synthetic methodologies for cyclized flavonoid synthesis like DMSO and iodine is one of the most common method for the formation of flavones [35]. In addition, the use of aq. NaOH solution with L-alanine has offered flavanone in excellent yields [36]. Aurone is synthesized by using mercury acetate and pyridine under reflux condition [37]. Reduction of 2'-Hydroxy Chalcones over Phase Transfer Catalysis catalysed condition offered Flavan-4-ols [38]. Dihydroflavonols prepared through H_2O_2 and diethyl amine in dioxane solvent [39] and flavanols synthesized *via* aq. Solution of NaOH and hydrogen peroxide in the presence of H_2O and Methanol [40].

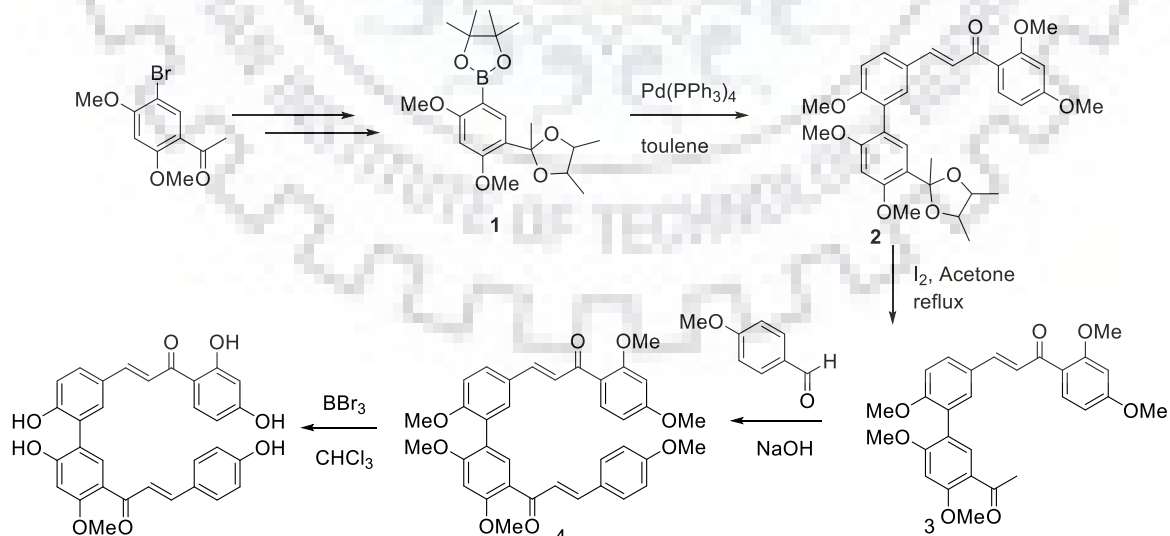
1.3.2.1.2. Synthesis of other heterocycles derivatives

Chalcones possess α , β -unsaturated carbonyl moieties and have two electrophilic centres which allows them to take part in addition reactions (both 1,2-addition and 1,4-conjugate addition) *via* delocalization of electron density in the $\text{C}=\text{C}-\text{C}=\text{O}$ system. Conjugate addition leading to the combination of potential biologically active five membered nitrogen containing heterocyclic ring in the presence of $\text{NH}_2\text{OH}\cdot\text{H}_2\text{O}$, $\text{NH}_2\text{NHCSNH}_2$, $\text{NH}_2\text{NH}_2\cdot\text{H}_2\text{O}$ and six membered nitrogen heterocyclic compounds due to NH_2CXNH_2 ($\text{X} = \text{S}, \text{O}$), with ethanol. Sometimes it is used for the synthesis of three membered heterocyclic compounds with aq. NaOH solution with Hydrogen peroxide [41].



Scheme.1.4. Various flavonoid derivatives from chalcone as starting material.

Abebaz and group described the total synthesis of bichalcone *i.e.* Rhuschalcone *via* acetophenone transferred into ketal form through $\text{H}_2\text{NSO}_3\text{H}$ / 2,3-butanediol in toluene. Halogen exchange into boronate ester by adding up of 2-isopropoxy-4,4,5,5-tetramethyl-1,3,2-dioxaborolane with *n*-BuLi. Compound **(1)** was coupled with bromo chalcone by Suzuki-Miyaura cross coupling using tetrakis(triphenylphosphine) as catalyst to give compound **(2)**.



Scheme.1.5. Synthesis of bichalcone.

Deprotected through molecular iodine in acetone produces acetophenone **(3)**. Condensation of compound **(3)** under solvent free condition in the presence of NaOH

converted into hexamethoxybichalcone (**4**) Finally, by demethylation, bichalcone converted into Rhuschalcone by using BBr_3 (Scheme 1.5) [42].

1.3.2.2. Biological Applications

Chalcone play a significant role as intermediates and key step in the synthesis and biosynthesis of cyclised flavonoids [43]. Major chalcone are phlorizin, arbutin, phloretin and chalconaringenin. It is an exclusive model that is associated with numerous pharmacological properties like anti-diabetic [44], anti-retroviral [45], anti-gout [46], anti-hypertensive [47], anti-histaminic [48], anti-inflammatory [49], anti-obesity [50], anti-oxidant [51], anti-neoplastic [52], anti-platelet [53], immunosuppressant [54], anti-fungal [55], anti-arrhythmic [56], anxiolytic [57], anti-parasital [58], anti-spasmodic [59], hypnotic [60], anti-malarial [61], anti-nociceptive [62], anti-tubercular [63], hypolipidemic [64].

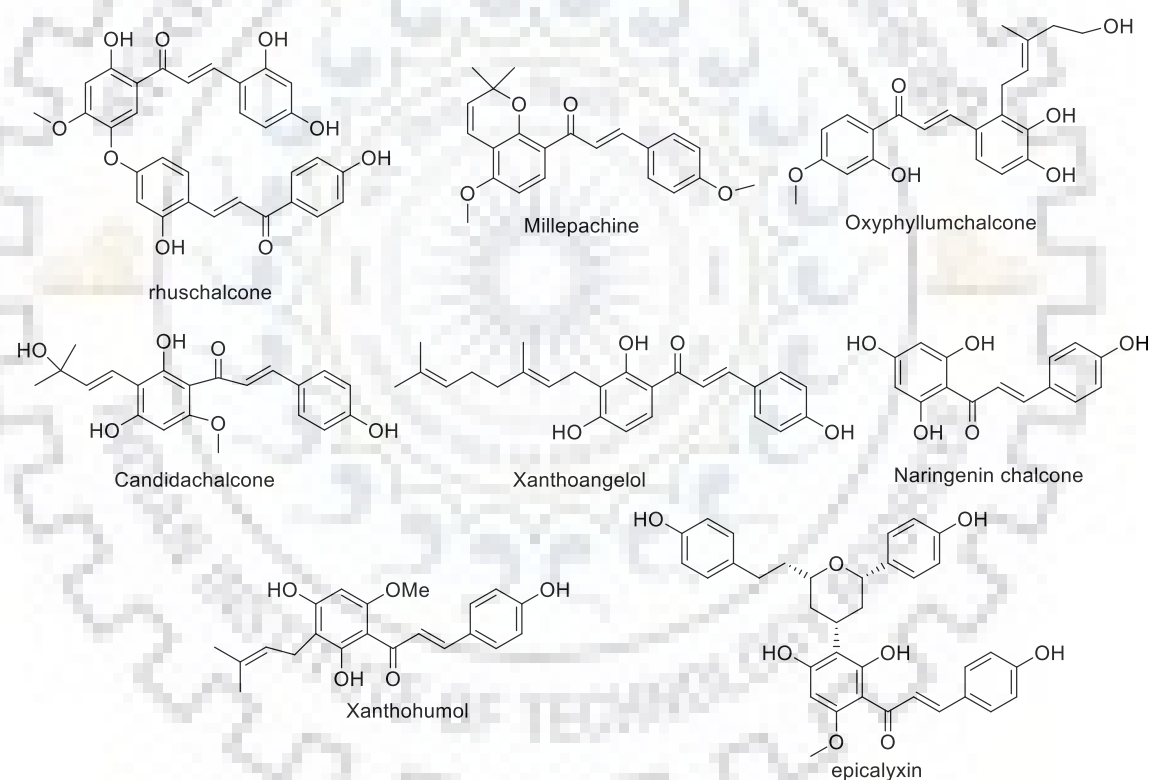


Figure.1.9. Some naturally occurring biologically active chalcone derivatives.

Some naturally occurring chalcones such as an oxygenated chalcone Licochalcone A obtained from the Chinese licorice root have been shown to inhibit the growth of both chloroquine-resistant (CQ^{R}) Dd2 and chloroquine-susceptible (CQ^{S}) 3D7 Plasmodium falciparum strains [40]. Some other chalcones were assessed for their potential inhibitory activities in contrast to the Inhibition of enzymes such as COX-1, COX-2, LOX s, PLA2-V, and release of pro-inflammatory cytokines like IL-6 and TNF- α show

ups the anti-inflammatory characteristics [65]. Chalcone is also used for the inhibition of Mitochondrial fumarate reductase enzyme which is responsible for production of succinate, leads to reduction of succinate level in parasites through suppressing glucose metabolism [66].

In 2003, Khan *et al.* described the synthesis of boronic acid chalcone (**5**) which shows anticancer activity against human breast cancer (MDA-MB-231) and (MCF7) cell line at micromolar concentration [67]. Domínguez and group prepared a series of Phenylurenyl chalcones (**6**) and used as antimalarial agent against *Plasmodium falciparum* [68]. Kumar and co-workers reported the preparation of 1*H*-1,2,3-triazole tethered β -lactam-phenyl styryl ketone bifunctional hybrids (**7**) and were estimated for their cytotoxic activity against a human lung cancer (A-549), colon cancer (Caco-2), leukaemia cancer (THP-1) and prostate cancer (PC-3) cell line [69].

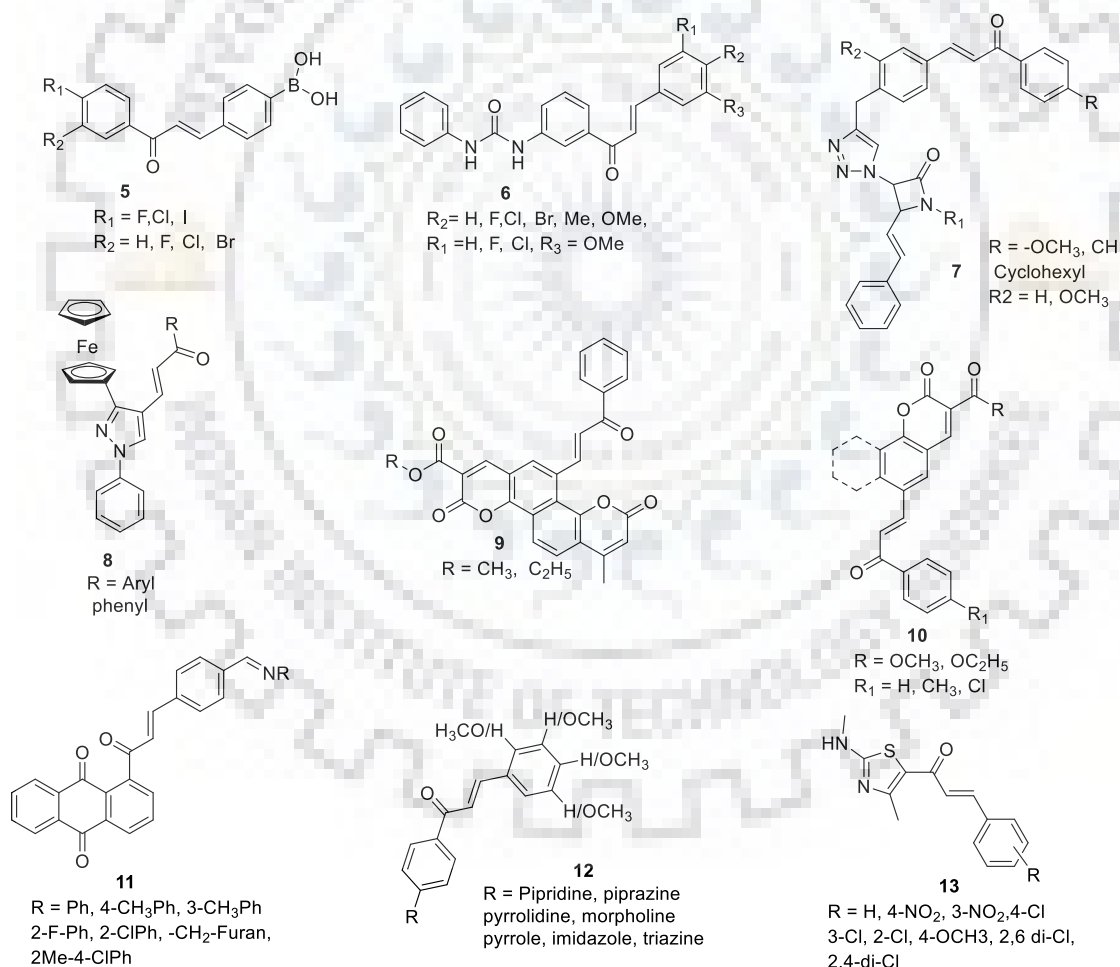


Figure.1.10. Some Synthetic biologically active chalcone derivatives.

Joksovic *et al.* described the synthesis, electrochemical study and antiproliferative activity against human cervix carcinoma (HeLa) and human myelogenous leukaemia (K562) of ferrocenyl pyrazole containing chalcone (**8**) derivatives [70]. A series of

biscoumarin chalcone (**9**) was synthesized by Shukla *et al.* exhibiting potential; anti-inflammatory and anti-oxidant agents [71]. Shashidhara and group reported the synthesis of coumarin based chalcone (**10**) and presented their biological evolution against one normal mouse embryo fibroblast (NIH3T3) and four Human cancer cell line such as oral squamous cell carcinoma (KB) breast adenocarcinoma (MCF-7), cervical carcinoma (C33A), lung cell line (A549) [72]. Joksovic' and Co-workers described the formation of chalcone (**11**) including an imine and anthraquinone group and were evaluated for cytotoxic activity in contrast to HeLa, non-small cell lung carcinoma (A549) and human colon carcinoma (LS174) cancer cells *in vitro* conditions [73]. Bhasin *et al.* described the preparation of novel chalcone derivatives (**12**) and assessed their anti-plasmodial activity against asexual blood stages of *Plasmodium Falciparum in vitro* [74]. Liaras and co-workers prepared a series of thiazole containing chalcones (**13**) and used them as potential antimicrobial active agent against Gram positive (*S. Aureus*, *Micrococcus flavus*, *Bacillus cereus*, *Leishmania monocytogenes*) and gram-negative bacteria (*Salmonella typhimurium*, *P. aeruginosa* *Enterococcus faecalis* and *E. coli*) and fungi (*Aspergillus fumigates*, *Penicillium funiculosum* and *Trichoderma viride*) [75]. Geranyl, Prenyl and farnesyl are important substituents that are connected with chalcone and are widely distributed in nature. They have shown a wide variety of pharmacological and biological activities like anti-diabetic, anti-reverse transcriptase, anti-fungal, anti-malarial, anti-tubercular, anti-bacterial, anti-tumor, anti-oxidative, anti-metastatic and anti-inflammatory [76].

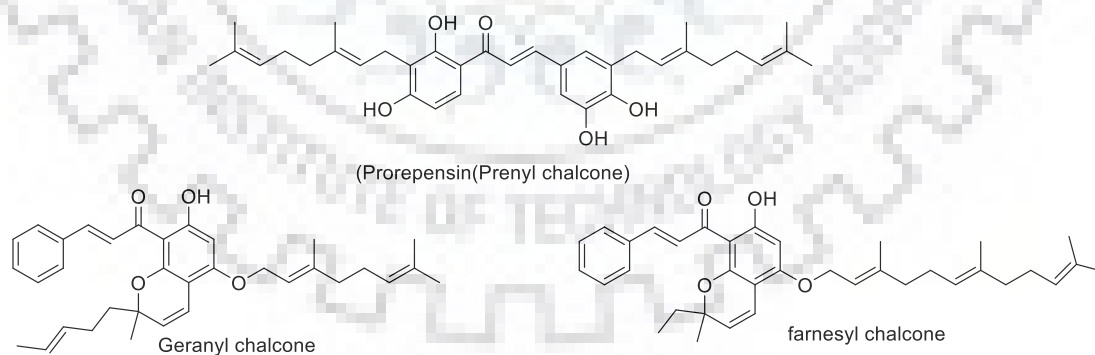
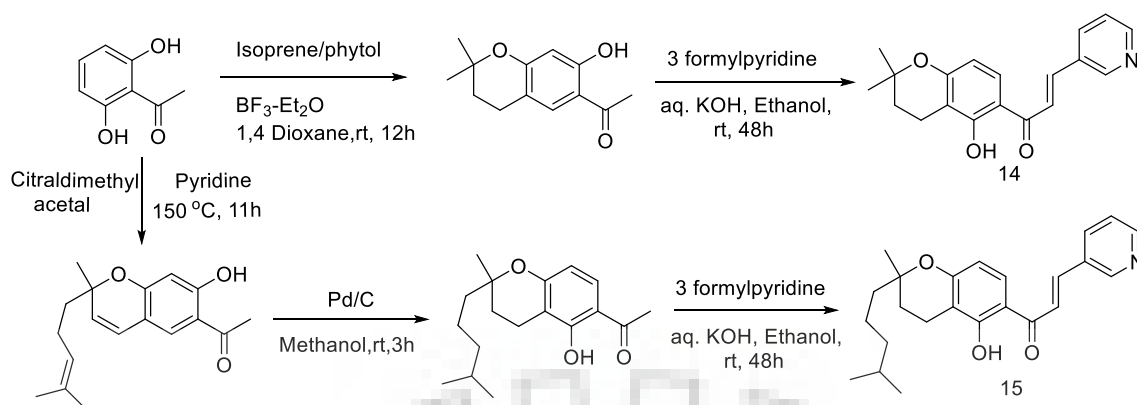


Figure.1.11. Prenyl, Geranyl and farnesyl chalcone.

Tadigoppula and co-workers reported the formation of chromano-chalcones (**14**) and (**15**) and screened their anti-malarial activity against *plasmodium falciparum in vitro* (Scheme 1.7) [77].



Scheme.1.6. Synthesis of Chromeno chalcones

1.4. Flavone

Flavone is one of the significant subgroups of flavonoids. The essential unit of flavone is pyrone, which is there as benzo-pyrone (chromone). If its C-2 position is substituted by phenyl group to give the first member, flavone (I) of the class Flavones (Figure 1.12). Flavones have a planar structure due to C-O-C bond angle 120.9° . The bond length of C-O is 1.376 \AA and dihedral angle of about 179.2° .

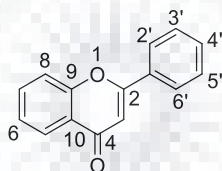
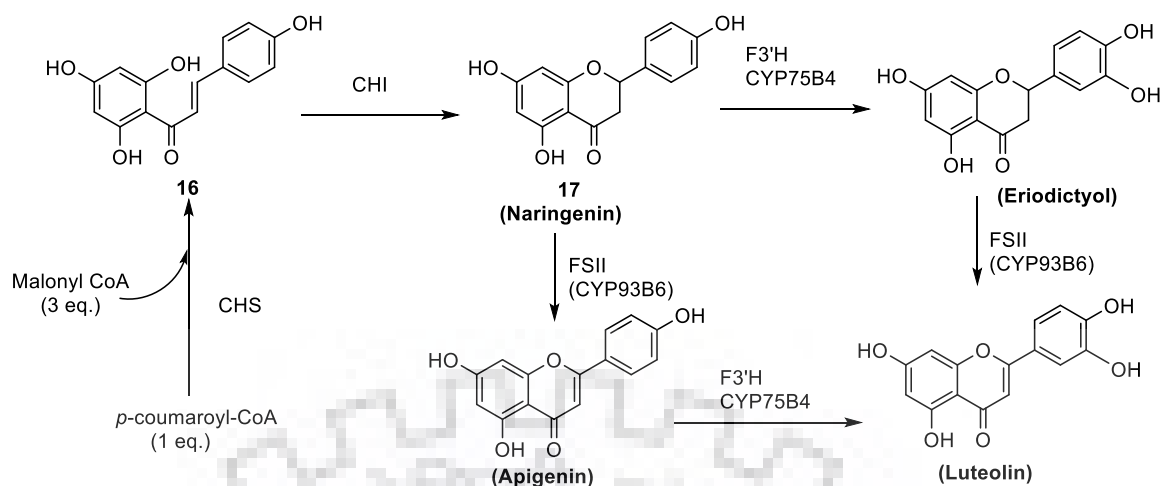


Figure.1.12. General Structure of flavone.

1.4.1. Methods for the synthesis of flavone

1.4.1.1. Biosynthetic method of flavone

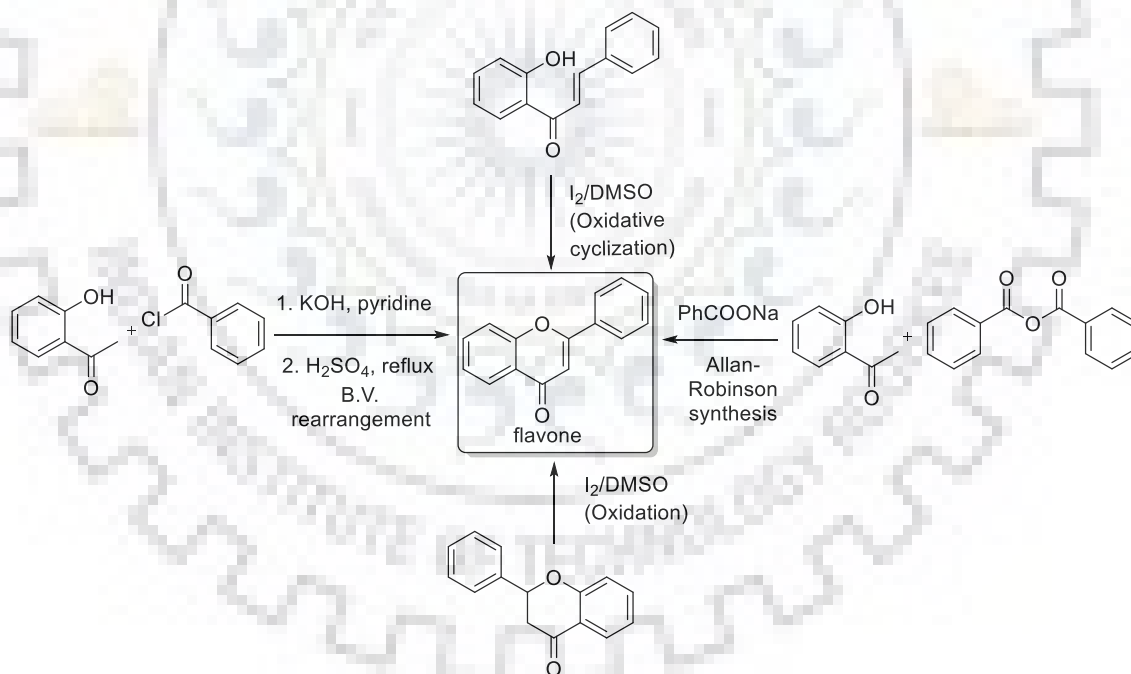
In flavone biosynthesis, *chalcone synthase* enzyme catalysed the flavone which is synthesised by 3eq. malonyl-CoA and 1 eq. *p*-Coumaroyl-CoA to forms chalcone (**16**) (naringenin chalcone), *via* cyclization *chalcone isomerase* enzyme to give flavanone (**17**) (naringenine) (Scheme1.7). Flavanone is the key intermediate for biosynthesis of flavone. Flavones are generated by introduction of a double bond between C-2 and C-3 *via* flavone synthase I enzyme (2-oxoglutarate-dependent dioxygenase) to flavone (Apigenin). In presence of *flavone 3'-hydroxylase* (F3'H) hydroxylation on apigenin proceeding to give luteolin [78].



Scheme.1.7. Biosynthesis pathway of flavone.

1.4.1.2 Synthetic Methods of flavone:

Many methods have been developed for the formation of flavones in the laboratory such as 2'-hydroxy chalcones give flavones by oxidative cyclization, in presence of iodine catalyst and DMSO at 130° C [36].



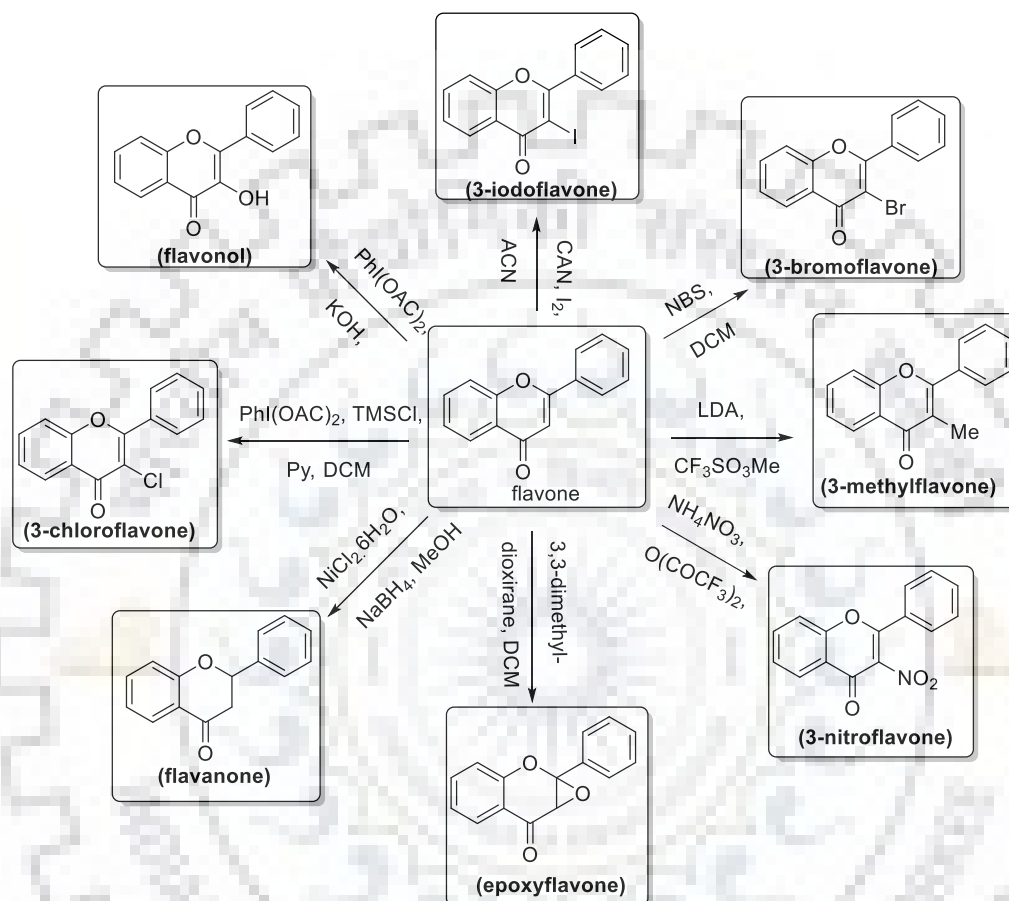
Scheme.1.8. Synthesis of flavone via different starting materials.

Another method is oxidation of flavanone *via* DMSO and Iodine [79]. Allan-Robinson method in which benzoic anhydride and 2'-hydroxyacetophenone reacts in presence of sodium salt of acid to afford flavone [80]. Baker-Venkatarman rearrangement in which 2'-hydroxy acetophenone and benzoyl chloride reacts in presence of base in pyridine forms 1,3-diketone which in presence of acidic medium cyclizes to afford flavone [81].

1.4.2. Application of flavone

1.4.2.1. Synthetic applications

In flavones, C-3 and α , β -unsaturated double bond is active center for electrophilic attack therefore, numerous reactions performed at C-3 position afford the 3-substituted flavone such as 3-iodoflavone by using I_2 CAN and ACN [82],



Scheme.1.9. Synthetic transformation from flavone.

next for 3-bromoflavone use NBS and DCM [86], methylation by using LDA/CF_3SO_3Me to afford 3-methylflavone [83], nitration by using NH_4NO_3 and trifluoroacetic anhydride to afford 3-nitroflavone [84], Chlorination using $TMSCl$ affords 3-chloroflavone [85], hydroxylation through (diacetoxyiodo) benzene and KOH to afford 3-hydroxy flavone [86], double bond reduction of α , β -unsaturated *via* $NaBH_4$ as reducing agents and $NiCl_2 \cdot 6H_2O$ as catalyst in methanol to afford flavanone [87]. Similarly, epoxidation of α , β -unsaturated double bond epoxidation can be carried out with dimethyldioxirane (Scheme 1.9) [88].

1.4.2.2. Biological applications

Flavones are mostly found in fruits, vegetables and cereals which we consume involuntarily in our day to day diet and they have an encouraging effect on our health

without any vital side effects. The major natural flavones are luteolin (3',4',5,7-tetrahydroxyflavone), chrysin (5,7-dihydroxyflavone) and apigenin (4',5,7-trihydroxyflavone), and show antioxidant activities at low concentrations due to presence of hydroxyl groups [89]. 6-hydroxy-flavone used in neurological disorder is obtained from leaves of *Barleria prionitis*. Some other natural occurring flavones are tangeritin (4',5,6,7,8- pentamethoxyflavone), Diosmetin (3',5,7 -trihydroxy-4-methoxy flavone), baicalein (5,6,7- trihydroxyflavone), wogonin (5,7-dihydroxy-8-methoxy flavone) and scutellarein (5,6,7,4'-tetrahydroxyflavone).

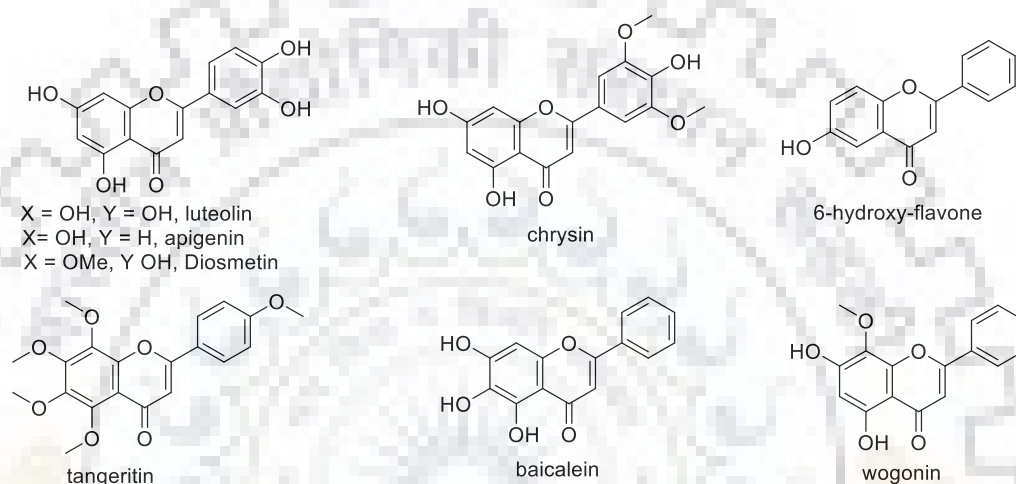


Figure.1.13. Some naturally occurring biologically active flavone derivatives

In 2007, Lewin and group reported the synthesis of piperazinyl flavones derivative (**18**) and tested its antimalarial activity against and resistant (FcB1, K1) *P. falciparum* strains and chloroquine-sensitive (Thai) ranging from micromolar to sub micromolar [90]. In 2012, Pratap *et.al.* described the preparation of Antidyslipidemic and Antidiabetic active aminopropanol based flavones (**19**) derivative [91]. Ertan and co-workers designed flavonyl-2,4-thiazolidinediones (**20**) and studied their insulin releasing and aldose reductase (AR) inhibitory activity effects *in vitro* [92]. Hillard and group synthesises ferrocenyl Flavone derivative (**21**) and showed cytotoxicity against the murine B16 melanoma cells. They are more cytotoxic as compared to the organic analogues and have IC_{50} value in micromolar range [93]. In 2015, our group synthesises flavones-estradiol conjugates (**22**) and studied their antiproliferative activity beside human cervical (HeLa cells) and estrogen-dependent breast cancer (MCF-7), with the estrogen-independent (MDA-MB-23) breast cancer cell line [94]. Prior, we also described the formation of triazole associated with flavone and tetrahydropyran (**23**), They have shown a wide variety of biological activity for example antiproliferative activity against human lymphoblastoid (KCL22), human breast (MDA-MB 231) and human cervical

(HeLa) carcinoma cell lines [95]. Prenylflavone (**24**) have shown a widespread variety of biological activities and pharmacological activities for example anti-diabetic, anti-reverse transcriptase, anti-fungal, anti-malarial, antitubercular, anti-bacterial, antitumor, anti-oxidative, anti-metastatic and anti-inflammatory. Ye *et al.* reported the synthesis of imidazole and indole flavones fused derivative (**25**) and significantly shown excellent antidepressant activity [96].

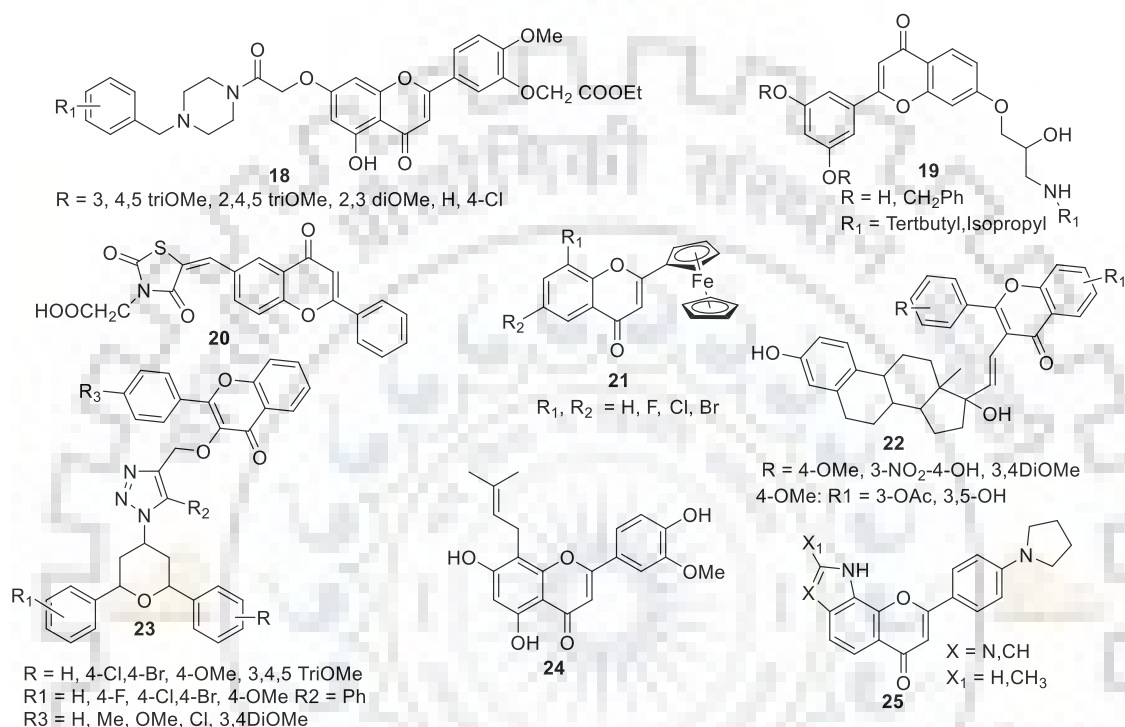
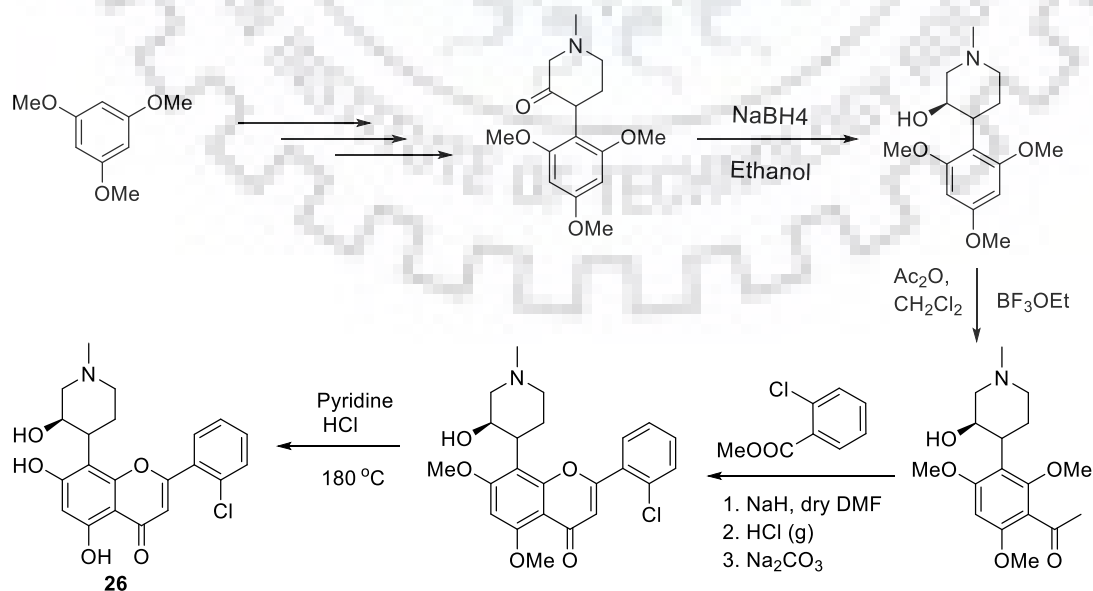


Figure.1.14. Some Synthetic biologically active Flavone derivatives.

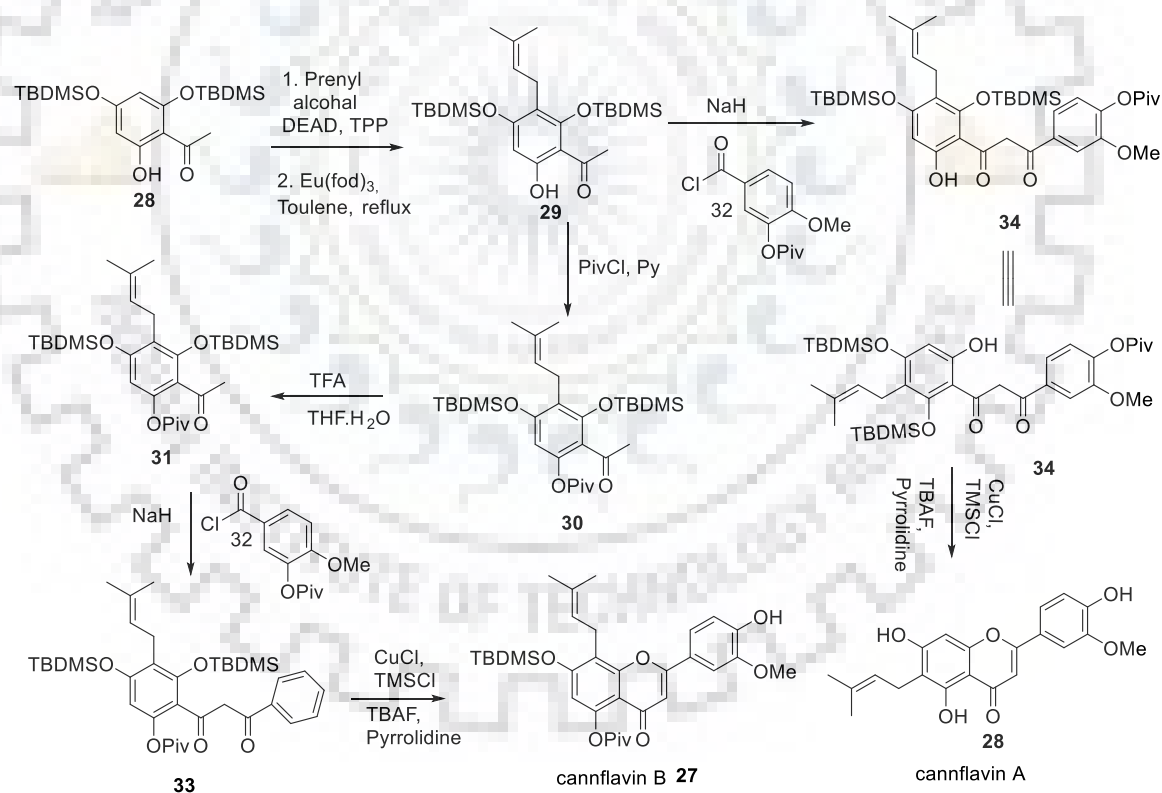
Kattige and group described the synthesis of flavopiridol anticancer agent (**26**) from



Scheme.1.10. Synthesis of flavopiridol alkaloid as anticancer agent.

1,3,5 trimethoxybenzene and *N*-Methylpiperidone *via* multistep process involving many organic reactions (Scheme 1.11) [97].

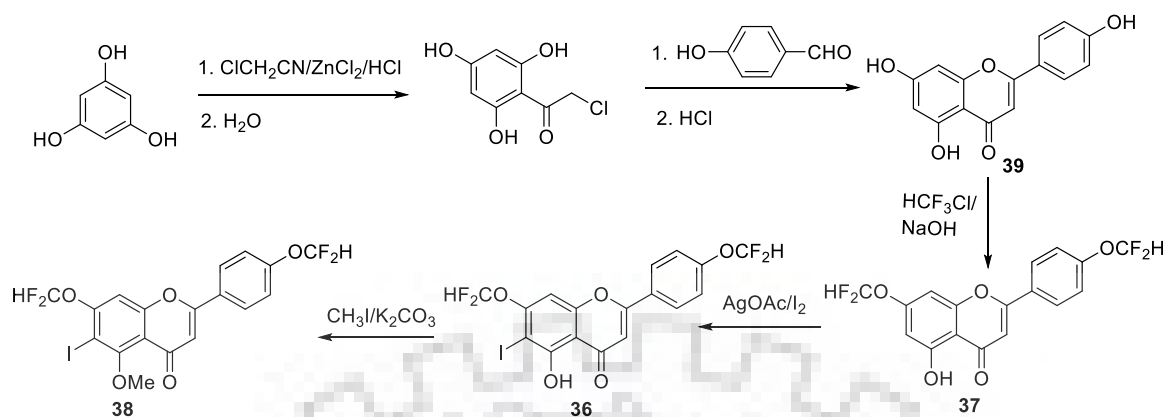
Iso-Prenylflavones, usually obtained from plants, have studied antioxidant properties and their synthesis is used for structure activity relationship (SAR) studies. Minassi *et al.* describes the formation of natural compound cannflavin B (**27**) and its regioisomer, cannflavin A (**28**) *i.e.* unnatural have isoprenyl group in ring A, potentially active for COX inhibiting. The *iso*-prenyl unit was introduced on protected acetophenone (**28**) through a Mitsunobu reaction followed by Cope-Claisen rearrangement to synthesized prenylated acetophenone (**29**). Regioselectively, the pivaloyl unit in (**30**) is used as a protecting group and the compound (**31**) is formed chemoselectively *via* *o*-desilylation through TFA into water/THF. Compound (**31**) and (**29**) react with benzoyl chloride (**32**) to give the diarylmethanes in the presence of NaH *i.e.* (**33**) and (**34**). Regioisomerically diarylmethanes (**33**) and (**34**) were cyclized to give compound (**27**) and (**28**) through Lewis acid TMS chloride and (CuCl₂) (Scheme 1.13) [98].



Scheme.1.11. Synthesis of iso-prenylflavone.

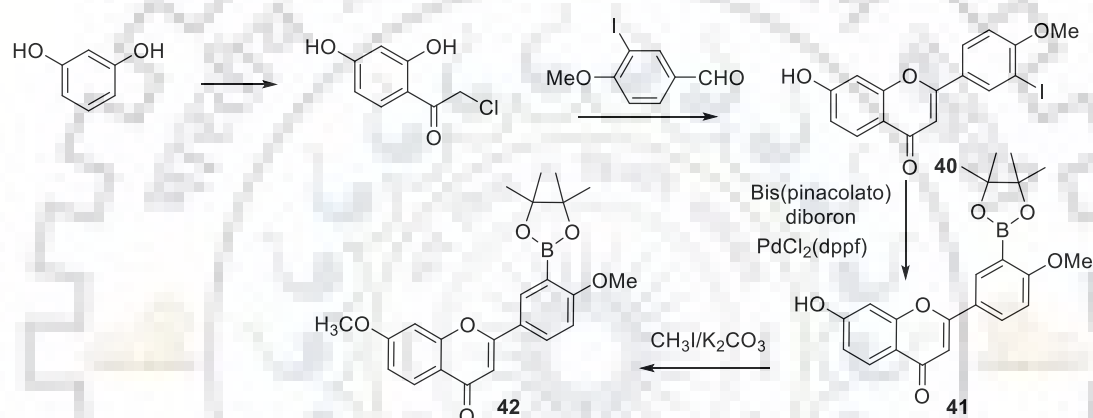
Biflavonoids have received great attention due to their varied biological application like antileishmanial, anti-inflammatory, antiviral, antiplasmodial and β -secretase inhibitory activity [99]. In general, biflavonoids activity is much higher as compared to individual

Step-1



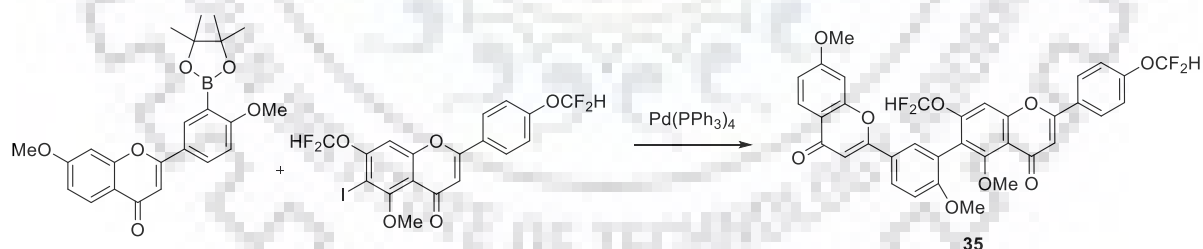
Scheme.1.12. Synthesis of 6-iodoflavone.

Step-2



Scheme.1.13. Synthesis of boronate flavone.

Step-3



Scheme.1.14. Synthesis of biflavone via Suzuki cross coupling reaction.

monomers [100]. Zheng *et al.* described the synthesis of *gem* Difluoromethylenated biflavone (35) in three steps. In 1st step they synthesized protected apigenin, hydroxyl group *via* difluoromethyl. The intermediate, 6-iodonated flavone (36) synthesized from (37) and intermediates *i.e.* flavone (39) which is synthesized by 2-chloroacetophenone and benzaldehyde, was regioselectively produced under mild reaction with I_2/AgOAc . Methylation of compound (37) was done in the presence of K_2CO_3 with CH_3I to give compound (38) (Scheme 1.12). In 2nd step protected boronate flavone (43) was synthesized from 3-iodonated flavone (41)

(Scheme 1.13). In 3rd Step they performed Suzuki cross coupling with 6-iodoflavone (39) and boronate flavone (43) by using tetrakis (triphenylphosphine)palladium (0) catalyst. (Scheme 1.14) [101].

1.5. Flavonol

Flavonol is a subgroup of flavonoid, chemically known as 3-Hydroxy flavone support (3-hydroxy-2-phenylchromen-4-one). Flavonols exist in a wide variety of fruits, red wine, tea and vegetables (Figure 1.10). Various fruits, leafy vegetables, tubers, bulbs spices and herbs in addition to wine and tea contain flavonols mostly in the form of glycosides [102]. Particularly peppers, onions, blueberries, cranberries, cherries, apples and grapes that have the flavonol at levels as high as around 350 ppm.

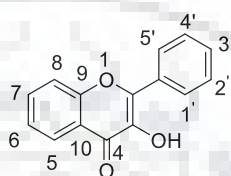
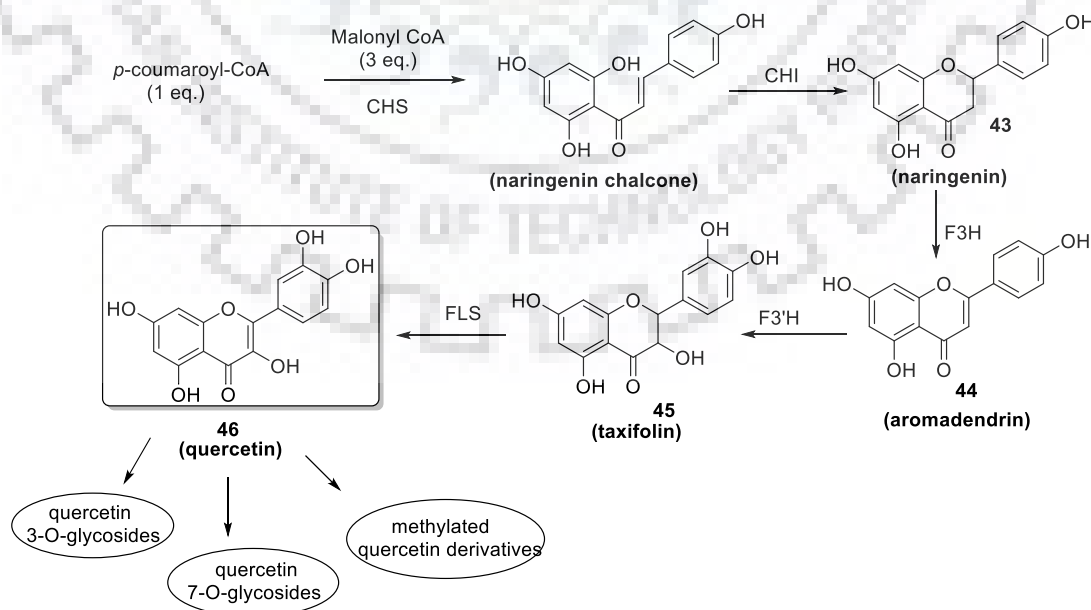


Figure.1.15. Basic skeleton of flavanol.

1.5.1. Methods for the synthesis of flavonol

1.5.1.1. Biosynthetic method of flavonol

The frame of flavonol is synthesized by reacting malonyl-CoA (3eq.) and *para*-coumaroyl-CoA (1eq.) in presence of CHS (*chalcone synthase enzyme*) to form Naringenin chalcone, which in the presence of *chalcone isomerase enzyme* (CHI) undergoes cyclization to afford flavanone(naringenin) (43). This compound (43) in the

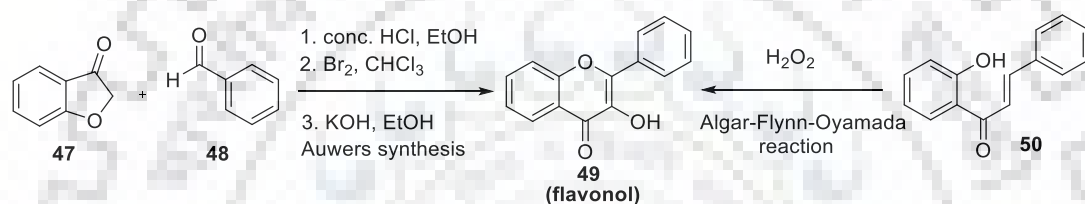


Scheme.1.15. Biosynthesis pathway of flavone.

presence of enzymes *flavone-3-hydroxylase (F3H)* and *flavone3'-hydroxylase (F3'H)* give rise to aromadendrin (**44**) and taxifolin (**45**) respectively. Finally, taxifolin (**45**) in the presence of *flavonol synthase (FLS)* furnishes quercetin (**46**) and this further can undergo various transformations to give glycosides (Figure 1.15) [103].

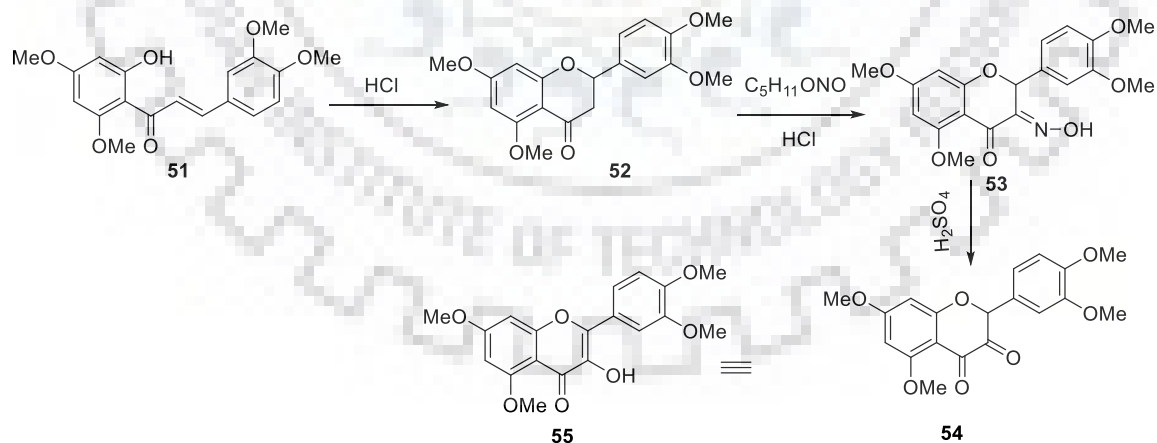
1.5.1.2. Synthetic methods of flavonol

In laboratory for the synthesis of flavonols several synthetic processes have been developed such as Auwers synthesis in which benzofuranone (**47**) reacts with benzaldehyde (**48**) in acidic medium followed by bromination and then rearrangement in presence of base to provide flavonol (**49**). [104] Algar-Flynn-Oyamada reaction in which the reaction of 2' hydroxychalcone (**50**) with H_2O_2 afforded chalcone oxiranes which undergo cyclization to give flavonol (scheme 1.16) [105].



Scheme.1.16. Synthesis of flavonol *via* Auwers synthesis and Algar-Flynn-Oyamada reaction.

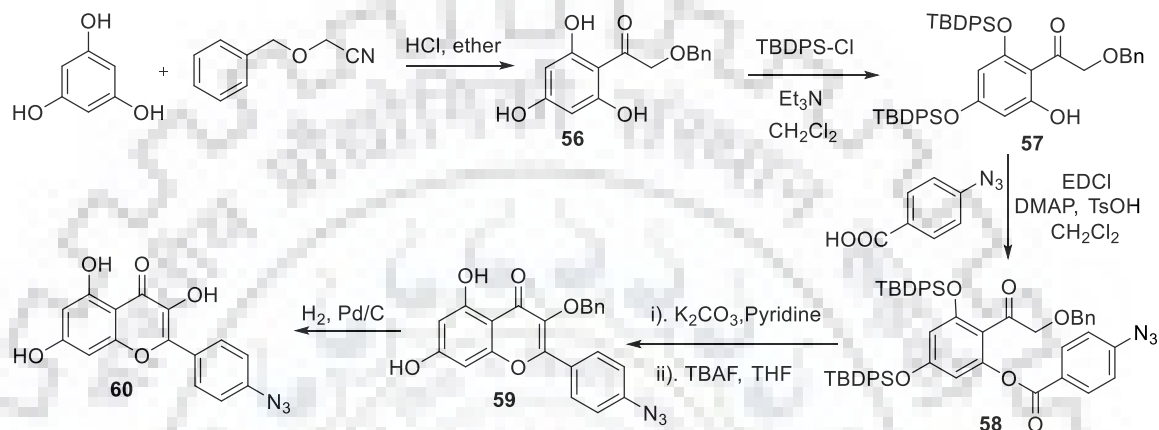
Kostanecki and group reported the synthesis of flavonol (**55**) *via* oximation of flavanone (**52**) which is synthesized from chalcone (**51**). Resulting Oximino ketone (**53**) subsequently by hydrolysis converted into a-diketone intermediate (**54**), which enolized to flavonol (**55**) (Scheme 1.17) [106].



Scheme.1.17. Synthesis of flavonol.

In 2000, Wandless *et al.* reported the synthesis of the substituted kaempferol (**60**) (3-hydroxyflavone) is shown in (Scheme 1.19). This reaction is carried out by benzyloxy acetonitrile and Phloroglucinol in ether, Ketone (**56**) is formed. The ketone (**56**) product when treated with triethylamine and *tert*-butylchlorodiphenylsilane gave bis-protected phenol (**57**) derivative. Phenol derivative (**57**) was acylated by 4-azidobenzoic acid,

using of EDCI and catalytic amount of DMAP and TsOH. In the presence of potassium carbonate and pyridine, acylated phenol (**58**) transformed into the protected flavonol *via* partial deprotection of the TBDPS ethers. Resulting mixture was treated with tetrabutylammonium fluoride (TBAF) in THF to give intermediate (**59**). The Azide group was reduced and benzyl ether was hydrogenolysed by using 5% palladium on carbon (Pd/C) under a hydrogen balloon to give the desired *p*-amino-substituted product (**60**) [107].

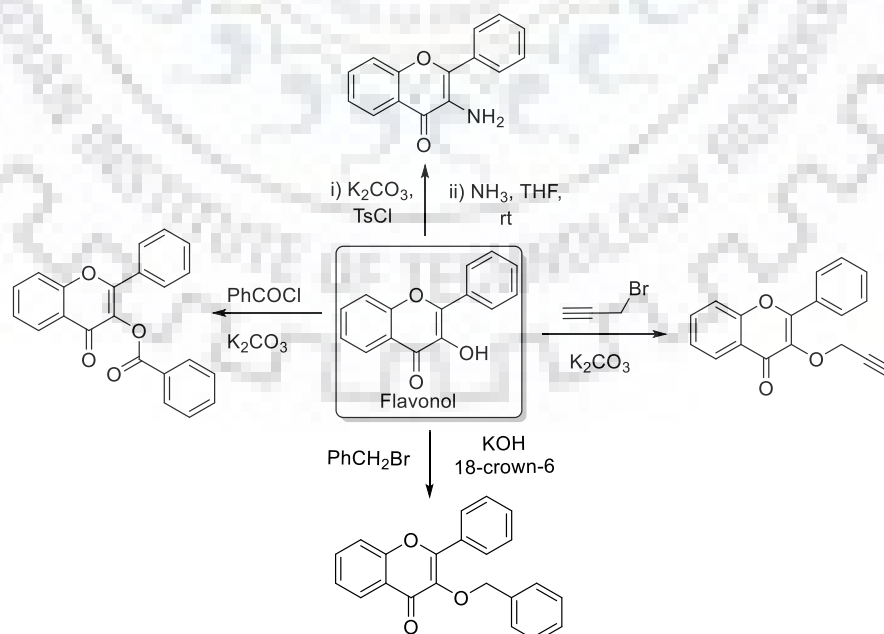


Scheme.1.18. Synthesis of kaempferol (**65**).

1.5.2. Application of flavonol

1.5.2.1. Synthetic Applications

In flavonol, the reactive site is 3-hydroxy group which undergoes various chemical transformations to give amination, ethers, esters and glycosylation.



Scheme.1.19. Synthetic transformations of flavonol.

Propargylation, benzylation, amination and benzylation of flavone can be obtained by reaction with ammonia solution [108], propargyl bromide [95], benzyl bromide [109], and benzoyl chloride [110] respectively in presence of base (scheme 1.19).

1.5.2.2. Biological Application

Flavonols afford several health benefits such as; increased consumption of flavonols is associated with lessened risk of cancer, stroke and cardiovascular diseases [111]. These can be attributed to their anti-oxidant properties due to occurrence of aromatic rings of the flavonoid molecule, which permit the acceptance and donation of electrons since free radical species. Furthermore, some flavanols approve bone health, healthy brain, prevent osteoporosis and possess anti-inflammatory and neuroprotective properties. Hence, ingesting of foods rich in flavanols is associated with long-term health profits. The major dietary flavanols are quercetin (**61**), myricetin (**62**), kaempferol (**63**), and rutin (**64**) (Figure 1.16).

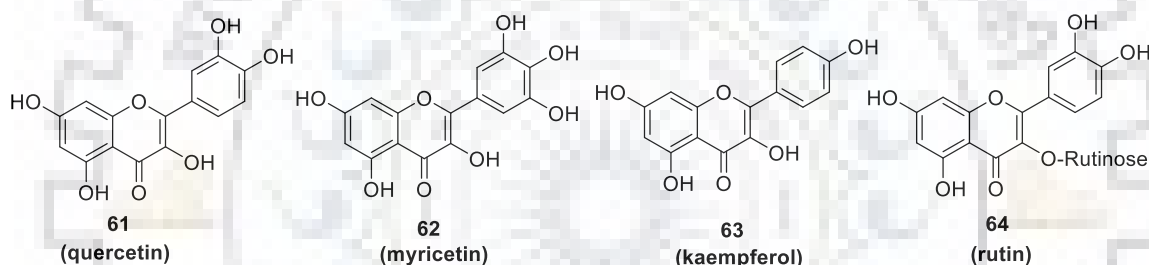


Figure.1.16. Biologically active structure of flavonol.

1.6 Aurone

Aurones *i.e.* 2-benzylidenebenzofuran-3(2H)-ones) are less common flavonoid derivatives in which chalcone is closed into a 5-membered ring as an alternative of the 6 membered ring that possess a benzofuran frame associated with a benzylidene linked in position 2. They are the resultant metabolites natural products go to the flavonoids family, and structurally they are isomers of flavones, distributed in flowers, fruits and vegetables anywhere they participate in the pigmentation of ornament flower like snapdragon, dahlia and cosmos [112].

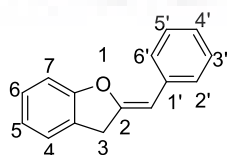
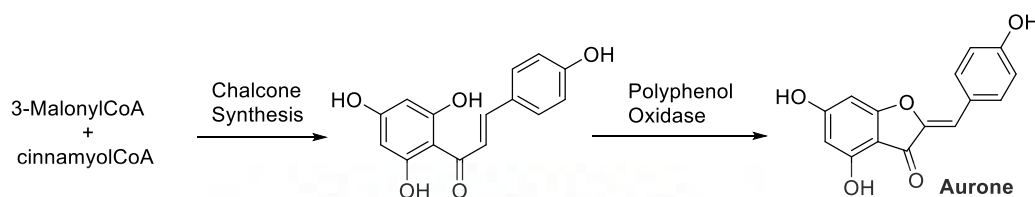


Figure.1.17. Basic skeleton of Aurone.

1.6.1. Methods for the Synthesis of Aurone

1.6.1.1. Biosynthetic method of Aurone

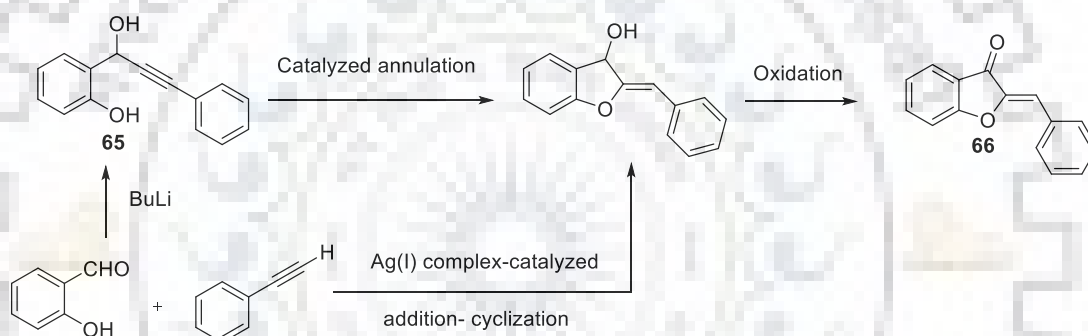
Aurones are obtained from biosynthesis of chalcone *via* rearrangement and oxidation as well as other flavonoids by aurone synthase [113], also found in numerous natural sources and show antioxidant activity by free radical's scavenger [114] (Scheme 1.21).



Scheme.1.20. Biosynthesis pathway of Aurone.

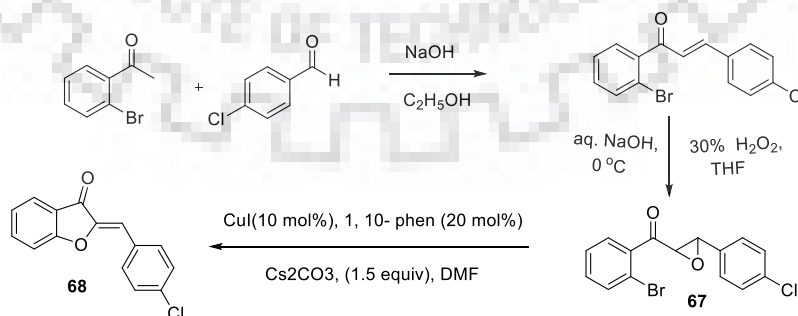
1.6.1.2. Synthetic method of Aurone

Yao *et al.* explained a highly simple and efficient phosphine ligand promoted method with silver nano-particle catalysed the annulation of 2-(1-hydroxy-3-arylprop-2-ynyl)phenol (**65**) behave as an intermediate in the formation of aurone (**66**) [115].



Scheme.1.21. Gold catalysed synthesis of (*Z*)-aurone *via* salicylaldehyde and phenyl acetylene.

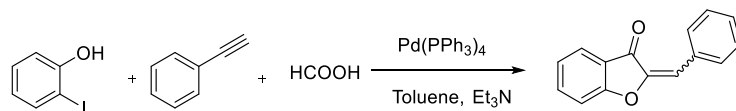
Su and group developed an efficient and expedient method for the preparation of (*Z*)-aurones (**68**) *via* intramolecular ring opening and cyclization reaction of (2-halogenphenyl)(3-phenyloxiran-2-yl) (**67**), yielding methanone (**67**) using copper iodide and 1,10 phenanthroline in DMF at heating [116].



Scheme.1.22. synthesis of (*Z*)-aurone through 2-bromo acetophenone and p-chlorobenzaldehyde.

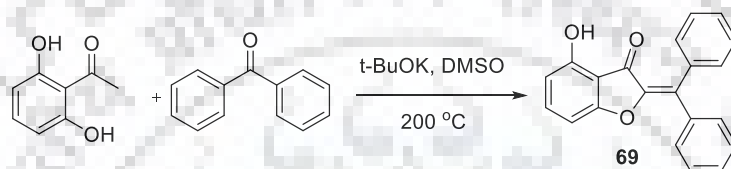
Qi and co-workers reported a universal and practical strategy to prepare aurone derivative through palladium catalyst with 2-iodophenol and terminal alkyne *via* formic

acid as the CO source through acetic anhydride used as an activator in moderate to good yields with high selectivity and good functional group tolerance [117].



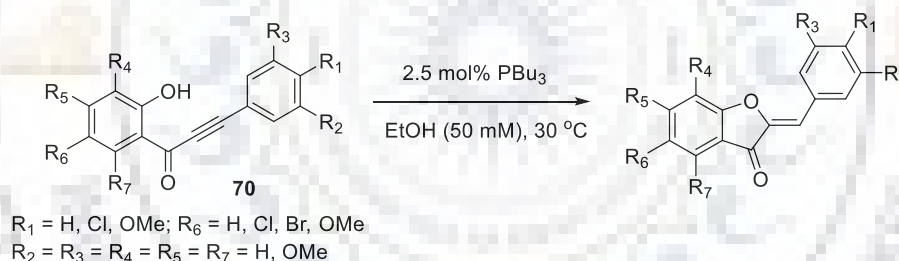
Scheme.1.23. Formation of aurone by 2-iodophenol and phenylacetylene.

Sauso group described the synthesis of aurone scaffold (2-(diphenylmethylene) -4-hydroxy benzo furan 3(2*H*)-one) (**69**) under thermal reaction condition *via* 2,6 - dihydroxy- acetophenone and aromatic ketone in the presence of potassium tertiary butoxide [118].



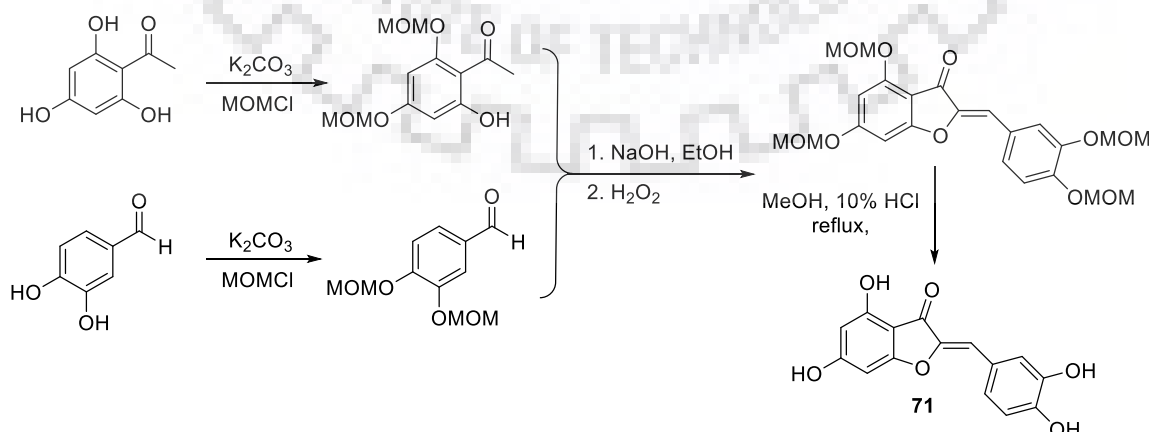
Scheme.1.24. Synthesis of (2-(diphenylmethylene) -4-hydroxy benzofuran 3(2*H*)-one).

Doi *et al.* reported the regioselective *exo*-Cyclization of *o*-Alkynoylphenols (**70**) with the catalytic amount of tributyl phosphine under ambident reaction condition [119].



Scheme.1.25. Synthesis of aurone by *exo*-cyclization of *o*-Alkynoylphenol.

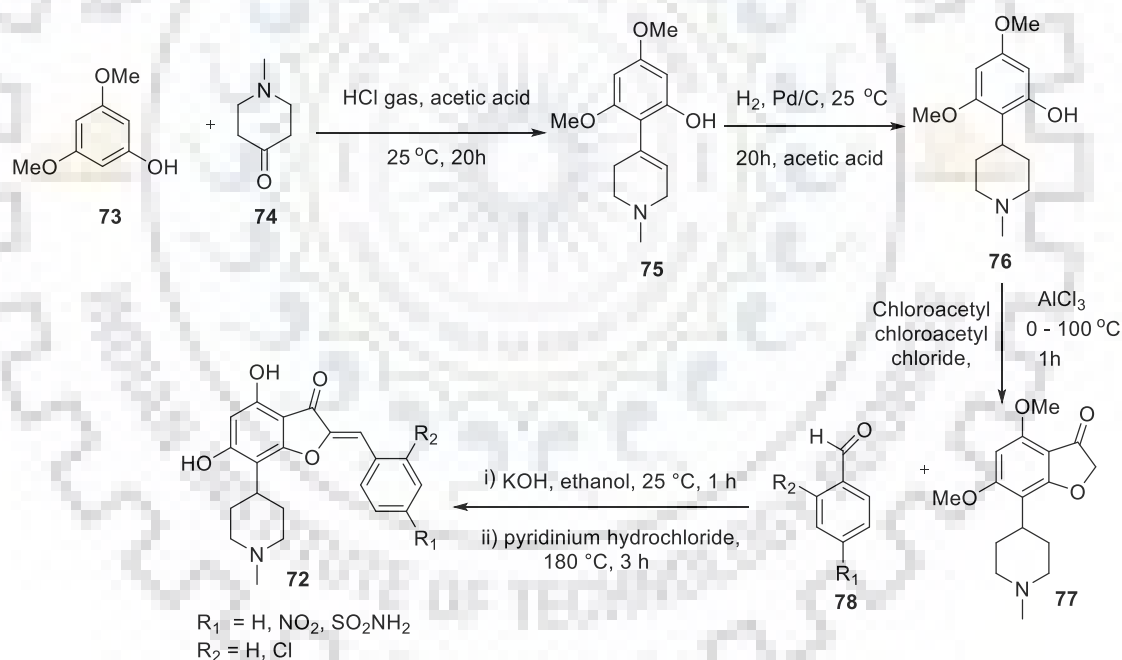
Li and group described the effective and simple formation of Aureusidine (**71**) in one pot



Scheme.1.26. Synthesis of Aureusidin by Algar–Flynn–Oyamada reaction.

synthesis from substituted benzaldehyde and acetophenone on account of a development of an Algar–Flynn–Oyamada reaction in the presence of base (NaOH), ethanol and H₂O₂ and H₂O at room temperature in 24h [120].

Seminally, Schoepfer *et al.* described the multistep synthesis of 2-benzylidene-benzofuran-3-ones (**72**) by mean of acid-catalysed condensation reaction of 1-methyl-4-piperidone (**74**) and dimethoxy phenol (**73**) yielding unsaturated derivative (**75**) in the presence of acetic acid. The compound (**75**) with Pd/C followed by hydrogenation in the presence of acetic acid gave (**76**). The benzo furanone (**77**) derivative synthesized when compound (**76**) consecutively react with aluminium trichloride and chloroacetyl chloride in a one-pot fashion. The compound (**77**) was condensed with substituted benzaldehyde (**78**) and synthesized 2-Benzylidene-benzofuran-3-ones (**72**) using two equivalents of potassium hydroxide and ethanol. Pyridinium hydrochloride is directly used for the deprotection of dimethoxy at 180 °C. This compound is used for the inhibition of CDKs. (Scheme 1.29) [121].



Scheme.1.27. Formation of 2-Benzylidene-benzofuran-3-ones as Flavopiridol Mimics.

1.6.2. Biological Applications

Naturally occurring cotinus coggygia leaves have been extensively utilized for injure therapeutic asset and antidiabetes that are rich in three aurones namely sulfurein (**79**), sulfuretin (**80**) and its dimer form disulfuretin (**81**) [122]. 3',4,4',6-Tetramethoxy aurone (**82**) is one of numerous constituents that has been obtained from the methanolic extract of *Cyperus radicans* (Cyperaceae) demonstrate insect antifeedant activity against *Spodoptera litura* larvae [123]. Li and group identified a prenyl derivative, pauciarone

A (**83**) which is derived from plant *i.e.* *Garcinia paucinervis*. They tested their cytotoxic activity in contrast to human leukaemia (NB4), human neuroblastoma (SH-SY5Y), Carcinomic human alveolar basal epithelial (A549), Human prostate (PC3), Human breast adenocarcinoma (MCF-7) cell lines [124].

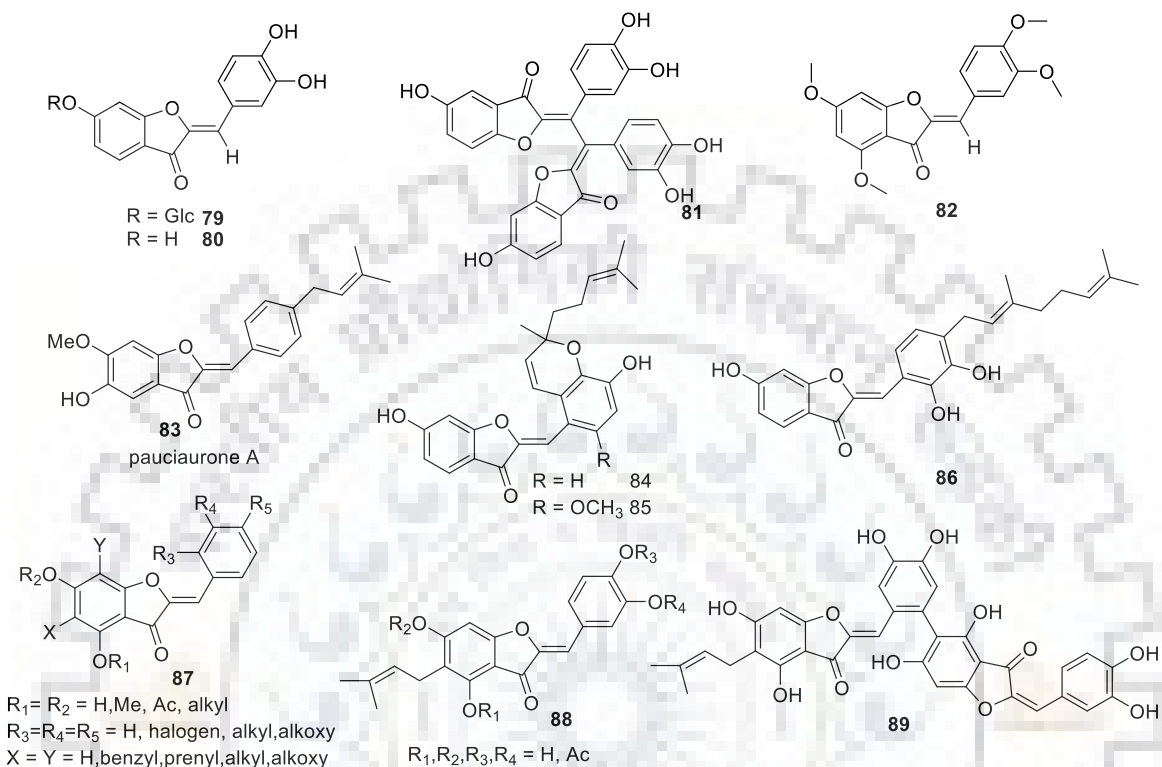


Figure.1.18. Some structure of naturally occurring aurone.

Huong and co-workers extracted and isolated three geranyl-aurones (**84**), (**85**) and (**86**) that were found in *Artocarpus altilis leaves*. These compounds are effective for α -glucosidase inhibitory ($\text{IC}_{50} = 4.9$ to $5.4 \mu\text{M}$) and Tyrosinase inhibitory activities and also used as anti-aging and anti-diabetic agents [125]. Its prenyl-aurone derivative displayed nitric oxide (NO) and 2,2-diphenyl-1-picrylhydrazyl (DPPH) radical scavenging activities [126]. Chu and group described the ability of aurones to prevent microbial infections, like bacterial and fungal infections. The Synthetic aurones (**87**) and (**88**) and naturally occurring dimer form of aurone (**89**) which is isolated from plant cell cultures. The capability to inhibit infections has been estimated in numerous bacterial and fungal (mycoses) agents on the basis of cell-based inhibition, by using an enzyme [127]. Subbaraza *et al.* described the synthesis of 3',4',6, 7 tetrahydroxy aurone and its analogues showing antioxidant activity *via* the superoxide NBT and DPPH free radical scavenger methods [128].

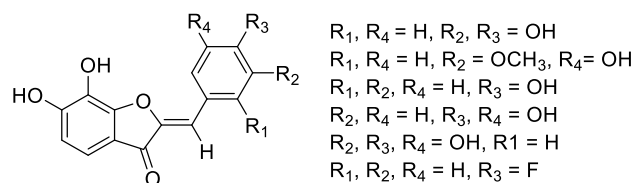


Figure.1.19. Structure of substituted aurone.

Okombi and group reported the formation of aurone scaffolds and used them as an inhibitor of Tyrosinase which is originated from Human Melanocytes. They developed 4,6,4'-trihydroxyaurone which is used for hyperpigmentation-related anomalies [129].

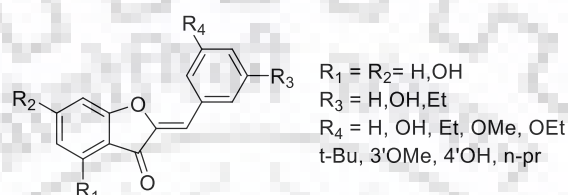


Figure.1.20. Structure of aurone.

Gilbert and group described the synthesis of aurone bind with chromene and coumarin scaffold *via* aldol type condensation reaction under catalytic amount of basic condition and evaluate biological activity against K562 human leukaemia cancer cell line [130].

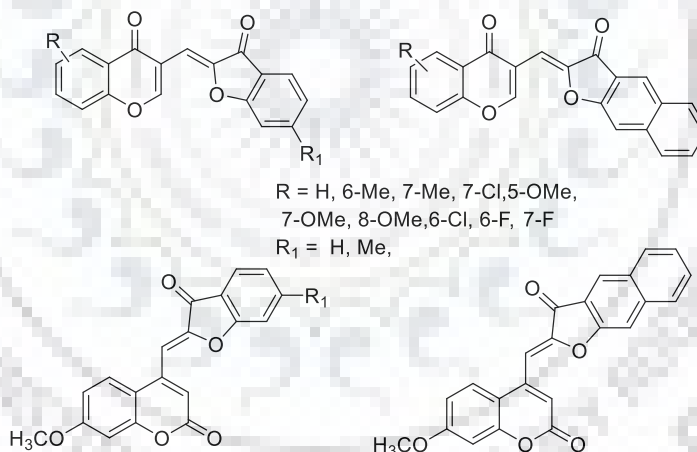


Figure.1.21. Structure of chromene and coumarin aurone scaffold.

Hillard *et.al.* explained the synthesis of ferrocene (organometallic) aurone (**90**) and organic aurone (**91**) using mercury (II) acetate at 80 °C in pyridine for 3-5 h with good yield. They evaluated their cytotoxic effect against estrogen receptor negative breast carcinoma (MDA-MB-231) ($IC_{50} = 2.8 \pm 0.5 - 3.8 \pm 0.1$) and human fetal lung cells (MRC-5) ($IC_{50} = 3.5 \pm 0.0 - 3.7 \pm 0.1$) of organic aurone at concentration ranging from 100 to 0.005 μM . Ferrocenyl aurones show antibacterial activity ranging from 2–32 mg L^{-1} against Gram positive bacteria and gram-negative bacteria for example *Staphylococci aureus* and *Escherichia coli* [131].

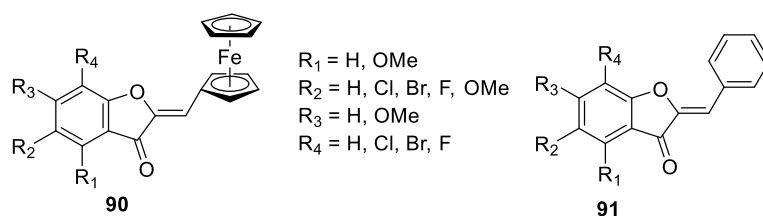
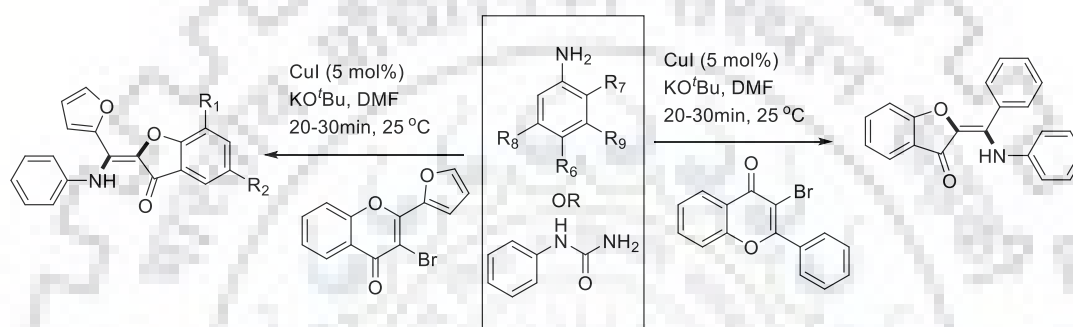


Figure.1.22. Structure of ferrocene (organometallic) and simple aurone.

Inspired by the inclusive range of medicinal and biological properties, electronic or photonic as fluorescence probes of aurone, we turned our attention to the synthesis of biologically active stereospecific aminated aurone under ambident reaction condition with strong base are discussed in chapters 3 (Scheme 1.28).



Scheme.1.28. Synthesis of substituted aminated aurone.

1.7. Polycyclic Benzofuran

Functionalized Polycyclic benzofuran systems are significant structural motifs in an enormous range of natural products such as Psoralidin (**92**), Medicarpin (**93**), plicadin (**94**), Anastatin (\pm) A (**95**) and Anastatins (\pm) B (**96**). Naturally obtained fused furan polycyclic heterocyclic compounds have been described to display intriguing and substantial biological activities like cardiotoxic, antibiotic, antiviral and protein tyrosine kinase inhibitory activities as got in halenaquinone and another allied natural compound (Figure 1.23) [132].

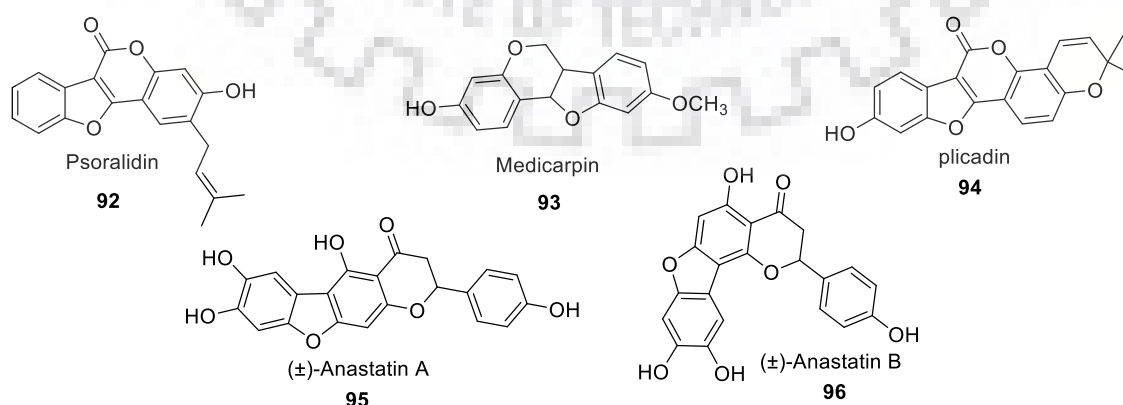
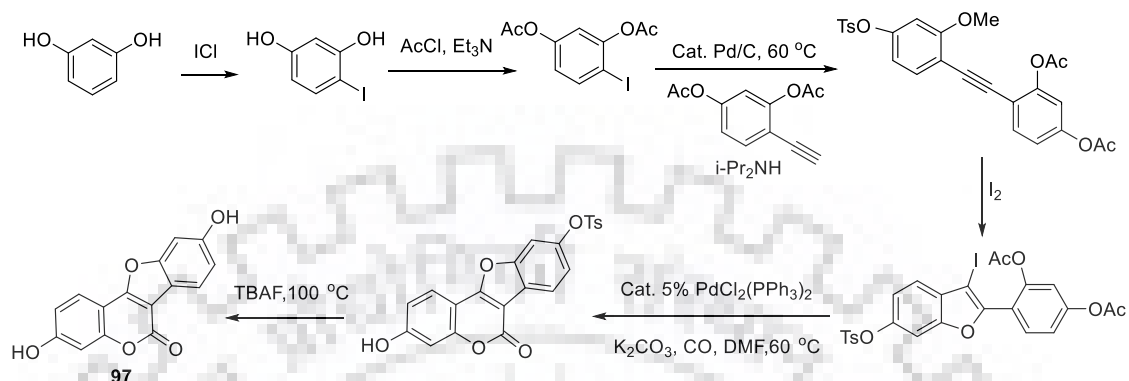


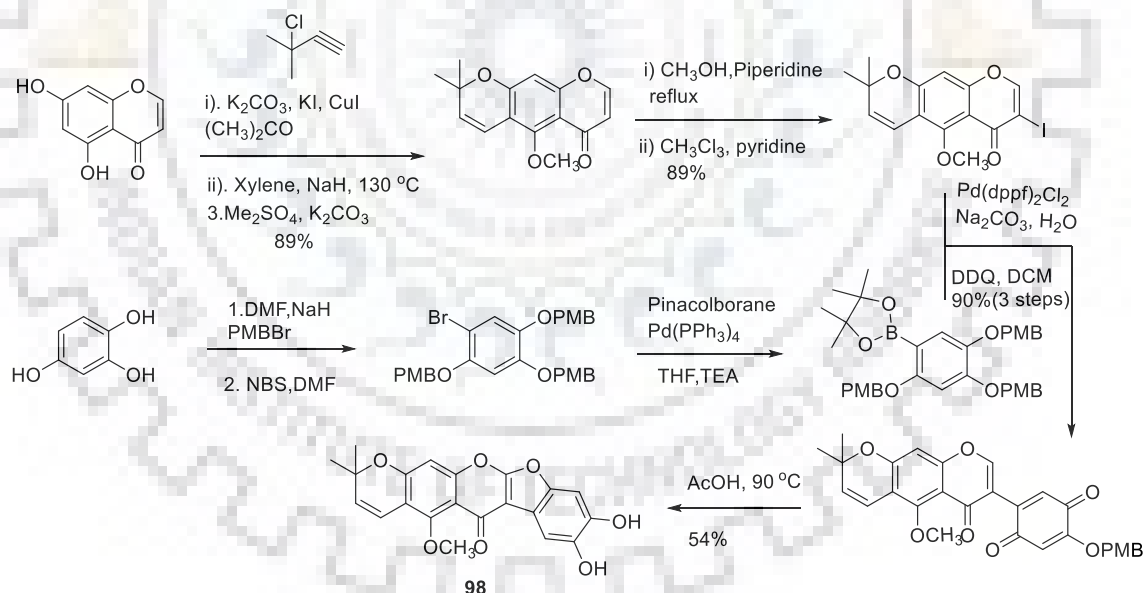
Figure.1.23. Some naturally occurring structure of Polycyclic Benzofuran derivative.

Larock *et al.* described the synthesis of naturally and biologically interesting polycyclic coumestrol (**97**), and their related derivatives that involve Sonogashira coupling reaction, followed by iodo-cyclization of acetoxy derivative, thereafter it undergoes palladium-catalysed carbonylation/lactonization [133].



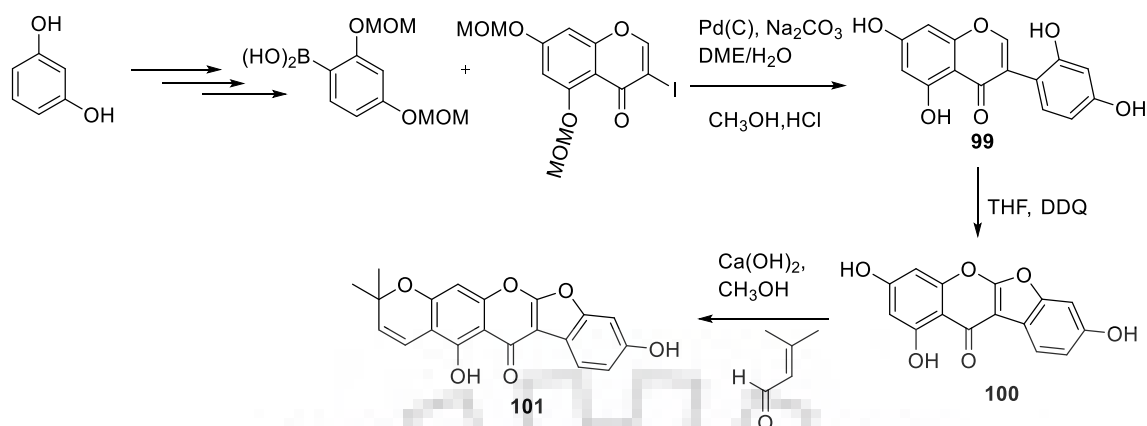
Scheme.1.29. Synthesis of naturally and biologically active coumestrol.

Zheng and Shen team described the total synthesis of hirtellanine A (**98**). At first the pyran ring was formed regioselectively, after that one-pot tandem boronation and Suzuki coupling reaction under palladium-catalyzed condition followed by tautomerism offered poly cyclic furan ring [134].



Scheme.1.30. Total synthesis of hirtellanine A.

Lupinalbin H (**101**) was synthesized *via* the formation of intermediate lupinalbin A (**100**) by regiospecific condensation with prenal. Lupinalbin A (**100**) prepared from prior synthesized 2'-hydroxygenistein (**99**) through oxidative cyclization [135].



Scheme.1.31. Total synthesis of lupinalbin H.

Pinto and co-workers reported the synthesis of tetracyclic furan such as novel and highly functionalized Psoralen analogues (**102**) and (**103**) and evaluated their antiproliferative activity against three human tumor cell lines like MCF-7 (breast cancer), SF-268 (CNS cancer), and NCI-H460 (non-small cell lung cancer) [136]. Similarly, Shchekotikhin *et al.* reported the synthesis of anthra[2,3-b]furan-3-carboxamides and its derivative (**104**) led to the evolution the antiproliferative activity of cervical HeLa and human leukaemia K562 cell line [137]. Shchekotikhin and group developed the synthesis of series of anthrafurandiones derivatives (**105**) that have ability to modulate topo I activity [138]. Nemoto and group designed and developed the synthesis of furan-fused tetracyclic (**106**) which shows antiviral activity. HVJ in LLC-MK2 cells was utilized for the evaluation [139].

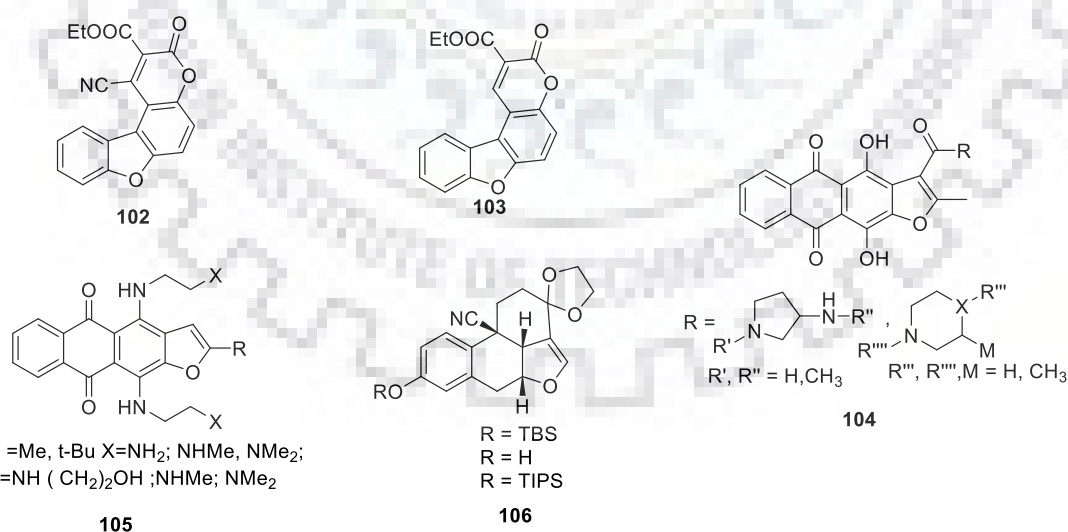
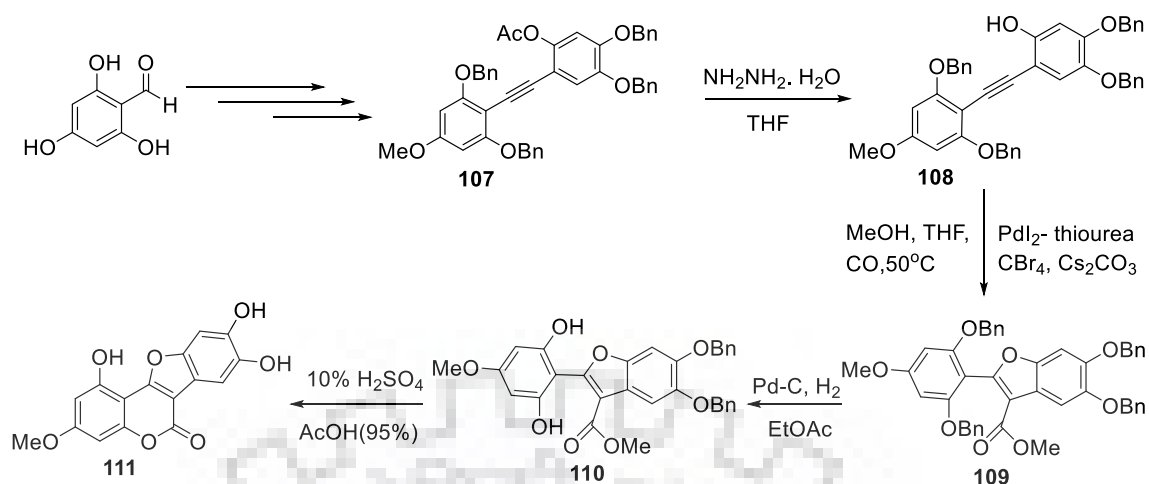


Figure.1.24. Some synthetic structure of Polycyclic Benzofuran derivative.

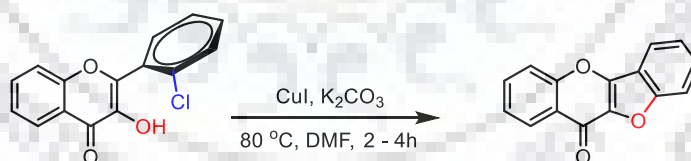
In 1952, Wedelolactone first obtained it from the extraction of *Wedelia calandulaceae* and which exhibits a wide range of biological activities including an antidote for snake venom.



Scheme.1.32. Synthesis of wadelolactone.

Yang *et al.* described the total synthesis of wedelolactone **111** via key steps **107** which is synthesized through palladium-catalysed Sonogashira cross coupling reaction. Compound **107** reacts with hydrazine hydrated in THF to give *o*-hydroxyaryl acetylene (**108**) after that through the palladium-catalysed carbonylation annulation reaction we got compound **109**. Wedelolactone **111** synthesized via when compound **110** was treated with 10% sulfuric acid in acetic acid [140].

In chapter 3, We also also synthesized the tetracyclic fused furan derivative via a simple and efficient Ullmann type coupling reaction involving the 3-hydroxyl flavone employing copper iodide at 80 °C in DMF under basic condition. This methodology has rewarded, high yields, less reaction time and easy and tentative experimental procedures over previous literature reports (described in chapter -2). (Scheme 1.37).



Scheme.1.33. Synthesis of tetracyclic fused furan derivative.

1.8. Chromene and Quinoline

In 2012, Miller and group described the synthesis and pharmacologically activity of 2-amino-7-(dimethylamino)-4-(naphthalen-1-yl)-4*H*-chromene-3-carbonitrile conjugates **112**. They studied their antiproliferative activity in two human prostate (LnCap and PC3) cancer cell lines and two human metastatic melanoma (A375 and WM164) cell lines with taxol resistant prostate (PC3-TxR) cancer cell line [141]. In 2008, again Cai and group described the synthesis of new Series of 4-Aryl-4*H*-chromenes **113**, **114** and **115** as novel anticancer agents. But they explore the (SAR) structural activity relationship on the basis of substituted pyrrole with alkyl fused at the 7,8- positions of

chromene [142]. In 2010, Foroumadi *et al.* synthesises the derivatives of 4- aryl-4H-chromene with 2-arylthiazol-4-yl **116** at 4-position, showing inhibitory action against colon adenocarcinoma cells SW480, breast cancer (MCF-7) and lung cancer (A549) cells with IC₅₀ values below 5 μ M [143].

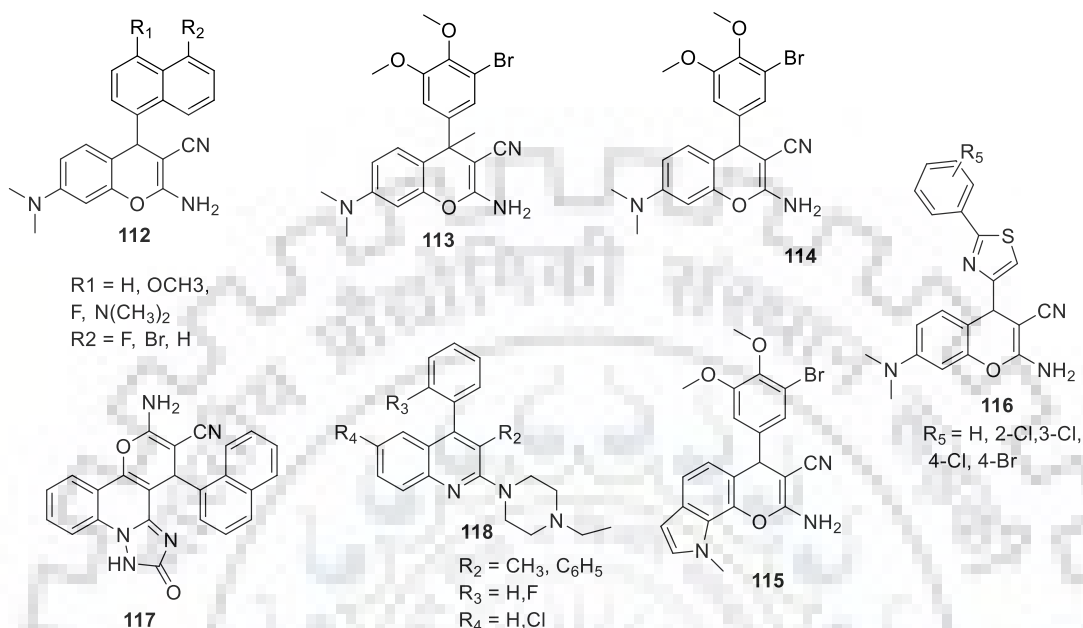


Figure.1.25. Synthesis of chromene and quinoline derivative.

Langer and groups reported the synthesis of [1,2,4]triazolo[1,5-*a*]quinoline-11-carbonitrile **117** and their analogs. They were used *in vitro* as anti-HIV-1 (strain IIIB) and anti-HIV-2 (strain ROD) activity in human cells (MT-4) depend on MTT assay [144]. In 2017, Zinjarde and co-workers synthesized quinoline with piperazine **118** scaffold with their antiproliferative activity against human breast cancer (MCF-7) cell line and human embryonic kidney (HEK293) cell line on the basis of MTT assay [145]. The synthesized series of compounds have antibacterial activity as tested against standard strains of *Staphylococcus aureus* (ATCC 25923), *Escherichia coli* (ATCC 25922) and *Pseudomonas aeruginosa* (ATCC 27853) *in vitro via* Broth Microdilution MIC method range between 64 and 128 μ g/ml. Having this range of pharmacological application by these derivatives, that framework is attractive for our particular attention.

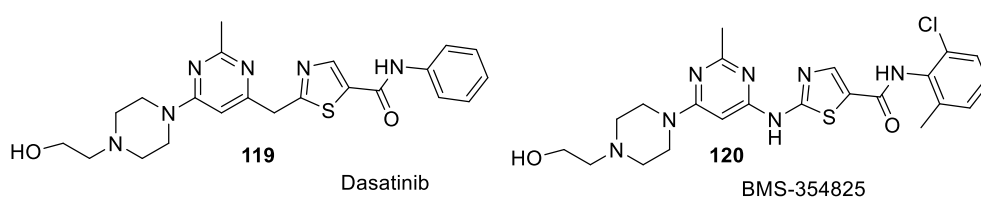


Figure.1.26. pyrimidine with piperazine derivative.

Dasatinib **119** is a potent pan-Src kinase inhibitors. Compound **120** was potentially active in K562 Xenograft model of CML (chronic myeloid leukaemia), demonstrating complete tumour reversion and little toxicity at multiple dose level [146].

Therefore, keeping all these details in mind about pyrimidine, piperazine, chromene and quinoline, we decided to join together these three moieties such as chromene, pyrimidine and piperazine to synthesize the diversely substituted chromene and quinoline pyrimidine piperazine conjugates **71** discussed in chapter 4 (Figure 1.25).

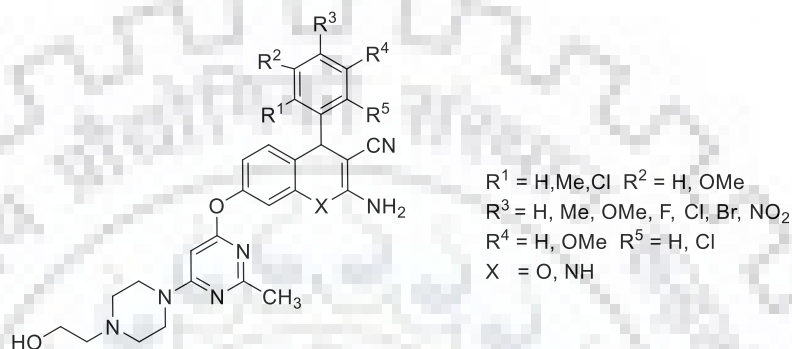
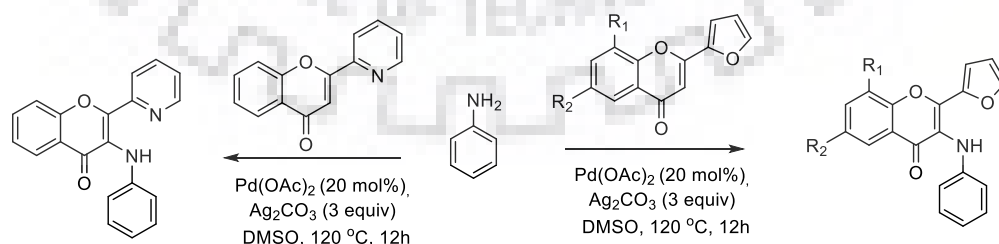


Figure.1.27. Chromene and quinoline pyrimidine piperazine conjugates.

The products were evaluated for their anti-proliferative activities and molecular docking. Bioassay results exhibited excellent activities against both hormone-dependent MCF-7 and hormone-independent MDA-MB-231 cancer cells and human embryonic kidney cell line (HEK293). To see the biological applications of flavone in above literature we join flavone with aniline and show biological activities in chapter 5.

We describe a series of 3-aminated flavone through Pd-mediated oxidative coupling using 2-heteroarylchromones and anilines as selective human Microtubule affinity regulating kinase 4 (MARK4) enzyme inhibitors, a recently identified anti-cancer drug target. Synthesized molecules were identified as hit and exhibited excellent *in vitro* inhibitory effect against MARK4 with IC₅₀ value (50% of ATPase activity).



Scheme.1.34. Synthesis of 3-N-aryl substituted-2-heteroarylchromones and their Microtubule Affinity Regulating Kinase 4 for human breast cancer cell line, human liver carcinoma cells and human embryonic kidney cell line.

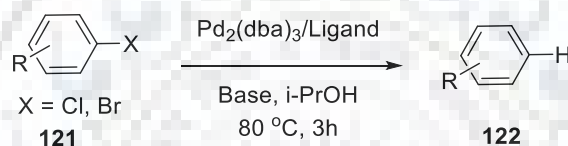
The fluorescence binding and dot blot assay were found in μM range. *In vitro* studies against the cancerous cells (MCF-7 and HepG2) inhibits the cell viability, induce

apoptosis and tau-phosphorylation.

1.9. Dehalogenation Reactions

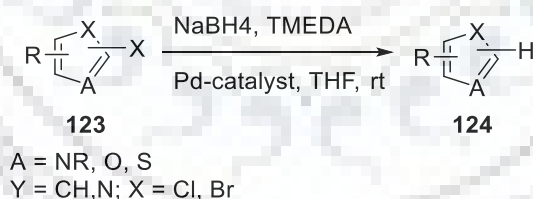
Organic halides compounds (charcoal) that have carbon-halogen bond, firstly synthesized by Justus von Liebig by chlorination of ethanol in 1832. After that, organohalides have achieved a great attention [147]. Organohalides are normally used as biodegradables, refrigerants, pesticides, chemical reagents – solvents, and polymers and soil fumigants [148]. It has been classified as pollutant in spite of their extensive use in numerous applications. Because of this, dehalogenation reaction plays a vital role to convert toxic organohalides to nontoxic products.

Lee and group used sterically hindered phosphites ligand and palladium as a catalyst for the aryl bromide and chloride **121** in isopropanol at 80 °C to afford corresponding dehalogenated product **122** in 3 hours [149].



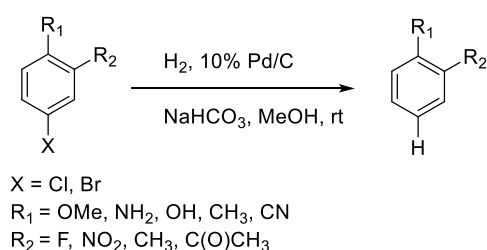
Scheme.1.35. Dehalogenation of aryl chlorides using palladium/phosphite catalyst.

Ruiu *et al.* established a novel methods for the hydrodehalogenation of halo-heteropentalenes **123** with NaBH_4 -TMEDA serve as a hydride source using $\text{PdCl}_2(\text{dppf})$ as a catalyst in THF to give Heteropentalenes **124** [150].



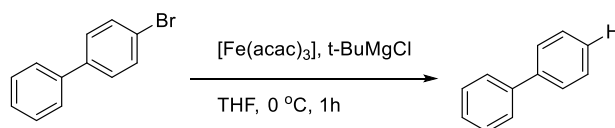
Scheme.1.36. Hydrodehalogenation of Halogenated Heteropentalenes.

Jimenez co-workers developed a Pd/C catalyzed dehalogenation strategy for the synthesis of different substituted arenes under basic condition at room temperature. [151].



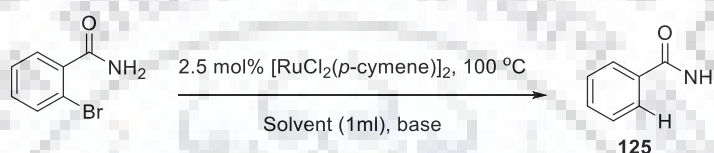
Scheme.1.37. Hydrodehalogenation of halobenzenes with molecular hydrogen.

The hydrodehalogenation of aryl halide reaction was performed by Wangelin and Co-workers in the presence of iron and commercially available *t*-BuMgCl as a hydride source with β -hydride elimination under milder reaction conditions [152].



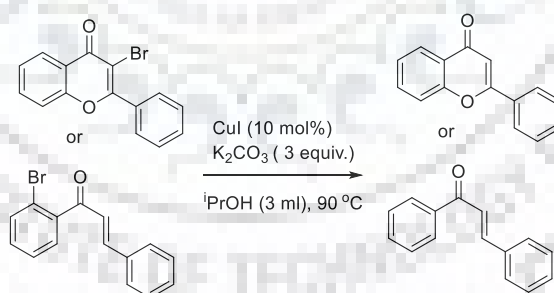
Scheme.1.38. Fe-catalysed hydrodehalogenation of aryl halide.

Xia *et al.* describe the dehalogenation adduct **125** by Ru(II)-catalyst with 2-propanol as a solvent and hydride source by transfer hydrodehalogenation of organic halides [153].



Scheme.1.39. Ru-catalysed hydrodehalogenation of aromatic halide.

In chapter 6, An operationally simple copper-catalysed hydro dehalogenation adduct has been developed with isopropanol used as a solvent and also serve as a hydride source in basic medium at 90 °C with high selectivity. By this reagent combination, Iodide, bromide and chloride can be reduced without any ligand involving good to excellent yield. The reduction is companionable with numerous electron-withdrawing or electron-donating groups of natural products.



Scheme.1.40. Synthesis of β' -dehalogenated chalcone and α flavone product.

1.10. References

1. Thada, R.; Chockalingam, S.; Dhandapani, R. K.; Panchamoorthy, R. "Extraction and Quantitation of Coumarin from Cinnamon and its Effect on Enzymatic Browning in Fresh Apple Juice: A Bioinformatics Approach to Illuminate its Antibrowning Activity" *J. Agric. Food Chem.* **2013**, *61*, 5385–5390.
2. Khan, F. A.; Ahmad, S., Kodipelli, N.; Shivange, G.; Anindya, R. "Syntheses of a Library of Molecules on the Marine Natural Product Ianthelliformisamines

- Platform and Their Biological Evaluation” *Org. Biomol. Chem.* **2014**, *12*, 3847–3865.
3. Newman, D. J.; Cragg, G. M.; Snader, K. M. “Natural Products as Sources of New Drugs over the Period” *J. Nat. Prod.* **2003**, *66*, 1022–1037.
 4. Thakkar, K.; Cushman, M. “A Novel Oxidative Cyclization of 2-Hydroxychalcones to 4,5-Dialkoxyaurones by Thallium(III) Nitrate” *J. Org. Chem.* **1995**, *60*, 6499–6510.
 5. Seijas, J. A.; Vazquez-Tato, M. P.; Carballido-Reboredo, R. “Solvent-Free Synthesis of Functionalized Flavones under Microwave Irradiation” *J. Org. Chem.* **2005**, *70*, 2855–2858.
 6. Cushman, M.; Nagarathnam, D.; Burg, D. L.; Geahlen, R. L. “Synthesis and Protein-Tyrosine Kinase Inhibitory Activities of Flavonoid Analogues” *J. Med. Chem.* **1991**, *34*, 798–806.
 7. Brown, D. E.; Rashotte, A. M.; Murphy, A. S., Normanly, J.; Tague, B. W.; Peer, W. A.; Taiz, L., Muday, G. K. “Flavonoids act as negative regulators of auxin transport in vivo in Arabidopsis” *Plant Physiol.* **2001**, *126*, 524–535.
 8. Davies, K. M.; Albert, N. W.; Schwinn, K. E. “From landing lights to mimicry: The molecular regulation of flower colouration and mechanisms for pigmentation patterning. *Funct.*” *Plant Biol.* **2012**, *39*, 619–638.
 9. Agati, G.; Azzarello, E.; Pollastri, S; Tattini, M. “Flavonoids as antioxidants in plants: Location and functional significance” *Plant. Sci.* **2012**, *196*, 67–76.
 10. Gudapati, V.; Badrappa, N. S.; Venkateshappa, C.; Reddy, G. C. “Synthesis of (±) Abyssinone I and related compounds: Their anti-oxidant and cytotoxic activities” *Eur. J. Med. Chem.* **2009**, *44*, 2239–2245.
 11. Gudapati, V.; Badrappa, S., N.; Venkateshappa, C.; Reddy. C. G. “Synthesis of (±)Abyssinone I and related compounds: Their anti-oxidant and cytotoxic activities” *Eur. J. Med. Chem.* **2009**, *44*, 2239; (b) Middleton E. J. “Effect of plant flavonoids on immune and inflammatory cell function” *Adv Exp Med Biol.* **1998**, *439*, 175–182.
 12. Jiang, W.; Wei, H.; He, B. “Dietary flavonoids intake and the risk of coronary heart disease: A dose-response meta-analysis of 15 prospective studies” *Thromb. Res.* **2015**, *135*, 459–463.
 13. Ansari, M. M; Neha, H. A.; Khan, N. H. A. “Quercetin alleviate oxidative stress and inflammation through upregulation of antioxidant machinery and down-

- regulation of COX2 and NF- κ B expression in collagen induced rheumatoid arthritis” *Int. J. Drug Dev. Res.* **2014**, *6*, 215–232.
14. Paris, D.; Mathura, V.; Ait-Ghezala, G.; Beaulieu-Abdelahad, D.; Patel, N.; Bachmeier, C.; Mullan, M. “Flavonoids lower Alzheimer's $\alpha\beta$ production via an NF κ B dependent mechanism” *Bioinformation* **2011**, *6*, 229–236.
 15. B.; Orlikova, D.; Tasdemir, F.; Golais, M.; Dicato, M.; Died. “Dietary chalcones with chemopreventive and chemotherapeutic potential” *Genes & Nutrition* **2011**, *6*, 210.
 16. Pinheiro, P. F.; Justino, G. C. “Structural analysis of flavonoids and related compounds-A review of spectroscopic applications, phytochemicals-A global perspective of their role in nutrition and health, Dr. Venketeshwer Rao (Ed.)” 33–56.
 17. Viana, G. B. S.; Bandeira, M. A.; Matos, F. J. “Analgesic and anti-inflammatory effects of chalcones isolated from *Myracrodruon urundeuva* allemão” *Phytomedicine* **2003**, *10*, 189–195.
 18. Jung, D. Y.; Elli, M. L. “Inhibition of tumour invasion and angiogenesis by epigallocatechin gallate (EGCG), a major component of green tea” *Int. J. Clin Exp Pathol.* **2001**, *82*, 309–316.
 19. Vermeer, A. M.; Mulder, J. P. T.; Molhuizen, F. O. H. “Theaflavins from black tea, especially theaflavin-3-gallate, reduce the incorporation of cholesterol into mixed micelles” *J. Agric. Food Chem.* **2008**, *56*, 12031–12036.
 20. Patil, D. A.; Freyer, J. A.; Killmer, L.; Offen, P.; Taylor, B. P.; Votta, J. B.; Johnson K. R. “A New Dimeric Dihydrochalcone and a New Prenylated Flavone from the Bud Covers of *Artocarpus altilis*: Potent Inhibitors of Cathepsin K.” *J. Nat. Prod.* **2002**, *65*, 624–627.
 21. Bayon, Y.; Ortiz, A. M.; Lopez-Hernandez, J. F.; Gao, F.; Karin, M.; Pfahl, M.; Piedrafita, J. F. “Inhibition of IB Kinase by a New Class of Retinoid-Related Anticancer Agents That Induce Apoptosis” *Mol. Cell. Biol.* **2003**, *23*, 1061–1074.
 22. Poerwono, H.; Sasaki, S.; Hattori, Y.; Higashiyama, K. “Efficient microwave-assisted prenylation of pinostrobin and biological evaluation of its derivatives as antitumor agents” *Bioorg Med. Chem. Lett.* **2010**, *20*, 2086–2089.
 23. Chen, C. C.; Huang, Y.-L.; Ou, J.-C.; Lin, C.-F.; Pan, T. M. “A New Dimeric Dihydrochalcone and a New Prenylated Flavone from the Bud Covers of

- Artocarpus altilis: Potent Inhibitors of Cathepsin K” *J. Nat. Prod.* **1993**, *56*, 1594–1597.
24. Monteiro, R.; Azevedo, I.; Calhau, C. “Modulation of Aromatase Activity by Diet Polyphenolic Compounds” *J. Agric. Food Chem.* **2006**, *54*, 3535–3540.
25. Kellis, T. J.; Vickery, E. L. “Purification and characterization of human placental aromatase cytochrome P-450” *J. Biol. Chem.* **1987**, *262*, 4413–4420.
26. Kostanecki, S. V.; Tambor, J. “Ueber die sechs isomeren monooxybenzalacetophenone (Monooxychalkone)” *Chem. Ber.* **1899**, *32*, 1921–1926.
27. Schroder, J.; Raiber, S.; Berger, T.; Schmidt, A.; Schmidt, J.; Soares-Sello, M. A.; Bardshiri, E.; Strack, D.; Simpson, J. T.; Veit, M.; Schro, G. “Plant Polyketide Synthases: A Chalcone Synthase-Type Enzyme Which Performs a Condensation Reaction with Methylmalonyl-CoA in the Biosynthesis of C-Methylated Chalcones” *Biochemistry* **1998**, *37*, 8417–8425.
28. Wu, F. X.; Neumann, H.; Spannenberg, A.; Schulz, T.; Jiao, J. H.; Beller, M. “Development of a general palladium-catalyzed carbonylative Heck reaction of aryl halides” *J. Am. Chem. Soc.* **2010**, *132*, 14596–14602.
29. Selepe, A. M.; Heerden, V. R. F. “Application of the Suzuki-Miyaura reaction in the synthesis of flavonoids” *Molecules* **2013**, *18*, 4739–4765.
30. Moriyama, K.; Takemura, M.; Togo, H. “Selective Oxidation of Alcohols with Alkali Metal Bromides as Bromide Catalysts: Experimental Study of the Reaction Mechanism” *J. Org. Chem.* **2014**, *79*, 6094–6104.
31. Zhang, W. C.; Viswanathan, G. S.; Li, C. J. “Scandium triflate catalyzed in situ Prins-type cyclization: Formations of 4-tetrahydropyrans and ethers” *Chem. Commun.* **1999**, 291–292.
32. Bukhari, A. N. S.; Jasamai, M.; Jantan, I.; Ahmad, W. “Review of methods and various catalysts used for chalcone synthesis Mini Rev.” *Org. Chem.* **2013**, *10*, 73–83.
33. Schramm, G. O. “Multi-component Heterocycle Syntheses Based upon Sonogashira Coupling Isomerization” Ruprecht-Karls University, Heidelberg, Germany, 200.
34. Thiot, C.; Mioskowski, C.; Wagner, A. “Sequential Hiyama Coupling/Narasaka Acylation Reaction of (*E*)-1,2-Disilylethene: Rapid Assembly of α , β -Unsaturated Carbonyl Motifs” *Eur. J. Org. Chem.* **2009**, *19*, 3219–3227.

35. Lokhande D. P.; SakateKiran S. S.; Taksande N. K.; Navghare, B. "Dimethylsulfoxide-iodine catalysed deprotection of 2'-allyloxychalcones: synthesis of flavones" *Tetrahedron Lett.* **2005**, *46*, 1573–1574.
36. Tanaka, K.; Sugino, T. "Efficient conversion of 2'-hydroxychalcones into flavanones and flavanols in a water suspension medium" *Green Chem.* **2001**, *3*, 133–134.
37. Patel, A. K.; Patel, N. H.; Patel, M. A.; Brahmabhatt, D. I. "Synthesis of Some 3-(4-Aryl-benzofuro[3,2-*b*] pyridin-2-yl) coumarins and Their Antimicrobial Screening" *J. Heterocycl. Chem.* **2012**, *49*, 504–510.
38. Jyotsna, D. D.; Rao, S. V. A. "Reduction of 2'-Hydroxy Chalcones Under Phase Transfer Catalysis-A new Method for the Synthesis of Flavan-4-OLS" *Synth. Commun.* **2006**, *18*, 1009–1014.
39. Saxena, S.; Makrandi, J. K.; Grover, S. K. "A Facile One-Step Conversion of Chalcones into 2,3-Dihydroflavonols" *Synthesis* **1985**, 110–111.
40. Tanaka, K.; Sugino, T. "Efficient conversion of 2'-hydroxychalcones into flavanones and flavanols in a water suspension medium" *Green Chem.* **2001**, *3*, 133–134.
41. Albuquerquea, T. M. H.; Clementina-Santosa, M. M.; Cavaleiroa S. A. J.; Silva S. M. A. "Chalcones as Versatile Synthons for the Synthesis of 5 and 6-membered Nitrogen Heterocycles." *Curr. Org. Chem.* **2014**, *18*, 2750–2775.
42. Mihigo, O. S.; Mammo, W.; Bezabih, M.; Andrae-Marobela, K.; Abegaz, M. B. "Total synthesis, antiprotozoal and cytotoxicity activities of rhuschalcone VI and analogs" *Bioorganic Med. Chem.* **2010**, *18*, 2464–2473.
43. Schroder, J.; Raiber, S.; Berger, T.; Schmidt, A.; Schmidt, J.; Soares-Sello, M. A.; Bardshiri, E.; Strack, D.; Simpson, J. T.; Veit, M.; Schro, G. "Plant Polyketide Synthases: A Chalcone Synthase-Type Enzyme Which Performs a Condensation Reaction with Methylmalonyl-CoA in the Biosynthesis of C-Methylated Chalcones" *Biochemistry* **1998**, *37*, 8417–8425.
44. Mahapatra, K. D.; Asati, V.; Bharti, K. S. "Chalcones and their role in management of diabetes mellitus: structural and pharmacological perspectives" *Eur. J. Med. Chem.* **2015**, *92*, 839–865.
45. Bukhari A. N. S.; Butt, M. A.; Amjad, B. W. M.; Ahmad, A.; Shah, H. V.; Trivedi, R. A. "Synthesis and evaluation of chalcone based pyrimidines as angiotensin converting enzyme inhibitors" *Pak. J. Pharm. Sci.* **2013**, *21*, 1368–1372.
46. Kim, W. D.; Curtis-Long, J. M.; Yuk, J. H.; Wang, Y.; Song, H. Y.; Jeong, H. S.; Park, H. K. "Quantitative analysis of phenolic metabolites from different parts of

- Angelica keiskei by HPLC-ESI MS/MS and their xanthine oxidase inhibition” *Food Chem.* **2014**, *153*, 20–27.
47. Kantevari, S.; Addla, D.; Bagul, K. P.; Sridhar, B.; Banerjee, K. S. “Synthesis and evaluation of novel 2-butyl-4-chloro-1-methylimidazole embedded chalcones and pyrazoles as angiotensin converting enzyme (ACE) inhibitors” *Bioorg. Med. Chem.* **2011**, *19*, 4772–4781.
48. Yamamoto, T.; Yoshimura, M.; Yamaguchi, F.; Kouchi, T.; Tsuji, R.; Saito, M.; Obata, A.; Kikuchi, M. “Anti-allergic activity of naringenin chalcone from a tomato skin extract” *Biosci. Biotechnol. Biochem.* **2004**, *68*, 1706–1711.
49. Israf, A. D.; Khaizurin, A. T.; Syahida, A.; Lajis, H. N.; Khozirah, S. “Cardamonin inhibits COX and iNOS expression via inhibition of p65NF-kB nuclear translocation and Ik-B phosphorylation in RAW 264.7 macrophage cells” *Mol. Immunol.* **2007**, *44*, 673–679.
50. Birari, B. R.; Gupta, S.; Mohan, G. C.; Bhutani, K. K. “Antiobesity and lipid lowering effects of glycyrrhizachalcones: experimental and computational studies” *Phytomedicine* **2011**, *18*, 795–801.
51. Aoki, N.; Muko, M.; Ohta, E.; Ohta, S. “C-Geranylated chalcones from the stems of *Angelica keiskei* with superoxide-scavenging activity” *J. Nat. Prod.* **2008**, *71*, 1308–1310.
52. Salum, B. L.; Altei, F. W.; Chiaradia, D. L.; Cordeiro, S. N. M.; Canevarolo, R. R.; Melo, S. P. C.; Winter, E.; Mattei, B.; Daghestani, N. H.; Santos-Silva, C. M.; Creczynski-Pasa, B. T.; Yunes, A. R.; Yunes, A. J.; Andricopulo, D. A.; Day, W. B.; Nunes, J. R.; Vogt, A. “Cytotoxic 3, 4, 5-trimethoxychalcones as mitotic arresters and cell migration inhibitors” *Eur. J. Med. Chem.* **2013**, *63*, 501–510.
53. Zhao, L.; Jin, H.; Sun, L.; Piao, H.; Quan, Z. “Synthesis and evaluation of antiplatelet activity of trihydroxychalcone derivatives” *Bioorg. Med. Chem. Lett.* **2005**, *15*, 5027–5029.
54. Luo, Y.; Song, R.; Li, Y.; Zhang, S.; Liu, J. Z.; Fu, J.; Zhu, L. H. “Design, synthesis, and biological evaluation of chalcone oxime derivatives as potential immunosuppressive agents” *Bioorg. Med. Chem. Lett.* **2012**, *22*, 3039–3043.
55. Lahtchev, V. K.; Batovska, I. D.; Parushev, P. S.; Ubiyvovk, M. V.; Sibirny, A. A. “Antifungal activities of chalcones: a mechanistic study using various yeast strains” *Eur. J. Med. Chem.* **2008**, *43*, 2220–2228.

56. Yarishkin, V. O.; Ryu, W. H.; Park, J.; Yang, S. M.; Hong, S.; Park, H. K. "Sulfonate chalcone as new class voltage-dependent K_p channel blocker" *Bioorg. Med. Chem. Lett.* **2008**, *18*, 137–140.
57. Jamal, H.; Ansari, H. W.; Rizvi, J. S. "Evaluation of chalcones-a flavonoid subclass, for their anxiolytic effects in rats using elevated plus maze and open field behaviour tests" *Fundam. Clin. Pharmacol.* **2008**, *22*, 673–681.
58. Zhai, L.; Chen, M.; Blom, J.; Theander, G. T.; Christensen, B. S.; Kharazmi, A. "The antileishmanial activity of oxygenated chalcones and their mechanism of action" *J. Antimicrob. Chemother.* **1999**, *43*, 793–803.
59. Sato, Y.; He, X. J.; Nagai, H.; Tani, T.; Akao, T. "Isoliquiritigenin, one of the antispasmodic principles of Glycyrrhiza ularensis roots, acts in the lower part of intestine" *Biol. Pharm. Bull.* **2007**, *30*, 145–149.
60. Cho, S.; Kim, S.; Jin, Z.; Yang, H.; Han, D.; Baek, I. N.; Jo, J.; Cho, W. C.; Park, H. J.; Shimizu, M.; Jin, H. Y. "Isoliquiritigenin, a chalcone compound, is a positive allosteric modulator of GABAA receptors and shows hypnotic effects" *Biochem. Biophys. Res. Commun.* **2011**, *413*, 637–642.
61. Tomar, V.; Bhattacharjee, G.; Kamaluddin, Rajakumar, S.; Srivastava, K.; Puri, K. S. "Synthesis of new chalcone derivatives containing acridinyl moiety with potential antimalarial activity" *Eur. J. Med. Chem.* **2010**, *45*, 745–751.
62. Campos-Buzzi, D. F.; Padaratz, P.; Meira, V. A.; Correa, R.; Nunes, J. R.; Cechinel-Filho, V. "40-Acetamidochalcone derivatives as potential antinociceptive agents" *Molecules* **2007**, *12*, 896–906.
63. Mascarello, A.; Chiaradia, D. L.; Vernal, J.; Villarino, A.; Guido, V. R.; Perizzolo, P.; Poirier, V.; Wong, D.; Martins, G. P.; Nunes, J. R.; Yunes, A. R.; Andricopulo, D. A.; Av-Gay, Y.; Terenzi, H. "Inhibition of Mycobacterium tuberculosis tyrosine phosphatase PtpA by synthetic chalcones: kinetics, molecular modeling, toxicity and effect on growth" *Bioorg. Med. Chem.* **2010**, *18*, 3783–3789.
64. Sashidhara, V. K.; Palnati, R. G.; Sonkar, R.; Avula, R. S.; Awasthi, C.; Bhatia, G. "Coumarin chalcone fibrates: a new structural class of lipid lowering agents" *Eur. J. Med. Chem.* **2013**, *64*, 422–431.
65. Jantan, I.; Bukhari, A. N. S.; Adekoya, A. O.; Sylte, I. "Studies of synthetic chalcone derivatives as potential inhibitors of secretory phospholipase A₂, cyclooxygenases, lipoxygenase and pro-inflammatory cytokine" *Drug Des Devel Ther.* **2014**, *8*, 1405–1418.

66. Boveris, A.; Hertig, M. C.; Turrens, F. J. "Fumarate reductase and other mitochondrial activities in *Trypanosoma cruzi*" *Mol. Biochem. Parasitol.* **1986**, *19*, 163–169.
67. Kumar, K. S.; Hager, E.; Pettit, C.; Gurulingappa, H.; Davidson, E. N.; Khan, R. S. "Design, Synthesis, and Evaluation of Novel Boronic-Chalcone Derivatives as Antitumor Agents" *J. Med. Chem.* **2003**, *46*, 2813–2815.
68. Domínguez N. J.; León, C.; Rodrigues, J.; Gamboa N.; Domínguez, d.; Gut. J.; Rosenthal, J. P. "Synthesis and Evaluation of New Antimalarial Phenylurenyl Chalcone Derivatives" *J. Med. Chem.* **2005**, *48*, 3654–3658.
69. Singh, P.; Raj R.; Kumar V.; Mahajan P. M.; Bedi S. M. P.; Kaur, T.; axena, K. A. "1,2,3-Triazole tethered β -lactam-Chalcone bifunctional hybrids: Synthesis and anticancer evaluation" *Eur. J. Med. Chem.* **2012**, *47*, 594–600.
70. Ratković. Z.; Juranić, D. Z.; Stanojković, T.; Manojlović, D.; Vukićević, D. R.; Radulović, N.; Joksović, D. M. "Synthesis, characterization, electrochemical studies and antitumor activity of some new chalcone analogues containing ferrocenyl pyrazole moiety" *Bioorg. Chem.* **2010**, *38*, 26–32.
71. Sashidhara, V. K.; Ram, K. M.; Modukuri, K.; Sonkar, R.; Bhatia, G.; Khanna, K. A.; Rai, S.; Shukla, R. "Synthesis and anti-inflammatory activity of novel biscoumarin-chalcone hybrids" *Bioorg. Med. Chem Lett.* **2011**, *21*, 4480–4484.
72. Sashidhara, V. K.; Kumar, A.; Kumar, M.; Sarkar, J.; Sinha, S. "Synthesis and *in vitro* evaluation of novel coumarin-chalcone hybrids as potential anticancer agents" *Bioorg. Med. Chem Lett.* **2010**, *20*, 7205–7211.
73. Kolundžija, B.; Marković, V.; Stanojković, T.; Joksović, L.; Matić, I.; Todorović, N.; Nikolić, M.; Joksović D. M. "Novel anthraquinone based chalcone analogues containing an imine fragment: Synthesis, cytotoxicity and anti-angiogenic activity" *Bioorg. Med. Chem Lett.* **2014**, *24*, 65–71.
74. Yadav, N.; Dixit, K. S.; Bhattacharya, A.; Mishra, C. L.; Sharma, M.; Awasthi, K. S.; Bhasin, K. V. "Antimalarial Activity of Newly Synthesized Chalcone Derivatives *In Vitro*" *Chem. Biol. Drug Des.* **2012**, *80*, 340–347.
75. Guantai, M. E.; Ncokazi, K.; Egan, J. T.; Gut, J.; Rosenthal, J. P.; Bhampidipati, R.; Kopinathan, A.; Smith, J. P.; Chibale, K. "Enone and Chalcone Chloroquinoline Hybrid Analogues: In Silico Guided Design, Synthesis, Antiplasmodial Activity, in *Vitro* Metabolism, and Mechanistic Studies" *J. Med. Chem.* **2011**, *54*, 3637–3649.

76. Liaras, K.; Geronikaki, A.; Glamočlija, J.; Ćirić, A.; Soković, M. "Thiazole-based chalcones as potent antimicrobial agents. Synthesis and biological evaluation" *Bioorg. Med. Chem Lett.* **2011**, *19*, 3135–3140.
77. (a) Tadigoppula, N.; Korthikunta, V.; Gupta, S.; Kancharla, P.; Khaliq, T.; Soni, A.; Srivastava, R. K.; Srivastava, K.; Puri, S. K.; Raju, K. S. R.; Wahajuddin, Sijwali, P. S.; Kumar, V.; Mohammad, I. S. "Synthesis and insight into the structure-activity relationships of chalcones as antimalarial agents" *J. Med. Chem.* **2013**, *56*, 31-45. (b) Jung, E. M.; Lee, Y. R. "First total synthesis of prorepensin with a bis-geranylated chalcone" *Bull. Korean Chem. Soc.* **2009**, *30*, 2563–2566.
78. Ferreyra, F. L. M.; Rius, P. S.; Casati P. "Flavonoids: biosynthesis, biological functions, and biotechnological applications" *Front Plant Sci.* **2012**, *3*, 1–14.
79. Dao, T. T.; Chi, Y. S.; Kim, J.; Kim, H. P.; Kim, S.; Park, H. "Synthesis and inhibitory activity against COX-2 catalysed prostaglandin production of chrysin derivatives" *Bioorg. Med. Chem. Lett.* **2004**, *14*, 1165–1167.
80. Malik, S. B.; Sharma, P.; Seshadri, T. R. "Furanoflavonoids from the leaves of *Pongamia glabra*" *Indian J. Chem. Sect. B.* **1977**, *15B*, 536–538.
81. Joshi, A. J.; Gadhwal, M. K.; Joshi, U. J.; Dmello, P.; Sinha, R.; Govil, G. "Synthesis of B-ring substituted flavones and evaluation of their antitumor and antioxidant activities" *Med. Chem. Res.* **2013**, *22*, 4293–4299.
82. Pal, M.; Subramanian, V.; Parasuraman, K.; Yeleswarapu, K. R. "Palladium catalyzed reaction in aqueous DMF: synthesis of 3-alkynyl substituted flavones in the presence of prolinol" *Tetrahedron* **2003**, *59*, 9563–9570.
83. Bird, T. G. C.; Brown, B. R.; Stuart, I. A.; Tyrrell, A. W. R. "Reactions of flav-2-enes and flav-2-en-4-ones (flavones)" *J. Chem. Soc. Perkin Trans. 1* **1983**, 1831–1846.
84. Detty, M. R.; McGarry, L. W. "Direct lithiation of chalcogen chromones, -flavones, and pyranones. The interconversion and electrophilic capture of ring-opened and ring-closed anions" *J. Org. Chem.* **1988**, *53*, 1203–1207.
85. Patoilo, D. T.; Silva, A. M. S.; Cavaleiro, J. A. S. "Regioselective 3-nitration of flavones: A new synthesis of 3-nitro- and 3-aminoflavones" *Synlett* **2010**, 1381–1385.
86. Rho, H. S.; Ko, B. S.; Ju, Y. S. "A facile preparation of 3-halo flavones using hypervalent iodine chemistry" *Synth. Commun.* **2001**, *31*, 2101–2106.

87. Moriarty, R. M.; Prakash, O. "Oxidation of carbonyl compounds with organo hypervalent iodine reagents" *Organic Reactions* **1999**, *54*, 273–418
88. Khurana, J. M.; Sharma, P. "Chemoselective reduction of α , β -unsaturated aldehydes, ketones, carboxylic acids, and esters with nickel boride in methanol-water" *Bull. Chem. Soc. Jpn.* **2004**, *77*, 549–552.
89. Adam, W.; Golsch, D.; Hadjiarapoglou, L.; Patonay, T. "Epoxidation of flavones by dimethyldioxirane" *J. Org. Chem.* **1991**, *56*, 7292–7297.
90. Choi, R. C. Y.; Zhu, J. T. T.; Yung, A. W. Y.; Lee, P. S. C.; Xu, S. L.; Guo, A. J. Y.; Zhu, K. Y.; Dong, T. T. X.; Tsim, K. W. K. "Synergistic action of flavonoids, baicalein, and daidzein in estrogenic and neuroprotective effects: A development of potential health products and therapeutic drugs against alzheimer's disease" *Evid. Based Complement. Alternat. Med.* **2013**, Article ID 635694, [http:// dx.doi. org/ 10 .1155/2013/635694](http://dx.doi.org/10.1155/2013/635694).
91. Auffret, G.; Labaied, M.; Frappier, F.; Rasoanaivo, P.; Grellier, P.; Lewin G. "Synthesis and antimalarial evaluation of a series of piperazinyl flavones" *Bioorg. Med. Chem. Lett.* **2007**, *17*, 959–963.
92. Verma, K. A.; Singh, H.; Satyanarayana, M.; Srivastava, P. S.; Tiwari, P.; Singh, B. A.; Dwivedi, K. A.; Singh, K. S.; Srivastava, M.; Nath, C.; Raghbir, R.; Srivastava, K. A.; Pratap, R. "Flavone-Based Novel Antidiabetic and Antidyslipidemic Agents" *J. Med. Chem.* **2012**, *55*, 4551–4567.
93. Bozdağ-Dündar, O.; Verspohl, J. E.; Daş-Evcimen, N.; Kaup, M. R.; Bauer, K.; Sarıkaya, M.; Evranos, B.; Ertan R. "Synthesis and biological activity of some new flavonyl-2,4-thiazolidinediones" *Bioorg. Med. Chem Lett.* **2008**, *16*, 6747–6751.
94. Pathe, K. G.; Konduru, K. N.; Parveen, I.; Ahmed, N. "Anti-proliferative activities of flavone-estradiol Stille-coupling adducts and of indanone-based compounds obtained by SnCl₄/Zn-catalysed McMurry cross-coupling reactions" *RSC Adv.* **2015**, *5*, 83512–83521.
95. Ahmed, N.; Konduru K. N.; Ahmad S.; Owais M. "Design, synthesis and antiproliferative activity of functionalized flavone-triazole-tetrahydropyran conjugates against human cancer cell lines" *Eur. J. Med. Chem.* **2014**, *82*, 552–564.
96. Liu, X.; Chan, C-B.; Qi, Q.; Xiao, G.; Luo, R. H.; He, X.; Ye, K. "Optimization of a Small Tropomyosin-Related Kinase B (TrkB) Agonist 7,8- Dihydroxyflavone Active in Mouse Models of Depression" *J. Med. Chem.* **2012**, *55*, 8524–8537.

97. Kattige, S. L.; Naik, R. G.; Dohadwalla, A. N.; Rupp, R. H.; de-Souza, N. J. U.S. Patent 4, 727, 1990. 900.
98. Minassi, A.; Giana, A.; Ech-Chahad, A.; Appendino, G. "A Regiodivergent Synthesis of Ring A C-Prenylflavones" *Org. Lett.* **2008**, *10*, 2267–2270.
99. Ndoile, M. M.; Heerden, V. R. F. "Total synthesis of ochnaflavone" *Beilstein J. Org. Chem.* **2013**, *9*, 1346–1351.
100. Thapa, A.; Woo, E.-R.; Chi, E. Y.; Sharoar, Md. G.; Jin, H-G.; Shin, S. Y.; Park, I-S. "Biflavonoids Are Superior to Monoflavonoids in Inhibiting Amyloid- β Toxicity and Fibrillogenesis via Accumulation of Nontoxic Oligomer-like Structures" *Biochemistry* **2011**, *50*, 2445–2455.
101. Zheng, X.; Meng, W.; Qing, F. "Synthesis of gem-difluoromethylenated biflavonoid via the Suzuki coupling reaction" *Tetrahedron Lett.* **2004**, *45*, 8083–8085.
102. Vega, M. R. G.; Souza, A. E.; Vieira, I. J. C.; Mathias, L.; Filho, R. B.; Echevarria, A. "Flavonoids from *Annona dioica* leaves and their effects in Ehrlich carcinoma cells, DNA topoisomerase I and II" *J. Braz. Chem. Soc.* **2007**, *18*, 1554–1559.
103. Ferreyra, F. L. M.; Rius, P. S.; Casati P. "Flavonoids: biosynthesis, biological functions, and biotechnological applications" *Front Plant Sci.* **2012**, *3*, 1–14.
104. Li, J. J. "Auwers flavone synthesis" *Name Reactions in Heter. Chem.* **2005**, *53*, 262–265.
105. Wagner, H.; Farkas, L.; Harborne, J. B.; Mabry, T. J.; Mabry, H. "In the Flavonoids" Eds.; Academic Press: New York, **1975**, 127.
106. Kostanecki, S.; Lampe, V. "Synthese des 2-Oxyflavonols" *Ber.* **1904**, *37*, 773–778.
107. Tanaka, H.; Stohlmeyer, M. M.; Wandless, J. T.; Taylor, P. L. "Synthesis of flavonol derivatives as probes of biological processes" *Tetrahedron Lett.* **2000**, *41*, 9735–9739.
108. Atsushiz, T.; Hirosato, T.; Hideyoshi M.; Mitsuru S. "Synthesis of 3-Aminoflavones from 3-Hydroxyflavones via 3-Tosyloxy- or 3-Mesyloxyflavones" *Chem. Lett.* **2006**, *35*, 128–129.
109. Dziuba, D.; Benhida, R.; Burger, A. "A mild and efficient protocol for the protection of 3-hydroxychromones under phase-transfer catalysis" *Synthesis* **2011**, 2159–2164.

110. Jayashree, B. S.; Thejaswini, J. C.; Nayak, Y.; Kumar, D. V. "Synthesis of novel flavone acyl esters and correlation of log P value with antioxidant and antimicrobial activity" *Asian J. Chem.* **2010**, *22*, 1055–1066.
111. Sesso, H. D.; Gaziano, J. M.; Liu, S.; Buring, J. E. "Flavonoid intake and the risk of cardiovascular disease in women" *Am. J. Clin. Nutr.* **2003**, *77*, 1400–1408.
112. Nakayama, T.; Sato, T.; Fukui, Y.; Yonekura-Sakakibara, K.; Hayashi, H.; Tanaka, Y.; Kusumi, T.; Nishino, T. "Specificity analysis and mechanism of aurone synthesis catalyzed by aureusdin synthase a polyphenol oxidase homolog responsible for flower coloration" *FEBS Letters* **2001**, *499*, 107–111.
113. Nakayama, T. "Enzymology of aurone biosynthesis" *J. Biosci. Bioeng.* **2002**, *94*, 487–491.
114. Narsinghani, T.; Sharma, C. M.; Bhargav, S. "Synthesis, Docking studies and antioxidant activity of some chalcone and aurone derivatives" *Med Chem Res.* **2013**, *22*, 4059–4068.
115. Harkat, H.; Blanc, A.; Weibel, J.-M.; Pale, P. "Versatile and Expedient Synthesis of Aurones via AuI-Catalyzed Cyclization" *J. Org. Chem.* **2008**, *73*, 1620–1623.
116. Weng, Y.; Chen, Q.; Su, W. "Copper-Catalyzed Intramolecular Tandem Reaction of (2-Halogenphenyl)(3-phenyloxiran-2-yl)methanones: Synthesis of (Z)-Aurones" *J. Org. Chem.* **2014**, *79*, 4218–4224.
117. Qi, X.; Li R.; Wu X.-F. "Selective palladium-catalyzed carbonylative synthesis of aurones with formic acid as the CO source" *RSC Adv.* **2016**, *6*, 62810–62813.
118. Sousa, M. C.; Berthet, J.; Delbaere, S.; Coelho, J. P. "One pot synthesis of aryl substituted aurones" *Dyes pigm.* **2011**, *21*, 4520–4523.
119. Saito, K.; Yoshida, M.; Doi, T. "An Efficient Synthesis of Aurone Derivatives by the Tributylphosphine-catalyzed Regioselective Cyclization of *o*-Alkynoylphenols" *Chem. Lett.* **2015**, *44*, 141–143.
120. Zhao, X.; Liu, J.; Xie, Z; Li, Y. "A One Pot Synthesis of Aurones from Substituted Acetophenones and Benzaldehydes: A Concise Synthesis of Aureusidine" *Synthesis* **2012**, *44*, 2217–2224.
121. Schoepfer, J.; Fretz, H.; Chaudhuri, B.; Muller, L.; Seeber, E.; Meijer, L.; Lozach, O.; Vangrevelinghe, E.; Furet P. "Structure-Based Design and Synthesis of 2-Benzylidene-benzofuran-3-ones as Flavopiridol Mimics" *J. Med. Chem.* **2002**, *45*, 1741–1747.

122. Westenburg, E. H.; Lee, K.-J.; Lee, K. S.; Fong, S. H. H.; Breemen, V. B. R.; Pezzuto, M. J.; Kinghorn, D. A. "Activity-Guided Isolation of Antioxidative Constituents of *Cotinus coggygia*" *J. Nat. Prod.* **2000**, *63*, 1696–1698.
123. Morimoto, M.; Fukumoto, H.; Nozoe, T.; Hagiwara, A.; Komai K. "Synthesis and Insect Antifeedant Activity of Aurones against *Spodoptera litura* Larvae" *J. Agric. Food Chem.* **2007**, *55*, 700–705.
124. Hu, Q.; Meng, Y.; Yao, J.; Qin, Y.; Yang, Z.; Zhao, G.; Yang, Z.; Gao, X.; Li, T. "Flavonoids from *Garcinia paucinervis* and their biological activities" *Chem. Nat. Compd.* **2014**, *50*, 994–997.
125. Mai, T. T. N.; Hai, X. N.; Phan, H. D.; Trong, P. N. H.; Nhan, N. T. "Three new geranyl aurones from the leaves of *Artocarpus altilis*" *Phytochem Lett.* **2012**, *5*, 647–650.
126. Huong, T. T.; Cuong, X. N.; Tram, H. L.; Quang, T. T.; Duong, V. L.; Nam, H. N.; Dat, T. N.; Huong, T. T. P.; Diep, N. C.; Kiem, V. P.; Minh, V. C. "A new prenylated aurone from *Artocarpus altilis*" *J Asian Nat Prod Res.* **2012**, 923–928.
127. Chu, W.L.A.; Jensen, F.R.; Jensen, T.B.; Sokilde, B.; Santana-Sorenson, A. M.; McAlpine, J. PCT Int. Appl. WO 9904789 A11990204,2002. (b). Chu, W. L.A.; Jensen, F.R.; Jensen, T.B.; McAlpine, J. B.; Sokilde, B.; Santana-Surensen, A. M. Patent, U.S. US 6307070.2001.
128. Venkateswarlu, S.; Panchagnula, K. G.; Subbaraju V. G. "Synthesis and Antioxidative Activity of 3',4',6,7-Tetrahydroxyaurone, a Metabolite of *Bidens frondosa*" *Biosci. Biotechnol. Biochem.* **2004**, *68*, 2183–2185.
129. Okombi, S.; Rival, D.; Bonnet, S.; Mariotte, A.-M.; Perrier, E.; Boumendjel, A. "Discovery of Benzylidenebenzofuran-3(2H)-one (Aurones) as Inhibitors of Tyrosinase derived from Human Melanocytes" *J. Med. Chem.* **2006**, *49*, 329–333.
130. Zwergel, C.; Valente, S.; Salvato, A.; Xu, Z.; Talhi, O.; Mai, A.; Silva, A.; Altuccic, L.; Kirsch, G. "Novel benzofuran chromone and coumarin derivatives: synthesis and biological activity in K562 human leukemia cells" *Med. Chem. Commun.* **2013**, *4*, 1571–1579.
131. Tiwari, N. K.; Monserrat, J-P.; Hequet, A.; Ganem-Elbaz, C.; Cresteil, T.; Jaouen, G.; Vessières, A.; Hillard, A. E.; Jolival, C. "In vitro inhibitory properties of ferrocene-substituted chalcones and aurones on bacterial and human cell cultures" *Dalton Trans.* **2012**, *41*, 6451–6457.

132. Roll, D. M.; Scheuer, P. J.; Matsumoto, G. K.; Claedy, J. "Halenaquinone, a Pentacyclic Polyketide from a Marine Sponge" *J. Am. Chem. Soc.* **1983**, *105*, 6177–6178. (b) Schmits, F. J.; Bloor, S. "Xesto- and Halenaquinone Derivatives from a Sponge, *Adocia* sp., from Truk Lagoon" *J. Org. Chem.* **1988**, *53*, 3922–3925.
133. Yao, T.; Yue, D.; Larock, C. R.; "An Efficient Synthesis of Coumestrol and Coumestans by Iodocyclization and Pd-Catalyzed Intramolecular Lactonization" *J. Org. Chem.* **2005**, *70*, 9985–9989.
134. Zheng, S. Y.; Shen, Z. W. "Total synthesis of hirtellanine A." *Tetrahedron Lett.* **2010**, *51*, 2883–2887.
135. Selepe, M. A.; Drewes, S. E.; Heerden, v. F. R. "Total synthesis of the pyranocoumaronochromone lupinalbin H." *Tetrahedron* **2011**, *67*, 8654–8658.
136. Oliveira, G. A. M. A.; Raposo, M. M. M.; Oliveira-Campos, F. M. A.; Machado, H. E. A.; Puapairoj, P.; Pedro, M.; Nascimento, J. S. M.; Portela, C.; Afonso, C.; Pinto, M. "Psoralen analogues: synthesis, inhibitory activity of growth of human tumor cell lines and computational studies" *Eur. J. Med. Chem.* **2006**, *41*, 367–372.
137. Shchekotikhin, E. A.; Dezhenkova, G. L.; Tsvetkov, B. V.; Luzikov, N. Y.; Volodina, L. Y.; Tatarskiy, V. V.; Kalinina, A. A.; Treshalin, I. M.; Treshalina, M. H.; Romanenko, I. V.; Kaluzhny, N. D.; Kubbutat, M.; Schols, D.; Pommier, Y.; Shtil, A. A.; Preobrazhenskaya, N. M. "Discovery of antitumor anthra[2,3-b]furan-3-carboxamides: Optimization of synthesis and evaluation of antitumor properties" *Eur. J. Med. Chem.* **2016**, *112*, 114–129.
138. Shchekotikhina, E. A.; Glazunovab, A. V.; Dezhenkovaa, G. L.; Shevtsovac, K. E.; Traven'c, F. V.; Balzarinid, J.; Huang, H.-S.; Shtilb, A. A.; Preobrazhenskayaa, N. M. "The first series of 4,11-bis[(2-aminoethyl)amino]anthra[2,3-b]furan-5,10-diones: Synthesis and anti-proliferative characteristics" *Eur. J. Med. Chem.* **2011**, *46*, 423–428.
139. Matsuya, Y.; Sasaki, K.; Nagaoka, M.; Kakuda, H.; Toyooka, N.; Imanishi, N.; Ochiai, H.; Nemoto H. "Synthesis of a New Class of Furan-Fused Tetracyclic Compounds Using o-Quinodimethane Chemistry and Investigation of Their Antiviral Activity" *J. Org. Chem.* **2004**, *69*, 7989–7993.
140. Govindachari, T. R.; Nagurajan, K.; Pai, B. R. "Chemical examination of *Wedelia calendulacea*. Part I. Structure of wedelolactone" *J. Chem. Soc.* **1956**, 629–632. (b).

- Li, C. C.; Xie, X. Z.; Zhang, D. Y.; Chen, H. J.; Yang Z. "Total Synthesis of Wedelolactone" *J. Org. Chem.* **2003**, *68*, 8500–8504.
141. Patil, A. S.; Wang, J.; Li, S. X.; Chen J.; Jones, S. T.; Hosni-Ahmed, A.; Patil, R.; Seibel, L. W.; Li, W.; Miller, D. D. "New substituted 4*H*-chromenes as anticancer agents" *Bioorg Med Chem Lett*, **2012**, *22*, 4458–4461.
142. Kemnitzer, W.; Drewe, J.; Jiang, S.; Zhang, H.; Crogan-Grundy, C.; Labreque, D.; Bubenick, M.; Attardo, G.; Denis, R.; Lamothe, S.; Gourdeau, H.; Tseng, B.; Kasibhatla, S.; Cai, X. S. "Discovery of 4-Aryl-4*H*-chromenes as a New Series of Apoptosis Inducers Using a Cell and Caspase-Based High Throughput Screening Assay. Structure–Activity Relationships of *N*-Alkyl Substituted Pyrrole Fused at the 7,8-Positions" *J. Med. Chem.* **2008**, *51*, 417–423.
143. Mahmoodi, M.; Aliabadi, A.; Emami, S.; Safavi, M.; Rajabalian, S.; Mohagheghi, A. M.; Khoshzaban, A.; Samzadeh-Kermani, A.; Lamei, N.; Shafiee, A.; Foroumadi, A. "Synthesis and *in-vitro* Cytotoxicity of Poly-functionalized 4-(2-Arylthiazol-4-yl)-4*H*-chromenes" *Arch. Pharm. Chem. Life Sci.* **2010**, *343*, 411–416.
144. Al-Masoudi, A. N.; Mohammed, H. H.; Hamdy, M. A.; Akrawi, A. O.; Eleyab, N.; Spannenbergd, A.; Pannecouquee, C.; Langer, P. "Synthesis and anti-HIV Activity of New Fused Chromene Derivatives Derived from 2-Amino-4-(1-naphthyl)-5-oxo-4*H*,5*H*-pyrano[3,2-*c*]chromene-3-carbonitrile" *Z. Naturforsch.* **2013**, *68b*, 229–238.
145. Joshi, V. P.; Sayed, A. A.; Kumar, R. A.; Puranik, G. V.; Zinjarde, S. S. "4-Phenyl quinoline derivatives as potential serotonin receptor ligands with antiproliferative activity" *Eur. J. Med. Chem.* **2017**, *136*, 246–258.
146. Doggrell, A. S. "BMS-354825: a novel drug with potential for the treatment of imatinib-resistant chronic myeloid leukaemia" *Expert Opin Investig Drugs* **2005**, *14*, 89–91.
147. Klein, U. "Experiments, models, paper tools: Cultures of organic chemistry in the nineteenth century" *Stanford university press: California* **2003**, 191-193.
148. Castro, E. C. "Environmental Dehalogenation: Chemistry and Mechanism" *Rev. Environ. Contam. Toxicol.* **1998**, *155*, 1–67.
149. Moon, J.; Lee, S. "Palladium catalyzed-dehalogenation of aryl chlorides and bromides using phosphite ligands" *J. Organomet. Chem.* **2009**, *649*, 473–477.

150. Chelucci, G.; Baldino, S.; Ruiu A. “Room-Temperature Hydrodehalogenation of Halogenated Heteropentalenes with One or Two Heteroatoms” *J. Org. Chem.* **2012**, *77*, 9921–9925.
151. Ramanathan, A.; Jimenez, S. L. “Reductive Dehalogenation of Aryl Bromides and Chlorides and Their Use as Aryl Blocking Groups” *Synthesis* **2009**, 217–220.
152. Czaplik, W. M.; Grupe, S.; Mayer, M.; Wangelin, v. A. J. “Practical iron-catalyzed dehalogenation of aryl halides” *Chem. Commun.* **2010**, *46*, 6350-6352.
153. Yu, T.; Wang, Z.; Chen, J.; Xia Y. “Transfer Hydro-dehalogenation of Organic Halides Catalyzed by Ruthenium(II) Complex” *J. Org. Chem.* **2017**, *82*, 1340–1346.





Chapter-2

Route to Highly Functionalized stereospecific-Aminated Aurones from 3-bromo flavones with aniline and N-phenyl urea via a Domino- Aza Michael- ring opening-cyclization reaction

Synthesis **2018**, 50, A–K



Chapter-2

Route to Highly Functionalized stereospecific-Aminated Aurones from 3-bromo flavones with aniline and N-phenyl urea via a Domino- Aza Michael- ring opening-cyclization reaction

Synthesis **2018**, 50, A–K



Chapter-3

*CuI mediated synthesis of heterocyclic flavone-
benzofuran fused derivatives*

Tetrahedron Lett. **2017**, 58, 2302–2305

3.1. Introduction

Ullmann coupling reaction is one of the most significant tools for the carbon-carbon, carbon-oxygen, carbon-sulphur, carbon-selenium carbon-phosphorus and carbon-nitrogen bond formation in the synthesis of diverse heterocyclic compounds and natural products of biological importance [1]. Another application that is it used in organic synthesis, various industrial applications, bioactive heterocyclic compounds, organic semiconductor materials, natural products, alkaloids, drug like molecules, chiral auxiliaries and polymer chemistry etc. [2]. A classical Ullmann coupling reaction, however, suffers from several limitations such as high reaction temperature (125–220 °C), long reaction time, use of stoichiometric or greater quantities of the copper-complex, poor functional group tolerance, the little amount of the products only and less applications of Ullmann coupling products [3]. Recently, several reaction conditions have been developed for Ullmann coupling reactions for giving better yields using chelating ligands such as 8-Hydroxyquinoline [4], amino acids such as L-proline [5], *N,N*-dimethylglycine [6] and L-tyrosine [7], phenanthroline [8], 1,2 diamine [9], triphenylphosphine [10], 2,2,6,6-tetramethylheptane-3,5-dione [11], phosphazene P₄-t-Bu base [12], β-diketone [13], neocuproine [14], monodendate and bidentate ligands [15], β-ketoester [16], picolinic acid [17], aminophenols [18], DMPAO [19], diimine ligands [20], pivalic acid [21], salicylamides [22] to enhance the solubility of copper salts.

Oxygen-containing five membered heterocycles are important synthetic intermediates in an assorted range of naturally occurring and pharmacologically active molecules [23].

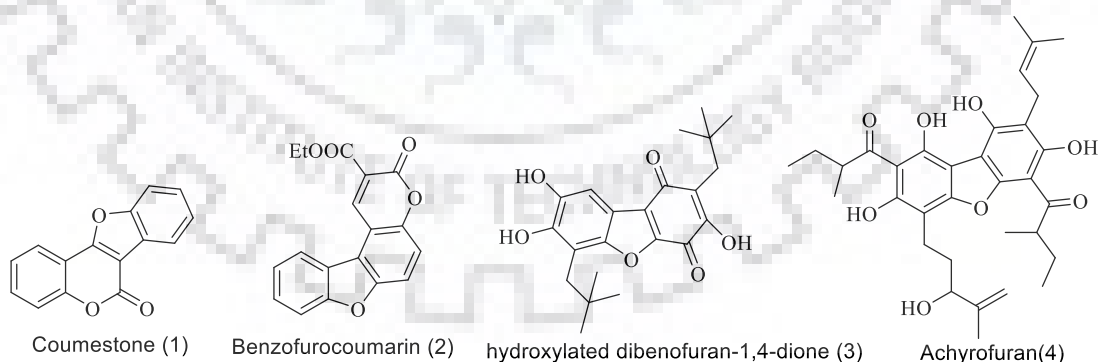
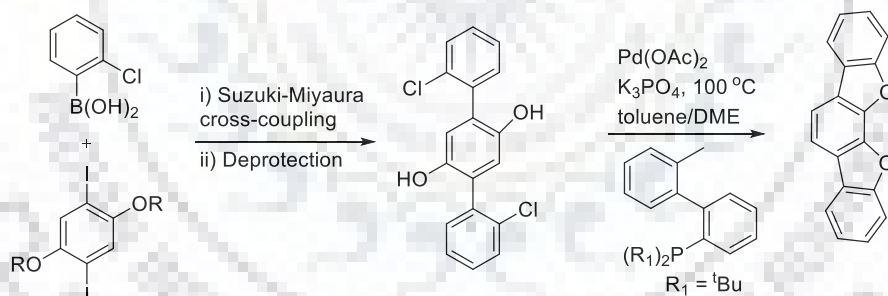


Figure.3.1. Biologically active benzofuro heterocyclic derivatives

Some synthetic and naturally occurring dibenzofuran derivatives shows different effects such as furan motifs with polycyclic ring skeleton like coumestan are resourceful intermediates in numerous natural products and therapeutic agents such as wedelolactone (1) used as inhibitor of IKK complex that contain LPS-persuaded caspase-11 expression [24]. Benzofurocoumarin (2) interestingly escorts to inhibit the growth of numerous

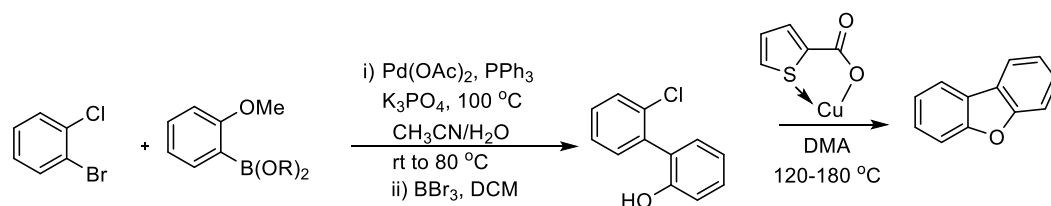
human cancer cell lines [25]. Hydroxylated dibenzofuran-1,4-dione (3) is central frame of Popolohuanone E to demonstrated the inhibition of topoisomerase II [26]. Achyrofuran (4) is conscientious for anti-diabetic [27].

Additionally, they possess a wide range of applications and act as antibacterial, antioxidant, antifungal, antibiotic, cardiogenic, protein tyrosine kinase inhibitory, anti-HIV, anti-Alzheimer and anticancer agents [28]. They are also employed as pharmaceutical agents in cyclic dependent kinase (CDK) inhibitors [29]. Some remarkable efforts have been made towards intramolecular C–O bond formations, involving transition metal catalysts. For example, through the dehalocoupling of diaryl ether *via* Benzyne-Tethered Aryl Lithiums intermediate formation [30]. Another approach is by the cyclization of *o*-iodophenols with silylaryl triflates [31] and oxidative coupling of diaryl ether [32]. Furthermore Pd-catalyzed reaction has been extensively used in the construction of furan ring *via* oxidative cyclisation of diaryl phenol in presence of air as oxidant [33] or 3-nitropyridine and tertbutylperoxybenzoate (BzOObu) as ligand and oxidant respectively [34]. Moreover, Nakano *et al.* have been developed a resourceful protocol for C–O coupling reactions with intramolecular O-arylation, generating ladder-type heteroacenes with palladium-catalyst and phosphine ligand [35].



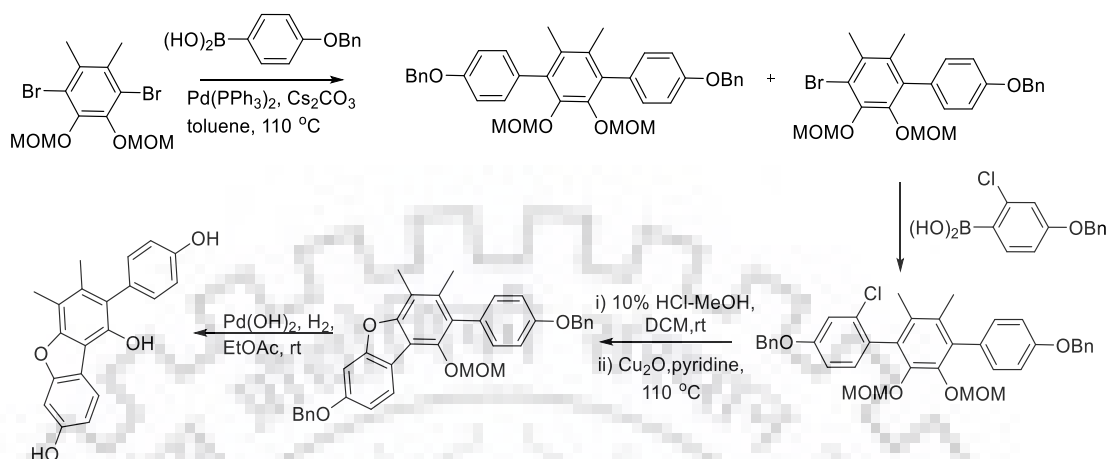
Scheme.3.1. Synthesis of ladder-type heteroacenes

Liu co-worker's successfully developed fused benzo[4,5]furoheterocycles with pre-synthesized copper(I) thiophene-2-carboxylate (CuTC)-complex *via* intramolecular cyclisation under inert atmosphere [36]. Zhu group explained CuBr catalyzed cyclo-etherification reaction using pivalic acid (PivOH) as additive [37].



Scheme.3.2. Synthesis of Dibenzofuran.

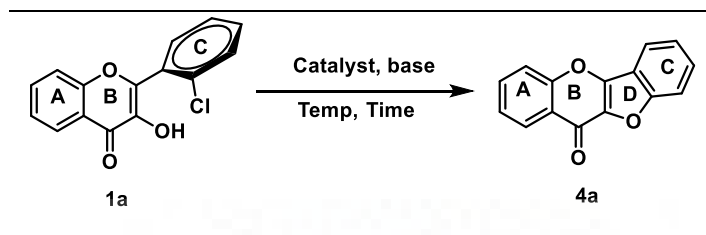
In 2017, Koshino and group described the synthesis of 3-phenyldibenzo[*b,d*]furan *i.e.* Vialinin B which is used as a tumor necrosis factor (TNF)- α production inhibitor. Phenylidibenzofuran moiety prepared through Cu_2O in pyridine [38].



Scheme.3.3. Synthesis of phenylidibenzofuran.

Recently, Hong *et al.* reported C–O cyclisation of flavones *via* C–H functionalization to form heterocyclic-annulated benzofuran skeleton. However, the product formation requires more than stoichiometric amount of $\text{Cu}(\text{OAc})_2$ along with $\text{Zn}(\text{OTf})_3$ as additive. Also, the reaction took longer time and high temperature (120 °C) [39]. Therefore, these methods undergo from several limitations such as inert atmosphere, expensive catalyst loading, high temperature (above 100-140 °C), oxidant, additive and requirement of sterically hindered ligands *etc.* To overcome these problems, many synthetic chemists have been attempted to develop economical, facile, efficient and environmentally benign protocols for the construction of benzofuran scaffolds. Hence, Expansion of an innovative catalytic process for the synthesis of flavanone fused benzofuran skeleton is highly desirable. Herein, we describe new protocol *i.e.* simple, efficient, easy, straightforward and ligand free copper-catalyzed Ullmann type coupling reactions for the intramolecular C–O bond formation between OH and Cl group to afford-biologically active flavone-benzofuran fused heterocyclic derivatives [40] from substituted 2-(2 chlorophenyl)-3-hydroxy-4*H*-chromen-4-ones relatively under mild reaction conditions with wide ranging of substrate scope.

3.2. Results and discussion

Table 3.1 Optimization of reaction conditions^a

Entry	Catalyst (10 mol%)	Base (3 equiv)	solvent	Temp (°C)	Time (h)	Yield (%) ^e
1	Pd(OAc) ₂	K ₂ CO ₃	DMSO	100 °C	24	
2	Cu(OAc) ₂	K ₂ CO ₃	DMSO	100 °C	24	-
3 ^b	Cu(OAc) ₂	- / K ₂ CO ₃	DMSO	100 °C	24	-
4	Cu(OAc)	K ₂ CO ₃	DMSO	80 °C	4	25%
5	CuBr ₂	Na ₂ CO ₃	DMSO	80 °C	3	40%
6	CuCl ₂	Na ₂ CO ₃	DMSO	80 °C	3	44%
7	CuBr ₂	K ₂ CO ₃	DMSO	80 °C	3	49%
8	CuCl ₂	K ₂ CO ₃	DMSO	80 °C	3	52%
9	CuCl	Na ₂ CO ₃	DMSO	80 °C	3	67%
10	CuBr	Na ₂ CO ₃	DMSO	80 °C	3	70%
11	CuI	Na ₂ CO ₃	DMSO	80 °C	3	72%
12	CuCl	K ₂ CO ₃	DMF	80 °C	3	75%
13	CuBr	K ₂ CO ₃	DMF	80 °C	2	79%
14	CuI	K₂CO₃	DMF	80 °C	2	90%
15	^c CuI	K ₂ CO ₃	DMF	80 °C	4	81%
16	^d CuI	K ₂ CO ₃	DMF	80 °C	12	85%

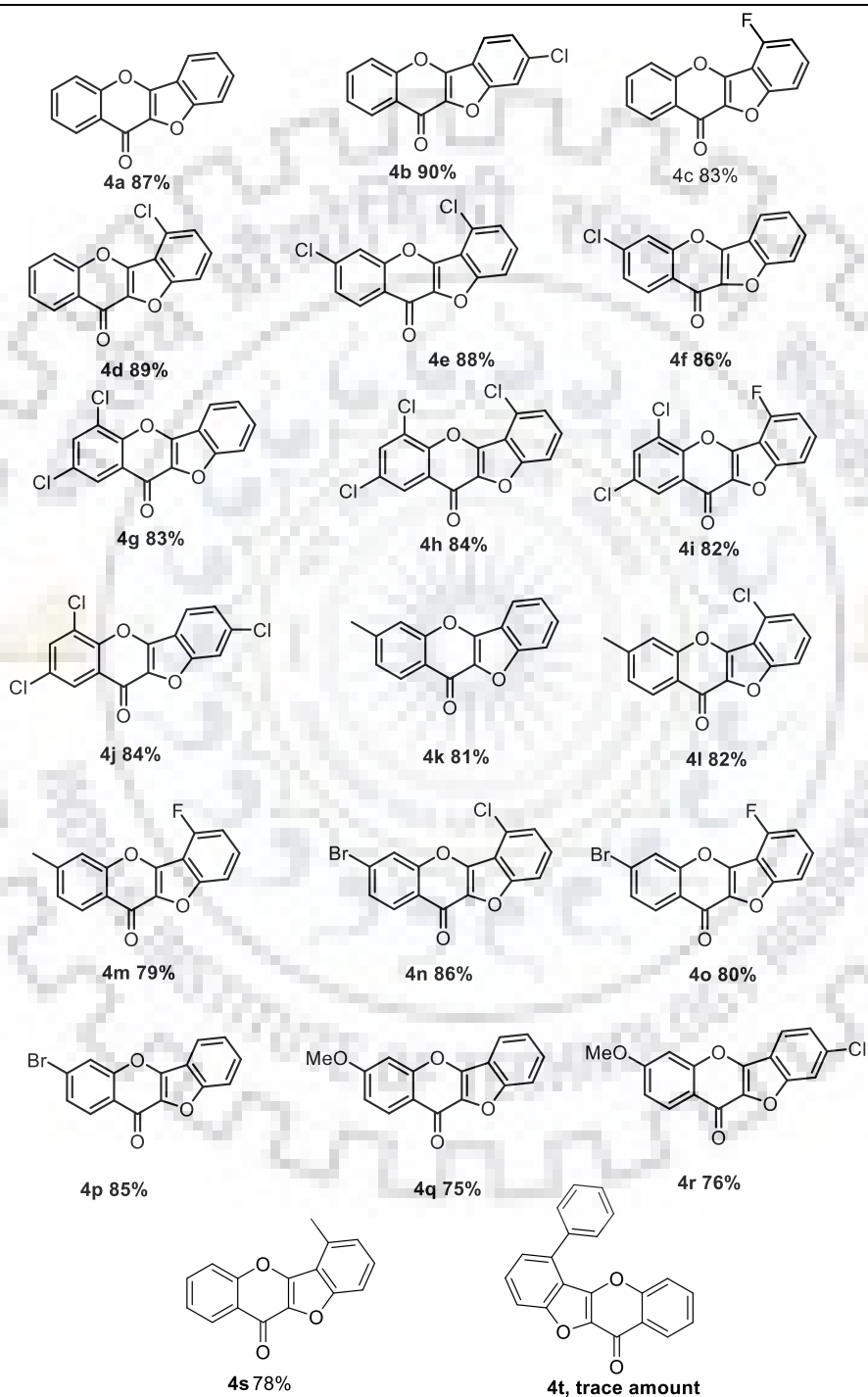
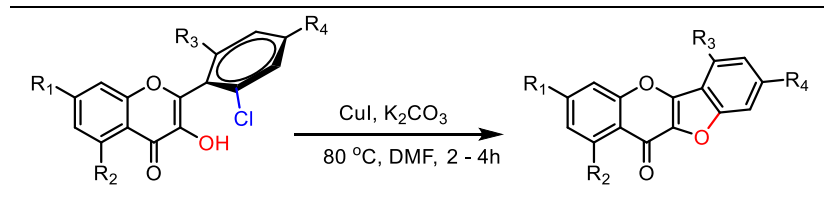
^aReaction were carried out at 1 mmol scale, catalyst (10 mol%), base (K₂CO₃) solvent (4ml), temperature, ^b Zn(OTf)₂ (20 mol %), ^cCuI (15 mol%), ^dCuI (5 mol%), ^eIsolated yield.

We commenced our reaction with 2-(2-chlorophenyl)-3-hydroxy-4*H*-chromen-4-one as a model substrate for the formation of product **4a** by using Pd(II)(OAc) in DMSO at 100 °C, but not succeeded to get the desired product (Table 3.1, entry 1). So we replaced Pd(OAc)₂ with Cu(II)acetate, but again we attained no product (Table 3.1, entry 2). Using Cu(II)acetate and Zn(OTf)₂ with or without a base *i.e.* K₂CO₃ was also vain as the

required product was not obtained (Table 3.1, entry 3). However, when we used Cu(I)acetate (10 mol%) the reaction furnished the product **4a** in 25% yield in 4h (Table 3.1, entry 4). Encouraged by the results, we investigated the reaction under different conditions. We proceed the reaction with different copper salts such as CuCl₂, CuBr₂ (10 mol%) in presence of base Na₂CO₃ and DMSO solvent. The yield of product formation slightly improved (30% and 34%) (Table 3.1, entry 5 and 6). Changing the base to K₂CO₃ as compare to Na₂CO₃, the product yield slightly improved (39% and 42% respectively) (Table 3.1, entry 7 and 8). The reaction was also performed with CuCl, CuBr (10 mol%) and CuI (10 mol%) in presence of base Na₂CO₃ which afforded the desired product in 67%, 70% and 72% respectively (Table 3.1, entry 9, 10 and 11). In order to improve the yield of the product formation, a comprehensive screening was adopted by changing the solvent and base conditions. It was also observed that with CuCl, and CuBr (10 mol%) in presence of K₂CO₃ the desired product was obtained in slightly better yield (75% and 79% respectively) as compared to Na₂CO₃ (Table 3.1, entry 12 and 13). Efficiency of the reaction was encouraging, when the reaction was carried out with CuI (10 mol%) in presence of base K₂CO₃ at 80 °C temperature in DMF for 2 hrs, excellent yield of product 90% was obtained (Table 3.1, entry 14). when reaction was carried out in presence of CuI with (15 mol%) and base K₂CO₃, no more variation in yields of the desired product was obtained (Table 3.1, entry 15). However, when we used CuI with (5 mol%) with base K₂CO₃ it improved the yield but took more time (10-12) hrs (Table 3.1, entry 16).

3.3. Substrate scope

Under optimized reaction conditions, we further focused on the scope of substrates in CuI catalyzed reaction of 2-(2-chlorophenyl)-3-hydroxy-4*H*-chromen-4-one derivatives for the synthesis of flavones-benzofuran fused derivatives (scheme 3.4). We explored the substrate scope for the tetracyclic flavone fused benzofuran compounds. The reaction exhibited wider substrate scope and showed good tolerance for both electron-donating and electron-withdrawing groups. Marginally, Electron withdrawing group –Cl and –Br substituted aryl ring A and ring C afforded products in higher yield (**4e**, **4f**, **4g**, **4h**, **4i**, **4j**, **4n**, **4o** and **4p**) than electron donating group –Me and –OMe substituted 2-(2-chlorophenyl)-3-hydroxy-4*H*-chromen-4-one (**4k**, **4l**, **4m**, **4q**, **4r**). The substituent at different positions of ring A also furnished products in satisfactory yields. We also performed reactions with ortho-substituted on C-ring like methyl and phenyl groups.



^aReaction condition: 1a (1 mmol, 272mg), K_2CO_3 (3 equiv., 414mg), CuI (0.1 mmol, 20mg) in DMF solvent (4 mL). ^bIsolated yield.

Scheme.3.4. Synthesis of heterocyclic flavones-benzofuran fused derivatives.

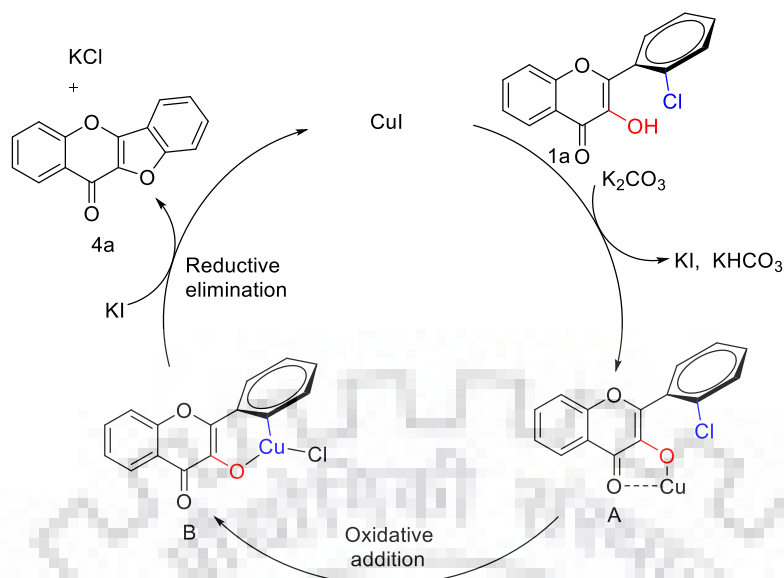
Methyl substituted reactant gave the product **4s** in moderate yield (78%) might be due to steric hinderance while a bulkier phenyl groups at ortho position failed to give the product.

3.4. Structure determination

The structure elucidation of $C_{15}H_7ClO_3$ (**4d**) and $C_{15}H_8Cl_2O_3$ (**1g**) was established on the basis of the collective information obtained from a variety of spectroscopic techniques such as U.V visible spectroscopy, FT-IR, 1H -NMR, ^{13}C -NMR and LC-MS. Compound **4d** was obtained as a white solid. UV-visible spectrum of **1g** demonstrate three absorption peaks at 245 nm, 307 nm and 343 nm on the other hand **4d** shows two absorption peaks at 245 nm (due to π - π^* transition) and 300 nm (due to n - π^* transition). The IR spectrum of **4d** showed absorptions at 1705, 1271, 1027, 751 cm^{-1} for carbonyl asymmetric stretching, C–O–C (ether) and C–Cl, symmetric stretching frequency respectively **1g** shows –OH at 3430 cm^{-1} and the disappearance of 3430 (–OH) cm^{-1} peak in **4d** confirmed the cyclization product. In 1H NMR–OH peak appear at 10.80 ppm in **1g**. Disappearance of –OH peak and some shifting shows of proton in aromatic region shows the formation of cyclized products. In ^{13}C -NMR spectrum, **1g** shows carbonyl peak (–C=O) at 180.2 ppm and thirteen signals due to symmetry of ring C, on the other hand **4d** exhibits carbonyl peak (–C=O) at 169.1 and fifteen signals due to loss of symmetry of ring C. Further the cyclized structure of the product $C_{15}H_7ClO_3$ was confirmed by LC–MS. The m/z molecular ion peak (M+1) at 271.2, 273.2 due to removal of one Cl-group from **1g** (expected = 271.0, 271.0).

3.5 Reaction mechanism

A plausible mechanism for the formation of product **4a** has been depicted on the basis of previous literature [41]. In the presence of K_2CO_3 , 2-(2-chlorophenyl)-3-hydroxy-4*H*-chromen-4-one converted into a potassium 2-(2-chlorophenyl)-4-oxo-4*H*-chromen-3-olate salt which reacted with CuI to form a copper (I) complex *i.e.* intermediate **A**. Copper (I) complex switched into copper (III) complex *i.e.* intermediate **B** *via* the oxidative addition of –Cl group of ring D. Finally, copper (III) complex's reductive elimination afforded the desired product **4a** and regenerated CuI for the next catalytic cycle (Scheme 3.5).



Scheme.3.5. Proposed mechanism

3.6. Conclusion

In summary, we have demonstrated an expedient copper-catalyzed intramolecular Ullman type-coupling reaction between $-OH$ and $-Cl$ group of substituted 2-(2-chlorophenyl)-3-hydroxy-4*H*-chromen-4-ones for the C-O bond formation to afford heterocycle flavones-benzofuran fused derivatives involving basic condition. Efficient and fast conversion under mild reaction conditions with excellent yield are great advantages of our method. Simplicity, reliability and Straightforwardness accomplish it an attractive tool for environmental and organic chemists. This path has wide substrate scope and should be appropriate for the synthesis of numerous pharmacologically interesting molecules.

3.7. Experimental Section

3.7.1. General information

All the required chemicals were purchased from Merck, Avra, Sigma aldrich and Himedia. IR spectra were recorded on a Thermo Nicolet FT-IR spectrophotometer with KBr. NMR was recorded on Bruker Spectrospin DPX 500 MHz and Jeol Resonance ECX 400 MHz spectrometer using $CDCl_3$ as solvent. In 1H NMR Chemical shifts were recorded in parts per million and referenced internally to the residual with tetramethylsilane (TMS δ -0.00 ppm) or proton resonance in $CDCl_3$ (δ -7.26ppm). ^{13}C NMR spectra were referenced to $CDCl_3$ (δ -77.0 ppm, the middle peak). Coupling constant are calculated in Hz. The following abbreviations are used to explain the multiplicities: s = singlet, d = doublet, dd = doublet of doublet, dt = doublet of triplet, t = triplet, q = quartet, m = multiplet. Mass spectra were measured with ESI ionization in MSQ LCMS mass spectrometer. Electronic

absorption spectra of **1j** and **3d** in dichloromethane solvent were recorded with an Evolution 600, Thermo scientific (shimadzu) UV. Visible spectrometer.

3.7.2. General procedure

3.7.2.1. Synthesis of Chalcone derivatives

To a solution of 10 millimole of o-hydroxy acetophenone (1.1ml) in 10 ml ethanol and 3 equiv. of sodium hydroxide, 1.1 millimole of benzaldehyde was added and the mixture was left overnight at 35- 40 °C. After regular TLC monitoring. The deep orange solution become appear that solution was poured into crushed ice and acidified with hydrochloric acid for neutralization. The yellow precipitate comes out and separated by filtration and recrystallized from methanol [42].

3.7.2.2. Synthesis of 3-hydroxy flavone derivatives

To a suspension of 1 millimole of chalcone in 10 ml of methanol was added 10 ml of 20% aqueous sodium hydroxide with stirring, after 15 min followed by the careful addition of 18 ml of 30% hydrogen peroxide over a period of 0.5 hours. After regular TLC monitoring. The reaction mixture was stirred for 3.5 hours at 30 °C and was poured into crushed ice containing 5 N hydrochloric acid for neutralization. The light-yellow colour precipitate was coming out then filtered, washed, dried and recrystallized from Methanol [43].

3.7.2.3. Synthesis of Flavone fused benzofuran derivatives

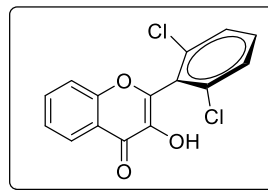
A round bottom flask with a magnetic stirring bar was charged with 2-(2-chlorophenyl)-3-hydroxy-4H-chromen-4-ones (1 mmol, 272 mg), K₂CO₃ (3 equiv., 414 mg), CuI (10 mol %, 0.1 mmol, 20 mg) in DMF solvent (4 mL). The reaction mixture was heated at 80 °C for 2-4 hrs. After regular TLC monitoring because of complete conversion of starting material, the mixture was poured into cold ice water and neutralized carefully using 1N hydrochloric acid which gave the precipitated product. It was filtered and washed with water under vacuum. The product was re-crystallized with methanol to get a light green colored solid because of copper iodide. Further purification by column chromatography (hexane/ethyl acetate, 9:1) afforded the desired product as a white solid with good to excellent yield.

3.8. Characterization data

2-(2,6-dichlorophenyl)-3-hydroxy-4H-chromen-4-one (1j): Yield: 96% as light yellow solid; mp: 242-244 °C; ¹H NMR (500 MHz, CDCl₃ ppm):

δ 10.80 (s, 1H), 8.45 (d, *J* = 7.9 Hz, 1H), 7.78–7.71 (m, 2H), 7.59–7.54 (m, 2H), 7.52–7.47 (m, 2H), 7.41 (d, *J* = 7.9 Hz, 1H);

¹³C NMR (100MHz, CDCl₃, ppm): δ 180.1, 156.0, 155.5, 148.0,

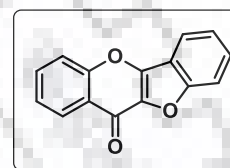


137.8, 133.7, 130.9, 127.8, 126.5, 125.0, 118.8, 117.0, 111.9; FT-IR (KBr): 3430, 1726, 1692, 1270, 1027, 918, 754, 657 cm⁻¹; LC-MS (ESI⁺): *m/z* calculated for C₁₅H₈O₃ [M+H]⁺: 306.9, found: 306.9.

11H-benzofuro [3, 2-b] chromen-11-one (4a): Yield: 87% as white solid; mp: 187-189 °C; ¹H NMR (500 MHz, CDCl₃ ppm): δ 8.48 (d, *J* = 7.9 Hz, 1H), 8.00

(d, *J* = 7.8 Hz, 1H), 7.76 (t, *J* = 7.5 Hz, 1H), 7.71–7.68 (m, 2H), 7.64

(t, *J* = 7.5 Hz, 1H), 7.52–7.45 (m, 2H); ¹³C NMR (100MHz, CDCl₃,



ppm): δ 167.3, 156.0, 155.5, 148.0, 137.8, 133.8, 130.9, 127.7, 126.5,

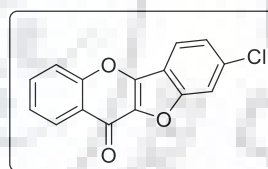
125.2, 125.0, 124.9, 118.8, 117.1, 112.0; FT-IR (KBr): 1705, 1670, 1270, 1027, 918, 754,

657 cm⁻¹; LC-MS (ESI⁺): *m/z* calculated for C₁₅H₈O₃ [M+H]⁺: 237.0, found: 237.2.

8-chloro-11H-benzofuro [3,2-b]chromen-11-one (4b): Yield: 90% as white solid; mp: 254–256°C; ¹H NMR (500 MHz, CDCl₃ ppm): δ

8.47 (d, *J* = 7.9 Hz, 1H), 7.92 (d, *J* = 8.4 Hz, 1H), 7.77 (t, *J* = 7.5 Hz, 1H), 7.70-7.69 (m, 2H), 7.51 (t, *J* = 7.5 Hz, 1H),

7.46 (d, *J* = 8.5 Hz, 1H); ¹³C NMR (100 MHz, CDCl₃ ppm):



δ 168.5, 156.4, 152.1, 141.6, 135.4, 130.4, 129.1, 126.4, 122.2, 121.3, 117.4, 117.1,

115.0, 112.7, 110.0; FT-IR (KBr): 1705, 1670, 1271, 1027, 918, 751, 658 cm⁻¹;

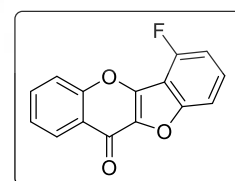
LC-MS (ESI⁺): *m/z* calculated for C₁₅H₇ClO₃ [M+H]⁺: 271.0, 273.0 found: 271.1,

273.2.

6-fluoro-11H-benzofuro [3,2-b]chromen-11-one (4c): Yield: 83% as white solid; mp: 232–234°C; ¹H NMR (400 MHz, CDCl₃ ppm): δ

8.45 (d, *J* = 7.9 Hz, 1H), 7.77-7.70 (m, 2H), 7.59-7.54 (m, 1H), 7.50-7.46 (m, 2H), 7.11 (t, *J* = 8.6 Hz, 1H); ¹³C NMR (100

MHz, CDCl₃ ppm): 167.1, 156.2(d, δ¹J_{C-F} = 242.8 Hz), 156.1,



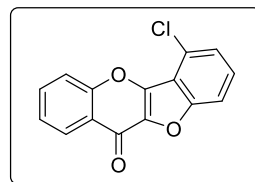
156.0, 155.0, 147.2, 137.2, 133.8, 131.2(d, ³J_{C-F} = 7.8 Hz), 126.5, 125.2, 118.6,

110.0,(d, ²J_{C-F} = 17.7 Hz), 109.2 (d, ³J_{C-F} = 4.3 Hz), 108.2 (d, ²J_{C-F} = 20.4 Hz) ppm;

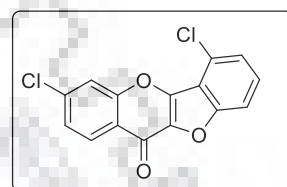
FT-IR (KBr): 1705, 1672, 1270, 1027, 918, 753, 658 cm⁻¹; LC-MS (ESI⁺): *m/z*

calculated for C₁₅H₇FO₃ [M+H]⁺: 255.0, found: 255.2.

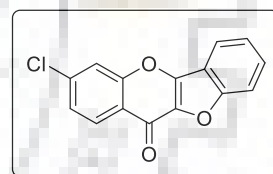
6-chloro-11H-benzofuro[3,2-b]chromen-11-one (4d): Yield: 89% as white solid; mp: 264–266°C; ^1H NMR (500 MHz, CDCl_3 ppm): δ 8.50 (d, $J = 7.9$ Hz, 1H), 7.82–7.77 (m, 2H), 7.63 (d, $J = 8.3$ Hz, 1H), 7.55–7.52 (m, 2H), 7.45 (d, $J = 7.6$ Hz, 1H); ^{13}C NMR (100 MHz, CDCl_3 ppm): δ 169.1, 154.4, 150.8, 141.1, 131.2, 126.6, 120.3, 115.2, 113.9, 112.1, 111.3, 110.3, 108.2, 107.6, 106.7; IR (KBr): 1703, 1672, 1270, 1027, 918, 753, 658 cm^{-1} ; LC-MS (ESI $^+$) m/z calculated for $\text{C}_{15}\text{H}_7\text{ClO}_3$ [M+H] $^+$: 271.0, 273.0, found-271.2, 273.2.



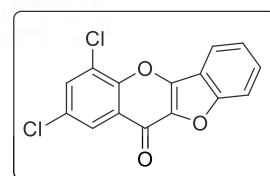
3, 6-dichloro-11H-benzofuro [3,2-b]chromen-11-one (4e): Yield: 88% as white solid; mp: 281–282°C; ^1H NMR (400 MHz, CDCl_3 ppm): δ 8.57 (s, 1H), 7.84 (d, $J = 8.8$ Hz, 1H), 7.63 (d, $J = 8.8$ Hz, 1H), 7.60–7.53 (m, 2H), 7.41 (d, $J = 7.2$ Hz, 1H); ^{13}C NMR (100 MHz, CDCl_3 ppm): 169.6, 152.0, 141.4, 135.0, 130.0, 129.9, 127.7, 126.5, 125.7, 122.8, 121.7, 120.7, 117.4, 114.6, 110.2; IR (KBr): 1705, 1672, 1270, 1027, 918, 753, 658 cm^{-1} ; LC-MS (ESI $^+$) m/z calculated for $\text{C}_{15}\text{H}_6\text{Cl}_2\text{O}_3$ [M+H] $^+$: 304.9 found: 304.9.



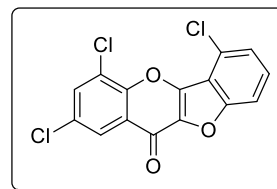
3-chloro-11H-benzofuro[3,2-b]chromen-11-one (4f): Yield: 86% as white solid; mp: 272–274°C; ^1H NMR (500 MHz, CDCl_3 ppm): δ 8.51 (s, 1H), 7.89 (d, $J = 7.8$ Hz, 1H), 7.74 (d, $J = 8.8$ Hz, 1H), 7.61–7.55 (m, 2H), 7.51 (d, $J = 8.8$ Hz, 1H), 7.39 (t, $J = 7.4$ Hz, 1H); ^{13}C NMR (100 MHz, CDCl_3 ppm): δ 166.1, 155.4, 154.8, 149.5, 137.2, 136.5, 131.0, 129.3, 124.5, 120.8, 120.3, 118.6, 117.9, 113.7; IR (KBr): 1703, 1672, 1270, 1027, 918, 753, 658 cm^{-1} ; LC-MS (ESI $^+$) m/z calculated for $\text{C}_{15}\text{H}_7\text{ClO}_3$ [M+H] $^+$: 271.0, 273.0, found-271.2, 273.2.



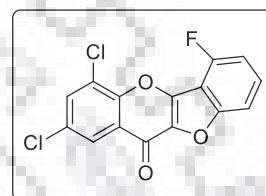
2,4-dichloro-11H-benzofuro[3,2-b]chromen-11-one (4g): Yield: 83% as white solid; mp: 261–263°C; ^1H NMR (400 MHz, CDCl_3 ppm): δ 8.16 (s, 1H), 7.86 (d, $J = 7.5$ Hz, 1H), 7.62 (s, 1H), 7.55 (s, 2H), 7.38–7.34 (m, 1H). ^{13}C NMR (100 MHz, CDCl_3 ppm): δ 165.1, 155.3, 150.0, 149.3, 136.8, 133.7, 131.3, 130.8, 127.2, 124.8, 124.7, 124.6, 120.8, 117.5, 113.5; IR (KBr): 1705, 1672, 1270, 1027, 918, 753, 658 cm^{-1} ; LC-MS (ESI $^+$) m/z calculated for $\text{C}_{15}\text{H}_6\text{Cl}_2\text{O}_3$ [M+H] $^+$: 304.9 found: 304.9.



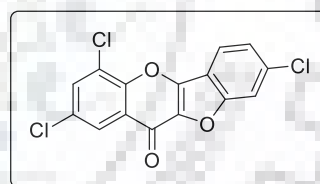
2,4,6-Trichloro-11H-benzofuro[3,2-b]chromen-11-one (4h) :Yield: 84% as white solid; mp: 273–275 °C, ^1H NMR (400 MHz, CDCl_3 ppm): δ 8.33 (s, 1H), 7.81 (s, 1H), 7.59 (d, $J = 6.0$ Hz, 2H), 7.45 (d, $J = 6.4$ Hz, 1H); ^{13}C NMR (100 MHz, CDCl_3 ppm): δ 165.2, 155.8, 150.3, 148.3, 137.3, 134.0, 131.5, 131.1, 128.0, 127.1, 125.3, 125.0, 124.6, 116.7, 112.0; IR (KBr): 1705, 1672, 1270, 1027, 918, 753; 658 cm^{-1} ; LC-MS (ESI $^+$) m/z calculated for $\text{C}_{15}\text{H}_5\text{Cl}_3\text{O}_3$ [M+H] $^+$: 338.9 found: 338.9.



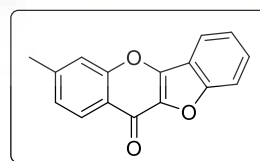
2,4-dichloro-6-fluoro-11H-benzofuro[3,2-b]chromen-11-one (4i): Yield: 82% as white solid; mp: 226–228 °C; ^1H NMR (400 MHz, CDCl_3 ppm): δ 8.17 (s, 1H), 7.75 (s, 1H), 7.51-7.45 (m, 1H), 7.37 (d, $J = 8.0$ Hz, 1H), 7.17 (t, $J = 8.6$ Hz, 1H); ^{13}C NMR (100 MHz, CDCl_3 ppm): 169.0, 160.8 (d, $^1J_{\text{C-F}} = 252$ Hz), 155.0, 140.8, 140.6, 137.0, 135.5 (d, $^3J_{\text{C-F}} = 3.6$ Hz), 132.8 (d, $^3J_{\text{C-F}} = 9.5$ Hz), 128.2, 125.8 (d, $^4J_{\text{C-F}} = 3.4$ Hz), 122.8, 120.5, 117.9 (d, $^2J_{\text{C-F}} = 18.6$ Hz), 118.2, 114.7 (d, $^2J_{\text{C-F}} = 21.5$ Hz); IR (KBr): 1705, 1672, 1270, 1027, 918, 753, 658 cm^{-1} ; LC-MS (ESI $^+$) m/z calculated for $\text{C}_{15}\text{H}_5\text{Cl}_2\text{FO}_3$ [M+H]: 322.9, found- 322.9.



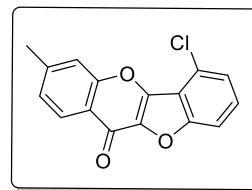
2,4,8-Trichloro-11H-benzofuro[3,2-b]chromen-11-one (4j): Yield: 84% as white solid; mp: 280–282 °C, ^1H NMR (400 MHz, CDCl_3 ppm): δ 8.27 (s, 1H), 7.91 (d, $J = 8.4$ Hz, 1H), 7.74 (s, 1H), 7.65 (s, 1H), 7.42 (d, $J = 8.4$ Hz, 1H); ^{13}C NMR (100 MHz, CDCl_3 ppm): δ 165.1, 155.3, 150.0, 148.9, 137.5, 137.4, 134.0, 131.1, 127.2, 125.9, 124.8, 124.6, 121.6, 116.3, 114.1; IR (KBr): 1705, 1672, 1270, 1027, 918, 753, 658 cm^{-1} ; LC-MS (ESI $^+$) m/z calculated for $\text{C}_{15}\text{H}_5\text{Cl}_3\text{O}_3$ [M+H]: 338.9, found- 338.9.



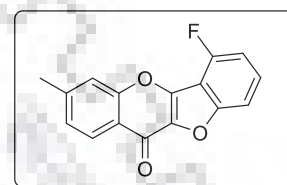
3-methyl-11H-benzofuro[3,2-b]chromen-11-one (4k): Yield: 81% as white solid, mp: 203–205 °C; ^1H NMR (400 MHz, CDCl_3 ppm): δ 8.24 (s, 1H), 7.96 (d, $J = 7.8$ Hz, 1H), 7.68–7.63 (m, 1H), 7.61–7.59 (m, 1H), 7.57–7.55 (m, 2H), 7.44 (t, $J = 7.0$ Hz, 1H), 2.49 (s, 1H); ^{13}C NMR (100 MHz, CDCl_3 ppm): δ 167.5, 155.2, 154.2, 149.1, 137.4, 135.0, 134.7, 130.5, 126.0, 124.9, 124.2, 120.6, 118.2, 118.1, 113.5, 21.0; IR (KBr): 1705, 1671, 1271, 1027, 918, 753, 657 cm^{-1} ; LC-MS (ESI $^+$): m/z calculated for $\text{C}_{16}\text{H}_{10}\text{O}_3$ [M+H] $^+$: 251.0 found: 251.2.



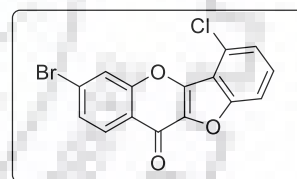
6-chloro-3-methyl-11H-benzofuro[3,2-b]chromen-11-one (4l): Yield: 82% as white solid; mp: 259–261 °C; ¹H NMR (400 MHz, CDCl₃ ppm): δ 8.05 (s, 1H), 7.60–7.56 (m, 2H), 7.53–7.50 (m, 1H), 7.42–7.38 (m, 2H), 2.48 (s, 3H); ¹³C NMR (101 MHz, CDCl₃ ppm): δ 165.9, 154.3, 144.3, 139.0, 137.1, 135.5, 134.9, 134.8, 132.5, 130.4, 128.3, 127.3, 124.7, 121.0, 118.3, 21.0; IR (KBr): 1705, 1670, 1271, 1029, 920, 753, 657 cm⁻¹; LC-MS (ESI⁺):m/z calculated for C₁₆H₁₀O₃ [M+H]⁺: 281.0 found: 281.2.



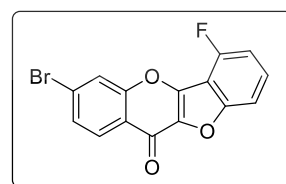
6-fluoro-3-methyl-11H-benzofuro[3,2-b]chromen-11-one (4m): Yield: 79% as white solid; mp: 240–242 °C; ¹H NMR (400 MHz, CDCl₃ ppm): δ 8.06 (s, 1H), 7.52 (d, *J* = 8.5 Hz, 1H), 7.45–7.40 (m, 2H), 7.35 (d, *J* = 7.8 Hz, 1H), 7.15 (t, *J* = 8.4 Hz, 1H); ¹³C NMR (100 MHz, CDCl₃ ppm): 169.0, 160.85 (d, ¹J_{C-F} = 253 Hz), 154.8, 140.1, 139.8, 135.6 (d, ³J_{C-F} = 3.8 Hz), 135.5, 134.8, 132.5 (d, ³J_{C-F} = 9.5 Hz), 125.8 (d, ⁴J_{C-F} = 3.4 Hz), 124.8, 121.1, 118.8 (d, ²J_{C-F} = 18.6 Hz), 118.4, 114.6 (d, ²J_{C-F} = 21.5 Hz), 21.0; IR (KBr): 1705, 1673, 1272, 1027, 918, 753, 658 cm⁻¹; LC-MS (ESI⁺) m/z calculated for C₁₆H₉FO₃ [M+H]⁺: 269.0 found: 269.2.



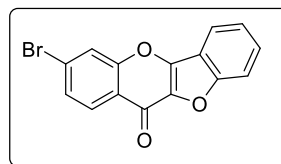
3-bromo-6-chloro-11H-benzofuro[3,2-b]chromen-11-one (4n): Yield: 86% as white solid; mp: 279–281 °C; ¹H NMR (400 MHz, CDCl₃ ppm): δ 8.58 (s, 1H), 7.85 (d, *J* = 8.8 Hz, 1H), 7.68–7.64 (d, *J* = 8.8 Hz, 1H), 7.69–7.54 (m, 2H), 7.42 (d, *J* = 7.2 Hz, 1H), 7.44 (t, *J* = 7.0 Hz, 1H); ¹³C NMR (100 MHz, CDCl₃ ppm): δ 165.9, 155.7, 154.8, 148.3, 137.6, 136.7, 131.2, 129.1, 127.7, 126.4, 125.1, 120.6, 118.8, 116.8, 112.0; IR (KBr): 1705, 1673, 1270, 1027, 918, 753, 658 cm⁻¹; LC-MS (ESI⁺) m/z calculated for C₁₅H₇BrClO₃ [M+H]⁺: 348.9 found :348.9.



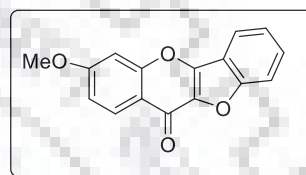
3-bromo-6-fluoro-11H-benzofuro[3,2-b]chromen-11-one (4o): Yield: 80% as white solid; mp: 226–228 °C; ¹H NMR (400 MHz, CDCl₃ ppm): δ 8.41 (s, 1H), 7.77–7.75 (m, 1H), 7.48–7.43 (m, 1H), 7.42–7.39 (m, 1H), 7.36–7.34 (m, 1H), 7.15 (t, *J* = 8.5 Hz, 1H); ¹³C NMR (100 MHz, CDCl₃ ppm): 169.0, 160.88 (d, ¹J_{C-F} = 254 Hz), 150.5, 140.9, 140.5, 135.6 (d, ³J_{C-F} = 3.6 Hz), 134.1, 133.0 (d, ³J_{C-F} = 9.5 Hz), 130.4, 125.5 (d, ⁴J_{C-F} = 3.5 Hz), 125.0, 123.7, 123.2, 117.9 (d, ²J_{C-F} = 18.5 Hz), 114.7 (d, ²J_{C-F} = 21.5 Hz); IR (KBr): 1704, 1672, 1270, 1025, 918, 753, 658 cm⁻¹; LC-MS (ESI⁺) calculated for m/z C₁₅H₇FO₃ [M+H]⁺: 339.9 found: 339.8.



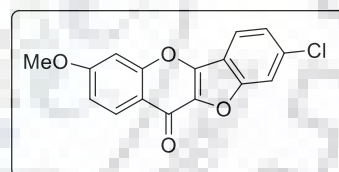
3-Bromo-11H-benzofuro[3,2-b]chromen-11-one (4p): Yield-85% as white solid; mp: 271–273 °C; ^1H NMR (500 MHz, CDCl_3 ppm): δ 8.63 (s, 1H), 8.02 (d, $J = 7.8$ Hz, 1H), 7.87 (d, $J = 8.7$ Hz, 1H), 7.74–7.69 (m, 2H), 7.64 (d, $J = 8.7$ Hz, 1H), 7.51 (t, $J = 7.1$ Hz, 1H); ^{13}C NMR (100 MHz, CDCl_3): δ 167.3, 157.0, 146.4, 140.0, 134.9, 134.8, 132.7, 131.5, 130.7, 127.8, 126.7, 125.7, 122.4, 119.6, 115.2; IR (KBr): 1702, 1672, 1270, 1027, 918, 753, 658 cm^{-1} ; LC-MS (ESI⁺) calculated for m/z $\text{C}_{15}\text{H}_7\text{BrO}_3$ $[\text{M}+\text{H}]^+$: 314.9, 316.9 found: 314.9, 316.9.



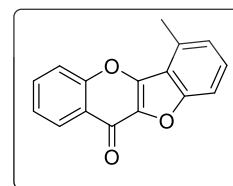
3-methoxy-11H-benzofuro[3,2-b]chromen-11-one (4q): Yield-75% as white solid; mp: 278–280 °C, ^1H NMR (400 MHz, CDCl_3 ppm): δ ^1H NMR (400 MHz,) δ 8.59 (s, 1H), 7.97 (d, $J = 7.9$ Hz, 1H), 7.82 (d, $J = 8.8$ Hz, 1H), 7.69 – 7.62 (m, 2H), 7.59 (d, $J = 8.8$ Hz, 1H), 7.46 (t, $J = 7.4$ Hz, 1H), 3.82 (s, 3H); ^{13}C NMR (100 MHz, CDCl_3 ppm): δ 170.3, 156.4, 152.1, 141.6, 135.4, 130.4, 129.0, 126.4, 122.2, 121.3, 119.9, 117.1, 115.0, 112.7, 110.0, 56.0; IR (KBr): 1705, 1672, 1270, 1027, 918, 753, 658 cm^{-1} ; LC-MS (ESI⁺) m/z calculated for $\text{C}_{16}\text{H}_{10}\text{O}_4$ $[\text{M}+\text{H}]^+$: 266.0 found: 266.3.



8-chloro-3-methoxy-11H-benzofuro[3,2-b]chromen-11-one (4r): Yield-76% as white solid; mp: 285–287 °C, ^1H NMR (400 MHz, CDCl_3 ppm): δ 8.57 (s, 1H), 7.83 (d, $J = 8.9$ Hz, 1H), 7.63 (d, $J = 8.9$ Hz, 1H), 7.60–7.53 (m, 2H), 7.60 (d, $J = 7.2$ Hz, 1H), 7.47 (t, $J = 7.3$ Hz, 1H); ^{13}C NMR (100 MHz, CDCl_3 ppm): δ 169.0, 158.8, 157.9, 151.5, 140.7, 139.9, 134.3, 132.2, 130.9, 129.6, 128.3, 123.8, 121.9, 119.9, 115.1, 55.4; IR (KBr): 1705, 1672, 1270, 1028, 918, 753, 658 cm^{-1} ; LC-MS (ESI⁺) m/z calculated for $\text{C}_{16}\text{H}_9\text{ClO}_4$ $[\text{M}+\text{H}]^+$: 301.0 found: 301.2.



6-methyl-11H-benzofuro[3,2-b]chromen-11-one (4s): Yield-76% as white solid; ^1H NMR (400 MHz, CDCl_3 ppm): δ 8.48 (d, $J = 6.8$ Hz 1H), 7.81–7.75 (m, 2H), 7.74–7.62 (m, 1H), 7.60–7.57 (m, 1H), 7.55–7.50 (m, 1H), 7.42 (t, $J = 7.6$ Hz, 1H); ^{13}C NMR (100 MHz, CDCl_3 ppm): δ 167.5, 155.2, 154.3, 149.2, 137.5, 135.1, 134.8, 130.5, 126.0, 124.9, 124.2, 120.7, 118.3, 118.2, 113.6, 21.0 cm^{-1} ; HRMS (ESI⁺) m/z calculated for $\text{C}_{16}\text{H}_{10}\text{NaO}_3$ $[\text{M}+\text{Na}]^+$: 273.0528 found: 273.0578



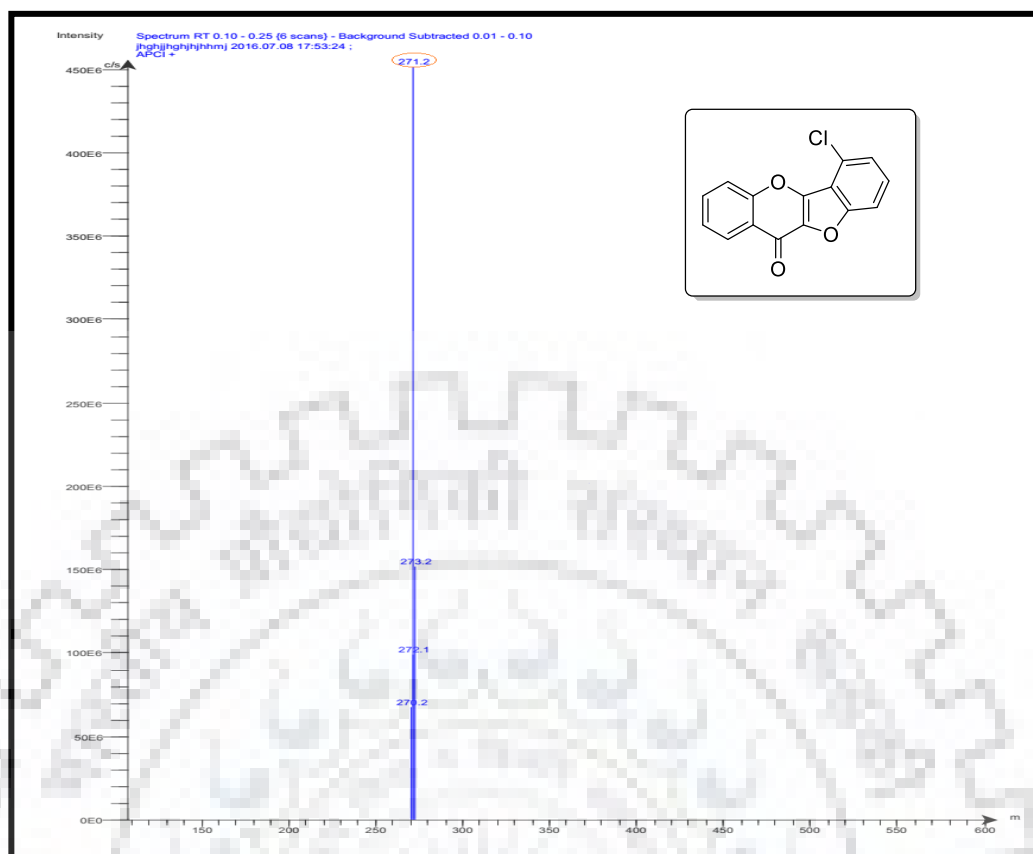


Figure.3.2. LC-MS spectra of **4d** compound.

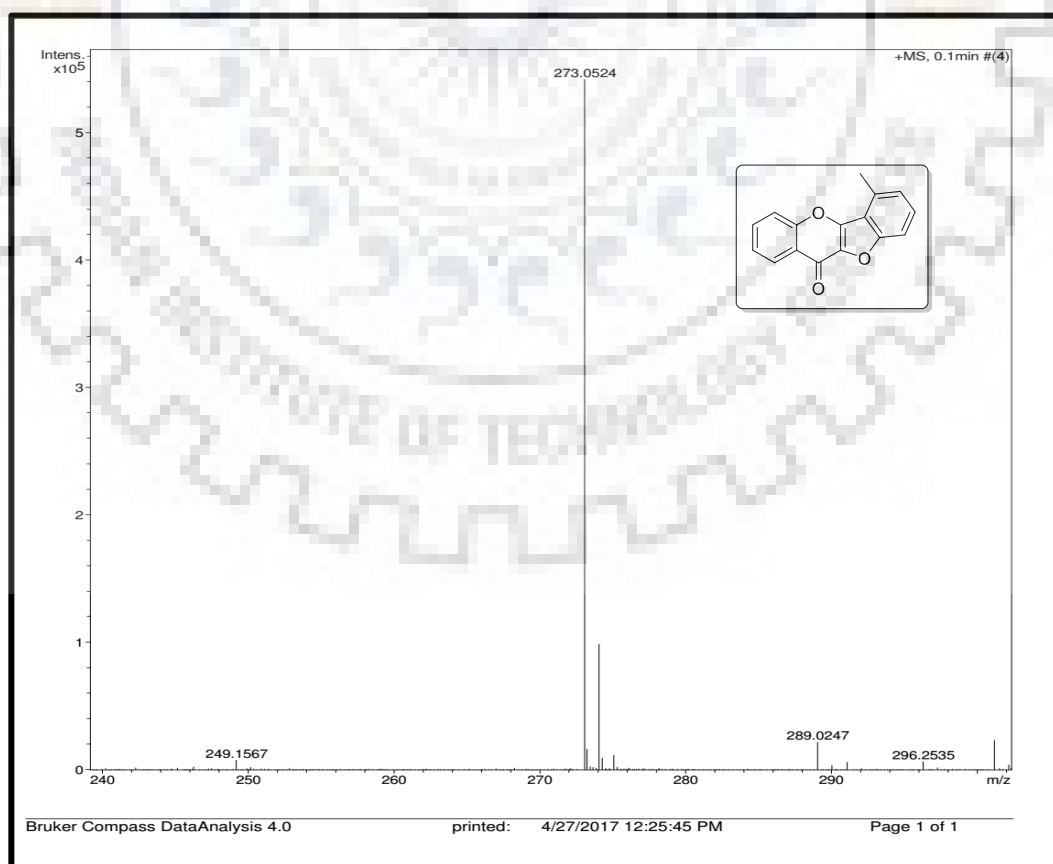


Figure.3.3. HRMS spectra of **4s** compound.

3.9. References

1. (a) Ullmann, F. "Ueber eine neue Bildungsweise von Diphenylaminderivaten" *Ber. Dtsch. Chem. Ges.* **1903**, *36*, 2382–2384; (b) Beletskaya, P. I.; Cheprakov, V. A. "Copper in cross-coupling reactions: The post-Ullmann chemistry" *Coord. Chem. Rev.* **2004**, *248*, 2337–2364.
2. (a) Nelson, D. T.; Meyers I. A. "The Asymmetric Ullmann Reaction. The Synthesis of Enantiomerically Pure C₂-Symmetric Binaphthyls" *J. Org. Chem.* **1994**, *59*, 2655–2658; (b) Satyanarayana, K.; Srinivas, K.; Himabindu, V.; Reddy M. G. "A Scaleable Synthesis of Dutasteride: A Selective 5 α -Reductase Inhibitor" *Org. Process Res. Dev.* **2007**, *11*, 842–845; (c) E vano, G.; Toumi, M.; Coste A. "Copper catalyzed cyclization reactions for the synthesis of alkaloids" *Chem. Commun.* **2009**, 4166–4175. (d) Yang, L.; Deng, G.; Wang, D.-X.; Huang, Z.-T.; Zhu, J.-P.; Wang, M.-X. "Highly Efficient and Stereoselective N-Vinylation of Oxiranecarboxamides and Unprecedented 8-endo-Epoxy-arene Cyclization: Expedient and Biomimetic Synthesis of Some *Clausena* Alkaloids" *Org. Lett.* **2007**, *9*, 1387–1390.
3. For reviews of copper-catalyzed reactions, see: (a) Lindley, J. "Copper assisted nucleophilic substitution of aryl halogen" *Tetrahedron* **1984**, *40*, 1433–1456; (b) Sawyer, J. S. "Recent Advances in Diaryl Ether Synthesis" *Tetrahedron.* **2000**, *56*, 5045–5065; (c) Monnier, F.; Taillefer, M. "Catalytic C=C, C=N, and C=O Ullmann-Type Coupling Reaction" *Angew. Chem. Int. Ed.* **2009**, *48*, 6954–6971.
4. (a) Fagan, P. J.; Hauptman, E.; Shapiro, R.; Casalnuovo, A. "Using Intelligent/Random Library Screening To Design Focused Libraries for the Optimization of Homogeneous Catalysts: Ullmann Ether Formation" *J. Am. Chem. Soc.* **2000**, *122*, 5043–5051; (b) Qian, C.; Xu, S.; Fang, D.; Zong, Q. "Copper-Catalyzed Synthesis of Triarylaminines from Aryl Halides and Arylaminines" *Chin. J. Chem.* **2012**, *30*, 1881–1885.
5. Ma, D.; Cai, Q. "L-Proline Promoted Ullmann-Type Coupling Reactions of Aryl Iodides with Indoles, Pyrroles, Imidazoles or Pyrazole" *synlett* **2004**, 0128–0130.
6. (a) Ma, D.; Cai, Q.; Zhang, H. "N,N-Dimethyl Glycine-Promoted Ullmann Coupling Reaction of Phenols and Aryl Halides" *Org. Lett.* **2003**, *5*, 3799–3802; (b) Cai, Q.; Zou, B.; Ma, D. "Mild Ullmann-Type Biaryl Ether Formation Reaction by Combination of ortho-Substituent and Ligand Effects" *Angew. Chem. Int. Ed.* **2006**, *45*, 1276–1279.

7. (a) Cai, Q.; He, G.; Ma, D. "Mild and Non-racemizing Conditions for Ullmann-type Diaryl Ether Formation between Aryl Iodides and Tyrosine Derivatives" *J. Org. Chem.* **2006**, *71*, 5268–5273; (b) Ma, D.; Zhang, Y.; Yao, J.; Wu, S.; Tao, F. "Accelerating Effect Induced by the Structure of R-Amino Acid in the Copper-Catalyzed Coupling Reaction of Aryl Halides with R-Amino Acids. Synthesis of Benzolactam-V8" *J. Am. Chem. Soc.* **1998**, *120*, 12459–12467.
8. (a) Altman, A. R.; Buchwald, L. S. "4,7-Dimethoxy-1,10-phenanthroline: An Excellent Ligand for the Cu-Catalyzed N-Arylation of Imidazoles" *Org. Lett.* **2006**, *8*, 2779–2782; (b) Wolter, M.; Nordmann, G.; Job, E. G.; Stephen, L.; Buchwald, L. S. "Copper-Catalyzed Coupling of Aryl Iodides with Aliphatic Alcohols" *Org. Lett.* **2002**, *4*, 973–976; (c) Kiyomori, A.; Marcoux, J. F.; Buchwald, S. L. "An efficient copper-catalyzed coupling of aryl halides with imidazoles" *Tetrahedron Lett.* **1999**, *40*, 2657–2660.
9. (a) Sedelmeier, J.; Bolm, C. "Efficient Copper-Catalyzed N-Arylation of Sulfoximines with Aryl Iodides and Aryl Bromide" *J. Org. Chem.* **2005**, *70*, 6904–6906; (b) Jiang, L.; Job, E.; Klapars, A. G.; Buchwald, L. S. "Copper-Catalyzed Coupling of Amides and Carbamates with Vinyl Halides" *Org. Lett.* **2003**, *5*, 3667–3669; (c) Antilla, C. J.; Baskin, M. J.; Barder, E. T.; Buchwald, L. S. "Copper-Diamine-Catalyzed N-Arylation of Pyrroles, Pyrazoles, Indazoles, Imidazoles, and Triazoles" *J. Org. Chem.* **2004**, *69*, 5578–5587; (d) Klapars, A. X.; Buchwald, L. S. "A General and Efficient Copper Catalyst for the Amidation of Aryl Halides" *J. Am. Chem. Soc.* **2002**, *124*, 7421–7428.
10. Gujadhur, R. K.; Venkataraman, D. "synthesis of diaryl ethers using an easy-to-prepare, air-stable, soluble copper(I) catalyst" *Synth. Commun.* **2001**, *31*, 2865–2879.
11. Buck, E.; Song, Z. J.; Tschäen, D.; Dormer, P. G.; Volante, R. P.; Reider, P. "Ullmann Diaryl Ether Synthesis: Rate Acceleration by 2,2,6,6-Tetramethylheptane-3,5-dione" *Org. Lett.* **2002**, *4*, 1623–1626.
12. Palomo, C.; Oiarbide, M.; Lopez, R.; Gomez-Bengoa, E. "Phosphazene P₄-Bu^t base for the Ullmann biaryl ether synthesis" *Chem. Commun.* **1998**, 2091–2092.
13. Shafir, A.; Buchwald, L. S. "Highly Selective Room Temperature Copper-Catalyzed C–N Coupling Reaction" *J. Am. Chem. Soc.* **2006**, *128*, 8742–8743.
14. Gujadhur, R. K.; Bates, C. G.; Venkataraman, D. "Formation of Aryl–Nitrogen, Aryl–Oxygen, and Aryl–Carbon Bonds Using Well-Defined Copper(I)-Based Catalysts" *Org. Lett.* **2001**, *3*, 4315–4317.

15. Rovira, M.; Soler, M.; Güell, I.; Wang, M.; Gomez, L.; Ribas X. “Orthogonal Discrimination among Functional Groups in Ullmann-Type C–O and C–N Couplings” *J. Org. Chem.* **2016**, *81*, 7315–7325; (b). Damkaci, F.; Sigindere, C.; Sobiech, T.; Vik, E.; Malone, J. “*N*-Picolinamides as ligands in Ullman type C–O coupling reactions” *Tetrahedron Lett.* **2017**, *58*, 3559–3564.
16. Lv, X.; Bao, W. A. “ β -Keto Ester as a Novel, Efficient, and Versatile Ligand for copper(I) catalyzed C–N, C–O and C–S Coupling Reactions” *J. Org. Chem.* **2007**, *7*, 3863–3867.
17. Maiti, D.; Buchwald S. L. “Cu-Catalyzed Arylation of Phenols: Synthesis of Sterically Hindered and Heteroaryl Diaryl Ethers” *J. Org. Chem.* **2010**, *75*, 1791–1794.
18. Qian, C.; Qin, L.; Zong, Q.; Wu, L.; Fang, D. “Aminophenols as Efficient Ligand for Copper-Catalyzed Ullmann-type Synthesis of Diaryl Ethers” *Bull. Korean Chem. Soc.* **2013**, *34*, 3915–3918.
19. Zhang, Y.; Yang, X.; Yao, Q.; Ma, D. “Cu/DMPAO-Catalyzed *N*-Arylation of Acyclic Secondary Amines” *Org. Lett.* **2012**, *14*, 3056–3059.
20. (a) Ouali, A.; Spindler, J. F.; Cristau, H. J.; Taillefer, M. “Mild Conditions for Copper-Catalyzed Coupling Reaction of Phenols and Aryl Iodides and Bromides” *Adv. Synth. Catal.* **2006**, *348*, 499–505; (b) Cristau, H. J.; Cellier, P. P.; Hamada, S.; Spindler, J. F.; Taillefer, M. “A General and Mild Ullmann-Type Synthesis of Diaryl Ethers” *Org. Lett.* **2004**, *6*, 913–916.
21. Aljaar, N.; Malakar, C. C.; Conrad, J.; Strobel, S.; Thomas Schleid, T.; Beifuss, U. “Cu-Catalyzed Reaction of 1,2-Dihalobenzenes with 1,3-Cyclohexanediones for the Synthesis of 3,4-Dihydrodibenzo[*b,d*]furan-1(2*H*)-ones” *J. Org. Chem.* **2012**, *77*, 7793–7803.
22. Kwong, F. Y.; Buchwald, S. L. “Mild and Efficient Copper-Catalyzed Amination of Aryl Bromides with Primary Alkylamines” *Org Lett.*, **2003**, *5*, 793–796.
23. Chen, Y.; Wei, X.; Xie, H.; Deng, H. “Antioxidant 2-Phenyl- benzofurans and a Coumestan from *Lespedeza virgata*.” *J. Nat. Prod.* **2008**, *71*, 929–932.
24. Li, C. C.; Xie, X. Z.; Zhang, D. Y.; Chen, H. J.; Yang, Z. “Total Synthesis of Wedelolactone” *J. Org. Chem.* **2003**, *68*, 8500–8504.
25. Oliveira, A. M. A. G.; Raposo, M. M. M.; Oliveira-Campos, A. M. F.; Machado, A. E. H.; Puapairoj, P.; Pedro, M.; Nascimento, M. S. J.; Portela, C.; Afonso, C.; Pinto,

- M. "Psoralen analogues: synthesis, inhibitory activity of growth of human tumor cell lines and computational studies" *Eur. J. Med. Chem.* **2006**, *41*, 367–372.
26. Anderson, C. J.; Denton M. R.; and Wilson, C. "A Biomimetic Strategy for the Synthesis of the Tricyclic Dibenzofuran-1,4-dione Core of Popolohuanone E" *Org. Lett.* **2005**, *7*, 123–125.
27. (a) Ergun, M.; Dengiz, C.; Ozer, M. S.; Sahin, E.; Balci, M. "Synthesis of thio- and furan-fused heterocycles: furopyranone, fuopyrrolone, and thienopyrrolone derivatives" *Tetrahedron* **2014**, *70*, 5993–5998; (b) Lombaert, D. S.; Blanchard, L.; Stamford, L. B.; Tan, J.; Wallace, E. M.; Satoh, Y.; Fitt, J.; Hoyer, D.; Simonsbergen, D.; Moliterni, J.; Marcopoulos, N.; Savage, P.; Chou, M.; Trapani, A. J.; Jeng, A. Y. "Potent and Selective Non-Peptidic Inhibitors of Endothelin-Converting Enzyme-1 with Sustained Duration of Action" *J. Med. Chem.* **2000**, *43*, 488–504; (c) Love, B. E. "Isolation and synthesis of polyoxygenated dibenzofurans possessing biological activity" *Eur. J. Med. Chem.* **2015**, *97*, 377–387.
28. Carney, R. J.; Krenisky, M. J.; Williamson, T. R.; Luo, J. "Achyrofurane, a New Antihyperglycemic Dibenzofuran from the South American Medicinal Plant *Achyrocline satureioides*" *J. Nat. Prod.* **2002**, *65*, 203–205.
29. (a) Voigt, B.; Meijer, L.; Lozach, O.; Schachtele, C.; Totzke, F.; Hilgeroth, A. "Novel CDK inhibition profiles of structurally varied 1-aza-9-oxafluorenes" *Bioorg. Med. Chem. Lett.* **2005**, *15*, 823–825. (b) Miller, C. P.; Collini, D. M.; Harris, A. H. "Constrained phytoestrogens and analogues as ER β selective ligands" *Bioorg. Med. Chem. Lett.* **2003**, *13*, 2399–2403.
30. Sanz, R.; Fernandez, Y.; Castroviejo, M. P.; Pe´rez, A.; Fan˜ana's, F. J. "A Route to Regioselectively Functionalized Carbazoles, Dibenzofurans, and Dibenzothiophenes through Anionic Cyclization of Benzyne-Tethered Aryllithiums" *J. Org. Chem.* **2006**, *71*, 6291–6294.
31. Zhang, Y.-M.; Razler, T.; Jackson, P. F. "Synthesis of pyrimido [4,5-*b*] indoles and benzo[4,5]furo[2,3-*d*]pyrimidines via palladium-catalyzed intramolecular arylation" *Tetrahedron Lett.* **2002**, *43*, 8235–8239.
32. De Lombaert, S.; Blanchard, L.; Stamford, L. B.; Tan, J.; Wallace, E. M.; Satoh, Y.; Fitt, J.; Hoyer, D.; Simonsbergen, D.; Moliterni, J.; Marcopoulos, N.; Savage, P.; Chou, M.; Trapani, A. J.; Jeng, A. Y. "Potent and Selective Non-Peptidic Inhibitors of Endothelin-Converting Enzyme-1 with Sustained Duration of Action" *J. Med. Chem.* **2000**, *43*, 488–504.

33. Xiao, B.; Gong, T.; Liu, Z.; Liu, J.; Luo, D.; Xu, J.; Liu, L. "Synthesis of Dibenzofurans via Palladium-Catalyzed Phenol-Directed C–H Activation/C–O Cyclization" *J. Am. Chem. Soc.* **2011**, *133*, 9250–9253.
34. Wei, Y.; Yoshika, N. "Oxidative Cyclization of 2-Arylphenols to Dibenzofurans under Pd(II)/Peroxybenzoate Catalysis" *Org. Lett.* **2011**, *13*, 5504–5507.
35. Kawaguchi, K.; Nakano, K.; Nozaki, K. J. "Synthesis of Ladder-Type π -Conjugated Heteroacenes via Palladium-Catalyzed Double N-Arylation and Intramolecular O-Arylation" *Org. Chem.* **2007**, *72*, 5119–5128.
36. Liu, J.; Fitzgerald, E. A.; Mani, S. N. J. "Facile Assembly of Fused Benzo[4,5]furo Heterocycles" *Org. Chem.* **2008**, *73*, 2951–2954.
37. Zhao, J.; Wang, Y.; He, Y.; Liu, L.; Zhu, Q. "Cu-Catalyzed Oxidative C(sp²)-H Cycloetherification of *o*-Arylphenols for the Preparation of Dibenzofurans" *Org. Lett.* **2012**, *14*, 1078–1081.
38. Takahashi, S.; Suda, Y.; Nakamura, T.; Matsuoka, K.; Koshino, H. "Synthesis of 3-phenyldibenzo[*b,d*]furan-type bioprobes utilizing vialinin B as a structural motif" *Synth. Commun.* **2017**, *47*, 22–28.
39. Moon, Y.; Kim, Y.; Hong, H.; and Hong, S. "Synthesis of heterocyclic-fused benzofurans via C–H functionalization of flavones and coumarins" *Chem. Commun.* **2013**, *49*, 8323–8325.
40. Miller, P. C.; Collini, D. M.; and Harris, A. H. "Constrained phytoestrogens and analogues as ER β selective ligands" *Bioorg. Med. Chem. Lett.* **2003**, *13*, 2399–2403.
41. Dai, C.; Sun, X.; Tu, X.; Wu, L.; Zhan, D.; Zeng, Q. "Synthesis of phenothiazines via ligand-free CuI-catalyzed cascade C–S and C–N coupling of aryl *ortho*-dihalides and *ortho*-aminobenzenethiols" *Chem. Commun.* **2012**, 5367–5369.
42. Yaeghoobi, M.; Frimayanti, N.; Chee, F. C.; Ikram, K. K.; Najjar, O. B.; Zain, M. S.; Abdullah, Z.; Wahab, A. H.; Rahman, A. N. "QSAR, in silico docking and vitro evaluation of chalcone derivatives as potential inhibitors for H₁N₁ virus neuraminidase" *Med. Chem. Res.* **2016**, *25*, 2133–2142.
43. Lokhande D. P.; SakateKiran S. S.; Taksande N. K.; Navghare, B. "Dimethylsulfoxide-iodine catalyzed deprotection of 2'-allyloxychalcones: synthesis of flavones" *Tetrahedron Lett.* **2005**, *46*, 1573–1574.





Chapter-4

*Synthesis, estrogen receptor binding affinity and
molecular docking of pyrimidine-piperazine-
chromene and -quinoline conjugates*

Bioorg. Med. Chem. Lett. **2017**, 27, 4493–4499

4.1. Introduction

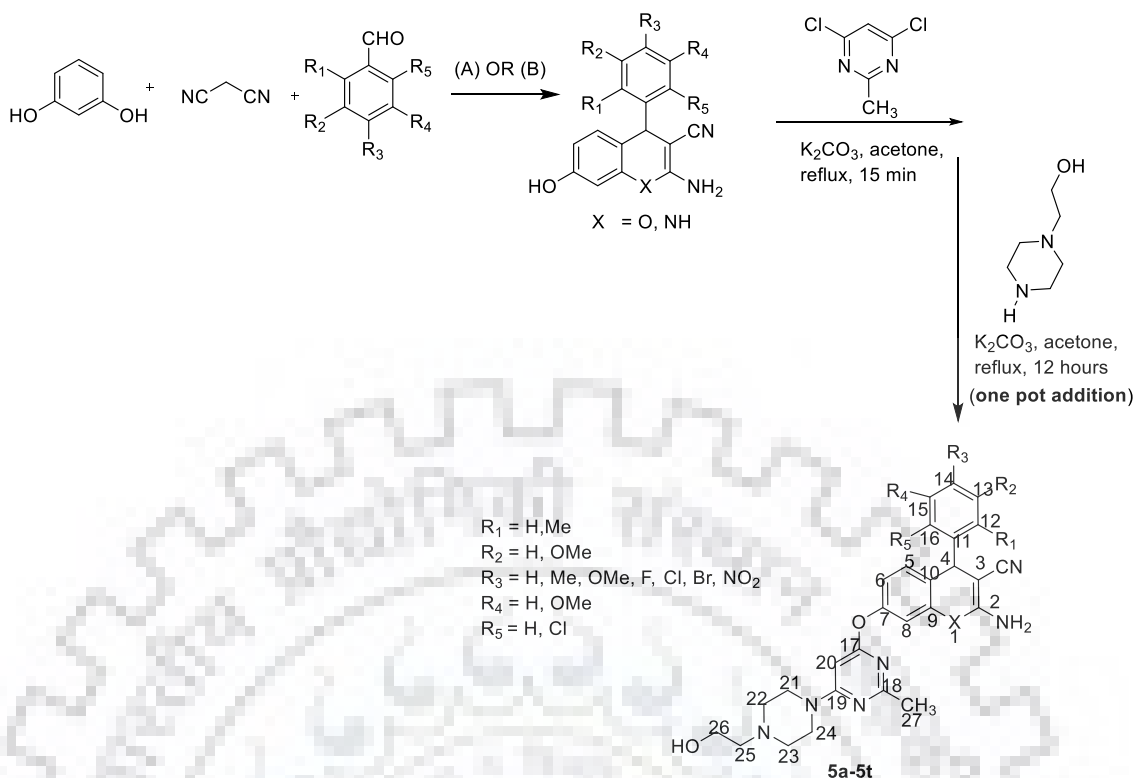
Cancer is deadliest disease and almost affects every society in every country. Breast cancer is the most prevalent cancer in women (25% of all cancers) with an approximately 1.67 million new cases diagnosed in 2012 [1]. The incidence of cancer cases is increasing day by day because of change in life style and other risk factors like overweight, physical inactivity, smoking, mutations in anticancer gene and aberrant expression of some proteins/protein kinases [2]. Estrogen, a female sex hormone, play vital role in the development and growth of breast tumors. Around 80% of breast cancers occur in post-menopausal women whose ovarian estrogen production has ceased with remaining estrogens originating in extra-glandular tissues. Several symptoms suggest that the tumorigenesis is a multi-step process that replicates genetic mutation and progressive alteration of normal human cells into a highly malignant derivatives [3]. It was also found that progesteron and estrogen receptors take part in proliferation of breast cancers. Approximately 80% estrogen receptor (called estrogen receptor a and estrogen receptor b) modulate the target gene expression *via* transcription factor and signal transducers [4]. However, ERa is a major regulator of breast cancer progression. It can be classified on the basis of their ERa status *i.e.* ERa-positive and ERa-negative, related with better prognosis and response to hormone therapy treatment [5]. ERa acts as a ligand-activated transcription which belong to the family of nuclear steroid receptors and binds towards 17b-estradiol (E₂), with specific DNA sequence (ERE), E₂-liganded-ER (E₂-ER) with co-activator proteins and RNA polymerase II components to transcription initiation complex in the promoters of target genes in the nucleus [6].The steroid hormone receptors (SHRs) also recognize the derivatives of naturally occurring non-steroidal and steroidal hormones, either as agonist and antagonists in the hormone dependent breast cancers (HDBC) prevention and cure, depending on their interaction with steroid hormone receptors (SHRs) [7–9]. Breast cancer diagnosis and development of selective estrogen receptors modulators (SERMs) has been improved through exploration of developing drug tamoxifen (TAM) and other selective ER modulators [10–12]. During chemotherapy, some unnecessary side effects are often observed where drugs failed to kill cancerous cells selectively without harming the normal cells. However, some unnecessary side effects are often observed where drugs failed to kill cancerous cells selectively. Therefore, it is a challenge to develop new cancer drugs for the pharmaceutical industry and the scientific community. During the past decades, bioconjugate biomolecules bearing unnatural organic structures have found an increasing

number of applications in molecular and cell biology. Conjugated groups provide biomolecules with novel properties that include fluorescence emission, catalytic activity, altered hydrophobicity or bio-affinity, resistance toward biodegradation and the ability to carry metal-ions [13]. 4-Aryl-4*H*-chromene and quinoline derivatives also showed wide range of biological applications [14] and used as potent apoptosis inducers [15]. In addition, an assortment of compounds bearing a pyrimidine ring [16-18] and substituted piperazine [19-24] have been shown cytotoxic effects against human cancers. Therefore, we synthesized a series of 2-amino-7-((6-(4-(2-hydroxyethyl) piperazine 1-yl)-2-methyl pyrimidin-4-yl)oxy)-4-phenyl-4*H*-chromene-3- carbonitriles and 2-amino-7-((6-(4-(2-hydroxyethyl)piperazin-1-yl)-2-methylpyrimidin-4-yl)oxy)-4-phenyl-1,4-dihydroquinoline-3-carbonitriles. Further, we accomplished SAR (Structure activity relationship) and molecular docking studies to get the best compounds **5f**, **5g** and **5o** against Bcl-2 protein, a breast cancer causing protein to see the interactions and to establish the correlations both in vitro and in silico studies.

4.2. Results and discussion

4.2.1. Chemistry

2-Amino-7-hydroxy-4-phenyl-4*H*-chromene-3-carbonitrile derivatives were synthesized using piperazine base and water solvent heated at 80 °C for 2 h. While, one pot synthesis for novel compounds 2-amino-7-((6-(4-(2-hydroxyethyl) piperazin-1-yl)- 2-methylpyrimidin-4-yl)oxy)-4-phenyl-4*H*-chromene-3-carbonitriles were obtained from a three-component reaction of 2-amino-7-hydroxy-4-phenyl-4*H*-chromene-3-carbonitrile, 4,6-dichloro-2- methyl pyrimidine and 2-(piperazin-1-yl)ethanol using acetone solvent in the presence of K₂CO₃ base under reflux condition for 12 h with excellent yield (90–97%). Similarly, 2-amino-7- hydroxy-4-phenyl-1,4-dihydroquinoline-3-carbonitrile derivatives were synthesized in the presence of ammonium acetate in water solvent, heated at 80 °C for 2 h. Then, 2-amino-7-((6-(4-(2-hydroxyethyl) piperazin-1-yl)-2-methyl pyrimidin-4-yl)oxy)-4-phenyl-1,4-dihydroquinoline-3-carbonitriles were synthesized using three components one pot reaction of 2-amino-7-hydroxy-4-phenyl-1,4- dihydroquinoline-3-carbonitrile, 4,6-dichloro-2-methyl pyrimidine and 2-(piperazin-1-yl) ethanol in acetone solvent with K₂CO₃ base under reflux condition for 12 h with excellent yield (91–94%) (Scheme 4.1)

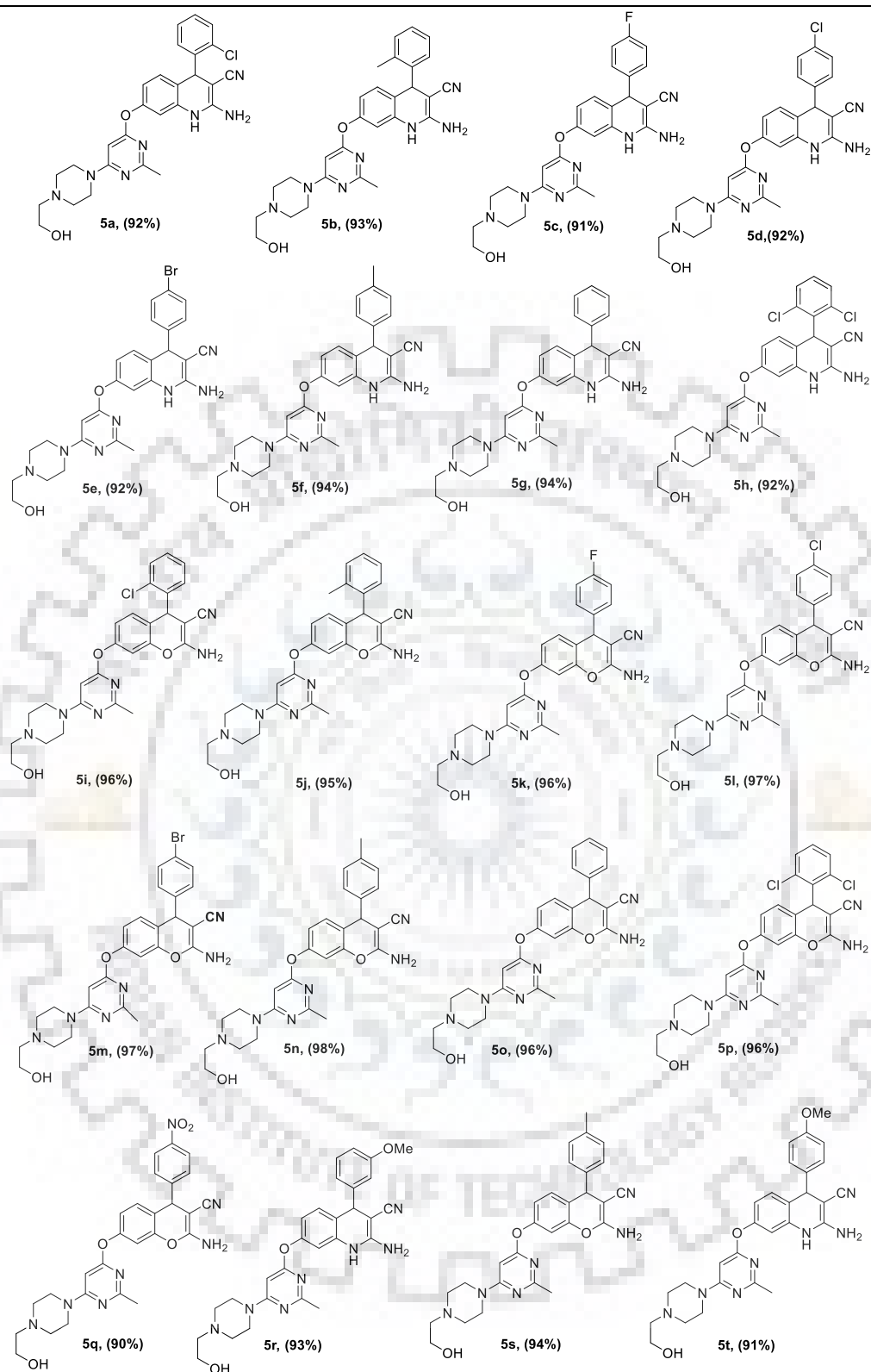


Condition (A) for X= O: piperazine, water (solvent), 80 °C and Condition (B) for X= NH: ammonium acetate, water (solvent), 80 °C.

Scheme: 4.1. Synthesis of pyrimidine-piperazine-chromene and -quinoline conjugates

4.2.1.1. Structure determination

The synthesized compounds were confirmed on the basis of their spectral data i.e. ¹H NMR, ¹³C NMR, IR spectra and APCI-ESI/Mass spectra. For example, compound **5e** i.e. 2-amino-4-(4-bromophenyl)-7-((6-(4-(2-hydroxyethyl)piperazin-1-yl)-2-methylpyrimidin-4-yl)oxy)-1,4-dihydroquinoline-3-carbonitrile in the ¹H NMR spectra, the characteristic singlet signal of -CH₃ (H-27) at 2.39 ppm and multiplet of six protons (H-22,23 and 25) at 2.59–2.53 ppm, triplet of four protons (H-21 and 24) at d 3.59 ppm and triplet of two proton (H-26) at d 3.64 ppm. Singlet of two proton of NH₂ at d 4.68 ppm attached with chromene moiety and singlet of tertiary carbon (H-13) of chromene moiety at d 4.69 ppm and singlet of (H-17) at d 5.71 ppm confirmed the structure of C₂₇H₂₈BrN₇O₂. In ¹³C NMR spectral signal of -CH₃ (C-27) at 26 and C-20 at 84.0, C-4 at 57.9, C-17 at 167.8 and C=O (C-7) at 169.9 ppm indicated the conformation of synthesized compound. In IR spectroscopy, peak at 3400 (-OH), 3200 (-NH₂ have two bend), 2217 (-C=N), 1640 (-C=C), 1542 (-C=N), 1100 (-C=O), 580 (C-Br) satisfied the product structure. Further, the product was concluded by APCI-MS mass spectroscopy.



Scheme 4.2. Substrate scope of pyrimidine-piperazine-chromene and -quinoline conjugates.

The molecular ion peak m/z at (M) 546.1 and (M+2) 548.1 of $C_{27}H_{28}BrN_7O_2$ (expected = 546.1, 548.1) was supported a molecular composition, provided the formation of the product.

4.2.2. Biology

4.2.2.1. MTT assay

Biological activity of all synthesized compounds **5a-5t** was confirmed by performing MTT assay on the human breast cancer cell lines (MCF-7). For cell cytotoxicity studies normal cells named human embryonic kidney cells (HEK293), was used. MTT assay was performed according to standard protocol [25]. In brief, exponentially growing MCF-7 and HEK293 cells were seeded in a 96-well micro liter plate (approximately 9000 cells per well). Subsequently cells were treated with varying concentrations (5 μ M to 200 μ M) of inhibitors. Curcumin was used as a positive control for both cytotoxicity and activity studies. After 48hrs, the whole mixture containing media and inhibitor was aspirated from the cells followed by 2 time washing with PBS, then 100 μ L DMEM and 20 μ L MTT (from 5mg/mL stock) was added to each well. Plates were incubated for 4-5hr at 37 °C in a CO₂ incubator.

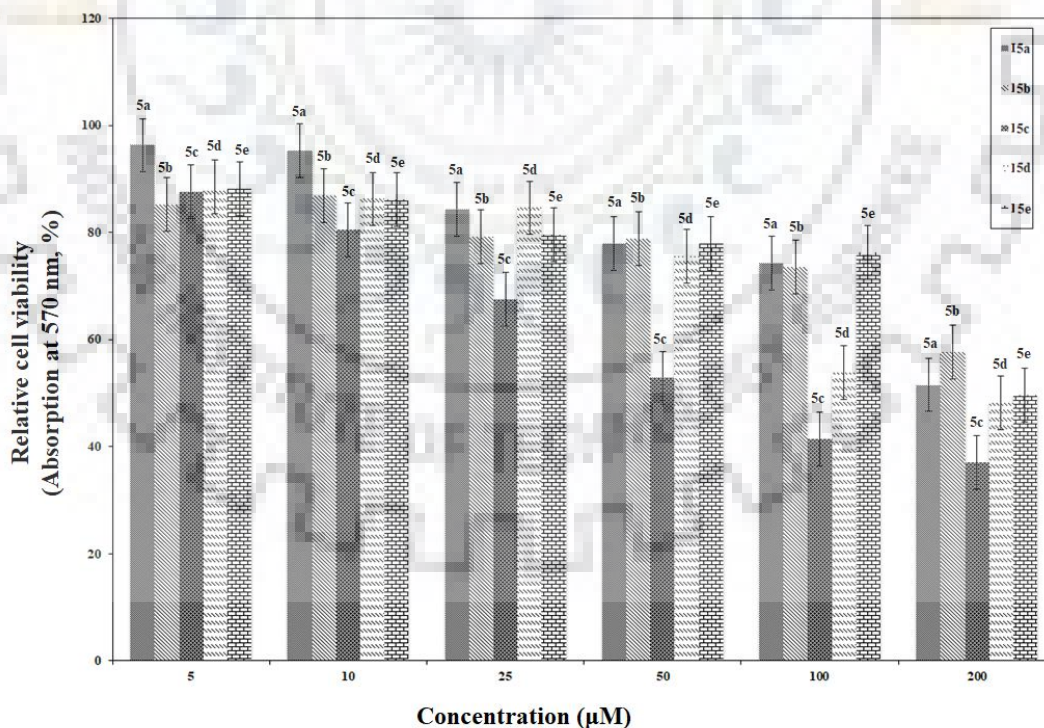


Figure.4.1. Effect of synthesized compounds **5a** to **5e** on the viability of HEK293 cells. HEK293 cells were incubated with the denoted concentrations of each compound for 48 h. The cell viabilities were evaluated by MTT assay. Data represent three independent sets of experiments and results are shown as the mean \pm SD.

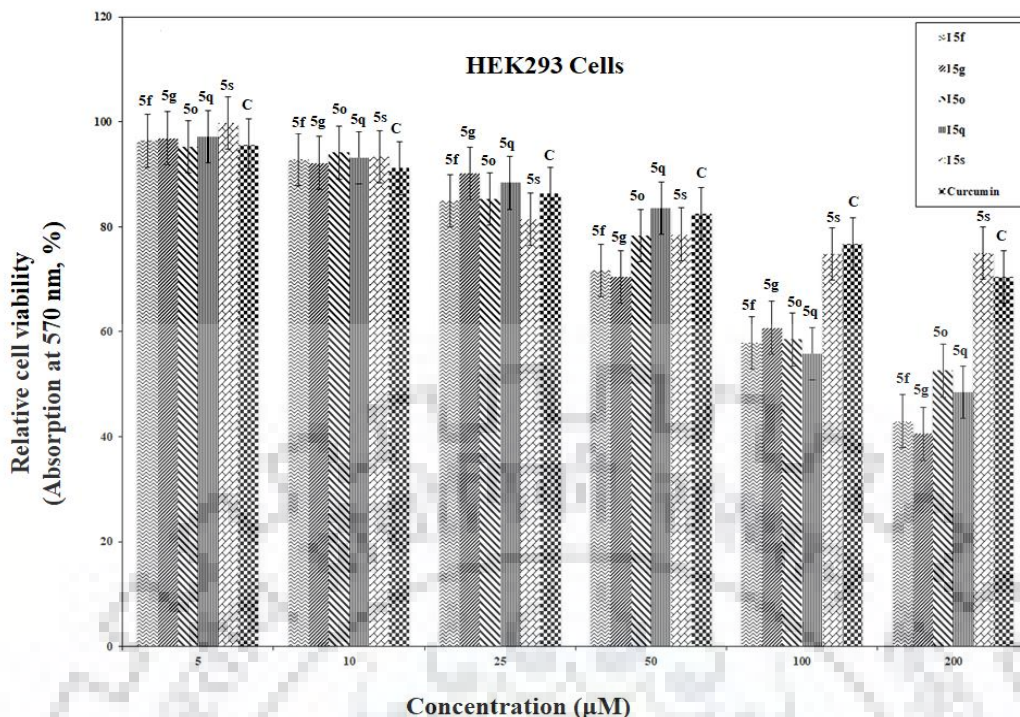


Figure.4.2. Effect of synthesized compounds **5f**, **5g**, **5o**, **5q** and **5s** on the viability of HEK293 cells. HEK293 cells were incubated with the denoted concentrations of each compound for 48 h. The cell viabilities were evaluated by MTT assay. Curcumin is used as a positive control. Data represent three independent sets of experiments and results are shown as the mean \pm SD.

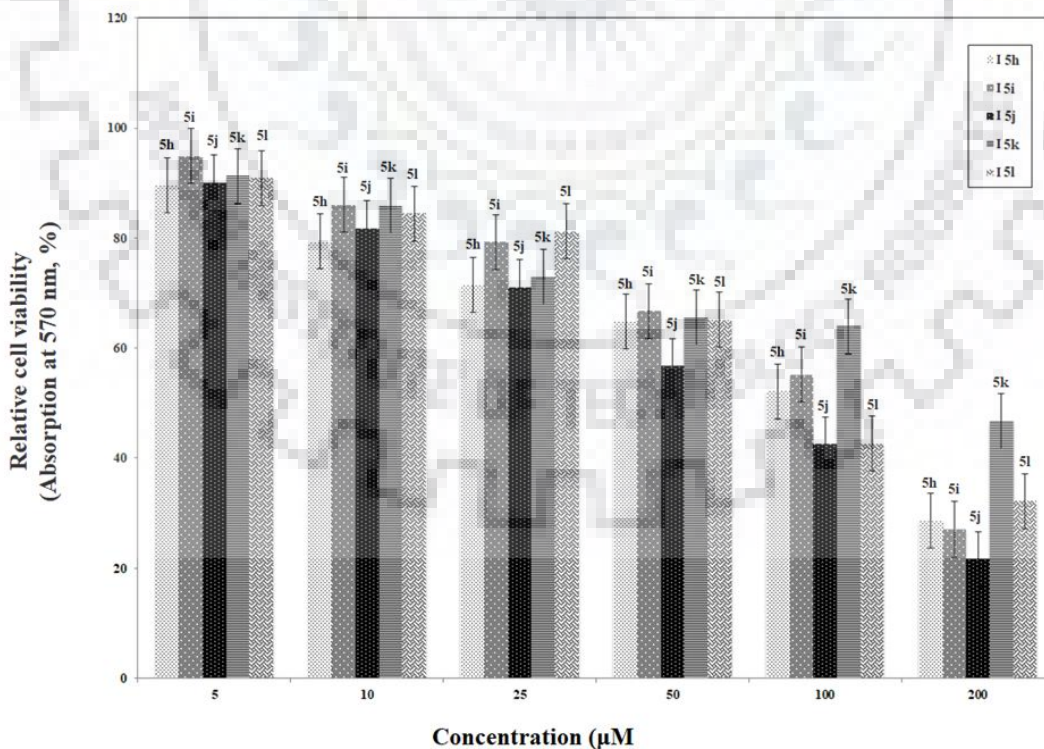


Figure.4.3. Effect of synthesized compounds **5h** to **5l** on the viability of HEK293 cells. HEK293 cells were incubated with the denoted concentrations of each compound for 48

h. The cell viabilities were evaluated by MTT assay. Data represent three independent sets of experiments and results are shown as the mean \pm SD.

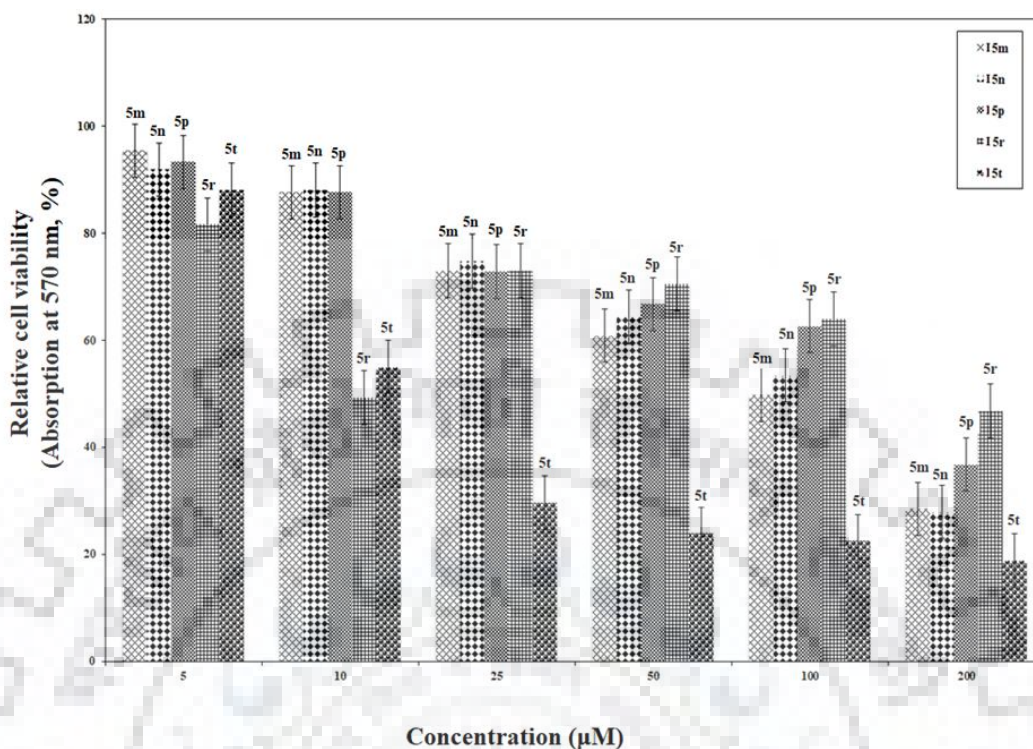


Figure.4.4. Effect of synthesized compounds **5m**, **5n**, **5p**, **5r** and **5t** on the viability of HEK293 cells. HEK293 cells were incubated with the denoted concentrations of each compound for 48 h. The cell viabilities were evaluated by MTT assay. Data represent three independent sets of experiments and results are shown as the mean \pm SD.

After that, the remaining medium was pipetted out using a multi-channel pipette carefully to leave the formazan crystals formed behind. Finally, to dissolve the formazan crystals, in each well, 100 μ L DMSO was added. The plates were then agitated for 15-20 minutes on an orbital plate shaker after which they were read immediately on titer plate reader (BioRad) at 570 nm.

The percentages of relative cell viabilities were estimated by comparing the viability of the treated cells with that of the control [26]. To study the functional significance of synthesized inhibitors, we examined the anti-cancer activity and cytotoxicity on human cancer cell line and normal cell lines respectively. To address the anti-cancerous activity of these inhibitors, we performed MTT on cancerous cell line (MCF-7) and to check the cytotoxic nature of synthesized inhibitors, HEK293 cells were used. As shown in Figure 3.2, no significant cytotoxicity was observed when varying concentration. Inhibitors **5f**, **5g**, **5o**, **5q** and **5s** were used in a dose-dependent manner.

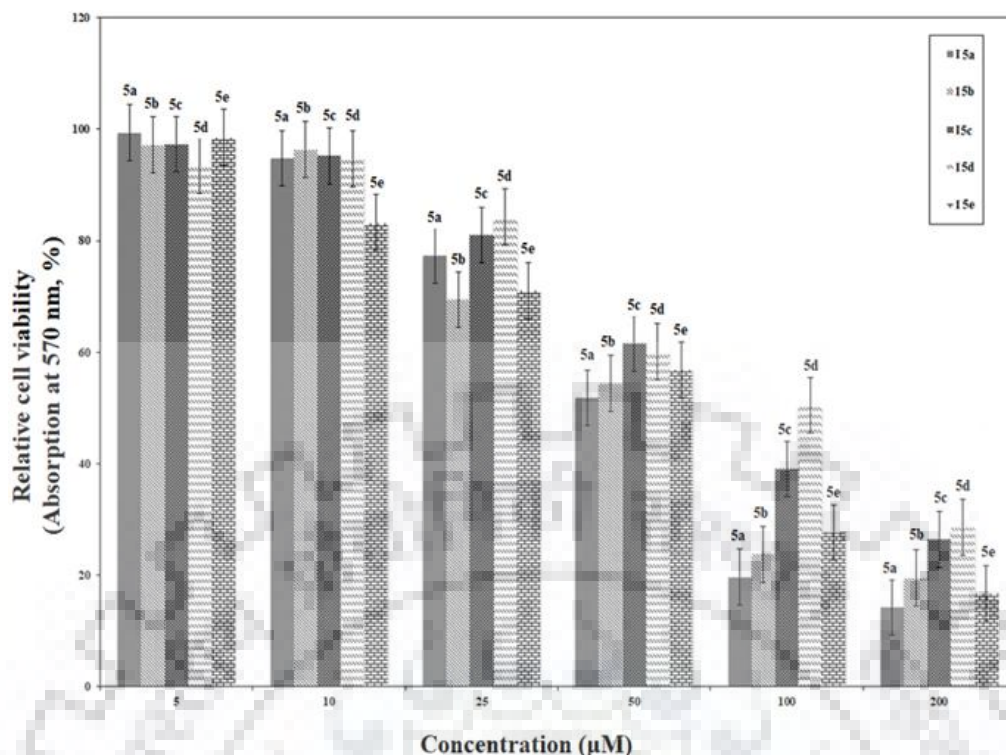


Figure.4.5. Effect of synthesized compounds **5a**, **5b**, **5c**, **5d** and **5e** on the viability of human breast cancer MCF-7 cells. MCF-7 cells were incubated with the denoted concentrations of each compound for 48 h. The cell viabilities were evaluated by MTT assay. Data represent three independent sets of experiments and results are shown as the mean \pm SD.

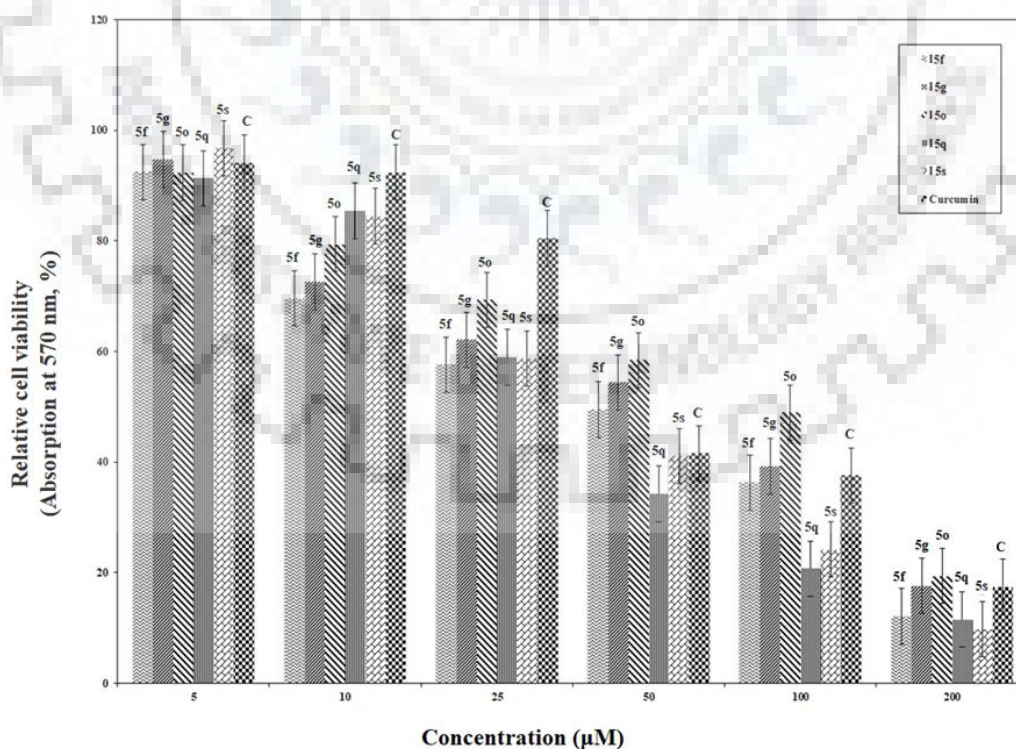


Figure.4.6. Effect of synthesized compounds **5f**, **5g**, **5o**, **5q** and **5s** on the viability of MCF-7 cells. MCF-7 cells were incubated with the denoted concentrations of each compound for 48 h. The cell viabilities were evaluated by MTT assay. Curcumin is used

as a positive control. Data represent three independent sets of experiments and results are shown as the mean \pm SD.

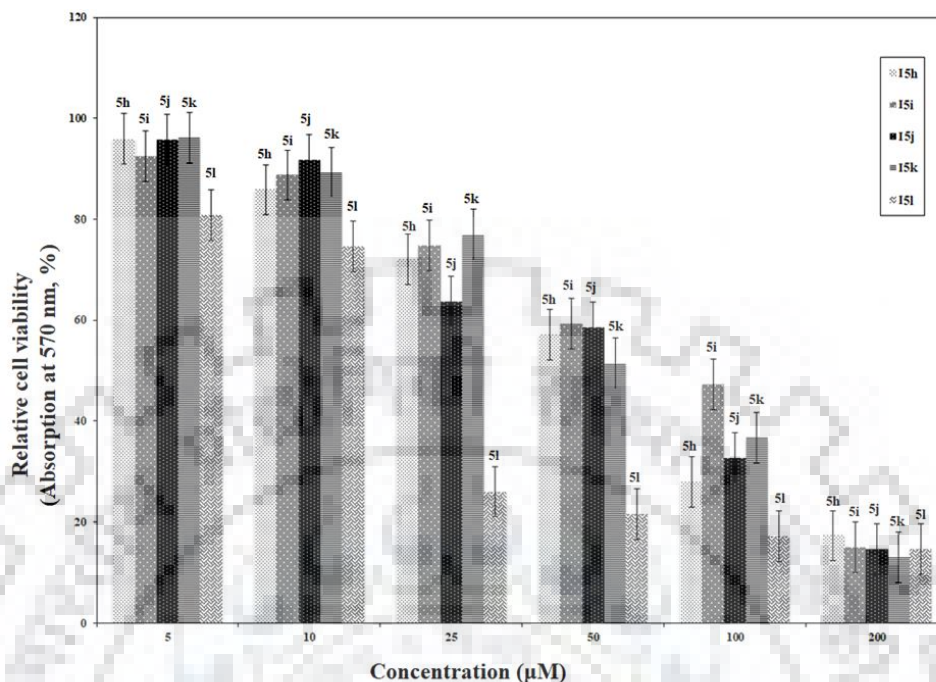


Figure.4.7. Effect of synthesized compounds **5h**, **5i**, **5j**, **5k**, and **5l** on the viability of human breast cancer MCF-7 cells. MCF-7cells cells were incubated with the denoted concentrations of each compound for 48 h. The cell viabilities were evaluated by MTT assay. Data represent three independent sets of experiments and results are shown as the mean \pm SD.

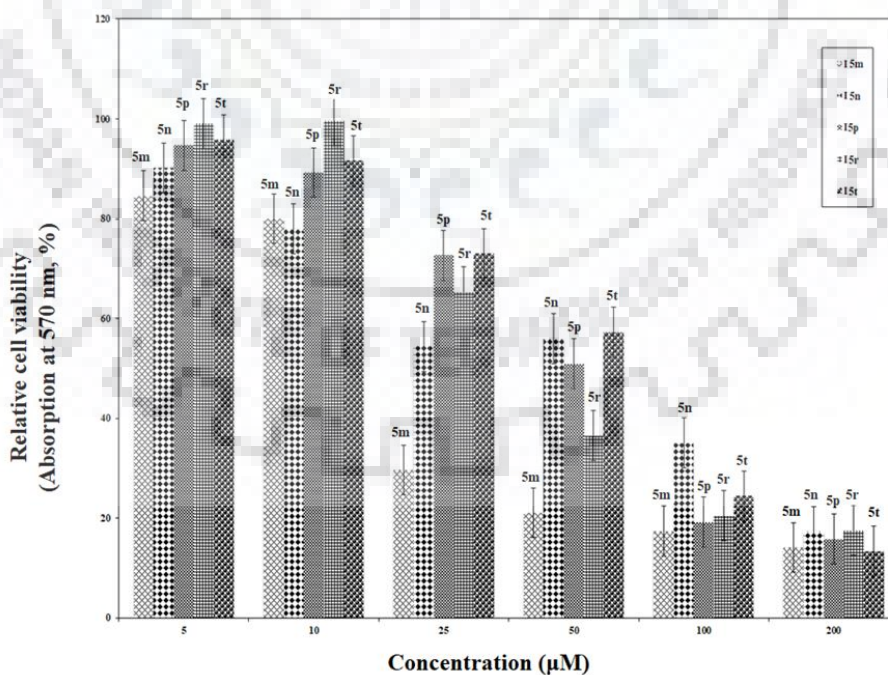


Figure.4.8. Effect of synthesized compounds **5m**, **5n**, **5p**, **5r** and **5t** on the viability of human breast cancer MCF-7 cells. MCF-7cells cells were incubated with the denoted concentrations of each compound for 48 h. The cell viabilities were evaluated by MTT

assay. Data represent three independent sets of experiments and results are shown as the mean \pm SD.

Table.4.1. Shows the calculated IC₅₀ values of synthesized compounds on MCF-7 and HEK-293 cells

S. No	R ₁	R ₂	R ₃	R ₄	R ₅	X	IC ₅₀ (μ M) (MCF -7 cells)	IC ₅₀ (μ M) (HEK-293 cells)
1	Cl	H	H	H	H	NH	190 \pm 2.01	70 \pm 1.22
2	Me	H	H	H	H	NH	198 \pm 1.83	57 \pm 1.23
3	H	H	F	H	H	NH	48 \pm 1.60	72 \pm 2.11
4	H	H	Cl	H	H	NH	170 \pm 1.71	95 \pm 2.10
5	H	H	Br	H	H	NH	193 \pm 3.22	62 \pm 1.80
6	H	H	Me	H	H	NH	48 \pm 1.70	140 \pm 3.22
7	H	H	H	H	H	NH	65 \pm 1.13	141 \pm 2.10
8	Cl	H	H	H	Cl	NH	102 \pm 1.77	62 \pm 1.22
9	Cl	H	H	H	H	O	119 \pm 1.22	79 \pm 1.77
10	Me	H	H	H	H	O	61 \pm 1.31	56 \pm 1.06
11	H	H	F	H	H	O	166 \pm 3.12	52 \pm 1.22
12	H	H	Cl	H	H	O	73 \pm 1.07	18 \pm 1.10
13	H	H	Br	H	H	O	91 \pm 1.13	19 \pm 1.80
14	H	H	OMe	H	H	O	104 \pm 2.08	55 \pm 1.62
15	H	H	H	H	H	O	92 \pm 1.18	>200
16	Cl	H	H	H	Cl	O	136 \pm 1.12	51 \pm 1.12
17	H	H	NO ₂	H	H	O	30 \pm 1.17	105 \pm 3.72
18	Cl	OMe	H	H	Cl	O	166 \pm 2.80	39 \pm 1.08
19	H	H	Me	H	H	O	16 \pm 1.10	>200
20	H	H	OMe	H	H	NH	12 \pm 1.11	62 \pm 1.10
21	Curcumin						48 \pm 1.11	>400

These results are comparable to natural anti-cancer compound curcumin; used as a positive control in this study. It can be easily observed from (Figure 3.6 & Figures 3.5, 3.7 and 3.8) that a significant anti-cancer activity of these synthesized compounds was perceived against the studied of human breast cancer cell lines. But if we compare the results, we found that from all of the studied compounds, compound **5f**, **5g**, **5o**, **5q** and **5s** showed the better activity as well as less cytotoxicity (Figure 3.2 & 3.6).

Results of percentage viabilities indicated that till 50 μM concentrations, all of these inhibitors are non-toxic for HEK293T cells (Figure 3.2). Whereas inhibitors **5a-5e**, **5h-5n**, **5p**, **5s** and **5t** showed significant levels of cytotoxicity (Figure 3.1, 3.3 and 3.4) even at low concentrations (below 50 μM). To check the anti-cancerous activity of these inhibitors, all the cells were treated with increasing concentrations of inhibitors (5 to 200 μM). Extent of cell proliferation with respect to concentration is shown in the Figure 3.6, 3.5, 3.7 and 3.8. From these results, percentage viability was calculated and determines the IC_{50} (50% inhibitory concentration) values for each inhibitor (Table 4.1).

4.2.2.2. Material and Methods

Bcl-2 appears to be a possible target for compounds **5f**, **5g**, **5o**, **5q** and **5s** as it induces the apoptosis by decreasing the level of anti-apoptotic protein Bcl-2 in MTT assay. Further, in silico molecular docking (MD) was performed using the three-dimensional structure of Bcl-2 from the Protein Data Bank (www.rcsb.org) (PDB ID: 4LVT) [27]. The steepest descent method from Gromacs 4.5.5 was used to optimize the coordinates and Bcl-2 protein was saved in. pdbqt format to carry docking analysis. AutoDock 4.2 with standard protocol was used to dock the test compounds with Bcl-2 [28]. The Lamarckian genetic algorithm (LGA) was applied to deal with protein-ligands interactions. The most favorable free binding energy and docking orientations lying within the range of 1.0 Å in root-mean square deviation (rmsd) tolerance were used to cluster the molecule and ranked accordingly. The lowest binding energy conformation was considered as the most favorable docking pose, after the docking search was completed. PyMOL was used to visualize molecular interactions.

4.2.2.3. Molecular Docking

Docking studies predicted the interaction of inhibitors with protein and residues involved in this complex. The orientation and conformation of inhibitors bound in the active site of the protein and formed protein-ligand complex with the highest binding energy value are the most important requirement for docking studies [29]. Therefore, optimal interactions and the best AutoDock score were used as criteria to interpret the best inhibitor. All the five compounds were docked into structure of Bcl-2. The docking results of Bcl-2 and inhibitors were shown in Table 3.2. Among the above docked compounds **5q** and **5s** had the highest binding energy with Bcl-2 protein while compounds **5f**, **5g** and **5o** showed the lowest binding energy. Docking poses of the best conformation of compounds **5f** and **5g** in binding site of Bcl-2 protein were shown in Figure 4.9 and 4.10 respectively.

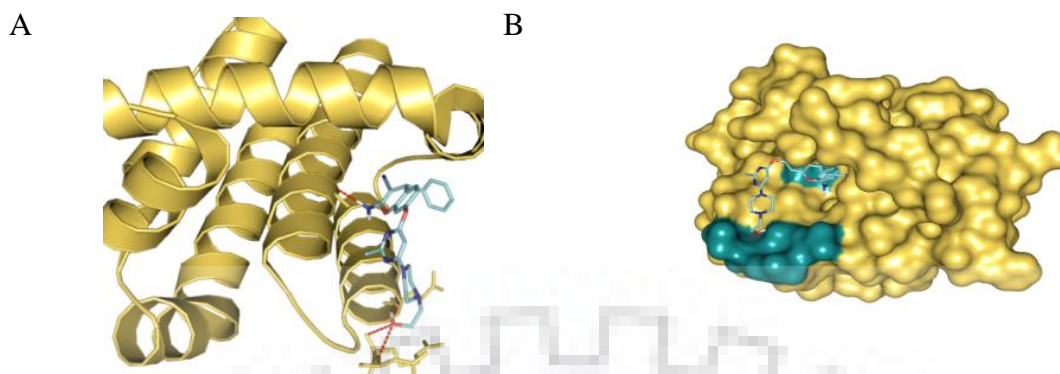


Figure.4.9. (A) 2-amino-7-((6-(4-(2-hydroxyethyl) piperazin-1-yl)-2-methylpyrimidin-4-yl)oxy)-4-(p-tolyl)-1,4-dihydroquinoline-3-carbonitriledocked with Bcl-2. (B) Surface representation of Bcl-2 docked with 2-amino-7-((6-(4-(2-hydroxyethyl)piperazin-1-yl)-2-methylpyrimidin-4-yl)oxy)-4-(p-tolyl)-1,4-dihydroquinoline-3-carbonitrile.

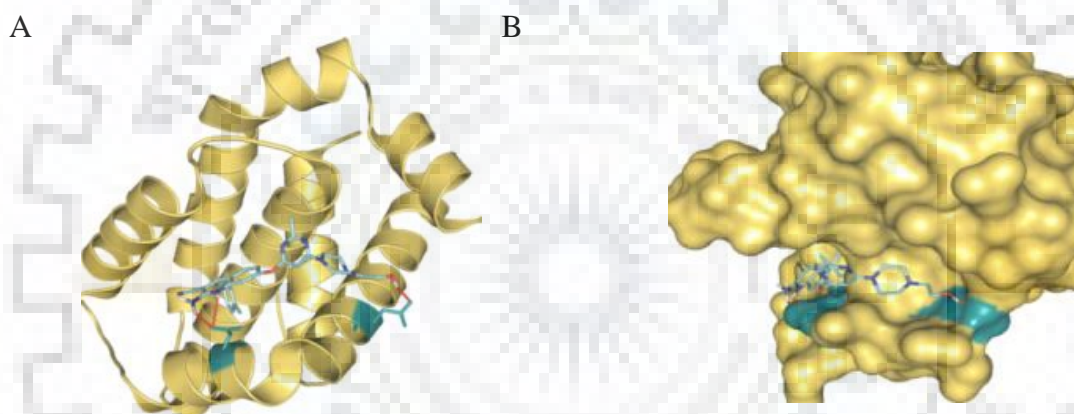


Figure: 4.10. (A) 2-amino-7-((6-(4-(2-hydroxyethyl)piperazin-1-yl)-2-methylpyrimidin-4-yl)oxy)-4-phenyl-1,4-dihydroquinoline-3-carbonitriledocked with Bcl-2. (B) Surface representation of Bcl-2 docked with 2-amino-7-((6-(4-(2-hydroxyethyl)piperazin-1-yl)-2-methylpyrimidin-4-yl)oxy)-4-phenyl-1,4-dihydroquinoline-3-carbonitrile.

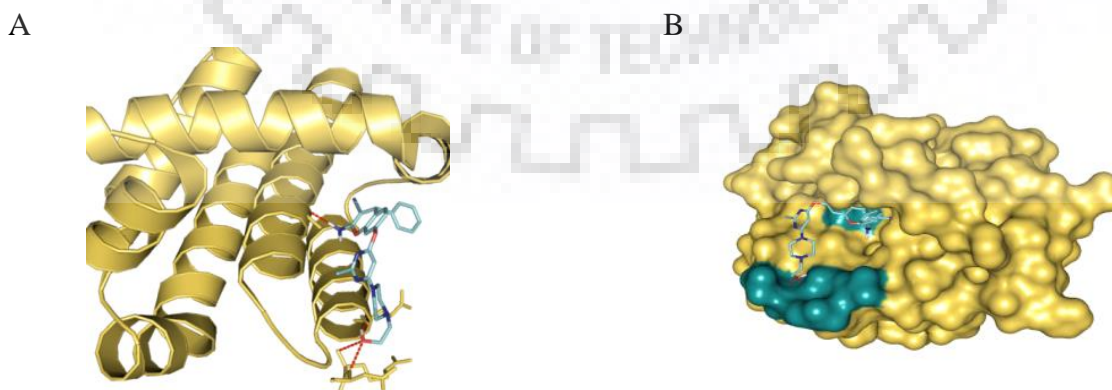


Figure.4.11. (A) 2-amino-4-(4-bromophenyl)-7-((6-(4-(2-hydroxyethyl)piperazin-1-yl)-2-methylpyrimidin-4-yl)oxy)-4H-chromene-3-carbonitriledocked with Bcl-2. (B) Surface representation of Bcl-2 docked with 2-amino-4-(4-bromophenyl)-7-((6-(4-(2-

hydroxyethyl)piperazin-1-yl)-2-methylpyrimidin-4-yl)oxy)-4H-chromene-3-carbonitrile.

The compounds **5f** and **5g** were nicely bound into the active site of Bcl-2 with minimum binding energy (ΔG) = **-9.08 kcal/mol (Ki = 221.60 μ M)** and (ΔG) = **-8.29 kcal/mol (Ki =705.90 μ M)** respectively (Table 3.2). The p-tolyl and phenyl group in compounds **5f** and **5g** formed three H-bond interactions one with Asp100 and two with Asp108, respectively (Figs. 3.9A, 3.10A). The residue Y199 of Bcl-2 protein form cation-p interactions with compounds **5f** and **5g** respectively and stabilizing the protein–ligand complex (Figs. 3.9B, 3.10B). Interestingly, compounds **5f** and **5g** exhibit good interactions of Bcl-2 which showed that these two compounds can bind strongly to the BH3 binding regions of Bcl-2 protein (Table 3.2). Compound **5o** also showed good interaction with binding energy (ΔG) **7.70 kcal/- mol, Ki = 2.26 mM**). The chromene ring in compound **5o**formed four H-bond interactions with Glu133, Arg136, Asp137 and Ala146 (Figure. 3.11).However, molecular docking results showed quite different orientation of compounds **5f**, **5g** and **5o** at the binding site of Bcl-2 due to substituent changing at 4-position of chromene derivatives. Therefore, concluding from the docking study that compounds **5f**, **5g** and **5o** have good binding with Bcl-2 among all five compounds. Compounds **5o** and **5t** possessing p-tolyl or phenyl group have similar biological activities but the docking studies results are quite different.

Table.4.2. Docking score of compounds **5f**, **5g** and **5o**.

S.No.	Compounds	Binding affinity (ΔG)	Estimated K_i
1	5f	-9.08 kcal/mol	221.60 μ M
2	5g	-8.29 kcal/mol	705.90 μ M
3	5o	-7.70 kcal/mol	2.26 μ M

This may be due to chromene derivatives with p-tolyl have different binding orientation than chromene derivatives which possessing phenyl group. Compound **5o** fits well in the binding pocket of Bcl-2 while compound **5t** binds also in pocket but less than compound **5o**. Compound **5t** have different stoichiometry than compound **5o** due to the presence of phenyl group. But In case of quinolone derivatives, p-tolyl or phenyl group do not have much different stoichiometry. Thus, these compounds have similar biological activities and the similar docking results. The compound **5t** contains p-tolyl group and due to the

presence of extra methyl group it fits perfectly in the pocket and methyl group increase the binding affinity [30].

4.3. Conclusion

In conclusion, we have synthesized highly functionalized novel pyrimidine-piperazine-chromene and -quinoline derivatives under multi-component one step reaction under mild reaction condition. Compounds were screened for their anti-proliferative activity against estrogen-responsive human breast cancer cell lines (MCF-7) and cytotoxicity in normal cell line i.e. human embryonic kidney cells (HEK293). Among them, compounds **5f**, **5g**, **5o**, **5q** and **5s** displayed good anti-proliferative activity (48 ± 1.70 , 65 ± 1.13 , 92 ± 1.18 , 30 ± 1.17 and 16 ± 1.10 mM) where chromene and quinoline moiety attached with 4,6-dichloro-2-methylpyrimidine and 2-(piperazin-1-yl)ethanol and other compounds also showed comparable enhanced activities to the standard drug curcumin (IC_{50} value 48 ± 1.11 mM). Concluding from the docking study, compounds **5f**, **5g** and **5o** showed good binding affinity ($\Delta G = 9.08$, 8.29 and 7.70 kcal/mol) with Bcl-2 among all synthesized compounds.

4.4. Experimental Section

4.4.1. General Information

All the required chemicals were purchased from Sigma Aldrich, Himedia and Aavra. IR spectra were recorded on a Thermo Nicolet FT-IR spectrophotometer with KBr. NMR was recorded on a Jeol Resonance ECX 400II spectrometer using $CDCl_3$ and DMSO as solvent. In 1H NMR Chemical shifts are recorded in parts per million and referenced internally to the residual with tetramethylsilane (TMS δ 0.00 ppm) or proton resonance in $CDCl_3$ (δ 7.26 ppm). ^{13}C NMR spectra were referenced to $CDCl_3$ (δ 77.0 ppm, the middle peak). Coupling constant were recorded in Hz. The following abbreviations are used to explain the multiplicities: s = singlet, d = doublet, dd = doublet of doublets, dt = doublet of triplets, t = triplet, q = quartet, m = multiplet. Mass spectra were measured with ESI ionization in MSQ LCMS mass spectrometer.

4.4.2. General procedure

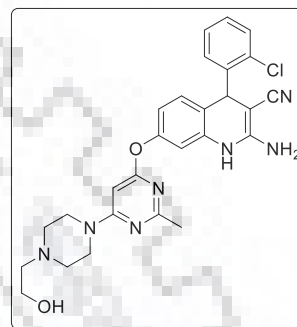
In a round bottom flask, 2-amino-7-hydroxy-4-phenyl-4H-chromene-3-carbonitrile or 2-amino-7-hydroxy-4-phenyl-1,4-dihydroquinoline-3-carbonitrile (1 mmol), K_2CO_3 (3 equiv.), acetone (3 mL) was charged and stirred at room temperature for 15 min. After 15 min., the color change and then 4,6-dichloro-2-methylpyrimidine was added and further stirred at 80 °C for 15 min in an oil bath, followed by 2-(piperazin-1-yl)ethanol was added. The reaction mixture was refluxed at 80 C until complete consumption of the

starting material, monitored by TLC using 10% chloroform and methanol. After completion of the reaction, the mixture was poured into crushed ice, precipitate formed, which was filtered under vacuum. The residue was purified by washing with diethyl ether (no need for column chromatography) with excellent yield (90–97%).

4.5. Characterization data

2-amino-4-(2-chlorophenyl)-7-((6-(4-(2-hydroxyethyl)piperazin-1-yl)-2-methylpyrimidin-4-yl)oxy)-1,4-dihydroquinoline-3-carbonitrile (5a) : Yield: 92% as pale yellow;

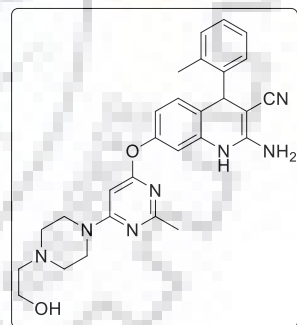
^1H NMR (400 MHz, CDCl_3 , δ): 7.37 (d, $J = 7.4$ Hz, 1H), 7.22 – 7.18 (m, 3H), 7.01 (d, $J = 8.0$ Hz, 1H), 6.79 – 6.77 (m, 2H), 5.67 (s, 1H), 5.38 (s, 1H), 4.68 (s, 2H), 3.65 (t, $J = 5.0$ Hz, 2H), 3.59 (t, $J = 4.1$ Hz, 4H), 2.59 – 2.54 (m, 6H), 2.39 (s, 1H); ^{13}C NMR (100 MHz, CDCl_3 , δ): 170.2, 167.9, 164.6, 159.1, 152.8, 149.2, 142.3, 135.6, 131.2, 130.2, 129.9, 127.4, 126.9, 119.8, 119.6, 118.1, 109.2, 83.8, 60.5, 59.5, 57.9, 52.6,



44.2, 37.1, 19.7; LC-MS (ESI^+): m/z calculated for $\text{C}_{27}\text{H}_{29}\text{ClN}_7\text{O}_3$ $[\text{M}+\text{H}]^+$: 518.2, 520.2 found: 518.1, 520.0.

2-amino-7-((6-(4-(2-hydroxyethyl)piperazin-1-yl)-2-methylpyrimidin-4-yl)oxy)-4-(o-tolyl)-1,4-dihydroquinoline-3-carbonitrile (5b) : Yield: 97% as Green color;

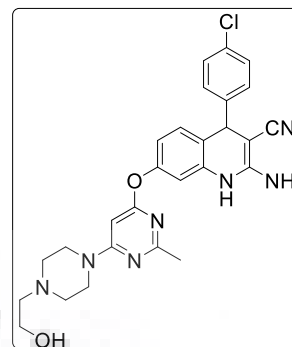
^1H NMR (400 MHz, CDCl_3 , δ): 7.14 – 7.13 (m, 3H), 7.06 – 7.03 (m, 1H), 6.85 – 6.83 (m, 1H), 6.79 – 6.74 (m, 2H), 5.68 (s, 1H), 4.70 (s, 2H), 4.55 (s, 1H), 3.64 (t, $J = 5.2$ Hz, 2H), 3.59 (t, $J = 4.7$ Hz, 4H), 2.58 – 2.53 (m, 6H), 2.40 (s, 1H), 2.39 (s, 1H); ^{13}C NMR (100 MHz, CDCl_3 , δ): 170.8, 168.5, 165.2,



159.7, 153.5, 149.8, 142.9, 136.2, 131.8, 130.8, 130.4, 128.0, 127.5, 120.4, 120.2, 118.7, 109.8, 84.4, 61.1, 60.1, 58.5, 53.2, 44.8, 37.7, 26.7, 20.4; FT-IR (KBr): 3400, 3200, 2217, 1640, 1542, 1100, 580 cm^{-1} ; LC-MS (ESI^+): m/z calculated for $\text{C}_{27}\text{H}_{29}\text{ClN}_6\text{O}_3$ $[\text{M}+\text{H}]^+$: 498.2 found: 498.1.

2-amino-4-(4-chlorophenyl)-7-((6-(4-(2-hydroxyethyl)piperazin-1-yl)-2-methylpyrimidin-4-yl)oxy)-1,4-dihydroquinoline-3-carbonitrile (5c): Yield: 92% as

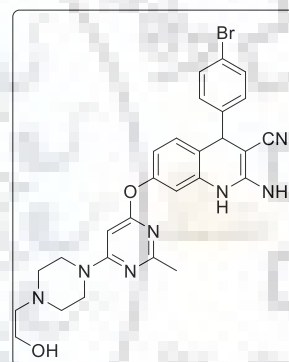
Pale yellow; ¹H NMR (400 MHz, CDCl₃, δ): 7.28 (d, *J* = 8.4 Hz, 2H), 7.14 (d, *J* = 8.4 Hz, 2H), 6.92 – 6.90 (m, 1H), 6.80 – 6.78 (m, 2H), 5.72 (s, 1H), 4.71 (s, 3H), 3.65 (t, *J* = 5.2 Hz, 2H), 3.60 (t, *J* = 4.7 Hz, 4H), 2.59 – 2.54 (m, 6H), 2.39 (s, 1H); ¹³C NMR (100 MHz, CDCl₃, δ): 169.9, 167.8, 164.6,



159.2, 153.1, 148.9, 143.0, 133.3, 130.4, 129.4, 129.1, 119.6, 118.7, 118.1, 109.3, 83.9, 60.1, 59.5, 57.9, 52.6, 44.2, 40.2, 26.0; FT-IR (KBr) : 3400, 3200, 2217, 1640, 1542, 1100, 578 cm⁻¹; LC-MS (ESI⁺): m/z calculated for C₂₇H₂₉ClN₇O₃ [M+H]⁺: 518.2, 520.2 found: 518.1, 520.0.

2-amino-4-(4-bromophenyl)-7-((6-(4-(2-hydroxyethyl)piperazin-1-yl)-2-methylpyrimidine-4-yl)oxy)-1,4-dihydroquinoline-3-carbonitrile (5d): Yield: 92% as Dark

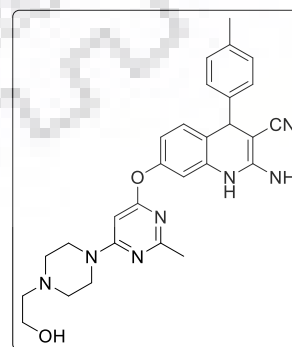
brown; ¹H NMR (400 MHz, CDCl₃, δ): 7.43 (d, *J* = 8.4 Hz, 2H), 7.08 (d, *J* = 8.4 Hz, 2H), 6.92 – 6.90 (m, 1H), 6.80 – 6.78 (m, 2H), 5.71 (s, 1H), 4.74 (s, 2H), 4.69 (s, 1H), 3.65 (t, *J* = 5.2 Hz, 2H), 3.60 (t, *J* = 4.6 Hz, 4H), 2.59 – 2.54 (m, 6H), 2.38 (s, 1H); ¹³C NMR (100 MHz, CDCl₃, δ) 169.9, 167.8, 164.6, 159.2,



153.2, 148.9, 143.5, 132.1, 132.0, 130.3, 129.8, 121.4, 118.6, 118.1, 109.3, 83.9, 60.2, 59.5, 57.9, 44.2, 40.3, 26.1; FT-IR (KBr): 3400, 3200, 2216, 1640, 1542, 1100, 580 cm⁻¹; LC-MS (ESI⁺): m/z calculated for C₂₇H₂₉BrN₇O₂ [M+H]⁺: 562.1, 564.1 found: 562.1, 564.1.

2-amino-7-((6-(4-(2-hydroxyethyl)piperazin-1-yl)-2-methylpyrimidin-4-yl)oxy)-4-(p-tolyl)-1,4-dihydroquinoline-3-carbonitrile (5e): Yield: 94% as Light Pink; ¹H NMR

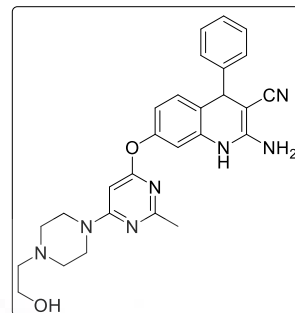
(400 MHz, CDCl₃, δ): 7.13 – 7.08 (m, 2H), 6.95 (d, *J* = 7.9 Hz, 2H), 6.79 – 6.76 (m, 4H), 5.68 (s, 1H), 4.68 (s, 2H), 4.63 (s, 1H), 3.64 (t, *J* = 5.2 Hz, 2H), 3.59 (t, *J* = 4.6 Hz, 4H), 2.59-2.53 (m, 6H), 2.39 (s, 1H), 2.30 (s, 1H); ¹³C NMR (100 MHz, CDCl₃, δ) 170.1, 167.9, 164.6, 159.0, 152.8, 149.0, 141.5,



137.1, 130.5, 129.6, 127.9, 119.53, 118.0, 109.2, 83.7, 61.1, 59.4, 57.9, 52.6, 44.2, 40.3, 26.1, 21.2; FT-IR (KBr): 3400, 3200, 2217, 1640, 1542, 1100, 580 cm⁻¹ LC-MS (ESI⁺): m/z calculated for C₂₈H₃₂N₇O₂ [M+H]⁺: 498.2 found: 498.2.

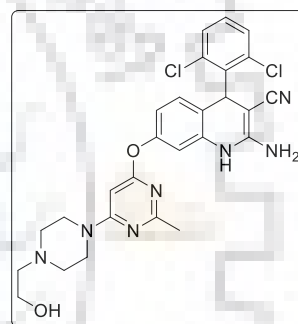
2-amino-7-((6-(4-(2-hydroxyethyl)piperazin-1-yl)-2-methylpyrimidin-4-yl)oxy)-4-phenyl-1,4-dihydro-quinoline-3-carbonitrile (5g): Yield: 94% as

Pale yellow; ^1H NMR (400 MHz, CDCl_3 , δ): 7.34 – 7.30 (m, 2H), 7.24 – 7.21 (m, 3H), 6.99 – 6.97 (m, 1H), 6.80 – 6.78 (m, 2H), 5.72 (s, 1H), 4.80 (s, 2H), 4.74 (s, 1H), 3.66 (t, $J = 5.3$ Hz, 2H), 3.61 (t, $J = 4.7$ Hz, 4H), 2.60– 2.55 (m, 6H), 2.41 (s, 1H); ^{13}C NMR (100 MHz, CDCl_3 , δ): 170.1, 167.8, 164.5, 159.3, 152.9, 149.0, 144.5, 130.5, 129.0, 128.1, 127.4, 120.0, 119.4, 118.0, 109.2, 83.8, 60.4, 59.4, 57.9, 52.6, 44.2, 40.7, 26.1; FT-IR (KBr): 3400, 3200, 2217, 1640, 1542, 1100, 580 cm^{-1} ; LC-MS (ESI⁺): m/z calculated for $\text{C}_{27}\text{H}_{30}\text{N}_7\text{O}_2$ $[\text{M}+\text{H}]^+$: 484.2, found: 484.2.



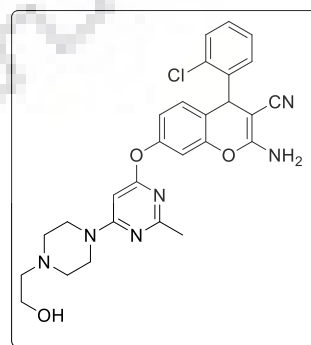
2-amino-4-(2,6-dichlorophenyl)-7-((6-(4-(2-hydroxyethyl)piperazin-1-yl)-2-methylpyrimidin-4-yl)oxy)-1,4-dihydroquinoline-3-carbonitrile (5h): Yield: 92% as pale

yellow; ^1H NMR (400 MHz, CDCl_3 , δ): 7.39 (d, $J = 7.9$ Hz, 1H), 7.23 (d, $J = 7.8$ Hz, 1H), 7.15 (t, $J = 7.9$ Hz, 1H), 6.87 (d, $J = 8.3$ Hz, 1H), 6.78 – 6.75 (m, 2H), 5.95 (s, 1H), 4.76 (s, 2H), 4.62 (s, 1H), 3.65 (t, $J = 5.2$ Hz, 2H), 3.59 (t, $J = 4.6$ Hz, 4H), 2.59 – 2.54 (m, 6H), 2.40 (s, 1H); ^{13}C NMR (100 MHz, $\text{CDCl}_3+\text{DMSO}-d_6$, δ): 169.6, 166.8, 163.9, 160.5, 152.7, 149.5, 137.3, 135.8, 135.1, 129.0, 128.5, 128.1, 117.0, 116.4, 108.4, 83.2, 59.9, 58.2, 53.3, 52.5, 43.6, 35.9, 25.6. FT-IR (KBr): 3400, 3200, 2217, 1640, 1542, 1100, 580 cm^{-1} LC-MS (ESI⁺): m/z calculated for $\text{C}_{28}\text{H}_{32}\text{N}_7\text{O}_3$ $[\text{M}+\text{H}]^+$: 552.2 found: 552.1



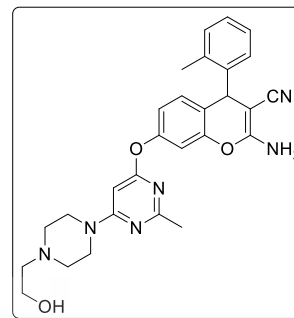
2-amino-4-(2-chlorophenyl)-7-((6-(4-(2-hydroxyethyl)piperazin-1-yl)-2-methylpyrimidin-4-yl)oxy)-4H-chromene-3-carbonitrile (5i): Yield: 96% as pale

yellow; ^1H NMR (400 MHz, CDCl_3 , δ): 7.37 (d, $J = 7.5$ Hz, 1H), 7.22 – 7.17 (m, 3H), 7.01 (d, $J = 8.1$ Hz, 1H), 6.79 – 6.77, (m, 2H), 5.67 (s, 1H), 5.38 (s, 1H), 4.68 (s, 2H), 3.64 (t, $J = 5.2$ Hz, 2H), 3.51 (t, $J = 4.4$ Hz, 4H), 2.59 – 2.53 (m, 6H), 2.39 (s, 1H); ^{13}C NMR (100 MHz, CDCl_3 , δ): 170.0, 167.7, 164.4, 158.9, 152.7, 149.0, 147.0, 142.0, 135.4, 131.0, 130.1, 129.7, 127.2, 126.7, 119.6, 119.5, 117.9, 109.0, 83.6, 60.3, 59.3, 57.7, 52.4, 44.0, 26.0; FT-IR (KBr): 3400, 3200, 2217, 1640, 1542, 1100, 580 cm^{-1} LC-MS (ESI⁺): m/z calculated for $\text{C}_{27}\text{H}_{29}\text{ClN}_6\text{O}_3$ $[\text{M}+\text{H}]^+$: 519.1, 521.1 found: 519.1, 521.2.



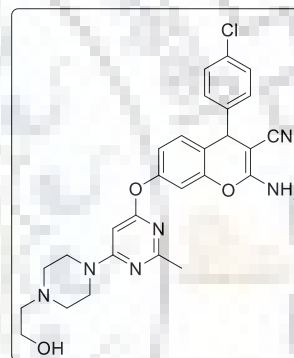
2-amino-7-((6-(4-(2-hydroxyethyl)piperazin-1-yl)-2-methylpyrimidin-4-yl)oxy)-4-(o-tolyl)-4H-chromene-3-carbonitrile (5j)

Yield: 97% as Green color; ¹H NMR (400 MHz, CDCl₃, δ): 7.13 – 7.13 (m, 3H), 7.05 – 7.04 (m, 1H), 6.85 – 6.83 (m, 1H), 6.78 – 6.73 (m, 2H), 5.68 (s, 1H), 5.05 (s, 1H), 4.70 (s, 2H), 3.64 (t, *J* = 5.2 Hz, 2H), 3.59 (t, *J* = 4.7 Hz, 4H), 2.58 – 2.53 (m, 6H), 2.40 (s, 1H), 2.39 (s, 1H); ¹³C NMR (100 MHz, CDCl₃, δ): 170.1, 167.8, 164.5, 159.1, 152.8, 149.2, 142.3, 135.5, 131.0, 130.2, 129.8, 127.3, 126.8, 119.8, 119.6, 118.1, 109.2, 83.7, 60.2, 59.5, 57.9, 52.6, 44.2, 37.1, 26.0, 19.7; FT-IR (KBr): 3400, 3200, 2217, 1640, 1542, 1100, 580 cm⁻¹; LC-MS (ESI⁺): *m/z* calculated for C₂₇H₂₉ClN₆O₃ [M+H]⁺: 499.2 found: 499.1.



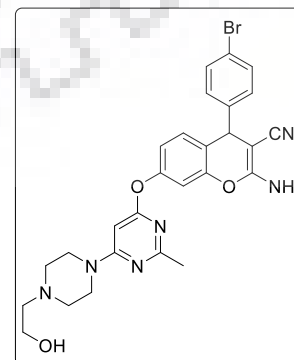
2-amino-4-(4-chlorophenyl)-7-((6-(4-(2-hydroxyethyl)piperazin-1-yl)-2-methylpyrimidin-4-yl)oxy)-4H-chromene-3-carbonitrile (5l)

Yield: 94% as Pale yellow; ¹H NMR (400 MHz, CDCl₃, δ): 7.39 (d, *J* = 7.9 Hz, 1H), 7.23 (d, *J* = 7.9 Hz, 1H), 7.15 (t, *J* = 7.9 Hz, 1H), 6.86 (d, *J* = 8.3 Hz, 1H), 6.78 – 6.77 (m, 1H), 6.76 – 6.74 (m, 2H), 5.94 (s, 1H), 5.62 (s, 1H), 4.67 (s, 2H), 3.64 (t, *J* = 5.2 Hz, 2H), 3.58 (t, *J* = 4.4 Hz, 4H), 2.59 – 2.53 (m, 6H), 2.40 (s, 1H); ¹³C NMR (100 MHz, CDCl₃ and DMSO-d₆ δ): 169.9, 167.2, 164.2, 160.5, 152.8, 149.7, 137.4, 136.1, 135.3, 129.0, 128.7, 128.2, 117.2, 116.6, 108.6, 83.2, 59.9, 58.2, 53.6, 52.6, 43.7, 36.0, 25.8; FT-IR (KBr): 3400, 3200, 2217, 1640, 1542, 1100, 580 cm⁻¹; LC-MS (ESI⁺): *m/z* calculated for C₂₇H₂₉ClN₆O₃ [M+H]⁺: 519.1, 521.1 found: 519.1, 521.2.



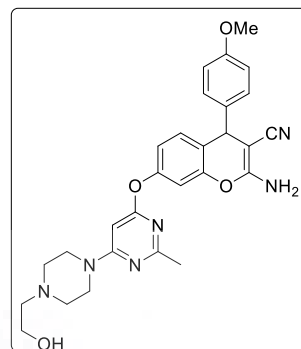
2-amino-4-(4-bromophenyl)-7-((6-(4-(2-hydroxyethyl)piperazin-1-yl)-2-methylpyrimidin-4-yl)oxy)-4H-chromene-3-carbonitrile (5m)

Yield: 95% as Pale yellow; ¹H NMR (400 MHz, CDCl₃, δ): 7.44 (d, *J* = 8.3 Hz, 2H), 7.09 (d, *J* = 8.4 Hz, 1H), 6.92 – 6.90 (m, 1H), 6.81 – 6.78 (m, 2H), 5.72 (s, 1H), 4.69 (s, 1H), 4.68 (s, 2H), 3.65 (t, *J* = 5.2 Hz, 2H), 3.60 (t, *J* = 4.7 Hz, 4H), 2.59 – 2.54 (m, 6H), 2.39 (s, 1H); ¹³C NMR (100 MHz, CDCl₃ δ): 169.9, 167.8, 164.6, 159.2, 153.1, 148.9, 143.5, 132.1, 130.3, 129.8, 121.4, 119.6, 118.6, 118.1, 109.3, 83.9, 60.2, 59.4, 57.9, 52.6, 44.2, 40.3, 26.1; FT-IR (KBr): 3400, 3200, 2217, 1640, 1542, 1100, 580 cm⁻¹; LC-MS (ESI⁺): *m/z* calculated for C₂₇H₂₉BrN₆O₃ [M+H]⁺: 563.1, 565.1 found: 563.1, 565.2.



2-amino-7-((6-(4-(2-hydroxyethyl)piperazin-1-yl)-2-methylpyrimidin-4-yl)oxy)-4-(4-methoxyphenyl)-1,4-dihydroquinoline-3-carbonitrile (5n) : Yield: 98% as Light

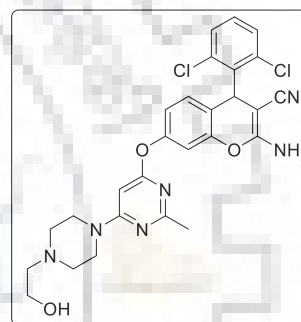
green; ^1H NMR (400 MHz, CDCl_3 , δ); 7.12 (d, $J = 8.6$ Hz, 2H), 6.95 – 6.93 (m, 2H), 6.83 (d, $J = 8.6$ Hz, 2H), 6.79 – 6.76 (m, 2H), 5.69 (s, 1H), 4.72 (s, 2H), 5.07 (s, 1H), 4.71 (s, 2H), 3.76 (s, 3H), 3.64 (t, $J = 5.3$ Hz, 2H), 3.59 (t, $J = 4.8$ Hz, 4H), 2.58 – 2.53 (m, 6H), 2.39 (s, 1H); ^{13}C NMR (100 MHz, CDCl_3 , δ) 170.0, 167.7, 164.4, 158.9, 158.7, 152.6, 148.8, 136.6, 130.3, 129.0, 119.8, 119.6, 117.8, 114.2, 109.0, 83.6, 60.7, 59.3, 57.7,



55.35, 52.4, 44.0, 39.8, 25.9; FT-IR (KBr): 3400, 3200, 2217, 1640, 1542, 1100, 580 cm^{-1} ; LC-MS (ESI $^+$): m/z calculated for $\text{C}_{28}\text{H}_{32}\text{N}_7\text{O}_3$ $[\text{M}+\text{H}]^+$: 514.2 found: 514.2.

2-amino-4-(2,6-dichlorophenyl)-7-((6-(4-(2-hydroxyethyl)piperazin-1-yl)-2-methylpyrimidin-4-yl)oxy)-4H-chromene-3-carbonitrile (5o):

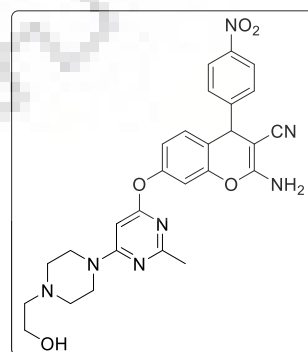
Yield: 93% as Pale yellow; ^1H NMR (400 MHz, CDCl_3 , δ); 7.38 (d, $J = 7.9$ Hz, 1H), 7.22 (d, $J = 7.9$ Hz, 1H), 7.14 (t, $J = 7.9$ Hz, 1H), 6.86 (d, $J = 8.3$ Hz, 1H), 6.77 – 6.74 (m, 2H), 5.93 (s, 1H), 5.62 (s, 1H), 4.75 (s, 2H), 3.64 (t, $J = 5.3$ Hz, 2H), 3.58 (t, $J = 4.3$ Hz, 4H), 2.58-2.53 (m, 6H), 2.39 (s, 3H). ^{13}C NMR



(100 MHz, DMSO and CDCl_3 , δ): 169.6, 166.7, 163.9, 160.4, 152.6, 149.5, 137.3, 135.8, 135.0, 128.9, 128.4, 128.0, 116.9, 116.3, 108.3, 83.2, 59.9, 58.2, 53.1, 52.5, 43.6, 35.9, 25.6; FT-IR (KBr): 3400, 3200, 2217, 1640, 1542, 1100, 580 cm^{-1} LC-MS (ESI $^+$): m/z calculated for $\text{C}_{27}\text{H}_{29}\text{Cl}_2\text{N}_6\text{O}_3$ $[\text{M}+\text{H}]^+$: 553.2 found: 553.1.

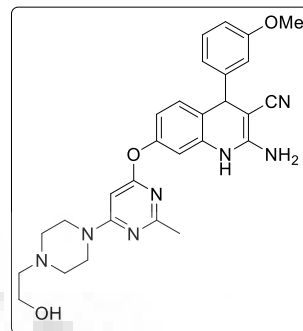
2-amino-7-((6-(4-(2-hydroxyethyl)piperazin-1-yl)-2-methylpyrimidin-4-yl)oxy)-4-(4-nitrophenyl)-4H-chromene-3-carbonitrile (5p): Yield: 90% as Light Yellow; ^1H

NMR (400 MHz, CDCl_3 , δ); 8.12 – 8.10 (m, 1H), 8.01 (s, 1H), 7.61 (d, $J = 7.5$ Hz, 1H), 7.51 (t, $J = 7.7$ Hz, 1H), 6.91 (d, $J = 8.1$ Hz, 1H), 6.83 – 6.81 (m, 2H), 5.73 (s, 1H), 5.12 (s, 1H), 4.91 (s, 2H), 3.65 (t, $J = 5.2$ Hz, 2H), 3.60 (t, $J = 4.9$ Hz, 4H), 2.58- 2.54 (m, 6H), 2.38 (s, 1H); ^{13}C NMR (100 MHz, CDCl_3 ,

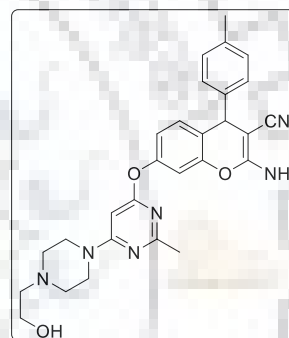


) : 169.9, 167.8, 164.6, 159.5, 153.5, 149.0, 148.8, 146.6, 134.8, 130.3, 130.0, 123.0, 122.7, 117.7, 109.6, 84.0, 59.0, 59.2, 57.9, 52.6, 44.2, 40.6, 26.1; FT-IR (KBr): 3400, 3200, 2217, 1640, 1542, 1100, 580 cm^{-1} ; LC-MS (ESI $^+$): m/z calculated for $\text{C}_{28}\text{H}_{27}\text{N}_7\text{O}_5$ $[\text{M}+\text{H}]^+$: 528.2 found: 528.2.

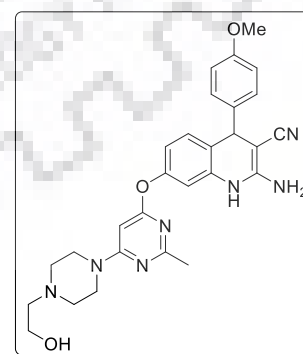
2-amino-7-(((6-(4-(2-hydroxyethyl)piperazin-1-yl)-2-methylpyrimidin-4-yl)oxy)-4-(3-methoxyphenyl)-4H-chromene-3-carbonitrile (5q) :Yield: 93% as Pale Yellow; ¹H NMR (400 MHz, CDCl₃, δ); 7.23 (d, *J* = 8.0 Hz, 1H), 6.99-6.97 (m, 1H), 6.81 – 6.75 (m, 4H), 6.73 – 6.72 (m, 1H), 5.69 (s, 1H), 5.13 (s, 1H), 4.74 (s, 2H), 3.76 (s, 3H), 3.64 (t, *J* = 5.2 Hz, 2H), 3.59 (t, *J* = 4.7 Hz, 4H), 2.58 – 2.53 (m, 6H), 2.39 (s, 1H); ¹³C NMR (100 MHz, CDCl₃, δ): 170.1, 167.8, 164.5, 160.0, 159.2, 152.9, 149.0, 130.5, 130.0, 120.5, 119.8, 119.2, 118.0, 114.2, 112.4, 109.2, 83.8, 60.9, 59.5, 57.9, 55.3, 52.6, 44.2, 40.7, 26.1; FT-IR (KBr): 3400, 3200, 2217, 1640, 1542, 1100, 580 cm⁻¹; LC-MS (ESI⁺): m/z calculated for C₂₈H₃₂N₆O₃ [M+H]⁺: 515.2 found: 515.0.



2-amino-7-(((6-(4-(2-hydroxyethyl)piperazin-1-yl)-2-methylpyrimidin-4-yl)oxy)-4-(p-tolyl)-4H-chromene-3-carbonitrile (5s) : Yield: 94% as Pale yellow; ¹H NMR (400 MHz, CDCl₃, δ): 7.13 – 7.12 (m, 3H), 7.05 – 7.03(m, 1H), 6.85 – 6.83 (m, 1H), 6.77 – 6.73(m, 2H), 5.69 (s, 1H), 5.06 (s, 1H), 4.75 (s, 2H), 3.64 (t, *J* = 5.2 Hz, 2H), 3.59 (t, *J* = 4.4 Hz, 4H), 2.58 – 2.53(m, 6H), 2.40 (s, 1H), 2.39 (s, 1H); ¹³C NMR (100 MHz, CDCl₃, δ) 170.1, 167.9, 164.6, 159.0, 152.8, 149.0, 141.5, 137.1, 130.5, 129.7, 127.9, 119.5, 118.0, 109.2, 83.7, 61.0, 59.4, 57.9, 52.5, 44.2, 40.3, 40.1, 26.1, 21.1; FT-IR (KBr): 3400, 3200, 2217, 1640, 1542, 1100, 580 cm⁻¹ LC-MS (ESI⁺): m/z calculated for C₂₈H₃₀N₆O₃ [M+H]⁺: 499.2 found: 499.1.



2-amino-7-(((6-(4-(2-hydroxyethyl)piperazin-1-yl)-2-methylpyrimidin-4-yl)oxy)-4-(4-methoxyphenyl)-4H-chromene-3-carbonitrile (5t) : Yield: 91% as Light green; ¹H NMR (400 MHz, CDCl₃, δ); 7.12 (d, *J* = 8.6 Hz, 2H), 6.95 – 6.93 (m, 1H), 6.83 (d, *J* = 8.6 Hz, 2H), 6.78 – 6.76 (m, 1H), 5.69 (s, 1H), 4.72 (s, 2H), 4.67 (s, 1H), 3.76 (s, 3H), 3.64 (t, *J* = 5.2 Hz, 2H), 3.59 (t, *J* = 4.8 Hz, 4H), 2.58- 2.53 (m, 6H), 2.39 (s, 1H); ¹³C NMR (100 MHz, CDCl₃): 170.0, 167.8, 164.5, 159.0, 158.9, 152.8, 148.9, 136.7, 130.5, 129.1, 119.9, 119.7, 117.9, 114.2, 109.2, 83.8, 60.9, 59.5, 57.8, 55.3, 44.1, 39.9, 26.0; FT-IR (KBr) : 3400, 3200, 2217, 1640, 1542, 1100, 580 cm⁻¹; LC-MS (ESI⁺): m/z calculated for C₂₈H₃₂N₆O₃ [M+H]⁺: 515.2 found:515.1.



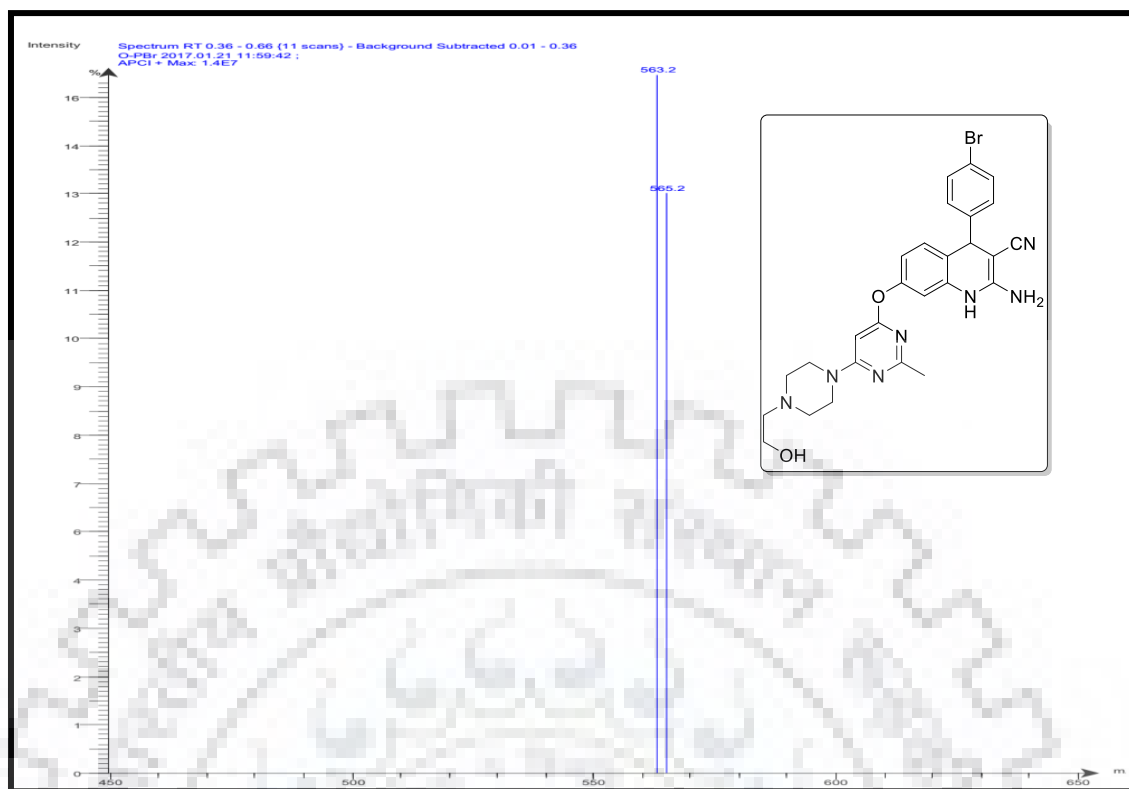


Figure.4.12. LC-MS spectra of **5d** compound.

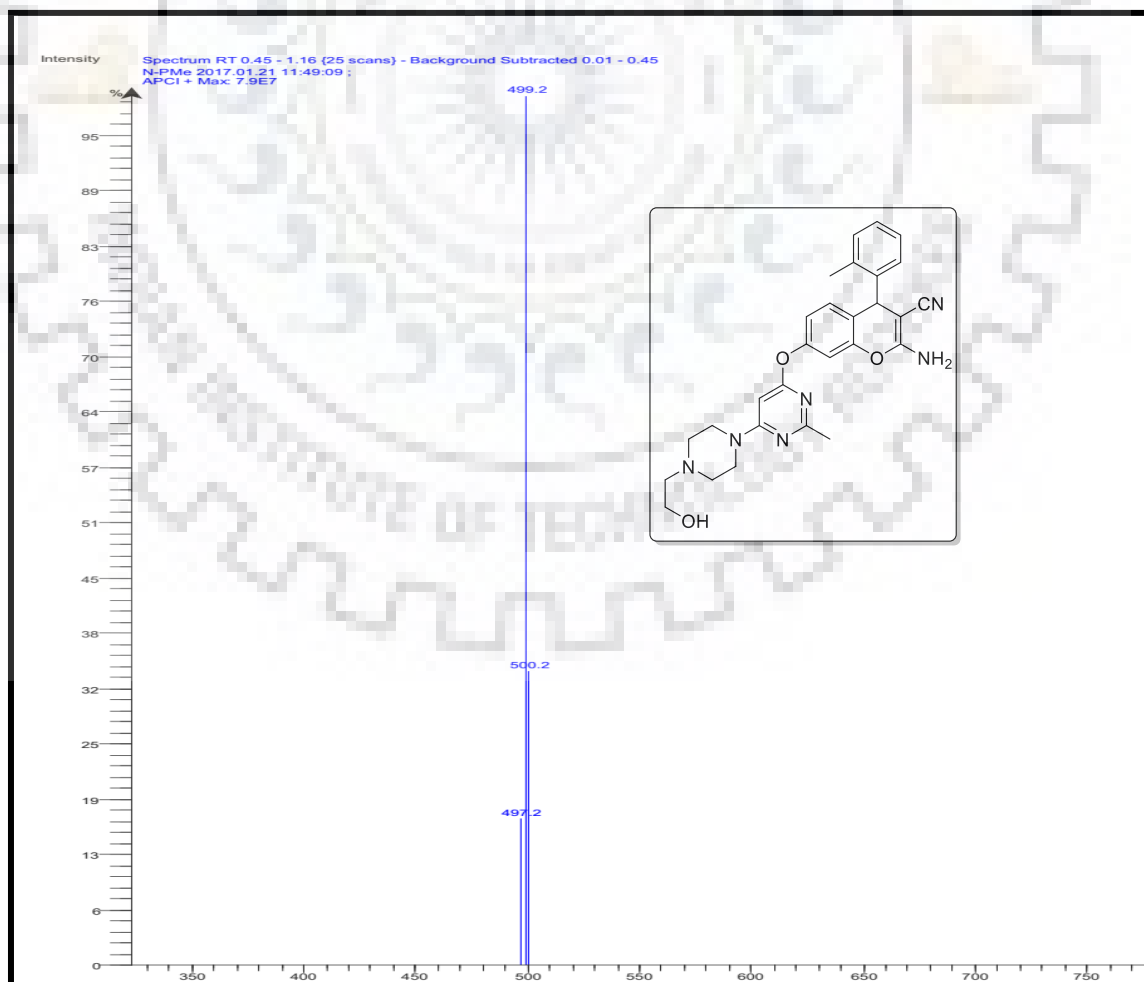


Figure.4.13. LC-MS spectra of **5j** compound.

4.6. References

1. Maggiolini, M.; Bonofiglio, D.; Marsico, S.; Panno, L. M.; Cenni, B.; Picard, D. “Estrogen Receptor α -Mediates the Proliferative but Not the Cytotoxic Dose-Dependent Effects of Two Major Phytoestrogens on Human Breast Cancer Cells” *Mol Pharmacol.* **2001**, *60*, 595–602; (b) Pathe, K. G.; Konduru, K. N.; Parveen, I.; Ahmed, N. “Anti-proliferative activities of flavone–estradiol Stille-coupling adducts and of indanone-based compounds obtained by SnCl_4/Zn -catalysed McMurry cross-coupling reactions” *RSC Adv.* **2015**, *5*, 83512–83521.
2. Torre, L. A.; Bray, F.; Siegel, R. L.; Ferlay, J.; Lortet-Tieulent, J.; Jemal, A. “Global cancer statistics” *CA Cancer J Clin.* **2012**, *65*, 87–108; (b) Torre, L. A.; Siegel, R. L.; Ward, E. M.; Jemal, A. “Global Cancer Incidence and Mortality Rates and Trends–An Update” *Cancer Epidemiol Biomarkers Prev.* **2016**, *25*, 16–27; (c) Hanahan, D.; Weinberg, R. A. “Hallmarks of cancer: the next generation” *Cell* **2011**, *144*, 646–674.
3. Hall, J. M.; Couse, J. F.; Korachk, S. “The Multifaceted Mechanisms of Estradiol and Estrogen Receptor Signaling” *J Biol Chem.* **2001**, *276*, 36869–36872.
4. (a) Nilsson; S.; Mäkelä, S.; Reuter, E.; Tujague, M.; Thomsen, J.; Andersson, G.; Enmark, E.; Pettersson, K.; Warner, M.; Gustafsson, J.-Å. “Mechanisms of Estrogen Action” *J Physiol Rev.* **2001**, *81*, 1535–1565; (b) Fisher, B.; Redmond, C.; Fisher, R. E.; Caplan, R. “Relative worth of estrogen or progesterone receptor and pathologic characteristics of differentiation as indicators of prognosis in node negative breast cancer patients: findings from National Surgical Adjuvant Breast and Bowel Project Protocol B-06.” *J Clin Oncol.* **1988**, *6*, 1076–1087.
5. Niemeier, L. A.; Dabbs, D. J.; Beriwal, S.; Striebel, J. M.; Bhargava, R. “Androgen receptor in breast cancer: expression in estrogen receptor-positive tumors and in estrogen receptor-negative tumors with apocrine differentiation” *Mod Pathol.* **2010**, *23*, 205–212.
6. Duffy, C.; Perez, K.; Partridge, A. “Implications of Phytoestrogen Intake for Breast Cancer” *Cancer J Clin.* **2007**, *57*, 260–277.
7. Spera, D.; Cabrera, G.; Fiaschi, R.; Carlson, E. K.; Katzenellenbogen, A. J.; Napolitano, E. “Estradiol derivatives bearing sulfur-containing substituents at the 11β or 7α positions: versatile reagents for the preparation of estrogen conjugates” *Bioorg Med Chem.* **2004**, *12*, 4393–4401.

8. Angelis, D. M.; Stossi, F.; Waibel, M.; Katzenellenbogen, S. B.; Katzenellenbogen, A. J. "Synthesis of Functionalized 1*H*-Isochromene Derivatives via an Au-Catalyzed Domino Cycloisomerization/Reduction Approach" *Bioorg Med Chem.* **2005**, *13*, 6529–6545.
9. Muthyala, R. S.; Ju, Y. H.; Sheng, S.; Williams, L. D.; Doerge, D. R.; Katzenellenbogen, B. S.; Helferich, W. G.; Katzenellenbogen, J. A. "Equol, a natural estrogenic metabolite from soy isoflavones: convenient preparation and resolution of R- and S- equols and their differing binding and biological activity through estrogen receptors alpha and beta" *Bioorg Med Chem.* **2004**, *12*, 1559–1567.
10. Fink, K. A.; Gurwitz, J.; Rakowski, W.; Guadagnoli, E.; Silliman, A. R. "Patient beliefs and tamoxifen discontinuance in older women with estrogen receptor-positive breast cancer" *J Clin Oncol.* **2004**, *22*, 3309–3315.
11. Burstein, H. J.; Temin, S.; Anderson, H.; Buchholz, T. A.; Davidson, N. E.; Gelmon, K. E.; Giordano, S. H.; Hudis, C. A.; Rowden, D.; Solky, A. J.; Stearns, V.; Winer, E. P.; Griggs, J. J. "Adjuvant Endocrine Therapy for Women with Hormone Receptor-Positive Breast Cancer: American Society of Clinical Oncology Clinical Practice Guideline Focused Update" *J Clin Oncol.* **2014**, *32*, 2255–2269.
12. (a) Doshi, J. M.; Tian, D.; Xing, C. "Structure–Activity Relationship Studies of Ethyl 2-Amino-6-bromo-4-(1-cyano-2-ethoxy-2-oxoethyl)-4*H*-chromene-3-carboxylate (HA 14-1), an Antagonist for Antiapoptotic Bcl-2 Proteins to Overcome Drug Resistance in Cancer" *J Med Chem.* **2006**, *49*, 7731–7739; (b) Kemnitzer, W.; Drewe, J.; Jiang, S.; Zhang, H.; Zhao, J.; Crogan-Grundy, C.; Xu, L.; Lamothe, S.; Gourdeau, H.; Denis, R.; Tseng, B.; Kasibhatla, S.; Cai, S. X. "Discovery of 4-Aryl-4*H*-chromenes as a New Series of Apoptosis Inducers Using a Cell and Caspase-Based High-Throughput Screening Assay. 3. Structure–Activity Relationships of Fused Rings at the 7,8-Positions" *J Med Chem.* **2007**, *50*, 2858–2864; (c) Kumar, R. R.; Perumal, S.; SenthilKumar, P.; Yogeeswari, P.; Sriram, D. "An atom efficient, solvent-free, green synthesis and antimycobacterial evaluation of 2-amino-6-methyl-4-aryl-8-[(*E*)-arylmethylidene]-5,6,7,8-tetrahydro-4*H*-pyrano[3,2-*c*]pyridine-3-carbonitriles" *Bioorg Med Chem Lett.* **2007**, *17*, 6459–6462; (d) Martínez-Grau, A.; Marco, J. L. "Friedländer reaction on 2-amino-3-cyano-4*H*-pyrans: Synthesis of derivatives of 4*H*-pyran [2,3-*b*] quinoline, new tacrine analogues" *Bioorg. Med Chem Lett.* **1997**, *7*, 3165–3170.

13. (a) Ahmed, N.; Dubuc, C.; Rousseau, J.; Bénard, F.; van Lier, J. E. "Synthesis, characterization, and estrogen receptor binding affinity of flavone-, indole-, and furan-estradiol conjugates" *Bioorg Med Chem Lett.* **2007**, *17*, 3212–3216; (b) Bhagat, M. K.; Roberts, J. C.; Mercer-Smith, J. A.; Knotts, B. D.; Vessella, R. L. "Preparation and biodistribution of copper-67-labeled porphyrins and porphyrin-A6H immunoconjugate" *Nucl. Med Biol.* **1997**, *24*, 179–185; (c) James, D. A.; Swamy, N.; Paz, N.; Hanson, R. N.; Ray, R. "Synthesis and estrogen receptor binding affinity of a porphyrin-estradiol conjugate for targeted photodynamic therapy of cancer" *Bioorg Med Chem Lett.* **1999**, *9*, 2379–2384.
14. Gao, M.; Miller, K. D.; Hutchins, G. D.; Zheng, Q.-H. "Synthesis of carbon-11-labeled 4-aryl-4*H*-chromens as new PET agents for imaging of apoptosis in cancer" *Appl Radiat Isot.* **2010**, *68*, 110–116.
15. (a) Hu, M.-J.; Zhang, B.; Yang, H.-K.; Liu, Y.; Chen, Y.-R.; Ma, T.-Z.; Lu, L. You, W.-W.; Zhao, P.-L. "Design, Synthesis and Molecular Docking Studies of Novel Indole–Pyrimidine Hybrids as Tubulin Polymerization Inhibitors" *Chem Biol Drug Des.* **2015**, *86*, 1491–1500; (b) Galmarini, M. C.; Jordheim, L.; Dumontet, C. "Pyrimidine nucleoside analogs in cancer treatment" *Expert Rev Anticancer Ther.* **2003**, *3*, 717–728; (c) Xie, F.; Zhao, H.; Zhao, L.; Lou, L.; Hu, Y. "Synthesis and biological evaluation of novel 2,4,5-substituted pyrimidine derivatives for anticancer activity" *Bioorg Med Chem Lett.* **2009**, *19*, 275–278; (d) Schenone, S.; Bruno, O.; Bondavalli, F.; Ranise, A.; Mosti, L.; Menozzi, G.; Fossa, P.; Donnini, S.; Santoro, A.; Ziche, M.; Manetti, F.; Botttaet, M. "Antiproliferative activity of new 1-aryl-4-amino-1*H*-pyrazolo[3,4-*d*] pyrimidine derivatives toward the human epidermoid carcinoma A431 cell line" *Eur J Med Chem.* **2004**, *39*, 939–946.
16. Weinberg, R. L.; Albom, S. M.; Angeles, S. T.; Husten, J.; Lisko, J. G.; McHugh, R. J.; Milkiewicz, K. L.; Murthy, S.; Ott, G. R.; Theroff, J. P.; Tripathy, R.; Underiner, T. L.; Zifcsak, C. A.; Dorsey, B. D. "Fused bicyclic derivatives of 2,4-diaminopyrimidine as c-Met inhibitors" *Bioorg Med Chem Lett.* **2011**, *21*, 164–167.
17. Boschi, D.; Tosco, P.; Chandra, N.; Chaurasia, S.; Fruttero, R.; Griffin, R.; Wang, L.-Z.; Gasco, A. "6-Cyclohexylmethoxy-5-(cyano-NNO-azoxy)pyrimidine-4-amine: A new scaffold endowed with potent CDK2 inhibitory activity" *Eur J Med Chem.* **2013**, *68*, 333–338.
18. Savall M. B; Chavez, F; Tays, K; Dunford, P. J.; Cowden, J. M.; Hack, M. D.; Wolin, R. L.; Thurmond, R. L.; Edwards, J. P. "Discovery and SAR of 6-Alkyl-2,4-

- diaminopyrimidines as Histamine H4 Receptor Antagonists” *J Med Chem.* **2014**, *57*, 2429–2439.
19. Marchetti, F.; Cano, C.; Curtin, J. N.; Marchetti, F.; Cano, C.; Golding, B. T.; Griffin, R. J.; Haggerty, K.; Newell, D. R.; Parsons, R. J.; Payne, S. L.; Wang, L. Z.; Hardcastle, I. R. “Synthesis and biological evaluation of 5-substituted O 4-alkylpyrimidines as CDK2 inhibitors” *Org Biomol Chem.* **2010**, *8*, 2397–2407.
20. Arris, E. C.; Boyle, T. F.; Calvert, H. A.; Curtin, N. J.; Endicott, J. A.; Garman, E. F.; Gibson, A. E.; Golding, B. T.; Grant, S.; Griffin, R. J.; Jewsbury, P.; Johnson, L. N.; Lawrie, A. M.; Newell, D. R.; Noble, M. E. M.; Sausville, E. A.; Schultz, R.; Yu, W. “Identification of Novel Purine and Pyrimidine Cyclin-Dependent Kinase Inhibitors with Distinct Molecular Interactions and Tumor Cell Growth Inhibition Profiles” *J Med Chem.* **2000**, *43*, 2797–2804.
21. Scagliotti, V. G.; Novello, S.; “The role of the insulin-like growth factor signaling pathway in non-small cell lung cancer and other solid tumors” *Cancer Treat Rev.* **2012**, *38*, 292–302; (b) Ali, Y.; Alam, S. M.; Hamid, H.; Husain, A.; Dhulap, A.; Bano, S.; Kharbanda, C. “Novel 2,4-dichlorophenoxy acetic acid substituted thiazolidin-4-ones as anti-inflammatory agents: Design, synthesis and biological screening” *Bioorg Med Chem Lett.* **2017**, *27*, 1017–1025.
22. Kerns, J. R.; Rybak, J. M.; Kaatz, W. G.; Vaka, F.; Cha, R.; Grucz, R. G.; Diwadkar, V. U. “Structural Features of Piperazinyl-Linked Ciprofloxacin Dimers Required for Activity Against Drug-Resistant Strains of *Staphylococcus aureus*” *Bioorg Med Chem Lett.* **2003**, *13*, 2109–2112.
23. Upadhayaya, S. R.; Sinha, N.; Jain, S.; Kishore, N.; Chandrab, R.; Arora, K. S. “Optically active antifungal azoles: synthesis and antifungal activity of (2R,3S)-2-(2,4-difluorophenyl)-3-(5-{2-[4-aryl-piperazin-1-yl]-ethyl}-tetrazol-2-yl/1-yl)-1-[1,2,4]-triazol-1-yl-butan-2-ol” *Bioorg Med Chem.* **2004**, *12*, 2225–2238.
24. (a) Upadhayaya, S. R.; Vandavasi, K. J.; Kardile, A. R.; Lahore, S. V.; Dixit, S. S.; Deokar, H. S.; Shinde, P. D.; Sarmah, M. P. “Novel quinoline and naphthalene derivatives as potent antimycobacterial agents” *Eur J Med Chem.* **2010**, *45*, 1854–1867; (b) Zyl, v. L. R.; Felix, H. I.; Monteagudo, E. S. “The combined effect of iron chelators and classical antimalarials on the *in-vitro* growth of *Plasmodium falciparum*” *J Antimicrob Chemother.* **1992**, *30*, 273–278.
25. Kumar, C. S. A.; Vinaya, K.; Chandra, N. J. S.; Thimmegowda, N. R.; Prasad, S. B. B.; Sadashiva, C. T.; Rangappa, K. S. “Synthesis and antimicrobial studies of novel

- 1-benzhydryl-piperazine sulfonamide and carboxamide derivatives” *J Enzym Inhib Med Chem.* **2008**, *23*, 462–469.
26. Naz, H.; Jameel, E.; Hoda, N.; Shandilya, A.; Khan, P.; Islam, A.; Ahmad, F.; Jayaram, B.; Hassan, M. I. “Structure guided design of potential inhibitors of human calcium-calmodulin dependent protein kinase IV containing pyrimidine scaffold” *Bioorg Med Chem Lett.* **2016**, *26*, 782–788.
27. Bava, S. V.; Puliappadamba, V. T.; Deepti, A.; Nair, A.; Karunagaran, D.; Anto, R. J. “Sensitization of Taxol-induced Apoptosis by Curcumin Involves Down-regulation of Nuclear Factor- κ B and the Serine/Threonine Kinase Akt and Is Independent of Tubulin Polymerization” *J Biol Chem.* **2005**, *280*, 6301–6308.
28. Souers, A. J.; Levenson, J. D.; Boghaert, E. R.; Ackler, S. L.; Catron, N. D.; Chen, J.; Dayton, B. D.; Ding, H.; Enschede, S. H.; Fairbrother, W. J.; Huang, D. C.; Hymowitz, S. G.; Jin, S.; Khaw, S. L.; Kovar, P. J.; Lam, L. T.; Lee, J.; Maecker, H. L.; Marsh, K. C.; Mason, K. D.; Mitten, M. J.; Nimmer, P. M.; Oleksijew, A.; Park, C. H.; Park, C. M.; Phillips, D. C.; Roberts, A. W.; Sampath, D.; Seymour, J. F.; Smith, M. L.; Sullivan, G. M.; Tahir, S. K.; Tse, C.; Wendt, M. D.; Xiao, Y.; Xue, J. C.; Zhang, H.; Humerickhouse, R. A.; Rosenberg, S. H.; Elmore, S. W. “ABT-199, a potent and selective BCL-2 inhibitor, achieves antitumor activity while sparing platelets” *Nat Med.* **2013**, *19*, 202–208.
29. Kumari, S.; Idrees, D.; Mishra, C. B.; Prakashb, A.; Wahiduzzamanb; Ahmad, F.; Hassan, M. I.; Tiwari, M. “Design and synthesis of a novel class of carbonic anhydrase-IXinhibitor 1-(3-(phenyl/4-fluorophenyl)-7-imino-3*H* [1,2,3] triazolo [4,5*d*] pyrimidin-6(7*H*)-yl)urea” *Mol Graph Model.* **2016**, *64*, 101–109.
30. Leung, C. S.; Leung, S. S. F.; Tirado-Rives, J.; Jorgensen, W. J. “Methyl Effects on Protein–Ligand Binding” *J Med Chem.* **2012**, *55*, 4489–4500.



Chapter-5

Design, Synthesis, Molecular docking and Molecular Insights Inhibition studies of Microtubule Affinity Regulating Kinase 4 of novel 3-N-aryl substituted-2-heteroaryl-chromones for Cancer Therapy

Eur. J. Med. Chem. **2018**, 159, 166-177

5.1. Introduction

Despite advances in the multi-modal management of a wide spectrum of human cancers, it remains a major global killer of human in almost all ages in every society, warranting the need for improved and targeted specific therapies. The incidence of cancer cases is increasing day by day because of changing in life style and other risk factors like overweight, physical inactivity, smoking, mutations in anti-cancer gene and aberrant expression of some proteins/protein kinases [1-2]. The cancer cells are distinguished by self-sufficiency in growth signals, and hypo-sensitivity to anti-growth signals, unlimited replicative potential, metastasis, sustained angiogenesis, and evasion of apoptosis. Many proteins are responsible for cancer growth and progression. However, kinases are main class that have been studied and exploited for the development of potential anticancer molecules [3-7].

Microtubules affinity regulated kinase 4 (MARK4) is the member of microtubule affinity-regulating kinases (MARKs) expressed in multiple tissues [8]. Besides microtubule dynamics regulation MARK4 is also implicated with signal transduction, adipogenesis, cell polarity and cell cycle progression has been also played by MARK4 [9-12]. Initially, the over-expression or dys-regulation of MARK4 was studied in neurological disorders like Alzheimer's disease [13]. But, it was also found that MARK4 is over-expressed in case of different type of cancer like hepatocellular carcinomas, gliomas and inhibits hippo signalling in breast cancer cells, suggesting the role for MARK4 in cancer progression and development [14-16]. Recent studies have shown that inhibition of MARK4 through small molecule inhibitors like chemically synthesized as well as natural molecules hindered the viability of cancerous cells [5,17,18]. Inhibition of MARK4 reduces the cell migration in breast cancer cells and increases the survival of breast and lung cancer patients [19]. These observations clearly suggested that MARK4 may be chosen as a molecular target for cancer prevention and treatment.

The discovery and development of new drugs that can be used in the treatment of cancer remains one of the biggest challenges for the scientific community. Interestingly, nature has demonstrated to be one of the best sources of molecules that can bind to the cancer specific targets [20]. Therefore, the search for new natural molecules, semi-synthetic and synthetic compounds that display specific activity against cancers are of great interest. For example, flavonoids based pyran derivatives that include epicalyxin F, calyxin F, epicalyxin G, calyxin G, epicalyxin K, calyxin K, calyxin L, calyxin I have previously been isolated from the seeds of *Alpinia blepharocalyx sp.* [21]. These plants are widely

distributed in south-western China and their seeds are commonly used in traditional medicine for the treatment of various stomach disorders [22]. Many of these natural products have shown interesting hepatoprotective activity and anti-proliferative activity against cancer cells [23]. Earlier studies further suggested that the flavone and its derivatives have wide-range of diverse biological applications such as anti-cancer activities, antiestrogenic [24] activities against aromatase enzyme [25] and interaction with estrogen receptors [26].

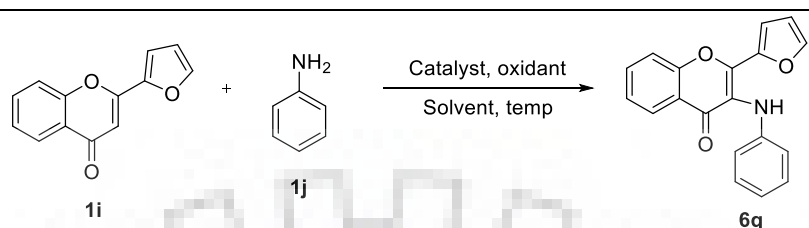
Due to our interest in this field [21, 27-28], we went on modifying the flavonoids scaffold in order to identify new compounds with comparable biological properties in the respect of natural molecules but with reduced or abolished side effects.

In recent years, metal catalysed direct functionalization of aryl C(sp²)-H bonds to diaryl amine have received great deal of attention. With this concept, a number of modifications to C-H amination were developed by Rhodium [29] and Iridium [30] mediated C(sp²)-H amination of benzamide with aryl azide and aniline, and others [31] reported with bidentate auxiliary and 8-amino quinoline-directed Cu(II)/air/Ag(I)catalysed C(sp²)-H amination with electron poor aniline and aliphatic amine and also described with copper catalysed C-H amination reaction on electron rich aniline with the influence of Ag(I)/TBAB. Still, it is challenging to create an inexpensive, efficient, and atom-economic amination method. Direct utilization of the instinctive nucleophilic characteristics of chromones via C-H bond functionalization could afford a valuable approach for preparing a series of varied related products with high site selectivity [32]. Keeping this in view, we explored biologically active natural products to investigate the 3-aminated flavones analogues. We performed amination reaction of flavones derivatives using reported methods but failed to get the product. Then, we tried amination of 2-heteroarylchromones using furan and pyridine as directing groups and hoped to create an efficient process for the synthesis of 3-aminated flavone derivatives. In this context, herein we developed a general method with the idea of utilizing flavone moiety for the amination *via* Pd(OAc)₂ used as a catalyst and Ag₂CO₃ as an oxidant to catalysed oxidative cross-coupling reactions. To discover and develop potent and selective Mark4 inhibitors for cancer therapy, we tried an efficient preparation of novel 3-N-aryl substituted-2-heteroarylchromones by carbon-heteroatom bond formation using 2-heteroarylchromones and anilines *via* transition metal mediated C-H functionalization reaction. Under optimal reaction conditions, 2-heteroarylchromones and anilines afforded the desired products in good to excellent yield (70-84%).

5.2. Results and discussion

5.2.1. Chemistry

Table 5.1. Optimization of reaction conditions



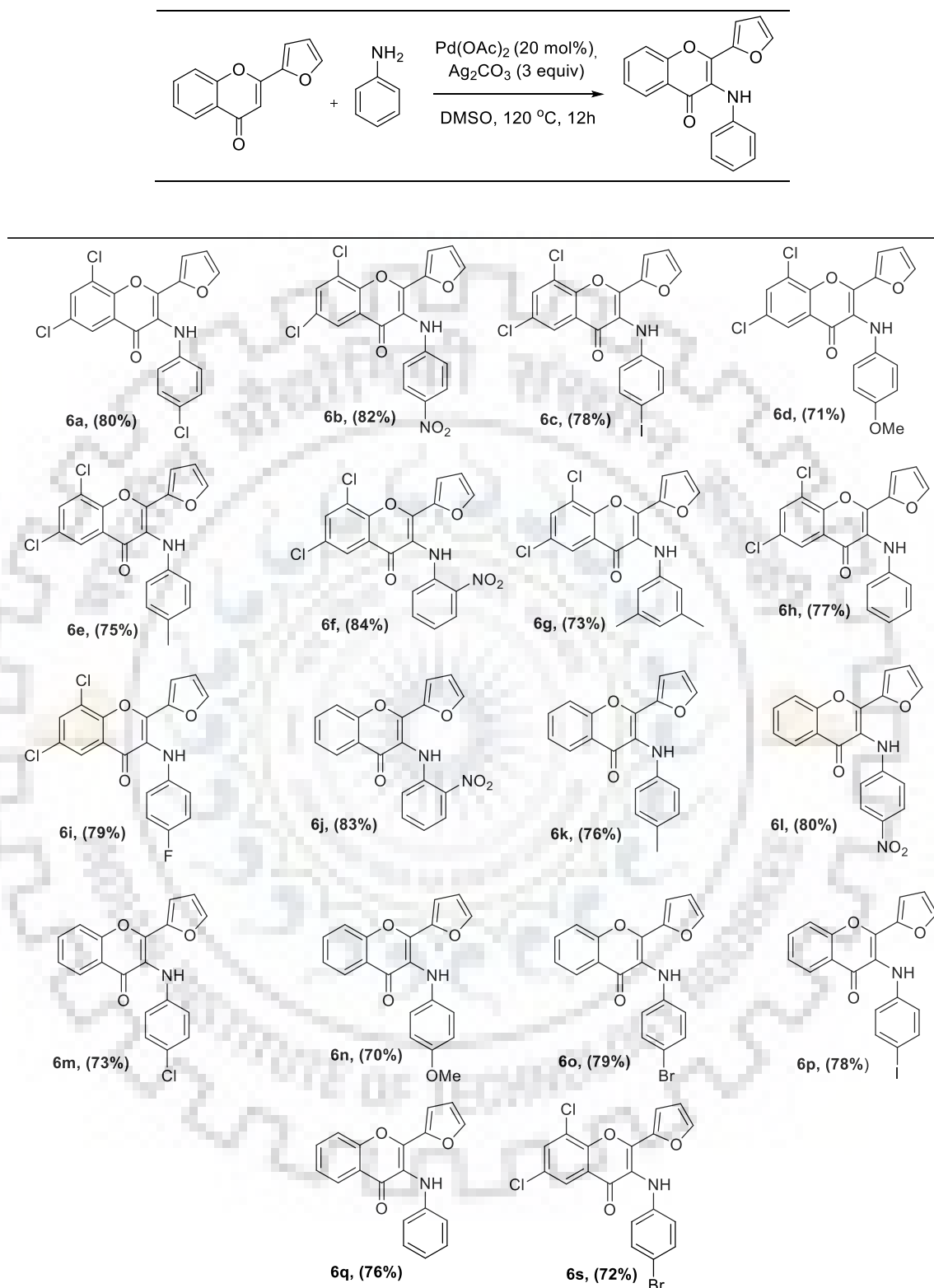
S. No.	Catalyst (20 mol%)	Oxidant (equiv)	solvent	Temp (°C)	yield ^d (%)
1	Pd(OAc) ₂	K ₂ S ₂ O ₈	DMF	120	-
2	Pd(OAc) ₂	Na ₂ S ₂ O ₈	DMSO	120	-
3	Pd(OAc) ₂	K ₂ S ₂ O ₈	DMF	120	-
4	Pd(OAc) ₂	Ag ₂ O (1)	DMSO	120	20
5	Pd(OAc) ₂	Ag ₂ O (2)	DMF	120	30
6	Pd(OAc) ₂	Ag ₂ NO ₃ (1)	DMF	120	35
7	Pd(OAc) ₂	Ag ₂ NO ₃ (1.5)	DMSO	120	41
8	Pd(OAc) ₂	Ag ₂ NO ₃ (2.0)	DMSO	120	45
9	Pd(OAc) ₂	Ag ₂ NO ₃ (3.0)	DMSO	120	47
10	Pd(OAc) ₂	Ag ₂ CO ₃ (1)	DMSO	120	42
11	Pd(OAc) ₂	Ag ₂ CO ₃ (1.5)	DMSO	120	49
12	Pd(OAc) ₂	Ag ₂ CO ₃ (2)	DMSO	120	67
13	Pd(OAc)₂	Ag₂CO₃ (3)	DMSO	120	84%
14	Pd(OAc) ₂	Ag ₂ CO ₃ (3)	DMSO	80	Trace
15	Pd(OAc) ₂	Ag ₂ CO ₃ (3)	DMSO	140	76
16	Pd(OAc) ₂ ^b	Ag ₂ CO ₃ (3)	DMSO	120	39
17	Pd(OAc) ₂ ^c	Ag ₂ CO ₃ (3)	DMSO	120	74
18	Pd(OAc) ₂	PhI(OAc) ₂ (1)	DCE	80	-
19	Pd(OAc) ₂	PhI(OAc) ₂ (2)	DCE	100	-
20	Pd(OAc) ₂	PhI(OAc) ₂ (3)	DCE	120	-

^aReaction were carried out at 1 mmol scale, catalyst (20 mol%), additive, solvent (4ml), temperature, ^bPd(OAc)₂10 mol %), ^cPd(OAc)₂ (30 mol%), ^dIsolated yield.

We commenced our reaction with 2-(furan-2-yl)-4H-chromen-4-one and aniline as a model substrate for the formation of product **6q** by using Pd(OAc)₂ (20 mol%) as a catalyst and K₂S₂O₈ (3 equiv.) as an oxidant in DMF at 120 °C, but failed to get the desired product (Table 5.1, entry 1). So, we replaced K₂S₂O₈ with Na₂S₂O₈ in 1,4-dioxane but we got no product improvement (Table 5.1, entry 2). Using Pd(OAc)₂ with K₂S₂O₈ (5 equiv.) in DMSO at 120 °C was also in vain as the desired product was not obtained (Table 5.1, entry 3). However, when we used Pd(OAc)₂ (20 mol%) with Ag₂O (5.1 and 2 equiv.) which furnished the product **3a** in 20% and 30% yields respectively in 12 h (Table 5.1, entry 4 and 5). Encouraged by the results, we investigated the reaction under various oxidants. We screened the reaction Pd(OAc)₂ (20 mol%) with different oxidant with different amount of silver salts such as Ag₂NO₃ (1 equiv.), Ag₂NO₃ (1.5 equiv.), Ag₂NO₃ (2 equiv.) and Ag₂NO₃ (3 equiv.) in the presence of DMSO solvent at 120 °C. The yield of product formation slightly improved (35%, 41%, 45% and 47% respectively (Table 5.1, entries 6, 7, 8 and 9). The yield was reduced sharply by changing the oxidant to Ag₂CO₃ (1 equiv.), (42%) (Table 5.1, entry 10). If we use Ag₂CO₃ (1.5 equiv.) and Ag₂CO₃ (2 equiv.) the product yield further improved (49% and 67%) respectively (Table 5.1, entry 11 and 12). Efficiency of the reaction was encouraging, when the reaction was carried out with Pd(OAc)₂ (20 mol%) in the presence of oxidant Ag₂CO₃ (3 equiv.), an excellent product yield 78% was obtained at 120 °C in DMSO for 12 h (Table 5.1, entry 13). Either lowering the temperature or increasing the temperature failed to give a better yield (Table 5.1, entries 14 and 15). The reaction with Pd(OAc)₂ (10 mol%) with Ag₂CO₃ (3 equiv.) afforded lower yield (39%) (Table 1, entry 16). No further increment in the desired product yield was also obtained when the reaction was performed in presence of Pd(OAc)₂ with (30 mol%) and oxidant Ag₂CO₃ (3 equiv.) in DMSO solvent at 120 °C (Table 1, entry 17). Similarly, no better yield was obtained with Pd(OAc)₂ (20 mol%) with different equivalent of phenyliododiacetate such as PhI(OAc)₂ (1 equiv.), PhI(OAc)₂ (2 equiv.) and PhI(OAc)₂ (3 equiv.) as an oxidant in dichloroethane (DCE) solvent at 80 °C, 100 °C and 120 °C (Table 5.1, entry 18, 19 and 20).

5.2.1.1. Substrate scope

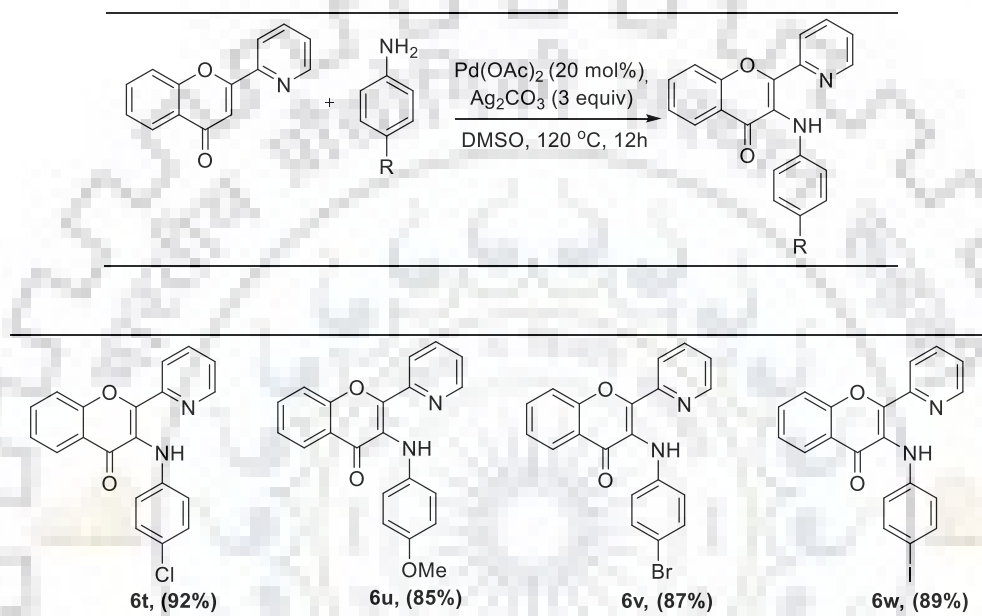
Under optimized reaction conditions, we further investigated the scope of substrates in Pd(OAc)₂ catalysed reaction of 2-(furan-2-yl)-4H-chromen-4-one and aniline derivatives for the synthesis of 3-aminoflavone derivatives (Scheme 5.1). The reaction exhibited wider substrate scope and showed good tolerance for electron-withdrawing groups, electron donating groups and without substrate at aniline.



Scheme 5.2. Scope of aniline for the direct C-H amination furan as a directing group.

Para substituted nitroaniline showed to be good substrate for this reaction (compounds **6b**, **6l**). To our surprise, ortho substituted nitroaniline delivered the corresponding aminated product in high yields (compounds **6f**, **6j**). The reaction proved good tolerance

toward halogenated substituents including F, Cl, Br and I to provide the corresponding aminated products in acceptable yields (compounds **6a**, **6c**, **6i**, **6m**, **6o** and **6p**). The substituent like $-\text{NO}_2$, and halogen groups such as $-\text{I}$, $-\text{Br}$ – Cl and F on aniline ring afforded products in good yield as compare to without substituent (compounds **8**, **17**) and the $-\text{Me}$ and $-\text{OMe}$ substituted products (compounds **6d**, **6e**, **6g**, **6k**, **6n** and **6s**). The products yield also varied depending upon the position of the substituents on flavones molecule.



Scheme 5.3. Scope of substrates for the direct C-H amination with pyridine as a directing group.

Additionally, we examined the scope of substrates in $\text{Cu}(\text{OAc})_2$ catalysed reaction of 2-(pyridin-2-yl)-4H-chromen-4-one and aniline derivatives for the synthesis of 3-aminoflavone derivatives (Scheme 5.2). The reaction showed extensive substrate scope with Cl, I, Me and OMe (**6t**, **6u**, **6v** and **6w**) with excellent yield (85-92%) in the presence of $\text{Pd}(\text{OAc})_2$ and Ag_2CO_3 at $120\text{ }^\circ\text{C}$ for 12h. We tried that reaction with copper acetate get acceptable yield in that case also (Scheme 5.3).

5.2.2. Biology

5.2.2.1. Expression and purification of protein

MARK4 was expressed and purified successfully. Purity of eluted protein was checked by running SDS-PAGE. Details of protein expression and purification have been described in our previous communications [34].

5.2.2.2. ATPase enzyme inhibition assay

Initially, all of the synthesized compounds were screened against MARK4 with the help of ATPase inhibition assay. We observed that out of 22 compounds, three compounds (**6b**, **6c** and **6n**) significantly inhibit the MARK4 activity. To evaluate the inhibitory potential of these selected compounds, enzyme assay of MARK4 was performed with increasing concentrations of each compound (0-10 μM). Subsequently, IC_{50} value (50% of ATPase activity) for compound (**6b**, **6c** and **6n**) was calculated as $2.12 \pm 0.22 \mu\text{M}$, $1.98 \pm 0.34 \mu\text{M}$, and $5.56 \pm 0.42 \mu\text{M}$, respectively (Figure 5.1A). These findings clearly suggested that selected compounds (**6b**, **6c** and **6n**) inhibits the activity of MARK4 and is presumably considered as potential inhibitor of MARK4.

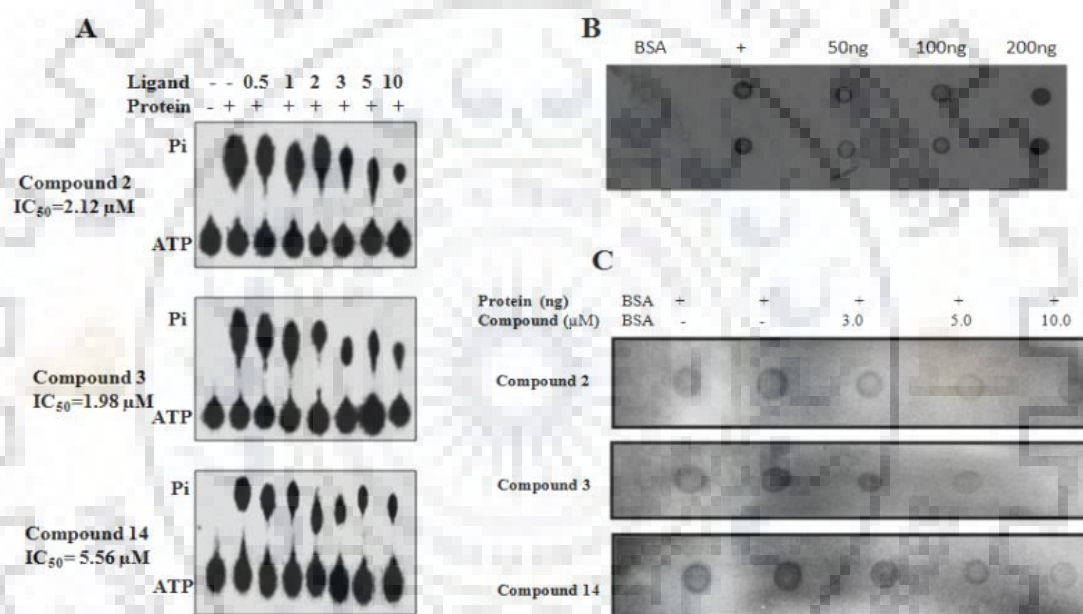


Figure.5.1. Kinase inhibition assay. (A). Shows the hydrolysis of Pi from ATP, position of Pi and ATP spots are indicated. Lane 1, negative control (without protein); lane 2, 100 nM MARK4 (positive control); and lanes labelled as 0.5,1.0, 2.0, 3.0, 5.0 and 10.0, shows the concentration of compound (**6b**, **6c** and **6n**). (B). Binding of MARK4 with radiolabelled oligos (C). Inhibition of kinase activity of MARK4 verified by DOT-blot assay by using radiolabelled oligos as substrate showing that all three selected molecules inhibits MARK4.

We have further screened MARK4 against radio labelled phosphate based oligos and found that it binds with oligos and hydrolyse phosphate significantly (Figure 5.1B). Thus, we studied the binding and inhibition of MARK4 by compounds (**6b**, **6c** and **6n**) with the help of dot blot assay. MARK4 was incubated with increasing the concentrations of these compounds and subsequently labelled oligos were added as a substrate. It was observed

that these compounds bind to MARK4 and significantly inhibit the release of phosphate from oligos (Figure 5.1C).

5.2.2.3. Binding of selected compounds to the MARK4

Molecular docking approaches have been used to see any molecular interaction exist between each synthesized compounds and residues lies in the active site cavity of MARK4.

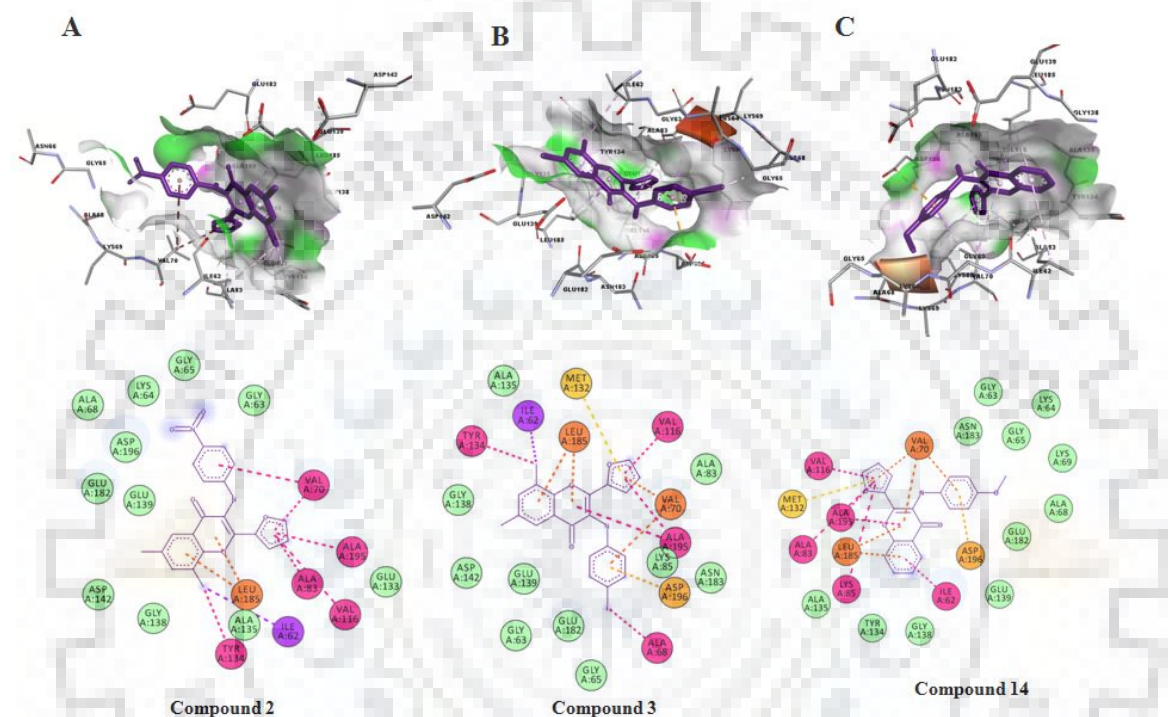


Figure 5.2. Molecular docking studies of (A) compound **6b**, (B) compound **6c** and (C) compound **6n**. Upper panel shows the pocket view of MARK4 binding with selected compounds. Lower panel is showing the 2D schematic diagram of interactions of MARK4 with selected compounds. Residues involved in hydrogen bonding, charge or polar interactions, van der Waals interactions are represented in different color.

We have used Autodock (version 4.2), an automated tool to perform docking which was installed on Windows 7 OS (on HP Proliant DL180 G6 workstation) [35]. It helps to estimate the intermolecular distance between the interacting residues and binding energies of each protein-ligand complex. Binding energy obtained from molecular docking and number of interacting residues helps us to select the best-docked complex among the selected synthesized compounds, results of docking are shown in Table 2.2. Analysis of docking results indicates a sufficient number of interactions are offered by the active site residues of MARK4 to the selected compounds (Figure 5.2). These observations clearly indicate that the synthesized compounds possess high binding

affinity for the MARK4 and specifically bind to the active site residues, which may significantly inhibit its activity.

Table.5.2. Molecular docking results showing binding energy and interacting residues from the active site of MARK4 with **6b**, **6c** and **6n** derivatives.

Compound number	Binding energy(kcal/mol)	Protein ligand interaction			
		No. of H bonds	Amino acid residues	Distance (Å)	Other interacting residues
6b	-8.8	2	Glu139 Glu182	3.4 3.5	Ala68, Lys64, Gly63, Gly65, Val70, Ala195, Glu133, Ala83, Val116, Ile62, Ala135, Leu185, Tyr134, Gly138, Asp142, Glu139, Glu182, Asp196
6c	-8.4	1	Glu182	3.5	Gly65, Glu182, Gly63, Glu139, Asp142, Gly138, Tyr134, Ala135, Ile62, Met132, Leu185, Val116, Ala83, Val70, Ala195, Lys85, Asn183, Asp196, Ala68
6n	-8.2	1	Asp196	3.2	Gly138, Tyr134, Lys85, Ala135, Leu185, Ala83, Ala195, Met132, Val116, Val70, Asn183, Gly63, Lys64, Gly65, Lys69, Ala68, Glu182, Glu139, Ile62

5.2.2.4. Fluorescence binding studies

To see the binding affinities of synthesized compounds with MARK4, we used fluorescent emission spectra measurements. Protein was excited at 280 nm and emission spectra were recorded in the range of 300-400 nm with the increasing concentrations of each compound (0-100 μ M). A decrease in fluorescence intensity with increasing the concentration of each compound is fitted in the modified Stern-Volmer equation (1) to calculate the binding constant, K_a and number of binding site per protein molecule (n).

$$\log(F_0 - F)/F = \log K_a + n \log [Q] \quad (1)$$

Where F_0 is the fluorescence intensity of protein and F is the fluorescence intensity of ligand, K_a is the binding constant and n is the number of binding sites, Q represents quenching constant. For the ligand-protein complex, the values for K_a and n can be derived from the intercept and slope.

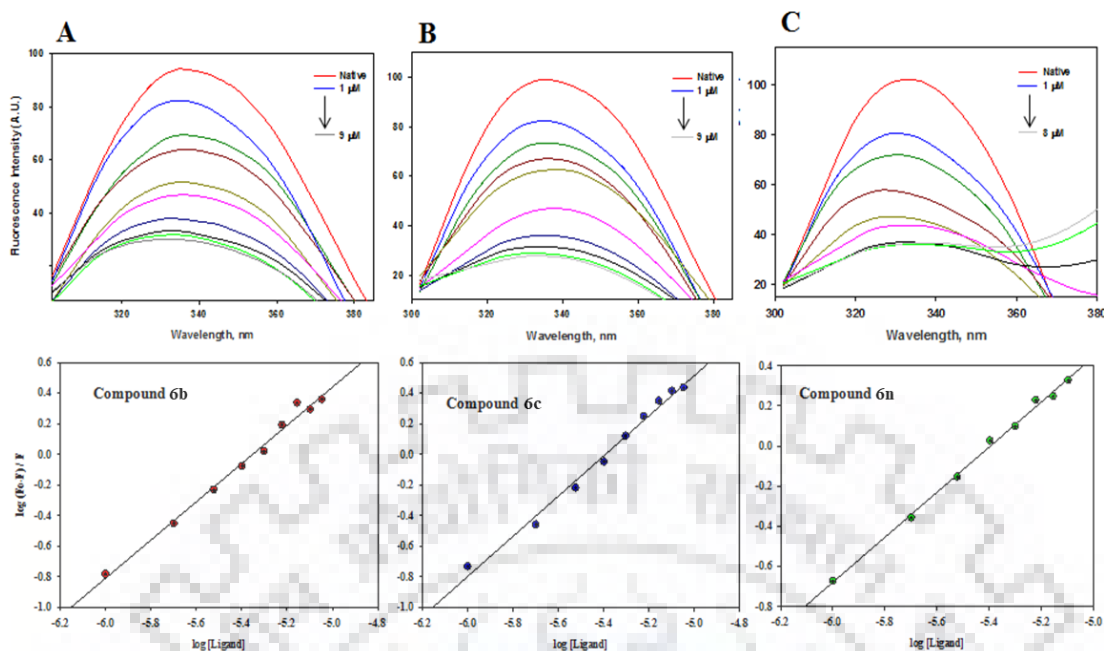


Figure.5.3. Fluorescence binding studies. Fluorescencespectra of MARK4 (5 μM) with increasing concentration of (A) Compound **6b**, (B) Compound **6c** and Compound **6n** (0–10 μM). Excitation wavelength was fixed to 280 nm and emission was recorded in the range 300–400 nm. Lower panel shows Modified Stern-Volmer plot used to calculate binding affinity (K_a) and number of binding sites (n).

The binding affinities of selected compounds have been studied by fluorescence binding (Figure 5.3). However, it was found that for each compound a single binding site has been present on MARK4. It is interesting to note that the results of fluorescence binding are consistent with that of enzyme activity results and suggested that the high binding affinity compounds significantly inhibit the enzyme activity of MARK4. Further, it was concluded from the dot blot assay, docking studies and fluorescence based binding assay that these compounds bind with the active site cavity of MARK4 and this binding hinders the substrate accessibility to MARK4. This observation also confirms our notion that binding of these compounds leads to the enzyme inhibition [5].

5.2.2.5. Cell proliferation assay

Initially, the selected synthesized compounds were evaluated for their cytotoxicity potential on MCF-7 (Human breast cancer cell line), HepG2 (human liver cancer cell line), and HEK293 (Human embryonic kidney cells) cell lines by MTT assay. For HEK293 cells, these compounds were screened in the concentration range of 0–200 μM, and treatments were given for 24 and 48 h. Whereas, in case of MCF-7 and HepG2 cells the compounds **6b**, **6c** and **6n** as selected by binding and enzyme inhibition assays are studied in detail. The results had shown that the studied concentration range of these

compounds inhibit the proliferation of MCF-7 as well as HepG2 cells (Figure 5.4). Consistent with earlier studies, cell proliferation studies also showed that compound **6b**, **6c** and **6n** provoked superior toxicity in a concentration dependent manner on MCF-7 and HepG2 cells. It was also interesting that in the studied sub-micromolar concentration range these compounds don't show considerable cytotoxicity towards HEK293 cell lines.

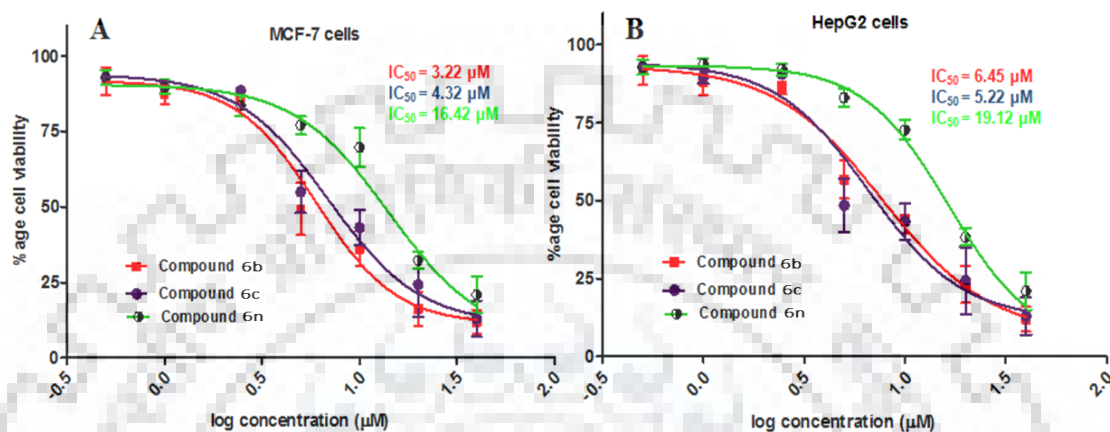


Figure.5.4. Cell proliferation studies. Effect of compound **6b**, **6c** and **6n** (A) MCF-7 (Breast Cancer) and (B) HepG2 (Liver cancer) cells. Cells were treated with increasing concentrations of compound **6b**, **6c** and **6n** (0–200 µM) for 48 h. Cell viabilities were shown as a percentage of the number of viable cells to that of the control. Each data point shown is the mean \pm SD from $n = 3$.

The IC₅₀ values for compound **6b**, **6c** and **6n** were found to be 3.22 ± 0.42 , 4.32 ± 0.23 µM, and 16.22 ± 1.33 for MCF-7 cells, and 6.45 ± 1.12 , $5.22 \pm .72$ µM, and 19.12 ± 1.43 for HepG2 cells. Cytotoxicity of these selected compounds at their respective IC₅₀ value were also studied on HEK293 cells. It was observed that more than 85% of embryonic kidney cells were viable even after 72 h of treatment. Cytotoxicity results clearly suggested that these compounds are non-toxic to normal cells and specifically bears toxicity for cancerous cells. Thus, compound **6b**, **6c** and **6n** were taken for further cell-based studies such as apoptosis and reactive oxygen species (ROS) production.

5.2.2.6. Apoptosis assay

Evasion of apoptosis is a striking hallmark of cancerous cells, it is an essential process that controls abnormal growth of cells, but impaired signalling helps the cancerous cells to escape apoptosis [36]. MARK4 over-expression also supports the growth and evasion of cancerous cells [37]. Thus, the probability of apoptosis induction by inhibiting MARK4 was studied. MCF-7 and HepG2 cells were starved in reduced serum medium and treated with IC₅₀ dose of each compounds for 24 h and subsequently annex in-V staining was used to assess the apoptotic potential of these compounds.

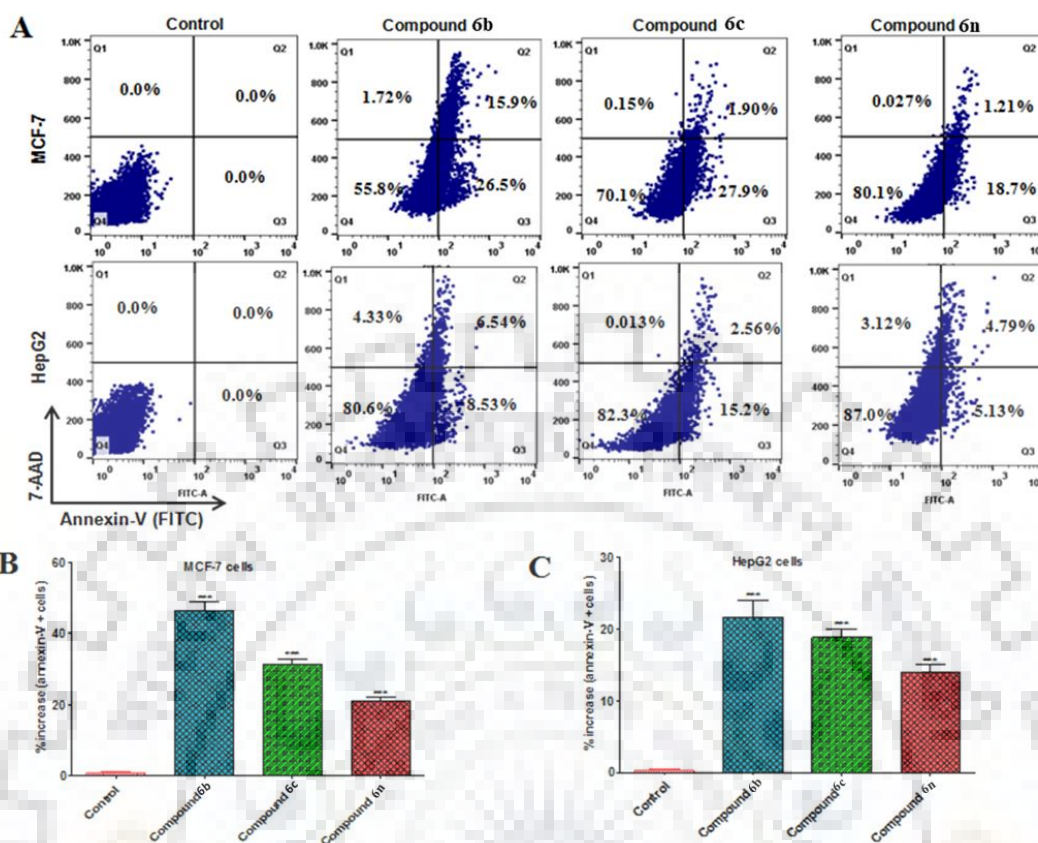


Figure 5.5. Apoptosis studies. (A) Annexin-V staining of MCF-7 and HepG2 cells; cells were treated with IC₅₀ concentrations of each compound for 48 h and subsequently stained with FITC Annex in-V. Stimulation of apoptosis was quantified by flow cytometry. Representative flow images showing FITC-Annex in-V labeled cells, which directly corresponds to the percentage of apoptotic cells. Bar graphs of (B) MCF-7 and (C) HepG2 cells represents the percentage of apoptotic cells stained with Annex in-V for duplicate measurements \pm SD. $**p < 0.001$, compared with the control (untreated cells). Statistical analysis was done using one-way ANOVA and t-test for unpaired samples. For anticancer activities doxorubicin has been taken as positive control.

Stained cells were analysed by flow cytometry and it was found that the treatment of compound **6b**, **6c** and **6n** considerably induces the apoptosis in the MCF-7 as well as HepG2 cells (Figure 5.5). Analysis of results suggested that treatment of compound **6b**, **6c** and **6n** induces apoptosis in 44.12%, 29.95% and 22.00 %, of MCF-7 cells, and 19.40%, 17.77% and 13.04 %, of HepG2 cells respectively as compared to the control cells (Figure 5.5). These observations clearly indicate that these three compounds induce apoptosis in MCF-7 and HepG2 cells.

Consistent to the results of binding, enzyme inhibition and cell proliferation, apoptosis assays also suggested that compound **6b** and **6c** induces apoptosis in more number of

cells (Figure 5.5). Though these three compounds elicited the apoptosis in highly significant number of cells but compound **6b** and **6c** found to be activates apoptosis more prominently. Inference from the decreased cell proliferation as a result of selected compound treatment also suggests that these molecules may inhibit the MARK4.

Because MARK4 is recently identified to inhibit hippo signalling in MCF-7 cell [37] and also acts as the negative regulator of mTORC1 [38], these two pathways are accountable for rapid cell proliferation and migration of cancer cells. So the molecule which inhibits the MARK4 might also be responsible to regulate these pathways. Thus, our results are in consistency with these earlier reports that MARK4 inhibition considerably reduces that cell proliferation and induces apoptosis in MCF-7 cells.

5.2.2.7. Tau-phosphorylation assay

Cell free *in vitro* ATPase inhibition studies clearly suggested that compound **6b**, **6c** and **6n** inhibit the MARK4 significantly.

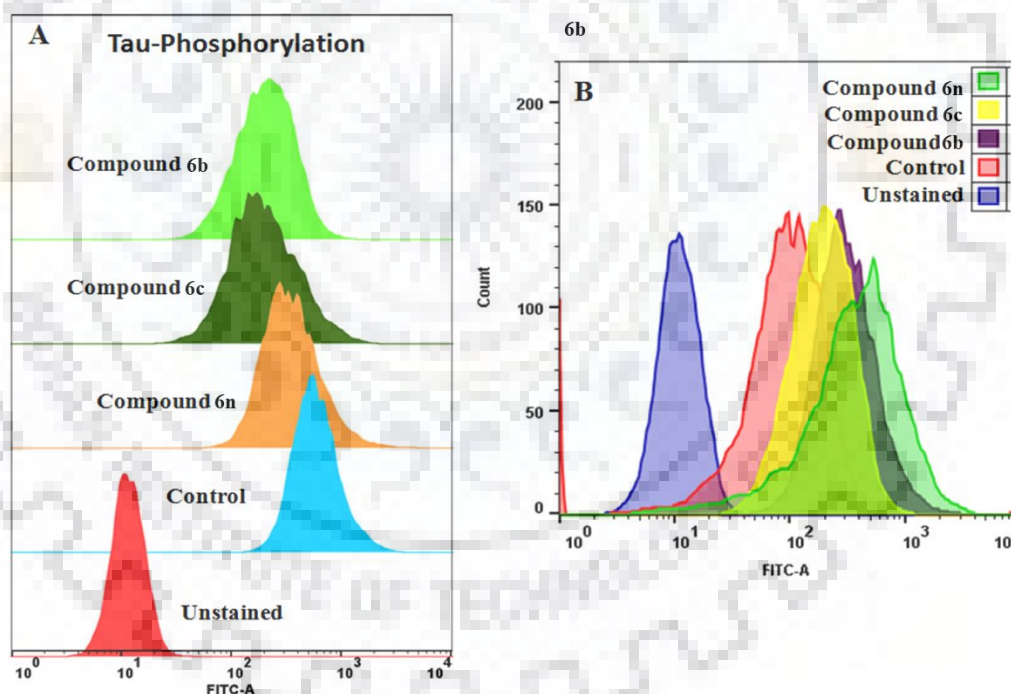


Figure.5.6. (A) Representative flow cytometry histogram of MCF-7 cell fractions stained with phosphorylated anti-tau antibodies, each histogram represents the phosphorylation status of tau under different treatments as mentioned in inset. (B). Showing the concentration of ROS at different concentrations of selected compounds.

In order to confirm this observation, enzyme inhibition activity is extended to a cell system-based tau-phosphorylation assay. Tau proteins act as the substrate for MARK4

mediated phosphorylation. For this cell were allowed to grow in presence of compound **6b**, **6c** and **6n**, subsequently phosphorylation of tau has been assessed with the help of flow cytometry. It was found that compound **6b**, **6c** and **6n** inhibit the phosphorylation of tau (Figure 5.6A). Result presented in the Figure 7A shows that treatment of compounds **6b**, **6c** and **6n** shifts the position of histogram towards the lower side of untreated cells (shown by red color: control). These results signify compounds **6b**, **6c** and **6n** inhibit the phosphorylation of tau. MARK4 phosphorylates the Tau: so, we study the effect of MARK4 inhibition on Tau phosphorylation.

5.2.2.8. Estimation of levels of reactive oxygen species

The respiratory cycle of mitochondria is the foremost source of reactive oxygen species (ROS), and ROS has the potential to induce cell apoptosis [38]. Thus it was speculated that the treatment of selected compounds might leads to the production of ROS. The MCF-7 cells were treated with IC₅₀ dose of compound **6b**, **6c** and **6n** for 5-6 h incubation (Figure 5.6B). ROS levels were quantified with the help of flow cytometry by using 2-Dichlorofluorescein diacetate (DCFDA) staining. Interestingly, it was found that treatment of compound **6b**, **6c** and **6n** increases the production of ROS. Representative histogram was shown in Figure 6B, which suggests that incubation of MCF-7 cells with compound **6b**, **6c** and **6n** shifts the position of respective histogram towards right (higher value), that shows an increase in the levels of ROS. Results of ROS measurement suggested that compound **6b**, **6c** and **6n** considerably increases the levels of ROS that might be also a reason for cellular death of MCF-7. Generation and accumulation of ROS result in oxidative stress and play a crucial role in the governing of cancer cell behaviour. Increased levels of ROS can activate a sequence of pro-apoptotic pathways, like mitochondrial dysfunction and ER stress and, which eventually leads to deterioration of cell function and apoptosis [39]. Taken together, all these observations suggesting that the inhibitory potential of these compounds against cancerous cells.

5.3. Conclusion

In conclusion, we developed an efficient method for the synthesis of novel 3-N-aryl substituted-2-heteroarylchromones via Pd-mediated oxidative coupling using 2-heteroarylchromones and anilines. Among the 22 synthesized compounds, compounds **6b**, **6c** and **6n** gave excellent results used as enzyme inhibition aligned with human MARK4 with IC₅₀ value $2.12 \pm 0.22 \mu\text{M}$, $1.98 \pm 0.34 \mu\text{M}$, and $5.56 \pm 0.42 \mu\text{M}$ with better binding affinity. They also showed anti-proliferative activity against human breast cancer line with 3.22 ± 0.42 , 4.32 ± 0.23 , and $16.22 \pm 1.33 \mu\text{M}$ and human liver carcinoma cells

with 6.45 ± 1.12 , 5.22 ± 0.72 , and $19.12 \pm 1.43 \mu\text{M}$. This study ensued in the identification of potential lead compounds for prospective *in vitro* and *in vivo* anticancer studies suggesting MARK4 as promising anti-cancer target.

5.4. Experimental section

5.4.1. General Information

All the required chemicals were purchased from Sigma Aldrich, Himedia and Aavra. IR spectra were recorded on a Thermo Nicolet FT-IR spectrophotometer with KBr. NMR was recorded on a Jeol Resonance ECX 400II spectrometer using CDCl_3 as solvent. In ^1H NMR Chemical shifts are recorded in parts per million and referenced internally to the residual with tetramethylsilane (TMS δ 0.00 ppm) or proton resonance in CDCl_3 (δ 7.26 ppm). ^{13}C NMR spectra were referenced to CDCl_3 (δ 77.0 ppm, the middle peak). Coupling constant were recorded in Hz. The following abbreviations are used to explain the multiplicities: s = singlet, d = doublet, dd = doublet of doublets, dt = doublet of triplets, t = triplet, q = quartet, m = multiplet. Mass spectra were measured with ESI ionization in MSQ LCMS mass spectrometer.

5.4.1.1. Chemistry

5.4.1.1.1. General procedure

A round bottom flask with a magnetic stirring bar was charged with flavone (1 mmol), $\text{Pd}(\text{OAc})_2$, (10 mol%), Ag_2CO_3 used as an oxidant (3 equivalent), DMSO solvent (3 mL) and the reaction was stirred at 120 °C temperature after 10 min aniline (1.5 mmol) is added. The reaction mixture was refluxed at 120 °C until complete consumption of the starting material as detected by TLC. TLC checked in 10% hexane and ethyl acetate. After completed the reaction, the mixture was poured into water and extract with water. The residue was purified *via* column chromatography with good to excellent yield (**6a-6w**).

5.4.1.2. Biology

5.4.1.2.1. ATPase assay

ATPase assay was performed to evaluate the enzyme activity of MARK4 in the presence of different compounds; for this previously published protocol from our group has been followed [4, 16]. Briefly, we measured ^{32}P i released from $[\gamma\text{-}^{32}\text{P}]$ ATP hydrolysis, which was catalysed by MARK4. After incubating proteins with ice-cold ATP (1 mM) and $[\gamma\text{-}^{32}\text{P}]$ ATP (specific activity 222 TBq mmol^{-1}) for 2 h at 37 °C thin layer chromatography was performed. We first preceded our experiment in the presence of increasing concentrations of all the synthesized compounds with MARK4. Finally, after initial

screening, MARK4 were incubated with increasing concentrations of selected compounds. These results were taken to measure the MARK4 inhibition in terms of percentage hydrolysis of ATP.

5.4.1.2.2. Molecular docking

Autodock Vina and Autodock 4 package was used for molecular docking (Trott and Olson, 2010). Autodock Vina uses an advanced docking algorithm and scoring function of protein ligand interactions. Atomic coordinates of MARK4 was retrieved from RCSB Protein Data Bank database (www.rcsb.org) using the PDB ID 5ES [40]. Prior to docking analysis, the structure was emended by removing the ligand and co-crystallized water molecules, followed by addition of polar hydrogens and Gasteiger charges using Auto Dock Tool (ADT). The 2D and 3D structures of all the synthesized compounds were generated and energy minimized by ChemBio3D Ultra 12.0. After preparing the coordinate files of MARK4 and respective compounds, they were subjected to molecular docking in order to see the bound conformations, binding affinity and possible protein-ligand interactions. PyMOL viewer (Schrödinger, LLC) and “Receptor-Ligand Interactions” modules of BIOVIA/Discovery Studio 2017R2 were used for the visualization and structure analysis of the docked complexes of MARK4 and to generate two-dimensional docking for the analysis of hydrogen bonds and hydrophobic interactions [41].

5.4.1.2.3. Fluorescence measurements

The binding study of synthesized compounds with recombinant MARK4 was carried out by monitoring fluorescence intensity change of emission spectrum of MARK4 by following our previously published protocol [33]. Each titration of protein was performed in triplicates and the average was taken for analysis. A significant decreased in fluorescence intensity of protein with increase in the concentration of selected compounds were used as the criteria to calculate the binding constant (K_a) as well as number of binding sites (n) present on the protein molecule using the modified Stern-Volmer equation [42]:

$$\log (F_0-F)/F = \log K_a + n \log [L] \quad (1)$$

where, F_0 = Fluorescence intensity of native protein, F = Fluorescence intensity of protein in the presence of ligand, K_a = Binding constant, n = number of binding sites, L = concentration of ligand. The values for binding constant (K_a) and number of binding sites (n) were derived from the intercept and slope, respectively.

5.4.1.2.4. Cell culture

HEK-293, HepG2 and MCF-7 human cell lines were grown and maintained in a DMEM supplemented with 10% heat-inactivated fetal bovine serum (Gibco) and 1% penicillin, streptomycin solution (Gibco), in a 5% CO₂ humidified incubator at 37°C. Cells were cultured, maintained and trypsinized not more than 30 passages.

5.4.1.2.5. Cell viability assay

To study the effect of synthesized compounds on cell viability and proliferation, standard MTT method was carried out. Cells were plated (8000-9000/well) in a 96-well plate and incubated overnight. On the next day, cells were treated with increasing concentrations (0.1–80 µM) of compounds in a final volume of 200 µl for 48 h at 37°C in a humidified chamber. At the end of treatment time point, 20 µl of MTT solution (from 5mg/ml stock solution in phosphate buffer saline, pH 7.4) was added to each well and incubated further for 4-5 h at 37°C in the CO₂ incubator. After stipulated time the supernatant was aspirated and the colored formazan crystal produced as a result of MTT reduction was dissolved in 100 µl of DMSO. The absorbance (A) of colored product was then measured at 570 nm on a multiplate ELISA reader (Bio-Rad). The percentage of viable cells was calculated and used to estimate the IC₅₀ (50% inhibitory concentration) values for studied compounds. For cell proliferation and anticancer activities paclitaxel has been taken as positive control.

5.4.1.2.6. Cell apoptotic assay

Annexin-V staining was used to analyse the apoptotic potential of selected synthesized compounds as described earlier [43]. Briefly, MCF-7 and HepG2 cells were treated with IC₅₀ dose of selected compound for 24 h at 37 °C, and the control cells were treated with the media only. After 24 h treatment, nearly 2.5 x 10⁶ cells were trypsinized and collected by centrifuging the cell suspension at 1800 rpm for 4 min. Collected cells were washed two times with 5 ml of PBS. Finally, cells were stained with FITC-Annex in-V with the help of FITC-Annex in-V kit according to the manufacturer's guidelines (BD-Biosciences, USA). Approximately, 10,000 events were analyzed for each sample through flow cytometry on BD LSR II Flow Cytometry Analyzer and FlowJo.

5.4.1.2.7. Tau-phosphorylation assay

For tau-phosphorylation inhibition assay, MCF-7 cells were grown in 6-well cell culture plate and treated with IC₅₀ dose of selected compounds. After 24 hrs, 1x 10⁶ cells were harvested and staining was done within 1 h of harvest. Followed by three times washing with PBS containing 2% BSA cells were fixed with fixation buffer (2%

paraformaldehyde) for 40 min (4 °C) and permeabilized with permeabilization buffer (eBioscience) and 0.5% saponin for 30 min at 4 °C. The cells were washed two times, re-suspended in incubation buffer and incubated with primary antibodies of anti-tau (pSer262), at 25 °C for 2 hr. After incubation cells were washed as before and labelled with FITC labelled goat anti-rabbit IgG secondary antibody for 30 min at room temperature. Flow cytometry analysis was performed on FlowJo (BD Bioscience, USA). At least 100,000 events were acquired for each sample.

5.4.1.2.8. Reactive oxygen species measurement

As DCF fluorescence helps to measure different types of reactive oxygen species (ROS), DCFDA staining was used to quantify the ROS level inside the cell as described earlier (Khan *et al.*, 2017). Briefly, the MCF-7 cells (70-80% confluent) were treated with IC₅₀ dose of each compound and positive control H₂O₂, respectively in a 24-well culture plate. After 5-6 h incubation of cells with respective compounds, cells were gently washed with 500 µl of prewarmed (at 37 °C) Krebs's Ringer buffer (20 mM HEPES, 2 mM MgSO₄, 10 mM dextrose, 127 mM NaCl, 1 mM CaCl₂ and 5.5 mM KCl), subsequently 10 µM DCFDA (Invitrogen Grand Island, NY) has been added to each well and incubated further for 30 min in dark at 37 °C in a humidified CO₂ incubator. After 30 min incubation, the cells were collected by trypsinization and ROS levels were quantified with the help of Flow Cytometry. Nearly 10,000 events for each sample were collected on BD LSR II Flow Cytometry Analyzer, and analyze with help of FlowJo.

5.5. Characterization data

6,8-dichloro-3-((4-chlorophenyl)amino)-2-(furan-2-yl)-4H-chromen-4-one (6a):

Yield: 80% as yellow solid; ¹H NMR (400 MHz, CDCl₃, δ): 10.8

(s, 1H), 7.71 (s, 1H), 7.54 (s, 1H), 7.48 (s, 1H), 7.44 – 7.43 (m,

1H), 7.38 (d, *J* = 8.7 Hz, 2H), 6.80 (d, *J* = 8.7 Hz, 2H), 6.67 –

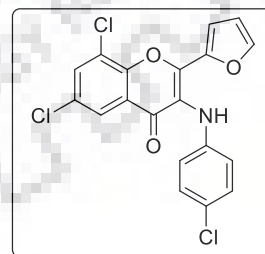
6.66 (m, 1H); ¹³C NMR (100 MHz, CDCl₃, δ): 177.8, 155.6,

145.8, 142.4, 139.1, 134.2, 133.2, 132.8, 132.0, 128.3, 126.3,

123.9, 121.4, 120.7, 118.9, 117.9, 111.6; IR (KBr): $\bar{\nu}$ = 3062, 2928, 1642, 1614, 1569,

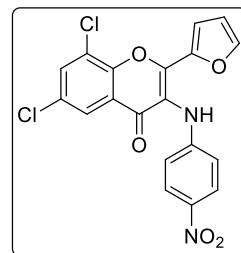
1500, 1451, 1367, 918, 771, 684 cm⁻¹; HRMS (ESI⁺): *m/z* calculated for C₁₉H₁₀Cl₃NO₃

[M+Na]⁺: 427.9624 found: 427.9647.

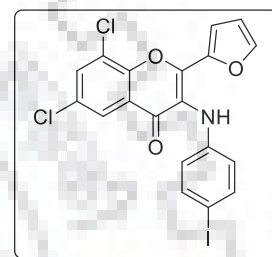


6,8-dichloro-2-(furan-2-yl)-3-((4-nitrophenyl)amino)-4H-chromen-4-one (6b):

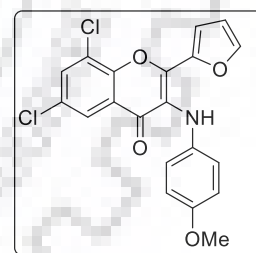
Yield: 82% as yellow solid; mp -142–144 °C; ¹H NMR (400 MHz, CDCl₃, δ): 10.6 (s, 1H), 8.13 (d, *J* = 9.0 Hz, 1H), 7.70 (s, 1H), 7.59 (s, 1H), 7.52 (s, 1H), 7.49 – 7.48 (s, 1H), 6.88 (d, *J* = 9.0 Hz, 2H), 6.73–6.70 (m, 1H); ¹³C NMR (100 MHz, CDCl₃, δ): 182.2, 146.4, 142.5, 141.7, 141.1, 135.0, 130.0, 129.7, 129.3, 16.5, 125.0, 124.0, 123.4, 122.8, 120.2, 111.2.; IR (KBr): $\bar{\nu}$ = 3061, 2926, 1641, 1614, 1569, 1500, 1451, 1367, 917, 771, 685 cm⁻¹; HRMS (ESI⁺): *m/z* calculated for C₁₉H₁₀Cl₂N₂O₅ [M+Na]⁺: 438.9864 found: 438.9894.

**6,8-dichloro-2-(furan-2-yl)-3-((4-iodophenyl)amino)-4H-chromen-4-one (6c):** Yield:

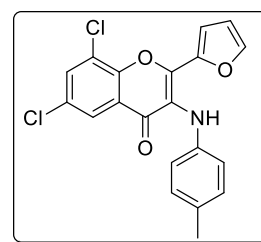
78% as yellow solid; mp - 183-185 °C; ¹H NMR (400 MHz, CDCl₃, δ): 10.8 (s, 1H), 7.70 (s, 1H), 7.56 (s, 1H), 7.54 – 7.53 (s, 2H), 7.48 (s, 1H), 7.43 – 7.42 (m, 1H), 6.67 – 6.65 (m, 3H); ¹³C NMR (100 MHz, CDCl₃, δ): 178.0, 155.7, 145.9, 145.6, 142.5, 140.0, 138.0, 134.1, 133.3, 128.4, 126.4, 124.2, 121.4, 120.8, 119.0, 113.1, 88.6; IR (KBr): $\bar{\nu}$ = 3063, 2924, 1641, 1614, 1569, 1501, 1451, 1367, 916, 771, 685 cm⁻¹. HRMS (ESI⁺): *m/z* calculated for C₁₉H₁₀Cl₂INO₃ [M+Na]⁺: 519.8980 found: 519.9020.

**6,8-dichloro-2-(furan-2-yl)-3-((4-methoxyphenyl)amino)-4H-chromen-4-one (6d):**

Yield: 71% as yellow solid; mp-156 - 158 °C; ¹H NMR (400 MHz, CDCl₃, δ): 10.91 (s, 1H), , 7.71 (s, 1H), 7.51 (s, 1H), 7.45 (s, 1H), 7.40 – 7.39(m, 1H), 7.07 (d, *J* = 8.1 Hz, 2H), 6.83 (d, *J* = 8.2 Hz, 2H), 6.64 – 6.62 (m, 1H), 3.91 (s, 3H); ¹³C NMR (100 MHz, CDCl₃, δ): 179.9, 154.8, 145.2, 143.2, 140.7, 137.9, 134.1, 133.5, 131.6, 123.9, 123.6, 123.5, 123.4, 122.7, 119.0, 112.8, 111.8, 55.5; IR (KBr): $\bar{\nu}$ = 3061, 2928, 1641, 1614, 1569, 1500, 1452, 1367, 918, 771, 685 cm⁻¹; HRMS (ESI⁺): *m/z* calculated for C₂₀H₁₃Cl₂NO₄ [M+Na]⁺: 424.0119 found: 424.0147.

**6,8-dichloro-2-(furan-2-yl)-3-(p-tolylamino)-4H-chromen-4-one (6e):** Yield:

75% as yellow semisolid; ¹H NMR (400 MHz, CDCl₃, δ): 11.06 (s, 1H), 7.71 (s, 1H), 7.51 (s, 1H), 7.45 (s, 1H), 7.40 – 7.39 (m, 1H), 7.07(d, *J* = 8.1 Hz, 2H), 6.83 (t, *J* = 8.2 Hz, 2H), 6.64 – 6.62 (m, 1H), 2.31 (s, 3H); ¹³C NMR (100 MHz, CDCl₃, δ): 179.59, 156.7, 146.6, 146.1, 143.4, 142.3, 138.0, 134.2, 131.2, 129.0, 125.9, 125.0, 121.8, 120.5, 119.2, 113.3, 111.6. IR (KBr): $\bar{\nu}$ =

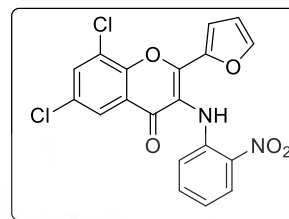


3061, 2929, 1642, 1615, 1569, 1502, 1451, 1367, 918, 771, 683 cm^{-1} ; HRMS (ESI⁺): m/z calculated for $\text{C}_{20}\text{H}_{13}\text{Cl}_2\text{NO}_3$ $[\text{M}+\text{Na}]^+$: 408.0170, found: 408.0202.

6,8-dichloro-2-(furan-2-yl)-3-((2-nitrophenyl)amino)-4H-chromen-4-one (6f):

Yield: 84% as yellow solid; mp -157–159 °C; ¹H NMR

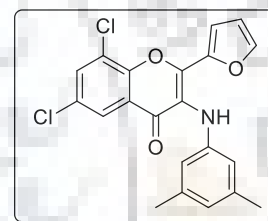
(400 MHz, CDCl_3 , δ): 11.08 (s, 1H), 7.70 (s, 1H), 7.51 (s, 1H), 7.45 (s, 1H), 7.40 – 7.39 (m, 1H), 7.07 (d, $J = 8.1$ Hz, 2H), 7.83 (d, $J = 8.2$ Hz, 2H), 6.64 – 6.62 (m, 1H), 2.31 (s, 3H); ¹³C NMR (100 MHz, CDCl_3 , δ): 180.2, 163.5, 145.2,



144.9, 144.0, 138.5, 138.3, 135.7, 133.8, 126.0, 125.5, 124.2, 123.5, 121.5, 118.3, 113.1, 111.4; IR (KBr): $\bar{\nu} = 3061, 2928, 1642, 1614, 1567, 1500, 1451, 1366, 918, 771, 685$ cm^{-1} ; HRMS (ESI⁺): m/z calculated for $\text{C}_{19}\text{H}_{10}\text{Cl}_2\text{N}_2\text{O}_5$ $[\text{M}+\text{Na}]^+$: 438.9864 found: 438.9892.

6,8-dichloro-3-((3,5-dimethylphenyl)amino)-2-(furan-2-yl)-4H-chromen-4-one (6h): Yield: 73% as yellow solid; mp - 162–164 °C; ¹H

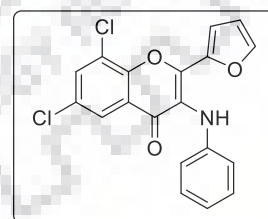
NMR (400 MHz, CDCl_3 , δ): 10.91 (s, 1H), 7.71 (s, 1H), 7.52 (s, 1H), 7.47 (s, 1H), 7.39–7.38 (m, 1H), 6.76 (s, 1H), 6.65 – 6.64 (m, 1H), 6.53 (s, 2H), 2.23 (s, 6H); ¹³C NMR (100 MHz, CDCl_3 , δ): 180.5, 161.9, 144.9, 143.2, 140.5, 133.6, 132.8,



128.9, 124.0, 123.9, 123.8, 122.4, 121.8, 118.7, 112.6, 112.4, 29.6. IR (KBr): $\bar{\nu} = 3062, 2928, 1642, 1614, 1569, 1500, 1451, 1367, 918, 771, 684$ cm^{-1} ; HRMS (ESI⁺): m/z calculated for $\text{C}_{21}\text{H}_{15}\text{Cl}_2\text{NO}_3$ $[\text{M}+\text{Na}]^+$: 422.0327 found: 422.0363

6,8-dichloro-2-(furan-2-yl)-3-(phenylamino)-4H-chromen-4-one (6i): Yield:

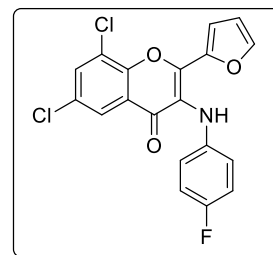
77% as semisolid; ¹H NMR (400 MHz, CDCl_3 , δ): 11.00 (s, 1H), 7.71 (s, 1H), 7.52 (s, 1H), 7.45 (s, 1H), 7.42 – 7.41 (m, 1H), 7.27 (t, $J = 7.6$ Hz, 1H), 7.13 (t, $J = 7.3$ Hz, 1H), 6.94 (d, $J = 7.9$ Hz, 2H), 6.65 – 6.64 (m, 1H); ¹³C NMR (100 MHz, CDCl_3 , δ): 177.4, 155.4, 145.7, 142.7, 139.9,



135.1, 133.2, 132.5, 129.1, 128.2, 126.6, 125.0, 122.7, 121.4, 120.5, 119.0, 111.4; IR (KBr): $\bar{\nu} = 3061, 2927, 1642, 1614, 1569, 1502, 1451, 1368, 918, 773, 684$ cm^{-1} . HRMS (ESI⁺): m/z calculated for $\text{C}_{19}\text{H}_{11}\text{Cl}_2\text{NO}_3$ $[\text{M}+\text{Na}]^+$: 394.0014 found: 394.0054.

6,8-dichloro-3-((4-fluorophenyl)amino)-2-(furan-2-yl)-4H-chromen-4-one

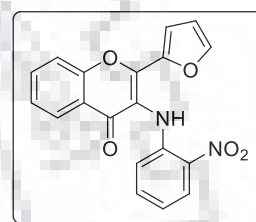
(6j): Yield: 73% as yellow solid; mp - 142–144 °C; ¹H NMR (400 MHz, CDCl₃, δ): 10.91 (s, 1H), 7.72 (s, 1H), 7.53 (s, 1H), 7.44–7.42 (m, 2H), 7.00–6.91 (m, 4H), 6.64–6.63 (m, 2H); ¹³C NMR (100 MHz, CDCl₃, δ): 171.49, 160.29 (¹J = 244.01 Hz), 155.4, 145.7, 142.6, 136.0, 135.5, 133.0, 132.6



(⁴J = 3.57 Hz), 128.3, 126.6, 124.7 (³J = 8.92 Hz), 121.4, 120.8, 119.0, 115.9 (²J = 22.91 Hz), 113.0; IR (KBr): $\bar{\nu}$ = 3062, 2928, 1642, 1614, 1569, 1500, 1451, 1367, 918, 771, 684 cm⁻¹; HRMS (ESI⁺): m/z calculated for C₂₁H₁₆FNO₃ [M+Na]⁺: 411.9919 found: 411.9955.

2-(furan-2-yl)-3-((2-nitrophenyl)amino)-4H-chromen-4-one (6k): Yield: 83%

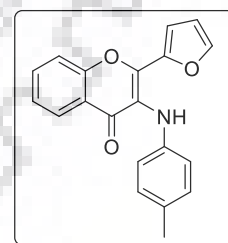
as yellow solid; mp - 172 -174 °C; ¹H NMR (400 MHz, CDCl₃, δ): 11.26 (s, 1H), 8.13 (d, *J* = 8.3 Hz, 1H), 7.83 (d, *J* = 7.8 Hz, 1H), 7.59 (t, *J* = 7.8 Hz, 1H), 7.46–7.44 (m, 3H), 7.32–7.26 (m, 1H), 7.20 (t, *J* = 7.4 Hz, 1H), 6.99 (t, *J* = 7.2 Hz, 1H), 6.64–6.62 (m, 2H); ¹³C NMR (100 MHz, CDCl₃, δ):



179.0, 159.3, 145.2, 144.9, 144.0, 138.5, 138.3, 135.7, 133.9, 126.2, 125.5, 124.2, 123.5, 121.5, 118.3, 113.1, 111.6; IR (KBr): $\bar{\nu}$ = 3062, 2928, 1642, 1614, 1569, 1500, 1451, 1367, 918, 771, 684 cm⁻¹; HRMS (ESI⁺): m/z calculated for C₁₉H₁₂N₂O₅ [M+Na]⁺: 371.0644 found: 371.0644.

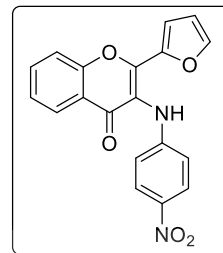
2-(furan-2-yl)-3-(p-tolylamino)-4H-chromen-4-one (6l): Yield: 76% as

semisolid; ¹H NMR (400 MHz, CDCl₃, δ): 10.88 (s, 1H), 7.84 (d, *J* = 7.7 Hz, 1H), 7.53 (t, *J* = 7.1 Hz, 1H), 7.47–7.46 (s, 1H), 7.29 (d, *J* = 8.3 Hz, 1H), 7.24–7.23 (m, 1H), 7.19 (d, *J* = 7.6 Hz, 1H), 7.02 (d, *J* = 7.6 Hz, 1H), 7.04 (d, *J* = 8.4 Hz, 2H), 6.78 (d, *J* = 8.3 Hz, 2H), 6.61–6.59 (m, 1H), 2.29 (s, 3H); ¹³C NMR

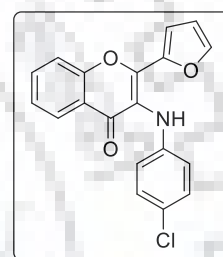


(100 MHz, CDCl₃, δ): 180.3, 154.7, 145.0, 144.3, 143.4, 137.9, 134.0, 133.5, 133.4, 129.6, 124.2, 123.4, 122.4, 122.0, 118.8, 112.7, 112.4, 21.0; IR (KBr): $\bar{\nu}$ = 3061, 2924, 1641, 1614, 1569, 1503, 1451, 1367, 918, 772, 685 cm⁻¹; HRMS (ESI⁺): m/z calculated for C₂₀H₁₅NO₃ [M+Na]⁺: 340.0988 found: 340.0431.

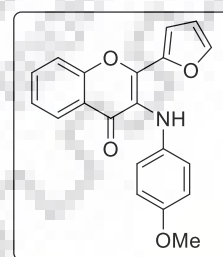
2-(furan-2-yl)-3-((4-nitrophenyl)amino)-4H-chromen-4-one (6m): Yield: 80% as yellow solid; mp - 159–161 °C; ¹H NMR (400 MHz, CDCl₃, δ): 10.47 (s, 1H), 8.08 (d, *J* = 8.4 Hz, 1H), 7.82 (d, *J* = 7.6 Hz, 1H), 7.60 (t, *J* = 7.6 Hz, 1H), 7.52 (s, 1H), 7.34 – 7.30 (m, 2H), 7.22 (t, *J* = 7.3 Hz, 1H), 6.79 (d, *J* = 8.4 Hz, 1H), 6.91 – 6.67 (m, 2H); ¹³C NMR (100 MHz, CDCl₃, δ): 179.7, 154.1, 147.4, 145.4, 143.0, 142.7, 135.2, 134.2, 128.5, 125.1, 124.0, 123.4, 123.1, 120.0, 119.0, 113.2, 112.0; IR (KBr): $\bar{\nu}$ = 3061, 2928, 1642, 1617, 1569, 1500, 1452, 1367, 918, 771, 683 cm⁻¹; HRMS (ESI⁺): *m/z* calculated for C₁₉H₁₂N₂O₅ [M+Na]⁺: 371.0644 found: 371.0644.



3-((4-chlorophenyl)amino)-2-(furan-2-yl)-4H-chromen-4-one (6n): Yield: 79% as yellow solid; mp -164–166 °C; ¹H NMR (400 MHz, CDCl₃, δ): 10.72 (s, 1H), 7.84 (d, *J* = 7.6 Hz, 1H), 7.59 – 7.57 (m, 1H), 7.48 (s, 1H), 7.32 – 7.29 (m, 2H), 7.20 (d, *J* = 8.5 Hz, 3H), 6.80 (d, *J* = 8.6 Hz, 2H), 6.63 – 6.63 (m, 2H); ¹³C NMR (100 MHz, CDCl₃, δ): 178.5, 154.6, 145.1, 143.2, 139.5, 134.0, 133.1, 132.1, 129.3, 129.0, 124.0, 123.6, 123.0, 122.6, 119.0, 112.8, 111.8; IR (KBr): $\bar{\nu}$ = 3061, 2928, 1642, 1615, 1569, 1503, 1451, 1367, 918, 771, 685 cm⁻¹; HRMS (ESI⁺): *m/z* calculated for C₁₉H₁₂ClNO₃ [M+Na]⁺: 360.0403 found: 360.0441.

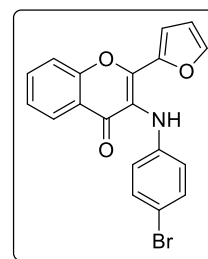


2-(furan-2-yl)-3-((4-methoxyphenyl)amino)-4H-chromen-4-one (6o): Yield: 70% as yellow solid; mp - 142–144 °C; ¹H NMR (400 MHz, CDCl₃, δ): 11.12 (s, 1H), 7.85 (d, *J* = 7.7 Hz, 1H), 7.53 (d, *J* = 7.9 Hz, 1H), 7.44 (s, 1H), 7.30 (d, *J* = 8.3 Hz, 1H), 7.23 – 7.22 (m, 1H), 7.19 (t, *J* = 7.4 Hz, 1H), 6.88 (d, *J* = 8.8 Hz, 1H), 6.79 (d, *J* = 8.8 Hz, 1H), 6.60 – 6.58 (m, 2H), 3.78 (s, 3H); ¹³C NMR (100 MHz, CDCl₃, δ): 180.5, 155.4, 145.1, 143.7, 141.2, 135.0, 132.2, 124.5, 124.1, 124.0, 124.0, 123.2, 119.5, 113.3, 112.4, 56.1; IR (KBr): $\bar{\nu}$ = 3061, 2927, 1641, 1615, 1569, 1500, 1451, 1367, 918, 771, 685 cm⁻¹; HRMS (ESI⁺): *m/z* calculated for C₂₀H₁₅NO₃ [M+Na]⁺: 356.0899 found: 356.0971.



3-((4-bromophenyl)amino)-2-(furan-2-yl)-4H-chromen-4-one (6p): Yield:

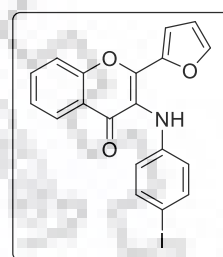
79% as semi-solid; ^1H NMR (400 MHz, CDCl_3 , δ): 10.71 (s, 1H), 7.83 (d, $J = 7.7$ Hz, 1H), 7.55 (t, $J = 7.5$ Hz, 1H), 7.46 (s, 1H), 7.30 – 7.27 (m, 2H), 7.21 – 7.18 (m, 3H), 6.80 – 6.78 (m, 2H), 6.62 – 6.61 (m, 2H); ^{13}C NMR (100 MHz, CDCl_3 , δ): 179.6, 154.6, 145.0, 143.1, 139.3, 133.9, 132.9, 131.9, 129.2, 128.9,



123.8, 123.4, 122.8, 122.5, 118.9, 112.6, 111.5; IR (KBr): $\bar{\nu} = 3061, 2928, 1641, 1614, 1570, 1502, 1451, 1367, 916, 771, 685$ cm^{-1} ; HRMS (ESI $^+$): m/z calculated for $\text{C}_{19}\text{H}_{12}\text{BrNO}_3$ $[\text{M}+\text{Na}]^+$: 403.9898 found: 403.9935.

2-(furan-2-yl)-3-((4-iodophenyl)amino)-4H-chromen-4-one (6q): Yield: 78%

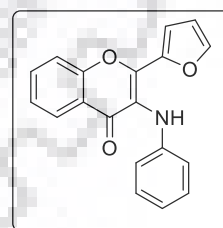
as yellow solid; mp - 149–151 $^\circ\text{C}$; ^1H NMR (400 MHz, CDCl_3 , δ): 10.66 (s, 1H), 7.83 (d, $J = 7.6$ Hz, 1H), 7.57 – 7.48 (m, 4H), 7.30 – 7.27 (m, 2H), 7.19 (t, $J = 7.2$ Hz, 1H), 7.22–7.19 (m, 3H), 6.63 – 6.62 (m, 2H), 6.61 – 6.59 (m, 2H); ^{13}C NMR (100 MHz, CDCl_3 , δ): 181.1, 162.3, 145.2, 143.2, 140.7, 138.0,



134.1, 133.1, 131.6, 124.0, 123.6, 123.5, 122.7, 119.0, 112.8, 112.7, 87.4; IR (KBr): $\bar{\nu} = 3061, 2927, 1642, 1614, 1569, 1500, 1451, 1367, 918, 772, 684$ cm^{-1} ; HRMS (ESI $^+$): m/z calculated for $\text{C}_{19}\text{H}_{12}\text{INO}_3$ $[\text{M}+\text{Na}]^+$: 451.9760 found: 451.9798.

2-(furan-2-yl)-3-(phenylamino)-4H-chromen-4-one (6s): Yield: 76% as semi-

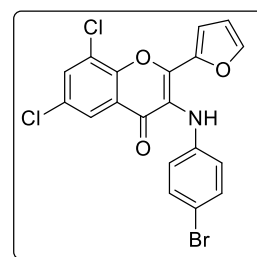
solid; ^1H NMR (400 MHz, CDCl_3 , δ): 10.82 (s, 1H), 7.85 (d, $J = 7.6$ Hz, 1H), 7.85 (d, $J = 7.6$ Hz, 1H), 7.55 (t, $J = 8.4$ Hz, 1H), 7.46 (s, 1H), 7.31 (d, $J = 8.4$ Hz, 1H), 7.27 – 7.26 (m, 1H), 7.24 (d, $J = 8.3$ Hz, 2H), 7.08 (t, $J = 7.4$ Hz, 1H), 6.99 (d, $J = 7.6$ Hz, 1H), 6.63 – 6.61 (m, 1H); ^{13}C NMR (100 MHz, CDCl_3 , δ): 178.0, 154.7, 145.0,



143.4, 140.6, 133.8, 132.9, 132.9, 129.0, 124.2, 124.1, 123.5, 122.5, 121.9, 118.8, 112.7, 111.8; IR (KBr): $\bar{\nu} = 3060, 2928, 1642, 1614, 1569, 1502, 1451, 1368, 918, 771, 684$ cm^{-1} ; HRMS (ESI $^+$): m/z calculated for $\text{C}_{19}\text{H}_{13}\text{NO}_3$ $[\text{M}+\text{Na}]^+$: 326.0793 found: 326.0829.

3-((4-bromophenyl)amino)-6,8-dichloro-2-(furan-2-yl)-4H-chromen-4-one

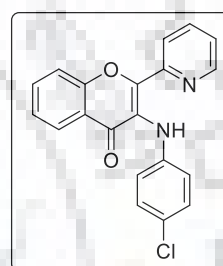
(6r): Yield: 72% as yellow solid; mp - 164–166 °C; ¹H NMR (400 MHz, CDCl₃, δ): 10.77 (s, 1H), 7.64 (s, 1H), 7.47 (s, 1H), 7.41 (s, 1H), 7.37 – 7.36 (m, 1H), 7.31 (d, *J* = 7.8 Hz, 2H), 6.80 (d, *J* = 7.8 Hz, 2H), 6.60 – 6.59 (m, 1H); ¹³C NMR (100 MHz, CDCl₃, δ): 177.9, 155.7, 145.8, 142.5, 139.2,



134.3, 133.3, 132.0, 128.4, 126.4, 124.1, 121.5, 120.7, 119.0, 118.0, 113.1, 111.6; IR (KBr): $\bar{\nu}$ = 3061, 2928, 1642, 1614, 1570, 1500, 1452, 1368, 918, 771, 685 cm⁻¹. HRMS (ESI⁺): *m/z* calculated for C₁₉H₁₀BrCl₂NO₃ [M+Na]⁺: 471.9119 found: 471.9157.

3-((4-chlorophenyl)amino)-2-(pyridin-2-yl)-4H-chromen-4-one (6u): Yield: 92% as

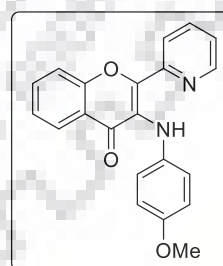
semi solid; ¹H NMR (400 MHz, CDCl₃, δ): 11.49 (s, 1H), 9.07 (d, *J* = 6.9 Hz, 1H), 7.78 (d, *J* = 9.0 Hz, 1H), 7.51 – 7.48 (m, 1H), 7.40 (d, *J* = 8.4 Hz, 2H), 7.28 (t, *J* = 7.4 Hz, 1H), 7.17 (d, *J* = 8.6 Hz, 3H), 7.05 (t, *J* = 6.9 Hz, 1H), 6.96 (d, *J* = 8.3 Hz, 1H), 6.35 (t, *J* = 7.6 Hz, 1H); ¹³C NMR (100 MHz, CDCl₃, δ): 190.1, 162.1, 152.2, 147.5,



136.2, 134.9, 133.1, 132.1, 131.3, 129.2, 128.6, 127.7, 119.6, 119.0, 118.7, 117.9, 117.8, 114.7; HRMS (ESI⁺): *m/z* calculated for C₂₀H₁₃ClN₂O₂ [M+Na]⁺: 371.0563 found: 371.0572; IR (KBr) $\bar{\nu}$ = 3061, 2923, 1642, 1629, 1570, 1517, 1455, 1368, 918, 771, 689 cm⁻¹.

3-((4-methoxyphenyl)amino)-2-(pyridin-2-yl)-4H-chromen-4-one (6v): Yield: 85%

as semi-solid; ¹H NMR (400 MHz, CDCl₃, δ): 11.55 (s, 1H), , 9.08 (d, *J* = 6.92 Hz, 1H), 7.75 (d, *J* = 8.9 Hz, 1H), 7.46 (t, *J* = 7.6 Hz, 1H), 7.24 – 7.21 (m, 3H), 7.11 (d, *J* = 8.2 Hz, 1H), 7.01 (t, *J* = 6.8 Hz, 1H), 6.94-6.91 (m, 2H), 6.70 (d, *J* = 8.3 Hz, 1H), 6.34 (t, *J* = 7.5 Hz, 1H), 3.81 (s, 3H); ¹³C NMR (100 MHz, CDCl₃, δ): 190.25,



161.9, 153.4, 149.5, 148.5, 147.5, 135.8, 133.2, 129.0, 127.6, 126.1, 123.0, 120.0, 118.5, 117.4, 114.3, 113.0, 110.8, 55.7; IR (KBr) $\bar{\nu}$ = 3061, 2923, 1642, 1629, 1570, 1517, 1455, 1368, 918, 771, 689 cm⁻¹. HRMS (ESI⁺): *m/z* calculated for C₂₁H₁₆N₂O₃ [M+Na]⁺: 367.1059 found: 367.1091.

3-((4-bromophenyl)amino)-2-(pyridin-2-yl)-4H-chromen-4-one (6w): Yield: 87% as semi-solid; mp - 142–144 °C; $^1\text{H NMR}$ (400 MHz, CDCl_3 , δ): 11.48 (s, 1H), 9.07 (d, $J = 6.9$ Hz, 1H), 7.78 (d, $J = 8.9$ Hz, 1H), 7.50 – 7.48 (m, 1H), 7.40 (d, $J = 8.4$ Hz, 2H), 7.29 – 7.25 (m, 1H), 7.16 (d, $J = 8.3$ Hz, 3H), 7.04 (t, $J = 6.9$ Hz, 1H), 6.94 (d, $J = 8.3$ Hz, 1H), 6.34 (t, $J = 7.6$ Hz, 1H); $^{13}\text{C NMR}$ (100 MHz, CDCl_3 , δ): 190.1, 162.1, 152.2, 147.5, 136.2, 134.9, 133.1, 132.3, 131.3, 129.2, 128.6, 127.7, 119.6, 119.0, 118.7, 117.9, 117.8, 114.7; HRMS (ESI $^+$): m/z calculated for $\text{C}_{20}\text{H}_{13}\text{BrN}_2\text{O}_2$ $[\text{M}+\text{Na}]^+$: 415.0058 found: 415.0096; IR (KBr) $\bar{\nu} = 3061, 2923, 1642, 1629, 1570, 1517, 1455, 1368, 918, 771, 689$ cm^{-1} .

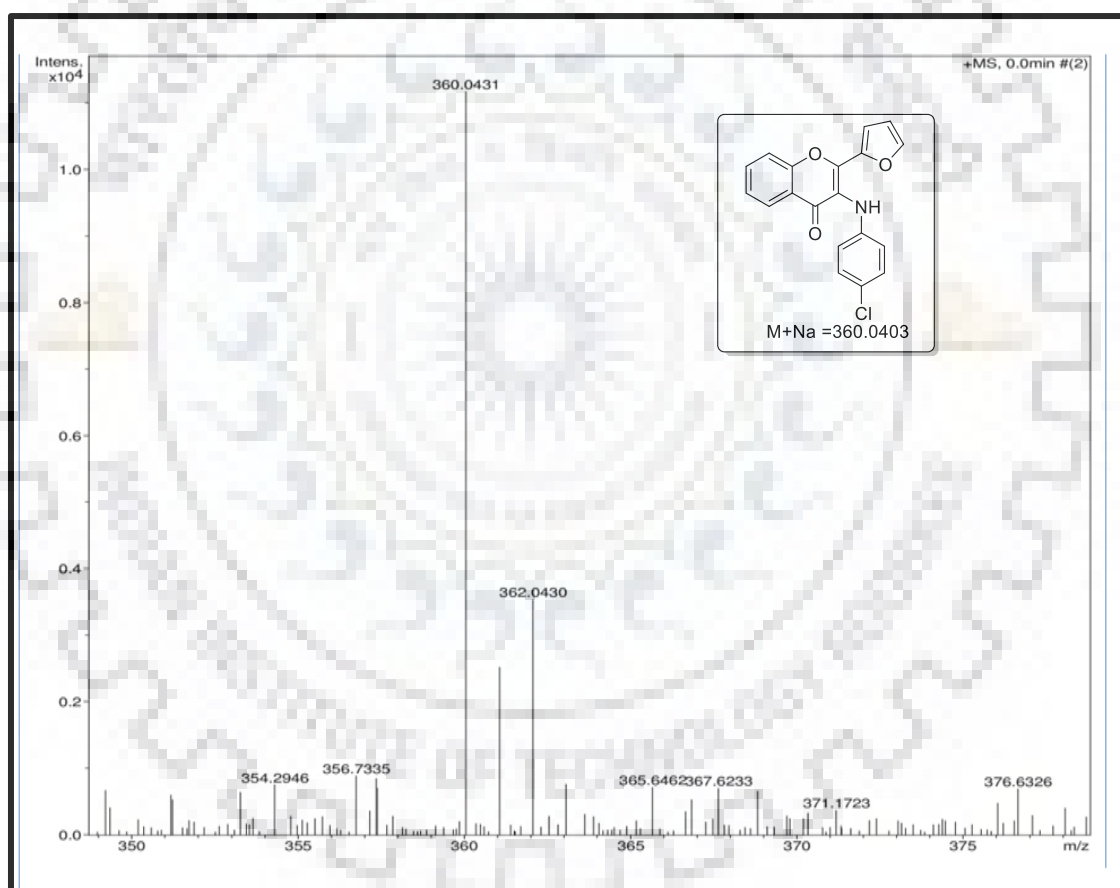
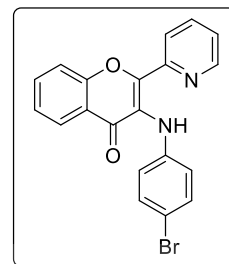


Figure.5.7. HRMS spectra of **6n** compound.

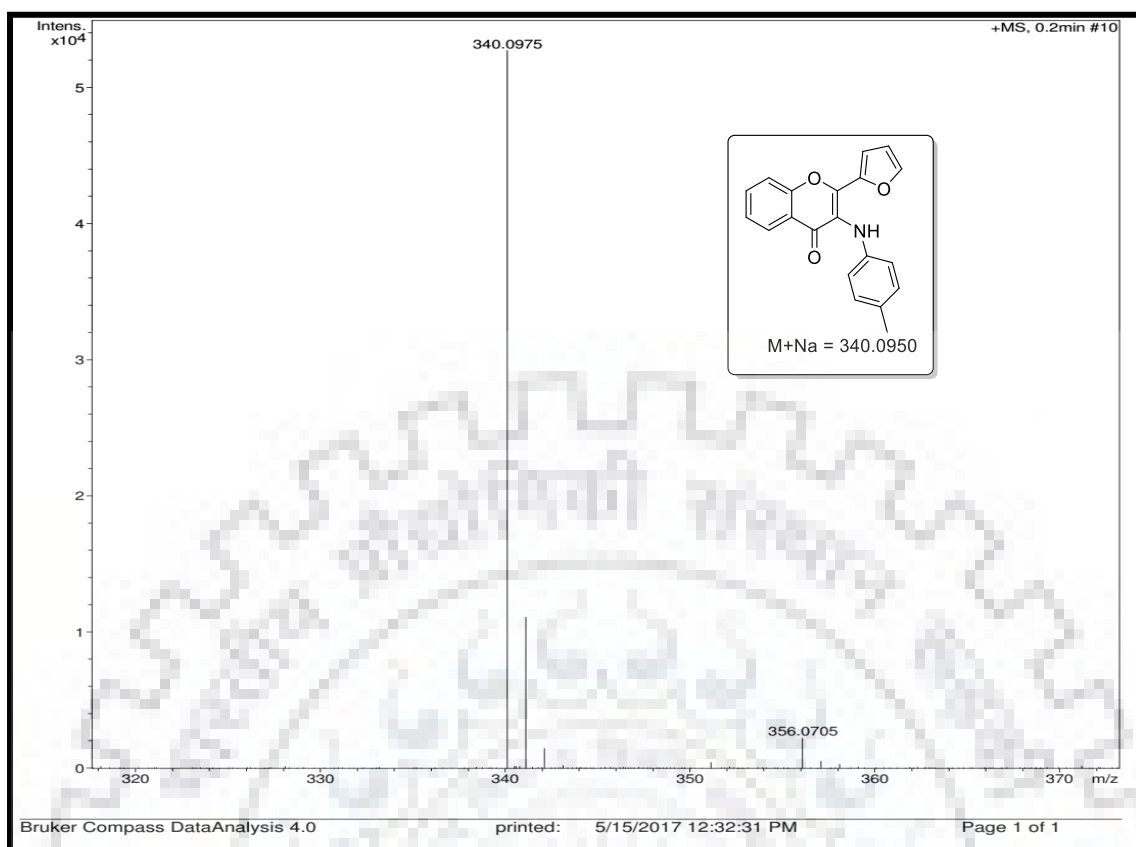


Figure.5.8. HRMS spectra of **6l** compound.

5.6. References

1. Torre, L. A.; Bray, F.; Siegel, R. L.; Ferlay, J.; Lortet-Tieulent, J.; Jemal, A. "Global cancer statistics" *CA Cancer J. Clin.* **2015**, *65*, 87–108.
2. Torre, L. A., Siegel, R. L., Ward, E. M., Jemal, A. "Global Cancer Incidence and Mortality Rates and Trends-An Update" *Cancer Epidemiol Biomarkers Prev.* **2016**, *25*, 16–27.
3. L'opez-Saez, F. J.; Torre, D. C.; Pincheira, J.; Gimenez-Martín, G. "Cell proliferation and cancer" *Histol. Histopathol.* **1998**, *13*, 1197–1214.
4. Naz, F. Khan, F. I.; Mohammad, T.; Khan, P.; Manzoor, S.; Hasan, G. M.; Lobb, K. A.; Luqman, S.; Islam, A.; Ahmad, F.; Hassan, M. I. "Investigation of molecular mechanism of recognition between citral and MARK4: A newer therapeutic approach to attenuate cancer cell progression" *Int J Biol Macromol.* **2018**, *107*, 2580–2589.
5. Naz, H.; Tarique, M.; Khan, P.; Luqman, S.; Ahamad, S.; Islam, A.; Ahmad, F.; Hassan, M. I. "Evidence of vanillin binding to CAMKIV explains the anti-cancer mechanism in human hepatic carcinoma and neuroblastoma cells" *Mol Cell Biochem.* **2018**, *438*, 35–45.

6. Giamas, G.; Stebbing, J.; Vorgias C. E.; Knippschild, U. "Protein kinases as targets for cancer treatment" *Pharmacogenomics* **2007**, *8*, 1005–1016; (b) Naz, H.; Jameel, E.; Hoda, N.; Shandilya, A.; Khan, P.; Islam, A.; Ahmad, F.; Jayaram, B.; Hassan, I. M. "Structure guided design of potential inhibitors of human calcium-calmodulin dependent protein kinase IV containing pyrimidine scaffold" *Bioorg Med Chem Lett.* **2016**, *26*, 782–788.
7. Hurov, J.; Piwnicka-Worms, H. "The Par-1/MARK family of protein kinases: from polarity to metabolism" *Cell cycle* **2007**, *6*, 1966–1969.
8. Drewes, G.; Ebneith, A.; Preuss, U.; Mandelkow, E. M.; Mandelkow, E. "MARK, a novel family of protein kinases that phosphorylate microtubule-associated proteins and trigger microtubule disruption" *Cell* **1997**, *89*, 297–308.
9. Tang, E. I.; Xiao, X.; Mruk, D. D.; Qian, X. J.; Mok, K. W.; Jenardhanan, P.; Lee, W. M.; Mathur, P. P.; Cheng, C. Y. "Microtubule affinity-regulating kinase 4 (MARK4) is a component of the ectoplasmic specialization in the rat testies" *Spermatogenesis* **2012**, *2*, 117–126.
10. Li, L.; Guan, K. L. "Microtubule-associated protein/microtubule affinity-regulating kinase 4 (MARK4) is a negative regulator of the mammalian target of rapamycin complex 1 (mTORC1)" *J Biol Chem.* **2013**, *288*, 703–708.
11. Liu, Z.; Gan, L.; Chen, Y.; Luo, D.; Zhang, Z.; Cao, W.; Zhou, Z.; Lin, X.; Sun, C. "Mark4 promotes oxidative stress and inflammation via binding to PPAR γ and activating NF- κ B pathway in mice adipocytes" *Sci Rep. 6* **2016**, 21382.
12. Sun, W.; Lee, S.; Huang, X.; Liu, S.; Inayathullah, M.; Kim, K.-M.; Tang, H.; Ashford, J. W.; Rajadas, J. "Attenuation of synaptic toxicity and MARK4/PAR1-mediated Tau phosphorylation by methylene blue for Alzheimer's disease treatment" *Sci. Rep. 6* **2016**.
13. Kato, T.; Satoh, S.; Okabe, H.; Kitahara, O.; Ono, K.; Kihara, C.; Tanaka, T.; Tsunoda, T.; Yamaoka, Y.; Nakamura, Y.; Furukawa Y. "Isolation of a novel human gene, MARKL1, homologous to MARK3 and its involvement in hepatocellular carcinogenesis" *Neoplasia* **2001**, *3*, 4–9.
14. Beghini, A.; Magnani, I.; Roversi, G.; Piepoli, T.; Di-Terlizzi, S.; Moroni, R. F.; Pollo, B.; Fuhrman-Conti, A. M.; Cowell, J. K.; Finocchiaro, G.; Larizza, L. "The neural progenitor-restricted isoform of the MARK4 gene in 19q13.2 is upregulated in human gliomas and overexpressed in a subset of glioblastoma cell lines" *Oncogene* **2003**, *22*, 2581–2591.

15. Heidary-Arash, E.; Shiban, A.; Song, S.; Attisano, L. "MARK4 inhibits Hippo signalling to promote proliferation and migration of breast cancer cells" *EMBO Rep.* **2017**, *18*, 420–436.
16. Naz, F.; Sami, N.; Naqvi, A. T.; Islam, A.; Ahmad, F.; Hassan, M. I. "Evaluation of human microtubule affinity-regulating kinase 4 inhibitors: fluorescence binding studies, enzyme and cell assays" *J Biomol Struct Dyn.* **2016**, 1–10.
17. Khan, P.; Rahman, S.; Queen, A.; Manzoor, S.; Naz, F.; Hasan, G. M.; Luqman, S.; Kim, J.; Islam, A.; Ahmad, F.; Hassan, M. I. "Elucidation of Dietary Polyphenolics as Potential Inhibitor of Microtubule Affinity Regulating Kinase 4: In silico and *In vitro* Studies" *Sci Rep.* **2017**, 9470.
18. Pardo, O. E.; Castellano, L.; Munro, C. E.; Hu, Y.; Mauri, F.; Krell, J.; Lara, R.; Pinho, F. G.; Choudhury, T.; Frampton, A. E.; Pellegrino, L.; Pshezhetskiy, D.; Wang, Y.; Waxman, J.; Seckl, M. J.; Stebbing, J. "miR-515-5p controls cancer cell migration through MARK4 regulation" *EMBO Rep.* **2016**, *17*, 570–584.
19. Gunasekera, P. S.; Paul, K. G.; Longley, E. R.; Isbrucker, A. R.; Pomponi, A. S. "Five New Discodermolide Analogues from the Marine Sponge *Discodermia* Species" *J. Nat. Prod.* **2002**, *65*, 1643–1648.
20. Devkota, P. K.; Covell, D.; Ransom, T.; McMahon, B. J.; Beutler, A. J. "Growth Inhibition of Human Colon Carcinoma Cells by Sesqui terpenoids and Tetralones of *Zygogynum calothyrsum*" *J. Nat. Prod.* **2013**, *76*, 710–714.
21. Ahmed, N.; Konduru, K. N.; Ahmad, S.; Owais, M. "Design, synthesis and antiproliferative activity of functionalized flavone-triazole-tetrahydropyran conjugates against human cancer cell lines" *Eur. J. Med. Chem.* **2014**, *82*, 552–564.
22. Tezuka, Y.; Gewali, B. M.; Ali, S. M.; Banskota, H. A.; Kadota, S. "Eleven Novel Diarylheptanoids and Two Unusual Diarylheptanoid Derivatives from the Seeds of *Alpinia blepharocalyx*" *J. Nat. Prod.* **2001**, *64*, 208–213.
23. Gewali, B. M.; Tezuka, Y.; Banskota, H. A.; Ali, S. M.; Saiki, I.; Dong, H.; Kadota, S. "Epicalyxin F and Calyxin I: Two Novel Antiproliferative Diarylheptanoids from the Seeds of *Alpinia blepharocalyx*" *Org. Lett.* **1999**, *1*, 1733–1736.
24. Middleton, E.; Chithan, K. "Free Radical Scavenging and Antioxidant Activity of Plant Flavonoids" Chapman and Hall, London **1993**, 145–166.
25. Chen, Z.-H.; Zheng, C.-J.; Sun, L.-P.; Piao, H.-R. "Synthesis of new chalcone derivatives containing a rhodanine-3-acetic acid moiety with potential anti-bacterial activity" *Eur. J. Med. Chem.* **2010**, *45*, 5739–5743.

26. Shashank, D.; Vishwanath, T.; Pasha, A.; Balasubramanian, V.; Nagendra, A.; Perumal, P.; Suthakaran, S. "Synthesis of some substituted benzothiazole derivatives and its biological activities" *Int. J. Chem Tech Res.* **2009**, *1*, 1224–1231.
27. Konduru, N. K.; Dey, S.; Sajid, M.; Owais, M.; Ahmed, N. "Synthesis and antibacterial and antifungal evaluation of some chalcone based sulfones and bisulfones" *Eur. J. Med. Chem.* **2013**, *59*, 23–30.
28. Ahmed, N.; Konduru, K. N. "Efficient, highly diastereoselective MS 4 Å-promoted one-pot, three-component synthesis of 2,6-disubstituted-4-tosyloxytetrahydropyrans via Prins cyclization" *Beilstein J. Org. Chem.* **2012**, *8*, 177–185.
29. Ryu, J.; Shin, K.; Park, H. S.; Kim, J. Y.; Chang, S. "Rhodium-Catalyzed Direct C-H Amination of Benzamides with Aryl Azides: A Synthetic Route to Diarylamines" *Angew. Chem., Int. Ed.* **2012**, *51*, 9904–9908.
30. Kim, H.; Shin, K.; Chang, S. "Iridium-Catalysed C-H Amination with Anilines at Room Temperature: Compatibility of Iridacycles with External Oxidants" *J. Am. Chem. Soc.* **2014**, *136*, 5904–5907.
31. Shang, M.; Sun, S.-Z.; Dai, H.-X.; Yu, J.-Q. "Cu(II)-Mediated C-H Amidation and Amination of Arenes: Exceptional Compatibility with Heterocycles" *J. Am. Chem. Soc.* **2014**, *136*, 3354–3357; (b). Trans, D. L.; Roane, J.; Daugulis, O. "Directed Amination of Non-Acidic Arene C-H Bonds by a Copper-Silver Catalytic System" *Angew. Chem. Int. Ed.* **2013**, *52*, 6043–6046; (c). Singh, K. B.; Polley, A.; Jana, R. "Copper(II)-Mediated Intermolecular C(sp²)-H Amination of Benzamides with Electron-Rich Anilines" *J. Org. Chem.* **2016**, *81*, 4295–4303.
32. Klier, L.; Bresser, T.; Nigst, A. T.; Karaghiosso, K.; Knochel, P. "Lewis Acid-Triggered Selective Zincation of Chromones, Quinolones, and Thiochromones: Application to the Preparation of Natural Flavones and Isoflavones" *J. Am. Chem. Soc.* **2012**, *134*, 13584–13587; (b) Geo, H.; Niphakis, J. M.; Georg I. G. "Palladium(II)-Catalysed Direct Arylation of Enaminones Using Organotrifluoroborates" *J. Am. Chem. Soc.*, **2008**, *130*, 3708–3709; (c) Moon, Y.; Kwon, D.; Hong, S. "Palladium-Catalysed Dehydrogenation/Oxidative Cross-Coupling Sequence of β -Heteroatom-Substituted Ketones" *Angew. Chem., Int. Ed.* **2012**, *51*, 11495–11498; (d) Chen, F.; Feng, Z.; He, C.-Y.; Wang, H.-Y.; Guo, Y.-L.; Zhang, X. "Pd-Catalysed Dehydrogenative Cross-Coupling of Polyfluoroarenes with Heteroatom-Substituted Enones" *Org. Lett.* **2012**, *14*, 1176–1179; (e) Min, M.; Kim, Y.; Hong, S. "Regioselective palladium-catalyzed olefination of coumarins via aerobic

- oxidative Heck reactions” *Chem. Commun.* **2013**, 49, 196–198; (f) Kim, D.; Hong, S. “Palladium(II)-Catalyzed Direct Intermolecular Alkenylation of Chromones” *Org. Lett.* **2011**, 13, 4466–4469.
33. Kónya, K.; Pajtás, D.; Attila Kiss-Szikszai, A.; Patonay, T. “Buchwald–Hartwig Reactions of Monohalo flavones” *Eur. J. Org. Chem.* **2015**, 828–839.
34. Khan, P.; Rahman, S.; Queen, A.; Manzoor, S.; Naz, F.; Hasan, G. M.; Luqman, S.; Kim, J.; Islam, A.; Ahmad, F.; Hassan, M. I. “Elucidation of Dietary Polyphenolics as Potential Inhibitor of Microtubule Affinity Regulating Kinase 4: In silico and In vitro Studies” *Sci Rep.* **2017**, 9470.
35. Morris, M. G.; Goodsell, S. D.; Halliday, S. R.; Huey, R.; Hart, E. W.; Belew, K. R.; Olson, J. A. “Automated docking using a Lamarckian genetic algorithm and an empirical binding free energy function” *J. Comput. Chem.* **1998**, 19, 1639–1662.
36. Hanahan, D.; Weinberg, R. A. “Hallmarks of cancer: the next generation” *Cell* **2011**, 144, 646–674.
37. Arash, H. E.; Shiban, A.; Song, S.; Attisano, L. “MARK4 inhibits Hippo signalling to promote proliferation and migration of breast cancer cells” *EMBO Rep.* **18**, **2017**, 420–436.
38. Li, L.; Guan, K. L. “Microtubule-associated protein/microtubule affinity-regulating kinase 4 (MARK4) is a negative regulator of the mammalian target of rapamycin complex 1 (mTORC1)” *J Biol Chem.* **2013**, 288, 703–708.
39. Circu, M. L.; Aw, T. Y. “Reactive oxygen species, cellular redox systems, and apoptosis” *Free Radic Biol Med.* **2010**, 48, 749–762.
40. Sack, J. S.; Gao, M.; Kiefer, S. E.; Jr, M. E. J.; Newitt, A. J.; Wu, S.; Yan, C. “Crystal structure of microtubule affinity-regulating kinase 4 catalytic domain in complex with a pyrazolopyrimidine inhibitor” *Acta Crystallogr F Struct Biol Commun.* **2016**, 72, 129–134.
41. Rigsby, E. R.; Parker, B. A. “Using the PyMOL application to reinforce visual understanding of protein structure” *Biochem Mol Biol Educ.* **2016**, 44, 433–437.
42. Boaz, H.; Rollefson, G. “The quenching of fluorescence. Deviations from the Stern-Volmer law” *J. Am. Chem. Soc.* **1950**, 72, 3435–3443.
43. Queen, A.; Khan, P.; Idrees, D.; Azam, A.; Hassan, M. I. “Biological evaluation of p-toluene sulphonylhydrazone as carbonic anhydrase IX inhibitors: An approach to fight hypoxia-induced tumors” *Int J Biol Macromol.* **2018**, 106, 840–850.





Chapter-6

*Regioselective Hydro-dehalogenation
of Aromatic α - and β - Halo carbonyl
Compounds by CuI in Isopropanol*

Eur. J. Org. Chem. **2019**, 759–764

6.1. Introduction

In the past decades, generally copper is innocuous, inexpensive and mild catalyst in diverse organic syntheses and has been found to be vastly effective for the carbon-carbon and C-heteroatom ($X = N, O, S, P, Se$ etc.) bond formation reactions [1]. Halides derivatives are extensively used as starting materials and intermediates in several chemical transformations, and the effective C-X ($X = Br, Cl, I$) bond formation has been actively studied. Still, substantial progresses are made towards the development of new dehalogenation protocols, to eliminate halogenated pollutants and for other synthetic applicabilities [2,3]. To date, set of different catalysts and reagents have been employed for the same. Traditionally, for hydride source molecular H_2 is used for dehalogenation of halides with Pd/C-Et₃N [4], and other palladium catalysts [5], palladium and rhodium nanoparticles [6,7]. Different Photocatalyzed methodologies are also been documented for the dehalogenation reactions with alcohols, amine and water as hydrogen transferring agents under light irradiation conditions [8-13].

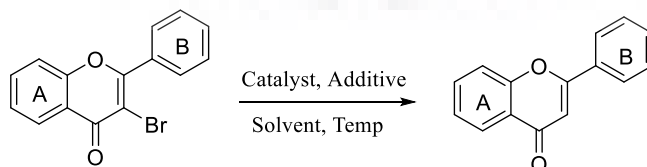
Strikingly, some alternative hydride source for carrying out the dehalogenation reactions with different transition metals have been also described, such as palladium with the usage of polymethylhydrosiloxane (PMHS) or sodium formate [14], Palladium, Rhodium and iridium complex with bidentate ligand involving silane [15], Pd(II) through cyclic amine [16], Pt(II) with hydrosilanes [17], Palladium involving DMF [18], Ruthenium(II) Phosphine Complex, Rh complex, palladium by phosphine and carbene ligand and Ni-Al clusters with alcohol [19], palladium and Nickel include alkoxides [20], halogen-metal exchange reaction [21], Pd/C contain hydrazine hydrochloride [22], indium-catalyzed dehalogenation of halo heteroarene in water [23], Pd(0) and iron with Grignard reagents through intramolecular β -hydride elimination of aryl halide [24], cobalt porphyrin in the presence of KOH [25], transition metals-catalyzed *via* metal hydride [26], Pd/C with sodium and ammonium formate [27] and NaBH₄ with TMEDA are usually accessible for this reductive dehalogenation transformation [28]. Recently, Xia *et al.* described a Ru-catalyzed dehalogenation protocol for the hydro-dehalogenation of organic halides [29]. All of these existing methods are allied with some of the serious drawbacks such as use of expensive catalyst, requirement of phosphine, carbene or other auxiliary ligands, which are either air sensitive, toxic or difficult to prepare. Hence, expansion of an innovative catalytic process for the selectively ortho-hydro-dehalogenation is highly desirable. Herein we report a new Cu-catalyzed protocol for the regioselectively hydro dehalogenation of β -halo-chalcone, α -halo-flavone and different

α -aryl halides using iso-propanol as a hydrogen donor solvent under milder reaction conditions.

6.2. Results and discussion

Our initial optimization commenced with the identification of proper catalyst and appropriate reaction conditions. A model reaction was performed with 3-bromoflavone (1K) using 10 mol % of copper iodide in the presence of formic acid as hydrogen donating solvent with K_2CO_3 at r.t. to 80 °C for 24 h (Table 6.1, entry 1). Unfortunately, the reaction failed to yield the desired product. Furthermore, the usage of acetic acid and TFA were also ineffective in producing any result (Table 6.1, entry 2 and 3). To our delight the formation of hydro-dehalogenated product flavone (**7a**) was obtained in 36% and 16% yield upon the usage of HCOOH/Et₃N (7:3 and 1:1 molar ratio) under similar conditions (Table 6.1, entry 4 and 5). Gratifyingly, the application of Isopropanol as a hydride source, under basic condition, using 3 mol % of CuI offers the desired product in 38% yield (Table 6.1, entry 6). Wherein, a noticeable betterment in the isolated yield up, to 71% was noticed with the gradual increase in the amount of catalysts loading from 3 mol % to 7 mol % at 80 °C for 24h (Table 6.1, entry 7 & 8). Delightfully, the employment of 10 mol % catalyst has offered the desired product in best yield of 92%, also reducing the reaction time to 12h (Table 6.1, entry 9). Moreover, further increment in the catalyst loading has not aid any amelioration in the yield (Table 6.1, entry 10). Notably, the reaction fails to proceed at all in the absence of catalyst and base, signifying the crucial importance of catalyst and base for the described transformation (Table 6.1, entry 11 & 12). (The use of other copper salt such as CuBr and CuCl results in the declination of isolated *i.e.* 75% and 64% respectively under similar reaction condition (Table 6.1, entry 13 and 14). Use of other hydrogen donating solvent such as; EtOH and MeOH failed in flourishing the desired product (**7a**). (Table 6.1, entry 15 & 16). The reaction was performed under nitrogen, and the reactions provided yield (89 %) of the product **7a**.

Table.6.1. Optimization of reaction condition:



Entry	Catalyst (10 mol %)	Additive (3 equiv.)	Solvent (hydrogen donor)	Temp.	Time (h)	Yield ^g (%)
1	CuI	K_2CO_3	HCOOH	rt to 80 °C	24	NR

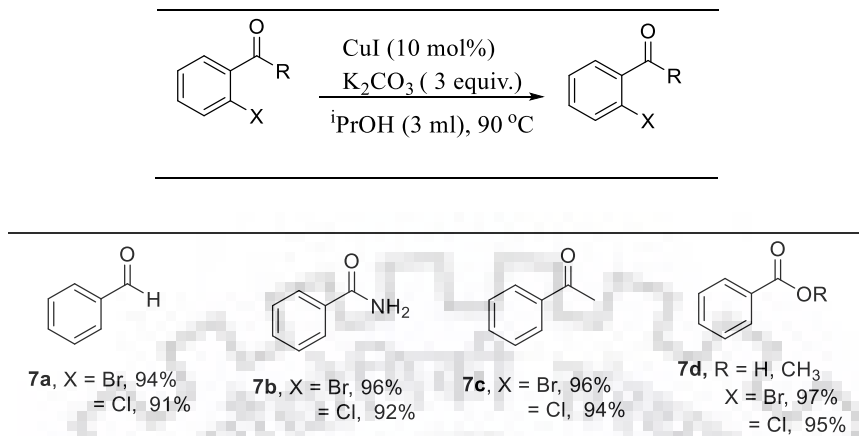
2	CuI	K ₂ CO ₃	CH ₃ COOH	rt to 80 °C	24	NR
3	CuI	K ₂ CO ₃	CF ₃ COOH	rt to 80 °C	24	NR
4	CuI	-	HCOOH/Et ₃ N (7:3)	rt to 80 °C	12-24	36
5	CuI	-	HCOOH/Et ₃ N (1:1)	rt to 80 °C	24	16
6 ^a	CuI	K ₂ CO ₃	ⁱ PrOH	90	24	38
7 ^b	CuI	K ₂ CO ₃	ⁱ PrOH	90	24	52
8 ^c	CuI	K ₂ CO ₃	ⁱ PrOH	90	24	71
9 ^d	CuI	K₂CO₃	ⁱPrOH	90	12	92
10 ^e	CuI	K ₂ CO ₃	ⁱ PrOH	90	24	91
11	-	-	ⁱ PrOH	rt to 90	24	NR
12	CuI	-	ⁱ PrOH	90	24	NR
13	CuBr	K ₂ CO ₃	ⁱ PrOH	90	12	75
14	CuCl	K ₂ CO ₃	ⁱ PrOH	90	12	64
15	CuI	K ₂ CO ₃	EtOH	90	36	NR
16	CuI	K ₂ CO ₃	MeOH	90	36	NR
17 ^f	CuI	K ₂ CO ₃	ⁱ PrOH	90	12	89

Reaction conditions unless specified otherwise: **1k** (1.0 mmol), catalyst, (10 mol%), additive (3 equiv.) Solvent as hydrogen donor (3ml) stirred at 80 °C for 12h. ^aCuI (1mol%). ^bCuI (3mol%). ^cCuI (5mol%). ^dCuI (7mol%). **1a** (1.0 mmol), catalyst, (10 mol%), additive (3equiv.) Solvent (DMF, 3ml), ^eL-Proline as hydrogen donor (1 equiv.) stirred at 80 °C for 12h. ^fUnder N₂. ^g Isolated yield.

With the optimal reaction conditions in hand, the substrate scope of the copper-catalysed dehalogenation of α -bromoketones are possible. The benzaldehyde, benzamide, acetophenone, benzoic acid and esters containing halo group next to the α carbon of the carbonyl group undergo dehalogenation reaction with excellent yield *i.e.* 97% - 91% yield (**Scheme 6.3.3**).

6.3. Substrate Scope

6.3.1. Substrate scope of α -halo arene derivative

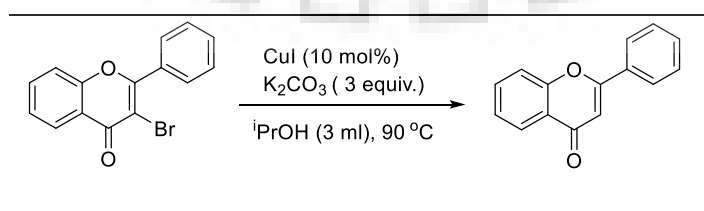


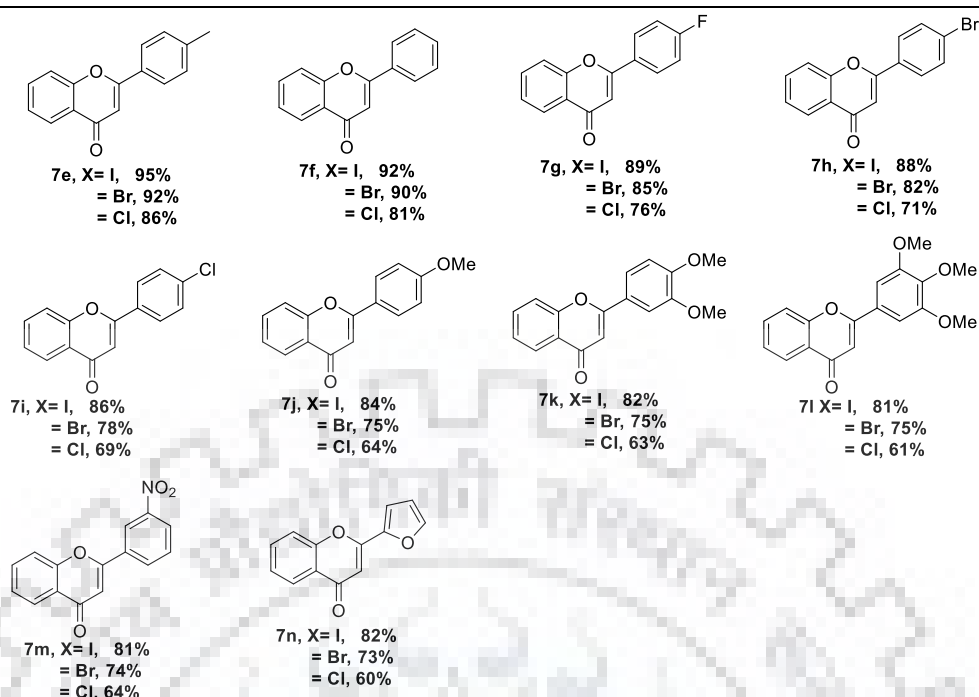
Reaction conditions: **11** (1.0 mmol), catalyst, (10 mol%), additive (3 equiv.) Solvent as hydrogen donor *i.e.* Isopropanol (3ml) stirred at 80°C for 12h.

Scheme.6.1. Dehalogenation reaction of α -halo arene derivative.

6.3.2. Substrate scope of 3-halo flavone

After α -halocarbonyls derivatives, we described the substrate scope for a series of 3-bromo flavone (α -halo carbonyl compounds) bearing different electron withdrawing and electron donating substituents (Scheme 6.2). As expected the reduction of the C–I bond is more efficiently achieved in comparison to C–Br and C–Cl bonds yielding the desired product **7e** in 95%, 92% and 86% yields respectively. Without substituent and the presence of halogen group (F, Br and Cl) on the 2-phenyl ring has not shown much alteration in yields of **7f-7i**. Seminally, presence of methoxy, dimethoxy, trimethoxy functional groups has also not shown noticeable variation, offering the described product **7j-7m** in 81-84% yields respectively. However, nitro containing derivative showcased sluggish reactivity resulting in the formation of targeted product **2i** in comparatively lower yields. Gratifyingly, the methodology was also successful with 3-bromo-2-(furan-2-yl)-4*H*-chromen-4-one, offering **7n** in 82% yield.



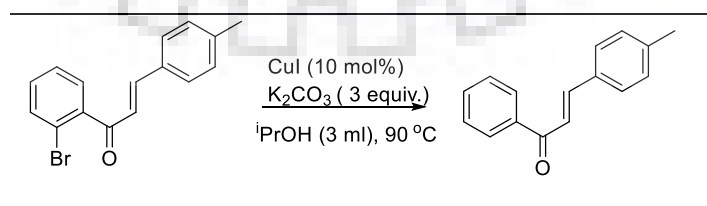


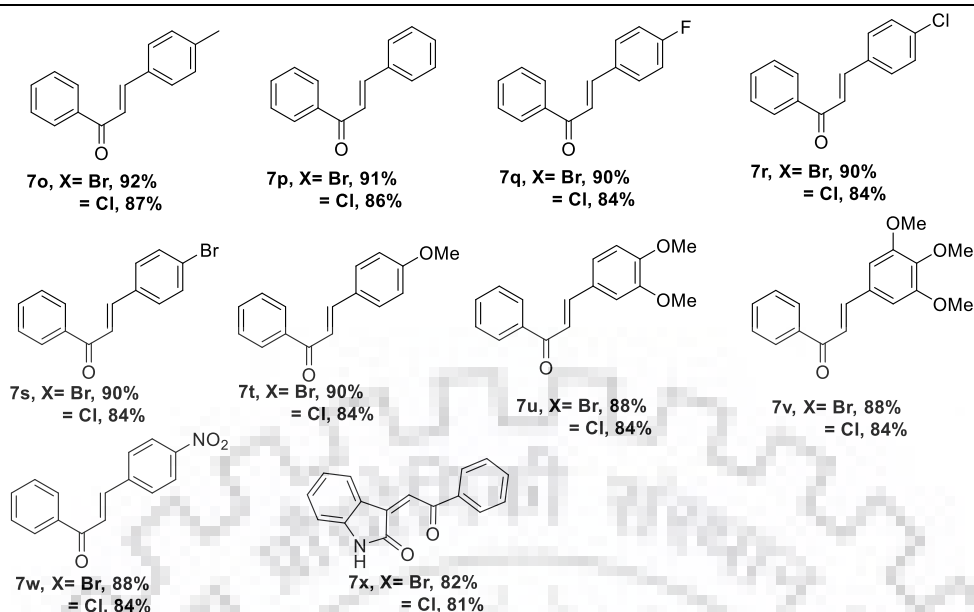
Reaction conditions: **1m** (1.0 mmol), catalyst, (10 mol%), additive (3 equiv.) Solvent as hydrogen donor *i.e.* Isopropanol (3ml) stirred at 80 °C for 12h.

Scheme.6.2. Dehalogenation reaction of 3-halo flavone.

6.3.3. Substrate scope of β -halo-chalcone

To extend the substrate scope of the present methodology, we explored the reaction with β' halo-chalcone derivatives, bearing different electron donating and withdrawing groups (Scheme 6.3). Under the present condition, reaction has not shown any noticeable impact of electronic environments, offering the respective products **7o-7w** in seminal yields (88-92%) (Scheme 3). Moreover, 2-haloIndoline Chalcone was also successfully dehalogenated under the current reaction conditions, affording product **7x** in 82% yield. It is noteworthy that the methodology showcased excellent selectivity in reducing the halogen functionalities, specifically reduces α and β halo functional group over the other.



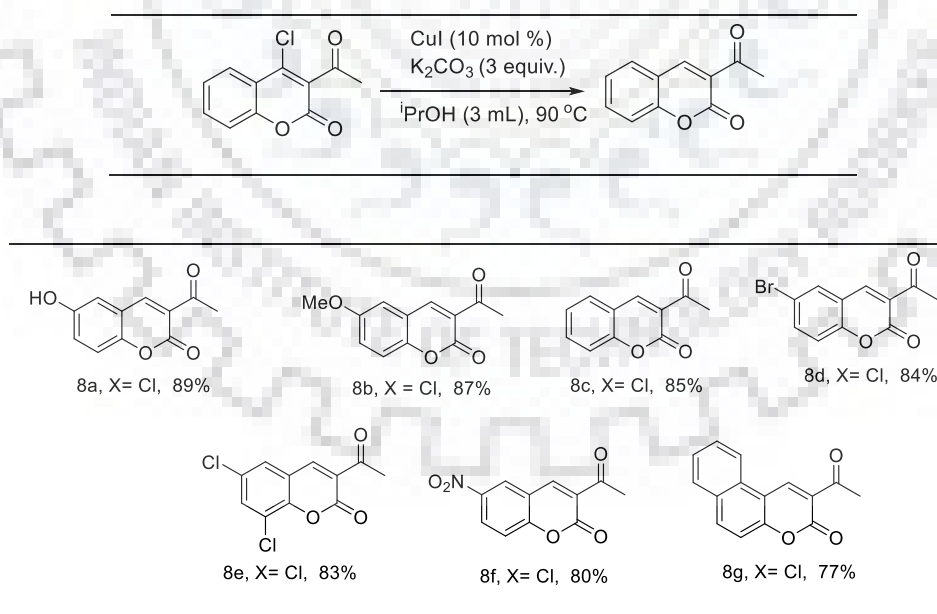


Reaction conditions: **1n** (1.0 mmol), catalyst, (10 mol%), additive (3 equiv.) Solvent as hydrogen donor *i.e.* Isopropanol (3ml) stirred at 80 °C for 12h.

Scheme.6.3. Dehalogenation reaction of β' -halochalcone.

6.3.4. Substrate scope of 3-acetyl-4-chlorocoumarin

Furthermore, the scope of the methodology was expanded by without and with substituted 4-Chloro-3-acetyl-4-chlorocoumarin (Scheme 6.4).



Reaction conditions: **1o** (1.0 mmol), catalyst, (10 mol %), additive (3 equiv.) Solvent as hydrogen donor *i.e.* Isopropanol (3ml) stirred at 90 °C for 12h.

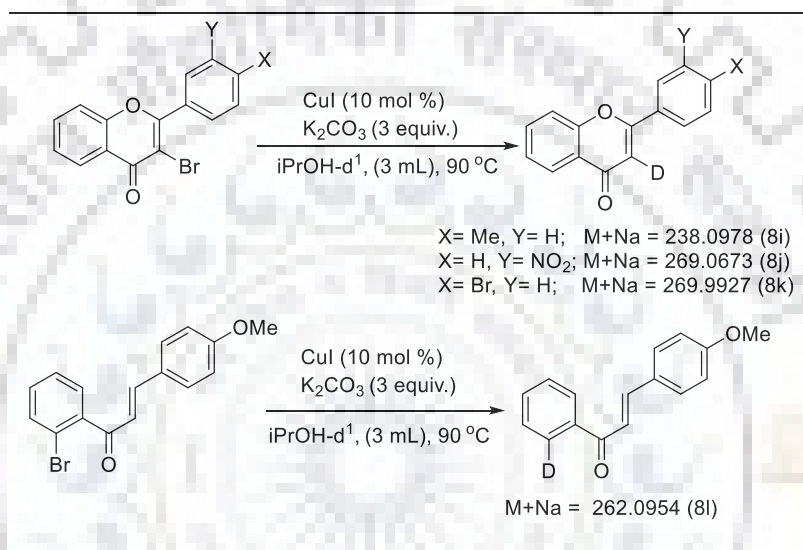
Scheme.6.4. Dehalogenation reaction of 3-acetyl-4-chlorocoumarin.

It was noted that, 4-Chloro-3-acetyl-4-chlorocoumarin bearing electron donating group like OH and -OMe and without group (**8a-8c**) offered the corresponding products

smoothly in 89% to 85% yields respectively. Wherein other derivatives containing Br, di-Cl and NO₂ functional groups (**8d-8f**) substituents. Contentedly, fused 4-Chloro-3-acetyl-4-chlorocoumarin also produces the same result, albeit in slight lesser yield *i.e.* 77%.

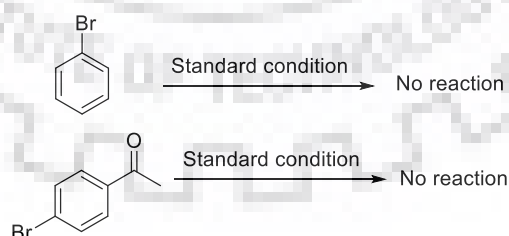
6.4. Controlled Experiment

In order to demonstrate the pathway of hydrogen transfer in reaction, we performed the control experiments using deuterated isopropanol and L-proline with different substrate group *i.e.* **8i-8l** (Scheme 6.6).



Scheme.6.5. Reaction of substituted flavone and chalcone with deuterated isopropanol.

Under observation we found the deuterated product instead of hydrogenation. This experiment confirm that hydrogen comes from isopropanol and L-proline. All deuterated compounds confirm by Mass. (**Figure 6.1 and 6.2**).



Scheme.6.6. reactivity of bromo derivatives.

In order to explore the reactivity of position of Bromo group some reactions were conducted (Scheme 6.6). Seemingly, the debromination reaction at *para* position of acetophenone and bromo benzene is fail to deliver the desired product.

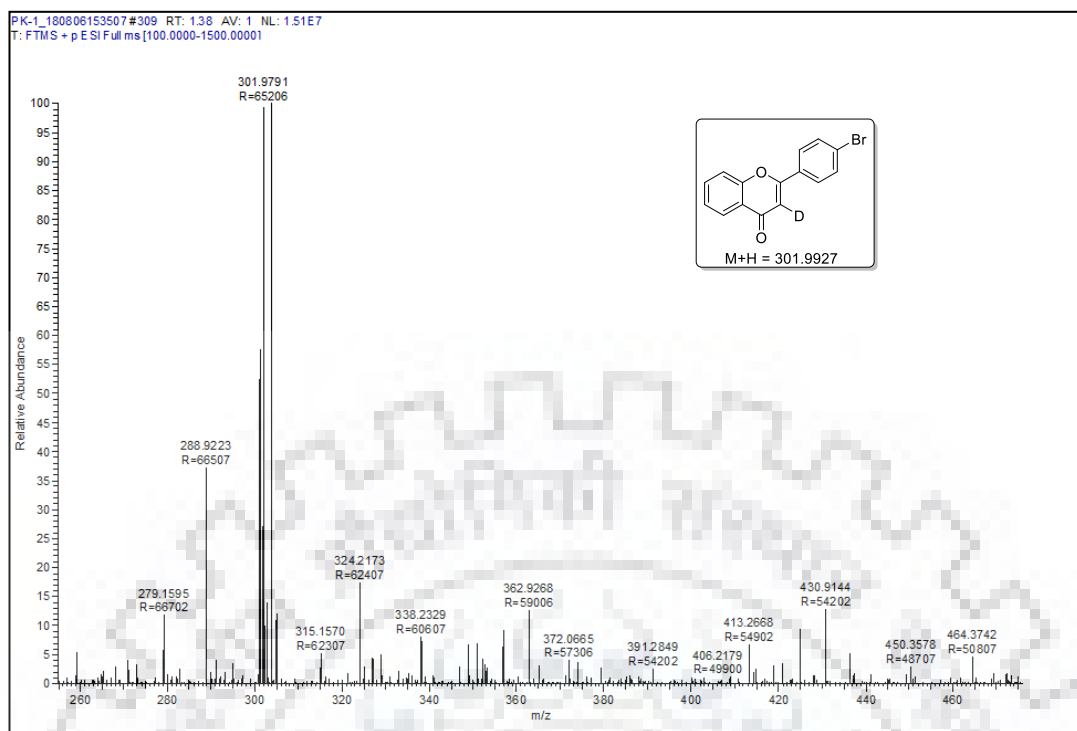


Figure.6.1. Deuterated HRMS spectrum of 8k.

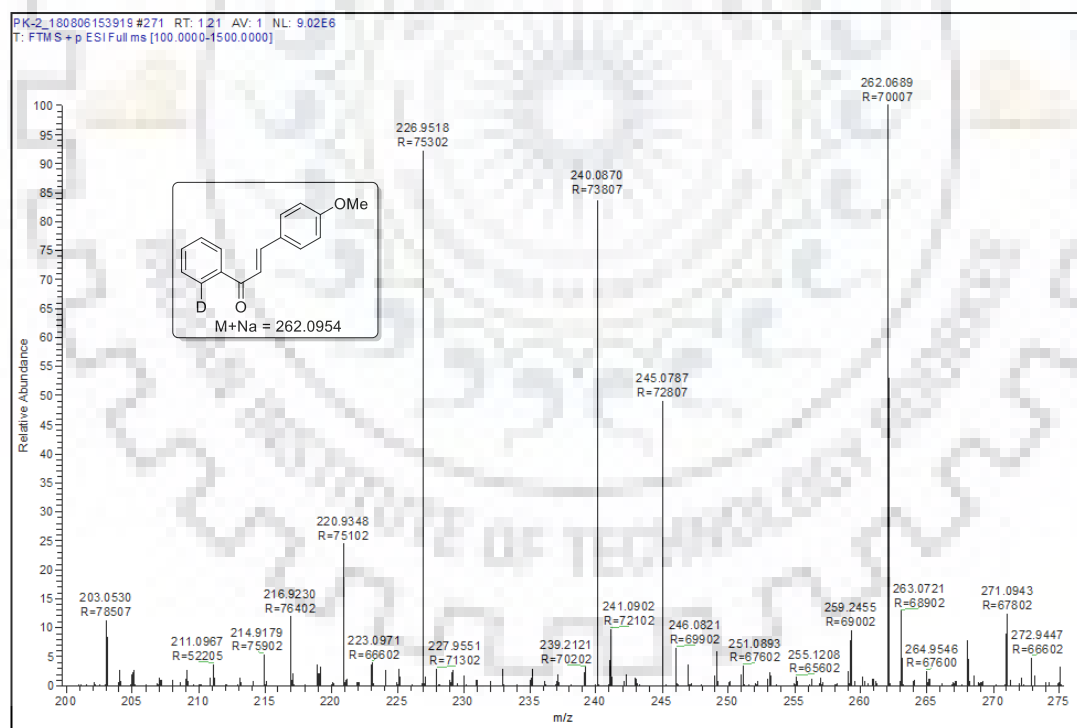
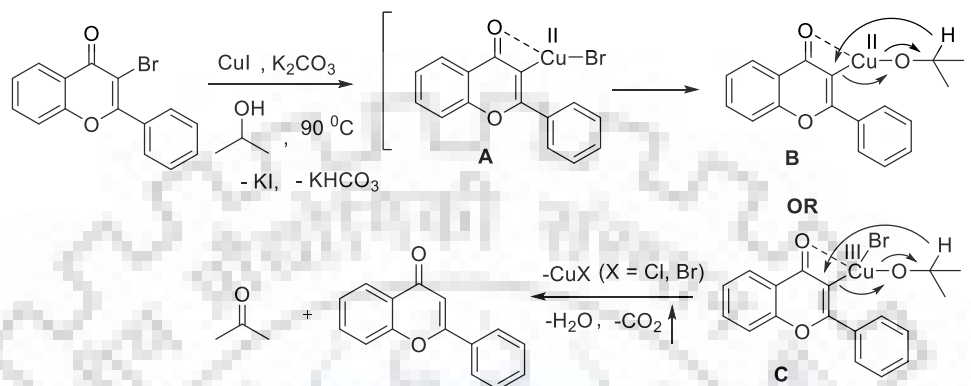


Figure.6.2. Deuterated HRMS spectrum of 8l.

6.5. Mechanism

On the basis of previous literature reports, a plausible mechanism for this copper catalyzed hydro-dehalogenation reaction is proposed in Scheme 6.7 [30]. Cu(I) iodide initially undergoes oxidative addition with halide to generate an intermediate A.

Thereafter, by mean of base isopropanol solvent was introduced into intermediate **A** in the form of isopropyl oxide ligand forming intermediate **B** or intermediate **C**. Followed by β -hydride elimination from isopropyl oxide, generating the final product with the elimination of acetone with the regeneration of catalyst which continues the cycle, which was confirmed by GC-MS.



Scheme.6.7. Proposed Mechanism

6.6. Conclusion

In summary, we have described an easy, efficient and simple hydrodehalogenation reaction of α -halocarbonyl compounds, α -haloflavone β' -halochalcone and substituted 4-Chloro-3-acetyl-4-chlorocoumarin derivative by copper iodide catalysis under transfer hydrogenation conditions. This method is featured with cheap and commercially available copper iodide catalyst with additive isopropanol turning both as the solvent and as the hydrogen source and without any additional ligand, broad substrate scope under mild reaction condition.

6.7. Experimental Section

6.7.1. General Information

All the required chemicals were purchased from Avra, Himedia and sigma Aldrich and available reagents were used without further purification. Thin layer chromatography was performed on 0.25 mm silica gel plates (60F-254) using UV light as the visualizing agent. Silica gel (100–200 mesh) was used for column chromatography. Melting points were determined on a capillary point apparatus equipped with a digital thermometer and are uncorrected. Nuclear magnetic resonance spectra were recorded on Jeol resonance ECX400MHz and Bruker spectrosin DPX 500 MHz spectrometer, and chemical shifts are reported in δ units, parts per million (ppm), relative to residual chloroform (7.26 ppm) in the deuterated solvent or with tetramethylsilane (TMS, δ 0.00 ppm) as the internal standard. ^{13}C NMR spectra were referenced to CDCl_3 (δ 77.00 ppm, the middle

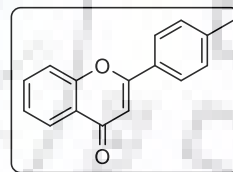
peak). Coupling constants were expressed in Hz. The following abbreviations were used to explain the multiplicities: s = singlet, d = doublet, t = triplet, m = multiplet. High resolution mass spectra were recorded with a micro TOF-Q analyzer spectrometer by using the electro-spray mode. IR spectra of the compounds were recorded on Thermo Nicolet FT-IR spectrometer with and are expressed as wave number (cm^{-1}).

6.7.2. General Procedure

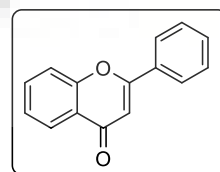
A round bottom flask with a magnetic stirring bar was charged with 3-bromo flavone (1 mmol), potassium carbonate (3 equivalent), isopropanol solvent and as a hydride transfer (3-4 ml), with copper iodide (10 mol%). The reaction mixture was stirred at 80 °C until complete consumption of the starting material as detected by TLC. TLC was checked in 10% Hexane and ethyl acetate. After completion of the reaction, The reaction mixture was cooled to ambient temperature and extract with ethyl acetate. The residue was purified *via* column chromatography with excellent yield (**7a-8g**).

6.8. Characterization data

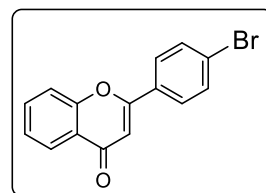
2-(p-tolyl)-4H-chromen-4-one (7e) [31]: Yield-92% as white solid; mp 109–111 °C; IR (KBr); 1666, 1376, 1095, 824, 753 cm^{-1} ; ^1H NMR (500 MHz, CDCl_3) δ 8.24 (d, $J = 7.8\text{Hz}$, 1H), 7.90 (d, $J = 8.8\text{ Hz}$, 2H), 7.70 (t, $J = 8.3\text{ Hz}$, 1H), 7.56 (d, $J = 8.3\text{ Hz}$, 1H), 7.42 (t, $J = 7.45\text{ Hz}$, 1H), 7.04 (d, $J = 8.8\text{ Hz}$, 2H), 6.76 (s, 1H), 2.41 (s, 3H); ^{13}C NMR (125 MHz, CDCl_3) δ 178.4, 163.4, 162.44, 156.2, 133.5, 128.0, 125.6, 125.0, 124.0, 123.9, 117.9, 114.4, 106.2, 21.9; HRMS (ESI): calcd for $\text{C}_{16}\text{H}_{12}\text{O}_2$ $[\text{M} + \text{Na}]^+$ 259.0753; found 259.0747.



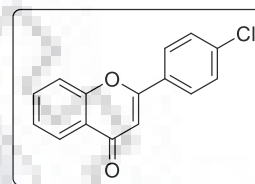
2-phenyl-4H-chromen-4-one (7f) [31]: Yield-90% as yellow solid; mp 100–102 °C; IR (KBr); 1689, 1376, 1095, 824, 755 cm^{-1} ; ^1H NMR (CDCl_3 , 400 MHz) δ 8.22 (d, $J = 7.9\text{ Hz}$, 1H), 7.92 (d, $J = 8.1\text{ Hz}$, 2H), 7.69 (t, $J = 7.8\text{ Hz}$, 1H), 7.56 (d, $J = 8.4\text{ Hz}$, 1H), 7.52 (d, $J = 6.0\text{ Hz}$, 3H), 7.41 (t, $J = 7.5\text{ Hz}$, 1H), 6.82 (s, 1H); ^{13}C NMR (CDCl_3 , 100 MHz) δ 178.6, 163.5, 156.3, 133.9, 131.9, 131.7, 129.1, 126.4, 125.8, 125.3, 124.0, 118.2, 1077; HRMS (ESI): calcd for $\text{C}_{15}\text{H}_{10}\text{O}_2$ $[\text{M} + \text{Na}]^+$ 245.0578; found 245.0594.



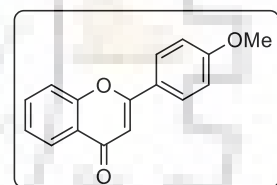
2-(4-bromophenyl)-4H-chromen-4-one (7h) [31]: Yield-82% as white solid; mp 185-189 °C; IR (KBr); 1666, 1376, 1095, 824, 753 cm^{-1} ; ^1H NMR (400 MHz); ^1H NMR (CDCl_3 , 400 MHz) δ 8.22 (d, $J = 7.9$ Hz, 1H), 7.87 (d, $J = 8.6$ Hz, 2H), 7.73–7.69 (m, 1H), 7.56 (d, $J = 8.4$ Hz, 1H), 7.50 (d, $J = 8.4$ Hz, 2H), 7.43 (t, $J = 7.5$ Hz, 1H), 6.80 (s, 1H); ^{13}C NMR (CDCl_3 , 100 MHz) δ 178.5, 162.3, 156.2, 138.0, 134.0, 130.3, 129.5, 127.6, 125.8, 125.5, 124.0, 118.2, 107.7; HRMS (ESI): calcd for $\text{C}_{15}\text{H}_9\text{BrO}_3$ [$\text{M} + \text{Na}$] $^+$ 322.9684; found 322.9708.



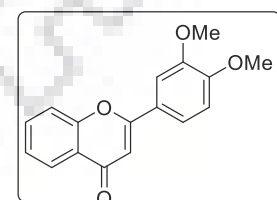
2-(4-chlorophenyl)-4H-chromen-4-one (7i) [31]: Yield-78% as white solid; mp 168-170 °C; IR (KBr); 1666, 1376, 1095, 824, 753 cm^{-1} ; ^1H NMR (CDCl_3 , 400 MHz) δ 8.21 (d, $J = 7.9$ Hz, 1H), 7.86 (d, $J = 8.6$ Hz, 2H), 7.72–7.68 (m, 1H), 7.56 (d, $J = 8.4$ Hz, 1H), 7.51–7.49 (m, 2H), 7.42 (t, $J = 7.6$ Hz, 1H), 6.79 (s, 1H); ^{13}C NMR (CDCl_3 , 100 MHz) δ 178.5, 162.4, 156.3, 138.0, 134.1, 130.3, 129.5, 127.3, 125.8, 125.5, 124.0, 118.2, 107.8; HRMS (ESI): calcd for $\text{C}_{15}\text{H}_9\text{ClO}_2$ [$\text{M} + \text{Na}$] $^+$ 279.0189; found 279.0205.



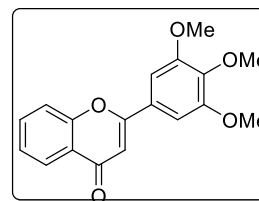
2-(4-methoxyphenyl)-4H-chromen-4-one (7j) [31]: Yield-75% as Pale-yellow solid; mp 134–136 °C; ^1H NMR (CDCl_3 , 500 MHz) δ 8.24 (d, $J = 7.8$ Hz, 1H), 7.91 (d, $J = 8.8$ Hz, 2H), 7.70 (t, $J = 8.3$ Hz, 1H), 7.57 (d, $J = 8.2$ Hz, 1H), 7.43 (t, $J = 7.35$ Hz, 1H), 7.04 (d, $J = 8.8$ Hz, 2H), 6.77 (s, 1H), 3.91 (s, 3H); ^{13}C NMR (CDCl_3 , 125 MHz) δ 178.9, 163.9, 162.9, 156.7, 134.0, 128.5, 126.2, 125.6, 124.5, 124.4, 118.4, 115.0, 106.7, 56.0; HRMS (ESI): calcd for $\text{C}_{16}\text{H}_{12}\text{O}_3$ [$\text{M} + \text{Na}$] $^+$ 275.0684; found 275.0706.



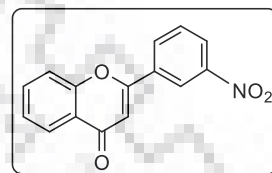
2-(3,4-dimethoxyphenyl)-4H-chromen-4-one (7k): Yield-75% as Pale yellow solid; mp 156–157 °C; ^1H NMR (CDCl_3 , 500 MHz) δ 8.25 (d, $J = 9.1$ Hz, 1H), 7.73–7.69 (m, 1H), 7.60 (d, $J = 6.3$ Hz, 2H), 7.45–7.42 (m, 2H), 7.02 (d, $J = 8.5$ Hz, 1H), 6.78 (s, 1H), 4.01 (s, 3H), 3.99 (s, 3H); ^{13}C NMR (CDCl_3 , 125 MHz) δ 178.4, 163.4, 156.2, 152.1, 149.3, 133.6, 125.7, 125.1, 124.3, 120.0, 118.0, 115.0, 111.2, 108.9, 106.5, 56.1, 56.0; HRMS (ESI): calcd for $\text{C}_{17}\text{H}_{14}\text{O}_4$ [$\text{M} + \text{Na}$] $^+$ 305.0790; found 305.0816.



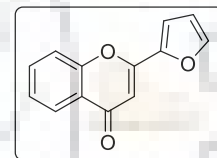
2-(3,4,5-trimethoxyphenyl)-4H-chromen-4-one (7l) [31]: Yield-75% as Pale yellow solid; mp 176–178 °C; $^1\text{H NMR}$ (CDCl_3 , 500 MHz) δ 8.25 (d, $J = 7.9$ Hz, 1H), 7.73 (t, $J = 8.4$ Hz, 1H), 7.61 (d, $J = 8.2$ Hz, 1H), 7.46 (t, $J = 7.8$ Hz, 1H), 7.16 (s, 2H), 6.80 (s, 1H), 3.99 (s, 6H), 3.95 (s, 3H); $^{13}\text{C NMR}$ (CDCl_3 , 125 MHz) δ 178.4, 163.3, 156.2, 153.6, 141.2, 133.76, 127.02, 125.7, 125.3, 123.9, 118.0, 107.4, 103.8, 61.05, 56.3; HRMS (ESI): calcd for $\text{C}_{18}\text{H}_{16}\text{O}_5$ $[\text{M} + \text{Na}]^+$ 335.0895; found 335.0920.



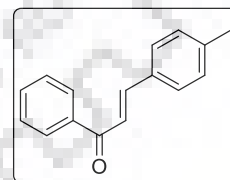
2-(3-nitrophenyl)-4H-chromen-4-one (7m): Yield-74% as White solid; mp 66-68 °C; $^1\text{H NMR}$ (CDCl_3 , 400 MHz,) δ 8.80 (s, 1H), 8.39 (d, $J = 8.1$ Hz, 1H), 8.22 (d, $J = 7.9$ Hz, 2H), 7.77-7.72 (m, 2H), 7.63 (d, $J = 8.4$ Hz, 1H), 7.46 (t, $J = 7.5$ Hz, 1H), 6.90 (s, 1H); $^{13}\text{C NMR}$ (CDCl_3 , 125 MHz,) δ 178.2, 160.6, 156.2, 148.8, 134.5, 133.7, 131.9, 130.4, 126.1, 125.9, 125.8, 123.9, 121.4, 118.3, 108.9; HRMS (ESI): calcd for $\text{C}_{15}\text{H}_{10}\text{NO}_4$ $[\text{M} + \text{Na}]^+$ 290.0429; found 290.0445.



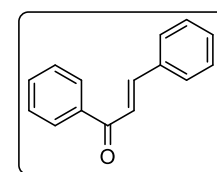
2-(furan-2-yl)-4H-chromen-4-one (7n): Yield-73% as white solid; mp 185-189 °C; $^1\text{H NMR}$ (CDCl_3 , 400 MHz) δ 8.19 (d, $J = 7.9$ Hz, 1H), 7.66 (t, $J = 7.4$ Hz, 1H), 7.61 (s, 1H), 7.48 (d, $J = 8.4$ Hz, 1H), 7.39 (t, $J = 7.5$ Hz, 1H), 7.13–7.12 (m, 1H), 6.73 (s, 1H), 6.60–6.59 (m, 1H); $^{13}\text{C NMR}$ (CDCl_3 , 100 MHz) δ 169.7, 143.4, 137.6, 136.9, 134.0, 132.8, 129.0, 128.9, 128.1, 126.5, 123.0, 120.7, 110.3; HRMS (ESI): calcd for $\text{C}_{13}\text{H}_8\text{O}_3$ $[\text{M} + \text{Na}]^+$ 235.0371; found 235.0393.



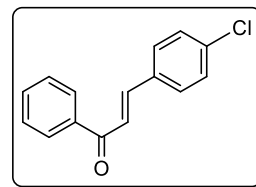
(E)-1-phenyl-3-(p-tolyl)prop-2-en-1-one (7o) [32]: Yield-92% as White solid; mp 95-96 °C; $^1\text{H NMR}$ (CDCl_3 , 500 MHz,) δ 8.01 (d, $J = 7.7$ Hz, 2H), 7.79 (d, $J = 15.7$ Hz, 1H), 7.58–7.55 (m, 1H), 7.54–7.46 (m, 5H), 7.21 (d, $J = 7.8$ Hz, 2H), 2.38 (s, 3H); $^{13}\text{C NMR}$ (CDCl_3 , 125 MHz,) δ 190.7, 144.9, 141.1, 138.4, 132.7, 132.2, 130.0, 129.7, 128.6, 128.5, 121.2, 21.5; HRMS (ESI): calcd for $\text{C}_{16}\text{H}_{14}\text{O}$ $[\text{M} + \text{Na}]^+$ 245.0942; found 245.0964.



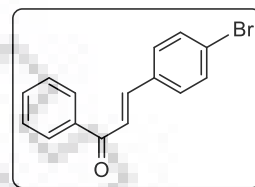
(2E)-1,3-Diphenylprop-2-en-1-one (7p) [32]: Yield-91% as Yellow needles; mp 55–57 °C; IR (KBr): 2935, 2877, 1585, 1266, 1088, 862, 733 cm^{-1} ; $^1\text{H NMR}$ (CDCl_3 , 400 MHz) δ 8.00 (d, $J = 7.8$ Hz, 1H), 7.74 (d, $J = 15.7$ Hz, 1H), 7.60–7.55 (m, 3H), 7.51–7.46 (m, 3H), 7.38 (d, $J = 8.0$ Hz, 1H); $^{13}\text{C NMR}$ (CDCl_3 , 100 MHz,) δ 190.4, 143.4, 138.1, 136.5, 133.4, 133.0, 129.7, 129.4, 128.9, 128.6, 122.5; HRMS (ESI): calcd for $\text{C}_{15}\text{H}_{12}\text{O}$ $[\text{M} + \text{Na}]^+$ 231.0786; found 231.0804.



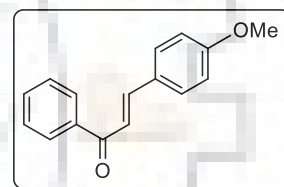
(E)-3-(4-chlorophenyl)-1-phenylprop-2-en-1-one (7r) [32]: Yield-90% as white solid; mp 113–115 °C; IR (KBr): 2954, 2880, 1610, 1271, 1107, 845, 729 cm^{-1} ; ^1H NMR (CDCl_3 , 400 MHz) δ 8.01 (d, $J = 7.8$ Hz, 2H), 7.75 (d, $J = 15.9$ Hz, 1H), 7.61 (t, $J = 7.4$ Hz, 1H), 7.57–7.50 (m, 7H); ^{13}C NMR (CDCl_3 , 100 MHz,) δ 190.2, 143.4, 137.9, 133.7, 133.0, 129.8, 128.5, 124.8, 122.5; (HRMS (ESI): calcd for $\text{C}_{15}\text{H}_{11}\text{ClO}_3$ [$\text{M} + \text{Na}$] $^+$ 265.0396; found 265.0418.



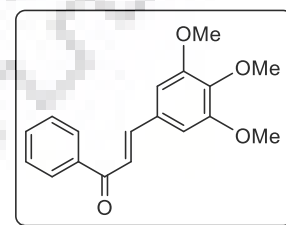
(E)-3-(4-bromophenyl)-1-phenylprop-2-en-1-one (7s) [32]: Yield-90% as pale yellow solid; mp 55–57 °C; IR (KBr): 2951, 2880, 1607, 1271, 1107, 843, 729 cm^{-1} ; ^1H NMR (CDCl_3 , 400 MHz,) δ 8.00 (d, $J = 7.8$ Hz, 2H), 7.72 (d, $J = 15.7$ Hz, 1H), 7.58 (t, $J = 7.4$ Hz, 1H), 7.55–7.48 (m, 7H); ^{13}C NMR (CDCl_3 , 100 MHz,) δ 190.3, 143.5, 138.1, 133.9, 133.0, 132.3, 129.9, 128.8, 128.6, 124.9, 122.6; (HRMS (ESI): calcd for $\text{C}_{15}\text{H}_{11}\text{BrO}$ [$\text{M} + \text{Na}$] $^+$ 308.9891; found 308.9905.



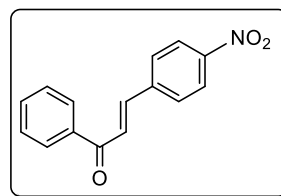
(E)-3-(4-methoxyphenyl)-1-phenylprop-2-en-1-one (7t): Yield-90% as White solid mp: 70–72 °C; IR (KBr): 3040, 1582, 1240, 1175, 1059, 1015, 854 cm^{-1} ; ^1H NMR (CDCl_3 , 400 MHz) δ 8.03 (d, $J = 8.9$ Hz, 2H), 7.80 (d, $J = 15.6$ Hz, 1H), 7.64 – 7.62 (m, 2H), 7.54 (d, $J = 15.6$ Hz, 1H), 7.41–7.39 (m, 3H), 6.97 (d, $J = 8.9$ Hz, 2H), 3.88 (s, 3H); ^{13}C NMR (CDCl_3 , 100 MHz) δ 188.8, 163.5, 144.1, 135.2, 131.2, 130.9, 130.4, 129.0, 128.4, 122.0, 113.9, 55.6; (HRMS (ESI): calcd for $\text{C}_{16}\text{H}_{14}\text{O}_2$ [$\text{M} + \text{Na}$] $^+$ 261.0891; found 261.0915.



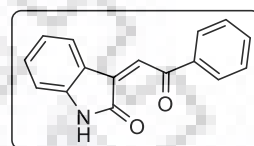
(E)-1-phenyl-3-(3,4,5-trimethoxyphenyl)prop-2-en-1-one (7v) [32]: Yield-88% white solid mp: 147–149 °C; IR (KBr): 3035, 1640, 1575, 1245, 1170, 1150, 1115 cm^{-1} ; ^1H NMR (CDCl_3 , 500 MHz,) δ 8.03 (d, $J = 7.9$ Hz, 2H), 7.74 (d, $J = 15.6$ Hz, 1H), 7.61 (t, $J = 6.9$ Hz, 1H), 7.53 (t, $J = 7.4$ Hz, 2H), 7.42 (d, $J = 15.6$ Hz, 1H), 6.89 (s, 2H), 3.94 (s, 6H), 3.92 (s, 3H); (HRMS (ESI): calcd for $\text{C}_{18}\text{H}_{18}\text{O}_4$ [$\text{M} + \text{Na}$] $^+$ 321.1103; found 321.1119.



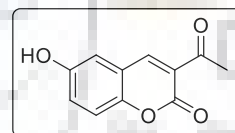
(E)-3-(4-nitrophenyl)-1-phenylprop-2-en-1-one (7w): Yield-88% as Pale yellow solid; mp 175-177 °C; IR (KBr): 3035, 1640, 1575, 1245, 1170, 1150, 1115 cm^{-1} ; ^1H NMR (CDCl_3 , 400 MHz) δ 8.28 (d, $J = 8.0$ Hz, 1H), 8.04 (d, $J = 7.9$ Hz, 2H), 7.91 (d, $J = 7.6$ Hz, 1H), 7.83 (d, $J = 15.7$ Hz, 1H), 7.66–7.59 (m, 4H), 7.53 (d, $J = 7.3$ Hz, 2H); ^{13}C NMR (CDCl_3 , 100 MHz,) δ 189.8, 141.7, 137.7, 136.7, 134.4, 133.4, 130.1, 128.9, 128.7, 124.7, 122.4; HRMS (ESI): calcd for $\text{C}_{15}\text{H}_{11}\text{NO}_3$ $[\text{M} + \text{Na}]^+$ 256.0637; found 256.0661.



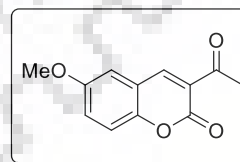
(Z)-3-(2-oxo-2-phenylethylidene)indolin-2-one (7x): Yield-82% as orange solid; mp 179-181 °C; IR (KBr): 2935, 1661, 1462, 1326, 1230, 1016, 862, 749 cm^{-1} ; ^1H NMR (CDCl_3 , 400 MHz) δ 8.55 (s, 1H), 8.29 (d, $J = 7.8$ Hz, 1H), 8.10 (d, $J = 7.1$ Hz, 2H), 7.85 (s, 1H), 7.64–7.60 (m, 1H), 7.52 (t, $J = 7.8$ Hz, 2H), 7.30 (t, $J = 7.7$ Hz, 1H), 7.00 (t, $J = 7.7$ Hz, 1H), 6.86 (d, $J = 7.8$ Hz, 1H); ^{13}C NMR (100 MHz, CDCl_3) δ 191.2, 169.7, 143.4, 137.6, 136.9, 134.0, 132.8, 129.0, 128.9, 128.1, 126.5, 123.0, 120.7, 110.3; HRMS (ESI): calcd for $\text{C}_{16}\text{H}_{11}\text{NO}_2$ $[\text{M} + \text{Na}]^+$ 272.0687; found 272.0705.



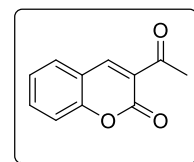
3-acetyl-7-hydroxy-2H-chromen-2-one (8a) [33]: Yield- 89% as Light pink solid; mp 236-237 °C; ^1H NMR ($\text{DMSO } d_6$, 400 MHz) δ ppm 8.58 (s, 1H), 7.77 (d, $J = 8.6$ Hz, 1H), 6.83 (d, $J = 8.6$ Hz, 1H), 6.73 (s, 1H), 2.54 (s, 3H); ^{13}C NMR ($\text{DMSO } d_6$, 100 MHz) δ ppm 194.7, 157.6, 149.8, 145.8, 134.1, 130.2, 127.7, 126.1, 122.8, 120.0, 30.6; HRMS (ESI): calcd for $\text{C}_{11}\text{H}_8\text{O}_4$ $[\text{M} + \text{Na}]^+$ 227.0320; found 227.0344.



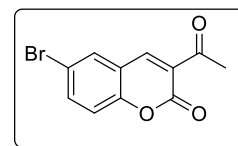
3-acetyl-8-methoxy-2H-chromen-2-one (8b) [33]: Yield-87% Light yellow solid; mp 167-168°C; ^1H NMR (CDCl_3 , 400 MHz) δ ppm 8.47 (s, 1H), 7.29-7.18 (m, 3H), 3.98 (s, 3H), 2.72 (s, 3H); ^{13}C NMR (CDCl_3 , 100 MHz) δ ppm 195.7, 158.8, 147.8, 147.7, 147.1, 145.0, 124.7, 121.4, 118.9, 115.9, 56.4, 30.6; HRMS (ESI): calcd for $\text{C}_{12}\text{H}_{10}\text{O}_4$ $[\text{M} + \text{Na}]^+$ 241.0477; found 241.0495.



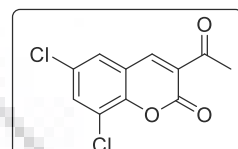
3-acetyl-2H-chromen-2-one (8c) [33]: Yield-85% as White solid; mp 121-122°C; ^1H NMR (CDCl_3 , 400 MHz) δ ppm 8.49 (s, 1H), 7.65-7.62 (m, 2H), 7.37-7.31 (m, 1H), 2.71 (s, 3H); ^{13}C NMR (CDCl_3 , 100 MHz) δ ppm 195.6, 159.3, 155.4, 147.6, 134.5, 130.3, 125.1, 124.6, 118.3, 116.7, 30.6; HRMS (ESI): calcd for $\text{C}_{11}\text{H}_8\text{O}_3$ $[\text{M} + \text{Na}]^+$ 211.0371; found 211.0393.



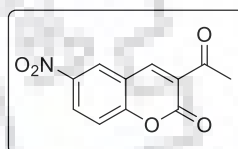
3-acetyl-6-bromo-2H-chromen-2-one (8d): Yield-84%; as White solid; mp 232-233°C; ^1H NMR (DMSO d_6 , 400 MHz) δ ppm 8.56 (s, 1H), 8.18 (s, 1H), 7.84 (d, $J = 8.6$ Hz, 1H), 7.40 (d, $J = 8.5$ Hz, 1H), 2.53 (s, 3H); ^{13}C NMR (DMSO d_6 , 100 MHz) δ ppm 195.2, 157.7, 149.5, 145.9, 133.6, 129.2, 129.0, 126.6, 121.3, 121.1, 30.2; HRMS (ESI): calcd for $\text{C}_{11}\text{H}_7\text{BrO}_3$ [$\text{M} + \text{Na}$] $^+$ 288.9476; found 288.9492.



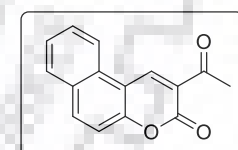
3-acetyl-6,8-dichloro-2H-chromen-2-one (8e): Yield-83% as White solid; mp 169-171°C; ^1H NMR (CDCl_3 , 400 MHz) δ ppm 8.38 (s, 1H), 7.69 (d, $J = 2.3$ Hz, 1H), 7.55 (d, $J = 2.3$ Hz, 1H), 2.73 (s, 3H); ^{13}C NMR (CDCl_3 , 100 MHz) δ ppm 194.8, 157.6, 149.6, 145.8, 134.1, 130.2, 127.7, 126.1, 122.8, 120.0, 30.6; HRMS (ESI): calcd for $\text{C}_{11}\text{H}_6\text{Cl}_2\text{O}_3$ [$\text{M} + \text{Na}$] $^+$ 278.9592; found 278.9618.



3-acetyl-6-nitro-2H-chromen-2-one (8f) [33]: Yield-80% as Light yellow solid; mp 167-168 °C; ^1H NMR (400 MHz, CDCl_3) δ 8.59-8.58 (m, 1H), 8.54 (s, 1H), 8.49 (dd, $J = 9.1, 2.6$ Hz, 1H), 7.51 (d, $J = 9.1$ Hz, 1H), 2.72 (t, 3H); ^{13}C NMR (CDCl_3 , 100 MHz) δ ppm 194.3, 158.5, 157.7, 146.0, 145.9, 128.6, 125.9, 118.3, 118.1, 118.0, 30.5; calcd for $\text{C}_{11}\text{H}_7\text{NO}_5$ [$\text{M} + \text{Na}$] $^+$ 256.0222; found 256.0240.



2-acetyl-3H-benzo[f]chromen-3-one (8g): Yield-77% as Light yellow solid; mp 185-187°C; ^1H NMR (CDCl_3 , 400 MHz) δ ppm 9.25 (s, 1H), 8.31 (d, $J = 8.4$ Hz, 1H), 8.06 (d, $J = 9.0$ Hz, 1H), 7.89 (d, $J = 8.0$ Hz, 1H), 7.71 (t, $J = 8.2$ Hz, 1H), 7.58 (t, $J = 7.8$ Hz, 1H), 7.42 (d, $J = 9.0$ Hz, 1H), 2.75 (s, 3H); ^{13}C NMR (CDCl_3 , 100 MHz) δ ppm 195.5, 159.4, 156.1, 143.2, 136.2, 130.1, 129.8, 129.2, 126.6, 122.4, 121.6, 116.4, 112.7, 30.6; HRMS (ESI): calcd for $\text{C}_{15}\text{H}_{10}\text{O}_3$ [$\text{M} + \text{Na}$] $^+$ 261.0528; found 261.0554.



6.9. References

- (a) Parveen, I.; Ahmed, N. "CuI mediated synthesis of heterocyclic flavone-benzofuran fused derivatives" *Tetrahedron Lett.* **2017**, *58*, 2302–2305; (b) Dai, C.; Sun, X.; Tu, X.; Wu, L.; Zhan, D.; Zeng, Q. "Synthesis of phenothiazines *via* ligand-free CuI-catalyzed cascade C–S and C–N coupling of aryl *ortho*-dihalides and *ortho*-aminobenzenethiols" *Chem. Commun.* **2012**, *48*, 5367–5369.
- (a) Pinder, R. A. "The Hydrogenolysis of Organic Halides" *Synthesis*, **1980**, 425452; (b) Hudlicky, M.; Trost, M. B.; Fleming, I. (Eds.), *Comprehensive Organic Synthesis*, Vol. 8, Pergamon, Oxford **1991**, 895, 922; (c) Alonso, F.; Beletskaya,

- P. I.; Yus, M. "Metal-Mediated Reductive Hydrodehalogenation of Organic Halides" *Chem. Rev.* **2002**, *102*, 4009–4091.
- Hitchman, L. M.; Spackman, A. R.; Ross, C. N.; Agra, C. "Disposal Methods for Chlorinated Aromatic Waste" *Chem. Soc Rev.* **1995**, 423–430.
 - (a) Monguchi, Y.; Kume, A.; Hattori, K.; Maegawa, T.; Sajiki, H. "Pd/C–Et₃N-mediated catalytic hydrodechlorination of aromatic chlorides under mild condition" **2006**, *62*, 7926–7933; (b) Marques, A. C.; Selva, M.; Tundo, P. "Facile Hydrodehalogenation with H₂ and Pd/C Catalyst under Multiphase Conditions. Part 2. Selectivity and Kinetics" *J. Org. Chem.* **1994**, *59*, 3830–3837; (c) Marques, A. C.; Selva, M.; Tundo, P. "Facile Hydrodehalogenation with H₂ and Pd/C Catalyst under Multiphase Conditions. 3. Selective Removal of Halogen from Functionalized Aryl Ketones. 4. Aryl Halide-Promoted Reduction of Benzyl Alcohols to Alkanes" *J. Org. Chem.* **1995**, *60*, 2430–2435.
 - (a) Jr., R. J. R.; Jr., M. E. R. "C–O Hydrogenolysis Catalyzed by Pd-PMHS Nanoparticles in the Company of Chloroarenes" *Tetrahedron Lett.* **2002**, *43*, 8823–8826; (b) Ariane-Angeloff, J.-J.; Brunet P.; Legars, D.; Neibecker, D.; Souyri, D. "Regioselective dechlorination of 2,3-dichloronitrobenzene into 3-chloronitrobenzene and regioselective dechlorination–hydrogenation into 3-chloroaniline" *Tetrahedron Lett.* **2001**, *42*, 2301–2303; (c) Zhang, Y.; Liao, S.; Xu, Y. "Highly active polymer anchored palladium catalyst for the hydrodehalogenation of organic halides under mild conditions" *Tetrahedron Lett.* **1994**, *35*, 4599–4602.
 - Nakao, R.; Rhee, H.; Uozumi, Y. "Hydrogenation and Dehalogenation under Aqueous Conditions with an Amphiphilic-Polymer-Supported Nanopalladium Catalyst" *Org. Lett.* **2005**, *7*, 163–165.
 - (a) Buil, L. M.; Esteruelas, A. M.; Niembro, S.; Oliván, M.; Orzechowski, L.; Pelayo, C.; Vallribera, A. "Dehalogenation and Hydrogenation of Aromatic Compounds Catalyzed by Nanoparticles Generated from Rhodium Bis(imino)pyridine Complexes" *Organometallics*, **2010**, *29*, 4375–4383; (b) Young, J. R.; Grushin, V. V. "Catalytic C–F Bond Activation of Nonactivated Monofluoroarenes" *Organometallics*, **1999**, *18*, 294–296; (c) Kvintovics, P.; Heil, B.; Palágyi, J.; Markó, L. "Rhodium-phosphine complexes as homogeneous catalysts: Homogeneous catalytic hydrodehalogenation of organic halides by molecular hydrogen" *J. Organomet. Chem.* **1978**, *148*, 311–315.

8. (a) Choi, W.; Hoffmann, M. R. "Photoreductive Mechanism of CCl_4 Degradation on TiO_2 Particles and Effects of Electron Donors" *Environ. Sci. Technol.* **1995**, *29*, 1646–1654; (b) Sun, C.; Zhao, J.; Ji, H.; Ma, W.; Chen, C. "Photocatalytic debromination of preloaded decabromodiphenyl ether on the TiO_2 surface in aqueous system" *Chemosphere* **2012**, *89*, 420–425.
9. (a) Chang, W.; Cun, S.; Pang, X.; Sheng, H.; Li, Y.; Ji, H.; Song, W.; Chen, C.; Ma, W.; Zhao, J. *Angew. Chem. Int. Ed.* **2015**, *54*, 2052–2056; (b) Sun, C.; Zhao, D.; Chen, C.; Ma, W.; Zhao, J. "TiO₂-Mediated Photocatalytic Debromination of Decabromodiphenyl Ether: Kinetics and Intermediates" *Environ. Sci. Technol.* **2009**, *43*, 157–162.
10. (a) Fuku, K.; Hashimoto, K.; Kominami, H. "Photocatalytic reductive dechlorination of chlorobenzene to benzene in 2-propanol suspension of metal-loaded titanium (IV) oxide nanocrystals in the presence of dissolve sodium hydroxide" *Chem. Commun.* **2010**, *46*, 5118–5120; (b) Shiraishi, Y.; Takeda, Y.; Sugano, Y.; Ichikawa, S.; Tanaka, S.; Hirai, T. "Highly efficient photocatalytic dehalogenation of organic halides on TiO_2 loaded with bimetallic Pd–Pt alloy nanoparticles" *Chem. Commun.* **2011**, *47*, 7863–7865.
11. (a) Yin, H.; Wada, Y.; Kitamura, T.; Yanagida, S. "Photoreductive Dehalogenation of Halogenated Benzene Derivatives Using ZnS or CdS Nanocrystallites as Photocatalysts" *Environ. Sci. Technol.* **2001**, *35*, 227–231; (b) Kuchmii, Y. S.; Korzhak, V. A.; Kryukov, I. A. "Coupled photocatalytic reactions for dehalogenation of polychlorinated hydrocarbons and generation of molecular hydrogen" *Theor. Exp. Chem.* **1999**, *35*, 153–157.
12. Zahran, E. M.; Bedford, N. M.; Nguyen, M. A.; Chang, Y. J.; Guiton, B. S.; Naik, R. R.; Bachas, L. G.; Knecht, M. R. "Light-Activated Tandem Catalysis Driven by Multicomponent Nanomaterials" *J. Am. Chem. Soc.* **2014**, *136*, 32–35.
13. Nguyen, M. A.; Zahran, E. M.; Wilbon, A. S.; Besmer, A. V.; Cendan, V. J.; Ranson, W. A.; Lawrence, R. L.; Cohn, J. L.; Bachas, L. G.; Knecht, M. R. "Converting Light Energy to Chemical Energy: A New Catalytic Approach for Sustainable Environmental Remediation" *ACS Omega* **2016**, *1*, 41–51.
14. (a) Pri-Bar, I.; Buchman, O. "Homogeneous, Palladium-Catalyzed, Selective Hydrogenolysis of Organohalides" *J. Org. Chem.* **1986**, *51*, 734; (b) Arcadi, A.; Cerichelli, G.; Chiarini, M.; Vico, R.; Zorzan, D. "Pd/C-Catalyzed Transfer

- Reduction of Aryl Chlorides with Sodium Formate in Water” *Eur. J. Org. Chem.* **2004**, 2004, 3404.
15. (a) Boukherroub, R.; Chatgililoglu, C.; Manuel, G. “PdCl₂-Catalyzed Reduction of Organic Halides by Triethylsilane” *Organometallics* **1996**, 15, 1508; (b) Yang, J.; Brookhart, M. “Iridium-Catalyzed Reduction of Alkyl Halides by Triethylsilane” *J. Am. Chem. Soc.* **2007**, 129, 12656.
 16. Imai, H.; Nishiguchi, T.; Tanaka, M.; Fukuzumi, K. “Transfer Hydrogenation and Transfer Hydrogenolysis. 14. Cleavage of Carbon-Halogen Bond by the Hydrogen Transfer from Organic Compounds Catalysed by Noble Metal Salts” *J. Org. Chem.* **1977**, 42, 2309.
 17. Stöhr, F.; Sturmayer, D.; Schubert, U. “C–Cl/Si–H Exchange catalysed by P, N-chelated Pt (II) complexes” *Chem. Commun.* **2002**, 2222.
 18. Zawisza, A. M.; Muzart, J. “Pd-catalysed reduction of aryl halides using dimethylformamide as the hydride source” *Tetrahedron Lett.* **2007**, 48, 6738–6742.
 19. (a) Cucullu, M. E.; Nolan, S. P.; Belderrain, T. R.; Grubbs, R. H. “Catalytic Dehalogenation of Aryl Chlorides Mediated by Ruthenium(II) Phosphine Complexes” *Organometallics* **1999**, 18, 1299; (b) Chen, J.; Zhang, Y.; Yang, L.; Zhang, X.; Liu, J.; Li, L.; Zhang, H. “A practical palladium catalyzed dehalogenation of aryl halides and α -haloketones” *Tetrahedron* **2007**, 63, 4266; (c) Cucullu, M. E.; Nolan, S. P.; Belderrain, T. R.; Grubbs, R. H. “Catalytic Dehalogenation of Aryl Chlorides Mediated by Ruthenium(II) Phosphine Complexes” *Organometallics* **1999**, 18, 1299; (d) Fujita, K.-I; Owaki, M.; Yamaguchi, R. *Chem. Commun.* **2002**, 2964; (e) Massicot, F.; Schneider, R.; Fort, Y.; Illy-Cherrey, S.; Tillement, O. “Synergistic Effect in Bimetallic Ni–Al Clusters. Application to Efficient Catalytic Reductive Dehalogenation of Polychlorinated Arenes” *Tetrahedron* **2000**, 56, 4765; (f) Navarro, O.; Marion, N.; Oonishi, Y.; Kelly, R. A., III; Nolan, S. P. “Suzuki–Miyaura, α -Ketone Arylation and Dehalogenation Reactions Catalyzed by a Versatile N-Heterocyclic Carbene–Palladacycle Complex” *J. Org. Chem.* **2006**, 71, 685.
 20. (a) Desmarests, C.; Kuhl, S.; Schneider, R.; Fort, Y. “Nickel(0)/Imidazolium Chloride Catalyzed Reduction of Aryl Halides” *Organometallics* **2002**, 21, 1554; (b) Viciu, M. S.; Grasa, G. A.; Nolan, S. P. “Catalytic Dehalogenation of Aryl Halides Mediated by a Palladium/Imidazolium Salt System” *Organometallics* **2001**, 20, 3607.

21. Lefebvre, O.; Marull, M.; Schlosser, M. "4-(Trifluoromethyl)quinoline Derivatives" *Eur. J. Org. Chem.* **2003**, *11*, 2115–2121.
22. Cellier, P. P.; Spindler, F. J.; Taillefer, M.; Cristau, J.-H. "Pd/C-catalyzed room-temperature hydrodehalogenation of aryl halides with hydrazine hydrochloride" *Tetrahedron Lett.* **2003**, *44*, 7191–7195.
23. Hirasawa, N.; Takahashi, Y.; Fukuda, E.; Sugimoto, O.; Tanji, K. "Indium-mediated dehalogenation of halo-heteroaromatics in water" *Tetrahedron Lett.* **2008**, *49*, 1492–1494.
24. (a) Hara, R.; Sato, K.; Sun, W.-H.; Takahashi, T. "Catalytic dechlorination of aromatic chlorides using Grignard reagents in the presence of $(C_5H_5)_2TiCl_2$ " *Chem. Commun.* **1999**, 845; (b) Guo, H.; Kanno, K.; Takahashi, T. "Iron-Catalyzed Dechlorination of Aryl Chlorides" *Chem. Lett.* **2004**, *33*, 1356; (c) Czaplik, W. M.; Grupe, S.; Mayer, M.; von Wangelin, A. J. "Practical iron-catalyzed dehalogenation of aryl halides" *Chem. Commun.* **2010**, *46*, 6350.
25. Chan, K. S.; Liu, C. R.; Wong, K. L. "Cobalt porphyrin catalyzed hydrodehalogenation of aryl bromides with KOH" *Tetrahedron Lett.* **2015**, *56*, 2728.
26. (a) Inoue, K.; Sawada, A.; Shibata, I.; Baba, A. "Indium(III) Chloride–Sodium Borohydride System: A Convenient Radical Reagent for an Alternative to Tributyltin Hydride System" *J. Am. Chem. Soc.* **2002**, *124*, 906–907; (b) Iranpoor, N.; Firouzabadi, H.; Azadi R. "Diphenylphosphinite ionic liquid (IL-OPPh₂): A solvent and ligand for palladium-catalyzed silylation and dehalogenation reaction of aryl halides with triethylsilane" *J. Organomet. Chem.* **2010**, *695*, 887–890.
27. Ahmed N.; Lier, v. E. J. *J. Chem. Res.* "Pd-C/ammonium formate: a selective catalyst for the hydrogenation of chalcones to dihydrochalcones" **2006**, 584–585.
28. (a) Chelucci, G.; Baldino, S.; Ruiu, A. "Room-Temperature Hydrodehalogenation of Halogenated Heteropentalenes with One or Two Heteroatoms" *J. Org. Chem.* **2012**, *77*, 9921–9925; (b) Chelucci, G.; Figus, S. "NaBH₄-TMEDA and a palladium catalyst as efficient regio- and chemoselective system for the hydrodehalogenation of halogenated heterocycles" *J. Mol. Catal.* **2014**, *393*, 191–209; (c) Chelucci, G. "Hydrodehalogenation of halogenated pyridines and quinolines by sodium borohydride/*N,N,N',N'*-tetramethylethylenediamine under palladium catalysis" *Tetrahedron Lett.* **2010**, *51*, 1562.

29. You, T.; Wang, Z.; Chen, J.; Xia, Y. "Transfer Hydro-dehalogenation of Organic Halides Catalyzed by Ruthenium(II) Complex" *J. Org. Chem.* **2017**, *82*, 1340–1346.
30. (a) Giri, R.; Brusoe, A.; Troshin, K.; Wang, Y. J.; Font, M.; Hartwig F. J. *J. Am. Chem. Soc.* 2018, *140*, 793–806; (b) Alonso, F.; Beletskaya, P. I.; Yus M.; *Chem. Rev.* 2002, *102*, 4009–4091.
31. Chimenti, F.; Fioravanti, R.; Bolasco, A.; Chimenti, P.; Secci, D.; Rossi, F.; Yanez, M.; Orallo, F.; Ortuso, F.; Alcaro, S.; Cirilli, R.; Ferretti, R.; Sanna. L. M. *Bioorg. Med. Chem.* **2010**, *18*, 1273-1279
32. Pathe, K. G.; Ahmed, N. *Tetrahedron Lett.* **2015**, *56*, 6202-6206.
33. Srikrishna, D.; Tasqeeruddin, S.; Dubey, K. P. *Lett. in Org. Chem.* **2014**, *11*, 556-563.



NMR SPECTRA OF SELECTED COMPOUNDS



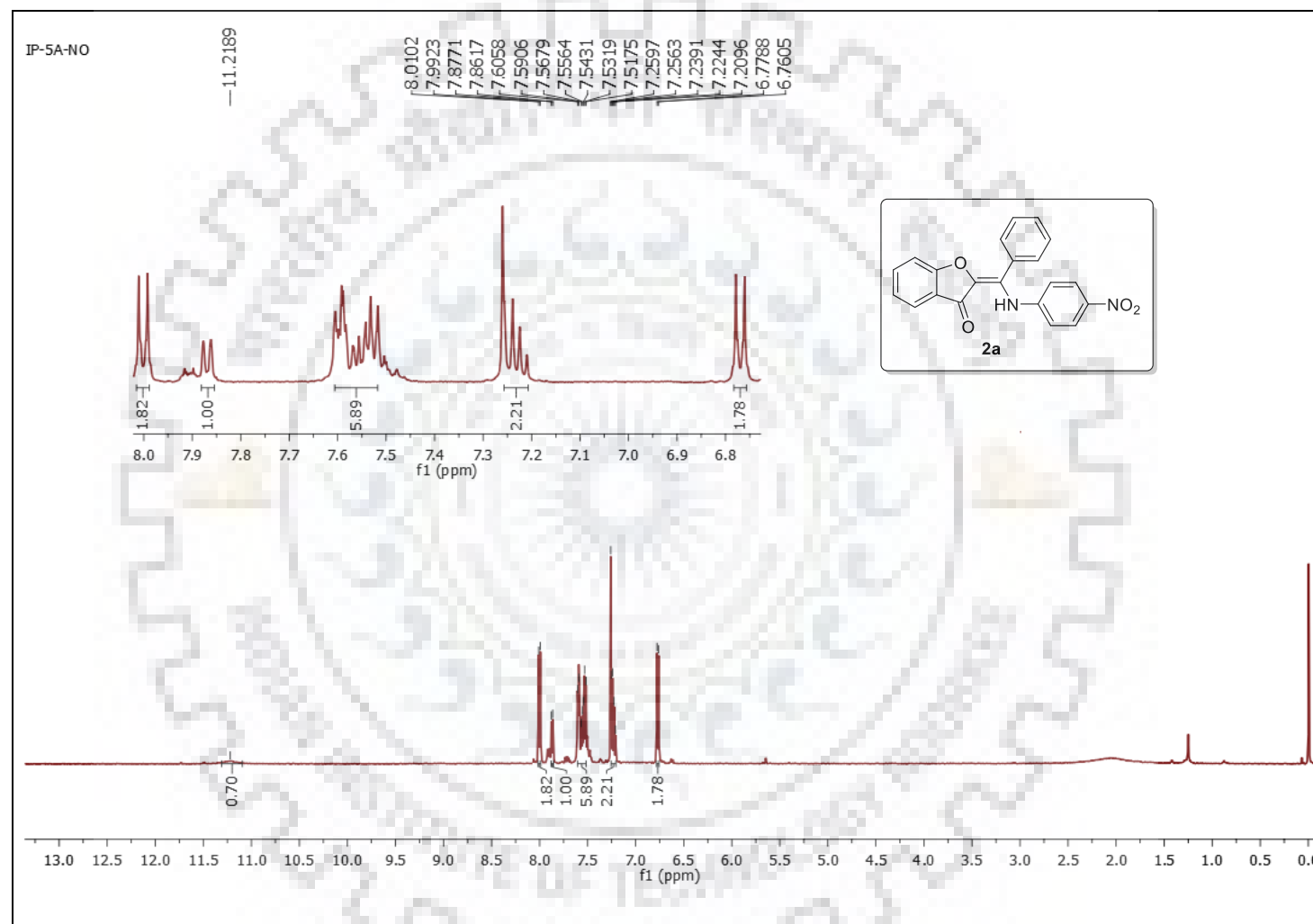


Figure S-1: ^1H NMR Spectrum of **2a**.

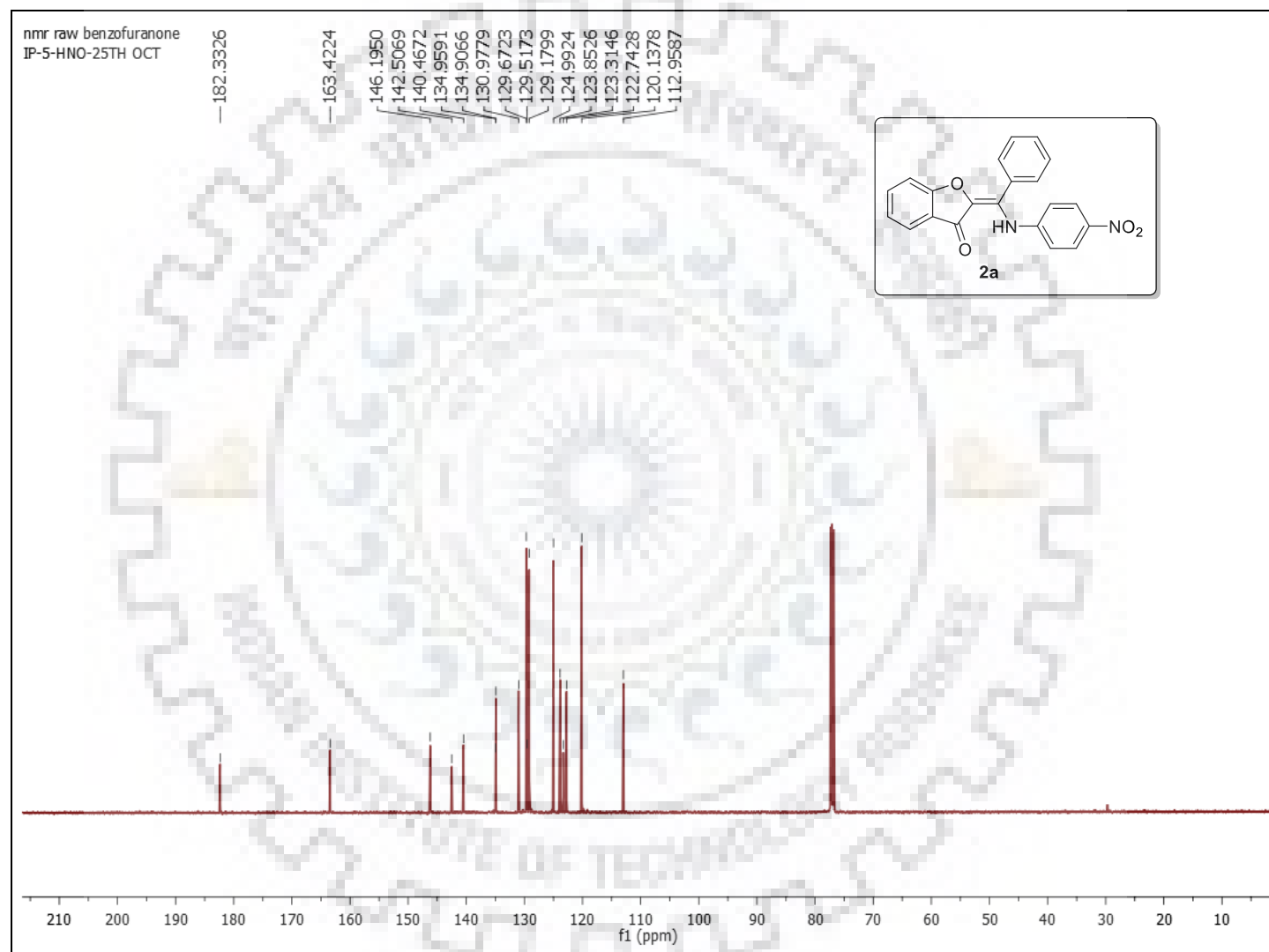


Figure S-2: ^{13}C Spectrum of **2a**.

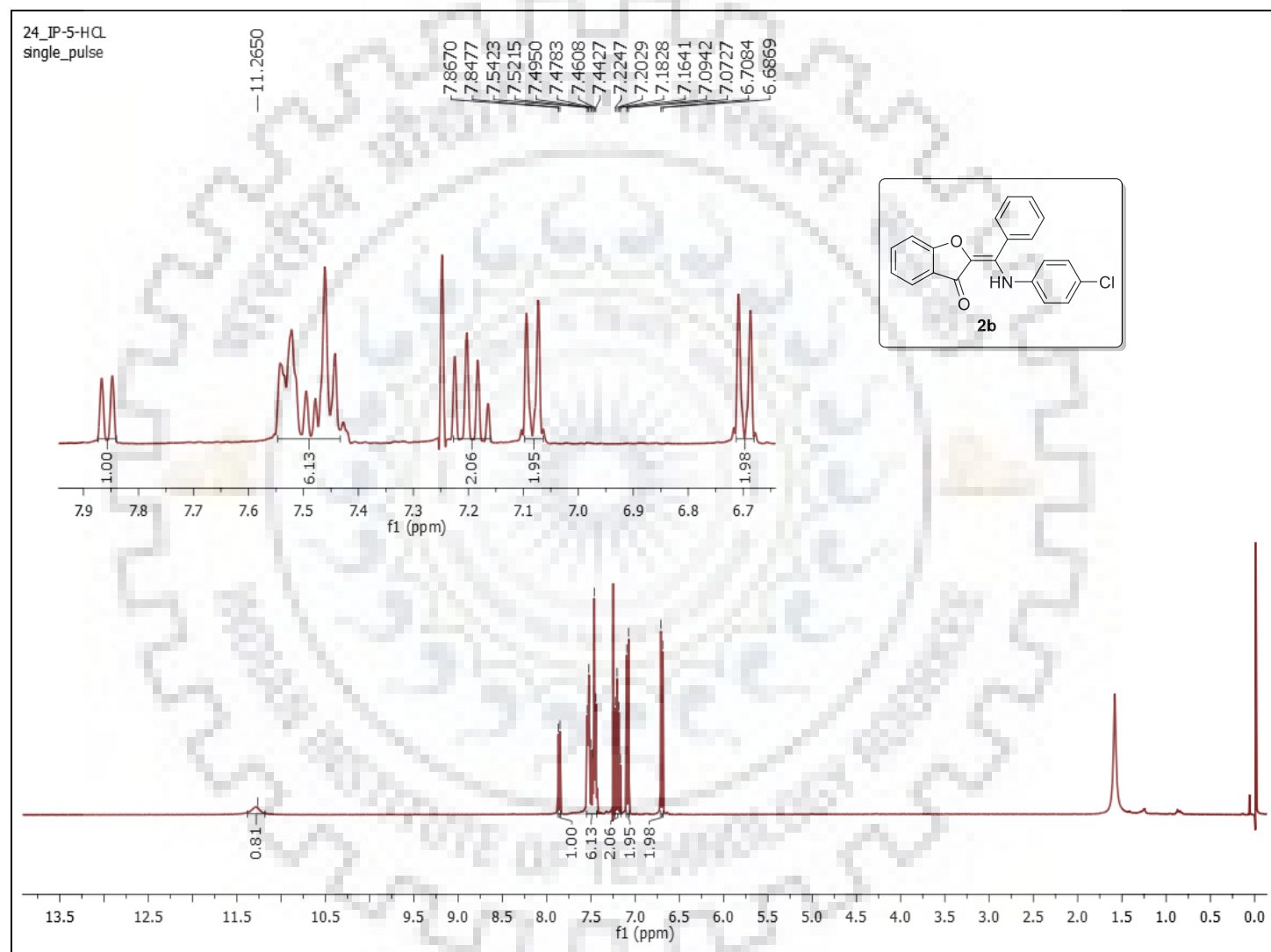


Figure S-3: ^1H NMR Spectrum of **2b**.

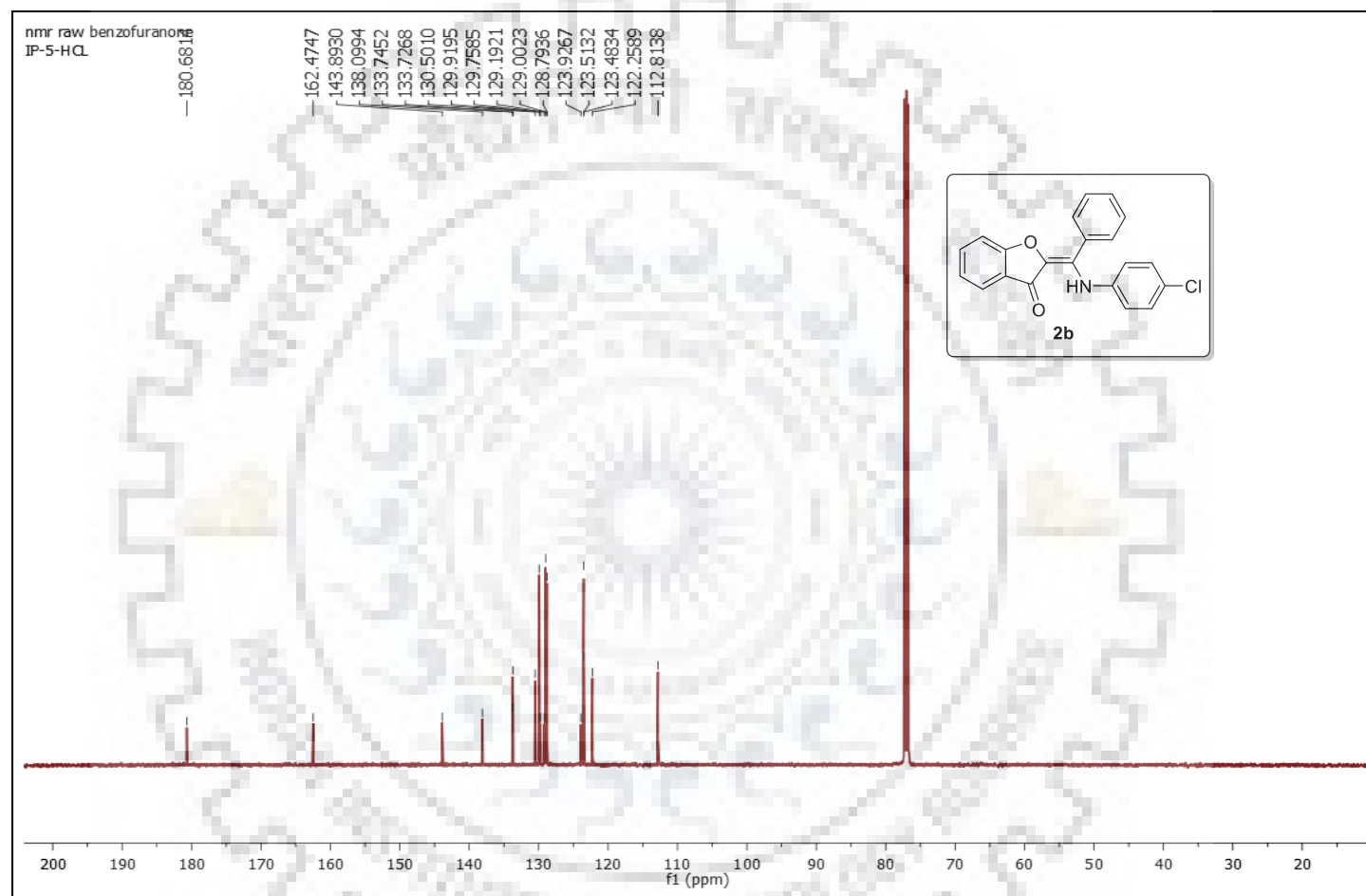


Figure S-4: ^{13}C Spectrum of **2b**.

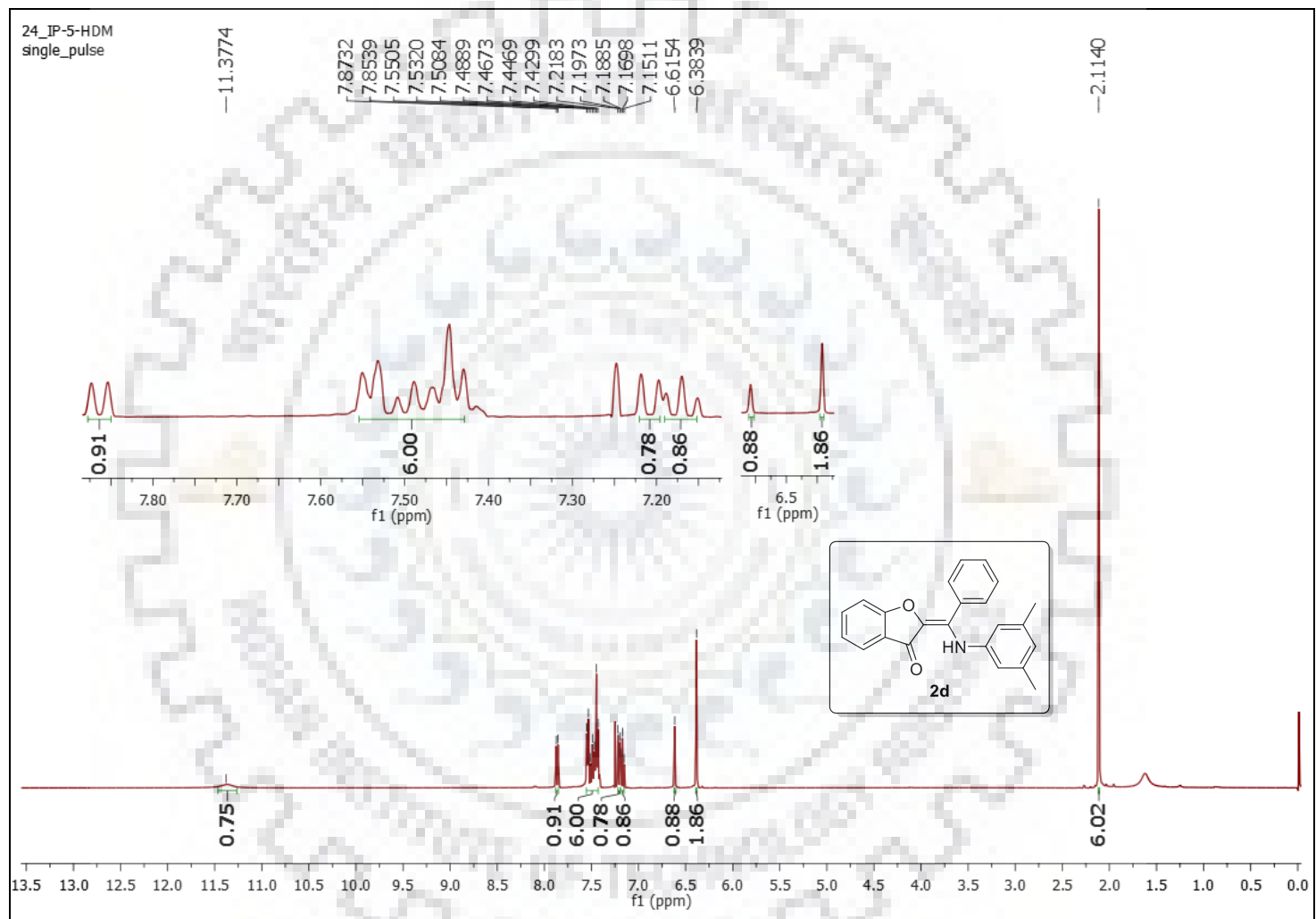


Figure S-5: ^1H NMR Spectrum of **2d**.

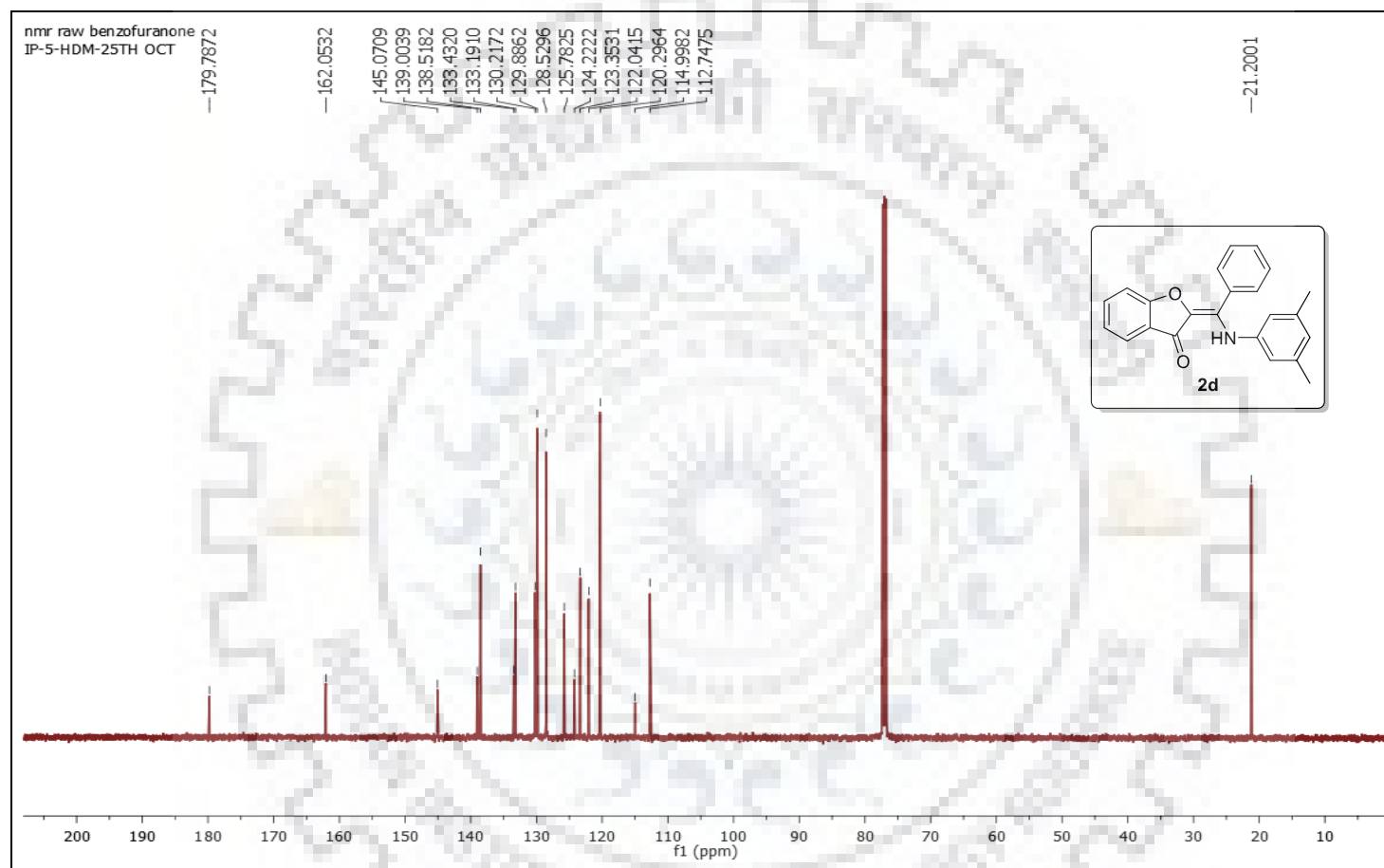


Figure S-6: ^{13}C Spectrum of **2d**.

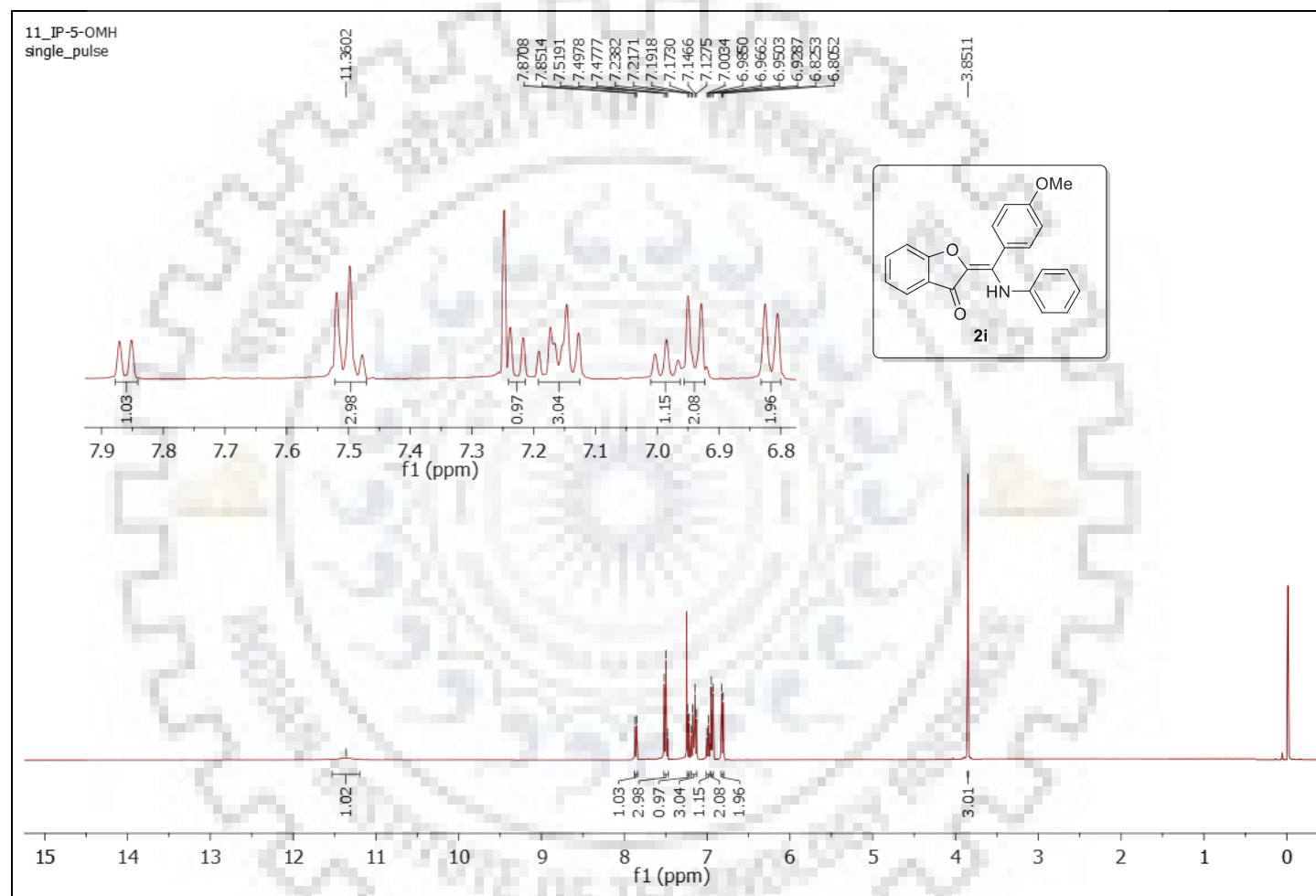


Figure S-9: ^1H NMR Spectrum of **2i**.

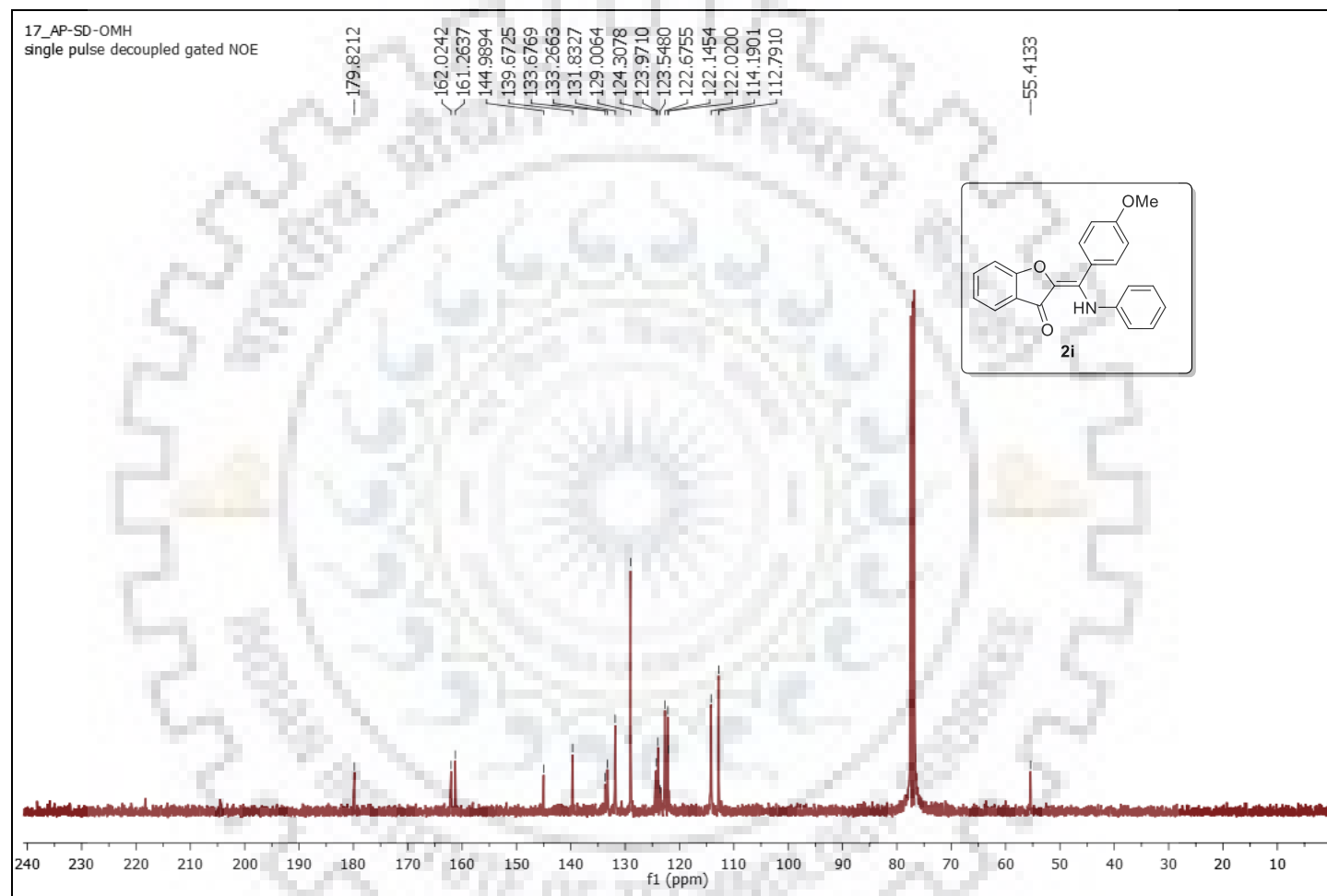


Figure S-10: ^{13}C Spectra of **2i**.

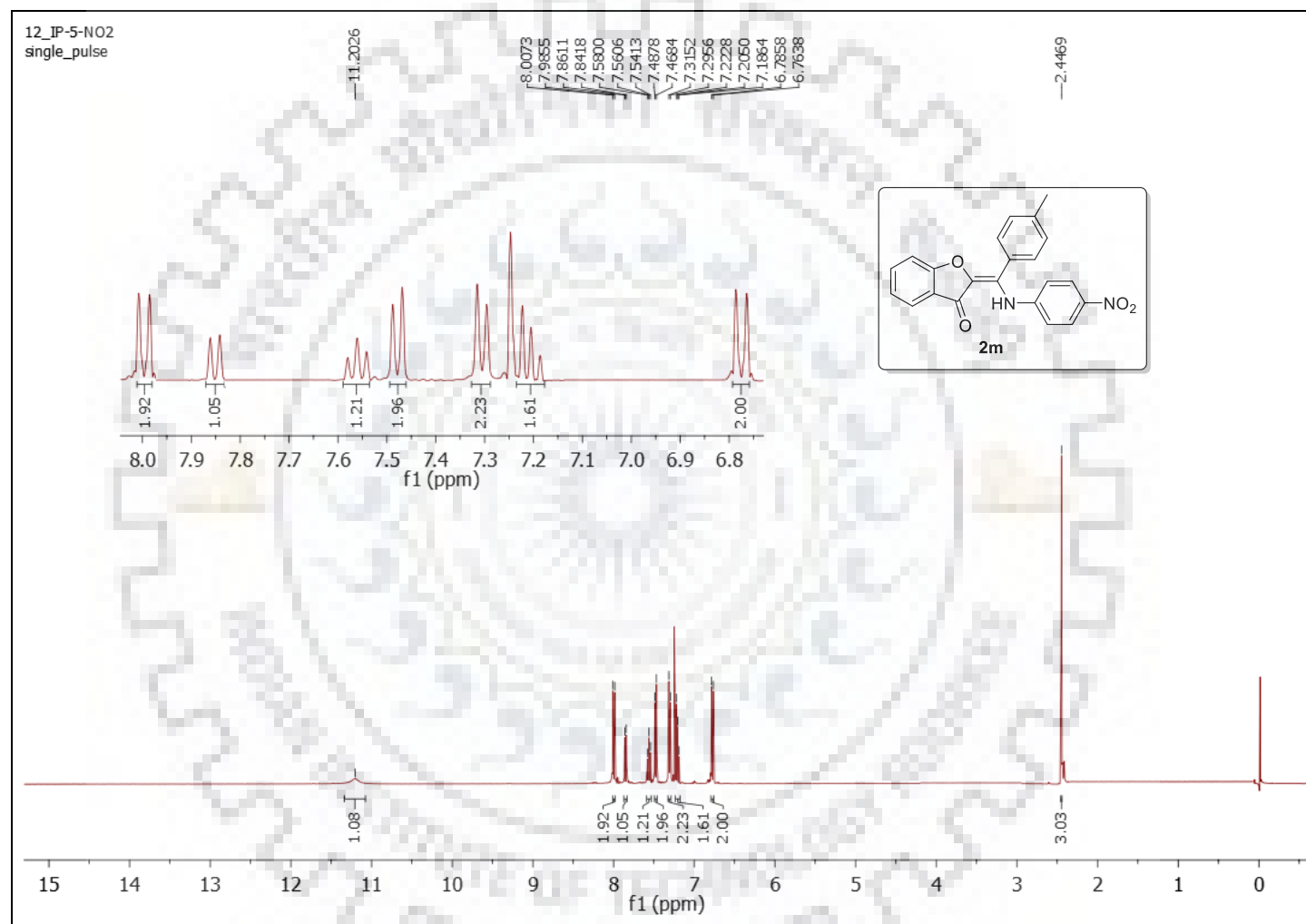


Figure S-11: ^1H NMR Spectrum of **2m**.

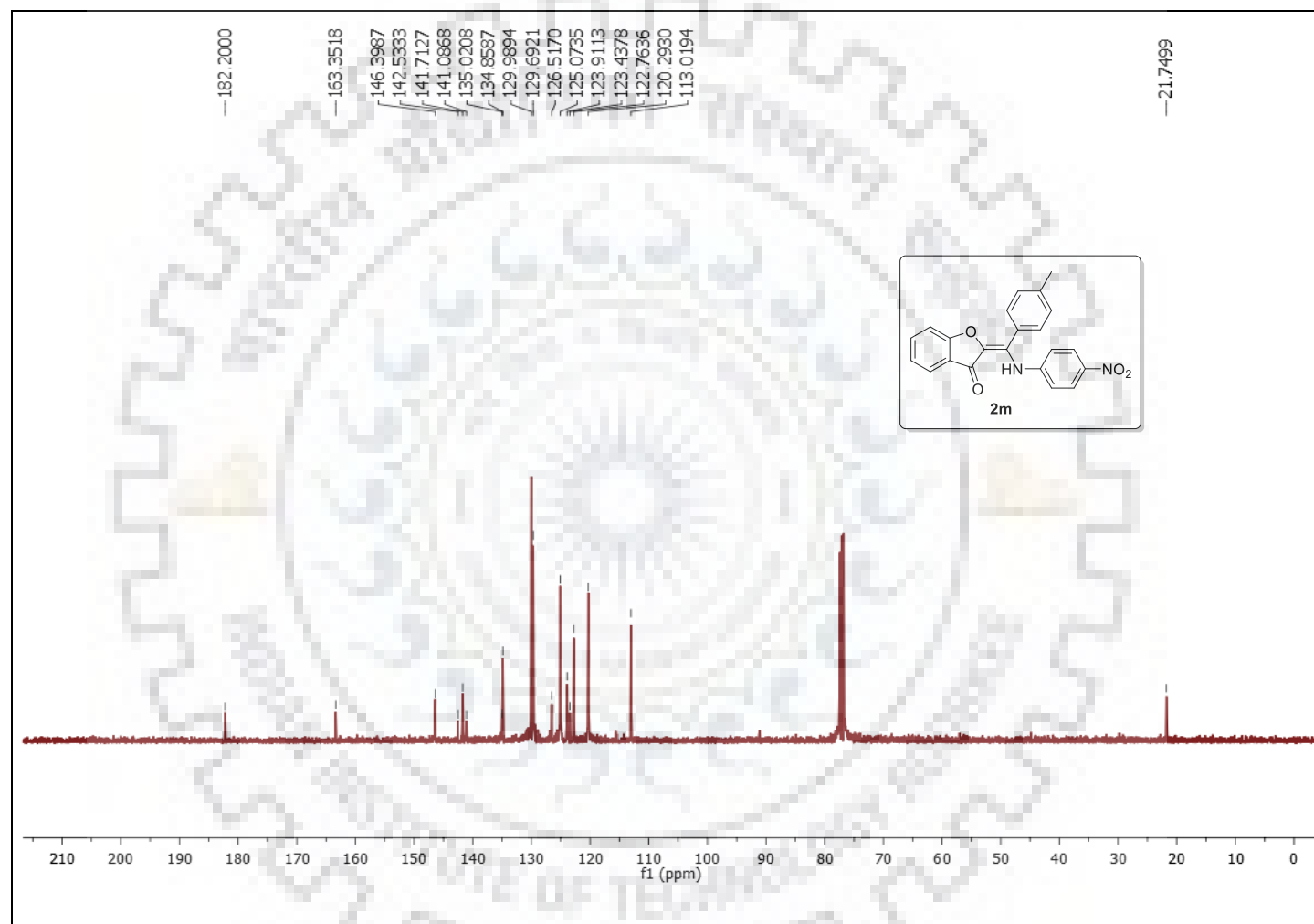


Figure S-12: ^{13}C Spectrum of **2m**.

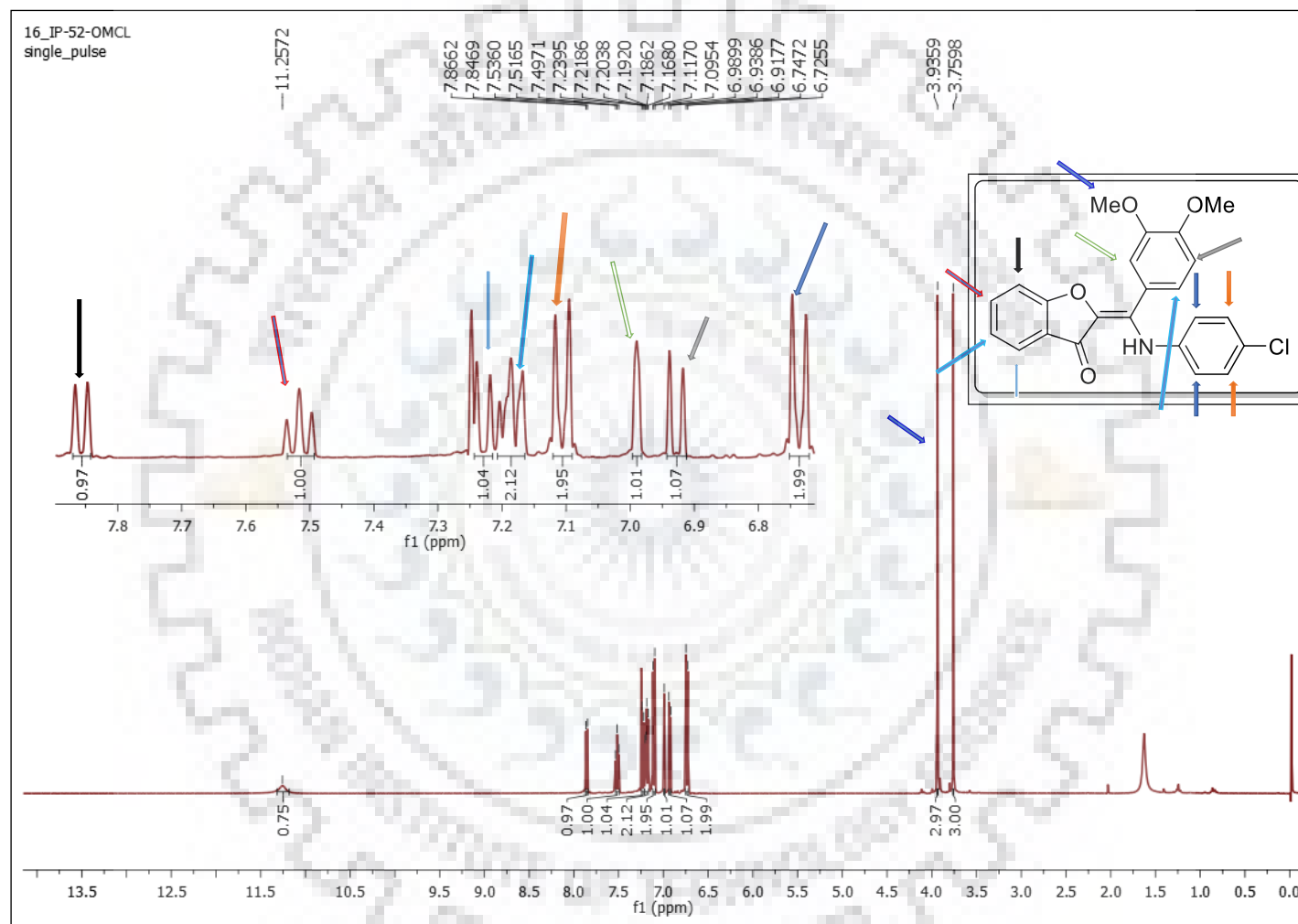


Figure S-13: ^1H NMR Spectrum of 2q.

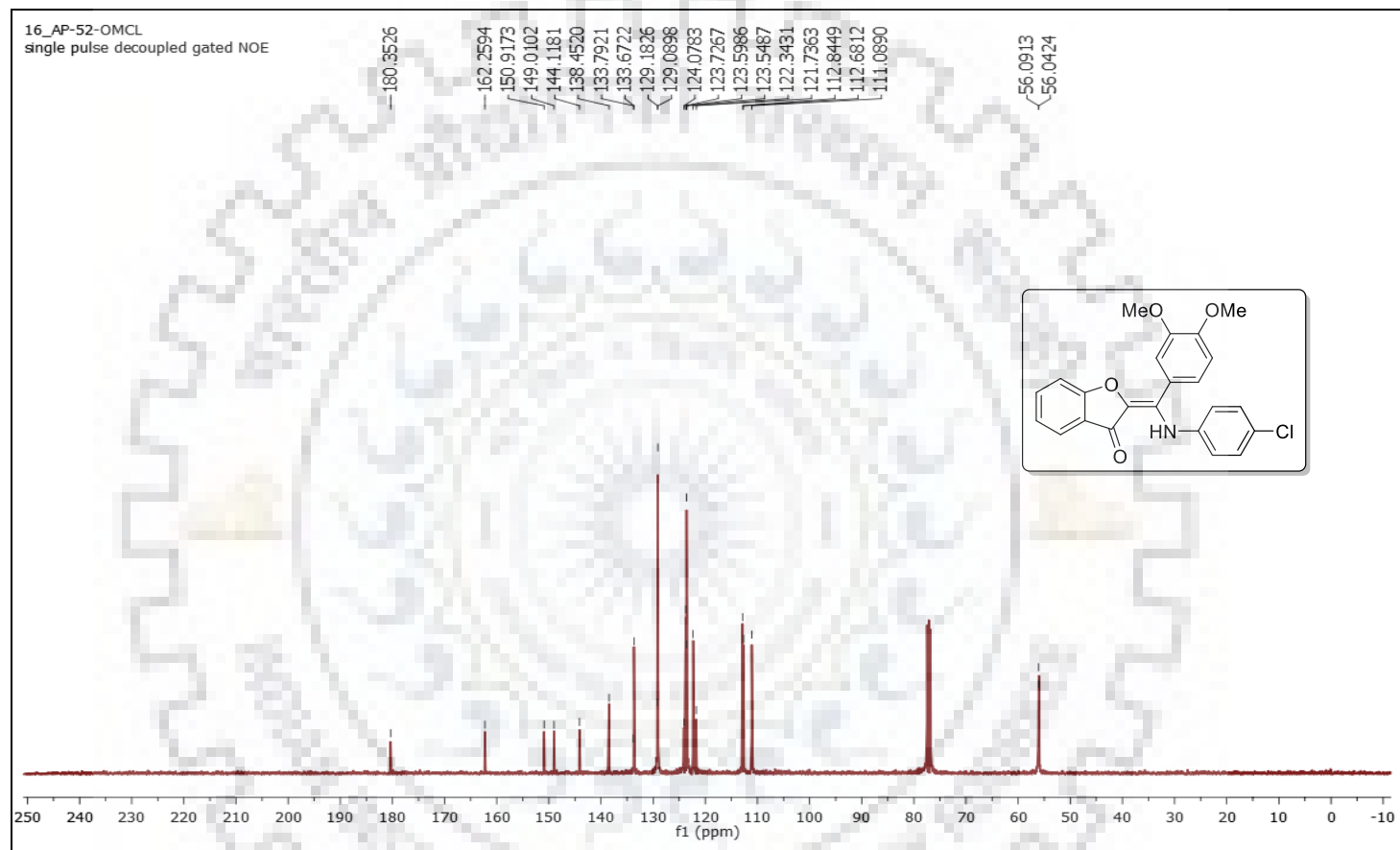


Figure S-14: ^1H NMR Spectrum of 2q.

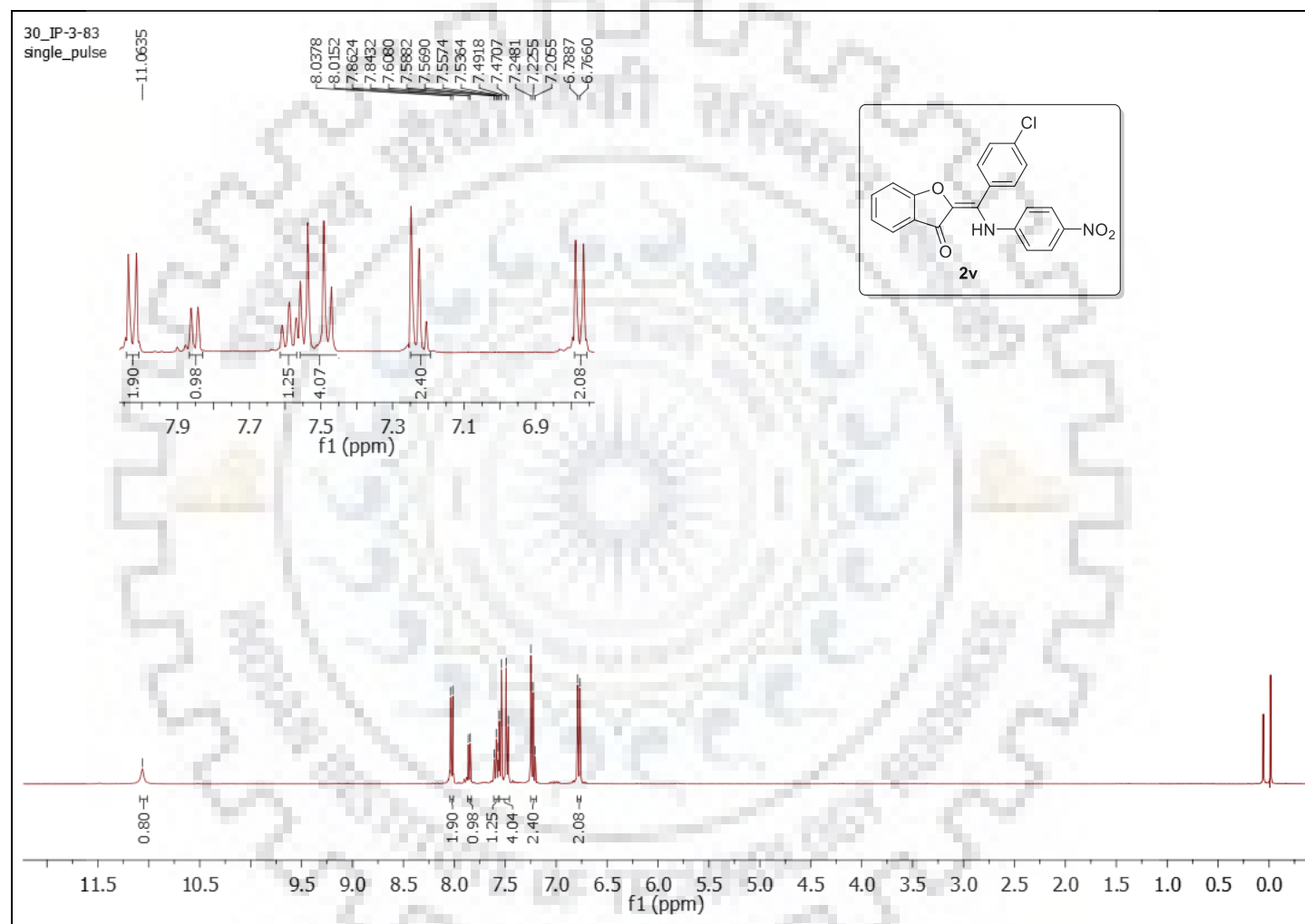


Figure S-15: ^1H NMR Spectrum of **2v**.

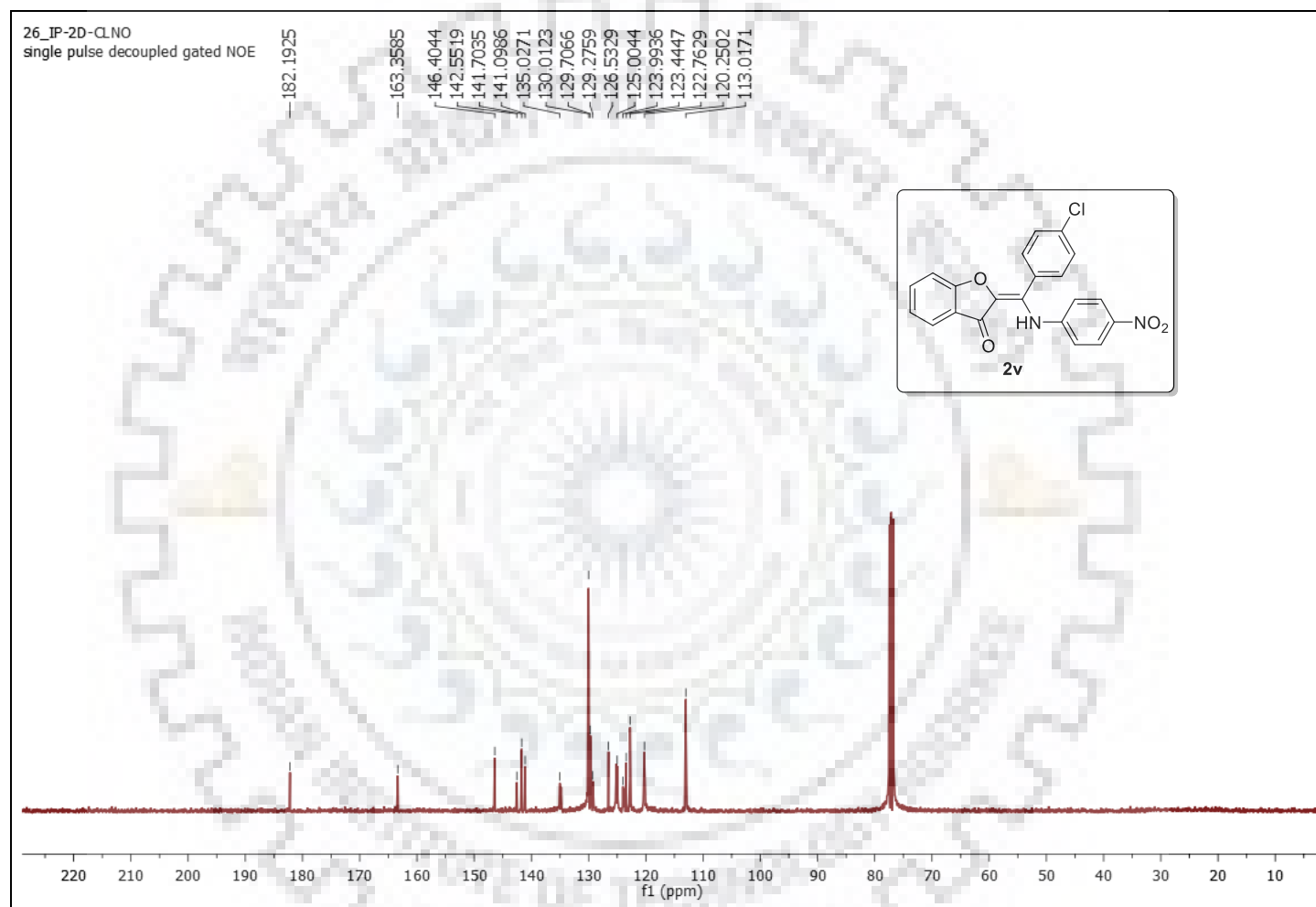


Figure S-16: ^{13}C Spectrum of **2v**.

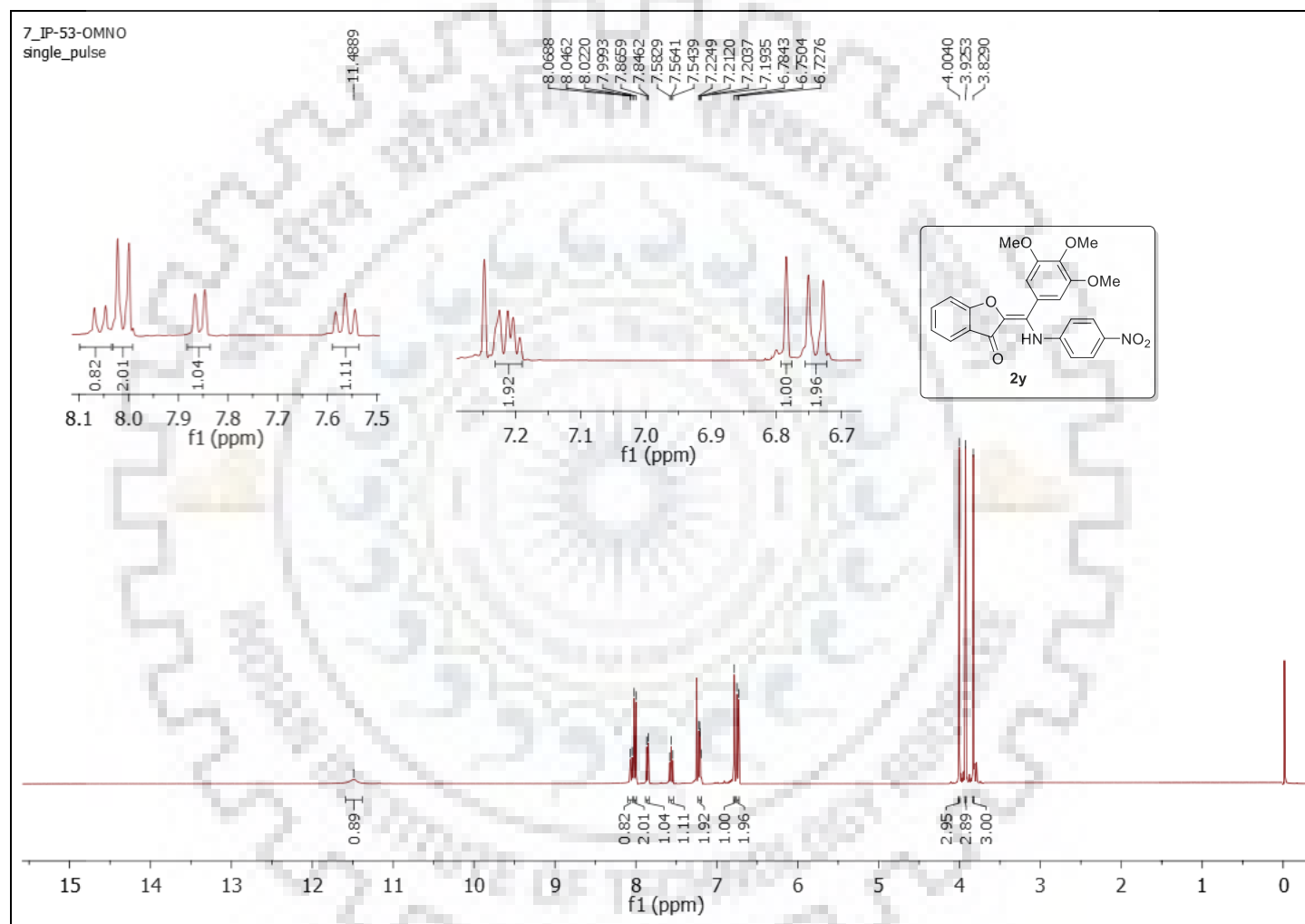


Figure S-17: ^1H NMR Spectrum of **2y**.

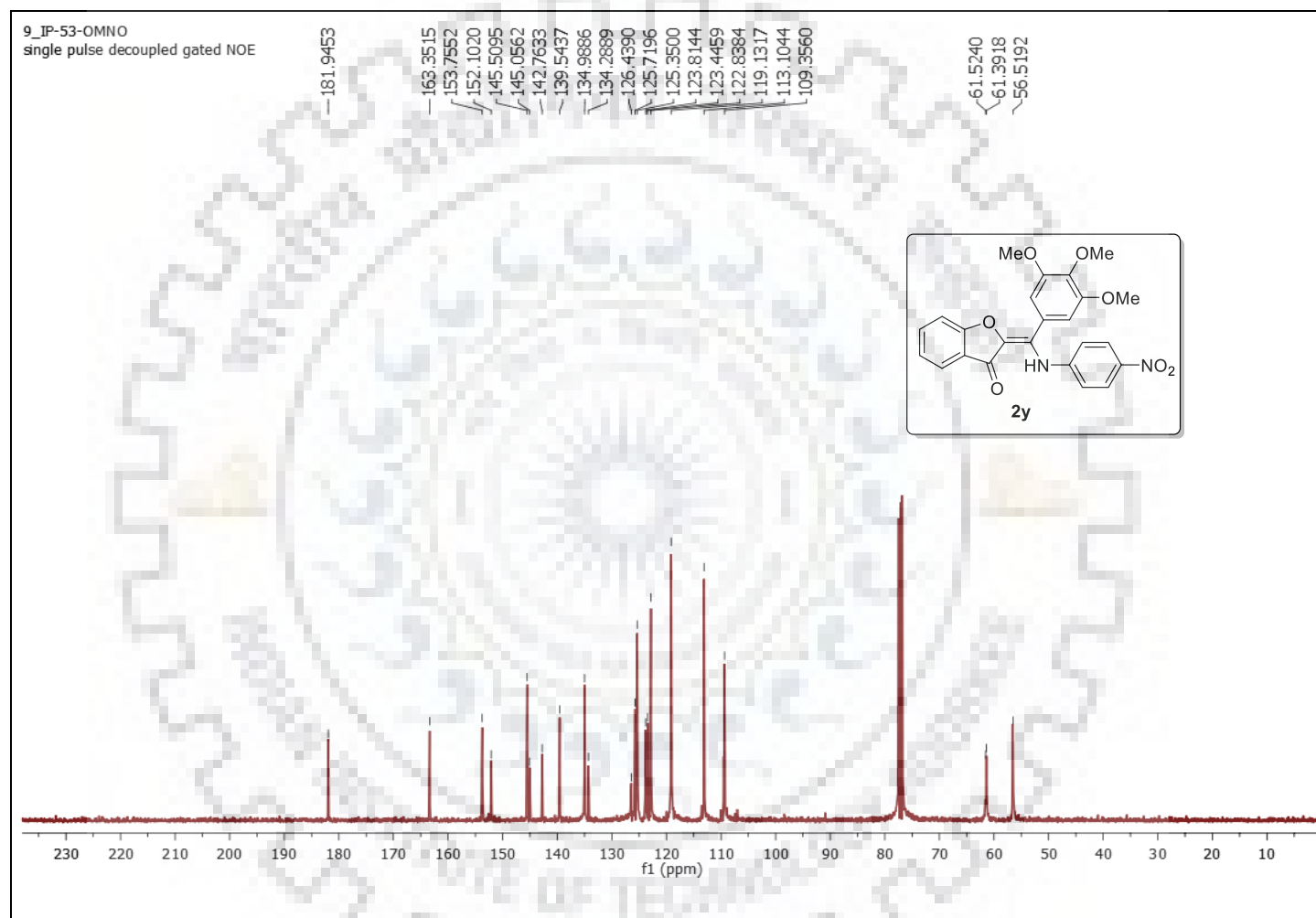


Figure S-18: ^{13}C Spectrum of **2y**.

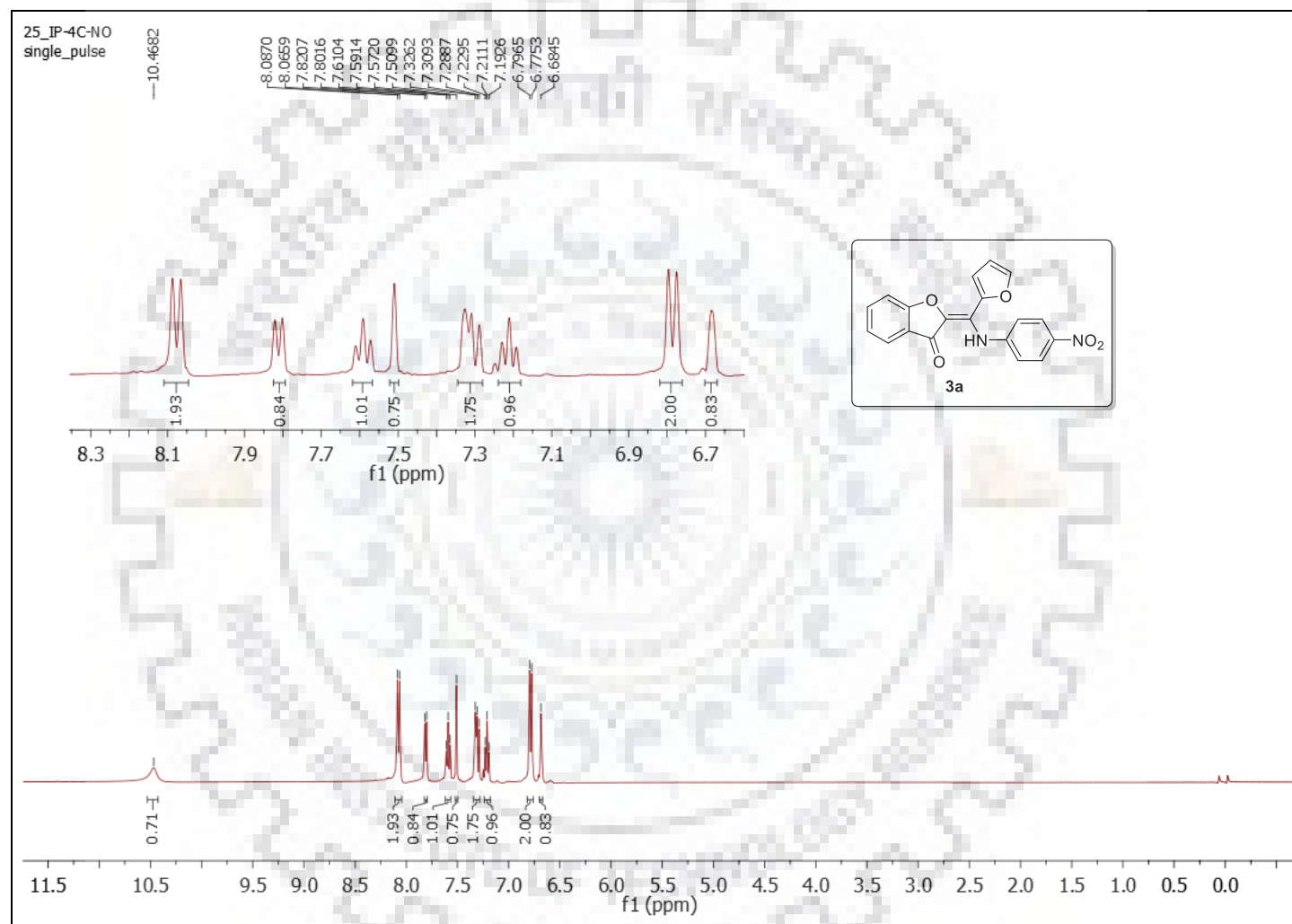


Figure S-19: ^1H NMR Spectrum of **3a**.

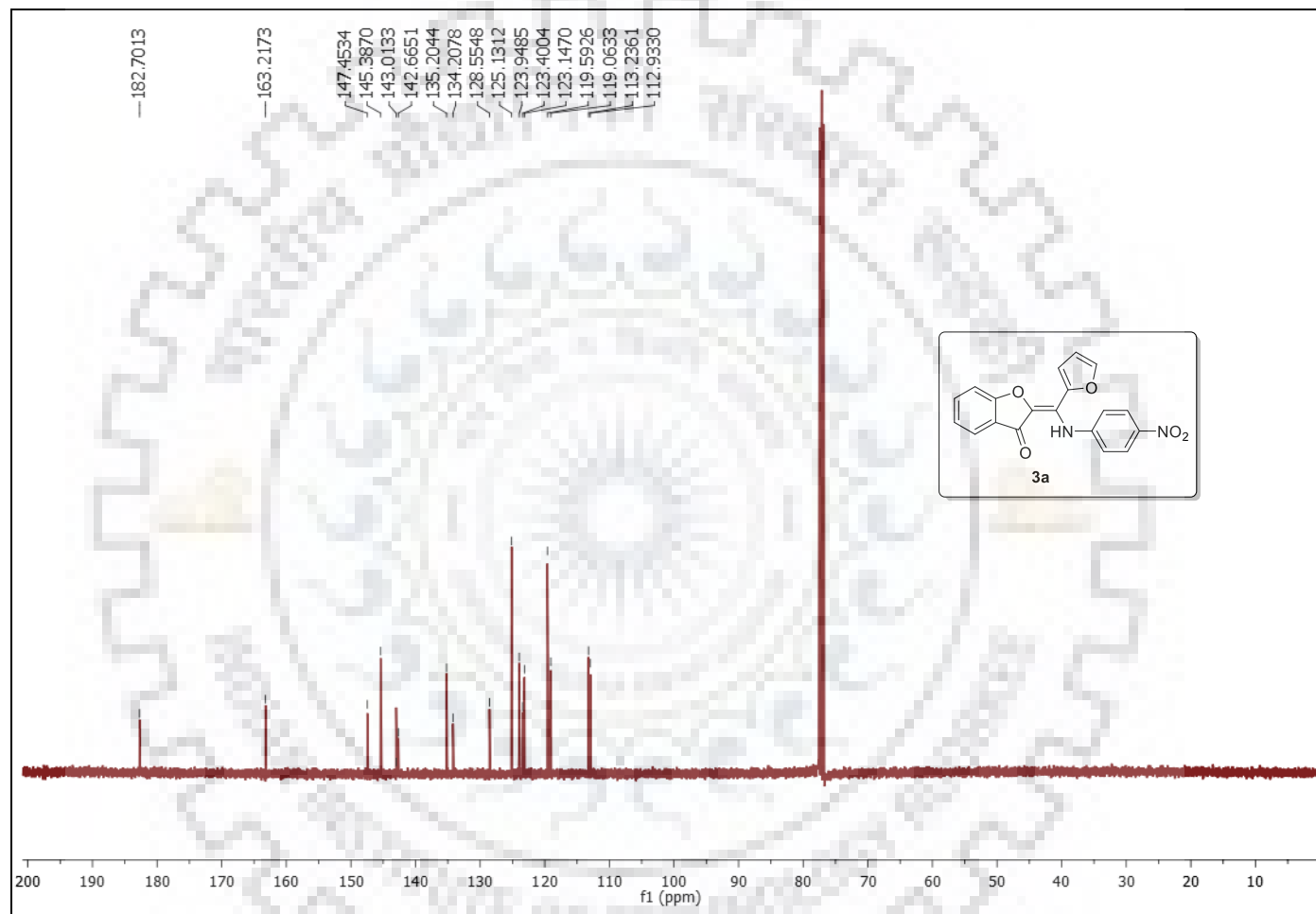


Figure S-20: ^{13}C Spectrum **3a**.

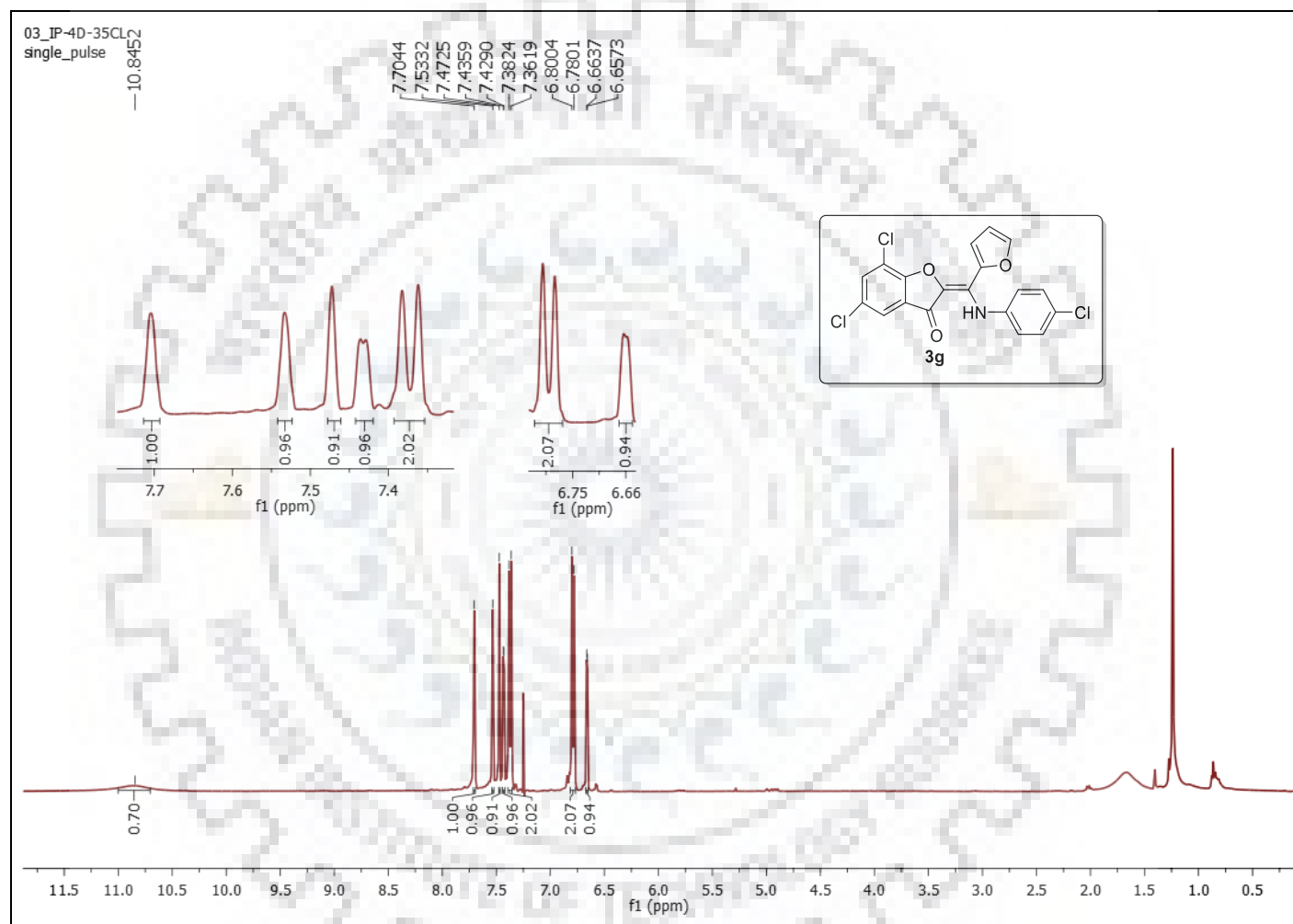


Figure S-21: ^1H NMR Spectrum of **3g**.

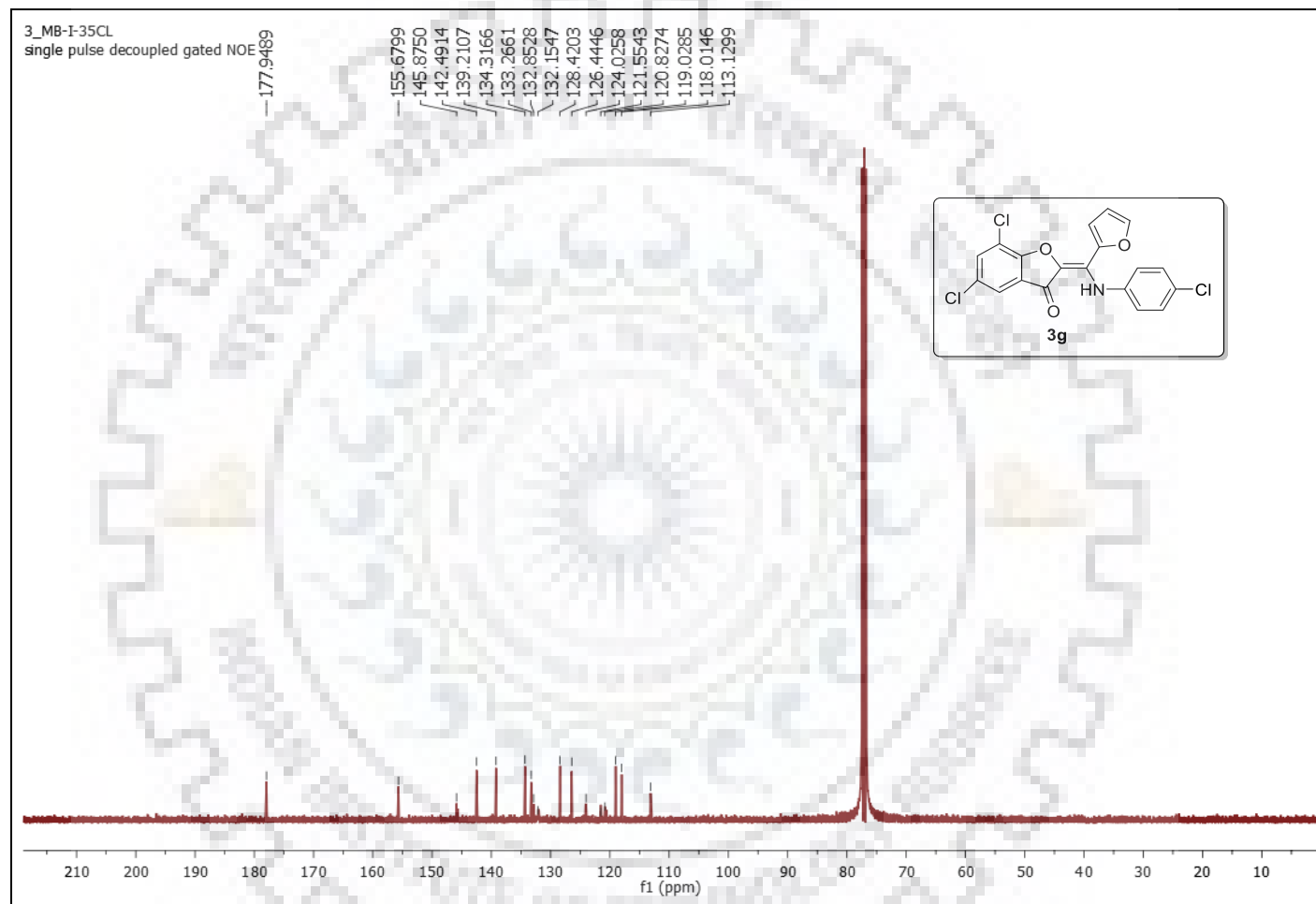


Figure S-22: ^{13}C Spectrum of **3g**.

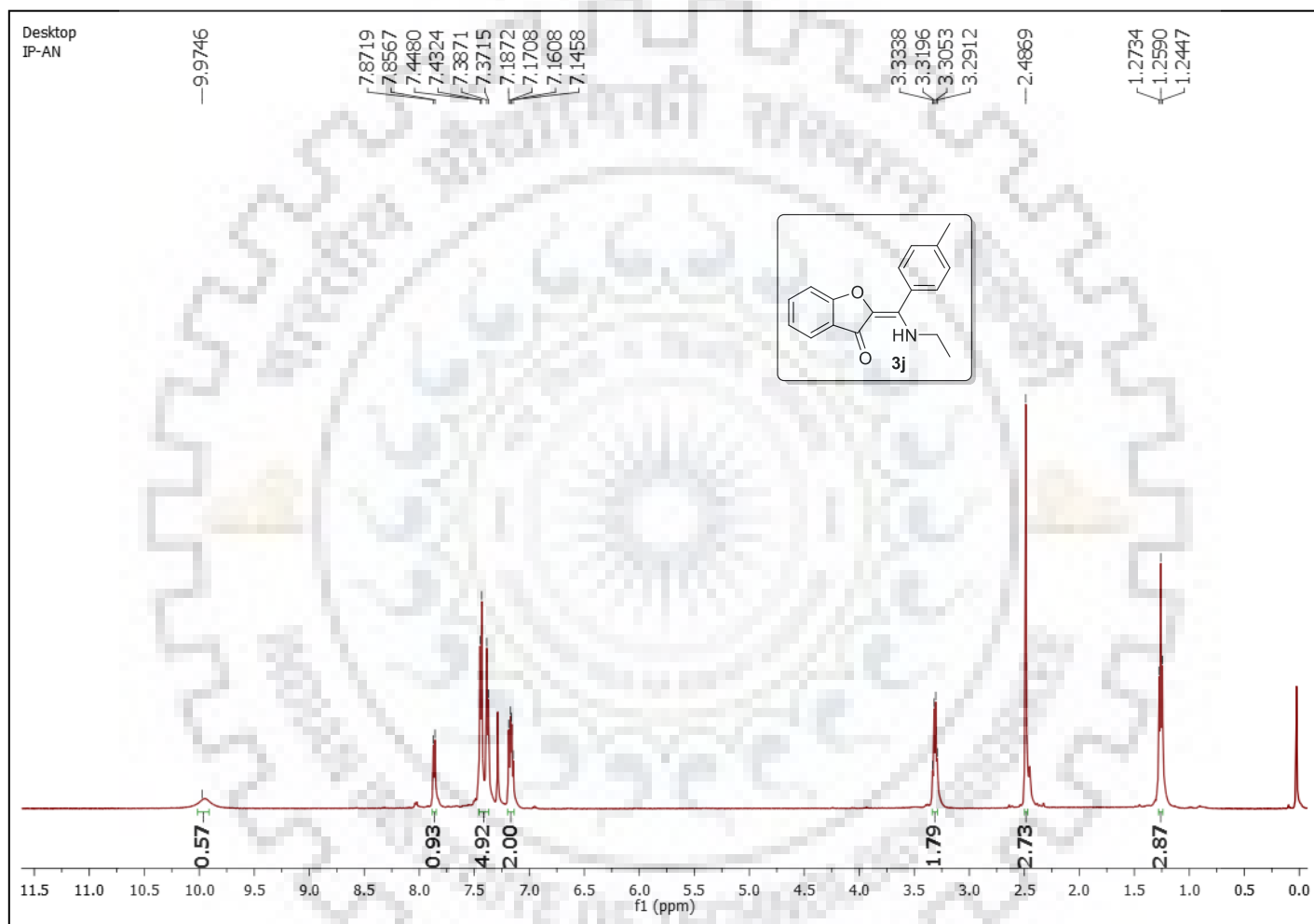


Figure S-23: ^1H NMR Spectrum of **3j**.

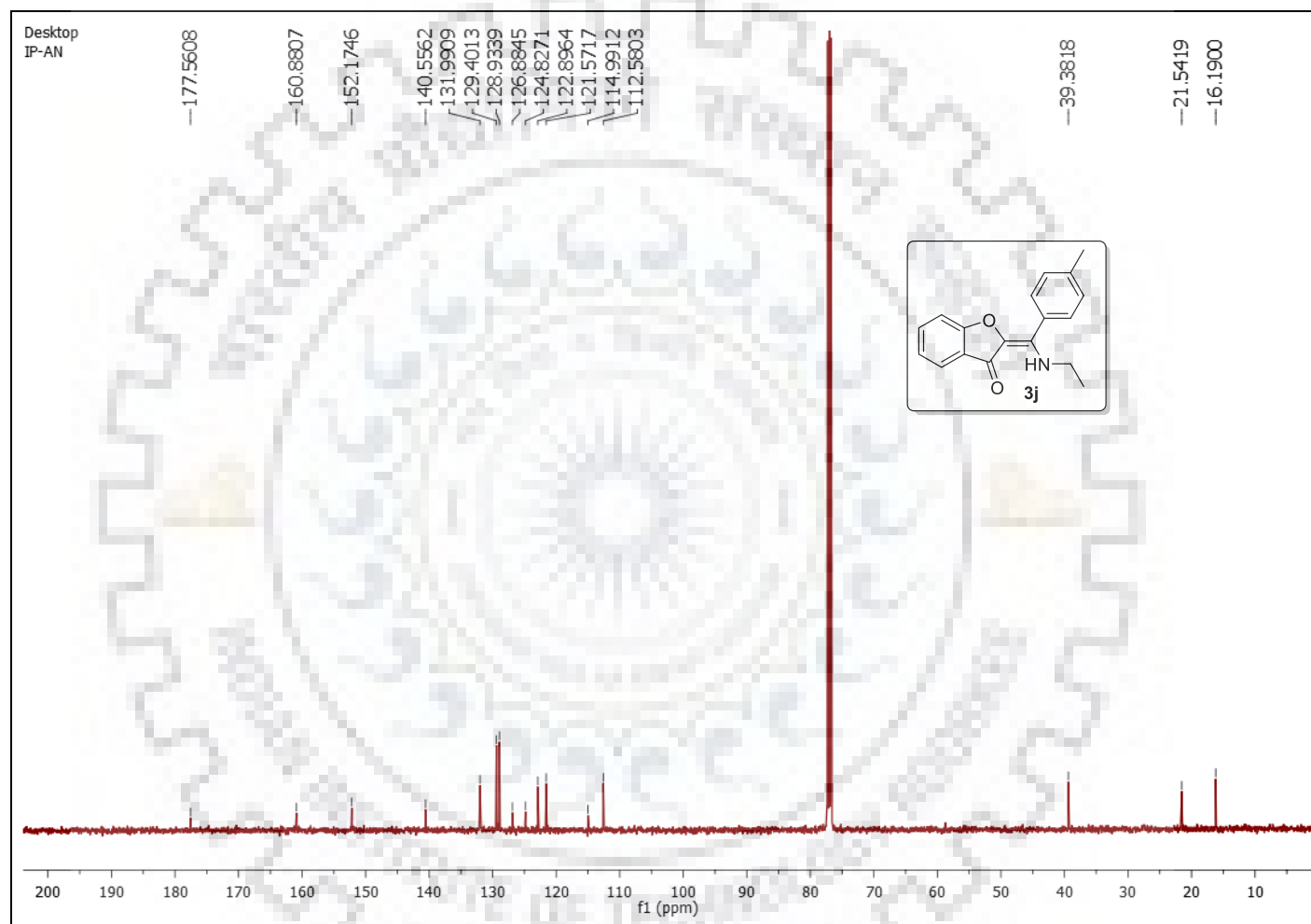


Figure S-24: ^{13}C Spectrum of **3j**.

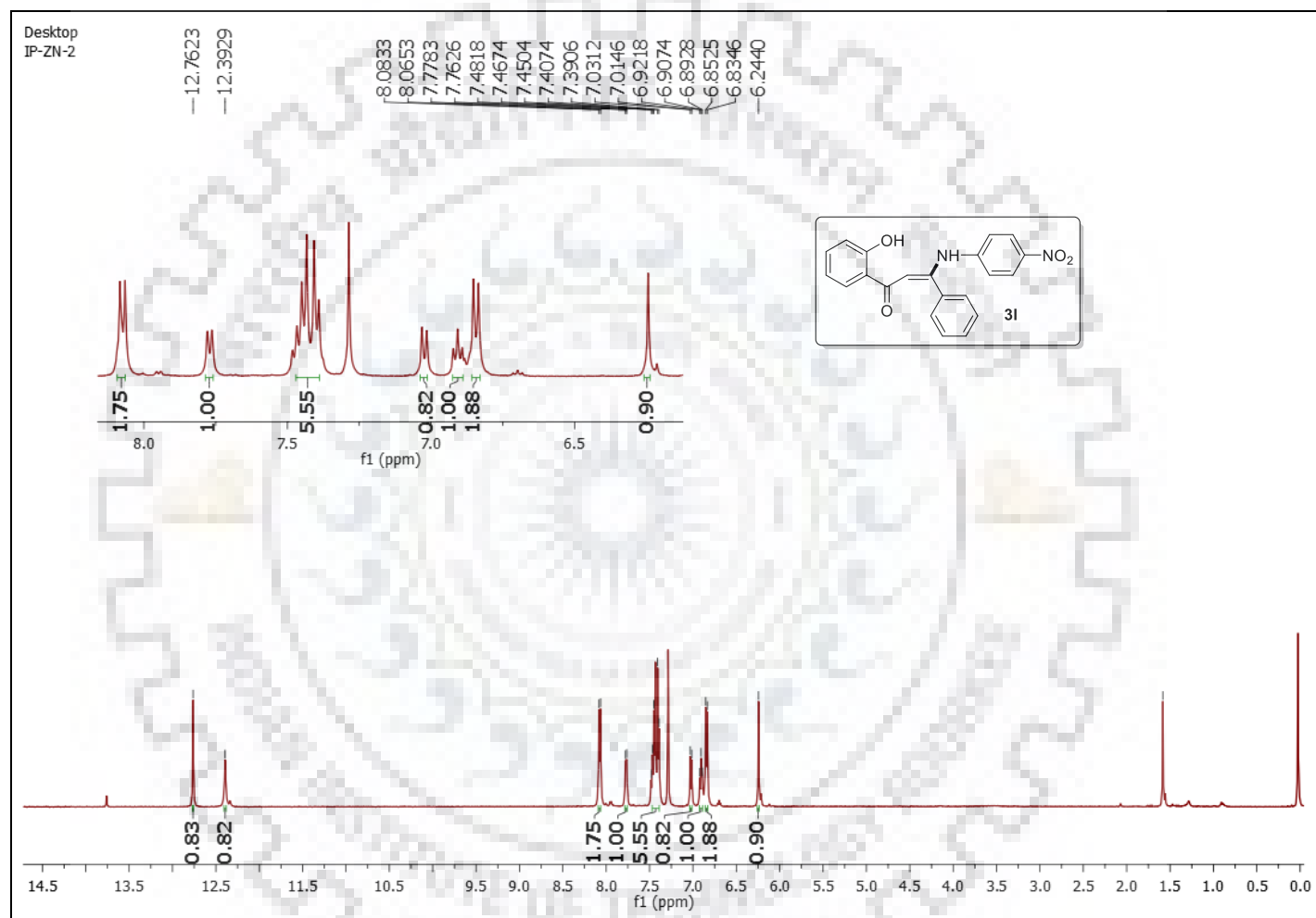


Figure S-25: ^1H NMR Spectrum of **31**.

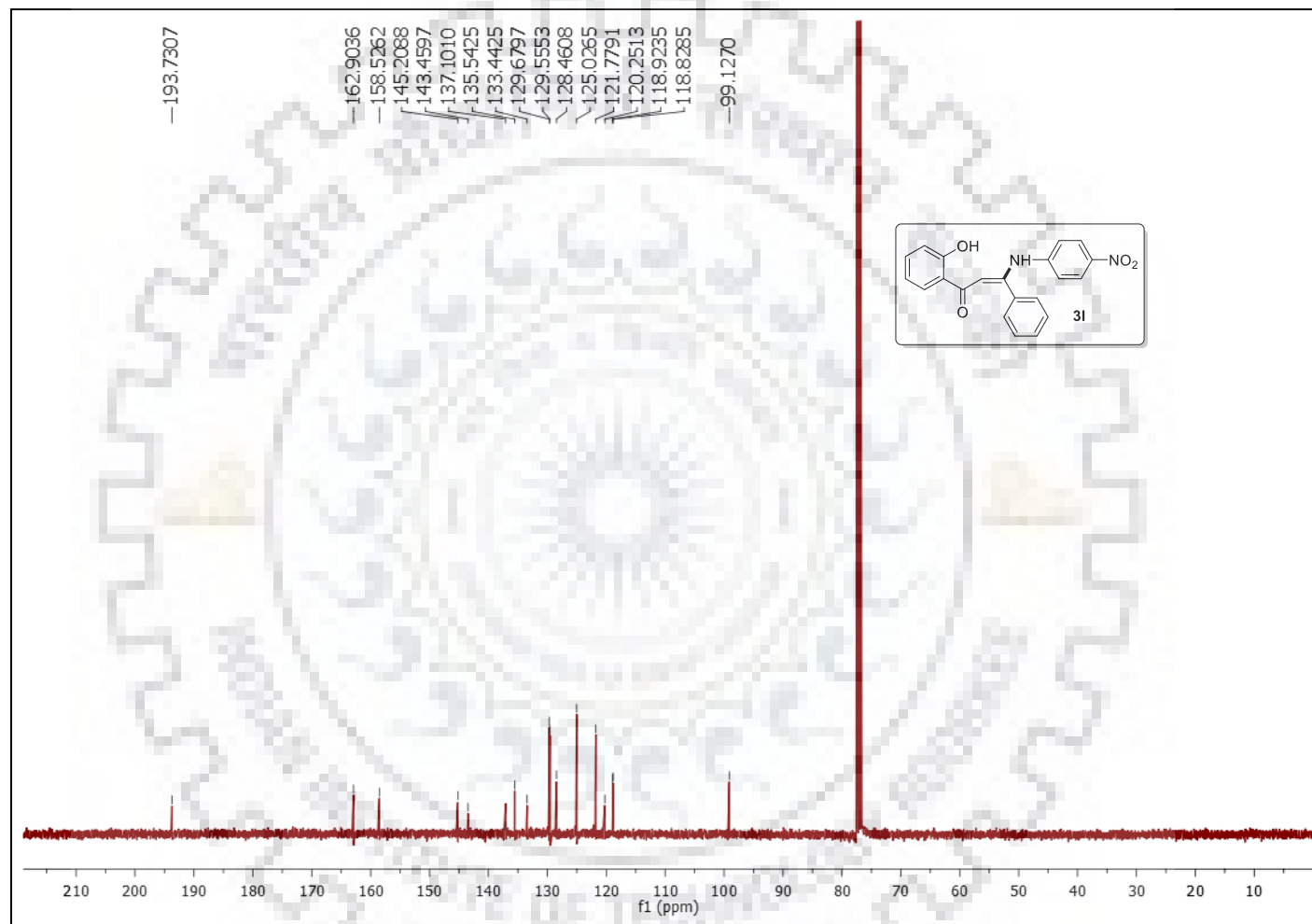


Figure S-26: ^{13}C Spectrum of **31**.

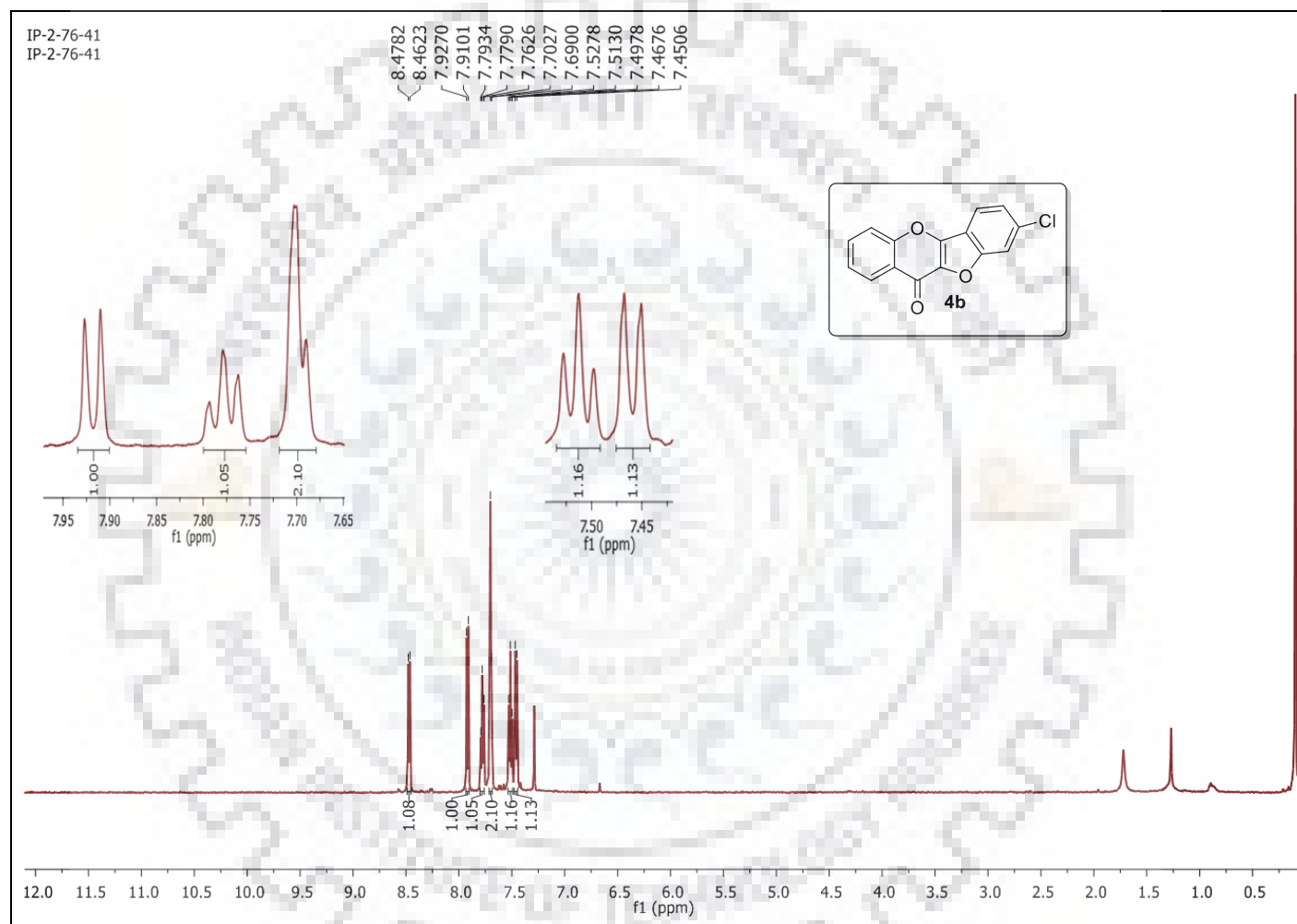


Figure S-27: ^1H NMR Spectrum of **4b**.

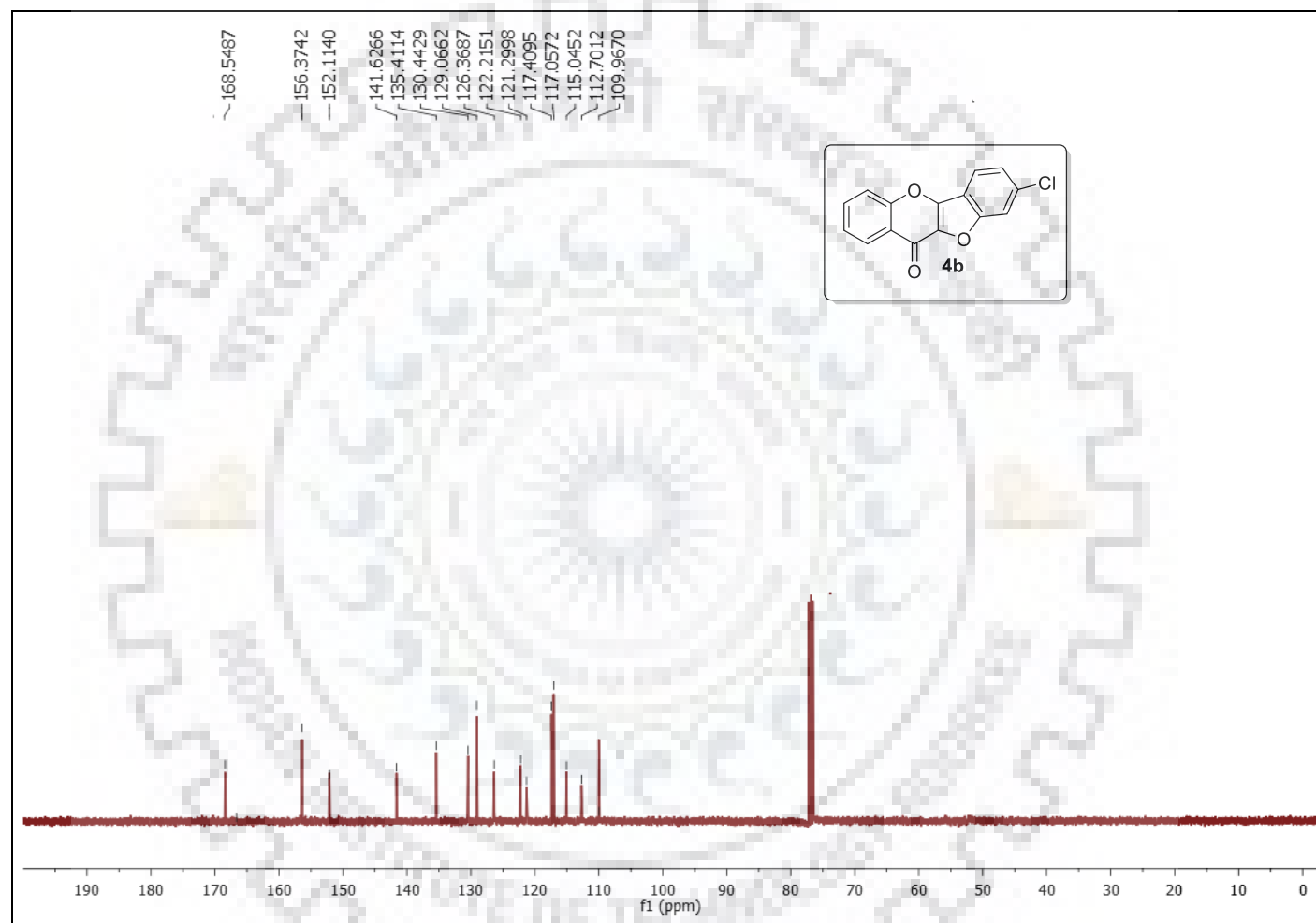


Figure S-28: ^{13}C Spectrum of **4b**.

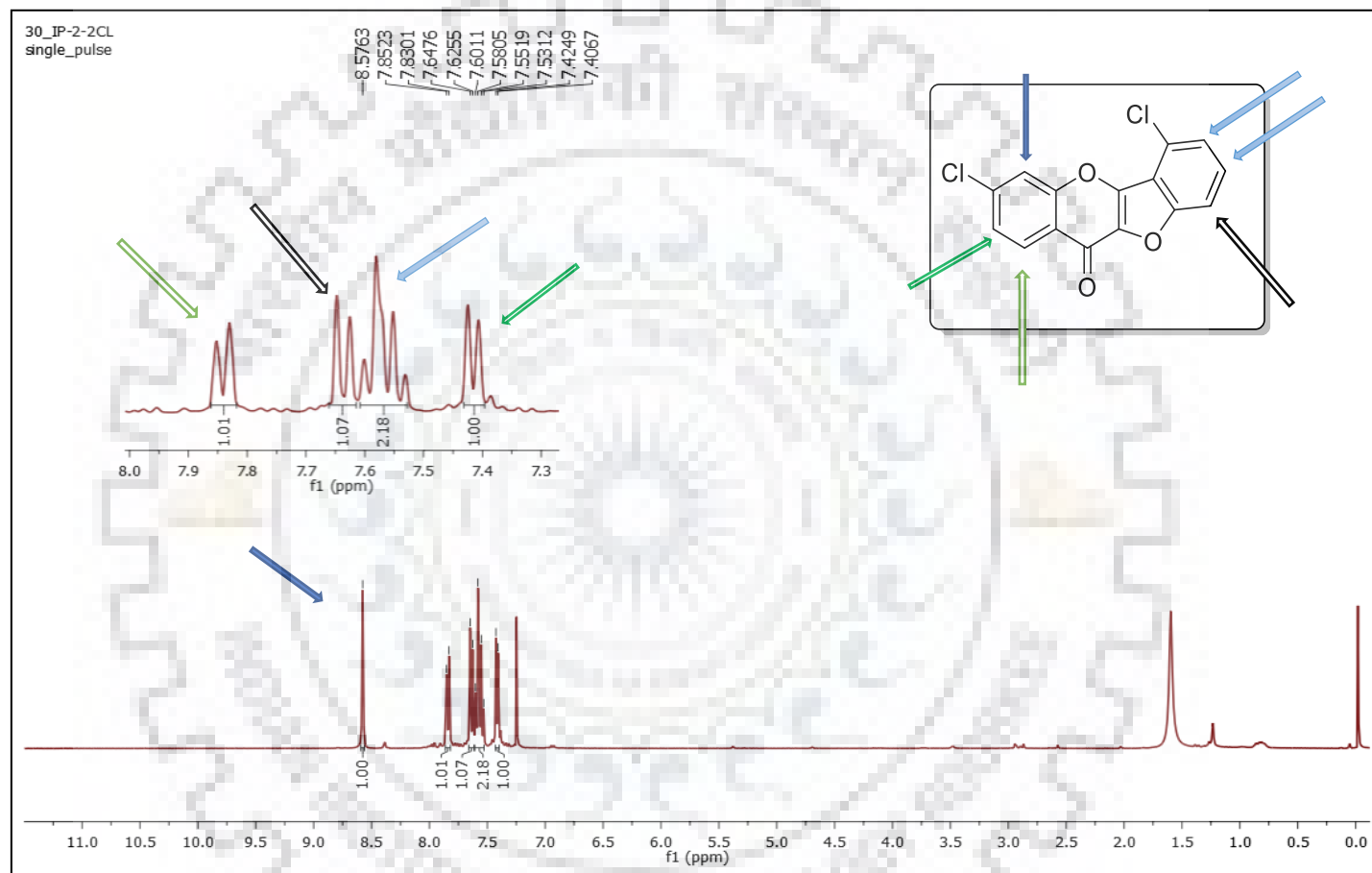


Figure S-29: ^1H NMR Spectrum of **4e**.

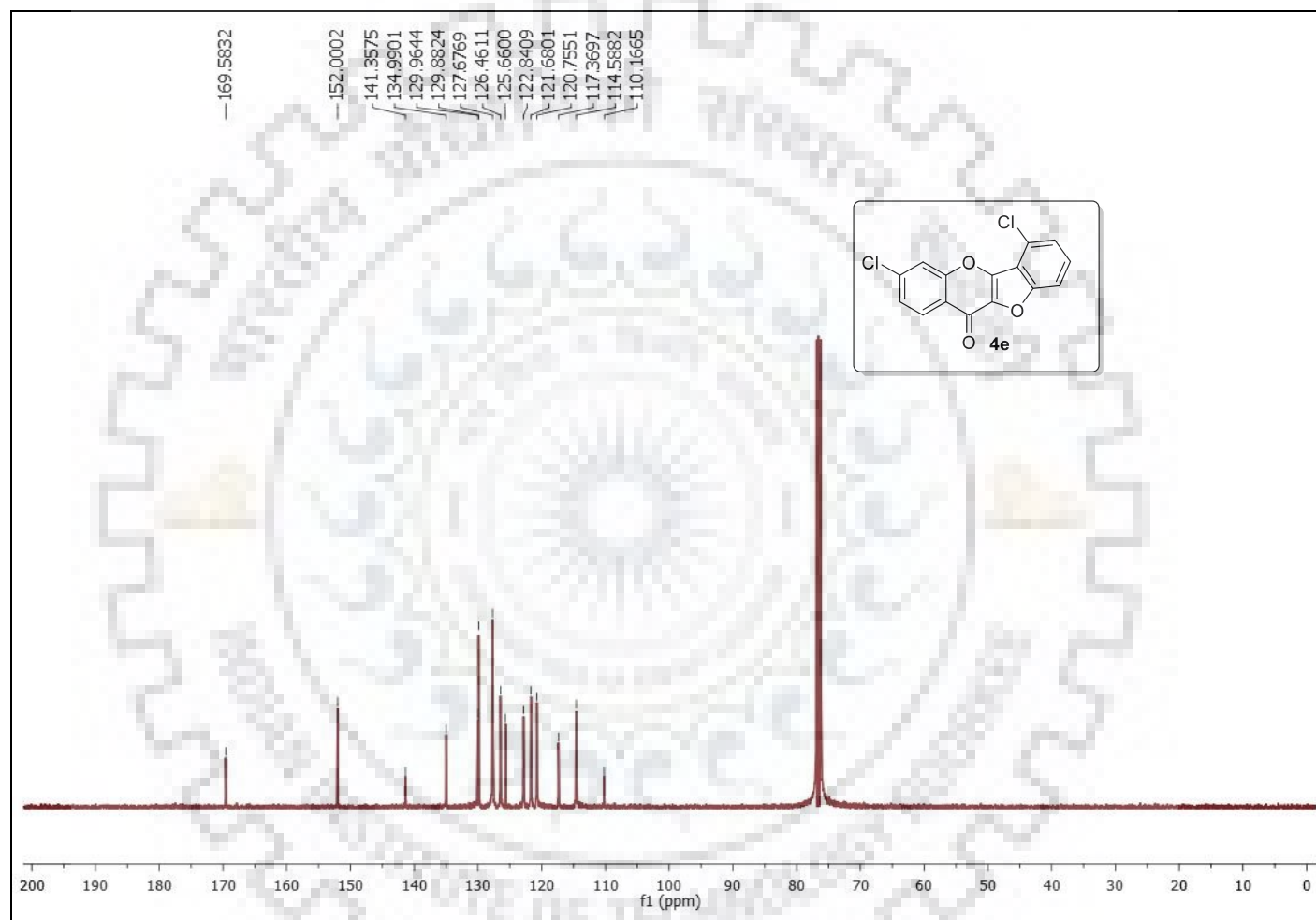


Figure S-30: ^{13}C Spectrum of **4e**.

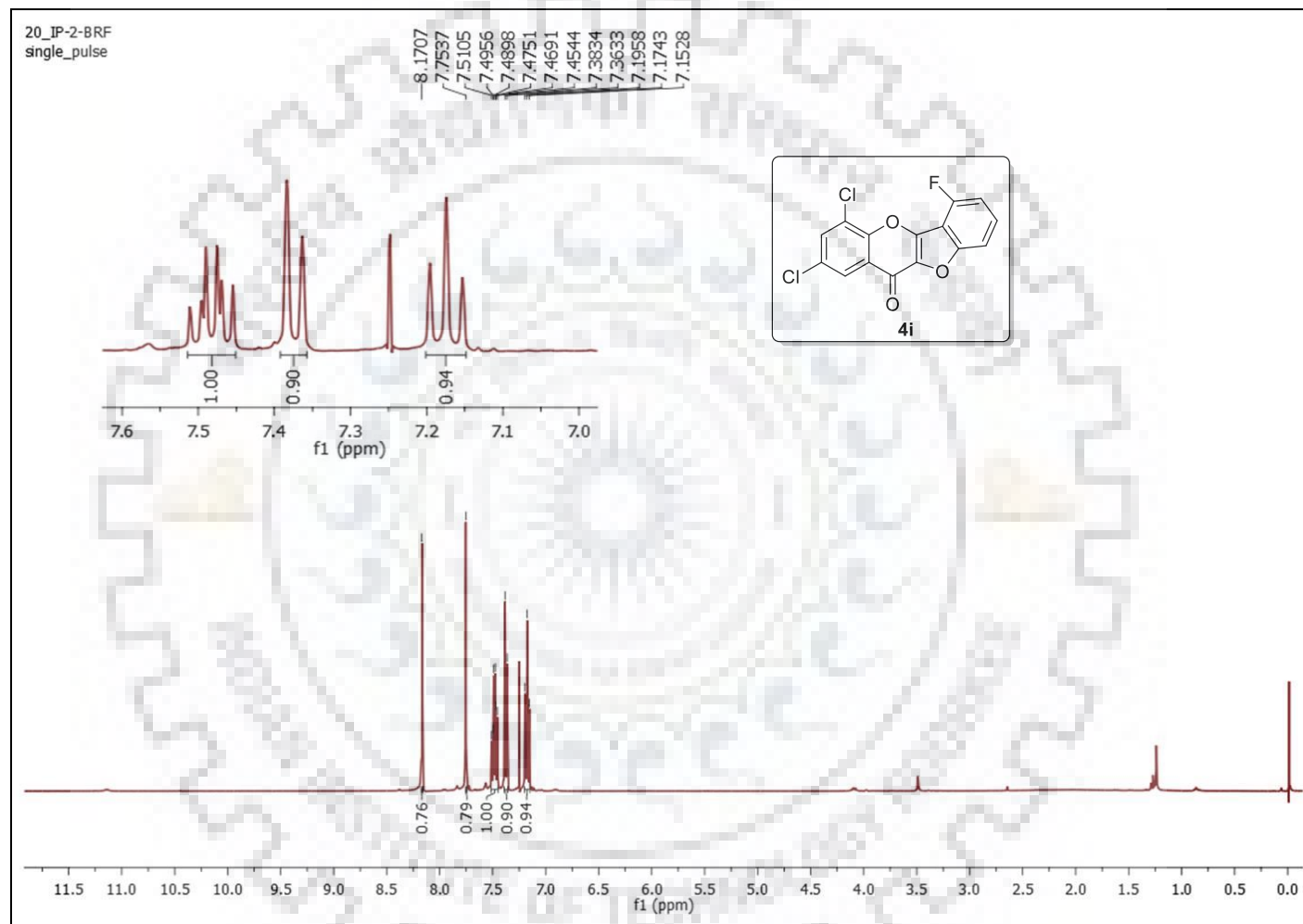


Figure S-31: ^1H spectrum of 4i.

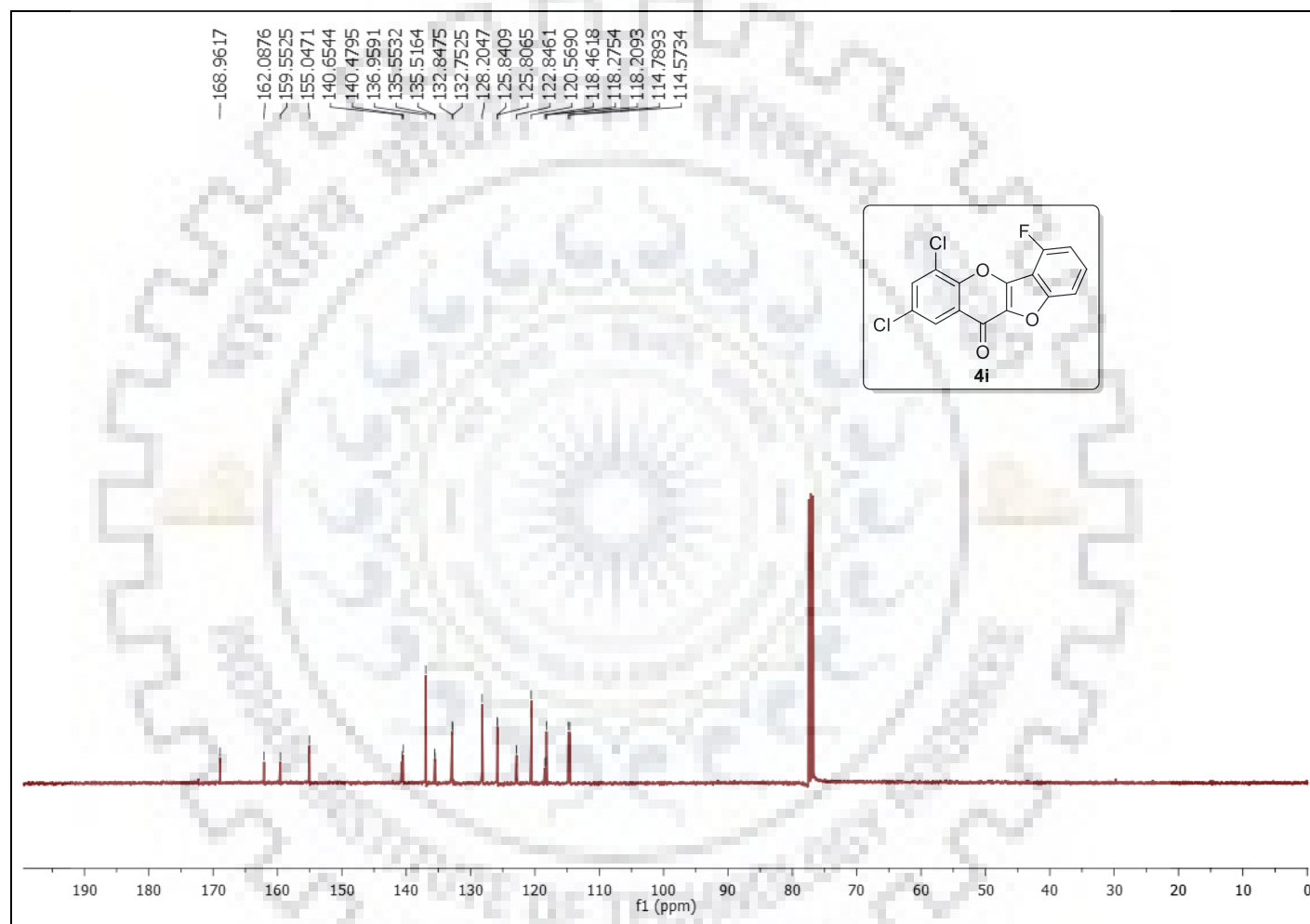


Figure S-32: ^{13}C spectrum of **4i**.

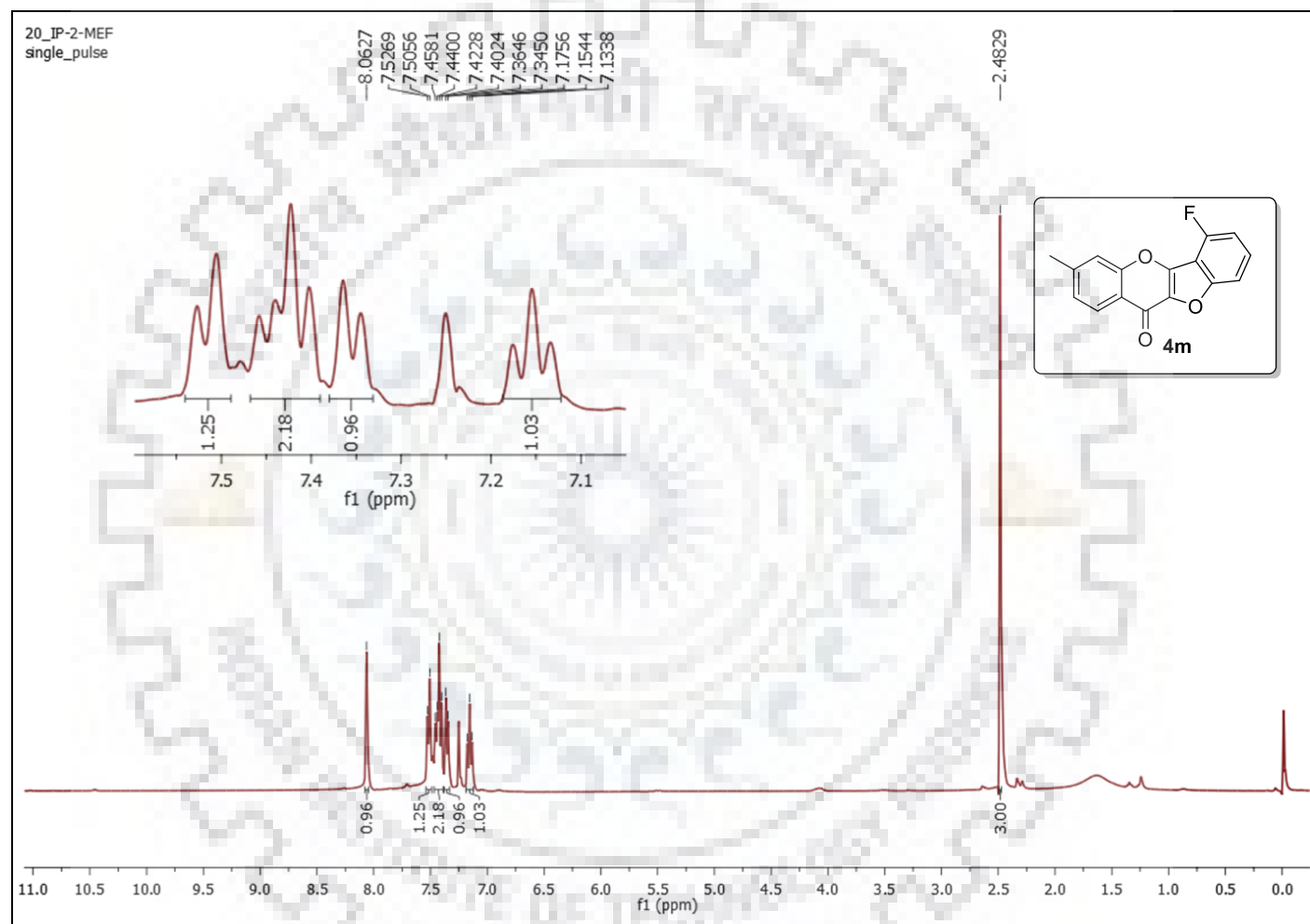


Figure S-33: ^1H spectrum of **4m**.

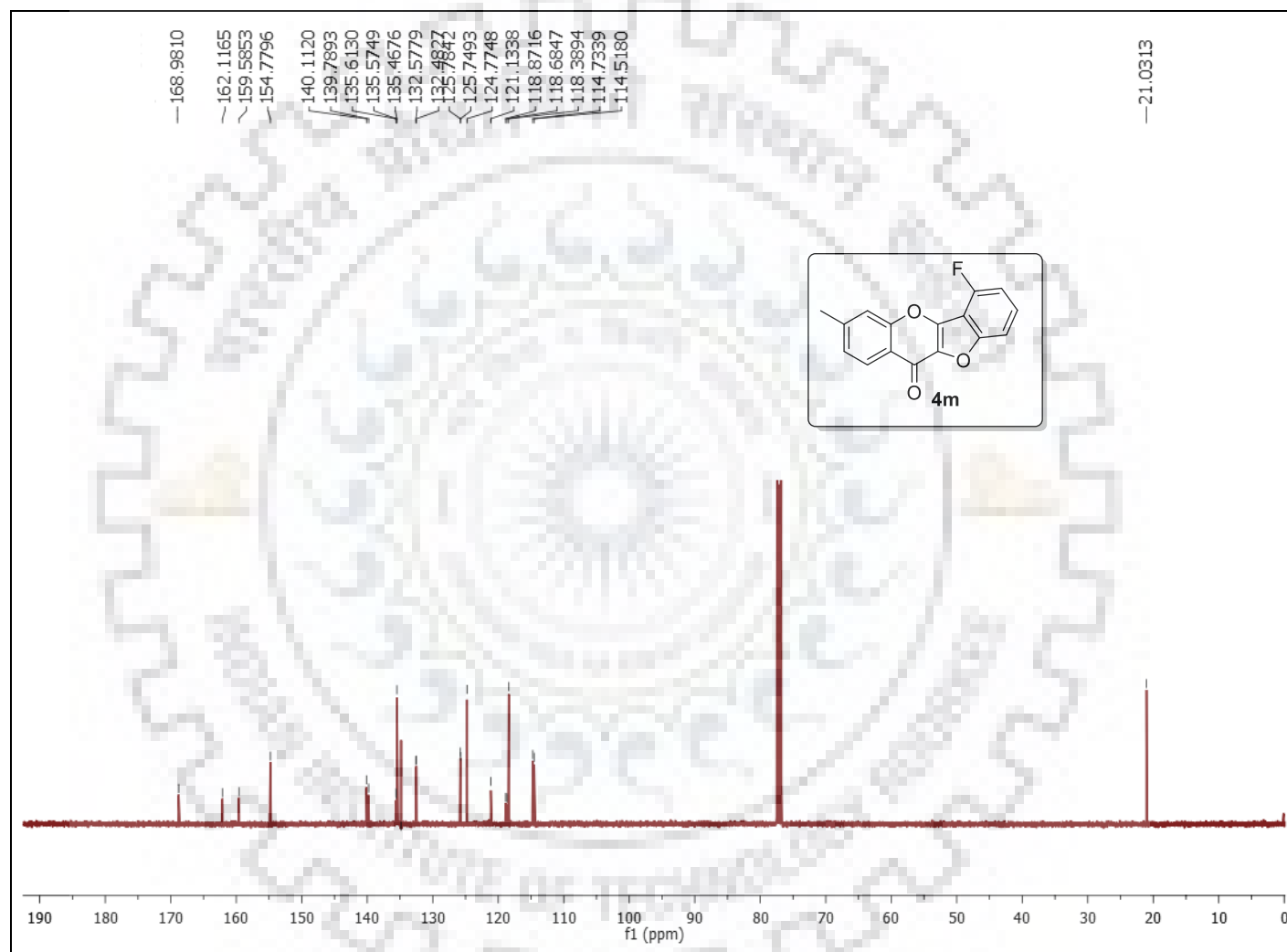


Figure S-34: ^{13}C spectrum of **4m**.

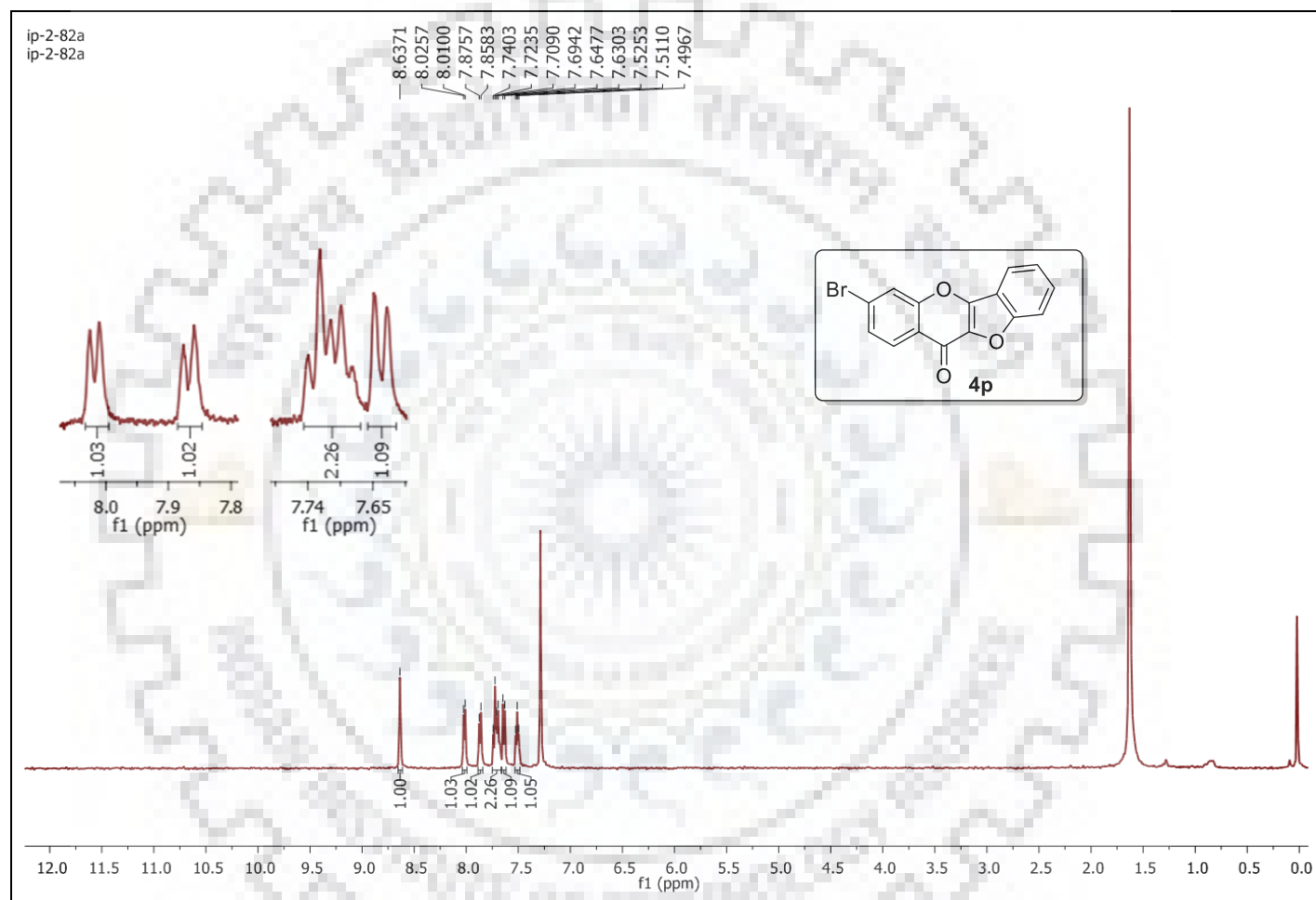


Figure S-35: ^1H spectrum of **4p**.

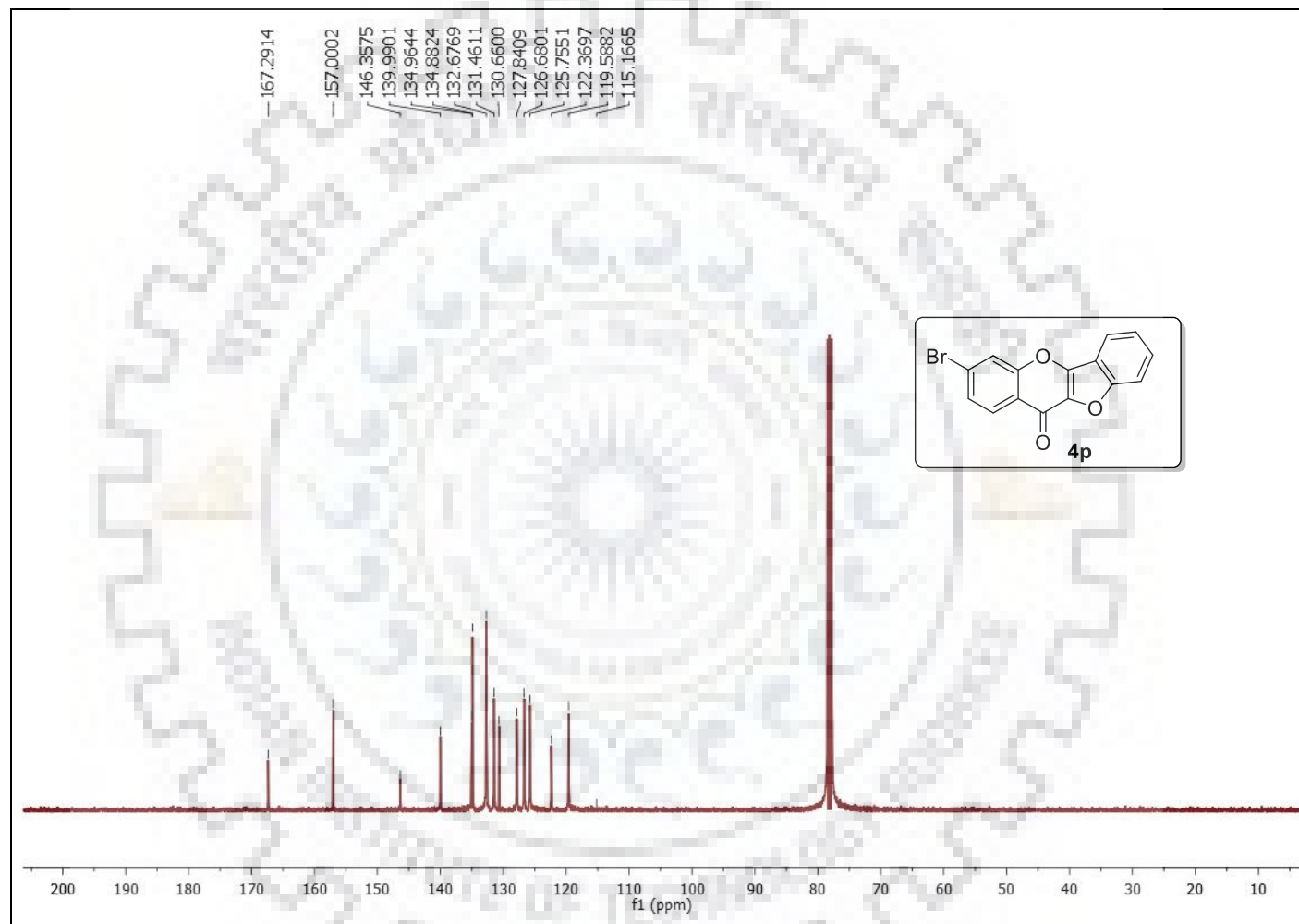


Figure S-36: ^{13}C spectrum of **4p**.

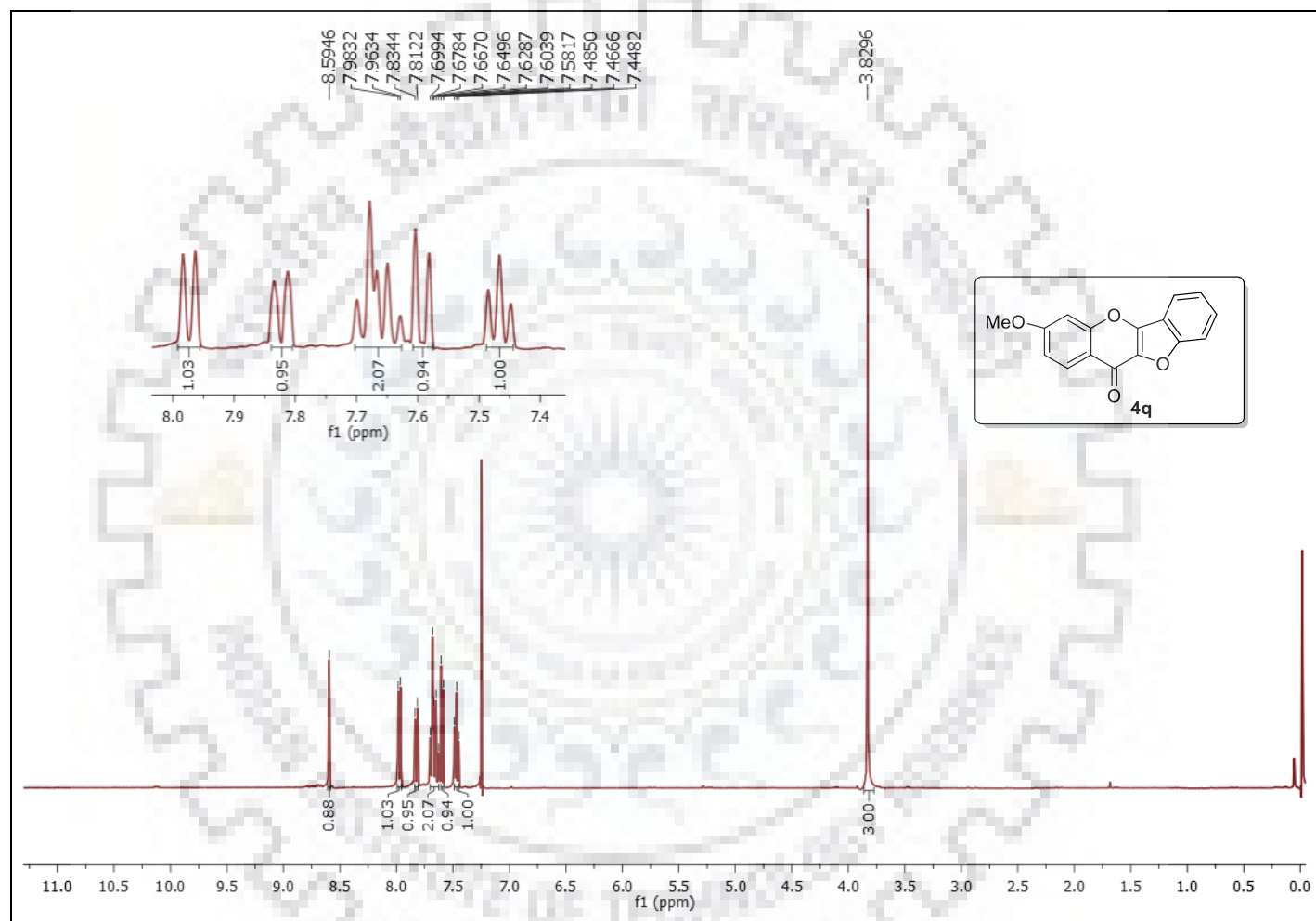


Figure S-37: ^1H spectrum of **4q**.

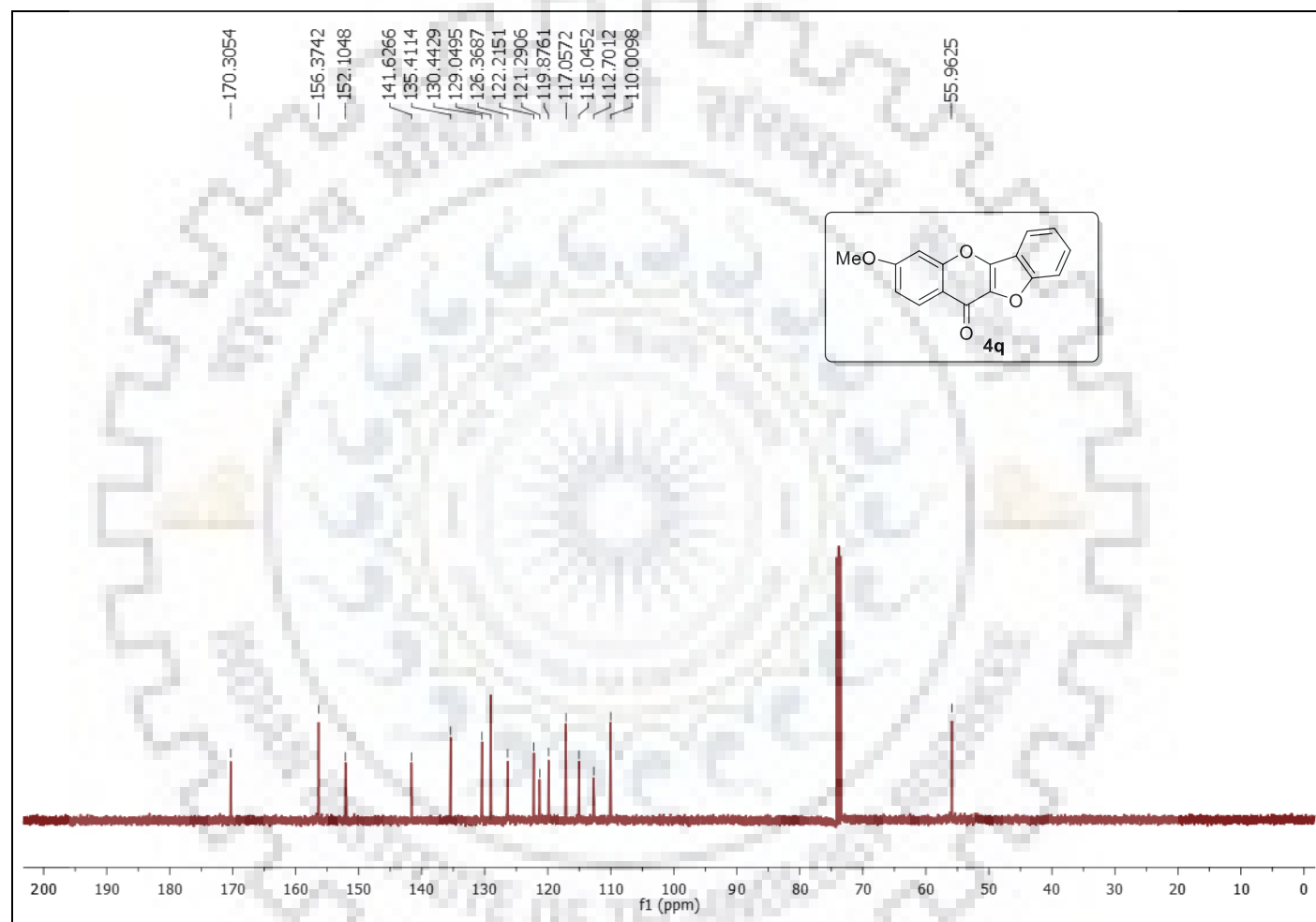


Figure S-38: ^{13}C spectrum of **4q**.

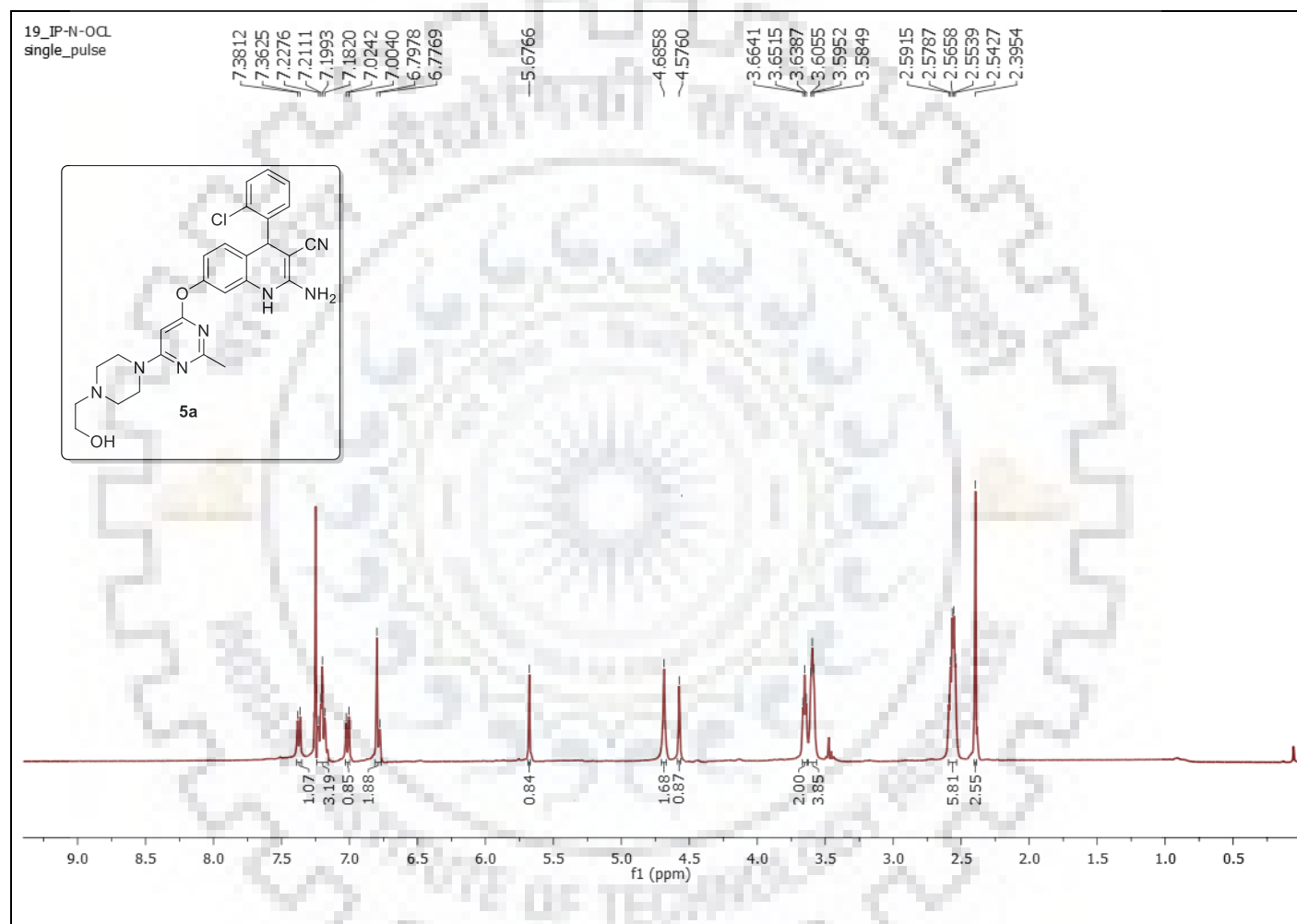


Figure S-39: ^1H NMR Spectrum of **5a**.

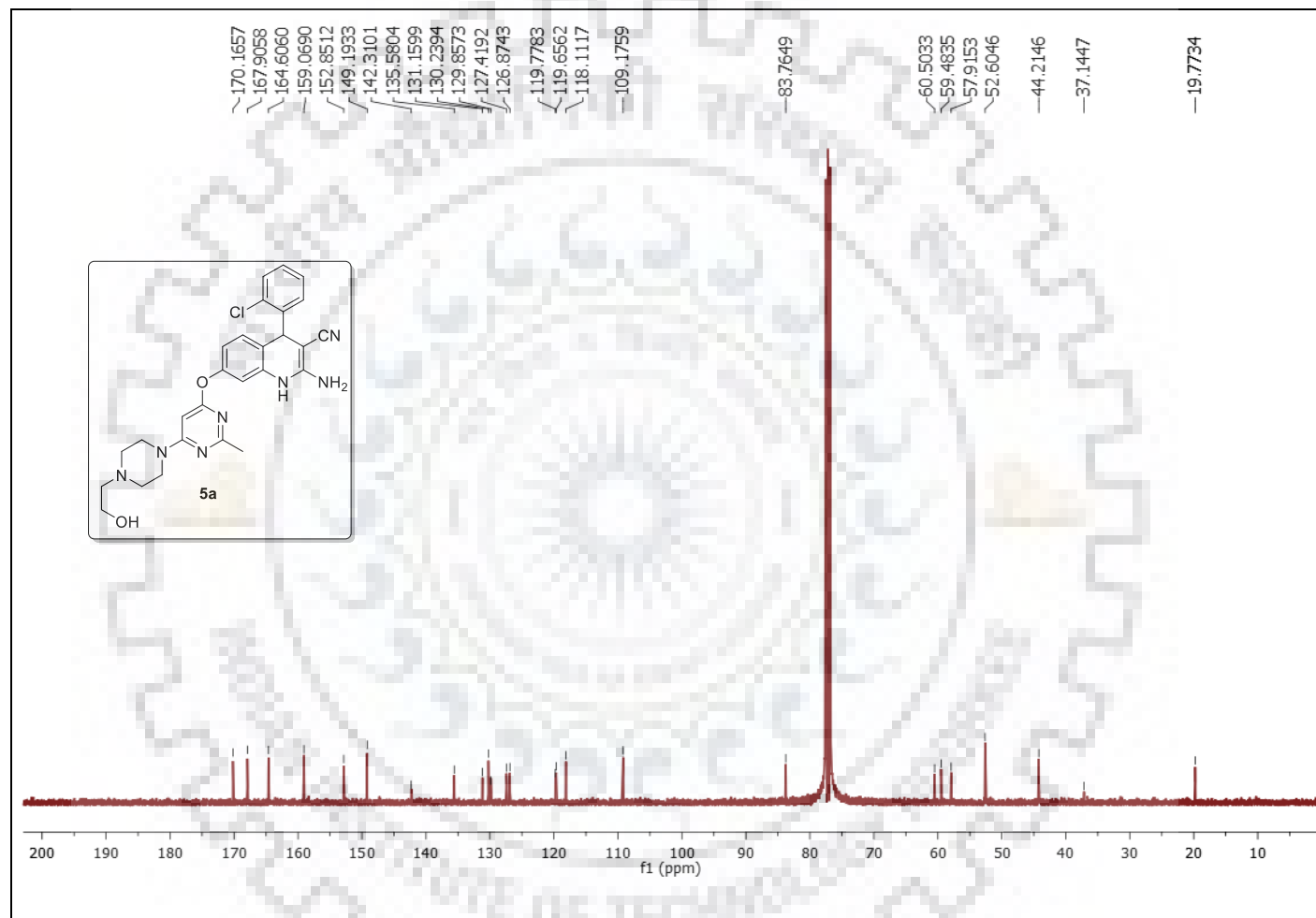


Figure S-40: ^{13}C Spectrum of **5a**.

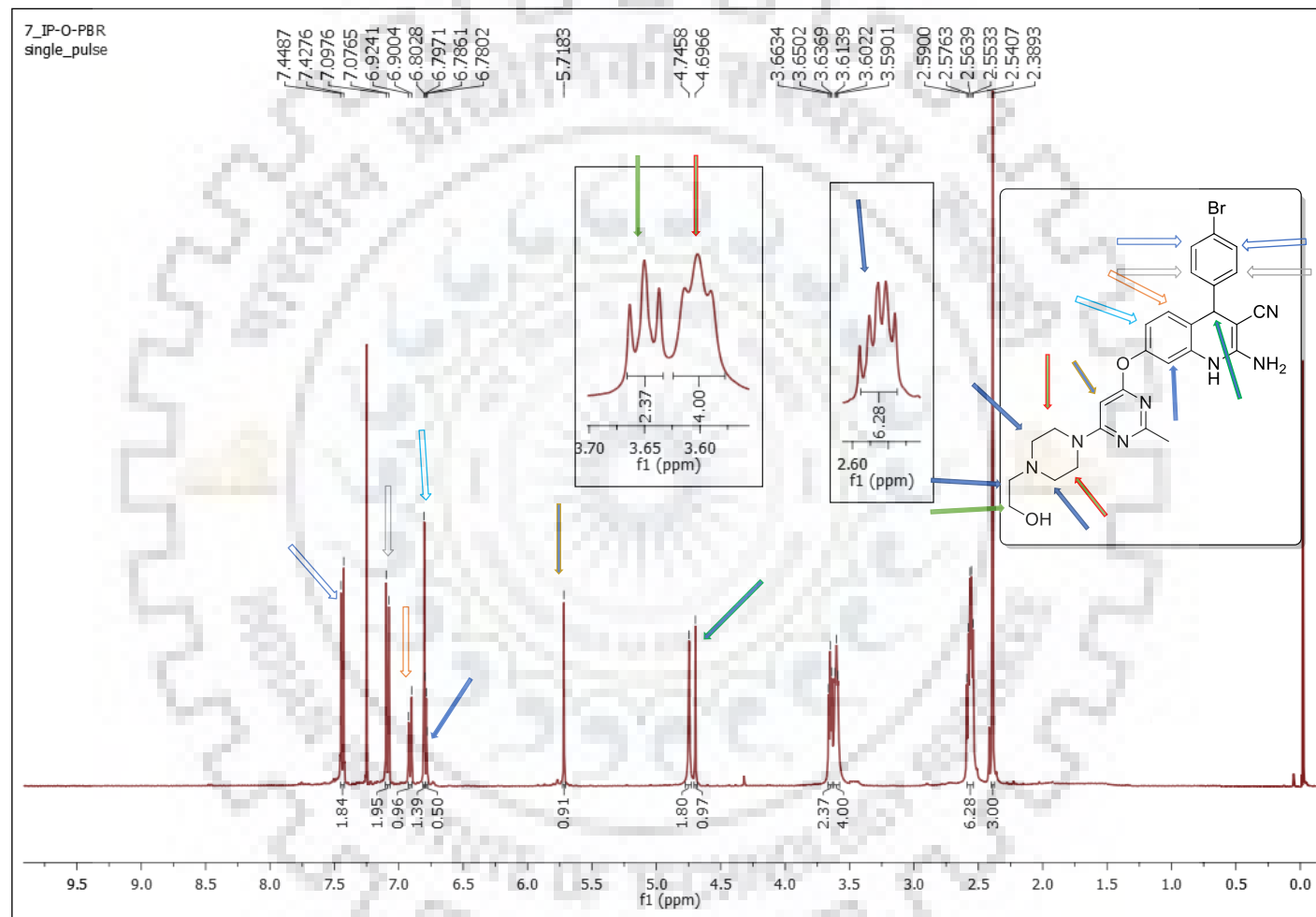


Figure S-41: ^1H NMR Spectrum of 5e.

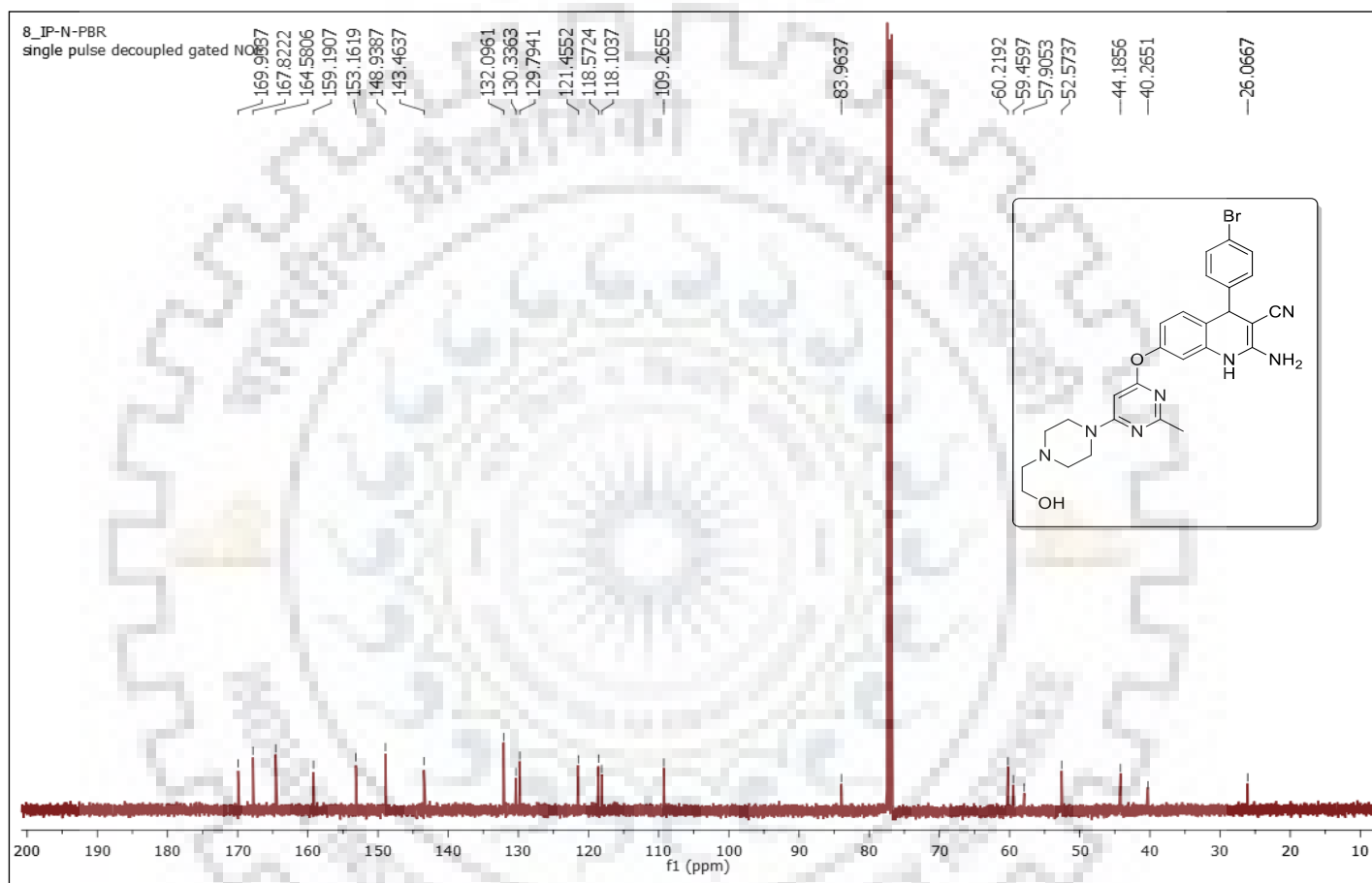


Figure S-42: ^1H NMR Spectrum of **5e**.

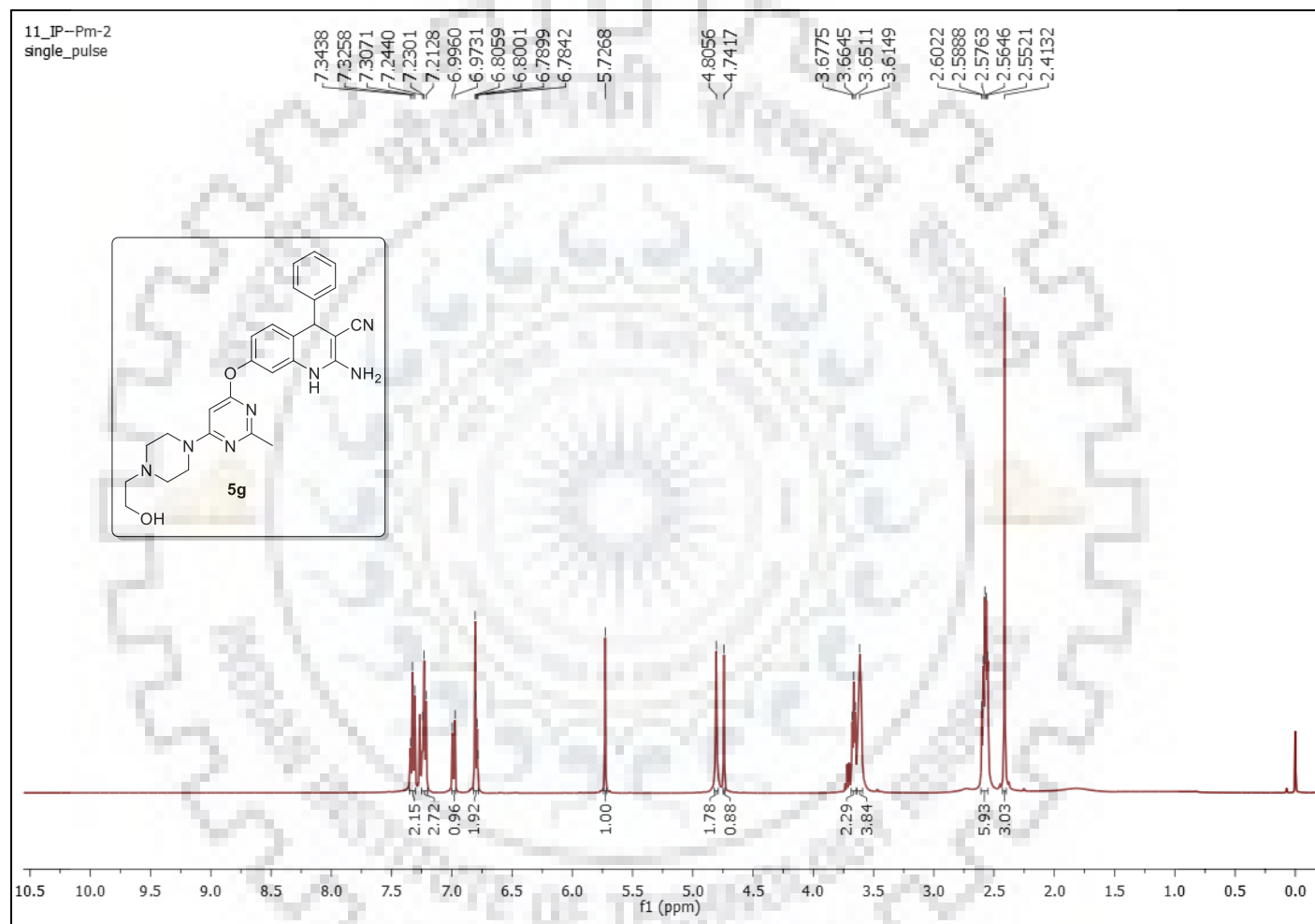


Figure S-43: ^1H NMR Spectrum of **5g**.

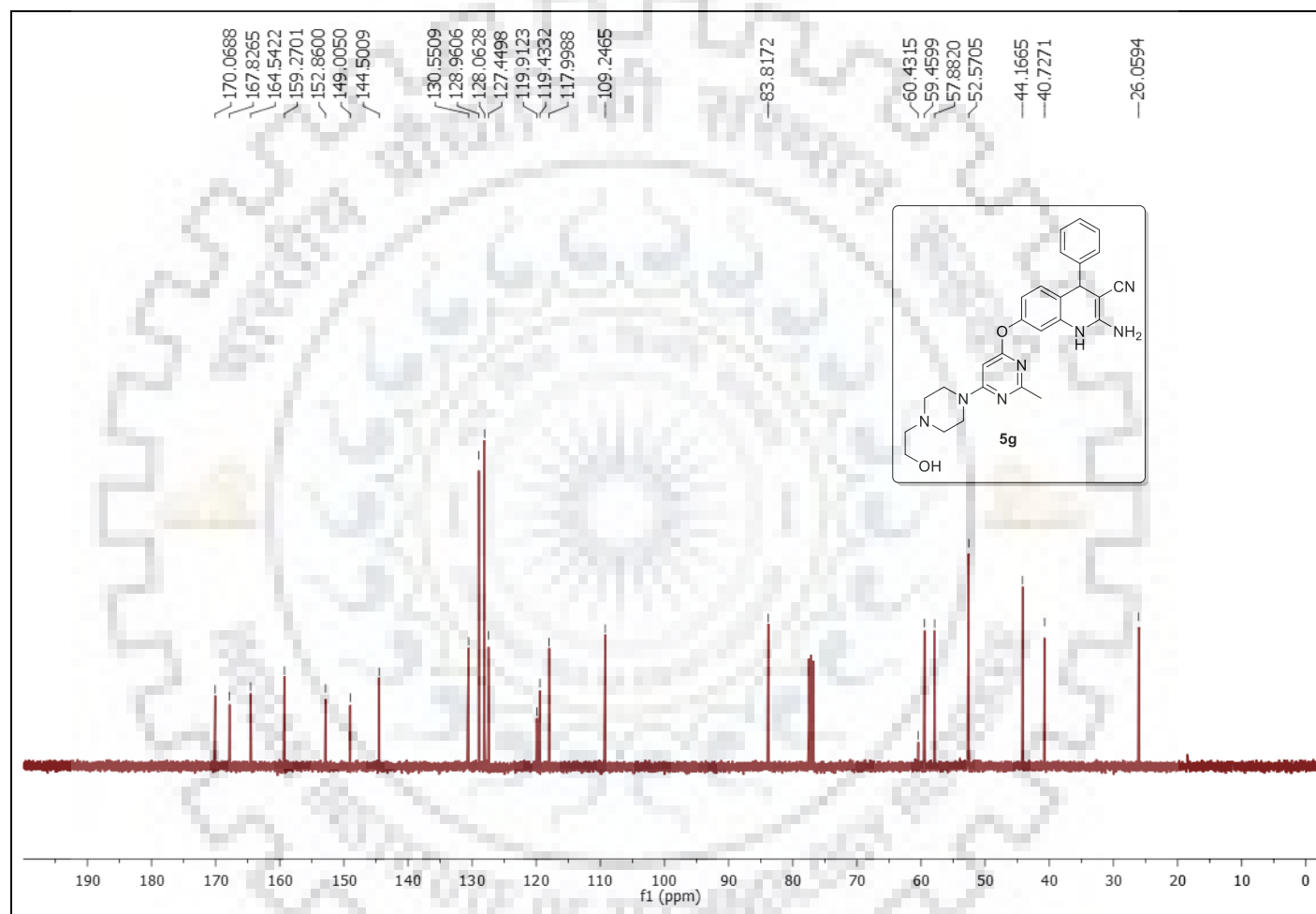


Figure S-44: ^{13}C Spectrum of **5g**.

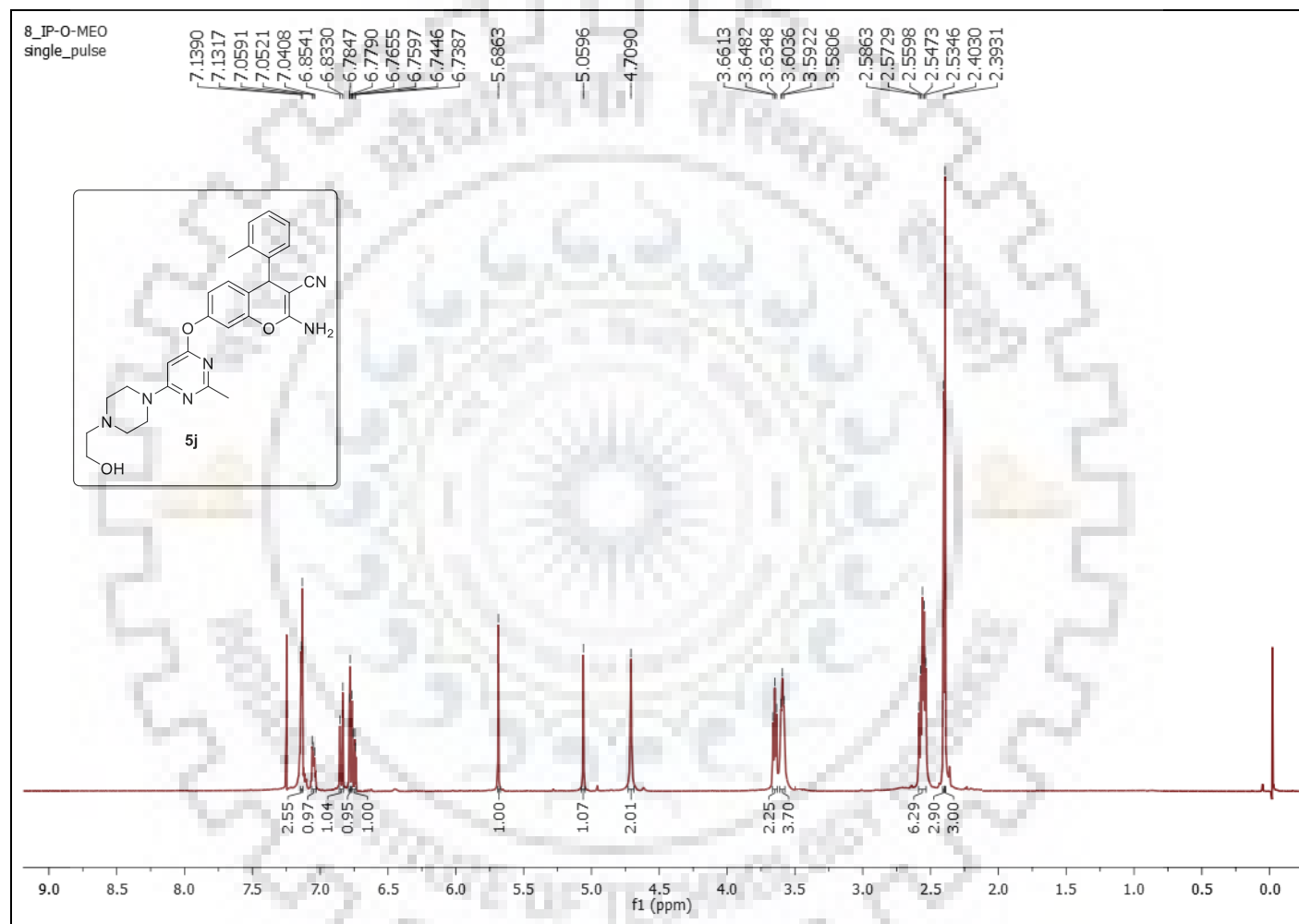


Figure S-45: ^1H NMR Spectrum of **5j**.

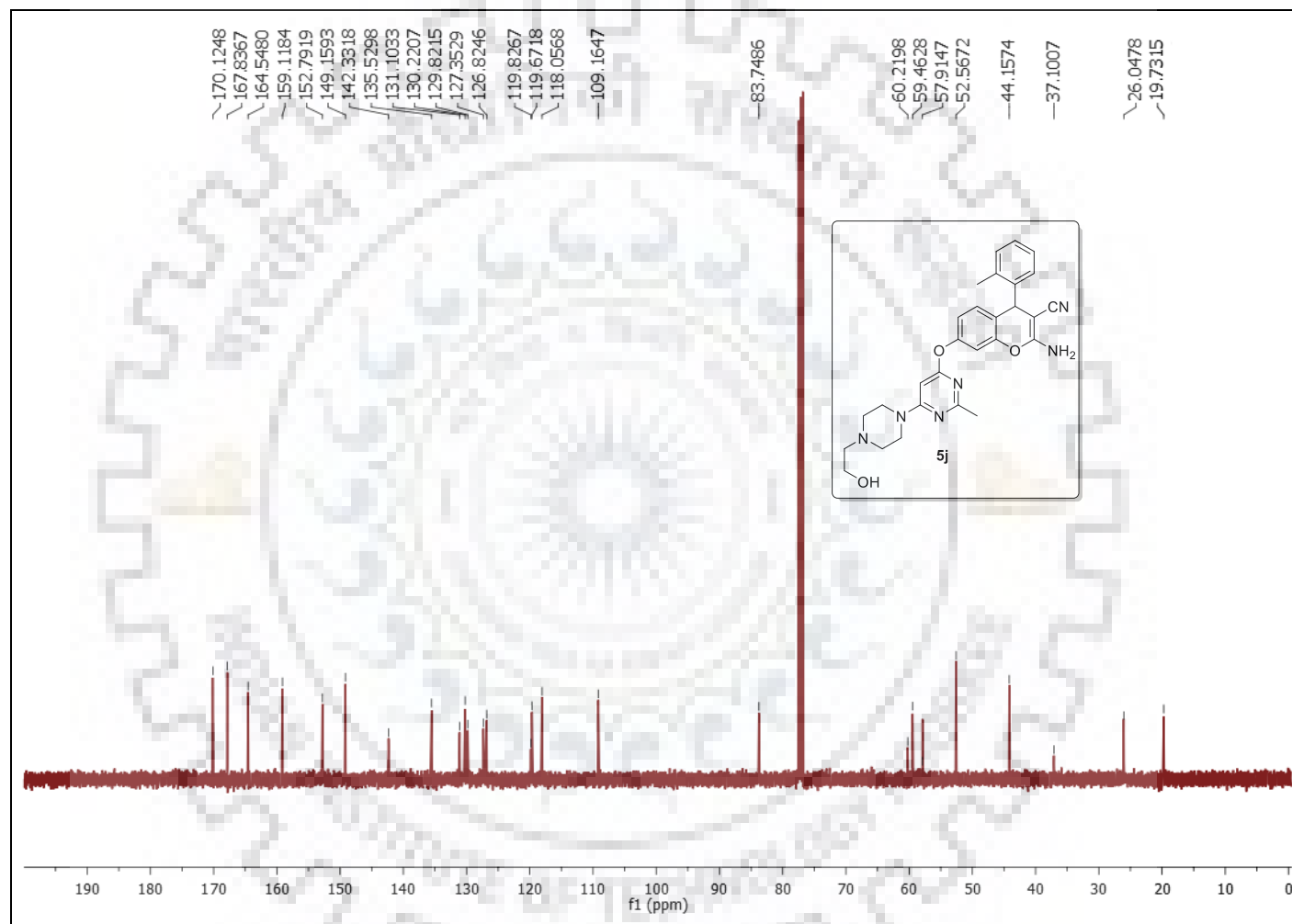


Figure S-46: ^{13}C Spectrum of 5j.

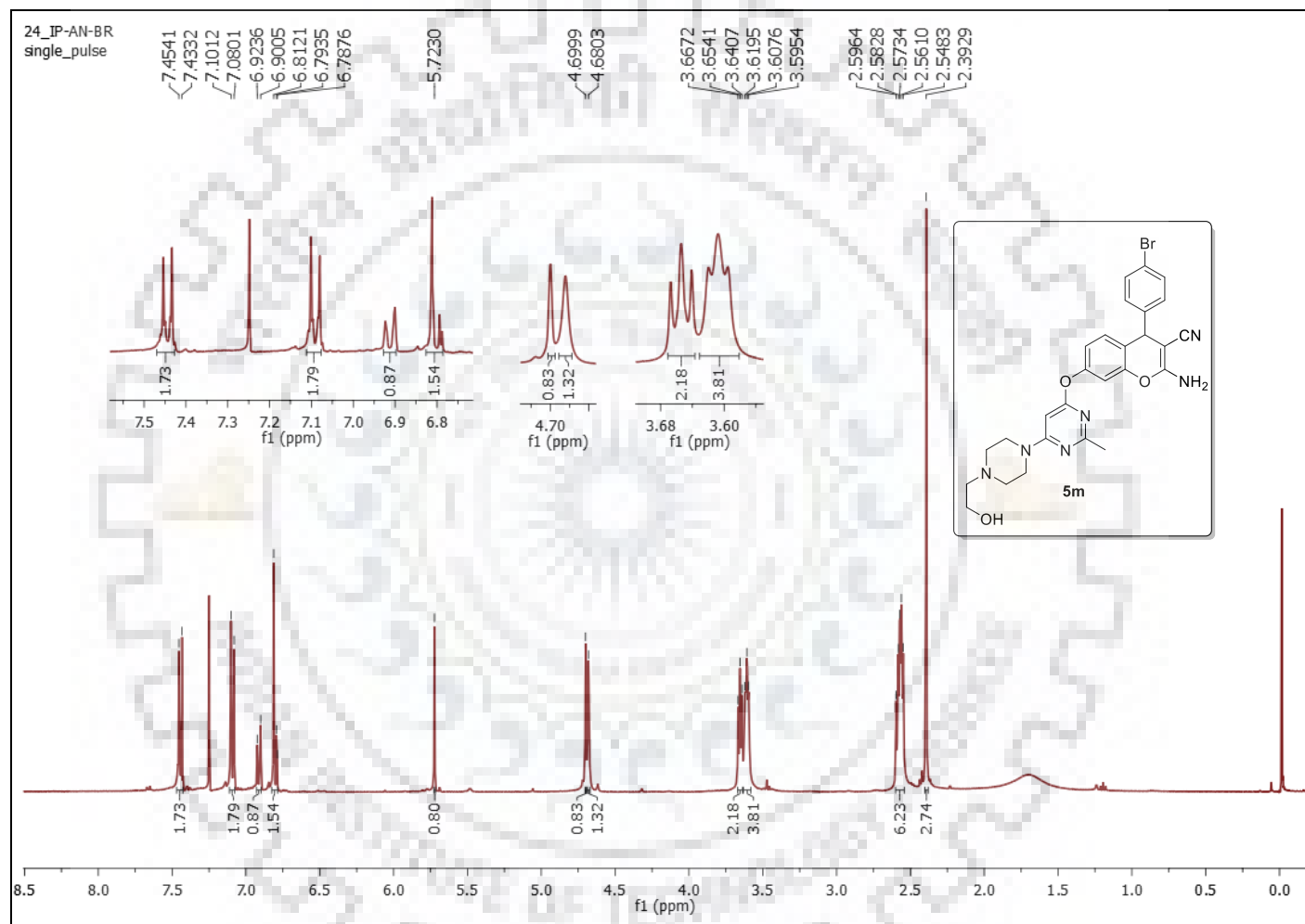


Figure S-47: ^1H NMR Spectrum of **5m**.

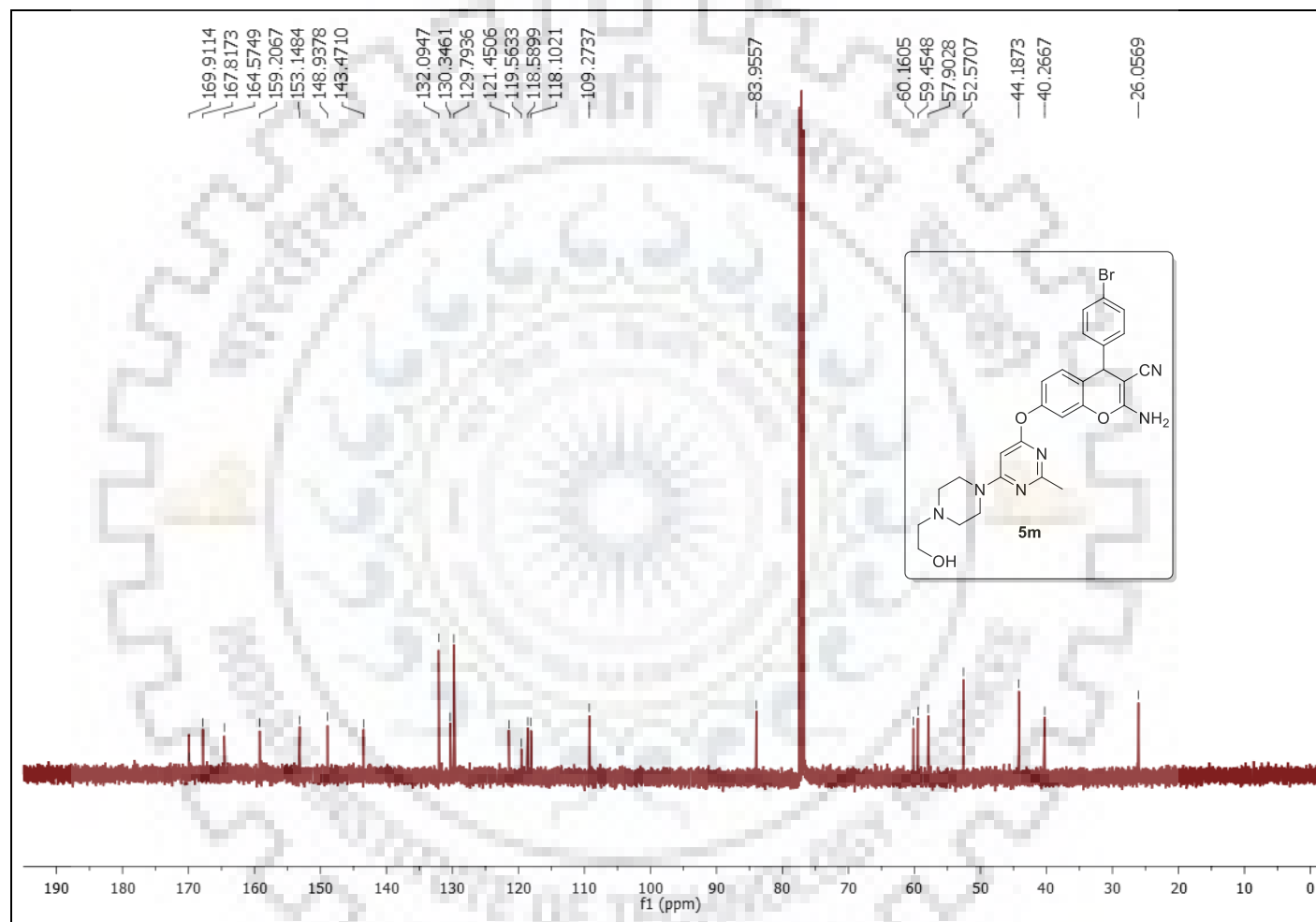


Figure S-48: ^{13}C Spectrum of **5m.**

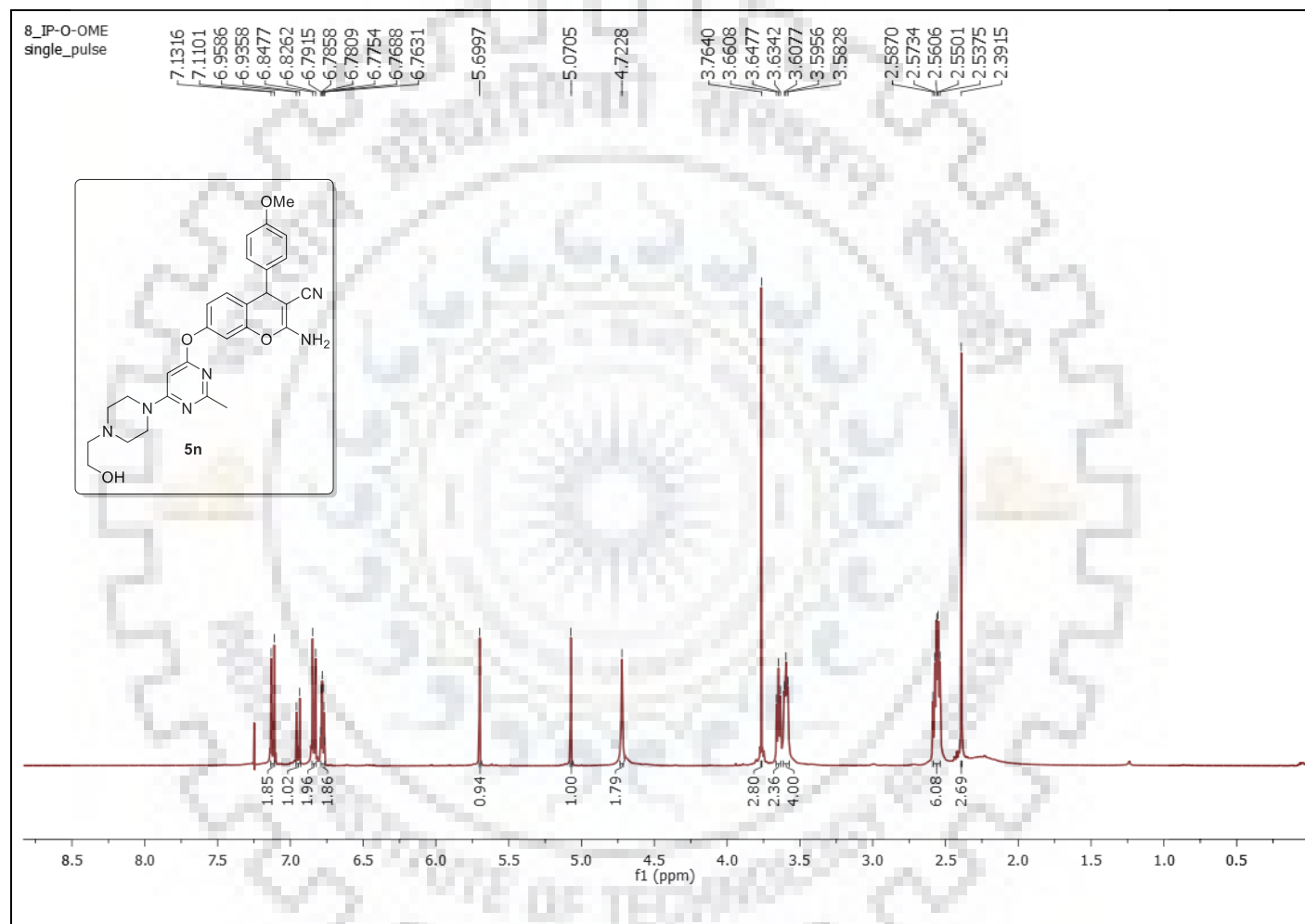


Figure S-49: ^1H Spectrum of **5n**.

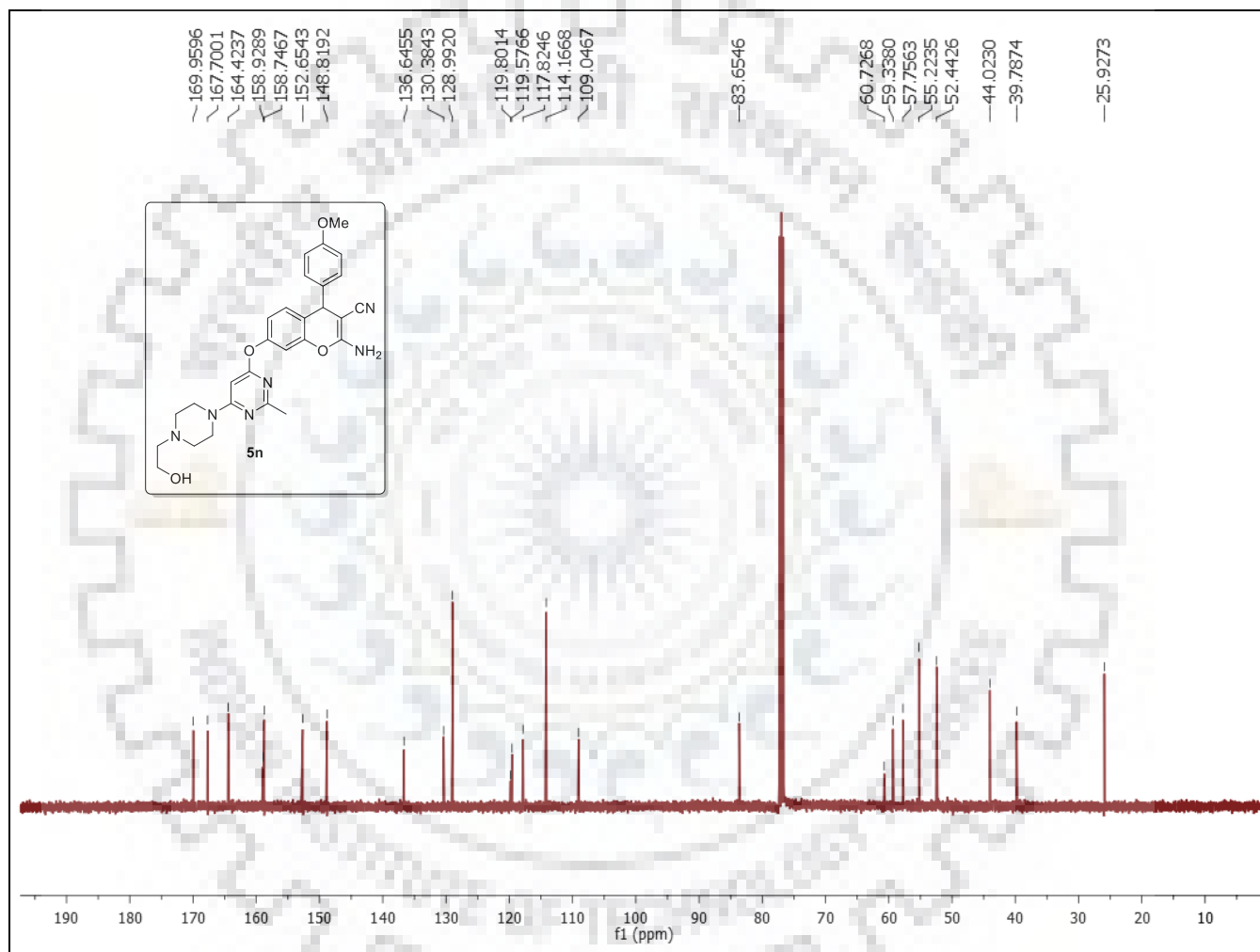


Figure S-50: ^{13}C Spectrum of 5n.

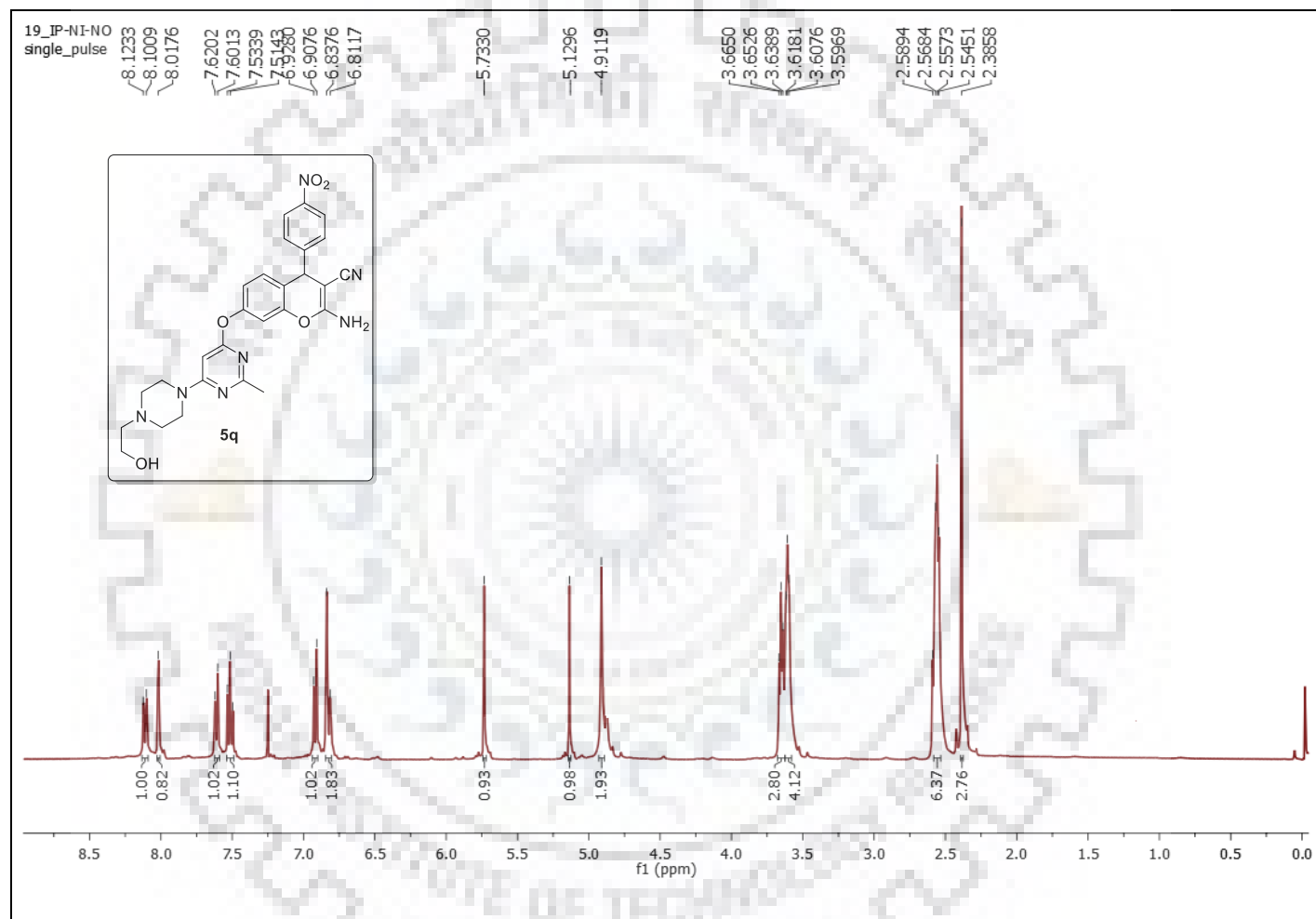


Figure S-51: ^1H NMR Spectrum of **5q**.

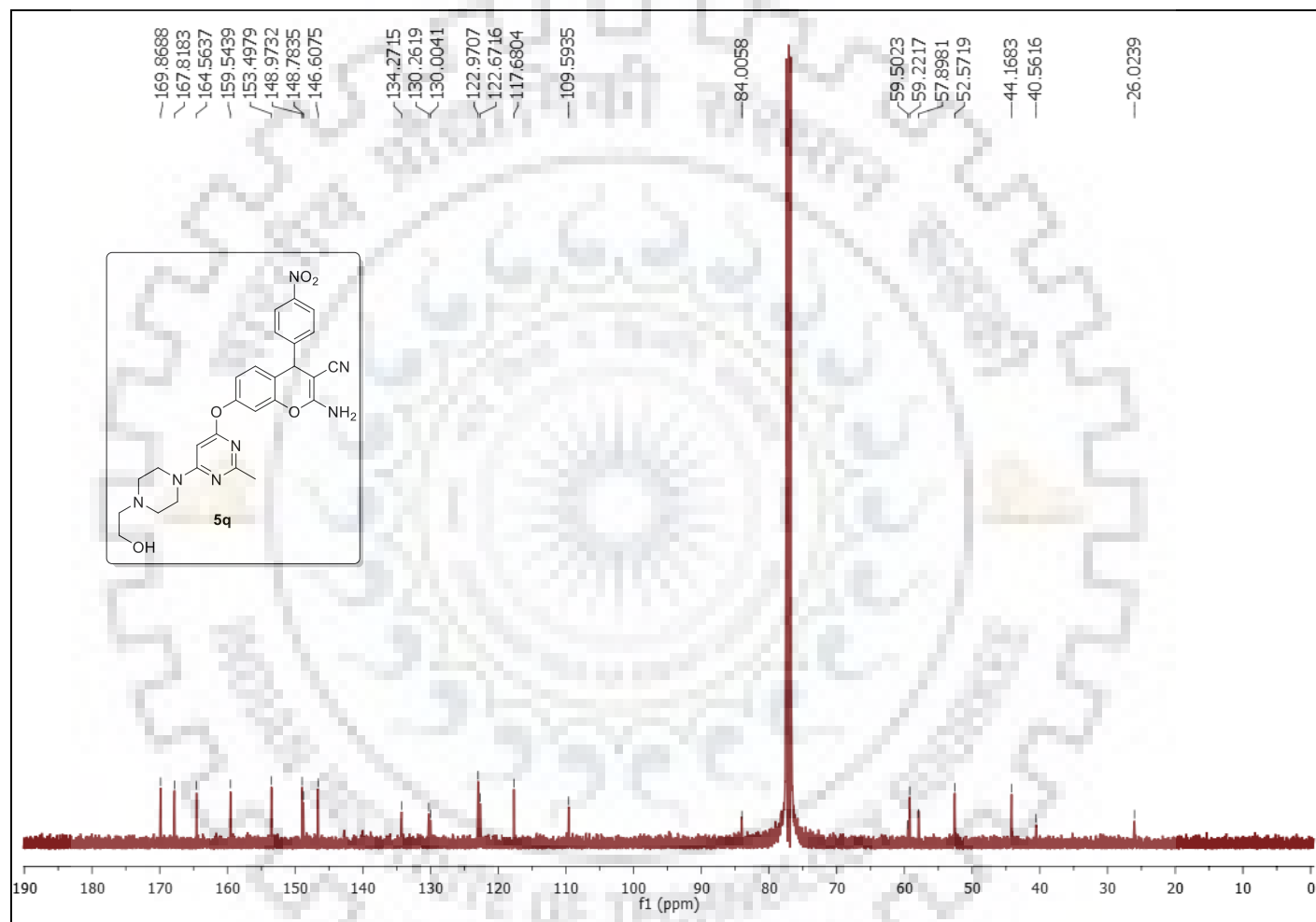


Figure S-52: ^{13}C Spectrum of **5q**.

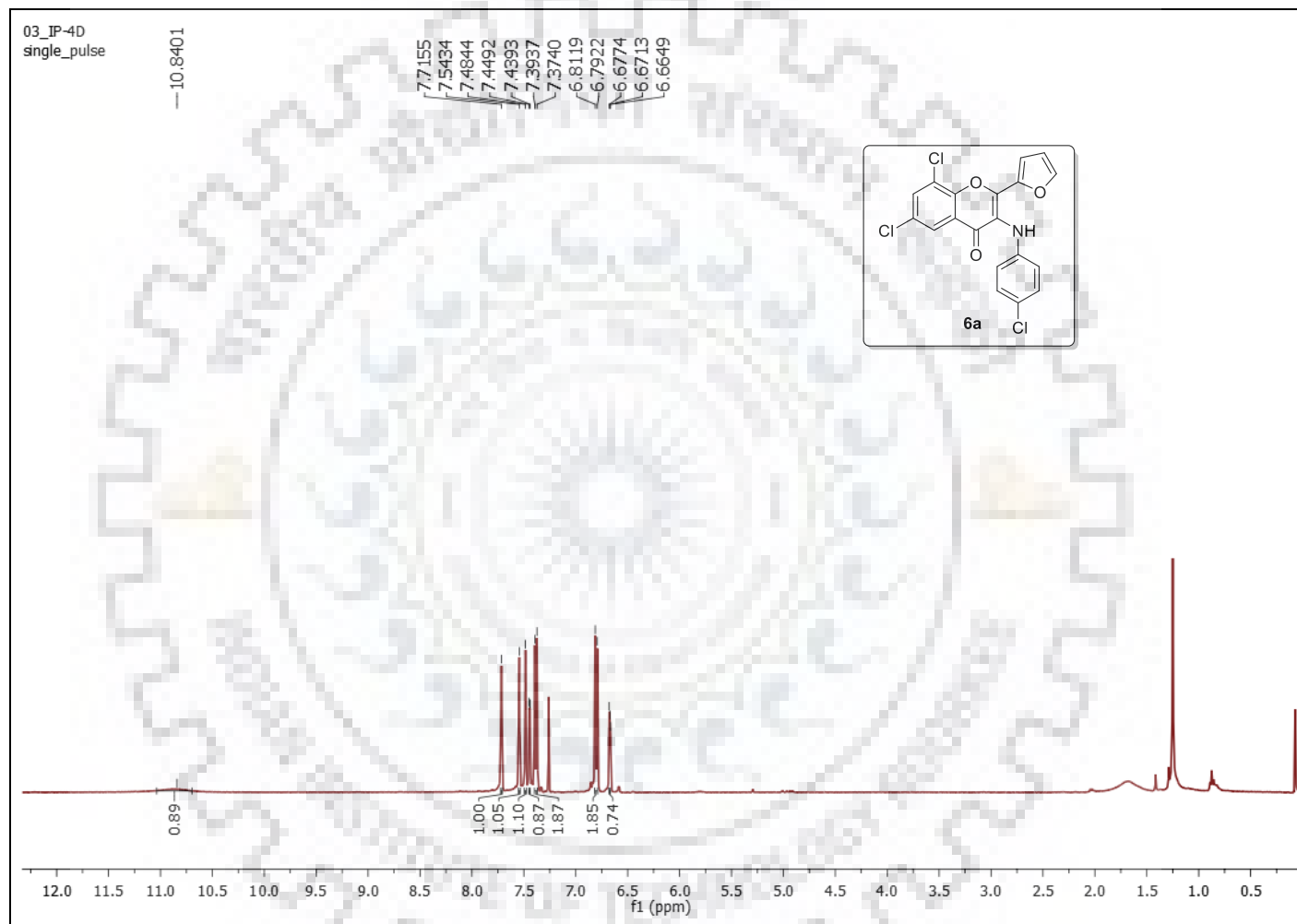


Figure S-53: ^1H NMR Spectrum of **6a**.

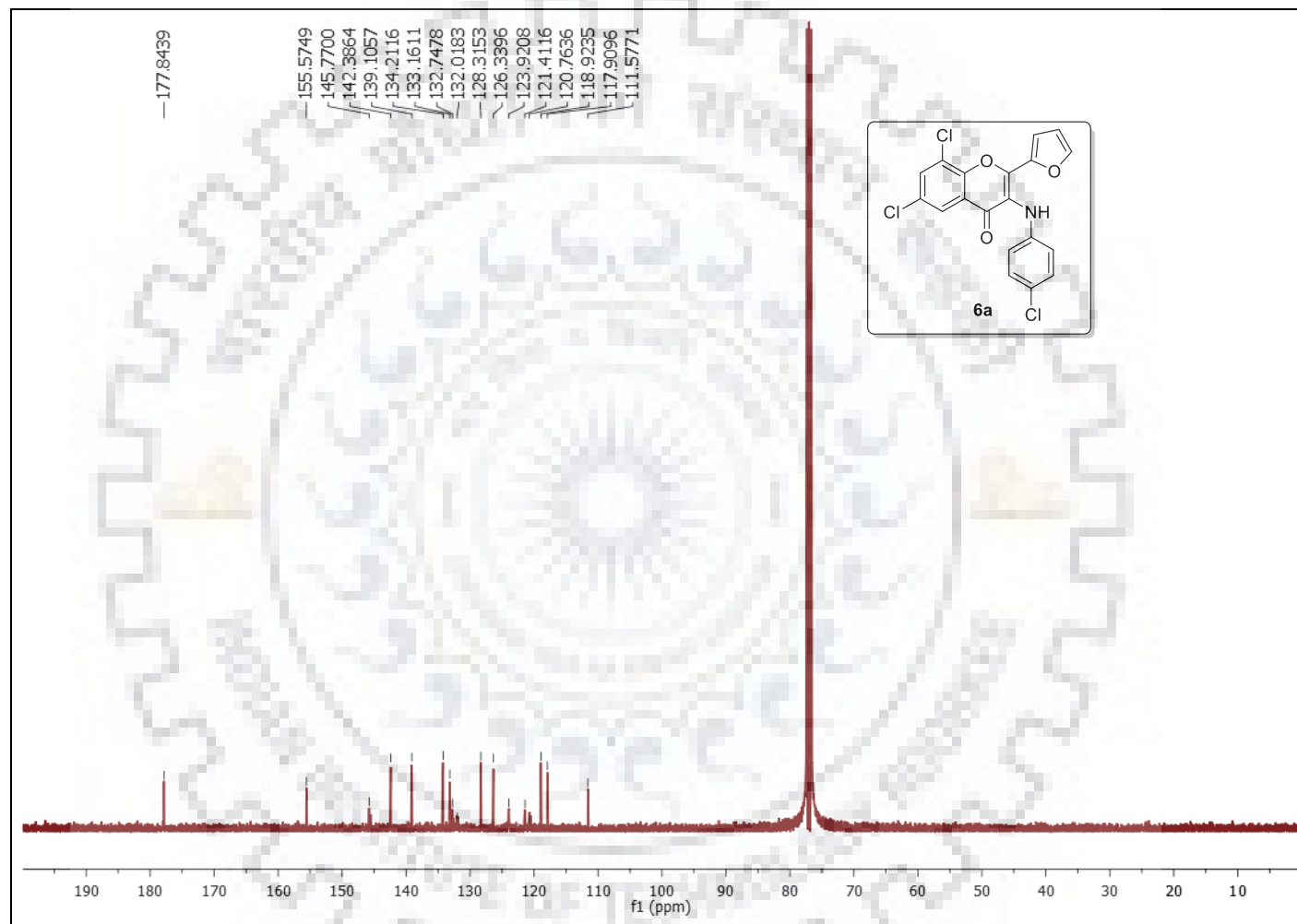


Figure S-54: ^{13}C Spectrum of **6a**.

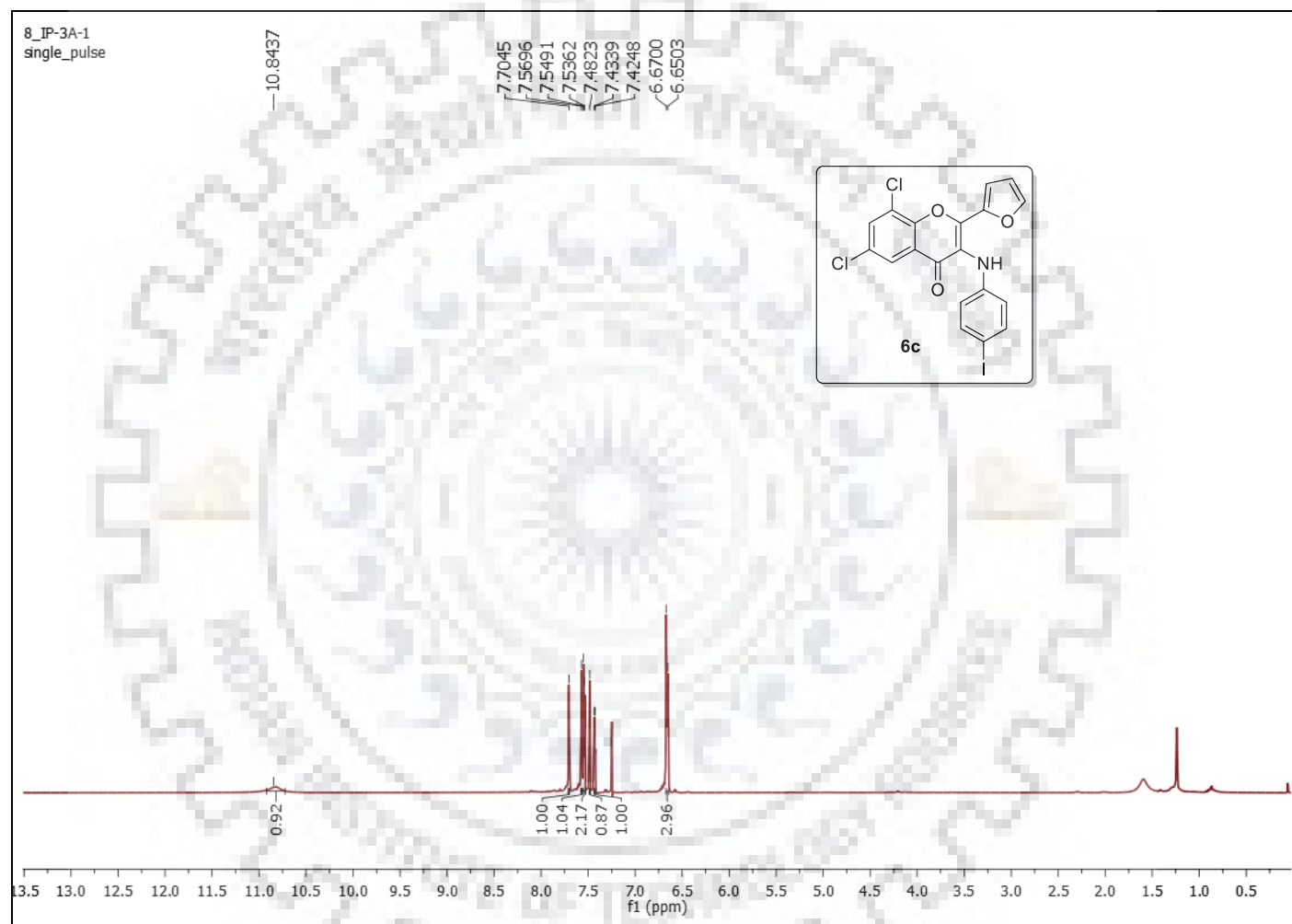


Figure S-55: ^1H NMR Spectrum of **6c**.

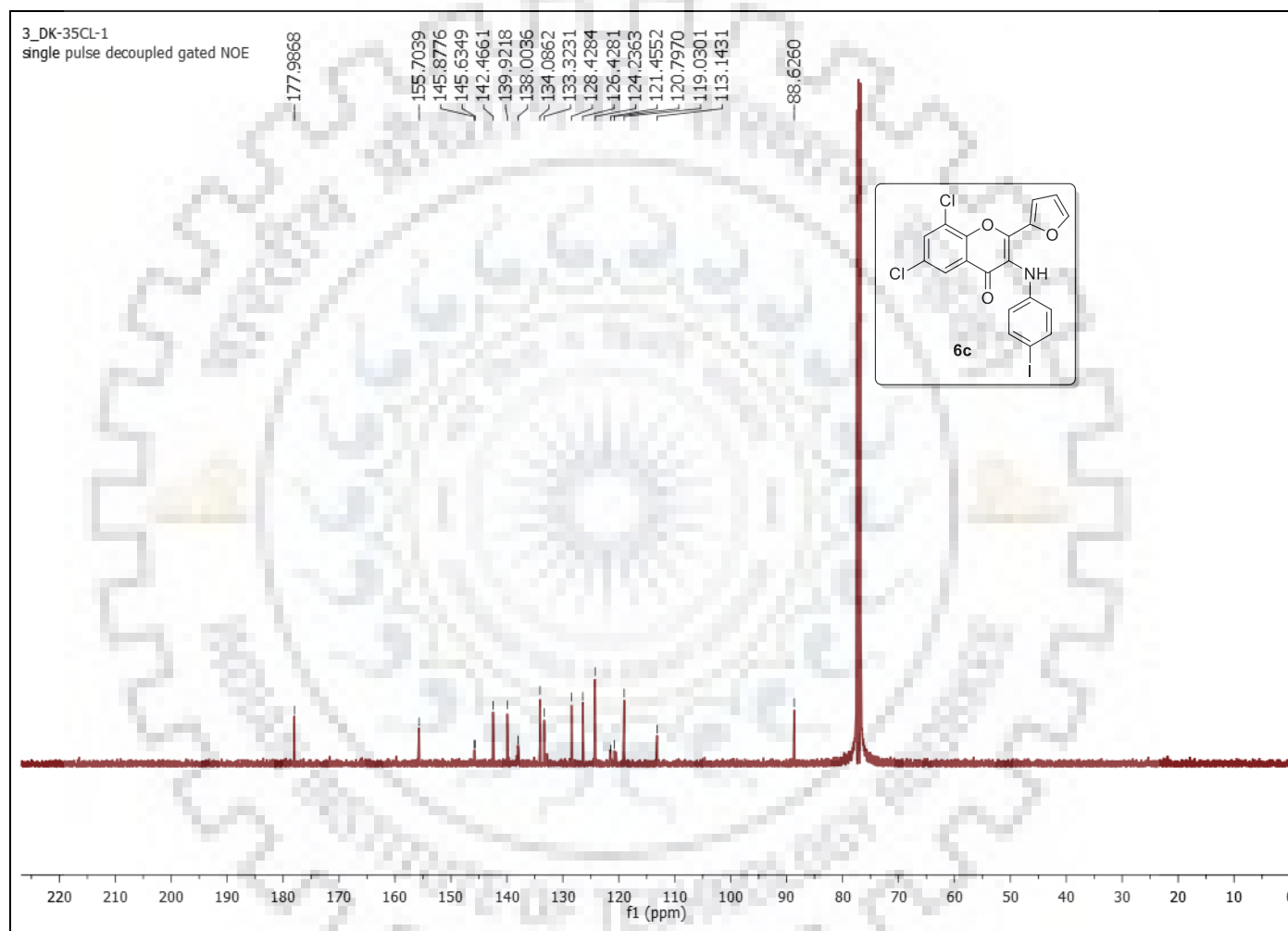


Figure S-56: ^{13}C Spectrum of **6c**.

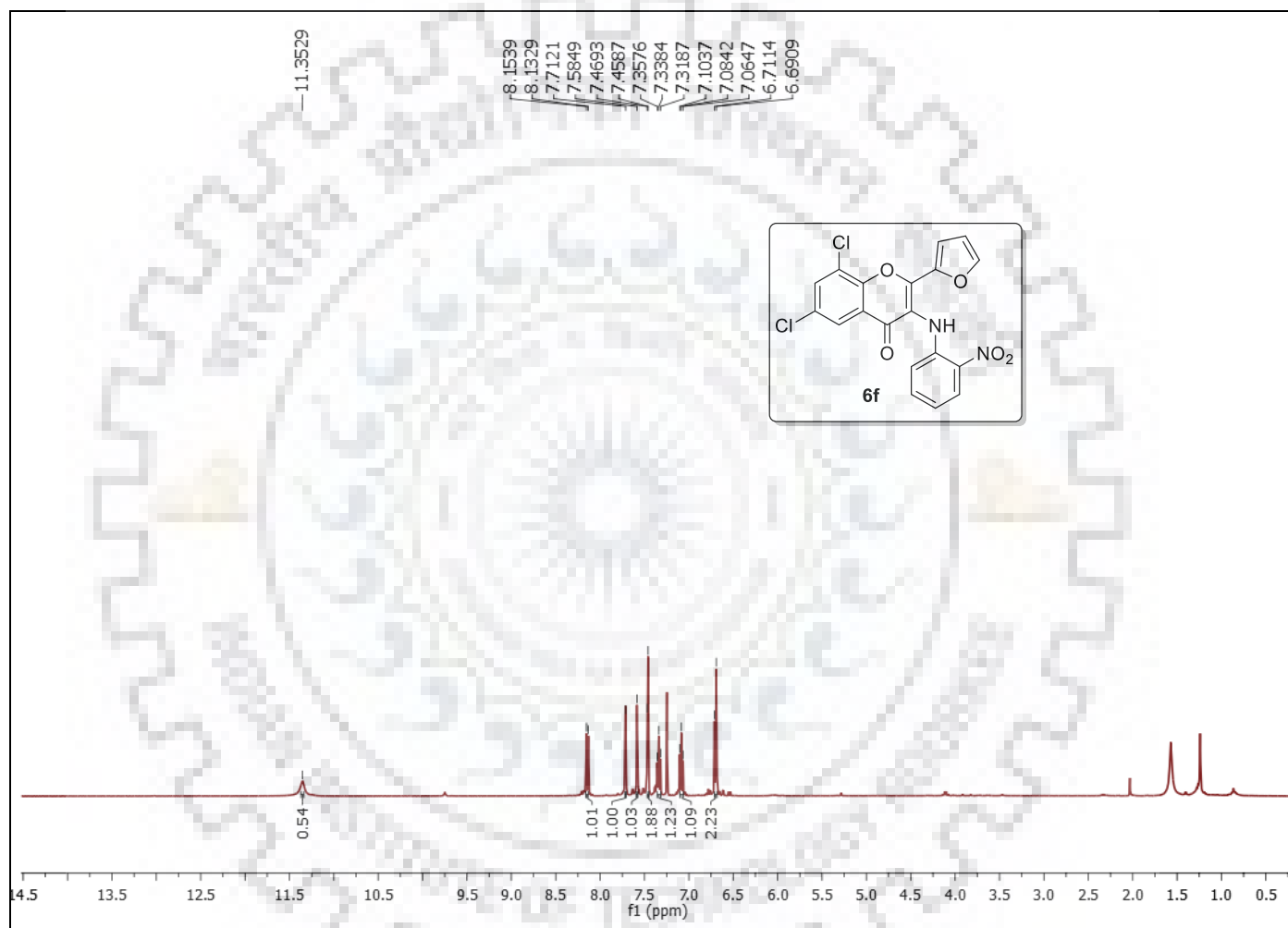


Figure S-57: ^1H NMR Spectrum of **6f**.

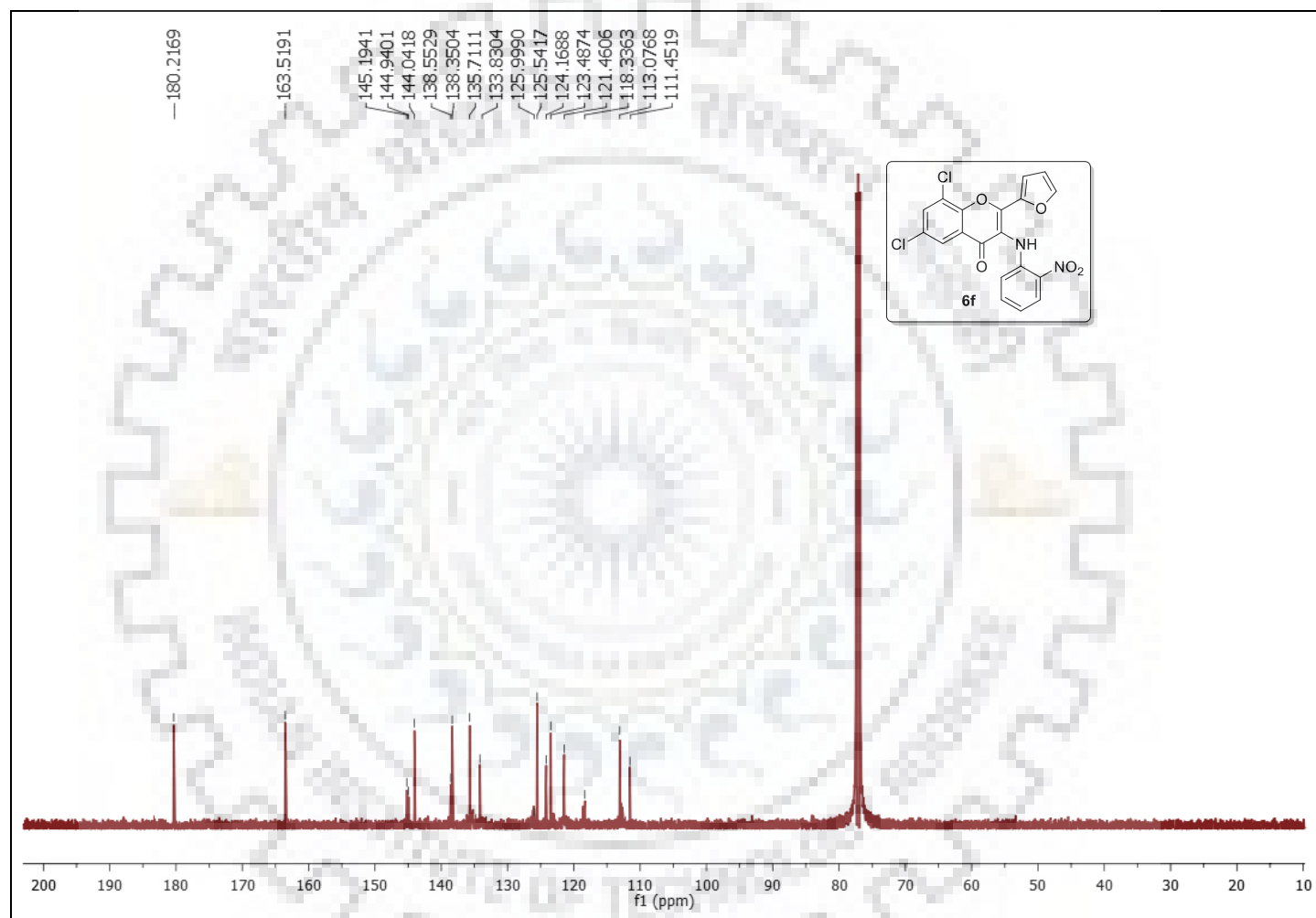


Figure S-58: ^{13}C Spectrum of **6f**.

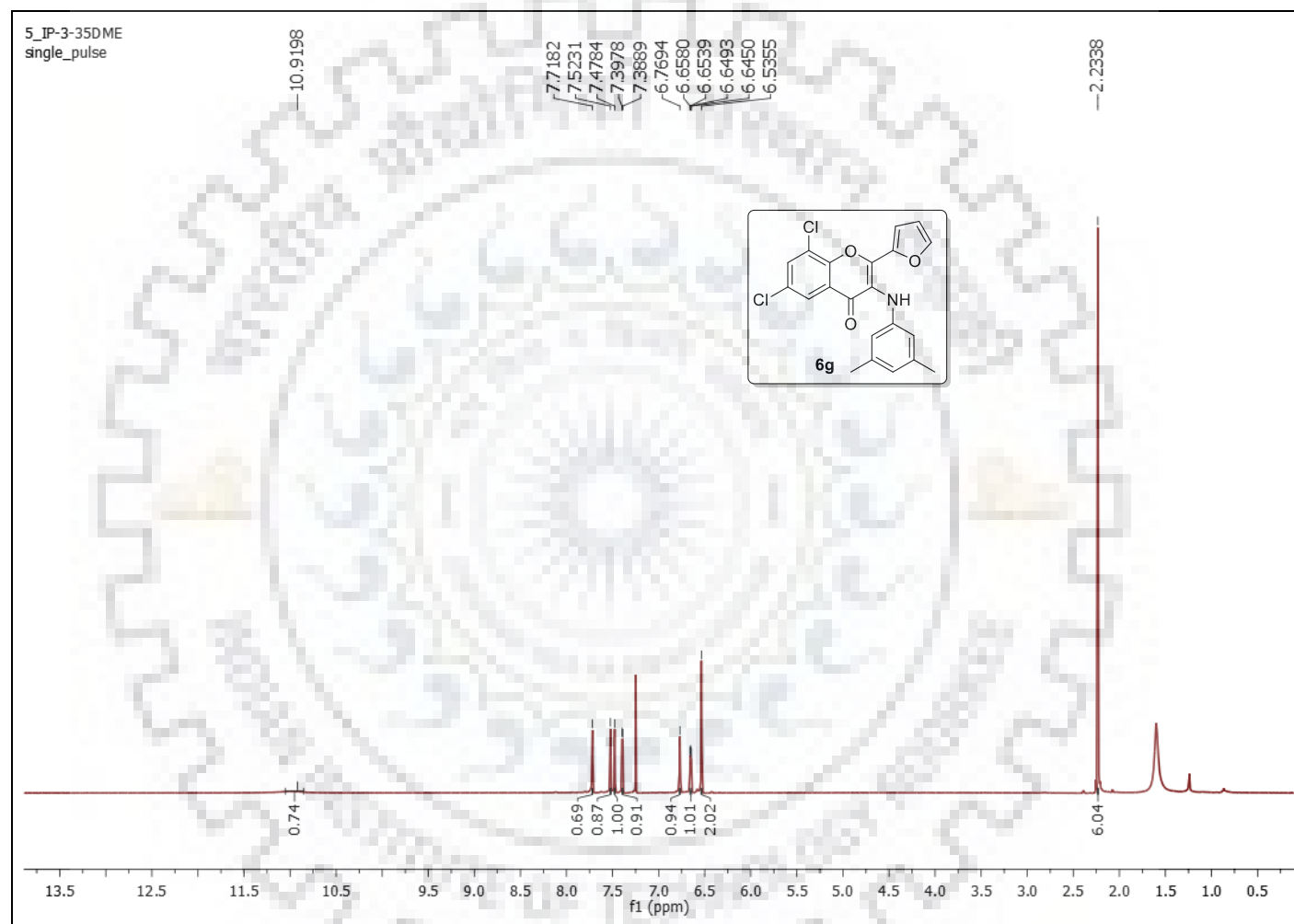


Figure S-59: ^1H NMR Spectrum of **6g**.

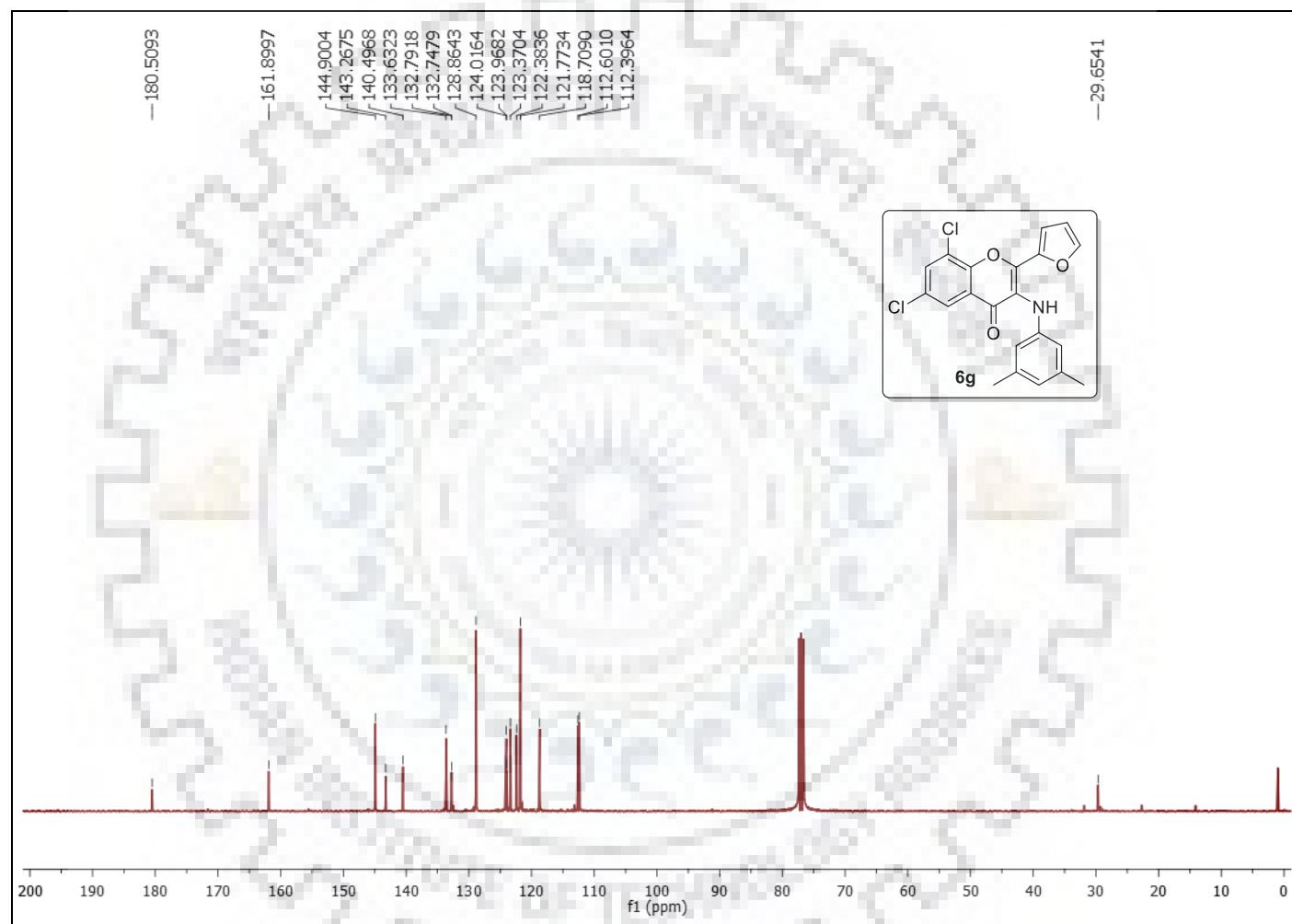


Figure S-60: ^{13}C Spectrum of **6g**.

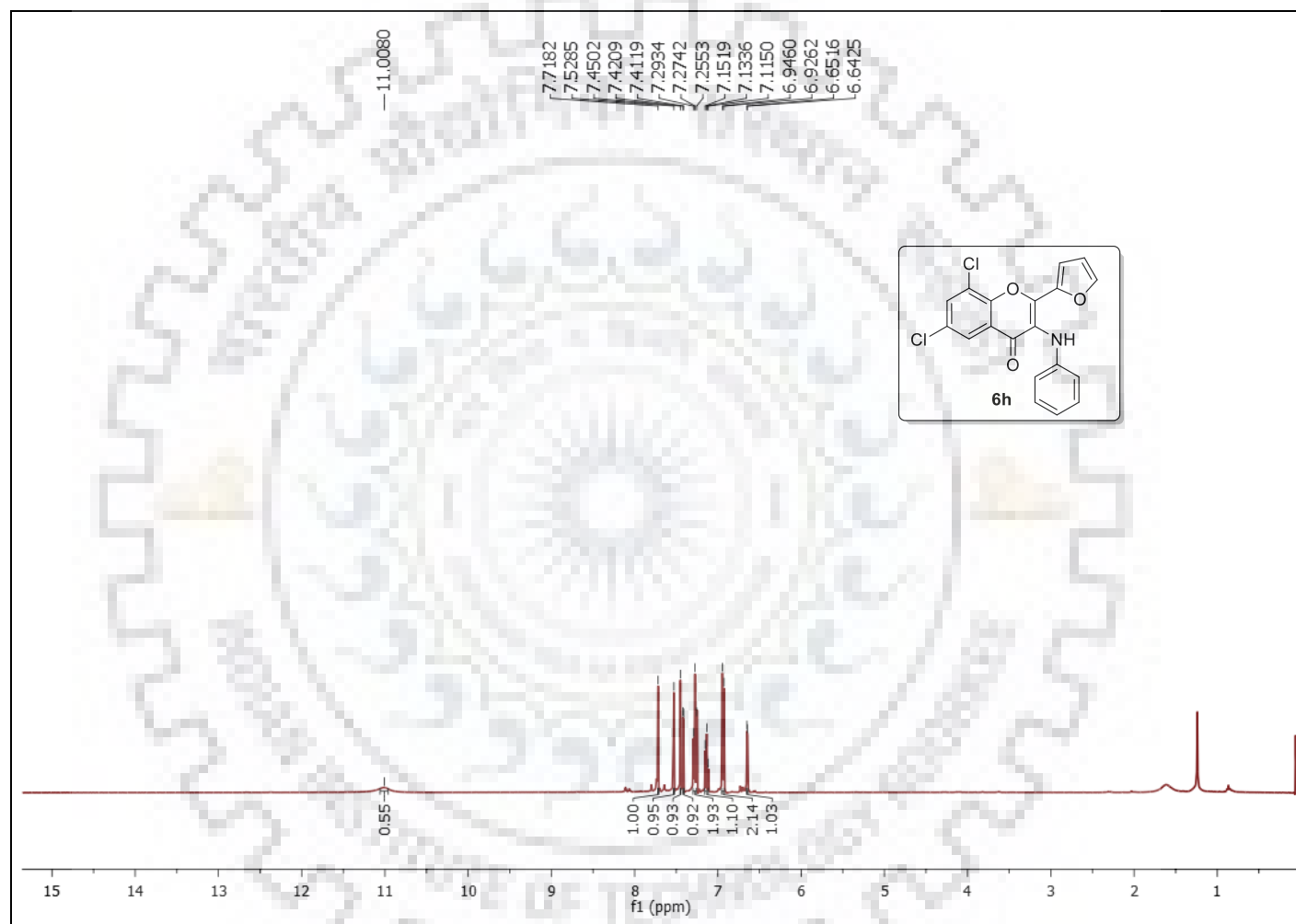


Figure S-61: ^1H NMR Spectrum of **6h**.

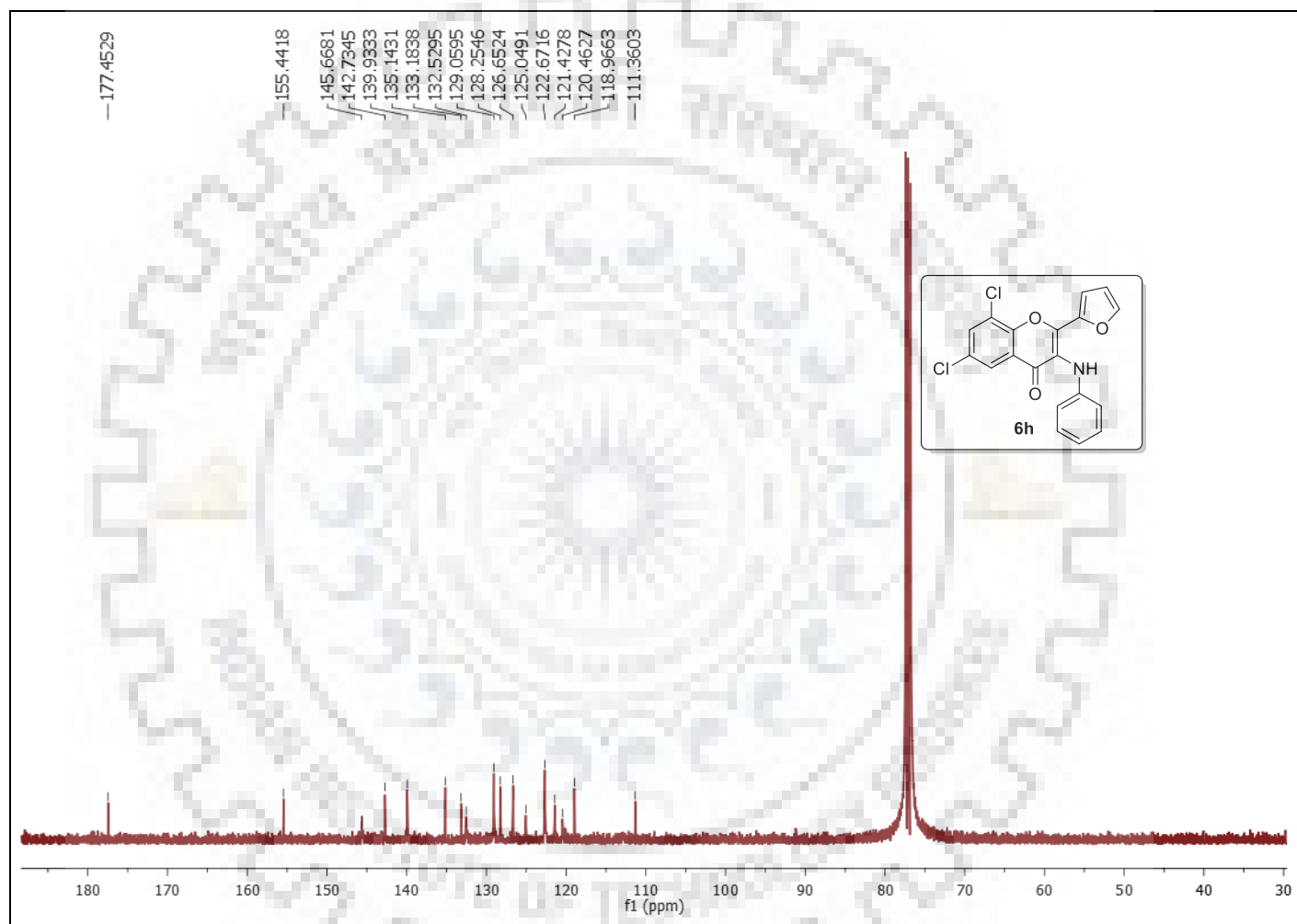


Figure S-62: ^{13}C Spectrum of **6h**.

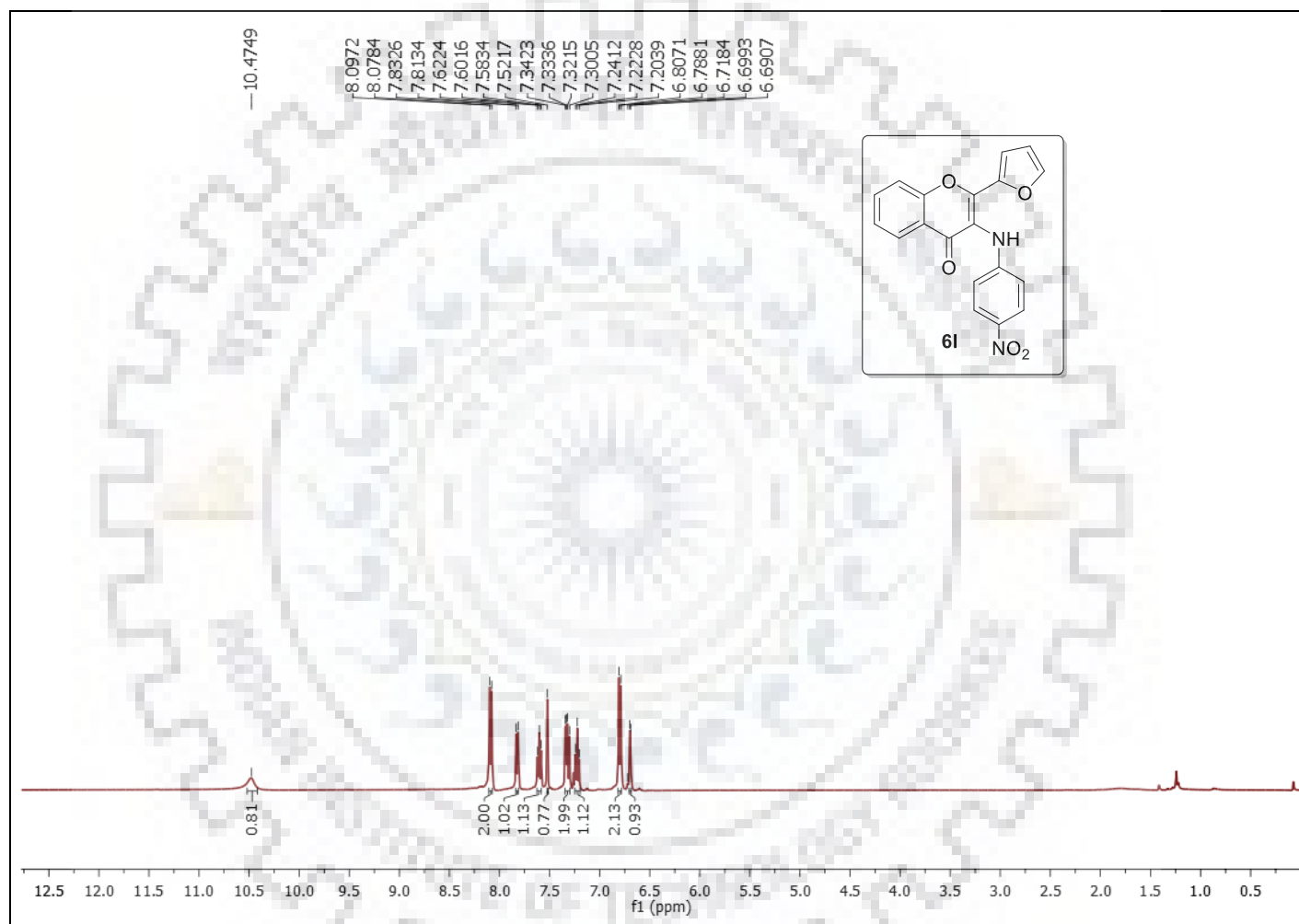


Figure S-63: ¹H NMR Spectrum of **6l**.

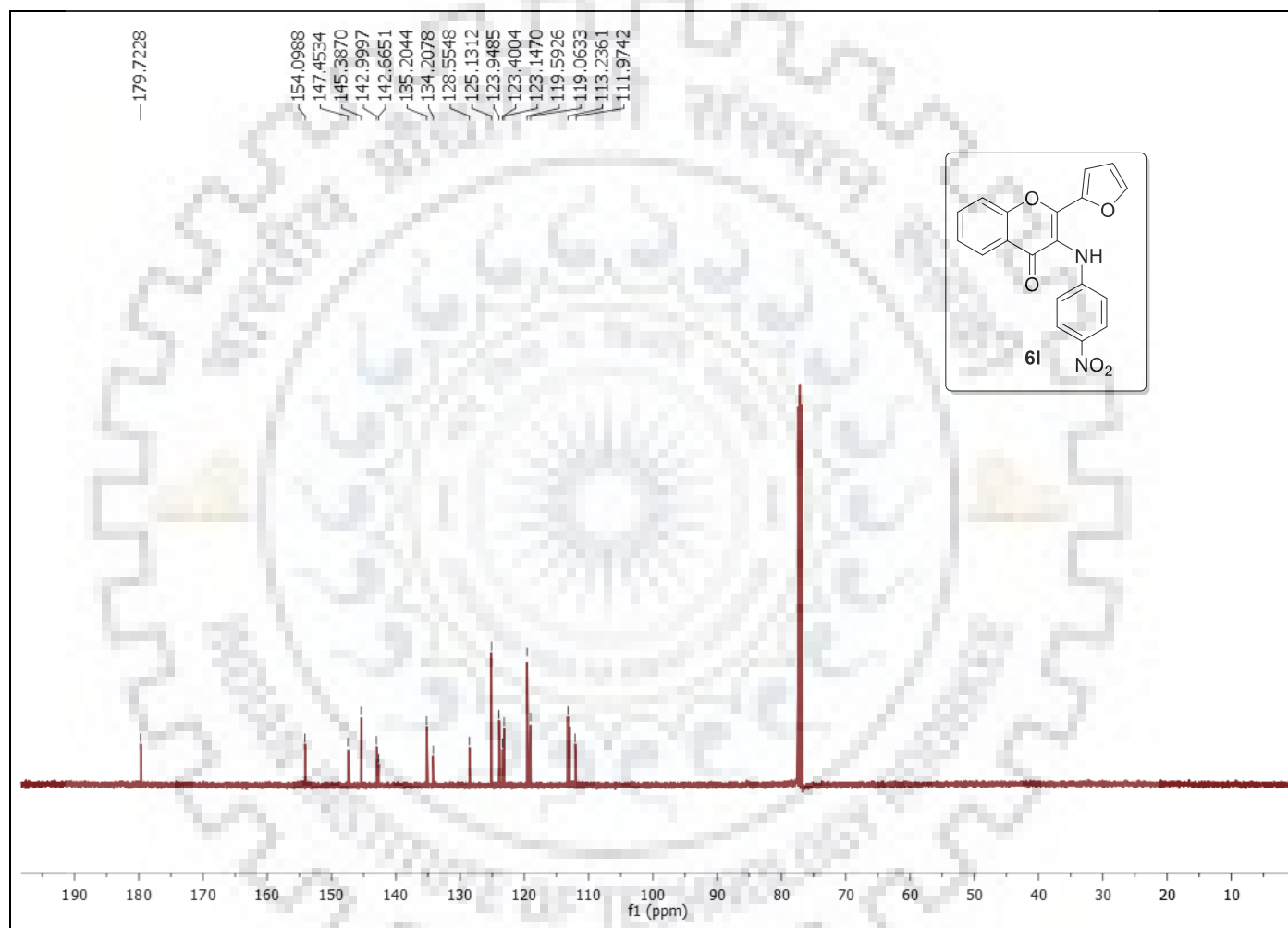


Figure S-64: ^{13}C Spectrum of **6l**.

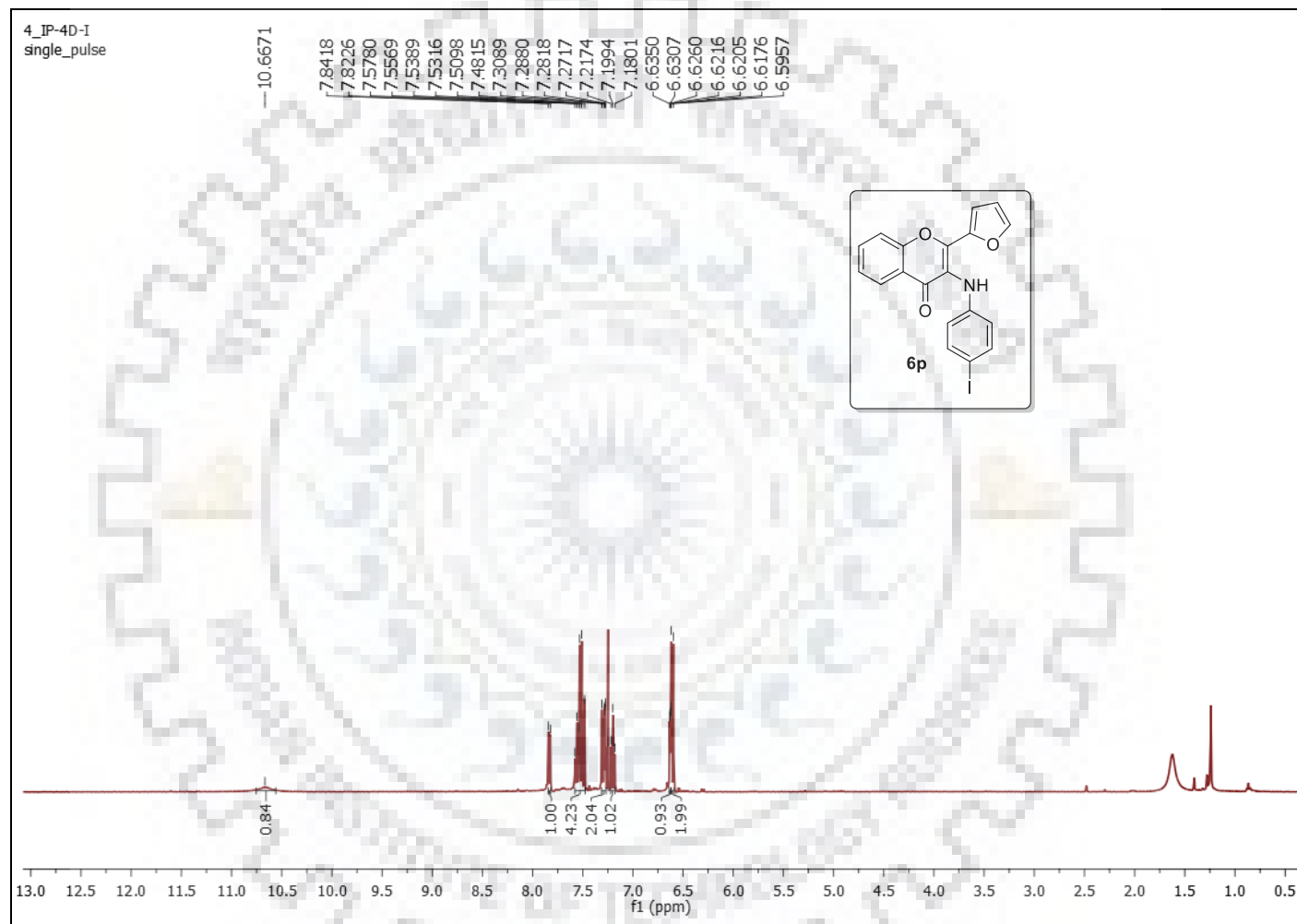


Figure S-65: ^1H NMR Spectrum of **6p**.

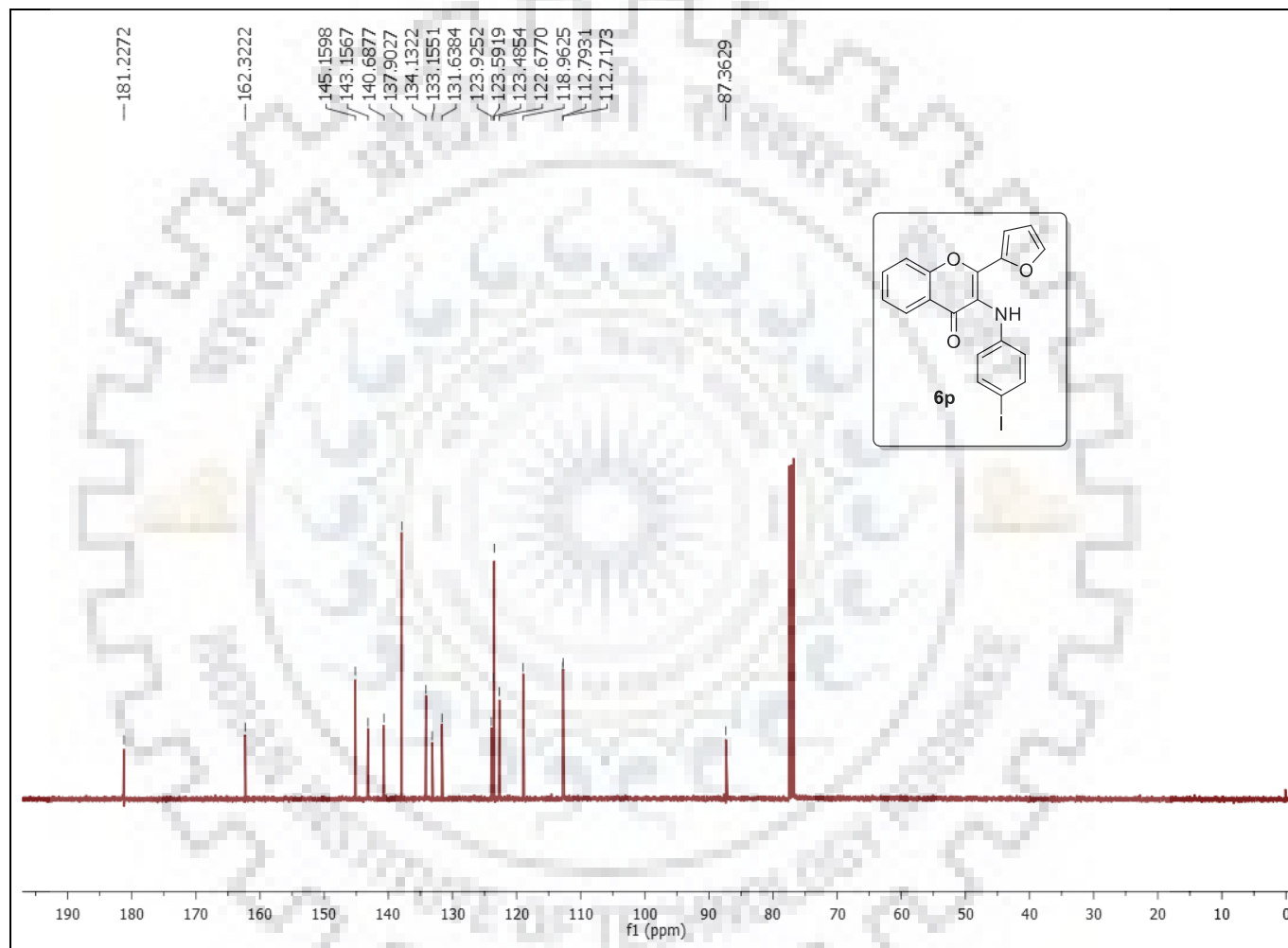


Figure S-66: ^{13}C Spectrum of **6p**.

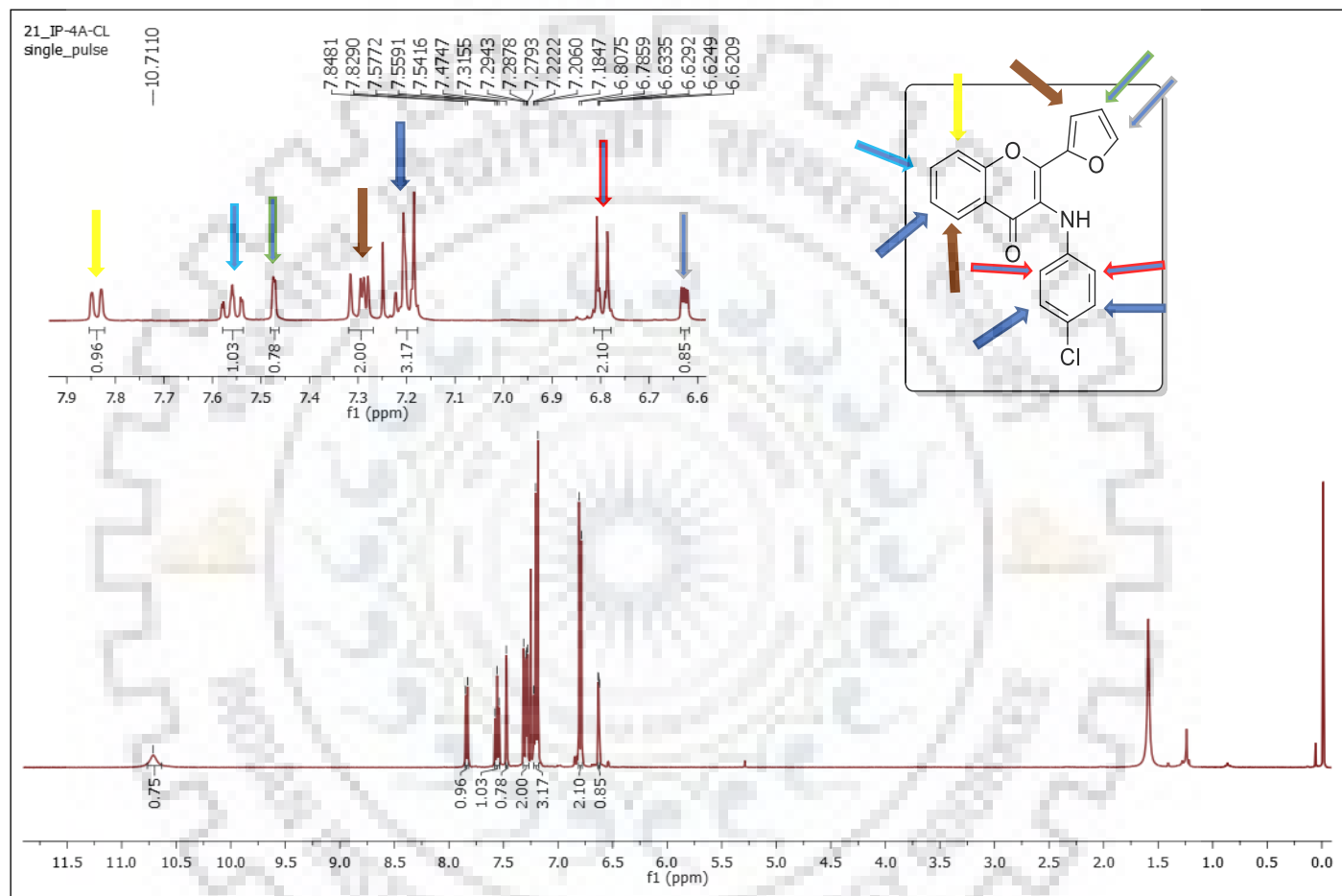


Figure S-67: ^1H NMR Spectrum of 6m.

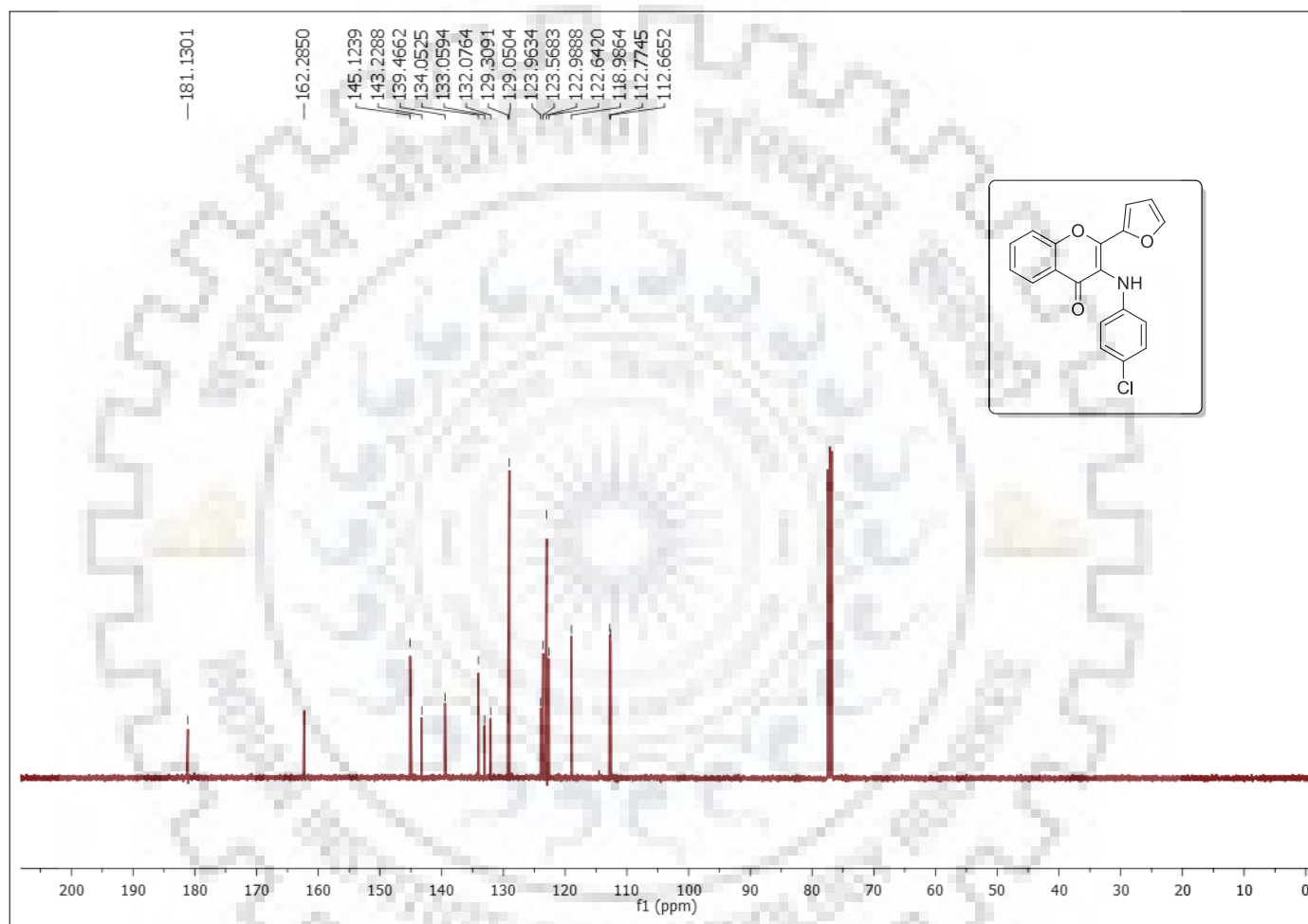


Figure S-68: ^{13}C NMR Spectrum of **6m**.

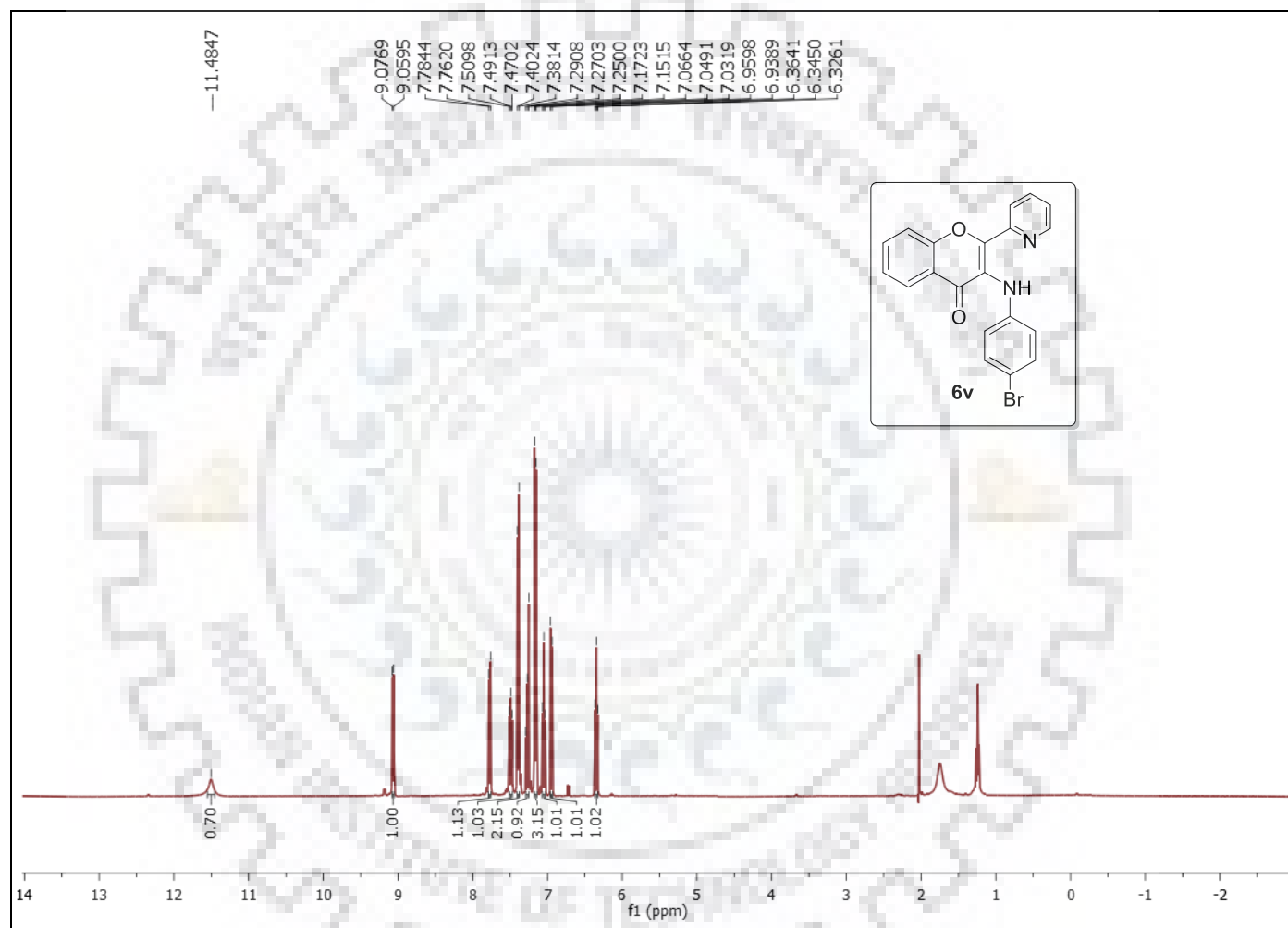


Figure S-69: ^1H NMR Spectrum of **6v**.

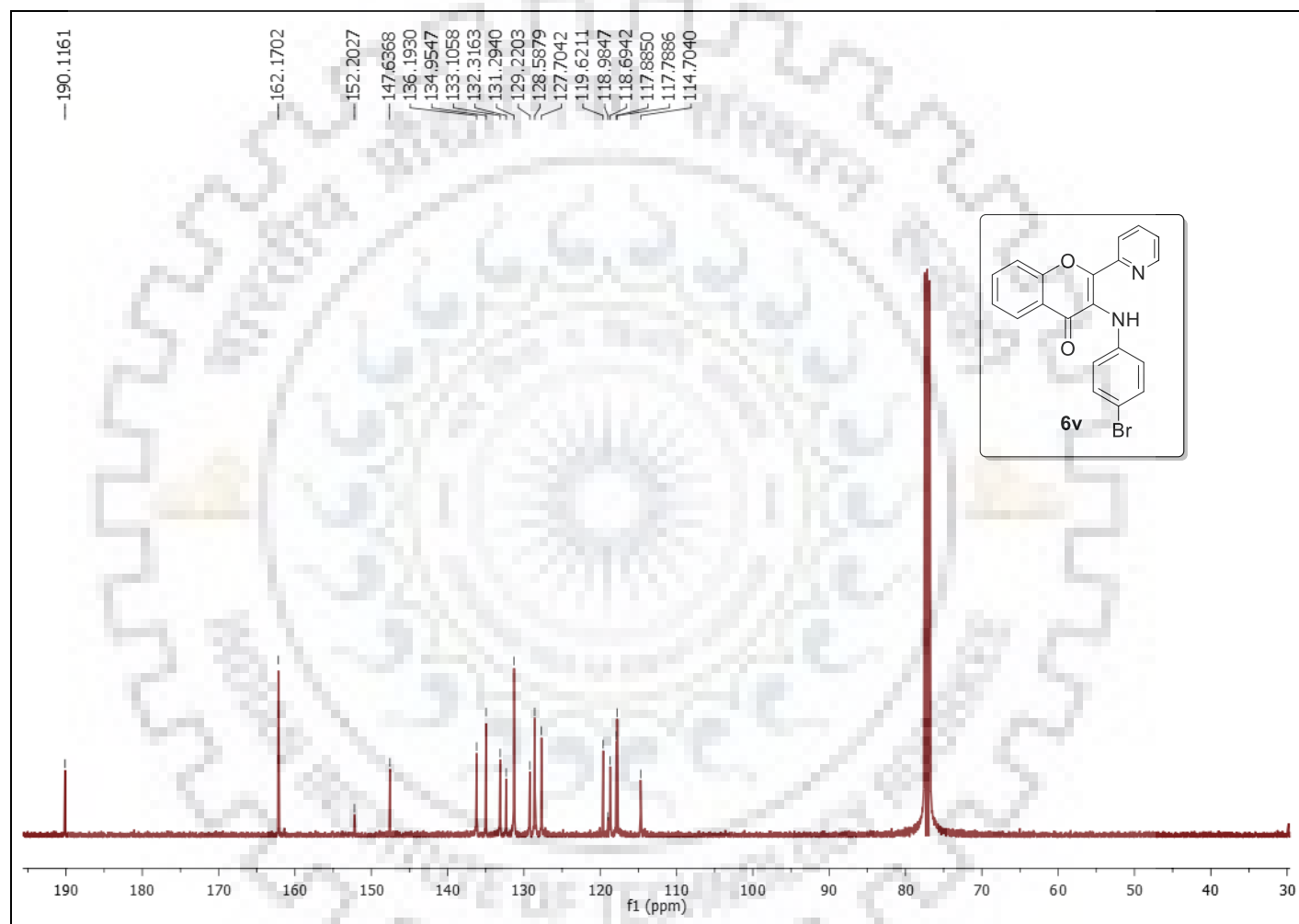


Figure S-70: ^{13}C Spectrum of 6v.

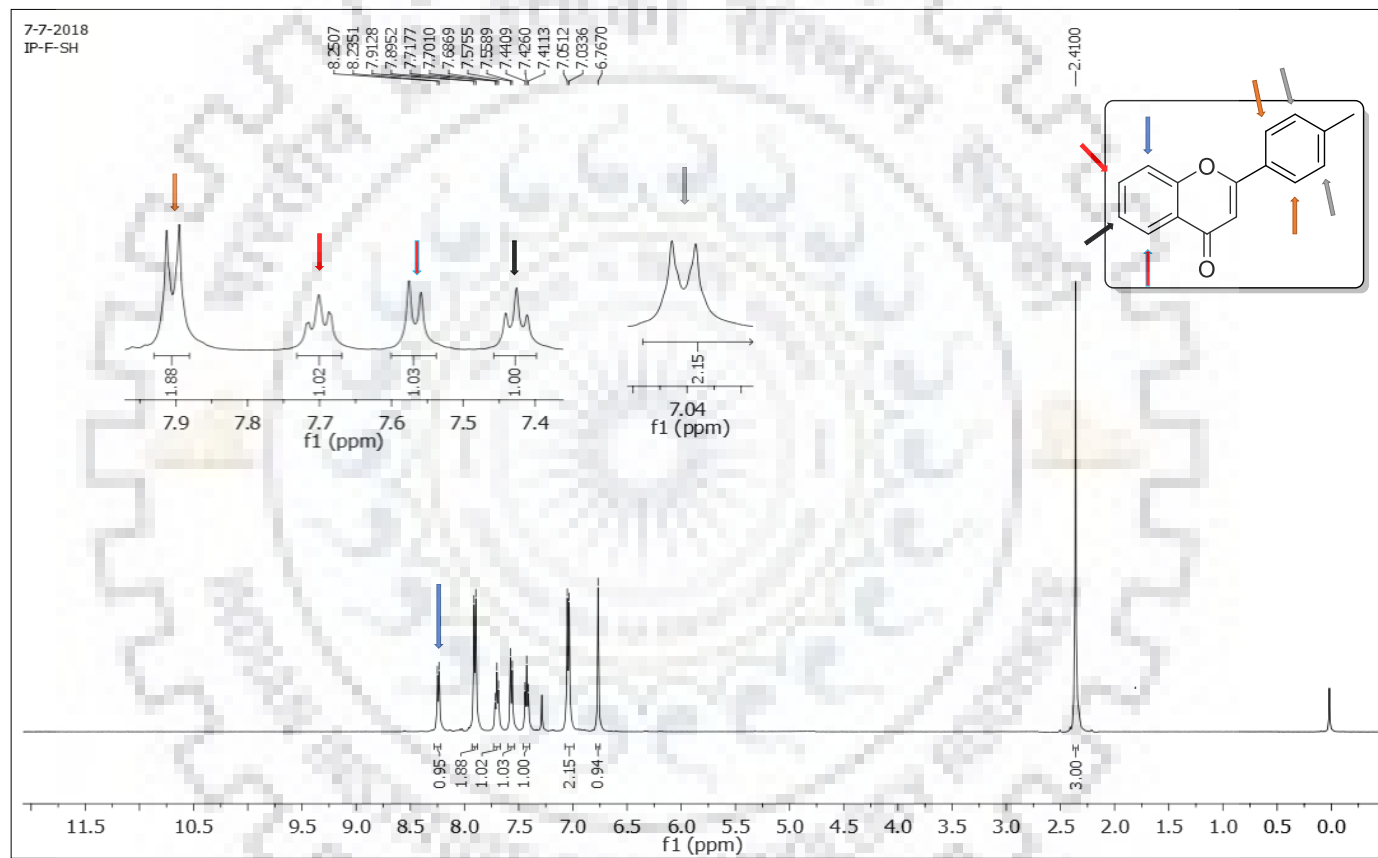


Figure S-71: ^{13}C Spectrum of **7e**.

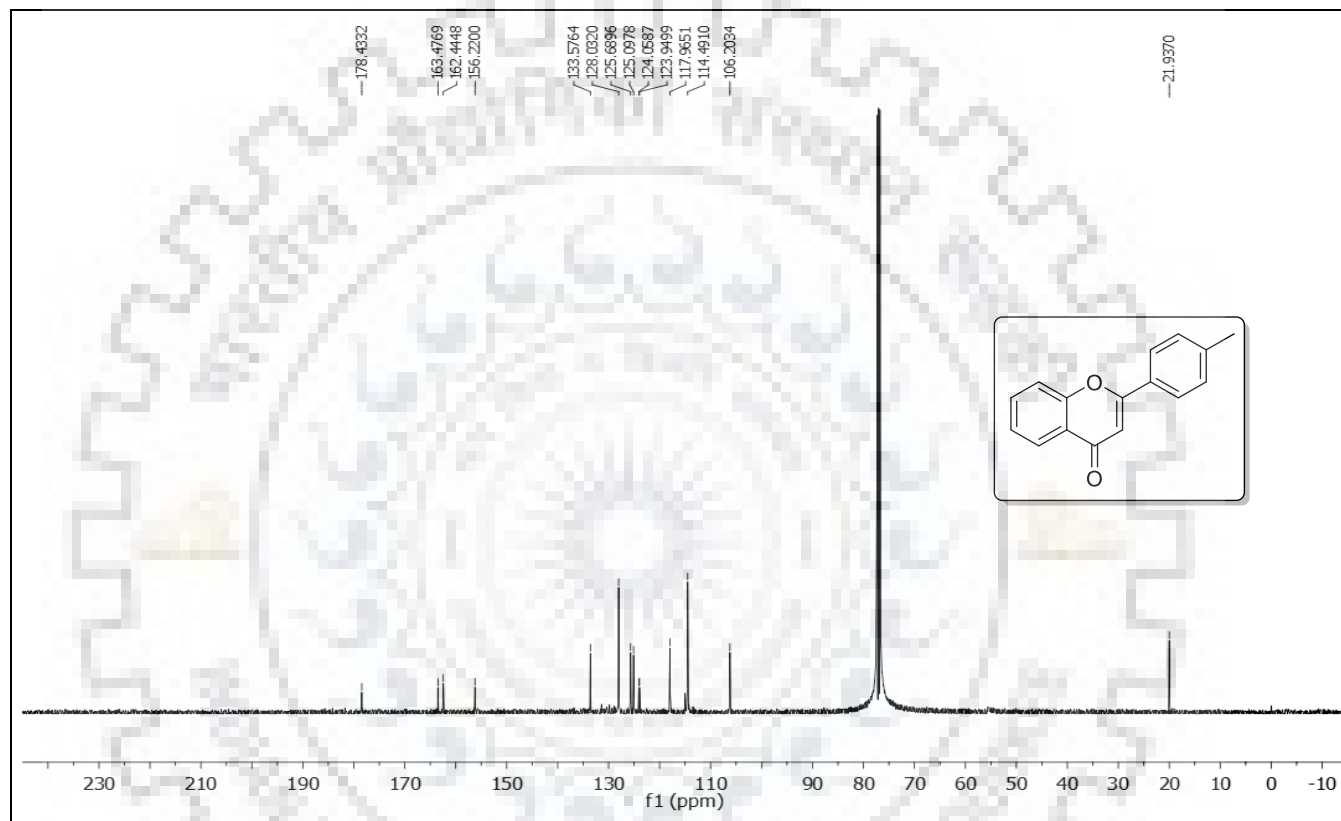


Figure S-72: ^{13}C Spectrum of 7e.

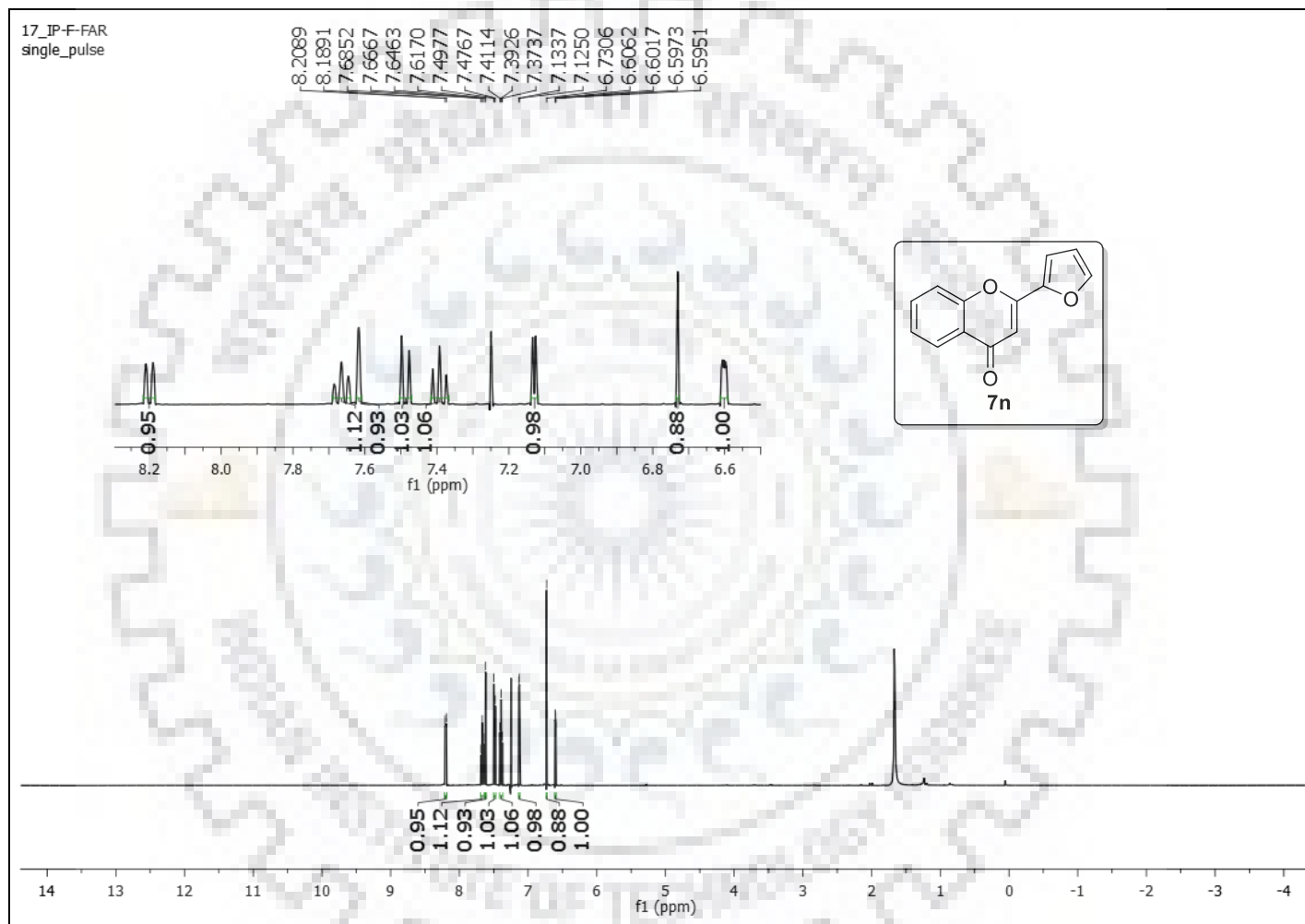


Figure S-73: ^{13}C Spectrum of **7n**.

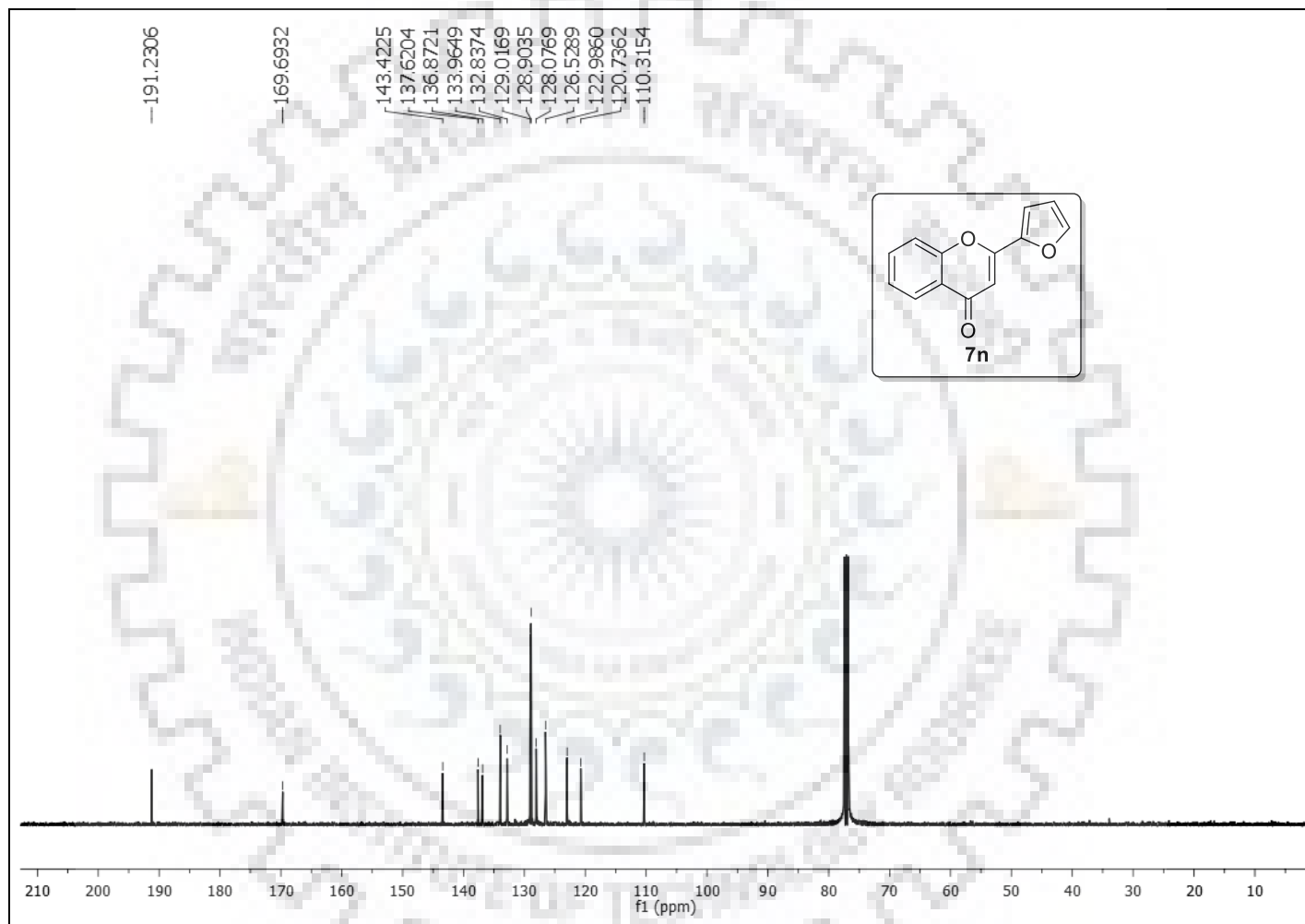


Figure S-74: ^{13}C Spectrum of **7n**.

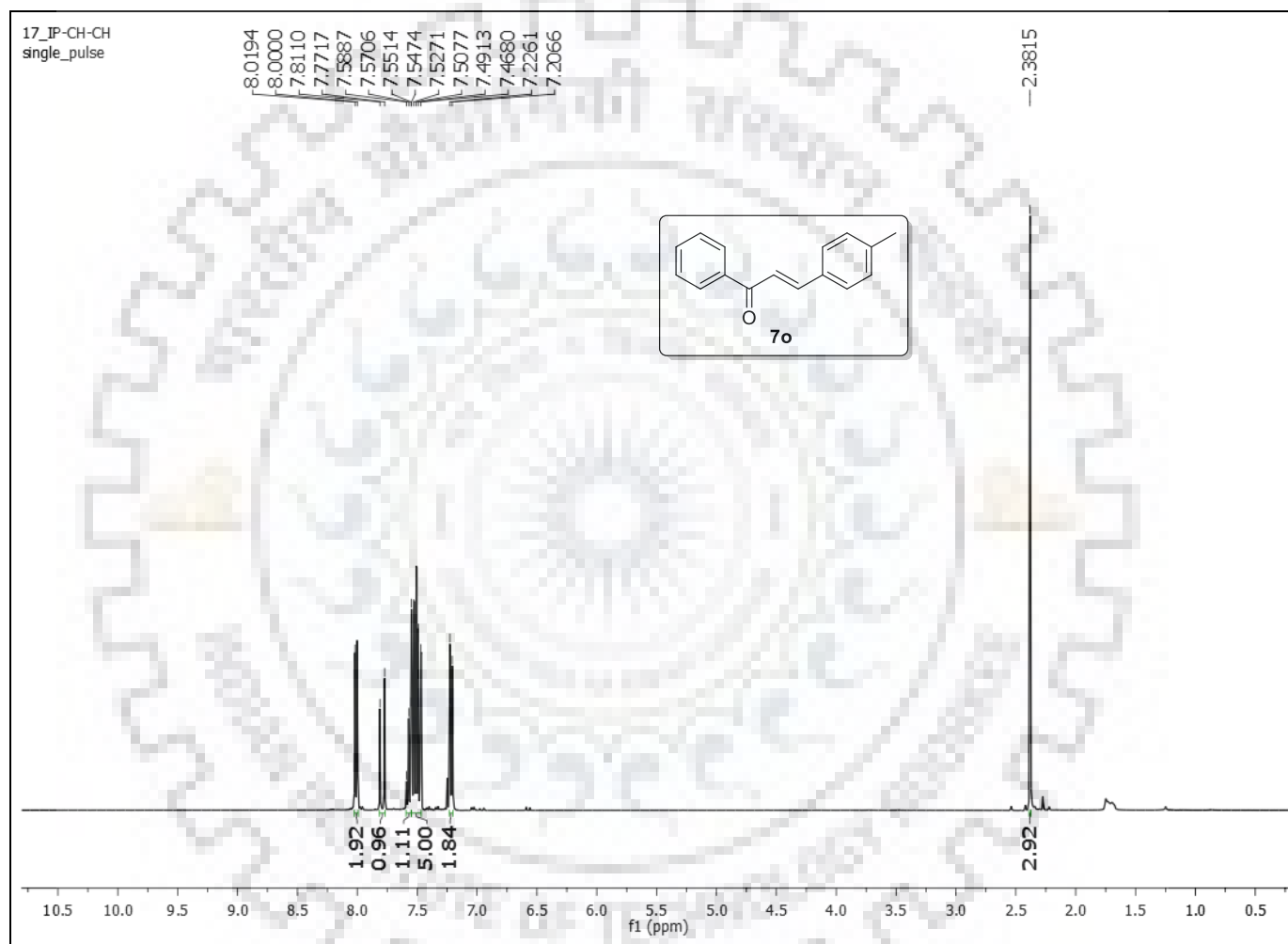


Figure S-75: ^{13}C Spectrum of **7o**.

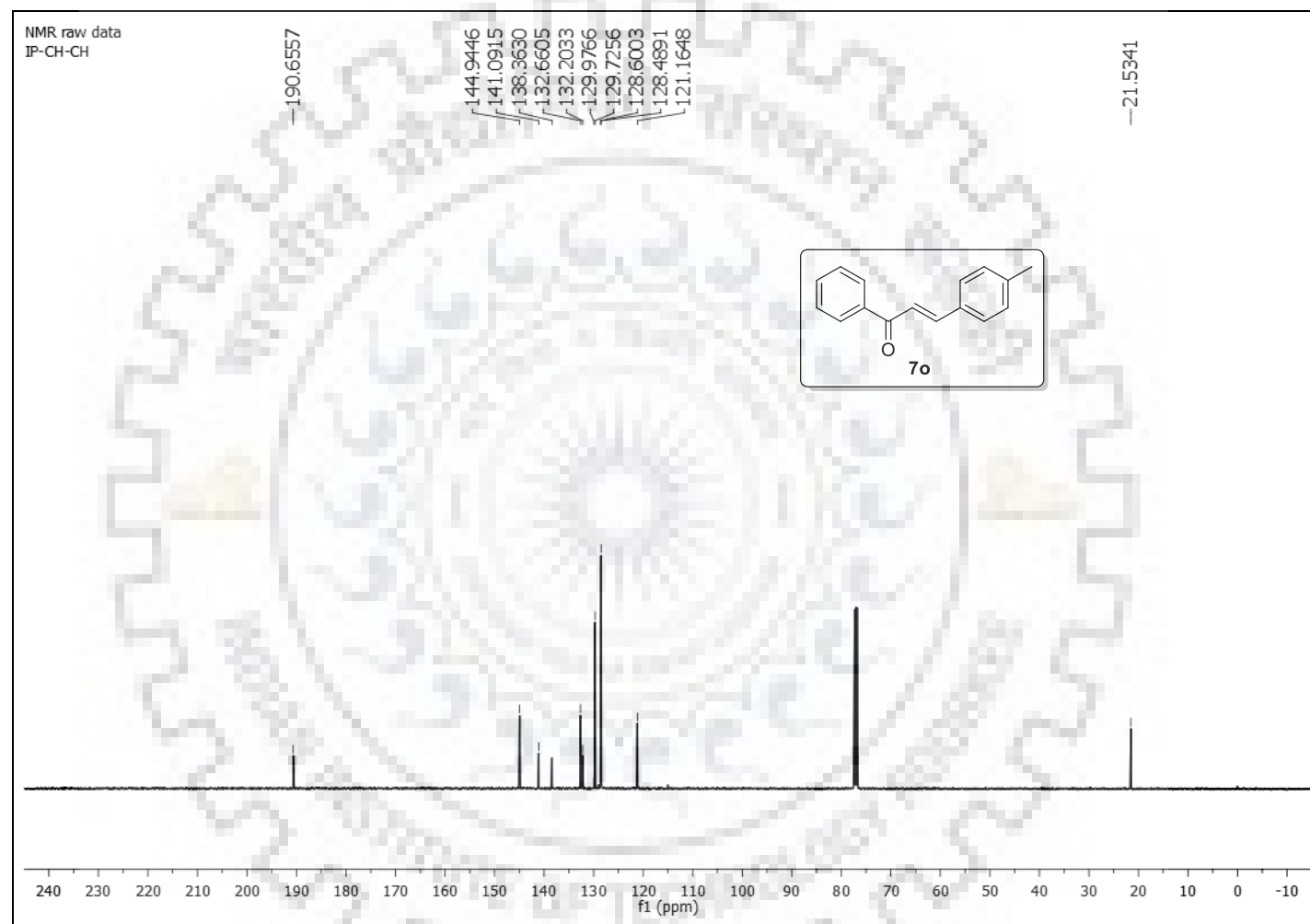


Figure S-76: ^{13}C Spectrum of **7o**.

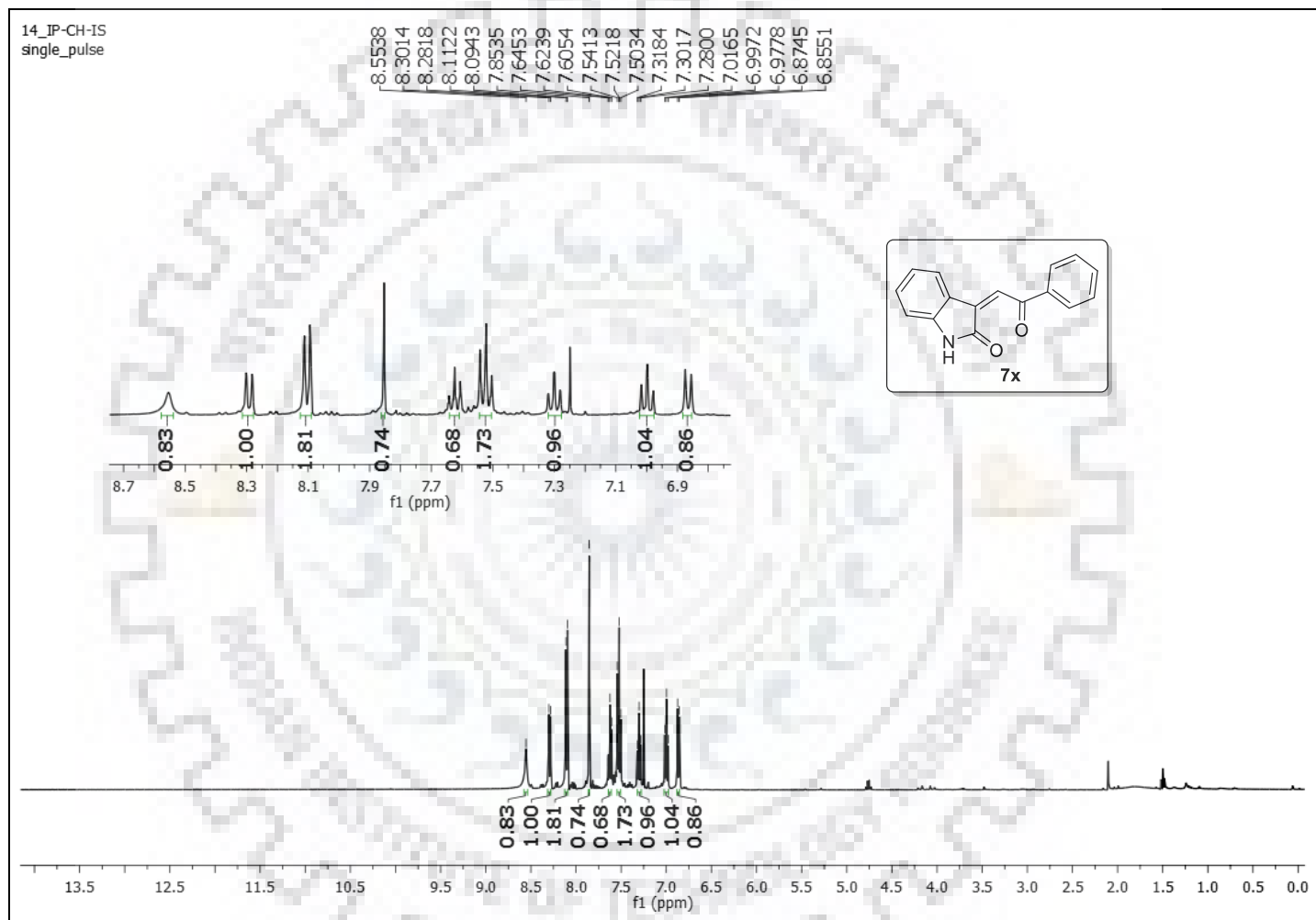


Figure S-77: ^{13}C Spectrum of 7x.

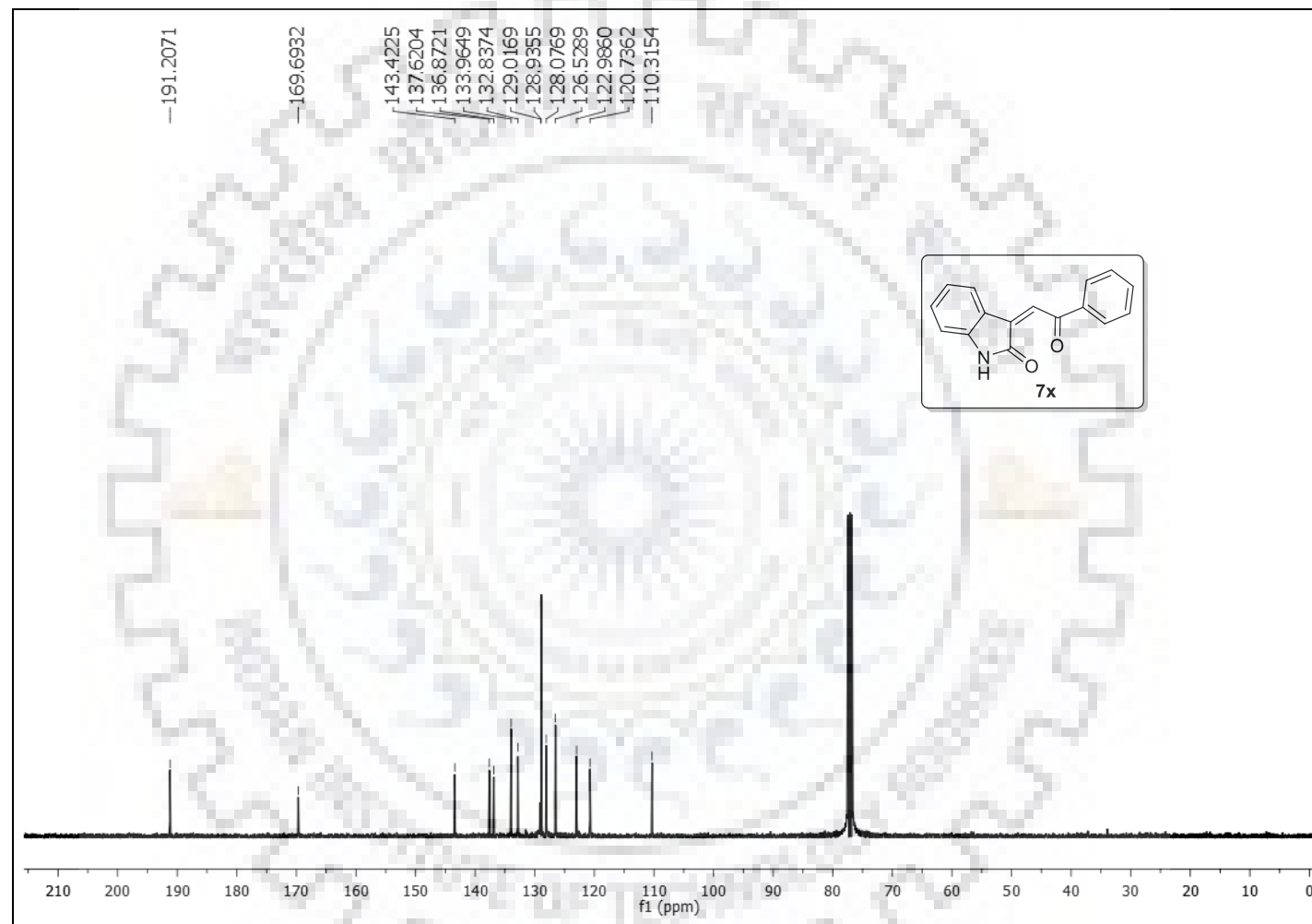


Figure S-78: ^{13}C Spectrum of 7x.

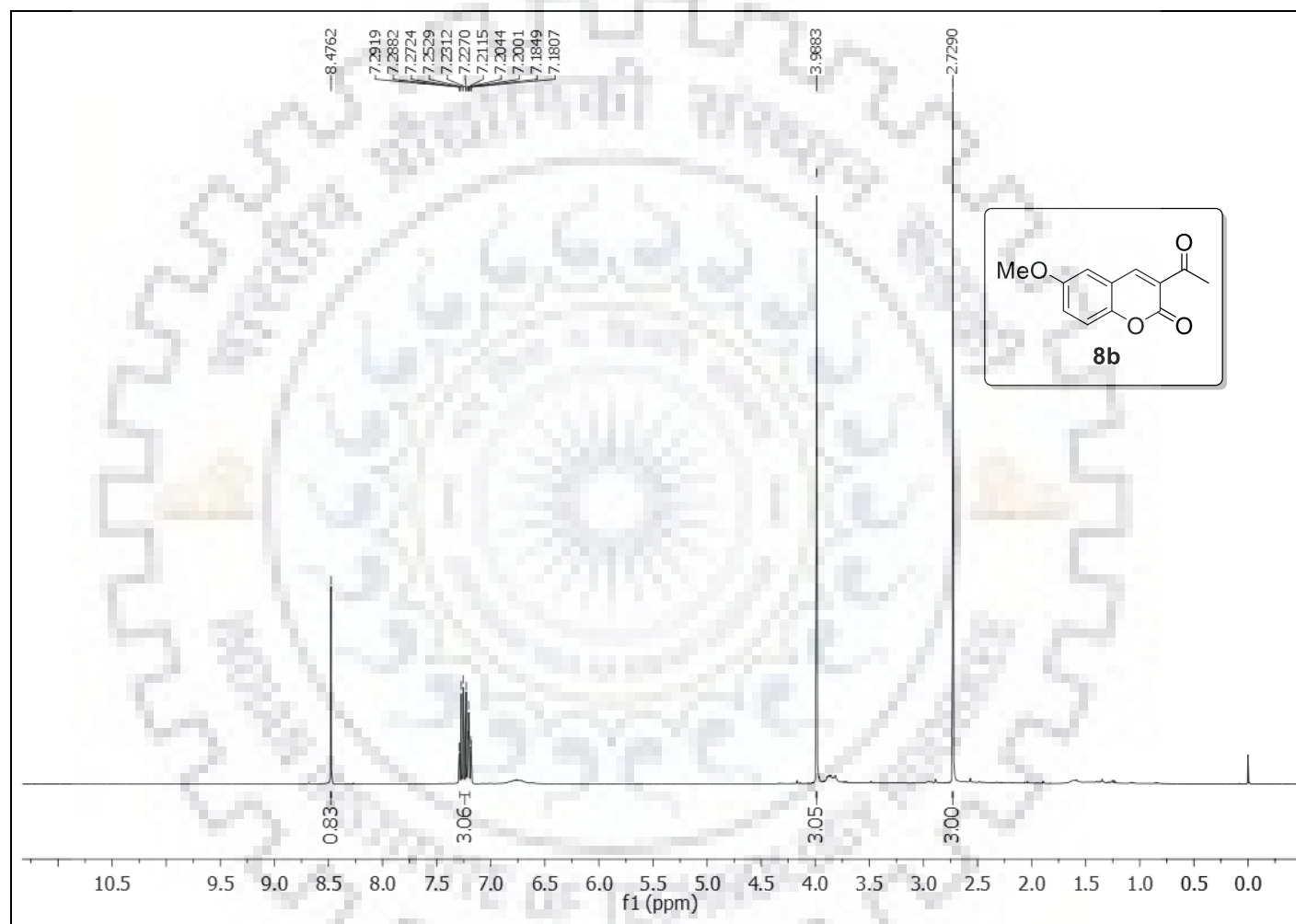


Figure S-79: ¹H Spectrum of **8b**.

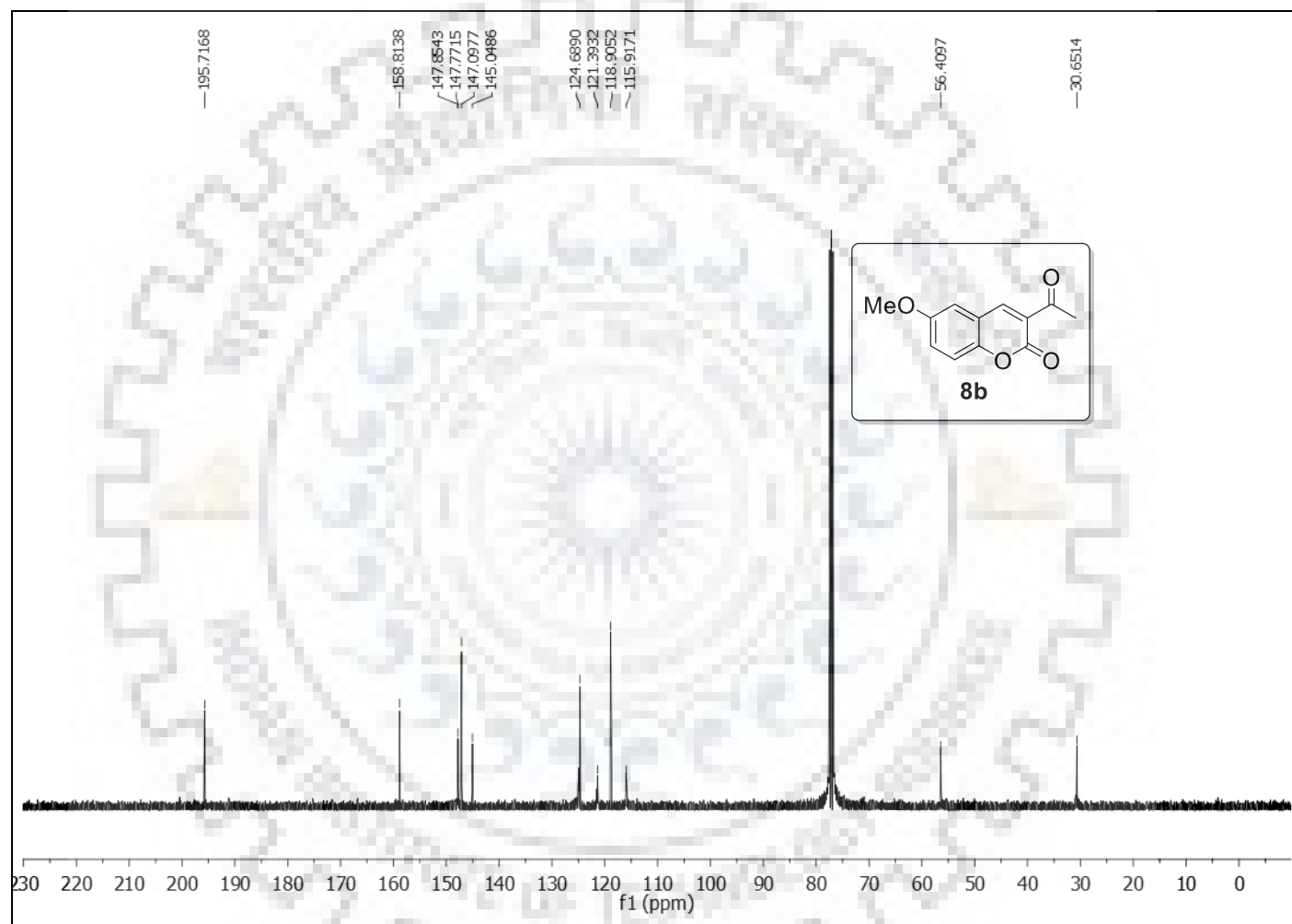


Figure S-80: ^{13}C Spectrum of **8b**.

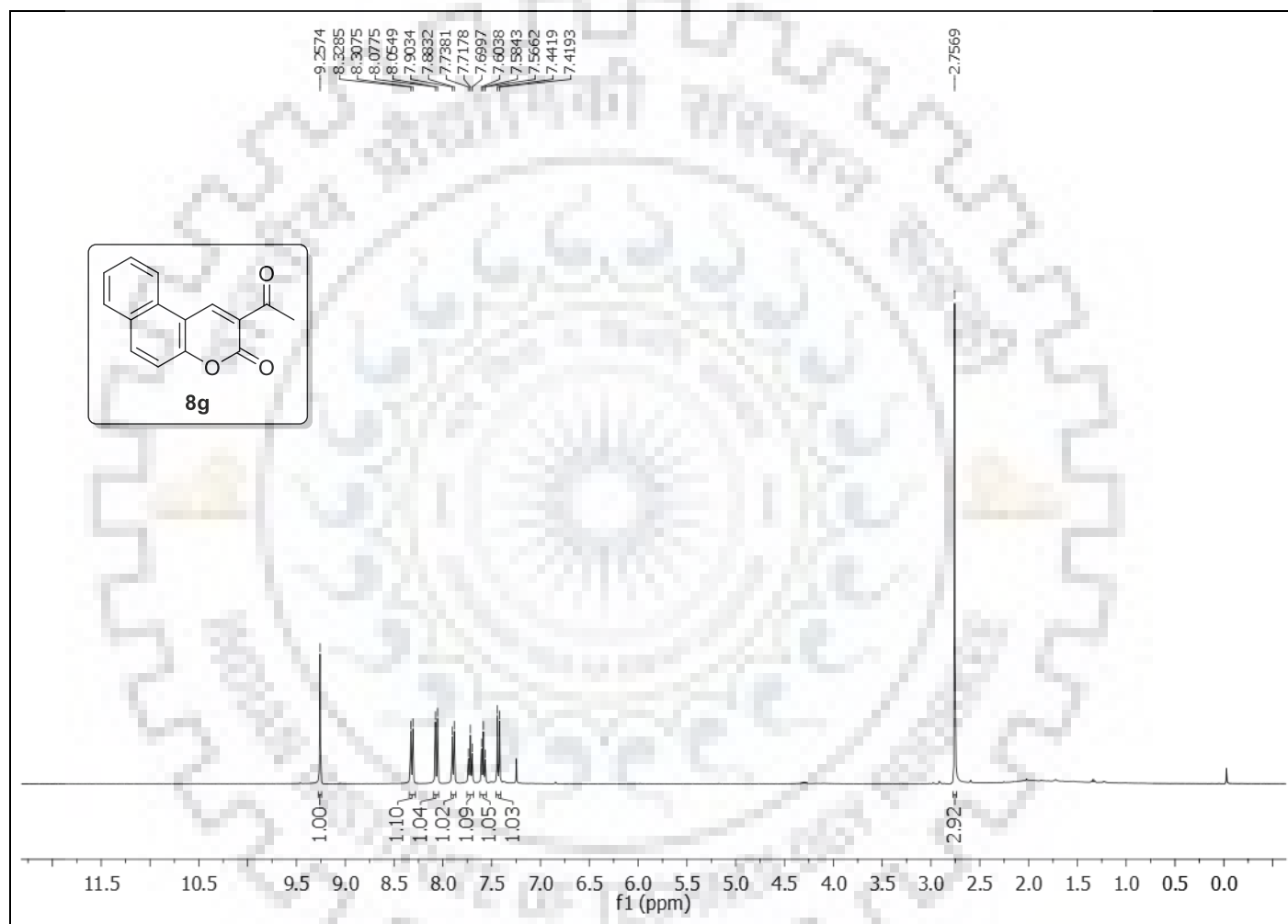


Figure S-81: ^1H Spectrum of **8g**.

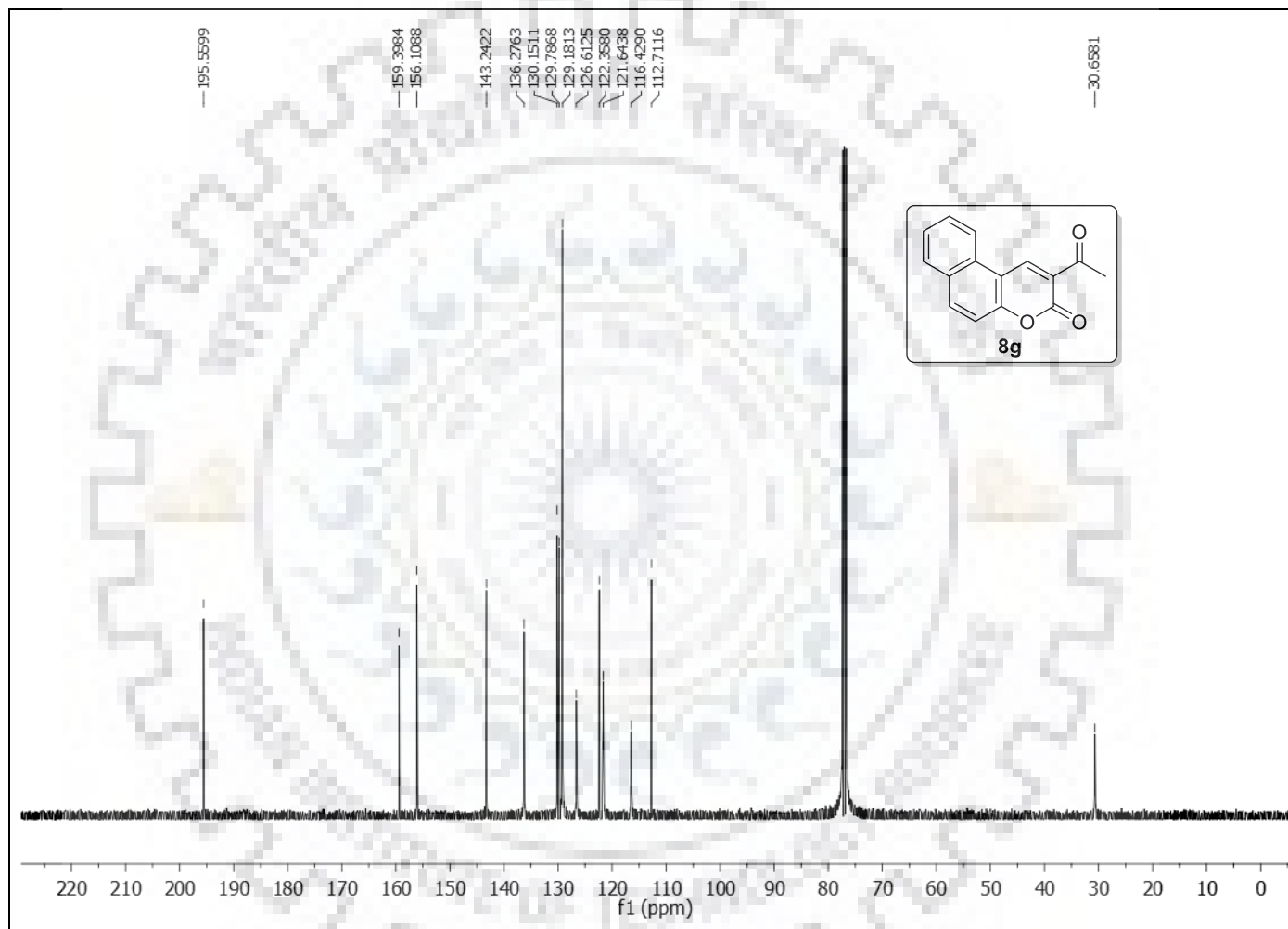


Figure S-82: ^{13}C Spectrum of **8g**.



SUMMARY

Natural products have many intriguing properties which have caught the attention of scientists and hence the study of natural products and related flavonoids has seen a huge surge in terms of the number of publications in the last decade or so. Flavonoids are polyphenolic stable aromatic species but at the same time reactive enough to allow modifications by different kinds of reactions known as functionalization methods. Flavonoids substituted with appropriate functional groups have been successfully explored for their use in medicine and drugs such as xanthokeyesmins A-C and dime fine for the treatment of bronchial asthma. In chapter 1, we have given a brief introduction regarding the synthetic methods and properties of flavonoids.

In Chapter 2 we described an unprecedented base catalysed domino C-O bond cleavage of 3-bromoflavone by insertion of substituted aniline and N-phenyl urea has been described. This method involves the formation of two new C-N and C-O bonds utilizing base and copper iodide for pharmacologically important stereospecific aminated aurone derivatives. These compounds were characterized by various spectroscopic techniques and single crystal XRD studies. Based on our extensive literature survey, aurone synthesis revealed harsh reaction condition, long reaction time, expensive catalyst loading. Our protocol is operationally successful with ease, avoids the requirement of additives, fast conversion and offers broad substrate scope.

In chapter 3, we synthesized biologically active tetracyclic flavone fused benzofuran derivative through mild condition. This reaction includes, sequential C-O bond formation followed by C-Cl bond cleavage. Diversely substituted flavone fused benzofuran are obtain in moderate to good yields. The compounds were characterized by various spectroscopic measurements. In comparison with the available methods for the, the present method is highly efficient and easy to operate with good substrate scope.

In chapter 4 we have developed multicomponent one pot synthetic route for the pharmacologically important pyrimidine-piperazine-chromene and -quinoline conjugates from readily available starting material. These synthesized compounds were assessed their antiproliferative activities against human embryonic kidney cells (HEK293) (Normal cell) and human breast cancer cell lines (MCF-7). The quinoline derivative with methyl group and without substitute and chromene derivative with methyl and nitro and without substituent show good activity than curcumin drug. Furthermore, quinoline derivative with methyl group and without substitute and chromene derivative gave good binding affinity against Bcl-2 protein.

SUMMARY

In chapter 5, we have reported the facile synthesis of 3-N-aryl substituted-2-heteroarylchromones *via* Pd-mediated through oxidative coupling reaction in good yield. These compounds show human Microtubule affinity regulating kinase 4 (MARK4) enzyme inhibitors. Among 22 synthesized molecules, compounds *para*-iodo, *para*-nitro and *para*-methyl were identified as hit and exhibited excellent *in vitro* inhibitory effect against MARK4 with IC₅₀ value (50% of ATPase activity) and through fluorescence binding and dot blot assay indicates a better binding affinity. *In vitro* studies against the cancerous cells (MCF-7 and HepG2) revealed that the compounds *para*-iodo, *para*-nitro and *para*-methyl substituted derivative inhibit the cell viability, induce apoptosis and tau-phosphorylation. Cell viability studies gave the growth inhibition of cancerous cells with good IC₅₀ for human breast cancer cells (MCF-7) and for human liver carcinoma cells (HepG2) respectively. Compounds *para*-iodo, *para*-nitro and *para*-methyl put the cancerous cells on oxidative stress as suggested by ROS quantification. Molecular docking of compounds *para*-iodo, *para*-nitro and *para*-methyl showed hydrogen bonding, charge or polar and vander waals interactions by the active site residues of MARK4. These observations clearly showed that the compounds fit nicely in the active site with high binding affinity. Thus, compounds may be as potential inhibitors and further explored to design novel therapeutic molecules in the drug discovery against MARK4-related diseases

In chapter 6, This chapter illustrates a novel copper catalyzed annulation reaction of α - and β -halo carbonyl compounds *via* isopropanol as a hydride donor and solvent under basic and mild condition. This reaction involve C-H bond formation followed by C-X bond cleavage. we performed the control experiments using deuterated isopropanol with different substrates. All deuterated products confirmed by HRMS spectroscopy.

ACKNOWLEDGEMENT

First and foremost, I am submissively bowing down to the almighty for bestowing me with innumerable blessings and uncountable favors throughout my life. I am sincerely grateful to Him for my skills and capabilities and for the many chances He gave me to arrive here and hold my head high with self-esteem.

I would like to express my sincere gratitude to my Supervisor Dr. Naseem Ahmed, Department of Chemistry, IIT Roorkee who was always available for discussions. He has contributed a great deal to my understanding in research through valuable discussions, ideas and useful comments, which were a great source of my inspiration.

I take the opportunity to express my gratitude to my Student Research Committee (SRC) members Dr. Anuj Sharma and Dr. Rama Krishna Peddinti, Department of Chemistry and Dr. Parsenjit Mondal, Department of Chemical engineering, IIT Roorkee for extending me all possible help and offering valuable suggestions during the entire course. I am highly grateful to Prof. M. R. Maurya, Head of the Department of Chemistry, for providing me with necessary facilities and support to carry out my work. I am thankful to Mr. S. P. Singh, Mr. Madan Pal, Mr. Tiwari and other staff members, Department of Chemistry, for giving a helping hand to me on all occasions.

I also thank to the Head, Institute instrumentation center, IIT Roorkee for providing NMR and other necessary instrumentation facilities. I would like to thanks Ms. Neetu Singh and Prof. U. P. Singh, IIT Roorkee, for single crystal X-ray data collection and discussion at various stage of my research work. I wish to put on record my gratitude to the Editors & Reviewers for their comments/suggestions during publishing manuscripts and conference proceedings.

I would like to thank my seniors and labmates Dr. S. M. Abdul shakoor, Dr. Naveen Konduru, Dr. Shaily, Dr. Nishant, Dr. Gulab, Dr. Sumit, Waheed, Mauzey, Danish, Khawaja and Bhawana. I thank you all for your cooperation, help, maintaining excellent working atmosphere in the lab and sparing time for me whenever I needed it from you. I am also grateful to all the members of Chemistry Department for their cooperation and timely help which provided a suitable environment to develop my skills as a researcher. True friendship is the soul of a beautiful life. I consider myself truly blessed as I have always been in a good company of friends. Their daily smiles and laughter have made my time intensely delightful and certainly unforgettable. I would like to gratefully thanks to my special friends Dr. Nirma Maurya, Dr. Mandeep Kaur, Dr. Surinder Pal Kaur, Dr. Divya singhal, Dr. Neha Gupta, Dr. Nitika Sharma, Dr. Ankita Saini, Dr. Himanshu, Dr. Tawseef Ahmed Dar, Mandeep Khan, Shweta, Manju, Kavita, Garima, Madhusudan,

ACKNOWLEDGEMENT

Anshu, Neha dua and Pratima with whom I have shared the best time of my life and who were always there in the hour of need. I extended my warm thanks to my friends Maheen, Khushnuma, Samya, Kanika, Huma, Gulista, Saima and all my batch mates at AMU.

It is a privilege to express my sincerest and warm gratitude to all the teachers who have taught me since childhood. I always value their patience, labour and dedicated efforts that they undertook to make me learn. Their advices and scoldings will always remain close to my heart and I will keep seeking them for further guidance and knowledge.

I am thankful to IITR and UGC, India for providing me the fellowship. I am grateful to IITR for providing necessary infrastructure for my research work.

I am incredibly lucky to have been born in a family of caring and loving members. My family deserves special mention for their unflagging love and support in my life. This work would simply have been impossible without them. I am indebted to my beloved mother Smt. Jannat Khatoon and father Sh. Inayat Hussain Ansari for their love, affection, constant inspiration, unconditional support throughout my life. I also thank to my family members Sh. Farooqe Ahmed and Smt. Akhtarun Nisha for their love, encouragement and innumerable prayers. I extend my gratefulness and love to my elder brothers Amjad Ali, Parvez Alam Ansari, Asad, Danish, Adil and cute younger sister Mahek for their love, affection and for all the sweet memories. I am exceedingly thankful to my special gratitude to my younger brother Javed Akhter for his loving support and encouragement and being a pillar of strength for me.

As I conclude, my apologies and honest gratitude to all those whose names have been unintentionally left. I hold all of them in high regards and I know they will swarm around me with their best efforts whenever I need them.

Finally, I am thankful to almighty GOD, for his mercy and grace bestowed upon me during my entire life.

Iram Parveen